COUPLING AND UNCOUPLING: DYNAMIC CONTROL OF MEMBRANE CONTACTS

EDITED BY: Dan Zhang, Yasunori Saheki, Benoît Kornmann and Junjie Hu

PUBLISHED IN: Frontiers in Cell and Developmental Biology

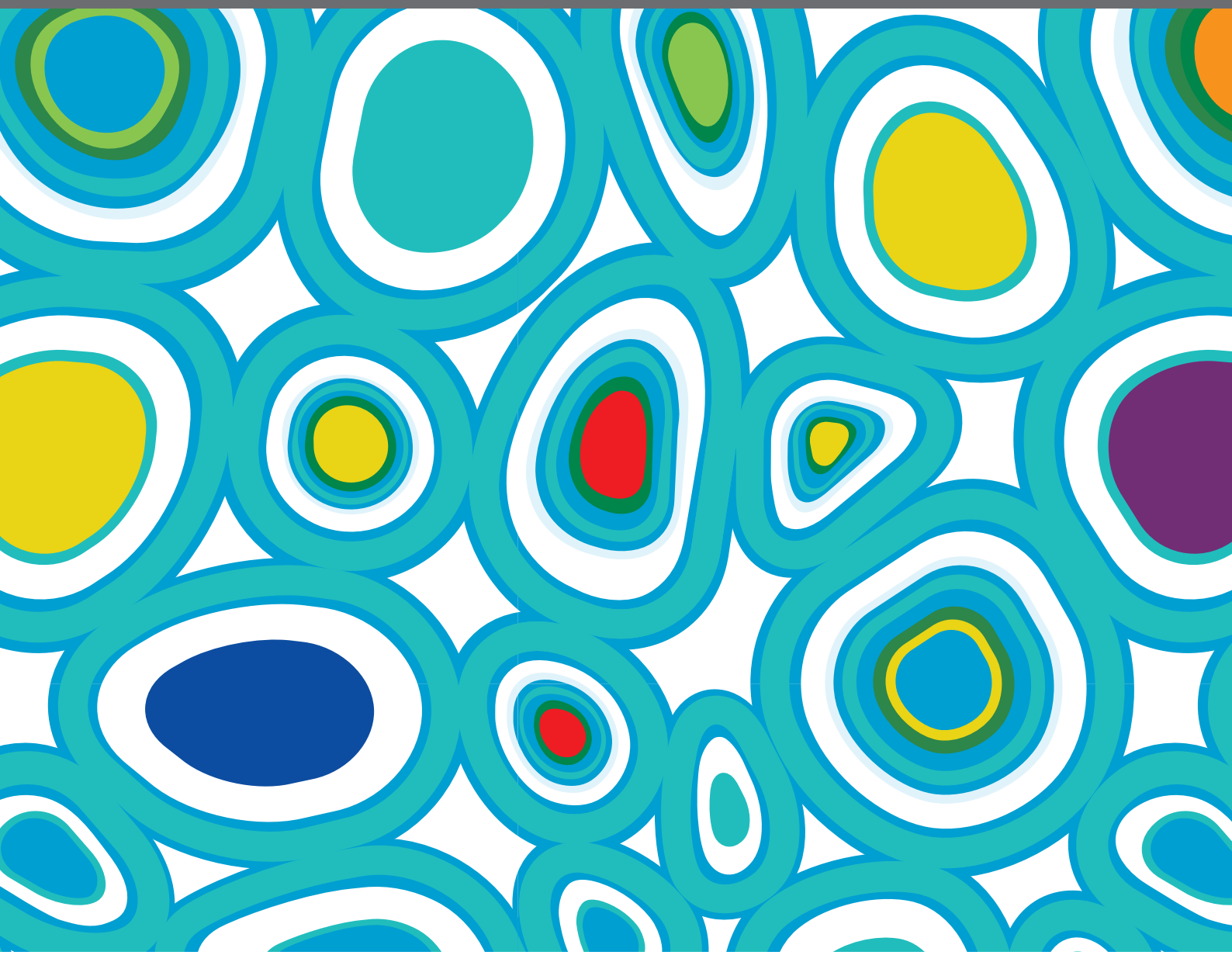

frontiers Research Topics

ISSN 1664-8714
ISBN 978-2-88971-213-7
DOI 10.3389/978-2-88971-213-7

About Frontiers

Frontiers is more than just an open-access publisher of scholarly articles: it is a pioneering approach to the world of academia, radically improving the way scholarly research is managed. The grand vision of Frontiers is a world where all people have an equal opportunity to seek, share and generate knowledge. Frontiers provides immediate and permanent online open access to all its publications, but this alone is not enough to realize our grand goals.

Frontiers Journal Series

The Frontiers Journal Series is a multi-tier and interdisciplinary set of open-access, online journals, promising a paradigm shift from the current review, selection and dissemination processes in academic publishing. All Frontiers journals are driven by researchers for researchers; therefore, they constitute a service to the scholarly community. At the same time, the Frontiers Journal Series operates on a revolutionary invention, the tiered publishing system, initially addressing specific communities of scholars, and gradually climbing up to broader public understanding, thus serving the interests of the lay society, too.

Dedication to Quality

Each Frontiers article is a landmark of the highest quality, thanks to genuinely collaborative interactions between authors and review editors, who include some of the world's best academicians. Research must be certified by peers before entering a stream of knowledge that may eventually reach the public - and shape society; therefore, Frontiers only applies the most rigorous and unbiased reviews.
Frontiers revolutionizes research publishing by freely delivering the most outstanding research, evaluated with no bias from both the academic and social point of view. By applying the most advanced information technologies, Frontiers is catapulting scholarly publishing into a new generation.

What are Frontiers Research Topics?

Frontiers Research Topics are very popular trademarks of the Frontiers Journals Series: they are collections of at least ten articles, all centered on a particular subject. With their unique mix of varied contributions from Original Research to Review Articles, Frontiers Research Topics unify the most influential researchers, the latest key findings and historical advances in a hot research area! Find out more on how to host your own Frontiers Research Topic or contribute to one as an author by contacting the Frontiers Editorial Office: frontiersin.org/about/contact

COUPLING AND UNCOUPLING: DYNAMIC CONTROL OF MEMBRANE CONTACTS

Topic Editors:
Dan Zhang, Temasek Life Sciences Laboratory, Singapore
Yasunori Saheki, Nanyang Technological University, Singapore
Benoît Kornmann, University of Oxford, United Kingdom
Junjie Hu, Chinese Academy of Sciences (CAS), China

Citation: Zhang, D., Saheki, Y., Kornmann, B., Hu, J., eds. (2021). Coupling and Uncoupling: Dynamic Control of Membrane Contacts. Lausanne: Frontiers Media SA. doi: 10.3389/978-2-88971-213-7

Table of Contents

frontiers in Cell and Developmental Biology

EDITORIAL
published: 24 August 2021
doi: 10.3389/fcell.2021.721546

Editorial: Coupling and Uncoupling: Dynamic Control of Membrane Contacts

Dan Zhang[1,2*†], *Yasunori Saheki*[3,4†], *Junjie Hu*[5,6†] *and Benoît Kornmann*[7†]

[1] Temasek Life Sciences Laboratory, National University of Singapore, Singapore, Singapore, [2] Department of Biological Sciences, National University of Singapore, Singapore, Singapore, [3] Lee Kong Chian School of Medicine, Nanyang Technological University, Singapore, Singapore, [4] Institute of Resource Development and Analysis, Kumamoto University, Kumamoto, Japan, [5] National Laboratory of Macromolecules, Institute of Biophysics, Chinese Academy of Sciences, Beijing, China, [6] College of Life Sciences, University of Chinese Academy of Sciences, Beijing, China, [7] Department of Biochemistry, University of Oxford, Oxford, United Kingdom

Keywords: membrane contact sites, organelle dynamics, membrane-cytoskeleton interactions, membrane contact remodeling, non-vesicular lipid transport

Editorial on the Research Topic

Coupling and Uncoupling: Dynamic Control of Membrane Contacts

OPEN ACCESS

Edited and reviewed by:
Vladimir Lupashin, University of Arkansas for Medical Sciences, United States

****Correspondence:***
Dan Zhang
zhangdan@tll.org.sg

†These authors have contributed equally to this work

Specialty section:
This article was submitted to Membrane Traffic, a section of the journal Frontiers in Cell and Developmental Biology

Received: *07 June 2021*
Accepted: *30 June 2021*
Published: *24 August 2021*

Citation:
Zhang D, Saheki Y, Hu J and Kornmann B (2021) Editorial: Coupling and Uncoupling: Dynamic Control of Membrane Contacts. Front. Cell Dev. Biol. 9:721546. doi: 10.3389/fcell.2021.721546

All living cells are dynamic assemblies in nature that continuously self-organize numerous molecules into various separate-yet-connected functional and homeostatic units. Many such membrane-bound units in eukaryotic cells, namely membranous organelles with characteristic morphologies, dynamics, and functions, together with the plasma membrane (PM) are physically interconnected at membrane contact sites (MCSs) without membrane fusion. MCSs are commonly regarded as interorganellar, though they can also be intraorganellar. To date, all membrane-bound organelles have been observed to make contacts with at least one other membrane type. The distribution and abundance of these interorganellar MCSs vary among cell types. Structurally, some MCSs could appear stable and constitutive [e.g., the endoplasmic reticulum (ER)-PM contacts in muscle cells and yeasts, etc]. However, membrane tethering as well as molecular assemblies at MCSs are often highly dynamic. For example, transient contacts between the ER and mitochondria (Mito) or endosomes (Endo) form during their respective fission. In mammalian cells, machineries for store-operated Ca^{2+} entry are rapidly assembled at ER-PM contacts upon reduction of Ca^{2+} levels in the ER lumen.

Close membrane apposition can be established in both an inter- and intraorganellar fashion through a variety of tethering machineries. Interorganellar tethering complexes facilitate direct transport of small molecules, such as lipids and ions at MCSs, which helps to maintain cellular homeostasis and guide associated signaling pathways and/or cellular events. Intraorganellar tethers on the other hand can support the architecture of organelles and hence their functions: They act either at the cytoplasmic interface to build stacked membranes [e.g., stacked ER cisternae albeit more prominently seen with the overexpression of ER resident proteins (Snapp et al., 2003) and Golgi stacks (Lee et al., 2014) etc.], or as intraluminal spacers to modulate lumen diameter [e.g., ER luminal spacer Climp63 (Zhao and Hu)], or in a complex manner to structure the interior of double-membrane-bound organelles, such as mitochondria (van der Laan et al., 2012). In all cases, spatial confinement at these membrane junctures could locally alter molecular dynamics and potentially involve microdomain formation for specialized activities.

With the discovery of major tethering complexes for various MCSs, one of the next major goals is to understand how cells spatiotemporally control assembly and disassembly of MCSs and coordinate the functions of various MCSs during different states of the cells. Many tethers have been pinpointed to couple membranes through protein-protein or protein-lipid interaction, however little is known quantitatively about the threshold of such interactions that suffices bona fide contact site formation. This is an important issue, as cross-membrane interactions essentially determine the membrane tethering strength and therefore could impact the abundance and dynamics of MCSs. Conceivably, modulation of such interactions at MCSs is likely the common mechanism for dynamic control of MCS formation in the cell. Thus, one should be cautious in interpreting findings that involve tethering proteins expressed at non-physiological levels for functional indication, as higher levels of tethers often induce the formation of ectopic and/or more stable MCSs, and vice versa, which may alter their functions. Intrinsic membrane remodeling capacity and cytoskeleton dynamics (Koppers et al.) could also affect the strength of membrane tethering at MCSs, possibly through imposing shear forces or cross-linking effects. Besides, organelle morphology, particularly the ER reticulation, appears crucial for MCS formation: For instance, membrane contacts are more frequently engaged with the tubular ER. Alteration in membrane curvature or geometry during organellar remodeling may locally promote the coupling or uncoupling between membranes.

Limited spacing at MCSs could obstruct space-demanding processes that involve large-sized protein assemblies (Zhang, 2020) or vesicles (Ng et al., 2018). It is conceivable that such physical roles would depend on the amount and plasticity of MCSs, and hence the disassembly and removal of MCS become an important step to finetune this barrier effect. While as for biochemical activities at MCSs, it is becoming clear that tethering of opposing membranes stimulates non-vesicular lipid transport mediated by lipid-transfer proteins (LTPs) (Ercan et al., 2021). How the assembly and disassembly of MCSs affect the global state of lipid transport, however, remains elusive. In fact, many LTPs have affinities for both membranes at MCSs through the binding of lipids or resident proteins, so they are often considered as part of the tethering machinery. However, most LTPs seem to have minor roles in sustaining MCSs under normal physiological conditions. One can envisage that non-vesicular lipid transfer could also occur via simple diffusion of LTPs following the lipid gradient between membranes. Indeed, some forms of non-vesicular lipid transport likely do not rely on MCSs (Dittman and Menon, 2017; Quon et al., 2018). Nevertheless, commonality of microniches created by juxtaposed membranes in lipid-related functions, including lipid transport, synthesis, and metabolism (discussed by Hewlett et al.; Nakatsu and Kawasaki; Xu and Huang), infers that MCSs should possess conserved advantages for these roles.

In this collection of articles, we see the latest summaries and perspectives on MCSs of various kinds covering their formation, dynamics, and functions, including ER-PM (Hewlett et al.; Li et al.), ER-Mito (Aoyama-Ishiwatari and Hirabayashi), ER-Endo (Shirane), ER-Golgi (Feng et al.), Mito-lipid droplet (LD) (Cui and Liu), and secretory vesicle-PM contacts (Ruan et al.), etc. In addition, Tashiro et al. developed an improved version of the split-GFP system in yeast and mammalian cells (which relies on lower expression of the split-GFP components), enabling quantitative analysis of various MCSs at near-native states in living cells. Cui and Liu further discuss potential molecular distinctions between dynamic and stable Mito-LD contacts from a structural point of view. Moreover, two articles particularly highlight anomalies of MCSs in various diseases, e.g., altered abundance of ER-Mito contacts being seen in different cell lineages associated with cardiovascular diseases (Liu et al.) and impaired endosomal homeostasis resulting from ER-Endo contact dysfunction perhaps underlying some forms of neurodegenerative disorders (Shirane). Finally, Wong et al. draw an interesting connection between host cell organelles and viral RNA-containing double-membrane vesicles (DMVs) for positive strand RNA viral replication, using severe acute respiratory syndrome coronavirus 2 as a major example. They review how these viruses hijack host lipid metabolic machineries and redirect lipids via assorted MCSs to generate DMVs for proliferation.

UNFATHOMED QUESTIONS AND CHALLENGES

Membrane-contact-related research has gained tremendous interest in recent years. While exciting advances have been made, many fundamental questions remain elusive. These include:

- How is the rate of non-vesicular lipid transport regulated in living cells? So far, lipid transfer has been primarily studied using reconstitution assays, but the rate of lipid transport observed *in vitro* is often slow. It is also intriguing to see how much of non-vesicular lipid transport is mediated at MCSs vs. by simple diffusion of LTPs *in vivo*. Further attempts will have to be made to establish methods for detecting and quantifying such lipid transfer in living cells.
- How does redundancy of multiple protein tethers contribute to their functional crosstalk at the same MCSs? The abundance and structural arrangement of individual tethers likely matter, especially when they differ in distances that they can stretch at MCSs. This question is pertinent to a common issue that many studies use depletion or over-expression of tethers to argue their functions. With potential interference among tethers (i.e., depletion or overexpression of tether A affecting tether B functions), we may need to re-evaluate some of the existing results.
- How does molecular interaction physically determine the extent of membrane tethering at MCSs? Addressing this question will provide mechanistic insights into the dynamic control of MCS remodeling.
- A general one–how do cells balance different MCSs in their quantity, distribution, dynamics, and functions, in harmony with their cellular states?

AUTHOR CONTRIBUTIONS

All authors listed have made a substantial, direct and intellectual contribution to the work, and approved it for publication.

ACKNOWLEDGMENTS

We thank all authors and reviewers for their contribution to the Research Topic.

REFERENCES

Dittman, J. S., and Menon, A. K. (2017). Speed limits for nonvesicular intracellular sterol transport. *Trends Biochem. Sci.* 42, 90–97. doi: 10.1016/j.tibs.2016.11.004

Ercan, B., Naito, T., Koh, D. H. Z., Dharmawan, D., and Saheki, Y. (2021). Molecular basis of accessible plasma membrane cholesterol recognition by the GRAM domain of GRAMD1b. *EMBO J.* 40:e106524. doi: 10.15252/embj.2020106524

Lee, I., Tiwari, N., Dunlop, M. H., Graham, M., Liu, X., and Rothman, J. E. (2014). Membrane adhesion dictates Golgi stacking and cisternal morphology. *Proc. Natl. Acad. Sci. U.S.A.* 111, 1849–1854. doi: 10.1073/pnas.1323895111

Ng, A. Y. E., Ng, A. Q. E., and Zhang, D. (2018). ER-PM contacts restrict exocytic sites for polarized morphogenesis. *Curr. Biol.* 28, 146–153.45. doi: 10.1016/j.cub.2017.11.055

Quon, E., Sere, Y. Y., Chauhan, N., Johansen, J., Sullivan, D. P., Dittman, J. S., et al. (2018). Endoplasmic reticulum-plasma membrane contact sites integrate sterol and phospholipid regulation. *PLoS Biol.* 16:e2003864. doi: 10.1371/journal.pbio.2003864

Snapp, E. L., Hegde, R. S., Francolini, M., Lombardo, F., Colombo, S., Pedrazzini, E., et al. (2003). Formation of stacked ER cisternae by low affinity protein interactions. *J. Cell Biol.* 163, 257–269. doi: 10.1083/jcb.200306020

van der Laan, M., Bohnert, M., Wiedemann, N., and Pfanner, N. (2012). Role of MINOS in mitochondrial membrane architecture and biogenesis. *Trends Cell Biol.* 22, 185–192. doi: 10.1016/j.tcb.2012.01.004

Zhang, D. (2020). Interplay between endoplasmic reticulum membrane contacts and actomyosin cytoskeleton. *Cytoskeleton* 77, 241–248. doi: 10.1002/cm.21623

Conflict of Interest: The authors declare that the research was conducted in the absence of any commercial or financial relationships that could be construed as a potential conflict of interest.

Publisher's Note: All claims expressed in this article are solely those of the authors and do not necessarily represent those of their affiliated organizations, or those of the publisher, the editors and the reviewers. Any product that may be evaluated in this article, or claim that may be made by its manufacturer, is not guaranteed or endorsed by the publisher.

frontiers in Cell and Developmental Biology

BRIEF RESEARCH REPORT
published: 16 June 2020
doi: 10.3389/fcell.2020.00500

Self-Association of Purified Reconstituted ER Luminal Spacer Climp63

Jinghua Zhao[1] *and Junjie Hu*[1,2]*

[1] Department of Genetics and Cell Biology, College of Life Sciences, Nankai University, Tianjin, China, [2] National Laboratory of Biomacromolecules, CAS Center for Excellence in Biomacromolecules, Institute of Biophysics, Chinese Academy of Sciences, Beijing, China

Membranes of the endoplasmic reticulum (ER) are shaped into cisternal sheets and cylindrical tubules. How ER sheets are generated and maintained is not clear. ER membrane protein Climp63 is enriched in sheets and routinely used as a marker of this structure. The luminal domain (LD) of Climp63 is predicted to be highly helical, and it may form bridges between parallel membranes, regulating the abundance and width of ER sheets. Here, we purified the LD and full-length (FL) Climp63 to analyze their homotypic interactions. The N-terminal tagged LD formed low-order oligomers in solution, but was extremely aggregation-prone when the GST tag was removed. Purified FL Climp63 formed detectable but moderate interactions with both the FL protein and the LD. When Climp63 was reconstituted into proteoliposomes with its LD facing out, the homotypic interactions were retained and could be competed by soluble LD, though vesicle clustering was not observed. These results demonstrate a direct self-association of Climp63, supporting its role as an ER luminal spacer.

Keywords: endoplasmic reticulum, sheet biogenesis, membrane tethering, homotypic interactions, reconstitution, Climp63

OPEN ACCESS

Edited by:
Wei Li,
Capital Medical University, China

Reviewed by:
Joji Mima,
Osaka University, Japan
Will Prinz,
National Institute of Diabetes and Digestive and Kidney Diseases, National Institutes of Health (NIH), United States

***Correspondence:**
Junjie Hu
huj@ibp.ac.cn

Specialty section:
This article was submitted to Membrane Traffic, a section of the journal Frontiers in Cell and Developmental Biology

Received: *06 April 2020*
Accepted: *25 May 2020*
Published: *16 June 2020*

Citation:
Zhao J and Hu J (2020) Self-Association of Purified Reconstituted ER Luminal Spacer Climp63. Front. Cell Dev. Biol. 8:500. doi: 10.3389/fcell.2020.00500

INTRODUCTION

The endoplasmic reticulum (ER) is composed by two interconnected morphological domains: tubules and sheets (Baumann and Walz, 2001; Shibata et al., 2006). Though the morphogenesis of the tubular ER network has been studied extensively (Shibata et al., 2009; Hu et al., 2011; Lin et al., 2012), little is known about how sheets are formed. ER sheets are cisternal structures bounded by two flattened parallel membranes, with a width of ∼30 nm in yeast and ∼50 nm in mammalian cells. Most sheets are decorated by translating ribosomes (Savitz and Meyer, 1990; Puhka et al., 2007), termed the rough ER, which links ER sheets to protein synthesis, a key function of the ER.

Investigation of professional secretory cells, such as pancreatic cells and plasma cells that contain massive ER sheets, sheds light on key regulators of sheet formation (Shibata et al., 2010). Three ER membrane proteins, cytoskeleton-linking membrane protein 63 (Climp63), p180, and kinectin, have been identified as sheet-enriched proteins that determine ER sheet formation. Climp63 is proposed to serve as a luminal ER spacer by forming luminal bridges. p180 and kinectin, both of which potentially contain extensive cytosolic coiled coil domains, are thought to flatten ER membranes using these coiled coils. In addition, the presence of polysomes on ER membranes likely promotes sheet formation (Shibata et al., 2010). Finally, the shaping of ER sheets may be facilitated

by tubule-forming proteins, which also localize to the edge of sheets and stabilize the high curvature there (Shibata et al., 2010). Among sheet-forming proteins, Climp63, which is also referred to as cytoskeleton associated protein 4 (CKAP4), is the most commonly used sheet marker in the ER. It rarely localizes to ER tubules (Gao et al., 2019; Schroeder et al., 2019) and is not observed in the nuclear envelope (Shibata et al., 2010). Climp63 is a 63 kDa type II transmembrane protein with a relatively short N-terminus (NT, 85 aa) and a long C-terminal luminal domain (LD, 472 aa; **Figure 1A**). Climp63 interacts with microtubules, as indicated by its name, through a region in the NT. The cytoskeleton linkage can be reversed by phosphorylation in the proximal region (Vedrenne et al., 2005) and potentially regulates translocon mobility (Nikonov et al., 2007) and ER positioning (Cui-Wang et al., 2012; Farías et al., 2019). Palmitoylation was also detected in the NT (Planey et al., 2009), but the physiological role is not entirely clear. Interestingly, Climp63 is also implicated in several signaling events (Nisha Gupta et al., 2006; Sandoz and van der Goot, 2015; Chavda et al., 2017), with some mechanisms requiring plasma membrane localization.

Importantly, the LD of Climp63 is expected to convey the most critical function, i.e., sheet morphogenesis. Depletion or deletion of Climp63 in cultured cells causes an ∼50% decrease in the luminal width of the ER (Shibata et al., 2010), and reintroduction of Climp63 with engineered LDs of different lengths results in ER sheets of corresponding width (Shen et al., 2019). The Climp63 LD is predicted to be mostly coiled coils (CCs), and homotypic zippering of these helices is naturally thought to be the basis for bridging the apposing lumen-forming membranes. However, purified LD was only analyzed in a denatured condition (Klopfenstein et al., 2001), and direct evidence of the existence of homotypic interactions is not available.

Here, we purified full-length (FL) Climp63 and the LD of Climp63 for biochemical analysis. We confirmed the helical nature of the LD and the self-association of Climp63 in both soluble and reconstituted forms, though the interactions were weaker than expected.

RESULTS

Purification of the Climp63 LD

To test the direct homotypic interaction of Climp63, we expressed GST-tagged mouse Climp63 LD (residues 104–575, **Supplementary Figure S1**) in *Escherichia coli*. When affinity-purified GST-Climp63 LD (theoretical molecular weight: 80.3 kDa) was subject to size exclusion chromatography, the protein was eluted as a relatively broad range (∼8–12 ml, **Figures 1B,C**), the peak of which correlates to a calibrated molecular weight of ∼1000 kDa. On the same column, a monomeric protein of 80 kDa would elute at ∼14 ml. These results suggest that the LD likely forms oligomers and/or adopts an extended configuration that shortens its retention time in the column compared to other globular proteins.

To avoid an influence by the GST tag, which is known to form weak dimers in solution (Sacchetta et al., 1993), on the oligomeric state of the LD, we attempted to remove the tag using protease 3C. As expected, the GST was efficiently separated from the LD by overnight cleavage on glutathione beads (**Supplementary Figure S2A**). The released LD severely precipitated, whereas uncleaved protein was stable in solution when eluted from the beads. These results indicate that isolated LD is aggregation-prone, likely due to a sticky surface that can be protected by the GST.

Tests of Self-Association Using Purified Climp63

Next, we tested the oligomeric state of the GST-Climp63 LD using analytical ultra-centrifugation (AUC). When 12.5 μM protein was loaded, the GST-Climp63 LD was mostly dimer (∼44%), but we also observed monomer (7.5%), trimer (∼28%) and tetramer (∼13%) species (**Figure 2A**). Because GST forms dimers (**Supplementary Figure S3A**), but not trimers (Sacchetta et al., 1993), these results suggest that Climp63 LD undergoes moderate self-association in addition to that by the GST. Furthermore, the oligomerization state was not affected in the presence of 2 mM Ca^{2+} (**Figure 2A**), which mimics the conditions with the ER lumen. The results also suggest that the high average molecular weight predicted by gel filtration analysis when similar protein concentrations were used is caused at least partly by an irregular shape of the protein, such as a rod, as proposed previously (Klopfenstein et al., 2001).

To further confirm the LD-mediated homotypic interactions, we performed pull-down assays using purified proteins. Because the GST-tag cannot be removed and its presence may cause background association, we expressed and purified GST-tagged FL mouse Climp63 (**Figure 1D**). Unlike the LD, the N-terminal GST could be cleaved efficiently without compromising the stability of the protein (**Supplementary Figure S2B**). We then engineered and purified FL Climp63 with either a C-terminal HA tag or Flag tag, the GST-Climp63 LD with a C-terminal Flag tag, and GST-Flag. FL Climp63-HA was attached to anti-HA antibody-conjugated agarose, incubated with individual Flag-tagged proteins, and the precipitates analyzed by SDS-PAGE and immunoblotting using anti-HA and anti-Flag antibodies. Both FL Climp63-Flag and GST-Climp63 LD-Flag were detected in the precipitates, but very little GST-Flag co-precipitated with FL Climp63-HA (**Figure 2B**). Notably, ∼0.5–1 μM total protein was used in these assays, and FL Climp63-HA was only able to pull down ∼1.0% of the FL Climp63-Flag or ∼2.6% of the LD that was supplied. When FL Climp63-HA was omitted in the assay, FL Climp63-Flag had a marginal attachment to the anti-HA agarose (**Figure 2B**). These results confirm a detectable, but relatively weak, homotypic interaction with Climp63.

The LD of Climp63 is predicted to be entirely α-helical with three potential CC regions (**Supplementary Figure S1**). To test whether deletion of the CC domains affects homotypic interactions, we preformed pull-down assays using deletion mutants in the context of FL Climp63 with an N-terminal Strep tag (**Supplementary Figure S3B**). As expected, Strep-FL Climp63 was able to co-sediment with FL Climp63-HA. Decreased binding was observed when CC2, the longest CC, was deleted, and the

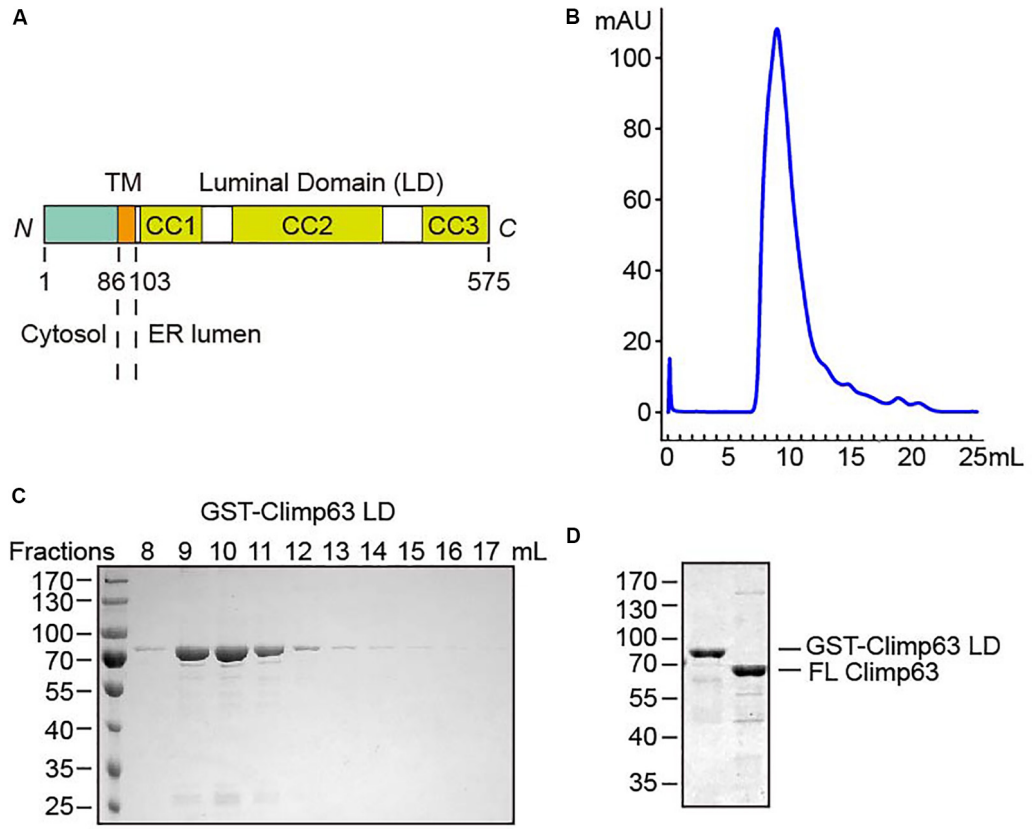

FIGURE 1 | Purification of Climp63. **(A)** Schematic diagram of *M. musculus* Climp63. The amino acids are numbered. TM, transmembrane; CC, coiled coil. **(B)** GST-Climp63 LD was purified through gel filtration analysis. **(C)** After gel filtration, the fractions were analyzed by SDS-PAGE and Coomassie blue staining. **(D)** GST-Climp63 LD and FL Climp63 were purified and the samples were analyzed by SDS-PAGE and Coomassie blue staining.

lack of both CC1 and CC2 caused a further reduction in self-association (**Supplementary Figure S3C**). These results suggest that redundant binding sites exist in the LD, and Climp63 self-association is sensitive to CC deletions.

Reconstitution of FL Climp63

We also tested whether Climp63 alters homotypic interactions in a membrane-bound setting. To achieve this goal, we performed directional reconstitution of the purified FL Climp63. Climp63 was solubilized by Fos-Choline-12 and subsequently exchanged into Triton X-100. In the reconstitution mixture, when the chosen detergent, including Triton X-100, is sufficient to be incorporated into pre-formed liposomes, but not enough to solubilize them, removal of the detergent could possibly cause directional insertion of membrane proteins into lipid bilayers (Rigaud and Levy, 2003). Using this method, we reconstituted FL Climp63 into proteoliposomes with bio-bead-aided detergent removal. Flotation analysis of the reconstituted sample indicated that Climp63 was successfully incorporated into membrane vesicles (**Figure 3A**). Climp63 contains one cysteine residue in the NT (C79, **Figure 3B**); accessibility of C79 by maleimide-linked Alexa Fluor 488 was used to probe the topology of reconstituted Climp63. Purified FL Climp63 was labeled efficiently. When Climp63-containing proteoliposomes were intact, no labeling was detected. Fluorescent labeling was resumed when the same sample was solubilized by 1% Triton X-100 (**Figure 3C**). We also mutated C79 to Ala and reintroduced a Cys at S124 in the LD domain. As expected, the reconstituted double mutant was readily labeled when the proteoliposomes were intact (**Supplementary Figure S4A**). Taken together, these results indicate that Climp63 was reconstituted into membranes with the LD/CT facing out.

Tests of Self-Association Using Reconstituted Climp63

Finally, Climp63-mediated interactions were measured in a proteoliposome-based pull-down assay. Vesicles containing either FL Climp63-HA or FL Climp63-Flag were isolated by collecting the top fraction in the flotation assay (**Supplementary Figure S4B**). Cryo-EM showed that proteoliposomes remained intact upon flotation, but no obvious tethering between vesicles was observed (**Supplementary Figure S4C**). These vesicles were then mixed and incubated with HA-agarose to pull-down FL Climp63-HA-containing vesicles (**Figure 4A**). A very low concentration of detergent (0.01% Triton X-100) was maintained, not to break vesicles, but to ensure binding

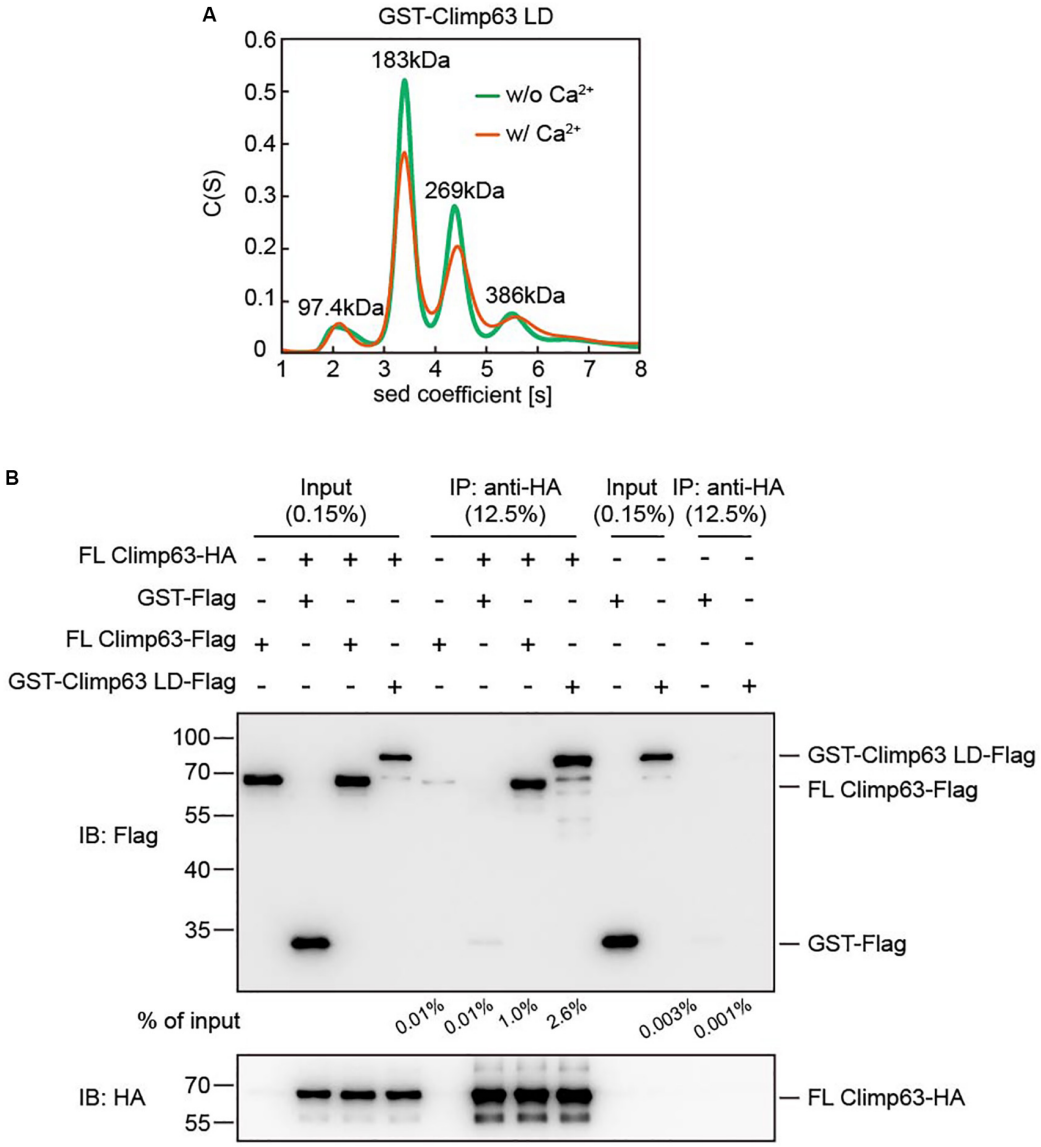

FIGURE 2 | Interactions between purified Climp63. **(A)** The size of GST-Climp63 LD (theoretical molecular weight: 80.3 kDa) was determined at 12.5 μM by analytical ultracentrifugation (AUC) with or without 2 mM $CaCl_2$. The estimated molecular masses are given above the peaks (in kilodaltons, kDa). **(B)** The interaction between purified FL Climp63-HA and FL Climp63-Flag was determined by co-immunoprecipitation. 5 μg of purified Climp63-HA (0.16 μM) was immunoprecipitated by anti-HA-agarose and then incubated with 10 μg of Flag-tagged protein, including FL Climp63-Flag (0.32 μM), GST-Climp63 LD-Flag (0.25 μM), or GST-Flag (0.8 μM), at 4°C for 1.5 h. The samples were analyzed by immunoblotting using the indicated antibodies. 0.15% of the input and 12.5% of the precipitate was loaded. The relative levels of co-precipitated Flag-proteins were quantified using the Gel-Pro analyzer software and normalized to the levels of input. Data are representative of three biological repeats.

fidelity in the assay. Consistently, HA-positive vesicles were able to co-sediment some Flag-positive vesicles (**Figure 4B**). In addition, when GST-Climp63 LD-Flag was incubated with FL Climp63-HA-containing vesicles, the LD was also detected in the HA-positive precipitates (**Figure 4B**). However, when the LD was present in 6-fold molar excess (**Figure 4C**), the interactions between HA-positive vesicles and Flag-positive vesicles were reduced (**Figure 4D**). Collectively, these results confirm that membrane-bound Climp63 is able to self-associate through its LD domain.

DISCUSSION

Our results provide definitive evidence that Climp63 may act as an ER luminal spacer by forming homotypic interactions through the ER LD. The self-association can reach at least tetramers in solution. We confirmed the interactions using the LD alone, between the LD and FL Climp63, and between differentially tagged FL Climp63 in the presence or absence of detergents. The assembly is likely specific, because purified proteins used in the binding assays did not form uncontrollable aggregations

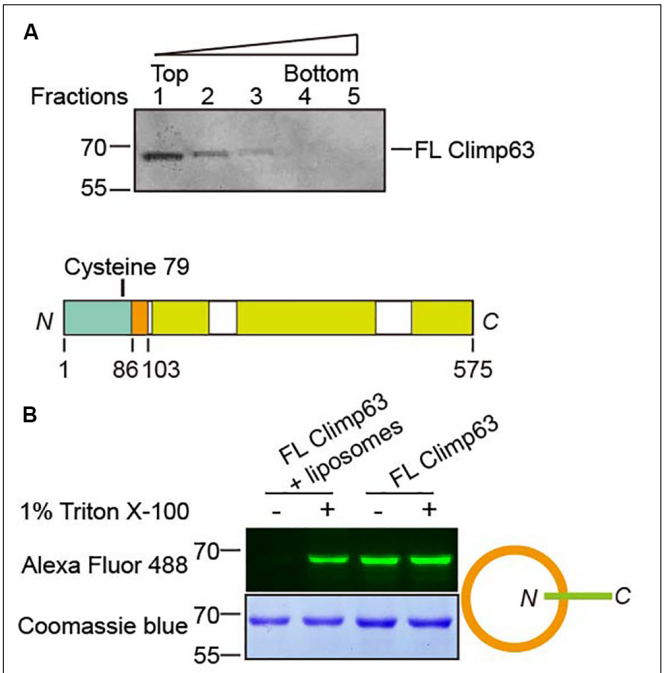

FIGURE 3 | Reconstitution of Climp63. **(A)** FL Climp63 was reconstituted into proteoliposomes followed by flotation analysis. Fractions were analyzed by SDS-PAGE and Coomassie blue staining. **(B)** The top panel shows a single cysteine in *M. musculus* Climp63. Purified and reconstituted FL Climp63 were labeled by a 10-fold molar excess of Alexa Fluor 488 C5 maleimide dye, with or without 1% Triton X-100, overnight at 4°C. The reactions were stopped by 2 mM BME. Samples were separated by SDA-PAGE and analyzed by fluorescent imaging (top) and Coomassie blue staining (bottom). The orientation of the reconstitution is indicated on the right.

and the assembly can be competed by the soluble LD and down-regulated by CC deletion.

Surprisingly, the measured affinity of the interaction was weaker than expected given that the LD is predicted to form extensive CCs. Marginal amounts of the LD or FL Climp63 were pulled down by HA-agarose-precipitated FL Climp63. Even when the protein concentration was 10-fold higher, the degree of oligomer formation by GST-Climp63 LD was maintained at low levels. These findings suggest that, although Climp63-mediated luminal bridges exist, they are less likely to be rigid and stable. Our results predict a self-association affinity of Climp63 that is weaker than micromolar. In contrast, a similar luminal bridge formed by KASH protein in the outer nuclear membranes and SUN protein in the inner nuclear membranes was reported to be ∼45 nM (Wang et al., 2012). When tethering factors, such as Climp63, are densely placed in apposed 2D faces, weak interactions may be combined to a reasonable level. Similar cases include Golgi stacking factors, the GRASP proteins. They are purified as monomers, but the crystal structures have revealed multiple assembly interfaces that are of physiological relevance in cells (Feng et al., 2013). Alternatively, the flexible bridges allow dynamic regulation of the ER luminal space.

We noticed that isolated LD exhibited severe aggregation when the GST tag was removed. These findings suggest possible strong *cis* interactions, i.e., self-association of Climp63 in the same side of the membrane, which might undermine *trans* interactions that were tested here and indeed needed as a luminal spacer. The width of ER sheets in mammalian cells is ∼50 nm in average. However, the previously purified Climp63 LD (in partial denatured conditions) was seen as 90-nm rods by EM, which less likely represents a functional spacer (Klopfenstein et al., 2001). If the LD forms one single straight helix, it would be estimated as 70 nm in length. Certain winding of the helical domain is therefore expected for a fit in 50 nm space.

Our findings imply that the Climp63 LD is most likely sticky and can bind to many other proteins in the ER lumen. The LD has been reported to bind to dicer (Pepin et al., 2012), integrin (Osugi et al., 2019), VE-cadherin (Lyu et al., 2019), and DKK1 (Kimura et al., 2016). Interestingly, Climp63 was recently shown to engage calumenin, a soluble ER chaperone (Shen et al., 2019), highlighting potential docking sites for luminal chaperones. Similarly, Climp63 was found to regulate the nanodomain distribution of ER-resident proteins (Gao et al., 2019). These observations suggest that Climp63 has functions beyond a ER luminal spacer, possibly linking to its ER sheet enrichment.

MATERIALS AND METHODS

Protein Expression and Purification

Full-length Climp63 (*Mus musculus*), CC-deleted mutants, and Climp63 LD (residues 104–575) were cloned into the pGEX6P-1 vector with an N-terminal GST tag. All constructs were transformed into bacterial strain BL21 (DE3) and cultures grown in Luria-Bertani media at 37°C to an OD600 of 0.8. Protein expression was induced by the addition of 0.35 mM IPTG for 24 h at 16°C. Cells were harvested, resuspended in lysis buffer (500 mM NaCl, 25 mM HEPES [pH 7.4], 10% glycerol), and lysed by ultrasonication. The lysate was centrifuged at 40,000 rpm for 1 h. For FL Climp63, the pellet was resuspended in lysis buffer containing 1% Fos-choline-12 and the insoluble components cleared by centrifugation. The recombinant protein was isolated by glutathione Sepharose (GE Healthcare), washed with lysis buffer containing 0.1% Triton X-100, and eluted by cleavage of the GST tag, where 180 μg protease 3C was incubated with the resuspended beads overnight at 4°C. For the GST-Climp63 LD, the supernatant was incubated with glutathione Sepharose after centrifugation. Sepharose was washed with lysis buffer (500 mM NaCl, 25 mM HEPES [pH 7.4]) and then eluted with buffer containing 10 mM glutathione. The protein was further purified by gel filtration chromatography (Superdex-200 Increase 10/300 GL; GE Healthcare) in 25 mM HEPES (pH7.4) and 500 mM NaCl with a flowrate of 0.5 mL/min at 4°C.

AUC

Purified 1 mg/mL GST-Climp63 LD (12.5 μM) and GST (40 μM) were used for AUC in a buffer containing 25 mM HEPES (pH7.4) and 500 mM NaCl. Sedimentation velocity experiments were performed at 4°C in Optima AUC (Beckman Coulter). All absorbance data at 280 nm were collected at 42,000 rpm in a

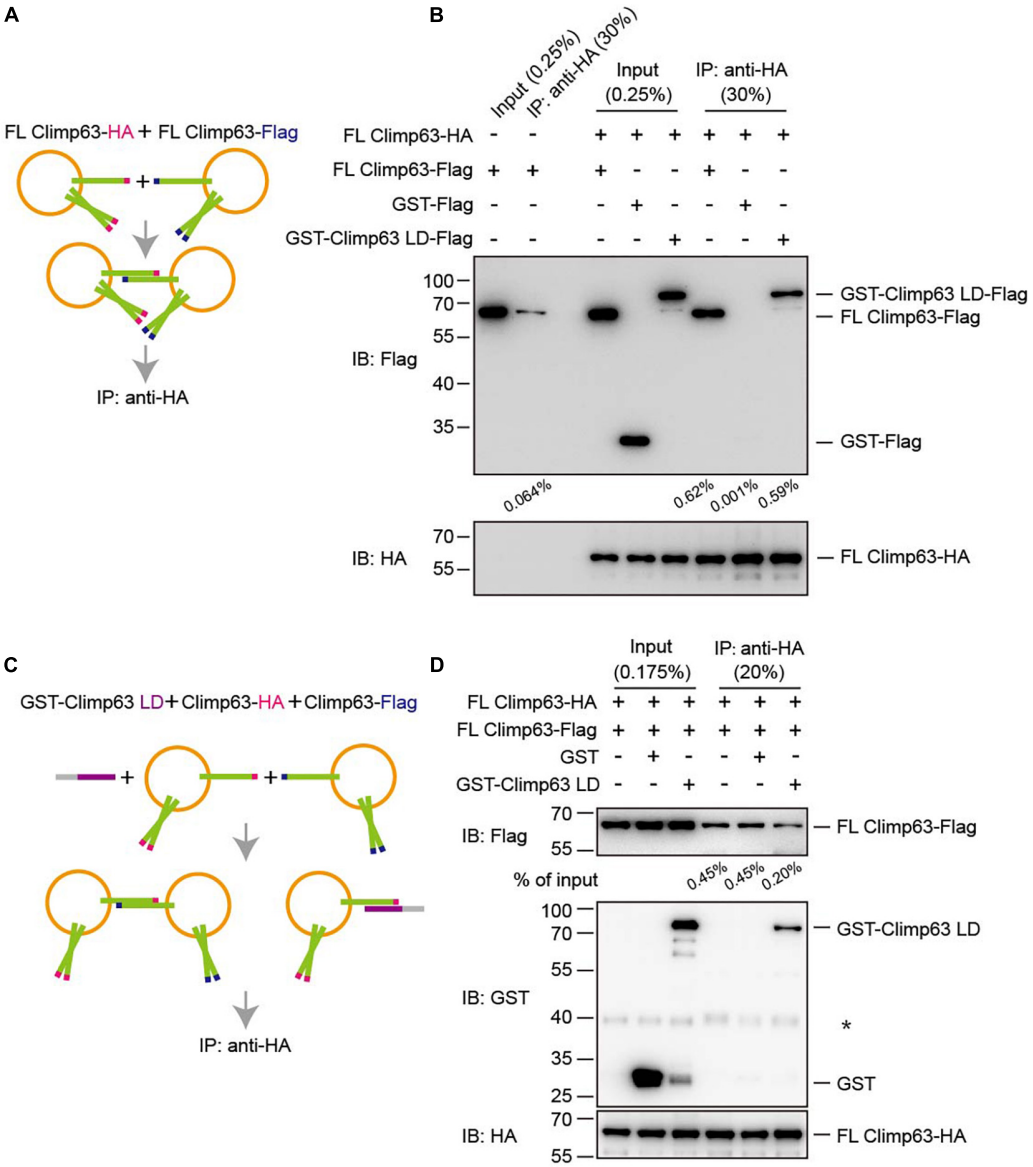

FIGURE 4 | Interactions between reconstituted Climp63. **(A)** Schematic diagram of the pull-down process shown in **(B)**. **(B)** FL Climp63-HA and FL Climp63-Flag were individually reconstituted into proteoliposomes and subjected to flotation. The top fractions (50 μl of 250 μl) were used for the pull-down assays. FL Climp63-HA-containing vesicles (~0.75 μg protein, 0.03 μM) were mixed with the indicated Flag-containing samples, including FL Climp63-Flag-containing vesicles (~1.5 μg protein, 0.06 μM), GST-Climp63 LD-Flag (1.5 μg, 0.05 μM), and GST-Flag (1.5 μg, 0.15 μM), and precipitated by anti-HA agarose. The samples were analyzed by immunoblotting using the indicated antibodies. 0.25% of the input and 30% of the precipitate was loaded. The relative levels of co-precipitated Flag-proteins were quantified using the Gel-Pro analyzer software and normalized to the levels of input. Data are representative of three biological repeats. **(C)** Schematic diagram of the pull-down process shown in **(D)**. **(D)** FL Climp63-HA and FL Climp63-Flag were individually reconstituted into proteoliposomes. FL Climp63-HA-containing vesicles (~0.1 μM) were mixed with FL Climp63-Flag-containing vesicles (~0.15 μM). GST-Climp63 LD (0.9 μM) was added for competition and GST (3 μM) was used as a control. The samples were analyzed by immunoblotting using the indicated antibodies. 0.175% of the input and 20% of the precipitate was loaded. The relative levels of co-precipitated Flag-proteins were quantified using the Gel-Pro analyzer software and normalized to the levels of input. The asterisk (*) indicates a non-specific band. Data are representative of three biological repeats.

rotor (An-50 Ti; Beckman Coulter) and analyzed by the program SEDFIT in terms of a continuous c(s) distribution.

Reconstitution of FL Climp63

POPC (1-palmitoyl-2-oleoyl-sn-glycero-3-phosphocholine), DOPS (1,2-dioleoyl-sn-glycero- 3-phospho-L-serine) and Rhod-PE [1,2-dioleoyl-sn-glycero-3-phosphoethanolamine-N-(lissamine rhodamine B sulfonyl)] were purchased from Avanti Polar Lipids. Lipid mixes (POPC:DOPS:Rhod-PE, 83.5:15:1.5 molar ratio) were dried to a film, hydrated with buffer (500 mM NaCl, 25 mM HEPES [pH 7.4], 10% glycerol), and extruded through polycarbonate filters with a pore size of 100 nm. FL

Climp63 in 0.1% Triton X-100 was mixed with preformed liposomes (protein:liposome, 1:1000 molar ratio) at an effective detergent to lipid ratio of ∼1. Protein and lipid were allowed to mix for 2 h at 4°C. The detergent was removed by adding Bio-Beads SM-2 adsorbent beads (Bio-Rad). The flotation of proteoliposomes was performed on a sucrose gradient to determine the reconstitution efficiency. Proteoliposomes (30 μl) were mixed with 100 μl of 1.9 M sucrose and overlaid with 100 μl of 1.25 M sucrose and 20 μl of lysis buffer. After centrifugation at 174,000 *g* for 75 min at 4°C in a rotor (TLS- 55; Beckman Coulter), the gradient was fractionated into five fractions and analyzed by SDS-PAGE and Coomassie blue staining.

Protein Labeling

Purified FL Climp63 and proteoliposomes were labeled with 10-fold molar excess of Alexa Fluor 488 C5 maleimide dye (Life Technologies) in the absence or presence of 1% Triton X-100 overnight at 4°C. The samples were separated by SDA-PAGE and analyzed by fluorescent imaging and Coomassie blue.

Immunoprecipitation

For immunoprecipitation of purified protein, 5 μg of FL Climp63-HA was immunoprecipitated by anti-HA-agarose at 4°C for 2 h. The agarose was washed twice with lysis buffer containing 0.1% digitonin and then incubated with 10 μg of Flag-tagged proteins in lysis buffer containing 1% digitonin at 4°C for 1.5 h. The agarose was washed four times with lysis buffer containing 0.1% digitonin. For immunoprecipitation of proteoliposomes, FL Climp63-HA and FL Climp63-Flag were reconstituted into liposomes and subjected to flotation. The top fractions were mixed in lysis buffer containing 0.0125% Triton X-100 at 4°C for 2 h. The mixture was then precipitated by anti-HA agarose at 4°C for 1.5 h. The agarose was washed four times with lysis buffer. Precipitated proteins were eluted with 2 × SDS-PAGE sample buffer and detected by Western blot. Band densities were quantified using Gel-Pro Analyzer version 4.0 (Media Cybernetics).

Cryo-Electron Microscopy

Full-length Climp63 was reconstituted into liposomes and subjected to flotation. The top fraction was applied to a glow discharged carbon grid. Each sample was plunge-frozen in liquid ethane using an automated system and visualized on a Tecnai 20 electron microscope operating at a voltage of 200 kV.

DATA AVAILABILITY STATEMENT

The original contributions presented in the study are included in the article/**Supplementary Material**, further inquiries can be directed to the corresponding author.

AUTHOR CONTRIBUTIONS

JZ and JH designed the research. JZ performed the experiments. JZ and JH analyzed the data. JH wrote the manuscript.

ACKNOWLEDGMENTS

We thank Dr. Sha Sun for technical assistance. JH is supported by the National Natural Science Foundation of China (Grant No. 91854202), the National Key Research and Development Program (Grant No. 2016YFA0500201), and the Strategic Priority Research Program of the Chinese Academy of Sciences (XDB39000000).

SUPPLEMENTARY MATERIAL

The Supplementary Material for this article can be found online at: https://www.frontiersin.org/articles/10.3389/fcell.2020.00500/full#supplementary-material

REFERENCES

Baumann, O., and Walz, B. (2001). Endoplasmic reticulum of animal cells and its organization into structural and functional domains. *Int. Rev. Cytol.* 205, 149–214. doi: 10.1016/s0074-7696(01)05004-5

Chavda, B., Ling, J., Majernick, T., and Planey, S. L. (2017). Antiproliferative factor (APF) binds specifically to sites within the cytoskeleton-associated protein 4 (CKAP4) extracellular domain. *BMC Biochem.* 18:13. doi: 10.1186/s12858-017-0088-y

Cui-Wang, T., Hanus, C., Cui, T., Helton, T., Bourne, J., Watson, D., et al. (2012). Local zones of endoplasmic reticulum complexity confine cargo in neuronal dendrites. *Cell* 148, 309–321. doi: 10.1016/j.cell.2011.11.056

Farías, G. G., Fréal, A., Tortosa, E., Stucchi, R., Pan, X., Portegies, S., et al. (2019). Feedback-driven mechanisms between microtubules and the endoplasmic reticulum instruct neuronal polarity. *Neuron* 102, 184.e8–201.e8.

Feng, Y., Yu, W., Li, X., Lin, S., Zhou, Y., Hu, J., et al. (2013). Structural insight into Golgi membrane stacking by GRASP65 and GRASP55 proteins. *J. Biol. Chem.* 288, 28418–28427. doi: 10.1074/jbc.m113.478024

Gao, G., Zhu, C., Liu, E., and Nabi, I. R. (2019). Reticulon and CLIMP-63 regulate nanodomain organization of peripheral ER tubules. *PLoS Biol.* 17:e3000355. doi: 10.1371/journal.pbio.3000355

Hu, J., Prinz, W. A., and Rapoport, T. A. (2011). Weaving the web of ER tubules. *Cell* 147, 1226–1231. doi: 10.1016/j.cell.2011.11.022

Kimura, H., Fumoto, K., Shojima, K., Nojima, S., Osugi, Y., Tomihara, H., et al. (2016). CKAP4 is a Dickkopf1 receptor and is involved in tumor progression. *J. Clin. Investig.* 126, 2689–2705. doi: 10.1172/jci84658

Klopfenstein, D. R., Klumperman, J., Lustig, A., Kammerer, R. A., and Hauri, H. P. (2001). Subdomain-specific localization of CLIMP-63 (p63) in the endoplasmic reticulum is mediated by its luminal helical segment. *J. Cell Biol.* 153, 1287–1299.

Lin, S., Sun, S., and Hu, J. (2012). Molecular basis for sculpting the endoplasmic reticulum membrane. *Int. J. Biochem. Cell Biol.* 44, 1436–1443. doi: 10.1016/j.biocel.2012.05.013

Lyu, Q., Xu, S., Lyu, Y., Choi, M., Christie, C. K., Slivano, O. J., et al. (2019). SENCR stabilizes vascular endothelial cell adherens junctions through interaction with CKAP4. *Proc. Natl. Acad. Sci. U.S.A.* 116, 546–555. doi: 10.1073/pnas.1810729116

Nikonov, A. V., Hauri, H. P., Lauring, B., and Kreibich, G. (2007). Climp-63-mediated binding of microtubules to the ER affects the lateral mobility of translocon complexes. *J. Cell Sci.* 120, 2248–2258. doi: 10.1242/jcs.008979

Nisha Gupta, Y. M., Kazi, A. S., Tao, J.-Q., Fisher, A. B., and Bates, S. R. (2006). Identification and characterization of p63 (CKAP4/ERGIC-63/CLIMP-63), a

surfactant protein A binding protein, on type II pneumocytes. *Am. J. Physiol. Lung. Cell Mol. Physiol.* 291, L436–L446.
Osugi, Y., Fumoto, K., and Kikuchi, A. (2019). CKAP4 Regulates Cell Migration via the Interaction with and Recycling of Integrin. *Mol. Cell. Biol.* 39:e00073-19.
Pepin, G., Perron, M. P., and Provost, P. (2012). Regulation of human Dicer by the resident ER membrane protein CLIMP-63. *Nucleic Acids Res.* 40, 11603–11617. doi: 10.1093/nar/gks903
Planey, S. L., Keay, S. K., Zhang, C.-O., and Zacharias, D. A. (2009). Palmitoylation of cytoskeleton associated protein 4 by DHHC2 regulates antiproliferative factor-mediated signaling. *Mol. Biol. Cell* 20, 1454–1463. doi: 10.1091/mbc.e08-08-0849
Puhka, M., Vihinen, H., Joensuu, M., and Jokitalo, E. (2007). Endoplasmic reticulum remains continuous and undergoes sheet-to-tubule transformation during cell division in mammalian cells. *J. Cell Biol.* 179, 895–909. doi: 10.1083/jcb.200705112
Rigaud, J. L., and Levy, D. (2003). Reconstitution of membrane proteins into liposomes. *Methods Enzymol.* 372, 65–86. doi: 10.1016/s0076-6879(03)72004-7
Sacchetta, P., Aceto, A., Bucciarelli, T., Dragani, B., Santarone, S., Allocati, N., et al. (1993). Multiphasic denaturation of glutathione transferase B1-1 by guanidinium chloride Role of the dimeric structure on the flexibility of the active site. *Eur. J. Biochem.* 215, 741–745. doi: 10.1111/j.1432-1033.1993.tb18087.x
Sandoz, P. A., and van der Goot, F. G. (2015). How many lives does CLIMP-63 have? *Biochem. Soc. Trans.* 43, 222–228. doi: 10.1042/bst20140272
Savitz, A. J., and Meyer, D. I. (1990). Identification of a ribosome receptor in the rough endoplasmic reticulum. *Nature* 346, 540–544. doi: 10.1038/346540a0
Schroeder, L. K., Barentine, A. E. S., Merta, H., Schweighofer, S., Zhang, Y., Baddeley, D., et al. (2019). Dynamic nanoscale morphology of the ER surveyed by STED microscopy. *J. Cell Biol.* 218, 83–96. doi: 10.1083/jcb.201809107
Shen, B., Zheng, P., Qian, N., Chen, Q., Zhou, X., Hu, J., et al. (2019). Calumenin-1 interacts with climp63 to cooperatively determine the luminal width and distribution of endoplasmic reticulum sheets. *iScience* 22, 70–80. doi: 10.1016/j.isci.2019.10.067
Shibata, Y., Hu, J., Kozlov, M. M., and Rapoport, T. A. (2009). Mechanisms shaping the membranes of cellular organelles. *Annu. Rev. Cell Dev. Biol.* 25, 329–354. doi: 10.1146/annurev.cellbio.042308.113324
Shibata, Y., Shemesh, T., Prinz, W. A., Palazzo, A. F., Kozlov, M. M., and Rapoport, T. A. (2010). Mechanisms determining the morphology of the peripheral ER. *Cell* 143, 774–788. doi: 10.1016/j.cell.2010.11.007
Shibata, Y., Voeltz, G. K., and Rapoport, T. A. (2006). Rough sheets and smooth tubules. *Cell* 126, 435–439. doi: 10.1016/j.cell.2006.07.019
Vedrenne, C., Klopfenstein, D. R., and Hauri, H. P. (2005). Phosphorylation controls CLIMP-63-mediated anchoring of the endoplasmic reticulum to microtubules. *Mol. Biol. Cell.* 16, 1928–1937. doi: 10.1091/mbc.e04-07-0554
Wang, W., Shi, Z., Jiao, S., Chen, C., Wang, H., Liu, G., et al. (2012). Structural insights into SUN-KASH complexes across the nuclear envelope. *Cell Res.* 22, 1440–1452. doi: 10.1038/cr.2012.126

Conflict of Interest: The authors declare that the research was conducted in the absence of any commercial or financial relationships that could be construed as a potential conflict of interest.

frontiers in Cell and Developmental Biology

REVIEW
published: 30 July 2020
doi: 10.3389/fcell.2020.00692

Mitochondrial Contact Sites in Inflammation-Induced Cardiovascular Disease

Hao Liu[1,2†], Xiao Liu[1,2†], Haixia Zhuang[2], Hualin Fan[2,3], Dongxing Zhu[4], Yiming Xu[5], Pengcheng He[6], Jinbao Liu[1,2] and Du Feng[1,2*]*

[1] Affiliated Cancer Hospital & Institute of Guangzhou Medical University, Guangzhou, China, [2] Guangzhou Municipal and Guangdong Provincial Key Laboratory of Protein Modification and Degradation, State Key Laboratory of Respiratory Disease, School of Basic Medical Sciences, Guangzhou Medical University, Guangzhou, China, [3] Guangdong Provincial People's Hospital, School of Medicine, South China University of Technology, Guangzhou, China, [4] Guangzhou Institute of Cardiovascular Diseases, The Second Affiliated Hospital, Key Laboratory of Cardiovascular Diseases, School of Basic Medical Sciences, Guangzhou Medical University, Guangzhou, China, [5] School of Basic Medical Sciences, Guangzhou Medical University, Guangzhou, China, [6] Department of Cardiology, Guangdong Cardiovascular Institute, Guangdong Provincial Key Laboratory of Coronary Heart Disease Prevention, Guangdong Provincial People's Hospital, Guangdong Academy of Medical Sciences, Guangzhou, China

The mitochondrion, the ATP-producing center, is both physically and functionally associated with almost all other organelles in the cell. Mitochondrial-associated membranes (MAMs) are involved in a variety of biological processes, such as lipid exchange, protein transport, mitochondrial fission, mitophagy, and inflammation. Several inflammation-related diseases in the cardiovascular system involve several intracellular events including mitochondrial dysfunction as well as disruption of MAMs. Therefore, an in-depth exploration of the function of MAMs will be of great significance for us to understand the initiation, progression, and clinical complications of cardiovascular disease (CVD). In this review, we summarize the recent advances in our knowledge of MAM regulation and function in CVD-related cells. We discuss the potential roles of MAMs in activating inflammation to influence the development of CVD.

Keywords: mitochondrial-associated membranes, mitochondria, autophagy, cardiovascular disease, inflammation, inflammasome

OPEN ACCESS

Edited by:
Junjie Hu,
Institute of Biophysics (CAS), China

Reviewed by:
Simone Patergnani,
University of Ferrara, Italy
Thomas Simmen,
University of Alberta, Canada

***Correspondence:**
Jinbao Liu
jliu@gzhmu.edu.cn
Du Feng
Fenglab@gzhmu.edu.cn;
feng_du@foxmail.com

†These authors share first authorship

Specialty section:
This article was submitted to Membrane Traffic, a section of the journal Frontiers in Cell and Developmental Biology

Received: *24 April 2020*
Accepted: *08 July 2020*
Published: *30 July 2020*

Citation:
Liu H, Liu X, Zhuang H, Fan H, Zhu D, Xu Y, He P, Liu J and Feng D (2020) Mitochondrial Contact Sites in Inflammation-Induced Cardiovascular Disease. Front. Cell Dev. Biol. 8:692. doi: 10.3389/fcell.2020.00692

INTRODUCTION

Inflammation is a universal phenomenon observed in CVDs, such as atherosclerosis (the primary underlying cause), AMI, cardiac I/R injury, stroke, and HF (Golia et al., 2014; Esposito et al., 2017; Zhou et al., 2018). Many experimental and clinical studies suggest that treatment with anti-inflammatory drugs is capable of reducing the risk of CVDs (Golia et al., 2014;

Abbreviations: AMI, acute myocardial infarction; AMPK, AMP-activated protein kinase; ASC, apoptosis-related speck-like protein; Bik, Bcl-2 interacting killer; BNIP3, BCL2/adenovirus E1B interacting protein 3; CAD, coronary artery disease; CaMKIIδ, $Ca2^{+}$/calmodulin regulated kinase δ; CVD, cardiovascular disease; CypD, cyclophilin D; DCM, dilated cardiomyopathy; FUNDC1, FUN14 domain containing 1; GSK3b, glycogen synthase kinase 3b; Hcy, homocysteine; HDL, high-density lipoprotein; HF, heart failure; HHcy, hyperhomocysteinemia; I/R injury, ischemia-reperfusion; IFN-γ, interferon γ; IP3R2, inositol 1,4,5-trisphosphate type 2 receptor; IRGM, immunity-related GTPase M; LDL, low-density lipoprotein; MAMs, mitochondrial-associated membranes; mtDNA, mitochondrial DNA; mt-ROS, mitochondrial reactive oxygen species; NgBR, Nogo-B receptor; NLRP3, NOD-like receptor family pyrin domain-containing protein 3; oxLDL, oxidative low-density lipoprotein; PACS-2, phosphofurin acidic cluster sorting protein 2; RyRs, ryanodine receptors; SR, sarcoplasmic reticulum; T2D, type 2 diabetes; Tet2, ten-eleven translocation 2; VDAC1, voltage-dependent anion-selective channel protein 1; VSMCs, vascular smooth muscle cells.

Maffia and Cirino, 2017; Ridker et al., 2017). Generally, inflammation is classified into classic inflammation (which is caused by infection and tissue injury) and para-inflammation (which is caused by tissue stress or malfunction); the latter is more responsible for chronic inflammatory disease, including T2D and CVDs (Medzhitov, 2008). The inflammasome, a critical factor in pro-inflammation, participates in a variety of inflammatory diseases and also serves as a possible therapeutic target for infectious and inflammatory diseases (Rathinam and Fitzgerald, 2016). In activated macrophages, NLRP3 is situated downstream of a series of signaling events including generation and releasing of mtROS (Tschopp and Schroder, 2010), cytosolic mtDNA release (Nakahira et al., 2011), lysosomal damage (Hornung and Latz, 2010), and cytosolic K^+ efflux (Petrilli et al., 2007; Shimada et al., 2012). Recent research has suggested that MAMs are crucial platforms for inflammasome formation. Impaired Ca^{2+} flux between mitochondria and the ER causes mitochondrial damage that, in turn, induces the activation of the NLRP3 inflammasome (Missiroli et al., 2018). In addition, the NLRP3 inflammasome is recruited to MAMs and activated by MAM-related effectors (Zhang et al., 2017). Given the importance of MAMs in the pathogenesis of CVDs, we hereby summarize the progress in understanding the specific roles of MAMs in inflammasome activation and the association between MAMs and the high-risk factors of CVDs. We also highlight some new research ideas in inflammasome-induced CVDs.

MAMs, INFLAMMASOMES, AND CVDs

About 2.5 billion years ago, a bacterium that used oxygen to convert organic molecules into energy turned into a mitochondrion after it was engulfed by an archaebacterium (McInerney et al., 2015). Eventually, it evolved into a double-membrane organelle inside eukaryotic cells, and provided energy for the cell while also participating in other cellular biological functions (Mills et al., 2017). This is a hypothesis of the origination of mitochondria which have been identified as the stable structures in cells and actively participate in cellular metabolism.

The organelles, including mitochondria and the ER in eukaryotic cells, are isolated from each other by their membranes, which allow individual organelles to have independent microenvironments to facilitate the appropriate biochemical reactions. Organelles are also tightly connected and work in a coordinated manner. When cells perform biological functions, some of the organelles need to be close to each other (Porter and Palade, 1957). In Bernhard and Rouiller (1956) first discovered Membrane Contact Sites (MCSs) with ultrastructural studies (Gatta and Levine, 2017). In 1969, John Ruby and his colleagues found a possible interaction between the outer mitochondrial membrane and the ER membrane (van Vliet et al., 2014). Shore and Tata used the same approach in rat liver homogenates with low-speed (640 g) to extract the rough and smooth ER fractions and found the major proportion of mitochondria was in this fractions at the end of the 1970s (Shore and Tata, 1977a,b). It was not until the last decade that the functions of MCSs have been gradually revealed (Gatta and Levine, 2017). MCSs are formed by interconnecting membrane protein complexes and lipids, which keep the two organelles in close contact without fusion (Annunziata et al., 2018). As one type of MCS, the MAM is the membrane contact between mitochondria and the ER, and it plays a role in exchange of materials and transport of ions between these organelles (Rizzuto et al., 1993). In recent years, MAMs have been found to be involved in intracellular phospholipid transport (Vance, 1990; Friedman et al., 2018), mitophagy (Missiroli et al., 2016; Wu et al., 2016), energy metabolism (Csordas and Hajnoczky, 2009), mitochondrial morphology (Liu et al., 2009), apoptosis (Theurey and Rieusset, 2017), and inflammasome formation (Zhou et al., 2011). These biological functions seem to be independent of each other, but they are inseparably linked. The MAM maintains the physiological function of normal cells within tissues, and the imbalance of MAMs is implicated in various diseases (Simmen and Tagaya, 2017; Wong et al., 2019). The disturbance of MAMs will lead to abnormal intracellular Ca^{2+} levels, impaired lipid transport, and the destruction of mitochondria. Consequently, the dysfunction of MAMs is associated with various diseases, such as cancers (Peretti et al., 2019), neurodegeneration (Krols et al., 2016), diabetes (Rutter and Pinton, 2014), infection (Jacobs and Coyne, 2013), and CVDs (Eisner et al., 2013).

In macrophages, the inflammasome transduces signals sensed by specific cytosolic proteins of the NLRP family into proteolytic activation of caspase-1 and -11, which can stimulate cells to yield and secrete cytokines including IL-1β, -18, and -1α (He et al., 2016; Yabal et al., 2019). During this process, there will be an increased level of mtROS and mtDNA released from mitochondria into the cytoplasm (Shimada et al., 2012). The increase of mtROS will recruit NLRP3 and cardiolipin to the outer membrane of mitochondria, as well as promoting K^+ efflux from mitochondria. Subsequently, ASC (apoptosis-related speck-like protein) accumulates at MAMs where the NLRP3-ASC complex is formed, stimulating caspase-1 activation (Zhou et al., 2011; Elliott et al., 2018; Namgaladze et al., 2019). These events lead to activation of macrophages. Due to changes in mitochondrial morphology and function, acetylation of tubulin occurs, which in turn increases the abundance of MAMs (Yabal et al., 2019; **Figure 1**). However, there are still many unexplored steps in this complex pathway. The molecular mechanisms that initiate the functional and morphological changes in mitochondria in activated macrophages have not yet been elucidated. These are, therefore, future research directions in this field.

ATHEROSCLEROSIS

Cardiovascular diseases, including CAD, cardiomyopathy, and HF, are associated with a high incidence of mortality (Mathers and Loncar, 2006; North and Sinclair, 2012). Atherosclerosis is a chronic disease that leads to progressive stenosis of arteries due to an imbalance in lipid metabolism (Guo et al., 2015). Immunocytes and cholesterol crystals accumulate on the arterial wall, leading to the development of an atherosclerotic plaque,

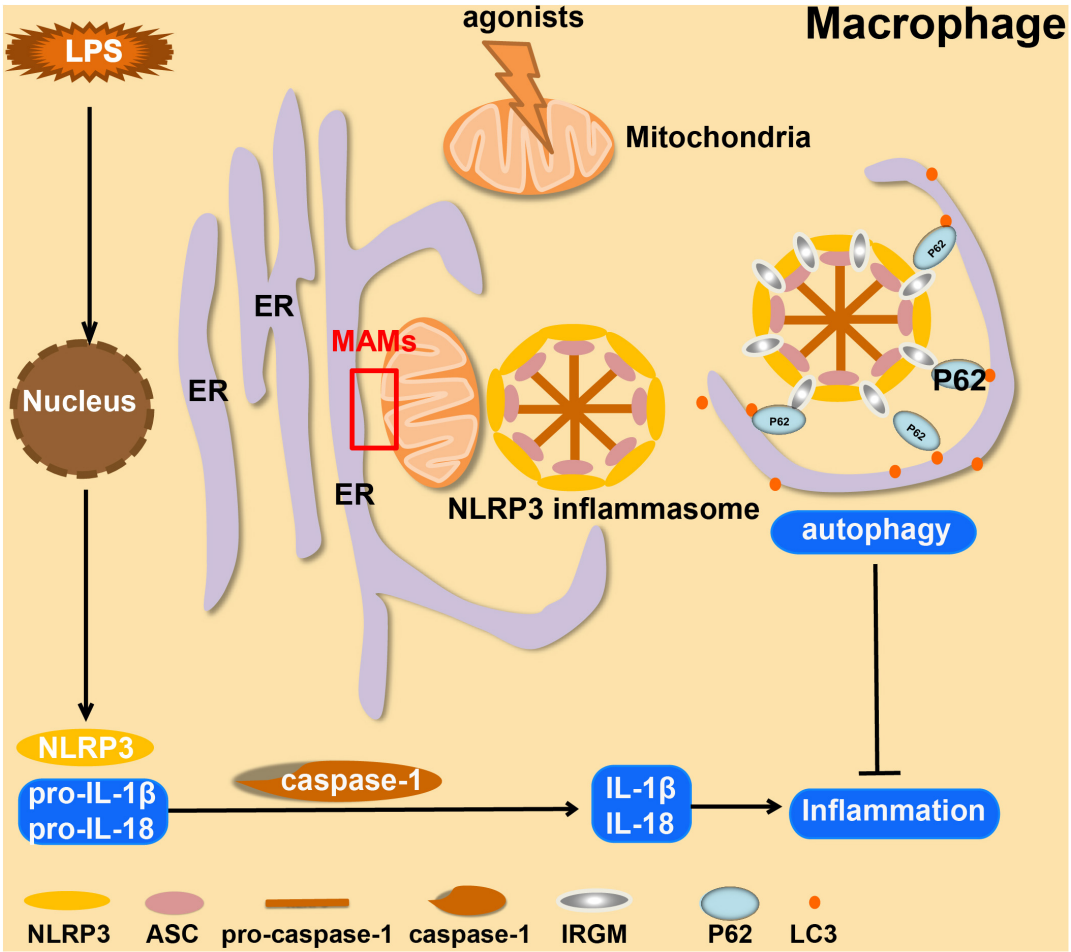

FIGURE 1 | Overview of the formation and autophagic clearance of inflammasomes. MAMs form in macrophages when they are stimulated by LPS and exposed to NLRP3 agonists (such as ATP, Alum, and Nigericin). Under these conditions, mitochondria usually become unstable, and then ASC and NLRP3 will be recruited at the MAM, which forms a positive-feedback loop. In Crohn's Disease, serving as a compensatory mechanism, IRGM promotes selective autophagy to suppress the formation of NLRP3 inflammasomes to limit inflammation.

which limits the flow of blood, and therefore of nutrients and oxygen, to various organs (Weber and Noels, 2011). Atherosclerosis can lead to further complications including life-threatening CVDs such as myocardial infarction and stroke (Sing et al., 2003; Guo et al., 2015). Atherosclerosis is more likely to occur in the colon germ-free animals, which suggests that atherosclerosis is closely related to inflammation caused by endogenous substances (Wright et al., 2000). Prevention and treatment of early atherosclerosis will deliver a breakthrough in the treatment of CVDs. NLRP3 is involved in the sterile inflammatory response in a variety of disease conditions (Liu et al., 2018). There are tiny cholesterol crystals in early atherosclerotic lesions. These crystals cause inflammation through activated caspase-1 which is cleaved by NLRP3 inflammasomes. The latter will lead to the secretion of cytokines like the IL family, which in turn will induce the formation and development of atherosclerotic plaques (Duewell et al., 2010). As the first signal for inflammasome activation, the abnormal accumulation of free fatty acids and LDL in human blood caused by imbalanced lipid metabolism can promote the production of pro-IL-1β through Toll-like receptors (Masters et al., 2011; **Figure 2**). Mice without LDL receptors are prone to develop atherosclerotic plaques. Compared to wild-type mice, atherosclerotic lesions were significantly reduced in NLRP3- or ASC- knockout mice after feeding them a high-cholesterol diet (Duewell et al., 2010). Similarly, the atherosclerotic lesions will shrink after depletion of IL-1β in ApoE-deficient mice (Kirii et al., 2003; Bhaskar et al., 2011). PACS-2 (phosphofurin acidic cluster sorting protein 2) regulates the distance between ER and mitochondria. Reduced expression of PACS-2 induces uncoupling of mitochondria from the ER and BAP31-dependent mitochondrial fission (Simmen et al., 2005). Upon stimulation with atherogenic lipids, PACS-2-associated MAM contacts increase in human VSMCs (Moulis et al., 2019). In VSMCs lacking PACS-2, MAM formation is impaired, leading to reduced mitophagosome formation and increased apoptosis induced by oxidized lipoprotein (Moulis et al., 2019). HHcy has been identified as a high-risk factor for CVDs from a mass

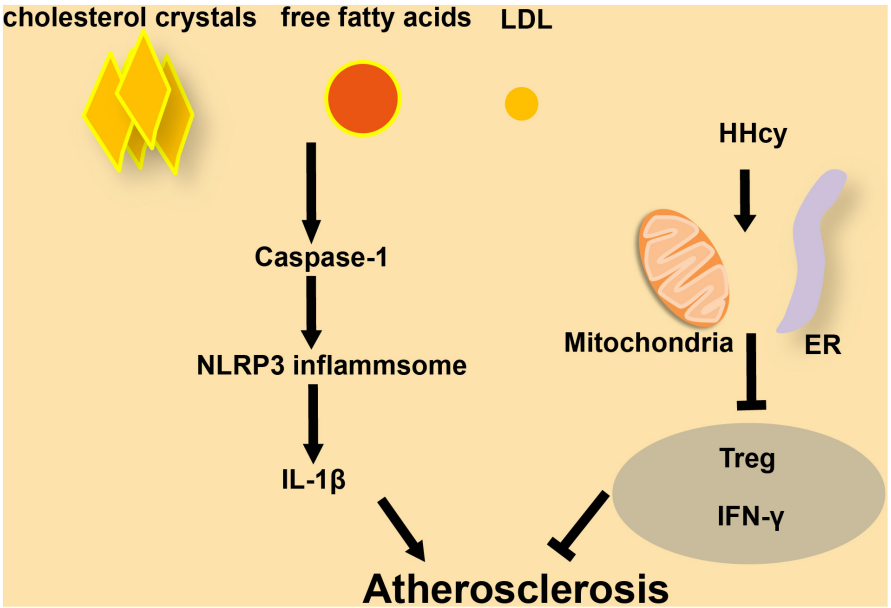

FIGURE 2 | The role of inflammasomes and MAMs in atherosclerosis. **(A)** In macrophages, cholesterol crystals, free fatty acids, and LDL increase the progression of atherosclerosis by activating caspase-1 and NLRP3 inflammasome formation, followed by release of secreted factors. **(B)** In T-cells, HHcy increases ER-mitochondria coupling, which attenuates IFN-γ secretion and suppresses Treg cells to accelerate atherosclerosis.

of clinical studies. In T-cells, Hcy increases the association of mitochondria with the ER. However, Nocodazole enlarges the distance between ER and mitochondria, leading to the inhibition of IFN-γ secretion and proliferation of T-cells. This effect shows that the balance of MAMs is essential for T-cell activation (Feng et al., 2016). Hcy accelerates atherosclerosis by increasing the release of chemokines/cytokines in monocytes and T-cells and results in the dysfunction of regulatory T-cells (Zeng et al., 2003; Feng et al., 2009; Ma et al., 2013; **Figure 2**). In macrophages from patients with CAD, the Ca^{2+} flux through MAMs maintains mitochondrial hyperactivity when GSK3b is inactivated, leading to the production of the collagenase cathepsin K that is related to CAD (Zeisbrich et al., 2018). According to existing research mentioned above (Moulis et al., 2019), the abundance of MAMs significantly increases in VSMCs and a subset of immune cells in atherosclerosis. At the same time, the increased MAMs in these immune cells will promote the release of inflammatory factors and further aggravate the development of atherosclerosis.

CARDIOMYOPATHY

Cardiomyopathy is defined as a myocardial disorder in which the heart muscle is functionally and structurally abnormal (McKenna et al., 2017). There are several different types of cardiomyopathies, and they can either be acquired, such as diabetic cardiomyopathy, or inherited, such as familial DCM (McKenna et al., 2017; Schaufelberger, 2019). Diabetic cardiomyopathy, one of the complications caused by diabetes, is closely related to the increased incidence of HF and arrhythmia in diabetic individuals (Boudina and Abel, 2007). Downregulation of the NLRP3 inflammasome restores cardiac function in diabetic cardiomyopathy models (Li et al., 2014; Yang et al., 2018; **Figure 3**). Metformin, the most widely used drug for treating T2D (Forslund et al., 2017), can inhibit NLRP3 by activating AMPK (AMP-activated protein kinase), thus increasing autophagy activity to promote the clearance of inflammasomes via inhibiting the mTOR pathway and alleviating the symptoms in diabetic cardiomyopathy (Yang et al., 2019a; **Figure 3**). Rosuvastatin can effectively delay the progress of diabetic cardiomyopathy through inhibition of NLRP3 inflammasomes (**Figure 3**; Luo et al., 2014). Familial DCM, a syndrome caused by genetic mutation, is characterized by an enlarged heart and impaired contractile function (Hershberger and Siegfried, 2011; Caragnano et al., 2019). DCM hearts are marked by the accumulation of lipoperoxidation products and the activation of both inflammasome and redox-responsive pathways (Caragnano et al., 2019). In mice, absence of the protein FUNDC1 (FUN14 domain containing 1) impaires the structure of MAMs, leads to the fusion of mitochondria and causes mitochondrial dysfunction, which results in DCM. In wild-type mice, MAM-localized FUNDC1 maintains the Ca^{2+} balance between mitochondria and the cytosol by influencing the function of IP3R2 (inositol 1,4,5-trisphosphate type 2 receptor). The absence of FUNDC1 at MAMs leads to the fusion of mitochondria and causes mitochondrial dysfunction, which results in DCM (Wu et al., 2017). FUNDC1 can also mediate diabetes-induced MAM formation and mitochondrial Ca^{2+} increase, resulting in impairment of cardiac structure and function (Munoz and Zorzano, 2017; **Figure 3**). Diabetes induces MAM formation through the downregulation of AMPK, and eventually causes diabetic cardiomyopathy (Wu et al., 2019).

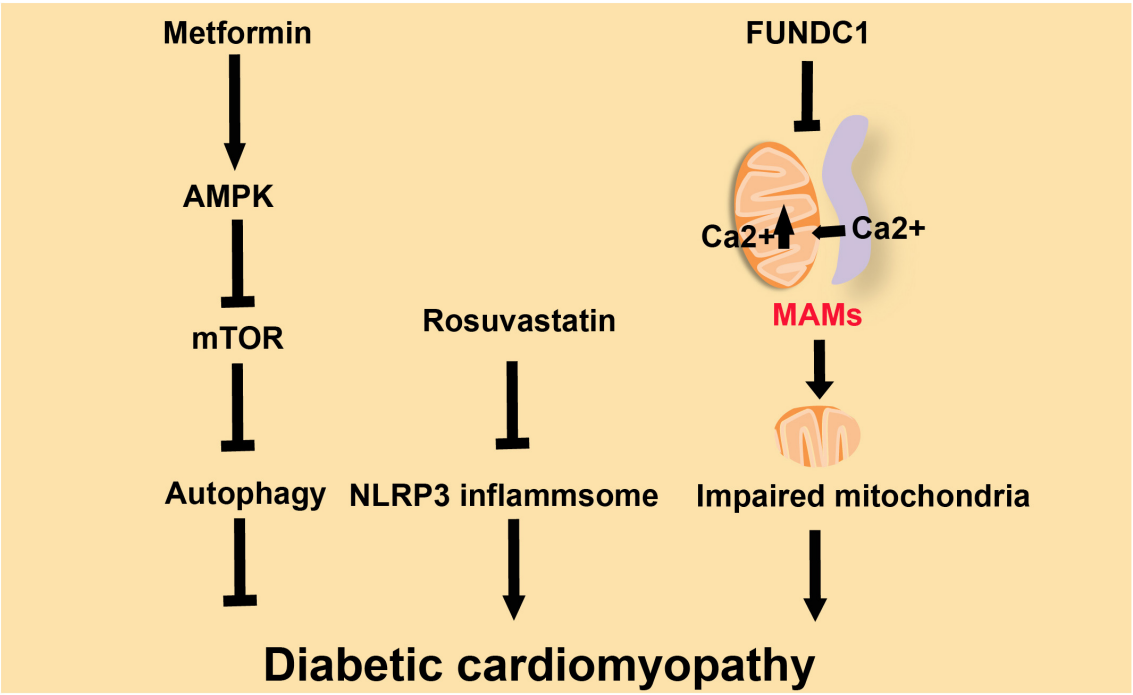

FIGURE 3 | Three factors influence diabetic cardiomyopathy. Metformin ameliorates diabetic cardiomyopathy via activation of AMPK, which inhibits mTOR and promotes autophagy. Rosuvastatin improves diabetic cardiomyopathy by repressing NLRP3-inflammasomes. FUNDC1 down-regulates Ca^{2+} flux and subsequently improves diabetic cardiomyopathy.

The inflammasome is essential to the development of diabetic cardiomyopathy and DCM (Li et al., 2014; Yang et al., 2018; Caragnano et al., 2019). The loss of NLRP3 will reduce heart damage in cardiomyopathy. The stability of MAMs is important for the structure and function of the heart. For example, an imbalance of MAMs will increase the concentration of Ca^{2+} in mitochondria, thereby destroying the mitochondria. The abundance of MAMs may affect the internal microenvironment of cardiomyocytes, including the ion levels and mitochondria-related events, in cardiomyopathy.

HEART FAILURE

The prevalence of HF is closely related to aging and approximately doubles with each decade. Due to the increase of the aging population, the threat of HF to humans will gradually increase in the coming decades (Sano et al., 2018). HF is related to chronic sterile inflammation induced by the activation of the inflammasome, which produces inflammatory cytokines that accelerate the process of myocardial apoptosis and ultimately lead to cardiac hypertrophy (Butts et al., 2018). Mice with Tet2 (Ten-eleven translocation 2)- deficient hematopoietic cells show more maladaptive cardiac remodeling and dysfunction in two HF models (transverse aortic constriction and the permanent ligation of the left anterior descending artery). IL-1β blockade or administration of an NLRP3 inflammasome inhibitor provided effective protection in these models (Sano et al., 2018). CaMKIIδ (Ca^{2+}/calmodulin-regulated kinase δ) will be activated in cardiomyocytes, followed by NLRP3 inflammasome activation (**Figure 4**). These responses promote macrophage recruitment, fibrosis, and HF induced by myocardial dysfunction (Suetomi et al., 2018). The SR, the ER in muscle cells, is associated with mitochondria, and this association is essential to the normal physiological functions of muscle cells (Dorn and Maack, 2013; Lopez-Crisosto et al., 2017). In noradrenaline-treated cardiomyocytes, cardiac metabolism is disordered due to the increased distance between the SR and mitochondria and the imbalanced Ca^{2+} homeostasis (Gutierrez et al., 2014). Overexpression of BNIP3 (BCL2/adenovirus E1B interacting protein 3) induces the oligomerization of VDAC1 (voltage-dependent anion-selective channel protein 1), which increases Ca^{2+} flux through MAMs into the mitochondria from SR. Based on this, BNIP3 induces mitochondrial dysfunction and apoptosis of cardiomyocytes, and eventually contributes to HF (Chaanine et al., 2013; **Figure 4**). In mice with leaky RYR2 (ryanodine receptor type 2) channels caused by genetic mutation, there is a detrimental increase in mitochondrial Ca^{2+} levels from the SR through MAMs. This Ca^{2+} leak also causes alterations of mitochondrial function and morphology (Santulli et al., 2015). Another report showed that Ca^{2+} released from the SR tunneled to mitochondria via RyRs, as IP3 receptors presented on mitochondrial and SR, leading to mitochondrial ATP production (Seidlmayer et al., 2016; **Figure 4**). MAMs are essential channels for Ca^{2+} to flow into the mitochondria from the SR. In cardiomyocytes, the excessive loading of Ca^{2+}

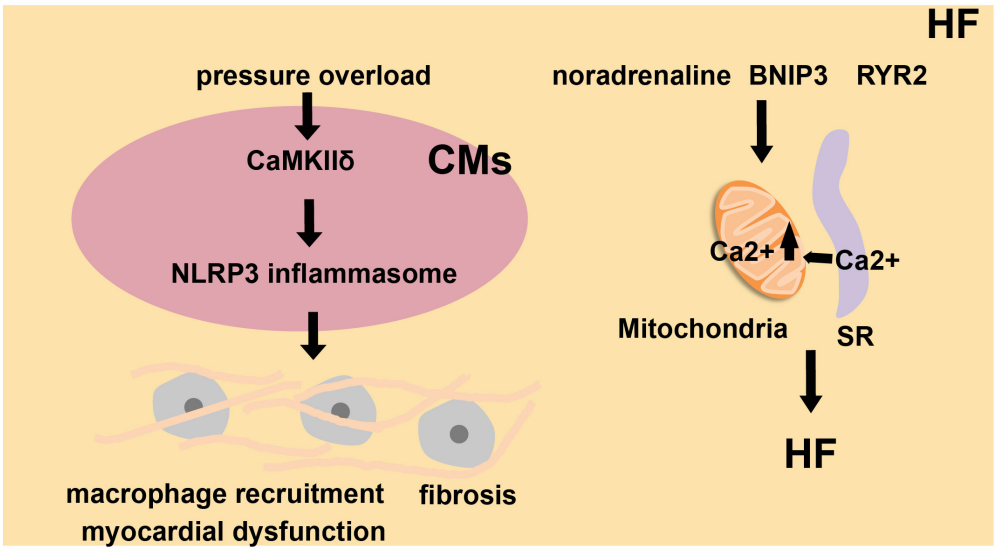

FIGURE 4 | The role of inflammasomes and MAMs in heart failure (HF). Under high blood pressure, cardiomyocytes (CMs) activate CaMKIIδ, trigger inflammatory gene expression and activate NLRP3 inflammasomes. This leads to macrophage recruitment, fibrosis, and myocardial dysfunction, which finally induces heart failure. Noradrenaline, BNIP3 and RYR2 channels influence SR-to-mitochondria Ca^{2+} transfer and also alter cardiac metabolism. These factors all contribute to HF.

into the mitochondria is a key contributor to mitochondrial imbalance, which in turn causes myocardial hypertrophy, and ultimately leads to HF.

AUTOPHAGY AND INFLAMMASOME CLEARANCE

Mitochondrial homeostasis is essential for heart health. Damaged mitochondria have reduced ATP production and yield dangerous amounts of ROS. Accumulated ROS may damage respiratory complex proteins, membrane lipids, and mtDNA, leading to catastrophic oxidative damage to the feed-forward cycle, and ultimately to cell death (Whelan et al., 2010; Morales et al., 2020). Damaged mitochondria, ubiquitinated in a Parkin-dependent manner, will be specifically recognized by p62, which induces autophagy (Zhong et al., 2016). The inflammasome components, ASC, NLRP3, and pro-caspase-1, accumulate at the MAMs (Zhou et al., 2011). In Crohn's Disease, the expression of IRGM (immunity-related GTPase M) is up-regulated to promote the accumulation of p62 and LC-3 around the NLRP3 inflammasome, which is then selectively removed by autophagy (Mehto et al., 2019a,b). Through this process, macrophages clear the MAM-associated inflammasomes, which is a cellular "self-defense" response to inflammatory stresses (Moulis et al., 2019; **Figure 1**). It is generally believed that a controlled inflammatory response is beneficial (for example, to protect against infection), but it can be harmful if dysregulated (for example, causing septic shock). Regardless of the cause, inflammation is presumably an adaptive response to restore homeostasis (Medzhitov, 2008). The NF-κB pathway is an inflammatory signaling pathway. In macrophages, activation of the NF-κB signaling pathway inhibits the inflammatory activity through p62-induced elimination of damaged mitochondria (Zhong et al., 2016).

CARDIOVASCULAR DRUGS AND MAM-RELATED CVDs

Several drugs are already in use to treat MAM-related CVDs. Nocodazole attenuates IFN-γ secretion and proliferation of T-cells (Feng et al., 2016) and reduces the inflammatory response by uncoupling MAMs. Consequently, it decreases the development of atherosclerotic plaques. Both Metformin (Yang et al., 2019a) and Rosuvastatin (Luo et al., 2014) can improve diabetic cardiomyopathy by inhibiting the formation of inflammasomes in diabetic patients. Noradrenaline, as an inducer of cardiac hypertrophy, alters Ca^{2+} handling and cardiac metabolism through MAMs (Gutierrez et al., 2014). Perhaps we could administer a norepinephrine inhibitor, such as Reboxetine, to improve the symptoms of HF patients. Recently, several clinical trials have reported that novel pharmacological therapies are associated with better outcomes in CVD patients. Canakinumab, an IL-1 antagonist, reduces the recurrence of ischemic events in patients with CVDs, and also reduces the hospitalization rate for HF (Abbate et al., 2020). Anakinra, a recombinant IL-1 receptor antagonist, has similar effects as canakinumab for CVD patients (Abbate et al., 2020). The influence of these therapies on the structure of MAMs in inflammation-induced CVDs should be further explored.

As described above, inflammation is a major factor in the occurrence and development of CVDs (Hansson and Hermansson, 2011), and cells need to repair themselves after exposure to inflammation. The formation and elimination of

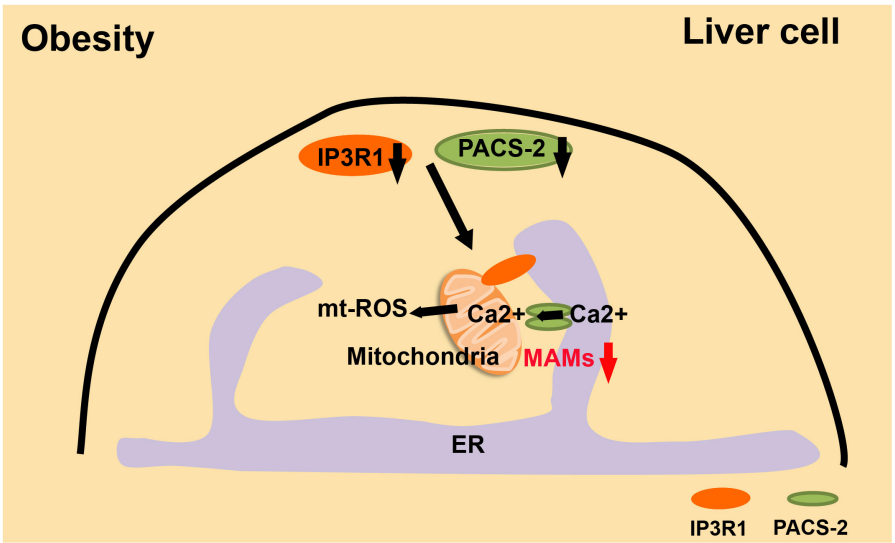

FIGURE 5 | MAMs and the development of obesity. In obesity, liver cells have excessive MAMs, high mtROS, and Ca^{2+}-overloaded mitochondria. These are all significantly relieved when IR3R1 and PACS2 are expressed at a lower level.

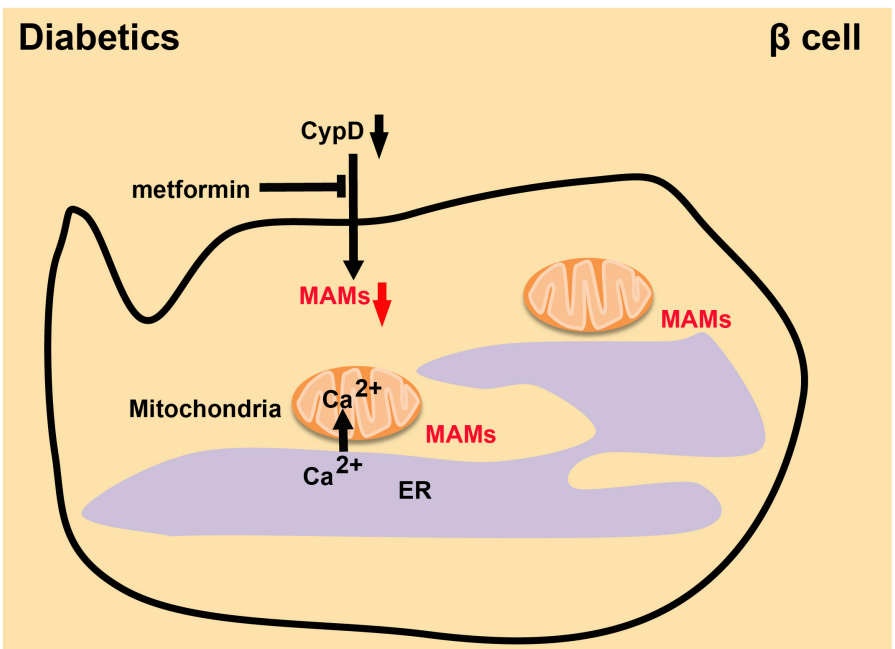

FIGURE 6 | The integrity of MAMs in diabetes. Absence of CypD decreases the quantity of MAMs and damages their integrity, while Metformin reverses this effect and leads to recovery of insulin sensitivity.

inflammasomes are completed at MAMs, which also participate in various biochemical functions such as Ca^{2+} communication and lipid transport. In summary, by studying the structure and function of MAMs, we may further understand the process of inflammasome formation and elimination. Interventions to inhibit the early inflammatory events would be beneficial to the treatment of CVD, and this will be a promising research direction in the CVD field in the future.

MAMs AND CVD RISK FACTORS

It has been shown that the abundance of inflammasomes increases in patients with a high risk of CVDs. The risk factors include obesity, smoking, diabetes, hypertension, and hypercholesterolemia. In the following sections, we will analyze the relationship between MAMs and these risk factors one by one.

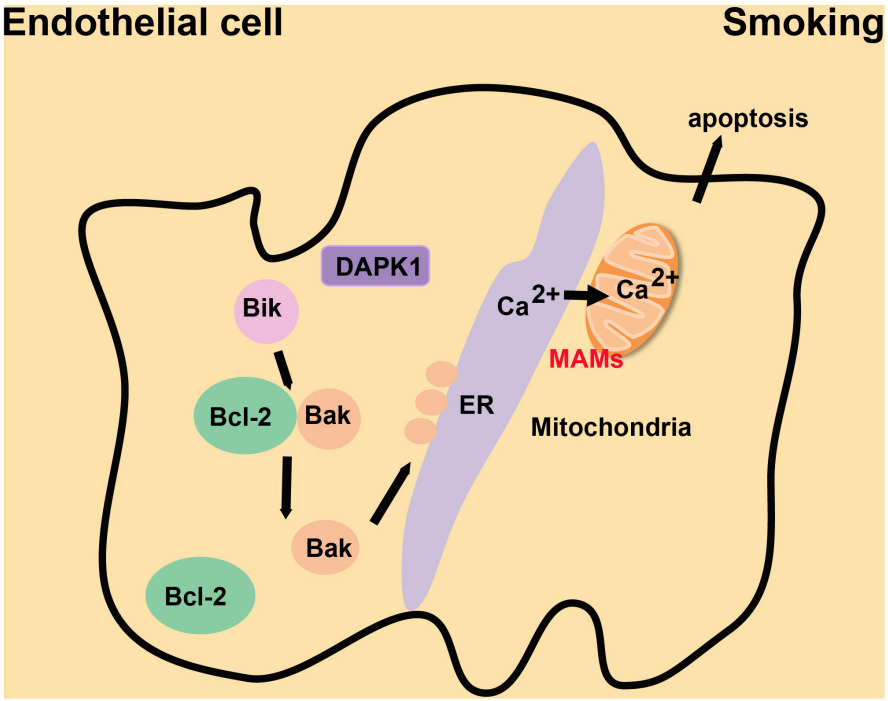

FIGURE 7 | The mechanism by which MAMs repress cigarette smoke-induced proliferation of endothelial cells. Bak is enriched at the ER following Bik-dependent dissociation of the Bak/Bcl-2 complex. Bak interacts with DPAK1 on the ER to increase the abundance of MAMs and Ca^{2+} flow from the ER to mitochondria, which suppresses the proliferation of endothelial cells induced by cigarette smoke.

OBESITY

The balance between the immune system and metabolism is disturbed in obese individuals, which increases the risk of CVD (Hotamisligil, 2006). Overnutrition leads to dysfunction of membrane-bound organelles, such as ER and mitochondria (Lowell and Shulman, 2005; Hotamisligil, 2010). In obesity, mitochondrial ROS is increased and mitochondria are significantly overloaded with Ca^{2+}. When the expression of IP3R1, the inositol triphosphate receptor, and PACS-2, the tethering protein of MAMs, is inhibited in obese mice, intracellular homeostasis is substantially improved, and obesity-induced metabolic imbalances are relieved (Arruda et al., 2014; **Figure 5**). The accumulation of MAMs is an early event in the process of obesity, and it is an adaptation process in the cell. However, long-term maintenance of MAMs will cause a series of mitochondrial dysfunctions, such as mitochondrial Ca^{2+} overload, reduced mitochondrial oxidative capacity, and increased mtROS.

In the pericentral zone of the liver, melatonin can convert macrosteatosis to microsteatosis. Melatonin increases the distance from ER to mitochondria, or decreases the abundance of MAMs, resulting in the improving of the structure and the metabolic functions of hepatic tissue (Stacchiotti et al., 2016). In summary, restoring the normal homeostasis of MAMs may reduce the degree of obesity and decrease the incidence of CVDs.

DIABETES

The risk of CVDs in diabetes increases 2–4 fold (Faria and Persaud, 2017). Controlling blood glucose and enhancing insulin resistance will significantly decrease the risk of CVDs in diabetic individuals (Gilca et al., 2017). Serving as a crucial intracellular regulator in the function of insulin secretion by pancreatic beta cells, Ca^{2+} is kept at low intracellular levels in normal conditions. In a high-glucose environment, beta cells will close ATP-sensitive K^{+} channels and inhibit plasma membrane depolarization to facilitate the precise increase in cytoplasmic Ca^{2+} levels, leading to the secretion of insulin (Rutter et al., 2017). However, dysfunctional MAMs will lead to abnormal Ca^{2+} transport and imbalanced Ca^{2+} levels in the cell, resulting in the pathogenesis of T2D, which is caused by decreased insulin sensitivity (Wang and Wei, 2017). Palmitate increases chemokine production from the islets, which promotes immune cell infiltration into the islets and increases the levels of immunocyte in the islets of patients, thus inducing insulin resistance (Rieusset et al., 2012; Tubbs et al., 2014; Khodabandehloo et al., 2016). In HuH7 hepatocellular carcinoma cells, increased MAM formation prevents the alteration of insulin signal transduction induced by palmitate (Tubbs et al., 2014). The integrity of MAMs is necessary for insulin signal transduction. Deletion of the gene encoding CypD, a mitochondrial protein in MAMs, reduced the abundance of MAMs and impaired their integrity. Interestingly, mice lacking CypD had insulin resistance and elevated hepatic neoglucogenesis in insulin tests. Treating CypD knockout mice

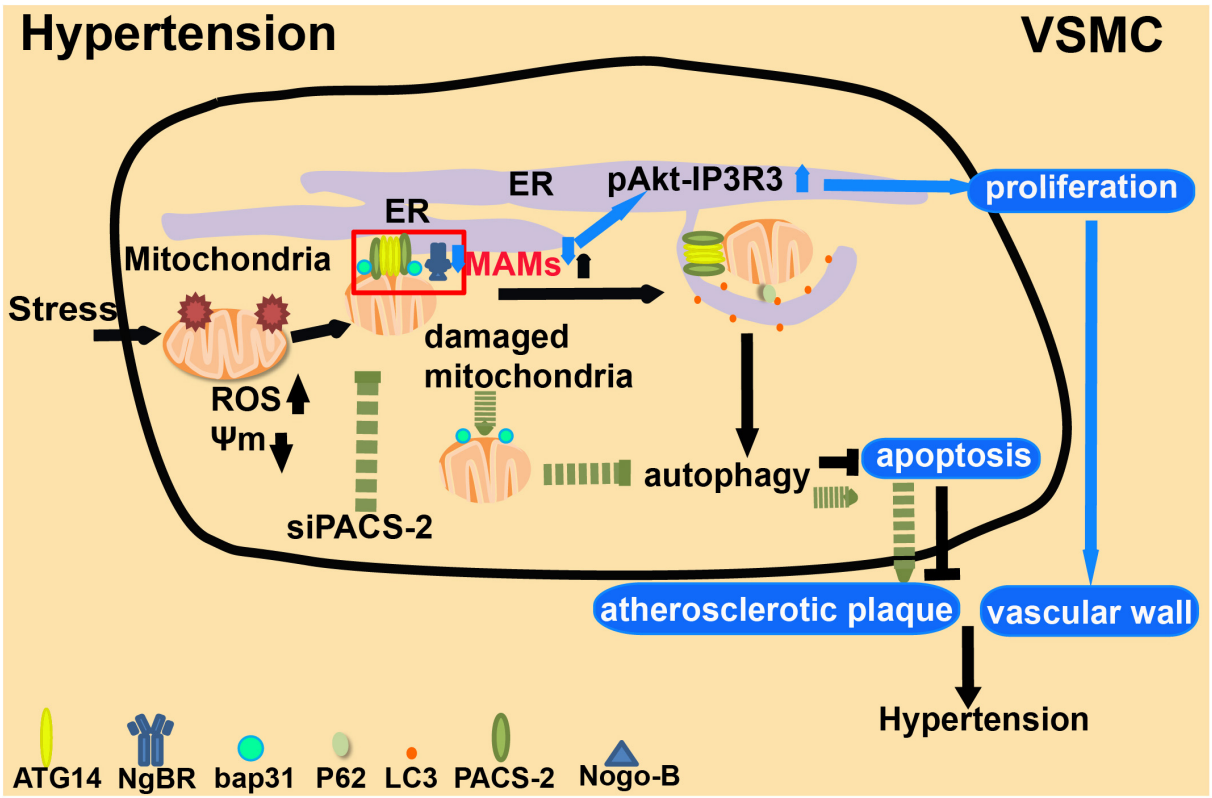

FIGURE 8 | The role of MAMs in hypertension. 1. Under extracellular stresses, PACS-2-associated MAM contacts are formed in VSMCs, which mediate mitophagy (autophagic degradation of mitochondria). 2. Depletion of PACS-2 decreases both mitophagy activity and the abundance of MAMs. This induces apoptosis and stimulates the formation of atherosclerotic plaques. 3. NgBR affects cell proliferation and migration by interacting with its ligand Nogo-B. Low expression of NgBR reduces the enrichment of MAMs and promotes pAkt-IP3R3 signaling, which enhances the proliferation of VSMCs and causes clinical symptoms.

with Metformin significantly improved the integrity of MAMs and the insulin sensitivity (Tubbs et al., 2014; Stacchiotti et al., 2018; **Figure 6**). Therefore, maintaining the stability of MAMs is a necessary condition for stabilizing intracellular Ca^{2+} and increasing insulin sensitivity. This is an essential direction for treating diabetes and reducing the incidence of CVDs.

SMOKING

Smoking is one of the critical risk factors in the occurrence and development of CVDs (Desgraz et al., 2017). Long-term smoking also inhibits the proliferation and repair responses of airway epithelial cells (Wang et al., 2001). Nicotine, as a standard component of cigarette smoke, induces bronchial epithelial cell senescence and apoptosis via ROS-mediated impairment of autophagy (Bodas et al., 2016). The Ca^{2+} reservoir in the ER is decreased in chronic obstructive pulmonary disease patients, and the Ca^{2+} influx is suppressed in epithelial cells from smokers (Petit et al., 2019; **Figure 7**). The following mechanism, based on a study of mice and cultured cells, may explain this phenomenon. Bik (Bcl-2 interacting killer) reduces the proliferation of epithelial cells by causing the release of Ca^{2+} stored in the ER. Bik dissociates the Bak/Bcl-2 complex, leading to the enrichment of Bak around the ER. Bak interacts with the kinase domain of DAPK1, increasing the abundance of MAMs and thus the flow of Ca^{2+} from the ER to mitochondria, which causes the apoptosis of proliferating epithelial cells to reduce cigarette smoke-induced mucous cell hyperplasia (Mebratu et al., 2017; **Figure 7**). Inhalation of cigarette smoke results in immune system imbalances which induce exaggerated and prolonged inflammation in the lung (Racanelli et al., 2018) and contribute to the development of CVDs. Some data suggest that folic acid and Vitamin B_{12} may combat oxidative stress caused by smoking via supplying essential nutrients, removing free radicals and inhibiting inflammation (Bhattacharjee et al., 2016). However, further exploration is required to determine whether these vitamins can regulate the proliferation and apoptosis of endothelial cells by affecting enrichment of MAMs in endothelial cells. Inhalation of cigarette smoke decreases the flow of Ca^{2+} and increases the production of ROS, which inhibits the proliferation and self-recovery ability of endothelial cells, and then causes apoptosis. The same effect will occur when MAMs are enriched in endothelial cells. Therefore, exploring the functional changes of MAM structure during inhalation of cigarette smoke will be important in devising methods to lessen the inflammatory damage and reduce complications such as CVDs.

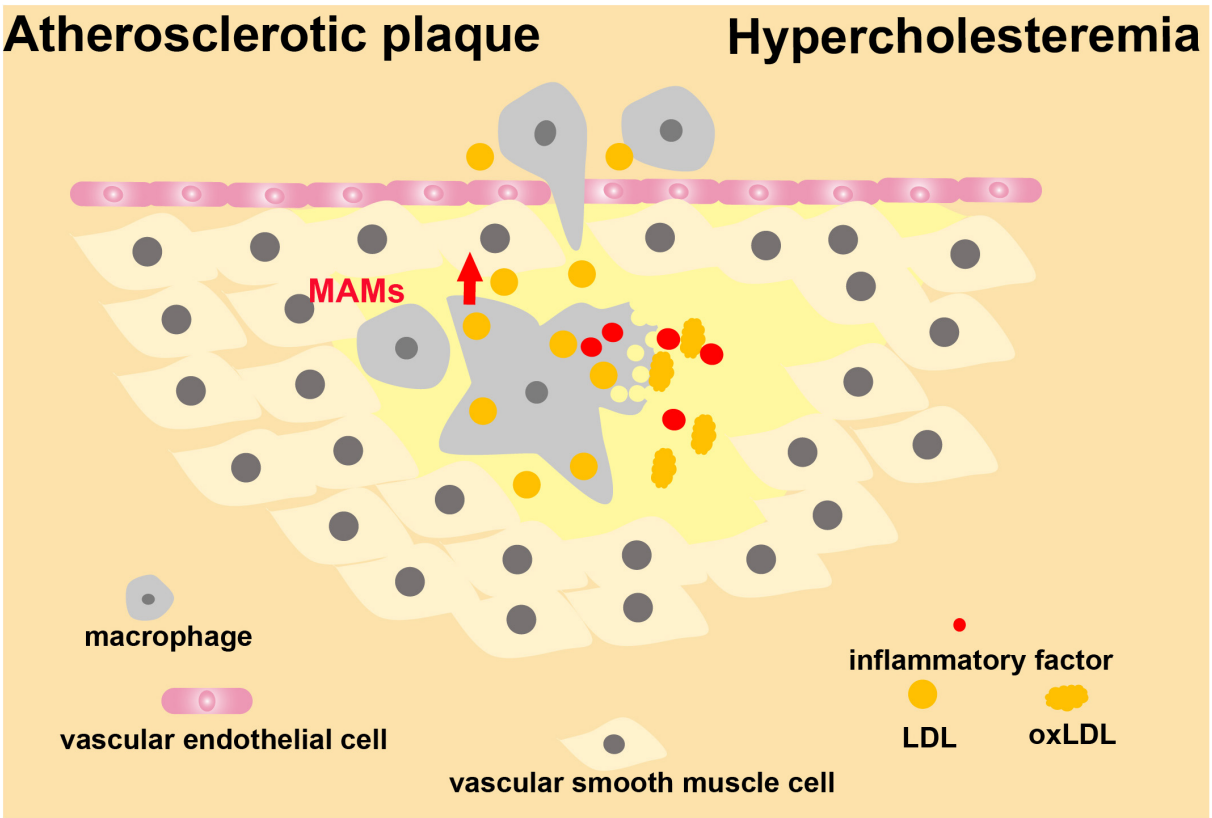

FIGURE 9 | MAMs in the development of atherosclerosis. MAMs are involved in signal transduction of macrophages during hypercholesteremia-induced chronic inflammation of the vascular wall.

HYPERTENSION

In pathology, hypertension is divided into two categories: primary hypertension and secondary hypertension. Primary hypertension, the main form of hypertension, is mainly due to structural and functional changes in small and large arteries, which cause high blood pressure (Laurent and Boutouyrie, 2015). Secondary hypertension, which affects about 5–10% of the hypertensive population, refers to hypertension caused by another disease or medical condition (Rimoldi et al., 2014). It includes renal vascular hypertension, primary aldosteronism, and diabetes-related hypertension (Laurent and Boutouyrie, 2015). Vascular constriction, diminished vasodilation reserve and stenosis, eutrophic remodeling, and changes in expandability are characteristics of small resistance arteries in patients with essential hypertension (Folkow, 1982, 1995; Mulvany and Aalkjaer, 1990; Schiffrin, 1992; Heagerty and Izzard, 1995; Mulvany et al., 1996; Rizzoni and Agabiti-Rosei, 2012). Proliferation, mild inflammation, fibrosis, and chronic vasoconstriction of VSMCs are implicated in the remodeling of hypertensive arterioles (Intengan and Schiffrin, 2001; Schiffrin and Touyz, 2004). These factors also affect the formation and development of atherosclerotic plaques. VSMCs control vascular homeostasis, including dilation, contraction, and remodeling (Moulis et al., 2019).

Recent studies also suggested a link between MAMs, autophagy and hypertension. PACS-2 maintains the migration of the autophagy-initiating ATG14 complex into the early autophagosome assembly region of the ER in the MAM structure (Hailey et al., 2010; Hamasaki et al., 2013). Depletion of PACS-2 induces BAP31-dependent mitochondrial fission and the dissociation of MAMs (Simmen et al., 2005). During stress, MAM structures will accumulate in VSMCs, and at the same time, PACS-2 will gather at MAMs. Depletion of PACS-2 will diminish mitochondrial autophagy in VSMCs and decrease the abundance of MAMs, thus inducing apoptosis (Moulis et al., 2019; Nahapetyan et al., 2019) and eventually leading to the development of hypertension (**Figure 8**). NgBR, localized in the ER, affects proliferation and migration by interacting with its ligand Nogo-B in VSMCs (Miao et al., 2006). NgBR is also required for angiogenesis (Zhao et al., 2010) and development (Rana et al., 2016). Its expression is low in the thickened pulmonary arteries of a hypoxic pulmonary hypertension rat model. Downregulation of NgBR expression reduces the abundance of MAMs in VSMCs, and meanwhile, promotes pAkt-IP3R3 signal transduction on the surface of MAMs, enhancing the proliferation ability of VSMCs (Yang et al., 2019b; **Figure 8**). Accumulating evidence indicates that MAMs may affect the functional structure of the vascular wall by regulating the proliferation, migration, and apoptosis of

VSMCs, which may cause clinical symptoms such as pulmonary hypertension. Reducing the accumulation of MAMs may have therapeutic value for ameliorating the structural damage of blood vessels, and may provide new strategies for preventing arterial hypertension (Yang et al., 2019c).

HYPERCHOLESTEREMIA

The lipoprotein transport system is vital to human health (Genest, 2003). Lipoproteins are classified according to size and density. HDL is relatively heavy as compared to LDL. However, chylomicrons, chylomicron residues, and VLDL are larger and lighter. Among lipoproteins, LDL particles are the main carriers of cholesterol to peripheral tissues, and loss-of-function analysis indicates that the LDL receptor is the main factor leading to hyperlipidemia (Geovanini and Libby, 2018). According to the lipid hypothesis, LDL is the key to reducing atherosclerotic plaque formation and limiting complications (Ridker, 2016). In hypercholesteremia, cholesterol-carrying LDL particles remain in the arterial wall (Williams and Tabas, 1995; Skalen et al., 2002; Hansson, 2005). This localization causes local inflammation within blood vessel walls, differentiation of monocytes into macrophages, accumulation of intracellular cholesterol, and production of inflammatory mediators (Libby et al., 2011). Consequently, immune cells are continuously recruited to secrete immune factors, leading to chronic inflammation (Stemme et al., 1995; Frostegard et al., 1999; Hansson and Hermansson, 2011). Oxidative stress stimulates vascular tissue to produce oxLDL, which is a critical trigger for atherosclerosis progression (Suciu et al., 2018). With the accumulation of oxLDL in the subendothelial region, the endothelium will become dysfunctional and undergo permeability changes (Palinski et al., 1989; Liao, 2013). At this stage, the role of MAMs in endothelial cells during the formation of atherosclerotic plaques remains unclear. However, during chronic inflammation of the vascular wall caused by hypercholesteremia, MAMs in macrophages are involved in transducing signals. Increasing evidence shows that the formation of NLRP3 inflammasomes is a key step in the process of atherosclerotic plaque formation caused by oxLDL (Lundberg and Yan, 2011; **Figure 9**). When inflammatory responses are triggered in macrophages, mitochondria lose their membrane potential, mtROS is upregulated, and the downstream pathways are activated to release inflammatory factors. Following the formation of inflammasomes at MAMs, NLRP3 accumulates at mitochondria, probably by sensing the increased calcium level (Triantafilou et al., 2013; Namgaladze et al., 2019). In patients with hypercholesteremia, new breakthroughs will be reached by studying the structure of MAMs in macrophages in the atherosclerotic plaque, and by understanding how MAMs regulate the development of chronic inflammation of blood vessels. We must also pay attention to the changes of MAM structures in vascular endothelial cells in atherosclerotic plaques, which may lead to new research directions.

CONCLUSION

Recently, the structure and function of MAMs have been intensively investigated. MAMs are involved in many aspects of cellular activities and are essential structures to maintain cell homeostasis and mutual communications between organelles. In certain circumstances, inflammation develops when the structure and function of MAMs are disturbed in some specialized types of cells, thus aggravating the progression of CVDs. Smoking, obesity, hyperglycemia, hypertension, hyperlipidemia, and other high-risk factors of CVDs will cause alterations of MAMs in different tissues, affecting the patient's prognosis. However, the growing body of recent experimental evidence mainly focuses on macrophages. Studies on vascular smooth muscle and endothelial cells are scarce, especially in the process of atherosclerosis. In the future, we need to explore the role of structural and functional changes in MAMs, and specific therapeutic strategies in smooth muscle and endothelial cells. MAMS are important places for mitochondrial fission, autophagy, intracellular energy metabolism, and material exchange; therefore, it is possible that controlling the structural changes of MAMs may be a key to treating patients with CVDs.

AUTHOR CONTRIBUTIONS

DF and JL conceived the review. HL, HF, and DF wrote the manuscript with the input from HZ, XL, DZ, YX, and PH. XL and HF drew the cartoons. All authors discussed the manuscript.

FUNDING

This work was supported by the NSFC (Nos. 91754115 and 31771531), by the Guangdong Province Universities and Colleges Pearl River Scholar Funded Scheme (GDUPS, 2018), by the Science and Technology Planning Project of Guangdong Province (2017B090901051 and 2016A020215152), by the Guangzhou Municipal "Ling Nan Ying Jie" Project (2018), and by Chuang Xin Qiang Xiao project of Guangzhou Medical University (2019KCXTD015).

REFERENCES

Abbate, A., Toldo, S., Marchetti, C., Kron, J., Van Tassell, B. W., and Dinarello, C. A. (2020). Interleukin-1 and the inflammasome as therapeutic targets in cardiovascular disease. *Circ. Res.* 126, 1260–1280. doi: 10.1161/circresaha.120.315937

Annunziata, I., Sano, R., and d'Azzo, A. (2018). Mitochondria-associated ER membranes (MAMs) and lysosomal storage diseases. *Cell Death Dis.* 9:328.

Arruda, A. P., Pers, B. M., Parlakgul, G., Guney, E., Inouye, K., and Hotamisligil, G. S. (2014). Chronic enrichment of hepatic endoplasmic reticulum-mitochondria contact leads to mitochondrial dysfunction in obesity. *Nat. Med.* 20, 1427–1435. doi: 10.1038/nm.3735

Bernhard, W., and Rouiller, C. (1956). Close topographical relationship between mitochondria and ergastoplasm of liver cells in a definite phase of cellular activity. *J. Biophys. Biochem. Cytol.* 2(4 Suppl.), 73–78. doi: 10.1083/jcb.2.4.73

Bhaskar, V., Yin, J., Mirza, A. M., Phan, D., Vanegas, S., Issafras, H., et al. (2011). Monoclonal antibodies targeting IL-1 beta reduce biomarkers of atherosclerosis in vitro and inhibit atherosclerotic plaque formation in Apolipoprotein E-deficient mice. *Atherosclerosis* 216, 313–320. doi: 10.1016/j.atherosclerosis.2011.02.026

Bhattacharjee, A., Prasad, S. K., Pal, S., Maji, B., Banerjee, A., Das, D., et al. (2016). Possible involvement of iNOS and TNF-alpha in nutritional intervention against nicotine-induced pancreatic islet cell damage. *Biomed. Pharmacother.* 84, 1727–1738. doi: 10.1016/j.biopha.2016.10.079

Bodas, M., Van Westphal, C., Carpenter-Thompson, R., Mohanty, M. D., and Vij, N. (2016). Nicotine exposure induces bronchial epithelial cell apoptosis and senescence via ROS mediated autophagy-impairment. *Free Radic. Biol. Med.* 97, 441–453. doi: 10.1016/j.freeradbiomed.2016.06.017

Boudina, S., and Abel, E. D. (2007). Diabetic cardiomyopathy revisited. *Circulation* 115, 3213–3223. doi: 10.1161/circulationaha.106.679597

Butts, B., Butler, J., Dunbar, S. B., Corwin, E., and Gary, R. A. (2018). Effects of exercise on ASC methylation and IL-1 cytokines in heart failure. *Med. Sci. Sports Exerc.* 50, 1757–1766. doi: 10.1249/mss.0000000000001641

Caragnano, A., Aleksova, A., Bulfoni, M., Cervellin, C., Rolle, I. G., Veneziano, C., et al. (2019). Autophagy and inflammasome activation in dilated cardiomyopathy. *J. Clin. Med.* 8:1519. doi: 10.3390/jcm8101519

Chaanine, A. H., Gordon, R. E., Kohlbrenner, E., Benard, L., Jeong, D., and Hajjar, R. J. (2013). Potential role of BNIP3 in cardiac remodeling, myocardial stiffness, and endoplasmic reticulum: mitochondrial calcium homeostasis in diastolic and systolic heart failure. *Circ. Heart Fail.* 6, 572–583. doi: 10.1161/circheartfailure.112.000200

Csordas, G., and Hajnoczky, G. (2009). SR/ER-mitochondrial local communication: calcium and ROS. *Biochim. Biophys. Acta* 1787, 1352–1362. doi: 10.1016/j.bbabio.2009.06.004

Desgraz, B., Collet, T. H., Rodondi, N., Cornuz, J., and Clair, C. (2017). Comparison of self-perceived cardiovascular disease risk among smokers with Framingham and PROCAM scores: a cross-sectional analysis of baseline data from a randomised controlled trial. *BMJ Open* 7:e012063. doi: 10.1136/bmjopen-2016-012063

Dorn, G. W. II, and Maack, C. (2013). SR and mitochondria: calcium cross-talk between kissing cousins. *J. Mol. Cell Cardiol.* 55, 42–49. doi: 10.1016/j.yjmcc.2012.07.015

Duewell, P., Kono, H., Rayner, K. J., Sirois, C. M., Vladimer, G., Bauernfeind, F. G., et al. (2010). NLRP3 inflammasomes are required for atherogenesis and activated by cholesterol crystals. *Nature* 464, 1357–1361. doi: 10.1038/nature08938

Eisner, V., Csordas, G., and Hajnoczky, G. (2013). Interactions between sarco-endoplasmic reticulum and mitochondria in cardiac and skeletal muscle - pivotal roles in Ca(2)(+) and reactive oxygen species signaling. *J. Cell Sci.* 126(Pt 14), 2965–2978. doi: 10.1242/jcs.093609

Elliott, E. I., Miller, A. N., Banoth, B., Iyer, S. S., Stotland, A., Weiss, J. P., et al. (2018). Cutting edge: mitochondrial assembly of the NLRP3 inflammasome complex is initiated at priming. *J. Immunol.* 200, 3047–3052. doi: 10.4049/jimmunol.1701723

Esposito, G., Cappetta, D., Russo, R., Rivellino, A., Ciuffreda, L. P., Roviezzo, F., et al. (2017). Sitagliptin reduces inflammation, fibrosis and preserves diastolic function in a rat model of heart failure with preserved ejection fraction. *Br. J. Pharmacol.* 174, 4070–4086. doi: 10.1111/bph.13686

Faria, A., and Persaud, S. J. (2017). Cardiac oxidative stress in diabetes: mechanisms and therapeutic potential. *Pharmacol. Ther.* 172, 50–62. doi: 10.1016/j.pharmthera.2016.11.013

Feng, J., Lu, S., Ding, Y., Zheng, M., and Wang, X. (2016). Homocysteine activates T cells by enhancing endoplasmic reticulum-mitochondria coupling and increasing mitochondrial respiration. *Protein Cell* 7, 391–402. doi: 10.1007/s13238-016-0245-x

Feng, J., Zhang, Z., Kong, W., Liu, B., Xu, Q., and Wang, X. (2009). Regulatory T cells ameliorate hyperhomocysteinaemia-accelerated atherosclerosis in apoE-/- mice. *Cardiovasc. Res.* 84, 155–163. doi: 10.1093/cvr/cvp182

Folkow, B. (1982). Physiological aspects of primary hypertension. *Physiol. Rev.* 62, 347–504. doi: 10.1152/physrev.1982.62.2.347

Folkow, B. (1995). Hypertensive structural changes in systemic precapillary resistance vessels: how important are they for in vivo haemodynamics? *J. Hypertens* 13(12 Pt 2), 1546–1559.

Forslund, K., Hildebrand, F., Nielsen, T., Falony, G., Chatelier, E. Le, Sunagawa, S., et al. (2017). Corrigendum: disentangling type 2 diabetes and metformin treatment signatures in the human gut microbiota. *Nature* 545:116. doi: 10.1038/nature22318

Friedman, J. R., Kannan, M., Toulmay, A., Jan, C. H., Weissman, J. S., Prinz, W. A., et al. (2018). Lipid homeostasis is maintained by dual targeting of the Mitochondrial PE biosynthesis enzyme to the ER. *Dev. Cell* 44, 261.e6–270.e6.

Frostegard, J., Ulfgren, A. K., Nyberg, P., Hedin, U., Swedenborg, J., Andersson, U., et al. (1999). Cytokine expression in advanced human atherosclerotic plaques: dominance of pro-inflammatory (Th1) and macrophage-stimulating cytokines. *Atherosclerosis* 145, 33–43. doi: 10.1016/s0021-9150(99)00011-8

Gatta, A. T., and Levine, T. P. (2017). Piecing together the patchwork of contact sites. *Trends Cell Biol.* 27, 214–229. doi: 10.1016/j.tcb.2016.08.010

Genest, J. (2003). Lipoprotein disorders and cardiovascular risk. *J. Inherit Metab. Dis.* 26, 267–287.

Geovanini, G. R., and Libby, P. (2018). Atherosclerosis and inflammation: overview and updates. *Clin. Sci.* 132, 1243–1252. doi: 10.1042/cs20180306

Gilca, G. E., Stefanescu, G., Badulescu, O., Tanase, D. M., Bararu, I., and Ciocoiu, M. (2017). Diabetic cardiomyopathy: current approach and potential diagnostic and therapeutic targets. *J. Diabetes Res.* 2017:1310265.

Golia, E., Limongelli, G., Natale, F., Fimiani, F., Maddaloni, V., Pariggiano, I., et al. (2014). Inflammation and cardiovascular disease: from pathogenesis to therapeutic target. *Curr. Atheroscler. Rep.* 16:435.

Guo, H., Callaway, J. B., and Ting, J. P. (2015). Inflammasomes: mechanism of action, role in disease, and therapeutics. *Nat. Med.* 21, 677–687. doi: 10.1038/nm.3893

Gutierrez, T., Parra, V., Troncoso, R., Pennanen, C., Contreras-Ferrat, A., Vasquez-Trincado, C., et al. (2014). Alteration in mitochondrial Ca(2+) uptake disrupts insulin signaling in hypertrophic cardiomyocytes. *Cell Commun. Signal.* 12:68. doi: 10.1186/preaccept-1950166084128344

Hailey, D. W., Rambold, A. S., Satpute-Krishnan, P., Mitra, K., Sougrat, R., Kim, P. K., et al. (2010). Mitochondria supply membranes for autophagosome biogenesis during starvation. *Cell* 141, 656–667. doi: 10.1016/j.cell.2010.04.009

Hamasaki, M., Furuta, N., Matsuda, A., Nezu, A., Yamamoto, A., Fujita, N., et al. (2013). Autophagosomes form at ER-mitochondria contact sites. *Nature* 495, 389–393. doi: 10.1038/nature11910

Hansson, G. K. (2005). Inflammation, atherosclerosis, and coronary artery disease. *N. Engl. J. Med.* 352, 1685–1695. doi: 10.1056/nejmra043430

Hansson, G. K., and Hermansson, A. (2011). The immune system in atherosclerosis. *Nat. Immunol.* 12, 204–212.

He, Y., Hara, H., and Nunez, G. (2016). Mechanism and regulation of NLRP3 inflammasome activation. trends biochem. *Sci* 41, 1012–1021. doi: 10.1016/j.tibs.2016.09.002

Heagerty, A. M., and Izzard, A. S. (1995). Small-artery changes in hypertension. *J. Hypertens* 13(12 Pt 2), 1560–1565.

Hershberger, R. E., and Siegfried, J. D. (2011). Update 2011: clinical and genetic issues in familial dilated cardiomyopathy. *J. Am. Coll Cardiol.* 57, 1641–1649. doi: 10.1016/j.jacc.2011.01.015

Hornung, V., and Latz, E. (2010). Critical functions of priming and lysosomal damage for NLRP3 activation. *Eur. J. Immunol.* 40, 620–623. doi: 10.1002/eji.200940185

Hotamisligil, G. S. (2006). Inflammation and metabolic disorders. *Nature* 444, 860–867. doi: 10.1038/nature05485

Hotamisligil, G. S. (2010). Endoplasmic reticulum stress and the inflammatory basis of metabolic disease. *Cell* 140, 900–917. doi: 10.1016/j.cell.2010.02.034

Intengan, H. D., and Schiffrin, E. L. (2001). Vascular remodeling in hypertension: roles of apoptosis, inflammation, and fibrosis. *Hypertension* 38(3 Pt 2), 581–587. doi: 10.1161/hy09t1.096249

Jacobs, J. L., and Coyne, C. B. (2013). Mechanisms of MAVS regulation at the mitochondrial membrane. *J. Mol. Biol.* 425, 5009–5019. doi: 10.1016/j.jmb.2013.10.007

Khodabandehloo, H., Gorgani-Firuzjaee, S., Panahi, G., and Meshkani, R. (2016). Molecular and cellular mechanisms linking inflammation to insulin resistance and beta-cell dysfunction. *Transl. Res.* 167, 228–256. doi: 10.1016/j.trsl.2015.08.011

Kirii, H., Niwa, T., Yamada, Y., Wada, H., Saito, K., Iwakura, Y., et al. (2003). Lack of interleukin-1beta decreases the severity of atherosclerosis in ApoE-deficient mice. *Arterioscler Thromb. Vasc. Biol.* 23, 656–660. doi: 10.1161/01.atv.0000064374.15232.c3

Krols, M., van Isterdael, G., Asselbergh, B., Kremer, A., Lippens, S., Timmerman, V., et al. (2016). Mitochondria-associated membranes as hubs for neurodegeneration. *Acta Neuropathol.* 131, 505–523. doi: 10.1007/s00401-015-1528-7

Laurent, S., and Boutouyrie, P. (2015). The structural factor of hypertension: large and small artery alterations. *Circ. Res.* 116, 1007–1021. doi: 10.1161/circresaha.116.303596

Li, X., Du, N., Zhang, Q., Li, J., Chen, X., Liu, X., et al. (2014). MicroRNA-30d regulates cardiomyocyte pyroptosis by directly targeting foxo3a in diabetic cardiomyopathy. *Cell Death Dis.* 5:e1479. doi: 10.1038/cddis.2014.430

Liao, J. K. (2013). Linking endothelial dysfunction with endothelial cell activation. *J. Clin. Invest.* 123, 540–541. doi: 10.1172/jci66843

Libby, P., Ridker, P. M., and Hansson, G. K. (2011). Progress and challenges in translating the biology of atherosclerosis. *Nature* 473, 317–325. doi: 10.1038/nature10146

Liu, D., Zeng, X., Li, X., Mehta, J. L., and Wang, X. (2018). Role of NLRP3 inflammasome in the pathogenesis of cardiovascular diseases. *Basic Res. Cardiol.* 113:5.

Liu, X., Weaver, D., Shirihai, O., and Hajnoczky, G. (2009). Mitochondrial 'kiss-and-run': interplay between mitochondrial motility and fusion-fission dynamics. *EMBO J.* 28, 3074–3089. doi: 10.1038/emboj.2009.255

Lopez-Crisosto, C., Pennanen, C., Vasquez-Trincado, C., Morales, P. E., Bravo-Sagua, R., Quest, A. F. G., et al. (2017). Sarcoplasmic reticulum-mitochondria communication in cardiovascular pathophysiology. *Nat. Rev. Cardiol.* 14, 342–360. doi: 10.1038/nrcardio.2017.23

Lowell, B. B., and Shulman, G. I. (2005). Mitochondrial dysfunction and type 2 diabetes. *Science* 307, 384–387.

Lundberg, A. M., and Yan, Z. Q. (2011). Innate immune recognition receptors and damage-associated molecular patterns in plaque inflammation. *Curr. Opin. Lipidol.* 22, 343–349. doi: 10.1097/mol.0b013e32834ada80

Luo, B., Li, B., Wang, W., Liu, X., Liu, X., Xia, Y., et al. (2014). Rosuvastatin alleviates diabetic cardiomyopathy by inhibiting NLRP3 inflammasome and MAPK pathways in a type 2 diabetes rat model. *Cardiovasc. Drugs Ther.* 28, 33–43. doi: 10.1007/s10557-013-6498-1

Ma, K., Lv, S., Liu, B., Liu, Z., Luo, Y., Kong, W., et al. (2013). , CTLA4-IgG ameliorates homocysteine-accelerated atherosclerosis by inhibiting T-cell overactivation in apoE(-/-) mice. *Cardiovasc. Res.* 97, 349–359. doi: 10.1093/cvr/cvs330

Maffia, P., and Cirino, G. (2017). Targeting inflammation to reduce cardiovascular disease risk. *Br. J. Pharmacol.* 174, 3895–3897. doi: 10.1111/bph.14039

Masters, S. L., Latz, E., and O'Neill, L. A. (2011). The inflammasome in atherosclerosis and type 2 diabetes. *Sci. Transl. Med.* 3:81s17.

Mathers, C. D., and Loncar, D. (2006). Projections of global mortality and burden of disease from 2002 to 2030. *PLoS Med.* 3:e442. doi: 0.1371/journal.pmed.0030442

McInerney, J., Pisani, D., and O'Connell, M. J. (2015). The ring of life hypothesis for eukaryote origins is supported by multiple kinds of data. *Philos. Trans. R. Soc. Lond. B Biol. Sci.* 370:20140323. doi: 10.1098/rstb.2014.0323

McKenna, W. J., Maron, B. J., and Thiene, G. (2017). Classification, epidemiology, and global burden of cardiomyopathies. *Circ. Res.* 121, 722–730. doi: 10.1161/circresaha.117.309711

Mebratu, Y. A., Leyva-Baca, I., Wathelet, M. G., Lacey, N., Chand, H. S., Choi, A. M. K., et al. (2017). Bik reduces hyperplastic cells by increasing Bak and activating DAPk1 to juxtapose ER and mitochondria. *Nat. Commun.* 8:803.

Medzhitov, R. (2008). Origin and physiological roles of inflammation. *Nature* 454, 428–435. doi: 10.1038/nature07201

Mehto, S., Chauhan, S., Jena, K. K., Chauhan, N. R., Nath, P., Sahu, R., et al. (2019a). IRGM restrains NLRP3 inflammasome activation by mediating its SQSTM1/p62-dependent selective autophagy. *Autophagy* 15, 1645–1647. doi: 10.1080/15548627.2019.1628544

Mehto, S., Jena, K. K., Nath, P., Chauhan, S., Kolapalli, S. P., Das, S. K., et al. (2019b). The Crohn's disease risk factor IRGM limits NLRP3 inflammasome activation by impeding its assembly and by mediating its selective autophagy. *Mol. Cell* 73, 429.e7–445.e7.

Miao, R. Q., Gao, Y., Harrison, K. D., Prendergast, J., Acevedo, L. M., Yu, J., et al. (2006). Identification of a receptor necessary for Nogo-B stimulated chemotaxis and morphogenesis of endothelial cells. *Proc. Natl. Acad. Sc.i U.S.A.* 103, 10997–11002. doi: 10.1073/pnas.0602427103

Mills, E. L., Kelly, B., and O'Neill, L. A. J. (2017). Mitochondria are the powerhouses of immunity. *Nat. Immunol.* 18, 488–498. doi: 10.1038/ni.3704

Missiroli, S., Bonora, M., Patergnani, S., Poletti, F., Perrone, M., Gafa, R., et al. (2016). PML at mitochondria-associated membranes is critical for the repression of autophagy and cancer development. *Cell Rep.* 16, 2415–2427. doi: 10.1016/j.celrep.2016.07.082

Missiroli, S., Patergnani, S., Caroccia, N., Pedriali, G., Perrone, M., Previati, M., et al. (2018). Mitochondria-associated membranes (MAMs) and inflammation. *Cell Death Dis.* 9:329.

Morales, P. E., Arias-Duran, C., Avalos-Guajardo, Y., Aedo, G., Verdejo, H. E., Parra, V., et al. (2020). Emerging role of mitophagy in cardiovascular physiology and pathology. *Mol. Aspects Med.* 71:100822. doi: 10.1016/j.mam.2019.09.006

Moulis, M., Grousset, E., Faccini, J., Richetin, K., Thomas, G., and Vindis, C. (2019). The multifunctional sorting protein PACS-2 controls mitophagosome formation in human vascular smooth muscle cells through mitochondria-er contact sites. *Cells* 8:638. doi: 10.3390/cells8060638

Mulvany, M. J., and Aalkjaer, C. (1990). Structure and function of small arteries. *Physiol. Rev.* 70, 921–961. doi: 10.1152/physrev.1990.70.4.921

Mulvany, M. J., Baumbach, G. L., Aalkjaer, C., Heagerty, A. M., Korsgaard, N., Schiffrin, E. L., et al. (1996). Vascular remodeling. *Hypertension* 28, 505–506.

Munoz, J. P., and Zorzano, A. (2017). FUNDC1: a novel protein in cardiac health. *Circulation* 136, 2267–2270. doi: 10.1161/circulationaha.117.031417

Nahapetyan, H., Moulis, M., Grousset, E., Faccini, J., Grazide, M. H., Mucher, E., et al. (2019). Altered mitochondrial quality control in Atg7-deficient VSMCs promotes enhanced apoptosis and is linked to unstable atherosclerotic plaque phenotype. *Cell Death Dis.* 10:119.

Nakahira, K., Haspel, J. A., Rathinam, V. A., Lee, S. J., Dolinay, T., Lam, H. C., et al. (2011). Autophagy proteins regulate innate immune responses by inhibiting the release of mitochondrial DNA mediated by the NALP3 inflammasome. *Nat. Immunol.* 12, 222–230. doi: 10.1038/ni.1980

Namgaladze, D., Khodzhaeva, V., and Brune, B. (2019). ER-mitochondria communication in cells of the innate immune system. *Cells* 8:1088. doi: 10.3390/cells8091088

North, B. J., and Sinclair, D. A. (2012). The intersection between aging and cardiovascular disease. *Circ. Res.* 110, 1097–1108. doi: 10.1161/circresaha.111.246876

Palinski, W., Rosenfeld, M. E., Yla-Herttuala, S., Gurtner, G. C., Socher, S. S., Butler, S. W., et al. (1989). Low density lipoprotein undergoes oxidative modification in vivo. *Proc. Natl. Acad. Sci. U.S.A.* 86, 1372–1376. doi: 10.1073/pnas.86.4.1372

Peretti, D., Kim, S., Tufi, R., and Lev, S. (2019). Lipid transfer proteins and membrane contact sites in human Cancer. *Front. Cell Dev. Biol.* 7:371. doi: 10.3389/fcell.2019.00371

Petit, A., Knabe, L., Khelloufi, K., Jory, M., Gras, D., Cabon, Y., et al. (2019). Bronchial epithelial calcium metabolism impairment in smokers and chronic obstructive pulmonary disease. decreased ORAI3 signaling. *Am. J. Respir. Cell Mol. Biol.* 61, 501–511. doi: 10.1165/rcmb.2018-0228oc

Petrilli, V., Papin, S., Dostert, C., Mayor, A., Martinon, F., and Tschopp, J. (2007). Activation of the NALP3 inflammasome is triggered by low intracellular potassium concentration. *Cell Death Differ.* 14, 1583–1589. doi: 10.1038/sj.cdd.4402195

Porter, K. R., and Palade, G. E. (1957). Studies on the endoplasmic reticulum. III. Its form and distribution in striated muscle cells. *J. Biophys. Biochem. Cytol.* 3, 269–300.

Racanelli, A. C., Kikkers, S. A., Choi, A. M. K., and Cloonan, S. M. (2018). Autophagy and inflammation in chronic respiratory disease. *Autophagy* 14, 221–232. doi: 10.1080/15548627.2017.1389823

Rana, U., Liu, Z., Kumar, S. N., Zhao, B., Hu, W., Bordas, M., et al. (2016). Nogo-B receptor deficiency causes cerebral vasculature defects during embryonic development in mice. *Dev. Biol.* 410, 190–201. doi: 10.1016/j.ydbio.2015.12.023

Rathinam, V. A., and Fitzgerald, K. A. (2016). Inflammasome complexes: emerging mechanisms and effector functions. *Cell* 165, 792–800. doi: 10.1016/j.cell.2016.03.046

Ridker, P. M. (2016). Residual inflammatory risk: addressing the obverse side of the atherosclerosis prevention coin. *Eur. Heart J.* 37, 1720–1722. doi: 10.1093/eurheartj/ehw024

Ridker, P. M., Everett, B. M., Thuren, T., MacFadyen, J. G., Chang, W. H., Ballantyne, C., et al. (2017). Antiinflammatory therapy with canakinumab for atherosclerotic disease. *N. Engl. J. Med.* 377, 1119–1131.

Rieusset, J., Chauvin, M. A., Durand, A., Bravard, A., Laugerette, F., Michalski, M. C., et al. (2012). Reduction of endoplasmic reticulum stress using chemical chaperones or Grp78 overexpression does not protect muscle cells from palmitate-induced insulin resistance. *Biochem. Biophys. Res. Commun.* 417, 439–445. doi: 10.1016/j.bbrc.2011.11.135

Rimoldi, S. F., Scherrer, U., and Messerli, F. H. (2014). Secondary arterial hypertension: when, who, and how to screen? *Eur. Heart J.* 35, 1245–1254. doi: 10.1093/eurheartj/eht534

Rizzoni, D., and Agabiti-Rosei, E. (2012). Structural abnormalities of small resistance arteries in essential hypertension. *Intern. Emerg. Med.* 7, 205–212. doi: 10.1007/s11739-011-0548-0

Rizzuto, R., Brini, M., Murgia, M., and Pozzan, T. (1993). Microdomains with high Ca2+ close to IP3-sensitive channels that are sensed by neighboring mitochondria. *Science* 262, 744–747. doi: 10.1126/science.8235595

Rutter, G. A., Hodson, D. J., Chabosseau, P., Haythorne, E., Pullen, T. J., and Leclerc, I. (2017). Local and regional control of calcium dynamics in the pancreatic islet. *Diabetes Obes Metab.* 19(Suppl. 1), 30–41. doi: 10.1111/dom.12990

Rutter, G. A., and Pinton, P. (2014). , Mitochondria-associated endoplasmic reticulum membranes in insulin signaling. *Diabetes* 63, 3163–3165. doi: 10.2337/db14-0812

Sano, S., Oshima, K., Wang, Y., MacLauchlan, S., Katanasaka, Y., Sano, M., et al. (2018). Tet2-mediated clonal hematopoiesis accelerates heart failure through a mechanism involving the IL-1beta/NLRP3 inflammasome. *J. Am. Coll Cardiol.* 71, 875–886. doi: 10.1016/j.jacc.2017.12.037

Santulli, G., Xie, W., Reiken, S. R., and Marks, A. R. (2015). Mitochondrial calcium overload is a key determinant in heart failure. *Proc. Natl. Acad. Sci. U.S.A.* 112, 11389–11394. doi: 10.1073/pnas.1513047112

Schaufelberger, M. (2019). Cardiomyopathy and pregnancy. *Heart* 105, 1543–1551.

Schiffrin, E. L. (1992). Reactivity of small blood vessels in hypertension: relation with structural changes. State of the art lecture. *Hypertension* 19, II1–II9.

Schiffrin, E. L., and Touyz, R. M. (2004). From bedside to bench to bedside: role of renin-angiotensin-aldosterone system in remodeling of resistance arteries in hypertension. *Am. J. Physiol. Heart Circ. Physiol.* 287, H435–H446.

Seidlmayer, L. K., Kuhn, J., Berbner, A., Arias-Loza, P. A., Williams, T., Kaspar, M., et al. (2016). Inositol 1,4,5-trisphosphate-mediated sarcoplasmic reticulum-mitochondrial crosstalk influences adenosine triphosphate production via mitochondrial Ca2+ uptake through the mitochondrial ryanodine receptor in cardiac myocytes. *Cardiovasc. Res.* 112, 491–501. doi: 10.1093/cvr/cvw185

Shimada, K., Crother, T. R., Karlin, J., Dagvadorj, J., Chiba, N., Chen, S., et al. (2012). Oxidized mitochondrial DNA activates the NLRP3 inflammasome during apoptosis. *Immunity* 36, 401–414. doi: 10.1016/j.immuni.2012.01.009

Shore, G. C., and Tata, J. R. (1977a). Two fractions of rough endoplasmic reticulum from rat liver. I. Recovery of rapidly sedimenting endoplasmic reticulum in association with mitochondria. *J. Cell Biol.* 72, 714–725. doi: 10.1083/jcb.72.3.714

Shore, G. C., and Tata, J. R. (1977b). Two fractions of rough endoplasmic reticulum from rat liver. II. Cytoplasmic messenger RNA's which code for albumin and mitochondrial proteins are distributed differently between the two fractions. *J. Cell Biol.* 72, 726–743. doi: 10.1083/jcb.72.3.726

Simmen, T., Aslan, J. E., Blagoveshchenskaya, A. D., Thomas, L., Wan, L., Xiang, Y., et al. (2005). PACS-2 controls endoplasmic reticulum-mitochondria communication and Bid-mediated apoptosis. *EMBO J.* 24, 717–729. doi: 10.1038/sj.emboj.7600559

Simmen, T., and Tagaya, M. (2017). Organelle communication at membrane contact sites (MCS): from curiosity to center stage in cell biology and biomedical research. *Adv. Exp. Med. Biol.* 997, 1–12. doi: 10.1007/978-981-10-4567-7_1

Sing, C. F., Stengard, J. H., and Kardia, S. L. (2003). Genes, environment, and cardiovascular disease. *Arterioscler Thromb. Vasc. Biol.* 23, 1190–1196.

Skalen, K., Gustafsson, M., Rydberg, E. K., Hulten, L. M., Wiklund, O., Innerarity, T. L., et al. (2002). Subendothelial retention of atherogenic lipoproteins in early atherosclerosis. *Nature* 417, 750–754. doi: 10.1038/nature00804

Stacchiotti, A., Favero, G., Lavazza, A., Garcia-Gomez, R., Monsalve, M., and Rezzani, R. (2018). Perspective: mitochondria-ER contacts in metabolic cellular stress assessed by microscopy. *Cells* 8:5. doi: 10.3390/cells8010005

Stacchiotti, A., Favero, G., Lavazza, A., Golic, I., Aleksic, M., Korac, A., et al. (2016). Hepatic macrosteatosis is partially converted to microsteatosis by melatonin supplementation in ob/ob mice non-alcoholic fatty liver disease. *PLoS One* 11:e0148115. doi: 10.1371/journal.pone.0148115

Stemme, S., Faber, B., Holm, J., Wiklund, O., Witztum, J. L., and Hansson, G. K. (1995). T lymphocytes from human atherosclerotic plaques recognize oxidized low density lipoprotein. *Proc. Natl. Acad. Sci. U.S.A.* 92, 3893–3897. doi: 10.1073/pnas.92.9.3893

Suciu, C. F., Prete, M., Ruscitti, P., Favoino, E., Giacomelli, R., and Perosa, F. (2018). Oxidized low density lipoproteins: the bridge between atherosclerosis and autoimmunity. Possible implications in accelerated atherosclerosis and for immune intervention in autoimmune rheumatic disorders. *Autoimmun. Rev.* 17, 366–375. doi: 10.1016/j.autrev.2017.11.028

Suetomi, T., Willeford, A., Brand, C. S., Cho, Y., Ross, R. S., Miyamoto, S., et al. (2018). Inflammation and NLRP3 inflammasome activation initiated in response to pressure overload by Ca(2+)/Calmodulin-dependent protein kinase II delta Signaling in cardiomyocytes are essential for adverse cardiac remodeling. *Circulation* 138, 2530–2544. doi: 10.1161/circulationaha.118.034621

Theurey, P., and Rieusset, J. (2017). Mitochondria-associated membranes response to nutrient availability and role in metabolic diseases. *Trends Endocrinol. Metab.* 28:32–45. doi: 10.1016/j.tem.2016.09.002

Triantafilou, K., Hughes, T. R., Triantafilou, M., and Morgan, B. P. (2013). The complement membrane attack complex triggers intracellular Ca2+ fluxes leading to NLRP3 inflammasome activation. *J. Cell Sci.* 126(Pt 13), 2903–2913. doi: 10.1242/jcs.124388

Tschopp, J., and Schroder, K. (2010). NLRP3 inflammasome activation: the convergence of multiple signalling pathways on ROS production? *Nat. Rev. Immunol.* 10, 210–215. doi: 10.1038/nri2725

Tubbs, E., Theurey, P., Vial, G., Bendridi, N., Bravard, A., Chauvin, M. A., et al. (2014). Mitochondria-associated endoplasmic reticulum membrane (MAM) integrity is required for insulin signaling and is implicated in hepatic insulin resistance. *Diabetes* 63, 3279–3294. doi: 10.2337/db13-1751

van Vliet, A. R., Verfaillie, T., and Agostinis, P. (2014). New functions of mitochondria associated membranes in cellular signaling. *Biochi.m Biophys. Acta* 1843, 2253–2262. doi: 10.1016/j.bbamcr.2014.03.009

Vance, J. E. (1990). Phospholipid synthesis in a membrane fraction associated with mitochondria. *J. Biol. Chem.* 265, 7248–7256.

Wang, C. H., and Wei, Y. H. (2017). Role of mitochondrial dysfunction and dysregulation of Ca(2+) homeostasis in the pathophysiology of insulin resistance and type 2 diabetes. *J. Biomed. Sci.* 24:70.

Wang, H., Liu, X., Umino, T., Skold, C. M., Zhu, Y., Kohyama, T., et al. (2001). Cigarette smoke inhibits human bronchial epithelial cell repair processes. *Am. J. Respir. Cell Mol. Biol.* 25, 772–779. doi: 10.1165/ajrcmb.25.6.4458

Weber, C., and Noels, H. (2011). Atherosclerosis: current pathogenesis and therapeutic options. *Nat. Med.* 17, 1410–1422. doi: 10.1038/nm.2538

Whelan, R. S., Kaplinskiy, V., and Kitsis, R. N. (2010). Cell death in the pathogenesis of heart disease: mechanisms and significance. *Annu. Rev. Physiol.* 72, 19–44. doi: 10.1146/annurev.physiol.010908.163111

Williams, K. J., and Tabas, I. (1995). The response-to-retention hypothesis of early atherogenesis. *Arterioscler Thromb. Vasc. Biol.* 15, 551–561. doi: 10.1161/01.atv.15.5.551

Wong, Y. C., Kim, S., Peng, W., and Krainc, D. (2019). Regulation and function of mitochondria-lysosome membrane contact sites in cellular homeostasis. *Trends Cell Biol.* 29, 500–513. doi: 10.1016/j.tcb.2019.02.004

Wright, S. D., Burton, C., Hernandez, M., Hassing, H., Montenegro, J., Mundt, S., et al. (2000). Infectious agents are not necessary for murine atherogenesis. *J. Exp. Med.* 191, 1437–1442. doi: 10.1084/jem.191.8.1437

Wu, S., Lu, Q., Ding, Y., Wu, Y., Qiu, Y., Wang, P., et al. (2019). Hyperglycemia-driven inhibition of AMP-activated protein kinase alpha2 induces diabetic cardiomyopathy by promoting mitochondria-associated

endoplasmic reticulum membranes in vivo. *Circulation* 139, 1913–1936. doi: 10.1161/circulationaha.118.033552

Wu, S., Lu, Q., Wang, Q., Ding, Y., Ma, Z., Mao, X., et al. (2017). Binding of FUN14 domain containing 1 with inositol 1,4,5-trisphosphate receptor in mitochondria-associated endoplasmic reticulum membranes maintains mitochondrial dynamics and function in hearts in vivo. *Circulation* 136, 2248–2266. doi: 10.1161/circulationaha.117.030235

Wu, W., Li, W., Chen, H., Jiang, L., Zhu, R., and Feng, D. (2016). FUNDC1 is a novel mitochondrial-associated-membrane (MAM) protein required for hypoxia-induced mitochondrial fission and mitophagy. *Autophagy* 12, 1675–1676. doi: 10.1080/15548627.2016.1193656

Yabal, M., Calleja, D. J., Simpson, D. S., and Lawlor, K. E. (2019). Stressing out the mitochondria: mechanistic insights into NLRP3 inflammasome activation. *J. Leukoc Biol.* 105, 377–399. doi: 10.1002/jlb.mr0318-124r

Yang, F., Qin, Y., Lv, J., Wang, Y., Che, H., Chen, X., et al. (2018). Silencing long non-coding RNA Kcnq1ot1 alleviates pyroptosis and fibrosis in diabetic cardiomyopathy. *Cell Death Dis.* 9:1000.

Yang, F., Qin, Y., Wang, Y., Meng, S., Xian, H., Che, H., et al. (2019a). Metformin inhibits the NLRP3 inflammasome via ampk/mtor-dependent effects in diabetic cardiomyopathy. *Int. J. Biol. Sci.* 15, 1010–1019. doi: 10.7150/ijbs.29680

Yang, Y. D., Li, M. M., Xu, G., Feng, L., Zhang, E. L., Chen, J., et al. (2019b). Nogo-B receptor directs mitochondria-associated membranes to regulate vascular smooth muscle cell proliferation. *Int. J. Mol. Sci.* 20:319.

Yang, Y. D., Li, M. M., Xu, G., Zhang, E. L., Chen, J., Sun, B., et al. (2019c). Targeting mitochondria-associated membranes as a potential therapy against endothelial injury induced by hypoxia. *J. Cell Biochem.* 120, 18967–18978. doi: 10.1002/jcb.29220

Zeisbrich, M., Yanes, R. E., Zhang, H., Watanabe, R., Li, Y., Brosig, L., et al. (2018). Hypermetabolic macrophages in rheumatoid arthritis and coronary artery disease due to glycogen synthase kinase 3b inactivation. *Ann. Rheum. Dis.* 77, 1053–1062. doi: 10.1136/annrheumdis-2017-212647

Zeng, X., Dai, J., Remick, D. G., and Wang, X. (2003). Homocysteine mediated expression and secretion of monocyte chemoattractant protein-1 and interleukin-8 in human monocytes. *Circ. Res.* 93, 311–320. doi: 10.1161/01.res.0000087642.01082.e4

Zhang, Z., Meszaros, G., He, W. T., Xu, Y., de Fatima, H., Magliarelli, L., et al. (2017). Protein kinase D at the Golgi controls NLRP3 inflammasome activation. *J. Exp. Med.* 214, 2671–2693.

Zhao, B., Chun, C., Liu, Z., Horswill, M. A., Pramanik, K., Wilkinson, G. A., et al. (2010). Nogo-B receptor is essential for angiogenesis in zebrafish via Akt pathway. *Blood* 116, 5423–5433. doi: 10.1182/blood-2010-02-271577

Zhong, Z., Umemura, A., Sanchez-Lopez, E., Liang, S., Shalapour, S., Wong, J., et al. (2016). NF-kappaB restricts inflammasome activation via elimination of damaged mitochondria. *Cell* 164, 896–910. doi: 10.1016/j.cell.2015.12.057

Zhou, H., Wang, S., Hu, S., Chen, Y., and Ren, J. (2018). ER-mitochondria microdomains in cardiac ischemia-reperfusion injury: a fresh perspective. *Front. Physiol.* 9:755. doi: 10.3389/fphys.2018.00755

Zhou, R., Yazdi, A. S., Menu, P., and Tschopp, J. (2011). A role for mitochondria in NLRP3 inflammasome activation. *Nature* 469, 221–225.

Conflict of Interest: The authors declare that the research was conducted in the absence of any commercial or financial relationships that could be construed as a potential conflict of interest.

frontiers in Cell and Developmental Biology

ORIGINAL RESEARCH
published: 20 November 2020
doi: 10.3389/fcell.2020.571388

Improved Split-GFP Systems for Visualizing Organelle Contact Sites in Yeast and Human Cells

*Shinya Tashiro[1], Yuriko Kakimoto[2], Manatsu Shinmyo[1], Shintaro Fujimoto[1] and Yasushi Tamura[1]**

[1] Faculty of Science, Yamagata University, Yamagata, Japan, [2] Department of Biochemistry and Molecular Biology, Graduate School of Medical Science, Yamagata University, Yamagata, Japan

Inter-organelle contact sites have attracted a lot of attention as functionally specialized regions that mediate the exchange of metabolites, including lipids and ions, between distinct organelles. However, studies on inter-organelle contact sites are at an early stage and it remains enigmatic what directly mediates the organelle-organelle interactions and how the number and degree of the contacts are regulated. As a first step to answer these questions, we previously developed split-GFP probes that could visualize and quantify multiple inter-organelle contact sites in the yeast and human cultured cells. However, the split-GFP probes possessed a disadvantage of inducing artificial connections between two different organelle membranes, especially when overexpressed. In the present study, we developed a way to express the split-GFP probes whose expressions remained at low levels, with minimal variations between different yeast cells. Besides, we constructed a HeLa cell line in which the expression of the split-GFP probes could be induced by the addition of doxycycline to minimize the artificial effects. The improved split-GFP systems may be faithful tools to quantify organelle contact sites and screen new factors involved in organelle-organelle tethering in yeast and mammalian cells.

Keywords: mitochondria, endoplasmic reticulum, organelle contact site, split GFP, yeast, peroxisome, vacuole, lipid droplet

OPEN ACCESS

Edited by:
Yasunori Saheki,
Nanyang Technological University, Singapore

Reviewed by:
Chris Stefan,
University College London, United Kingdom
Joe Costello,
University of Exeter, United Kingdom

***Correspondence:**
Yasushi Tamura
tamura@sci.kj.yamagata-u.ac.jp

Specialty section:
This article was submitted to Membrane Traffic, a section of the journal Frontiers in Cell and Developmental Biology

Received: *10 June 2020*
Accepted: *26 October 2020*
Published: *20 November 2020*

Citation:
Tashiro S, Kakimoto Y, Shinmyo M, Fujimoto S and Tamura Y (2020) Improved Split-GFP Systems for Visualizing Organelle Contact Sites in Yeast and Human Cells. Front. Cell Dev. Biol. 8:571388. doi: 10.3389/fcell.2020.571388

INTRODUCTION

Organelles are critical membrane-bound structures that developed in eukaryotic cells to allow them to efficiently perform multiple chemical reactions within single cells by isolating and concentrating specific enzymes and metabolites. In order to maintain the characteristic organelle functions, the spatial independence of individual organelles must be strictly maintained so that their contents do not mix via the non-specific fusion of different organelle membranes. However, recent studies have shown that distinct organelles directly interact with each other and form functionally specialized regions called the "organellar-contact sites" (Eisenberg-Bord et al., 2016; Murley and Nunnari, 2016; Cohen et al., 2018; Wu et al., 2018; Scorrano et al., 2019; Tamura et al., 2019; Prinz et al., 2020). For example, it has been revealed that the ERMES (ER-Mitochondria Encounter Structure) complex acts as a molecular tether between the mitochondrial outer membrane and the endoplasmic reticulum (ER) membrane and mediates phospholipid transport between these organelles in yeast (Kornmann et al., 2009; Kojima et al., 2016; Kawano et al., 2018;

Kornmann, 2020). In addition to the ER-mitochondria contacts, multiple organelle-contact sites as well as tethering factors have been identified in yeast. Although extensive studies have identified a number of factors that tether distinct organelle membranes, it is still unknown how the contact sites are regulated in terms of number and size. Besides, since we usually visualize organelle contact sites by using fluorescent protein fused to known organelle tethering factors in living cells, it is difficult to observe the contact sites in the absence of such organelle tethering factors. Therefore, we previously developed split-GFP probes that could visualize inter-organelle-contact sites as research tools to tackle these problems (Kakimoto et al., 2018). Our studies using the split-GFP probes in yeast suggest that one organelle forms contact sites with various organelles at the same time. We also showed that the split-GFP system was effective in visualizing the contact site between the mitochondria and the ER in HeLa cells. Similar studies using split-GFP were also performed by other research groups and demonstrated its usability for visualization and quantification of inter-organelle contacts (Cieri et al., 2018; Shai et al., 2018; Yang et al., 2018). In fact, a genome-wide screen using the fluorescent signals of split-Venus as an index of the mitochondria-peroxisome interactions successfully identified Fzo1 and Pex34 as the tethering factors between these organelles (Shai et al., 2018). However, since split-GFP hardly dissociates once it gets associated, it has a disadvantage of inducing artificial inter-organellar contacts, especially when overexpressed. Indeed, a previous study reported that the split-GFP probes expressed on peroxisome and the ER could act as an artificial tether and increase their organelle contacts (Bishop et al., 2019).

In this study, we tested different ways to express split-GFP probes to overcome the drawbacks of the original split-GFP systems. Specifically, we found that expressing split-GFP probes from the genome remarkably decreased the variation in the expression levels among cells and maintained a low expression level in yeast. We also constructed a HeLa cell line that was capable of a doxycycline-inducible expression of the split-GFP protein. By adjusting the doxycycline concentration and induction time, we succeeded in determining the appropriate conditions for observing the ER-mitochondria-contact sites in HeLa cells. Our improved split-GFP methods may be powerful tools for discovering novel organelle tethering factors and regulators.

MATERIALS AND METHODS

Plasmids

Plasmids and DNA oligos used in this study have been listed in **Tables 1**, **2**, respectively. To integrate the genes that express the organelle-targeted split-GFP fragments into the genomic DNA of yeast, we tandemly cloned the *GPD* promoter, the gene encoding the split-GFP protein, the *CYC1* terminator, and the hygromycin or clonNAT-resistant marker gene (*hphMX* or *natNT2*) into the pBlueScript SK(-) cloning vector (Agilent Technologies). We first amplified the DNA fragments encoding the *GPD* promoter, Tom71, Ifa38, Dpp1, the first 60 N-terminal residues of Pex3 and GFP1-10, and the *CYC1* terminator, using the plasmids pSFL22, 16, 100, 26, and 28 (Kakimoto et al., 2018), respectively, as templates and a pair of primers YU1390 and YU499. We also amplified the DNA fragments encoding *hphMX* and *natNT2* by PCR using pBS-hphMX and pBS-natNT2 (Kojima et al., 2019), respectively, as templates and the primer pairs YU501/YU503 and YU500/YU502, respectively. We further amplified the complete gene cassettes that encoded the promoter, the split-GFP fusion gene, the terminator, and the drug-resistance gene by an overlap extension PCR using the two DNA fragments previously mentioned as templates and the primer pairs YU1390/YU503 and YU1390/YU502, and inserted the products into the EcoRI/BamHI site of pBlueScript SK(-) using the In-Fusion® HD Cloning Kit, resulting in pYC135, pYC136, pYC137, pYC141, pYC143, and pYC144, respectively.

To express split-GFP fusion proteins on the ER membrane and the mitochondrial outer membrane (MOM) in HeLa cells, we prepared two plasmids, pMM186 and 189, that expressed ERj1N-V5-GFP1-10 and Tom70N-FLAG-GFP11, respectively. To construct pMM186 and 189, we first amplified the GFP1-10 and GFP11 genes from pSFL9 and pSFL11 (Kakimoto et al., 2018) using the primers YU944/945 and YU946/947, digested the product using NotI/XbaI, and ligated them into the NotI/XbaI sites of pMM77 and 76 (Kakimoto et al., 2018), resulting in pMM86 and pMM83, respectively. Next, we amplified the ERj1N-V5-GFP1-10 and Tom70N-FLAG-GFP11 genes from pMM86 and pMM83 by PCR using primer pairs YU1365/1481 and YU1414/1367, respectively. The DNA fragment encoding ERj1N-V5-GFP1-10 was cloned into an EcoRI/BamHI-cut pTETone vector (Takara Bio USA, Inc.) using the In-Fusion® HD Cloning Kit, resulting in pMM186. The DNA fragment encoding Tom70N-FLAG-GFP11 was digested with NheI/BamHI and ligated into the NheI/BamHI-cut pIRESNeo3 vector (Takara Bio USA, Inc.), resulting in pMM189.

To express mCherry-Vps39, we first prepared yeast expression vectors with the *ADH1* promoter and the *CYC1* terminator in *CEN*-plasmids, pRS316, resulting in pYU60. Then, we cloned the mCherry gene amplified by PCR using a pair of primer YU311/312 to the NotI/SpeI site of pYU60, resulting in pYU99. Finally, we cloned the *VPS39* gene amplified by PCR using a pair of primer YU2825/2827 to the BamHI/SalI site of pYU99, resulting in pFL92.

To express Su9-tagBFP protein in HeLa cells, we constructed pMM243 as follows. First, we amplified the tagBFP gene by PCR using pJW1513 (Williams et al., 2014) as the template and a pair of primers YU1724/1725, digested with NotI/XbaI, and then ligated to NotI-XbaI-digested pMM76 (Kakimoto et al., 2018), resulting in pMM220. We amplified the DNA fragment encoding the Su9 presequence by PCR using a pair of primers YU1773/1774, digested with BamHI/NotI and ligated to the BamHI/NotI site of pMM220 to replace the gene encoding N-terminal 70 amino acids of Tom70 and 3xFLAG tag to the gene encoding Su9. pJW1513 was a gift from Jonathan Weissman (Addgene plasmid # 62383[1]; RRID:Addgene_62383).

[1]http://n2t.net/addgene:62383

TABLE 1 | Plasmids used in this study.

Name1	Name2	Source
pFL8	pRS316-Su9-RFP	Kakimoto et al., 2018
pFL17	pRS316-BipN-mCherry-HDEL	Kakimoto et al., 2018
pFL92	pRS316-mCherry-Vps39	This study
pSFL9	pRS316-GPDp-GFP(1–10)	Kakimoto et al., 2018
pSFL11	pRS316-GPDp-GFP(11)	Kakimoto et al., 2018
pSFL16	pRS316-GPDp-Ifa38-GFP(1–10)	Kakimoto et al., 2018
pSFL22	pRS316-GPDp-Tom71-GFP(1–10)	Kakimoto et al., 2018
pSFL26	pRS316-GPDp-Pex3N-GFP(1–10)	Kakimoto et al., 2018
pSFL28	pRS316-GPDp-Erg6-GFP(1–10)	Kakimoto et al., 2018
pSFL71	pRS314-GPDp-Tom70N-3xFLAG-GFP(11)	Kakimoto et al., 2018
pSFL100	pRS316-GPDp-Dpp1-GFP(1-10)	Kakimoto et al., 2018
pYC135	pBS-GPDp-Ifa38-V5-GFP(11)-CyC1ter-natNT2	This study
pYC136	pBS-GPDp-Erg6-V5-GFP(11)-CyC2ter-natNT2	This study
pYC137	pBS-GPDp-Dpp1-V5-GFP(11)-CyC1ter-natNT2	This study
pYC141	pBS-GPDp-Ifa38-GFP(1–10)-CyC1ter-hphMX	This study
pYC143	pBS-GPDp-Tom71-GFP(1–10)-CyC1ter-hphMX	This study
pYC144	pBS-GPDp-Pex3N-GFP(1–10)-CyC1ter-hphMX	This study
pMM76	pCDNA3.1-Tom70(1–70)-3xFLAG-eGFP	Kakimoto et al., 2018
pMM77	pCDNA3.1-ERj1N(1–200)-V5-eGFP	Kakimoto et al., 2018
pMM78	pcDNA3.1-N-eGFP-V5-Cb5C	This study
pMM83	pCDNA3.1-Tom70(1–70)-3xFLAG-GFP(11)	This study
pMM86	pCDNA3.1-ERj1N(1–200)-V5-GFP(1–10)	This study
pMM186	pTETOne-ERj1N(1–200)-V5-GFP1-10	This study
pMM189	pIRESNeo3-Tom70(1–70)-3xFLAG-GFP11	This study
pMM220	pCDNA3.1-Tom70(1–70)-3xFLAG-tagBFP	This study
pMM243	pcDNA3.1-Su9-tagBFP	This study
pMM350	pcDNA3.1-mCherry-Cb5C	This study
pYU21	pBS-kanMX4	Kojima et al., 2019
pYU36	pFA6a-mCherry-kanMX6	Kakimoto et al., 2018
pYU60	pRS316-ADH1p-MCS-CYC1ter	This study
pYU99	pRS316-ADH1p-mCherry-MCS-CYC1ter	This study
pYU101	pFA6a-mScarlet-KanMX4	Kakimoto et al., 2018
pJW1513	pRS316-pTDH3-Su9-TagBFP	Williams et al., 2014

To express mCherry-Cb5C comprising of mCherry and C-terminal 104–134 residues of cytochrome b5 in HeLa cells, we constructed pMM350 as follows. First, we purchased pMM78, pcDNA3.1-N-eGFP vector in which the tandem genes encoding V5 tag and residues 104–134 of cytochrome b5, were cloned at the BamHI/NotI site from eurofin genomics. We then amplified the gene encoding mCherry by PCR using pMM27 (Kakimoto et al., 2018) as template and a pair of primers YU2500/2501, digested with NheI/BamHI and ligated to the NheI/BamHI-digested pMM78 to replace eGFP to mCherry.

Yeast Strains and Growth Media

A haploid SEY6210 strain (*MATα leu2-3,112 ura3-52 his3-Δ200 trp1-Δ901 suc2-Δ9 lys2-801; GAL*) was used in this study. To chromosomally express the split-GFP proteins in yeast, we transformed the wild-type yeast cells with DNA fragments amplified from pYC135, pYC136, pYC137, pYC141, pYC143, or pYC144 by PCR using the primer pairs YU1506/1507 or YU1510/1511. The genes for GFP1-10 and GFP11 were integrated into the *LEU2* and *URA3* loci, respectively. The transformants were selected on the yeast extract-peptone-dextrose (YPD) medium containing 200 μg/ml hygromycin B or 200 μg/ml clonNAT. The integration of the DNA cassettes into the correct sites was confirmed by PCR using the genomic DNA as template and the primer pairs YU1512/1513 for the *LEU2* locus and YU1514/1515 for the *URA3* locus. For the expression of the split-GFP probes from plasmids, yeast cells were cultivated on SCD-Trp-Ura (0.67% yeast nitrogen base without amino acids, 0.5% casamino acids, 2% glucose, 20 μg/ml each of adenine, L-histidine, and L-methionine, and 30 μg/ml each of L-leucine and L-lysine). For the expression of the split-GFP probes from chromosomes, yeast cells were cultivated in the SCD complete medium (0.67% yeast nitrogen base without amino acids, 0.5% casamino acids, 2% glucose, 20 μg/ml each of adenine, L-histidine, L-methionine, L-tryptophan, and uracil, and 30 μg/ml each of L-leucine and L-lysine). For starvation conditions, SD-N or S-NC medium, which omits ammonium sulfate or both ammonium sulfate and glucose from the SCD complete medium were used. To introduce mScarlet or mCherry-tag at C-terminus of Mmm1, Nvj1 and Sei1, we amplified DNA

TABLE 2 | Oligo DNAs used in this study.

Name1	Sequence
YU311	AATTGCGGCCGCATGGTGAGCAAGGGCGAGGAGG
YU312	CCCACTAGTCTTGTACAGCTCGTCCATGCCGCC
YU499	CGCCTCGACATCATCTGCCCGGCCGCAAATTAAAGCCTTC
YU500	GAAGGCTTTAATTTGCGGCCGAGCTCGATTACAACAGGTG
YU501	GAAGGCTTTAATTTGCGGCCGGGCAGATGATGTCGAGGCG
YU502	TAGAACTAGTGGATCCCGGGTTAATTAAGGCGCGC
YU503	TAGAACTAGTGGATCCAGTCTTGACGTGCGCAGCT
YU944	CATGCGGCCGCCGGTGGCACTAGTATGAGCAAAGG
YU945	CCCTCTAGATTACTTTTCGTTGGGATCTTTCG
YU946	CATGCGGCCGCCCGATGGAGGGTCTGGTGGCG
YU947	CCCTCTAGATTATGTAATCCCAGCAGCATTT
YU1365	CCCTCGTAAAGAATTCATGACTGCTCCGTGCTCTC
YU1367	GCAGAGATCTGGATCCTTATGTAATCCCAGCAGCA
YU1390	NNNGCTAGCGCCACCATGGGTGGCACTAG
YU1403	TAGATGCACAAGTGAACACTGAACAAGCATACTCTCAACCATTTAGATACCGGATCCCCGGGTTAATTAA
YU1404	CACCTCGTTGTAAGTGACGATGATAACCGAGATGACGGAAATATAGTACAGAATTCGAGCTCGTTTAAAC
YU1414	CTGCGGCCTAGCTAGCGCCACCATGGCCGCGTCCA
YU1481	GCAGAGATCTGGATCCTTACTTTTCGTTGGGATCT
YU1499	TTTGAAAGCGCCATAAGTGCGCGTGTTTGTGCCTTCTGATATGATATCGTGTTGTAAAACGACGGCCAGT
YU1500	CAATTACACTTTTTTTTTTAGATTGTTCGGTACTTAGTCAAGTTTTATTTCACAGGAAACAGCTATGACC
YU1506	CGCCGGAACCGGCTTTTCATATAGAATAGAGAAGCGTTCATGACTAAATGGTTGTAAAACGACGGCCAGT
YU1507	GAGCCATTAGTATCAATTTGCTTACCTGTATTCCTTTACATCCTCCTTTTCACAGGAAACAGCTATGACC
YU1510	TTTTGATTCGGTAATCTCCGAGCAGAAGGAAGAACGAAGGAAGGAGCACAGTTGTAAAACGACGGCCAGT
YU1511	AATTTTTTTTTTTTCGTCATTATAGAAATCATTACGACCGAGATTCCCGGCACAGGAAACAGCTATGACC
YU1512	AATTTCAGAGGTCGCCTGAC
YU1513	TCATGATTTTCTGTTACACC
YU1514	TGGTTTCAGGGTCCATAAAG
YU1515	TACTGTTACTTGGTTCTGGC
YU1724	NNNGCGGCCGCATGAGCGAGCTGATTAAGGAGAACATG
YU1725	NNNTCTAGATTAATTAAGCTTGTGCCCCAGTTTGCTAG
YU1773	NNNGGATCCATGGCCTCAACTCGCGTTCTTG
YU1774	NNNGCGGCCGCcGCTACTGTAGGCTCTCTTCTGGAAGG
YU2055	GTATGTGGCCACGTAGTAAAAATACGAGAGAAGAAAAGCCTACAGAGTTACGGATCCCCGGGTTAATTAA
YU2056	AGGCAGAGAAGATAGGAAAAAGATAGAACAAAAAATTTGTACATAAATATGAATTCGAGCTCGTTTAAAC
YU2500	NNNGCTAGCATGGTGAGCAAGGGCGAGGAG
YU2501	NNNGGATCCCTTGTACAGCTCGTCCATGCCGC
YU2825	NNNGGATCCATGTTAAGAGCTCAAAAGCTACACT
YU2827	NNNgtcgacTTACTTATTATTTAGCTCATTTATA
YU2933	AAAATGTGAATCCAAGGTTTCAAGAAAATAAGATAAAGTGAATAGGAAGGGTTGTAAAACGACGGCCAGT
YU2934	AGAAAATAACAGCTAGGTTTTAAAATTATATAGCGAGAAGTACAATTCTACACAGGAAACAGCTATGACC
YU2938	CTTCATCAGCAACTGTAGGAGGAGAAAGCAGGTATATAACTAGCCGCAATGTTGTAAAACGACGGCCAGT
YU2939	CATATTTCTATCATTCACTTGTTAGTGCATGAGAAGAAGTAATTGCAATACACAGGAAACAGCTATGACC
YU3018	ATCCTATGTAACGGTTGAAACAGATCATAAGCTGGCTTCAACTAATCCAAGTTGTAAAACGACGGCCAGT
YU3019	AAATGTTTGTTTTTTTATGTAGACACTATTTTCAAACTATCTTTGTTAAACACAGGAAACAGCTATGACC
YU3020	AAATGTTTGTTTTTTTATGTAGACACTATTTTCAAACTATCTTTGTTAAACACAGGAAACAGCTATGACC
YU3021	ATCGGAGAGTATGTATTTGTGTAGTTATGTACTTAGATATGTAACTTAATCACAGGAAACAGCTATGACC

fragments by PCR using pYU36 or pYU101 as the template and primer pairs YU2055/2056, YU1403/1404, YU2931/2932, respectively, and then introduced them into yeast cells expressing the split-GFP proteins. Similarly, to introduce the *mdm12*Δ, *mdm34*Δ, *sei1*Δ, *ldb16*Δ, and *mdm1*Δ mutations, we amplified the DNA cassettes harboring the *kanMX4* flanked by 50 bp of homologous sequences to the up- and down-stream of the *MDM12*, *MDM34*, *SEI1*, *LDB16*, and *MDM1* genes, respectively by PCR using pYU21 as the template DNA and primer pairs YU3018/3019, YU3020/3021, YU2933/2934, YU2938/2939, YU1499/1500, respectively, and introduced them into yeast cells expressing the split-GFP proteins.

Cell Culture and Transfection

HeLa cells were maintained at 37°C in the Dulbecco's Modified Eagle Medium (DMEM) with 10% FBS and antibiotics (100 U/ml penicillin and 100 μg/ml streptomycin). DNA transfection was performed using Lipofectamine 2000 (Invitrogen) according to the manufacturer's instructions. Briefly, 24 h before transfection, HeLa cells were seeded in 35-mm glass-bottom dishes (Iwaki) with a seeding density of 1.5×10^5 cells in 2 ml DMEM with 10% FBS and incubated at 37°C under 5% CO_2. Then, the HeLa cells were co-transfected with two plasmids for the expression of the GFP1-10 and the GFP11 fusion proteins (1.25 μg each/35-mm dish) and further incubated for 24 h for the microscopic analysis.

HeLa cells capable of stably expressing Tom70N-FLAG-GFP11 or expressing ERj1N-V5-GFP1-10 by induction were constructed as follows. First, the HeLa cells were transfected with pMM189 (pIRESNeo3/Tom70N-FLAG-GFP11) and selected with 500 μg/ml of G418. The resulting HeLa cells were further transfected with pMM186 (pTETone/ERj1N-V5-GFP1-10) and selected with 300 μg/ml of hygromycin.

Western Blotting

Whole cells extracts were prepared from logarithmically growing yeast cells as reported previously (Kushnirov, 2000). Proteins were separate by SDS-PAGE and were transferred to PVDF membranes (Immobilon-FL Millipore). After blocking with 1% skim milk in TBS-T buffer (10 mM Tris–HCl pH 7.5, 150 mM NaCl, and 0.05% Tween 20), the membranes were incubated with primary antibodies against V5, GFP, Tim23, Tom40, or Tom70 for 2 h at room temperature or for overnight at 4°C. After washing with TBS-T buffer three times and specific proteins were detected by Cy5-conjugated secondary antibodies, goat anti-rabbit or mouse IgG (H+L) (Thermo Fisher Scientific) and analyzed with Typhoon imager (GE Healthcare).

FACS Analysis

For FACS analysis using yeast cells, we used Cell Sorter SH800 (Sony). Briefly, logarithmically growing yeast cells were first evaluated by scattered light channels to obtain yeast cells of roughly similar cell size. After removal of dead cells showing high fluorescence of propidium iodide, cells were separated with FITC channel (488-nm laser, 525/50-nm band-pass filter). For each analysis, total 100,000 cells were analyzed at 2,000 cells per second.

Fluorescence Microscopy

We used an Olympus IX83 microscope with a CSU-X1 confocal unit (Yokogawa), 100×, 1.4 NA and 20×, 0.75 NA objectives (UplanSApo, Olympus), and an EM-CCD camera (Evolve 512; Photometrics) and an cMOS camera (Zyla-4, ANDOR) manipulated by Metamorph software (Molecular Devices). GFP or RFP/mCherry/Mitotracker were excited by 488-nm or 561-nm lasers (OBIS, Coherent), and the emissions were made to pass through a 520/35-nm or 617/73-nm band-pass filter, respectively. The confocal fluorescent sections were collected every 0.2 or 0.4 μm of the yeast cells or HeLa cells, respectively. We used the ImageJ software to generate maximum projection images from the obtained confocal images. For the MitoTracker staining, HeLa cells were incubated with 100 ng/ml of the MitoTracker Red CMXRos (Thermo Fisher Scientific) in an Opti-MEM for 30 min at 37°C in 5% CO_2. Cells were washed twice using DMEM with 10% FBS and subjected to a microscopic observation.

For immunofluorescence microscopy, 48 h before microscopic observation, HeLa cells were seeded in 35 mm glass-bottom dish (Iwaki, D141410) with a seeding density of 8×10^4 in 0.2 ml DMEM supplemented with 10% FBS and incubated. Then, the medium was exchanged to DMEM supplemented with 10% FBS and doxycycline for the expressions of GFP1-10 fusion protein and further incubated for 4, 6, or 8 h before the fixation. The HeLa cells were fixed with pre-warmed 4% PFA in phosphate buffer for 12 min at room temperature and washed three times with PBS. The cells were permeabilized with 0.5% Triton X100 in PBS for 12 min and washed three times with PBS. After blocking with 3% BSA containing PBS for 1 h, the cells were incubated with 1 μg/ml anti-Tom20 antibodies (SantaCruz, sc-11415) in blocking buffer for 15 h at 4°C. Cells were washed three times with PBS and incubated with 2 μg/ml Goat Anti-Rabbit IgG H&L (Alexa Fluor® 594), (abcam, ab150080) in blocking buffer for 1 h at RT. The HeLa cells were washed with PBS three times and observed under Olympus IX83 microscope with a CSU-X1 confocal unit (Yokogawa), a 100×, 1.4 NA, objective (UplanSApo, Olympus) and an cMOS camera (ZYLA-4, ANDOR).

To observe organelle-contact sites in yeast, yeast cells expressing the split-GFP probes from plasmid DNAs or the genomic DNA, were cultivated in SCD-Trp-Ura or SCD complete medium, respectively, to logarithmic phase. The yeast cells were collected by centrifugation (2,000 *g* for 5 s) at room temperature and immediately observed under the fluorescence microscope.

For live-cell imaging, HeLa cells expressing split GFP were stimulated by 300 ng/ml doxycycline 8 h before imaging. Mitochondria were stained with 25 nM MitoTracker Red CMXRos 30 min before imaging. The images of HeLa cells cultured at 37°C in 5% CO_2 were captured at a rate of one frame per 4s by BZ-X800 (Keyence, Japan), a 100×, 1.45 NA, objective (Nikon, Japan). GFP and Mitotracker were excited by 495-nm and 565-nm light and the emission was passed through 525/50-nm or 605/70-nm band-pass filter, respectively. Obtained images were analyzed with ImageJ or BZ-X800 Analyzer (Keyence, Japan) software.

RESULTS

The Overexpressed Split-GFP Probes Induce Artificial Organelle Interactions

It has been shown that the ER-mitochondria-contact sites in yeast cells can be observed as small discrete foci under a fluorescent microscope when a subunit of the ERMES complex is expressed as a fusion protein with a fluorescent protein like GFP (Kornmann et al., 2009). For example, when we expressed Mmm1, which is an ER-resident subunit of the ERMES complex, as a GFP-fusion protein, we could observe the "ERMES dots" that represented the ER-mitochondria-contact sites (**Figure 1A**). We previously assessed the usability of the split-GFP proteins

as a fluorescent probe that visualized the organelle-contact sites by using the ERMES dots as references. The split-GFP proteins expressed on the ER and the mitochondrial outer membrane (MOM) mostly showed dot-like signals like the ERMES dots (**Figure 1B, a**), indicating that the split-GFP proteins worked as a fluorescent probe for the ER-mitochondria-contact sites (**Figure 1C**). However, we also noticed that the reconstituted split-GFP proteins resulted in some large foci or elongated tubular signals, which were never observed for the ERMES dots, albeit only a minor portion of the total (∼10% of the total signals) (**Figure 1B, b**). These observations indicate that the split-GFP probes have a disadvantage of inducing artificial organelle-organelle interactions, which in turn affects the organelle morphologies and functions (**Figure 1D**). Additionally, the GFP signals varied widely among different cells, probably due to the fluctuation of the expression levels of the split-GFP probes, which also makes it difficult to precisely quantify the organelle-organelle interactions.

We previously confirmed that the split-GFP proteins could also visualize the ER-mitochondria-contact sites in human cultured cells. Similar to the ERMES dots, the split-GFP proteins expressed on the ER and the MOM in HeLa cells resulted in punctate signals on the mitochondria (**Figure 1E**; Kakimoto et al., 2018). This observation indicates that the organelle-targeted split-GFP proteins work as a probe that allows for the visualization of the organelle-contact sites not only in yeasts but also in human cultured cells. However, the overexpressed split-GFP proteins drastically altered the tubular shape of the mitochondria and the ER. We transiently expressed mCherry-Cb5C and Su9-BFP, which were ER and mitochondria marker proteins, respectively, and the split-GFP probes on the ER and MOM at the same time to monitor the organelle morphologies together with their contact sites. We noticed that the overexpressed split-GFP probes deformed both the ER and mitochondria from tubular to vesicular structures, which were hardly seen in normal cells. Besides, we noticed that the vesiculated ball-like mitochondria were completely enclosed by the highly curved ER membranes (**Figure 1F**). This clearly indicates that the split-GFP proteins affect the structure and function of organelles by inducing organelle-organelle interactions.

PCR Template Plasmids for the Expression of Split-GFP Probes From the Chromosomal DNA

A possible way to overcome the disadvantage of the existing method and for a more precise quantification of the interactions between different organelles using the split-GFP probes in yeast is to modulate the expression levels of the split-GFP probes as well as to lessen their variation among yeast cells. For these purposes, we decided to express the split-GFP probes from the chromosome instead of expression from a plasmid. First, we constructed various gene cassettes that tandemly combined the gene that expressed the split-GFP probe and the drug-resistant gene *hphMX* or *natMX* into the pBlueScript vector (**Figures 2A,B**). Then, we amplified the gene cassettes from the plasmids by PCR using appropriate primer pairs, as shown in **Figure 2** and **Table 1**. Finally, the purified DNA cassette was transformed into yeast cells by a regular lithium acetate method (Gietz and Schiestl, 2007). In this study, we integrated the GFP1-10 and GFP11 fusion genes into the *URA3* and *LEU2* genes, respectively, which are commonly used as auxotrophic marker genes in yeast (**Figure 2**).

Chromosomal Gene Integration Enables Low-Level Expression of the Split-GFP Probes in Yeast

We next tested whether integration of the split-GFP genes into the chromosome resulted in lower expression levels of the split-GFP probes and/or smaller variations in their levels among yeast cells. To this end, we selected the following six organelle pairs: mitochondria-ER (**Figure 3A**), mitochondria-vacuole (**Figure 3B**), ER-lipid droplets (LDs) (**Figure 3C**), peroxisome-vacuole, (**Figure 3D**) peroxisome-ER (**Figure 3E**), and peroxisome-LDs (**Figure 3F**). We then compared the reconstituted GFP signals observed at the organelle-contact sites when the split-GFP probes were chromosomally expressed with those obtained when they were expressed from plasmids. As we reported previously, split-GFP probes expressed from plasmids resulted in clear GFP signals between all the organelle pairs tested, although the signal intensities varied widely among different cells, probably due to different expression levels (Kakimoto et al., 2018). Although these results suggest the existence of organelle-contact sites between these organelle pairs, the strong GFP signals probably indicate the artificially induced tethering between these organelles (**Figure 1D**).

We found that in contrast to the plasmid-expressed split-GFP probes, the chromosomally expressed split-GFP probes exhibited uniform and small punctate GFP signals which were similar to the ERMES dots, indicative of the authenticity of the organelle-contact sites. Quantification of the total GFP intensities normalized to the cell area clearly showed low variations in the GFP signals (**Figure 3G**). We further confirmed these results by fluorescence-activated cell sorting (FACS). As shown in **Figure 3H**, we could separate populations of yeast cells with or without the plasmid- or genome-based expression of split-GFP probes. Yeast cells expressing the split-GFP probes from the plasmids showed higher fluorescent signals (**Figure 3H, p**) than those expressing them from the genomic DNA (**Figure 3H, g**) and those without the expression (**Figure 3H, n**). Similar to the result of microscopy-based analyses, the plasmid-based expressions caused large variabilities in the GFP signals and resulted in two peaks that showed different GFP signals in some cases. On the other hand, the population of yeast cells expressing the split-GFP probes from the genomic DNA was detected as a single sharp peak, indicating the low variations in the GFP signals. With the plasmid-based method, it has been impossible to judge whether no or very weak GFP signals are simply due to the low expression levels of the split-GFP proteins or abnormal organelle contacts because the variations in the expression levels of the split-GFP proteins in each cell are large. The genome-based split-GFP system, however, made it possible to count all yeast cells for quantification because we can detect similar levels of

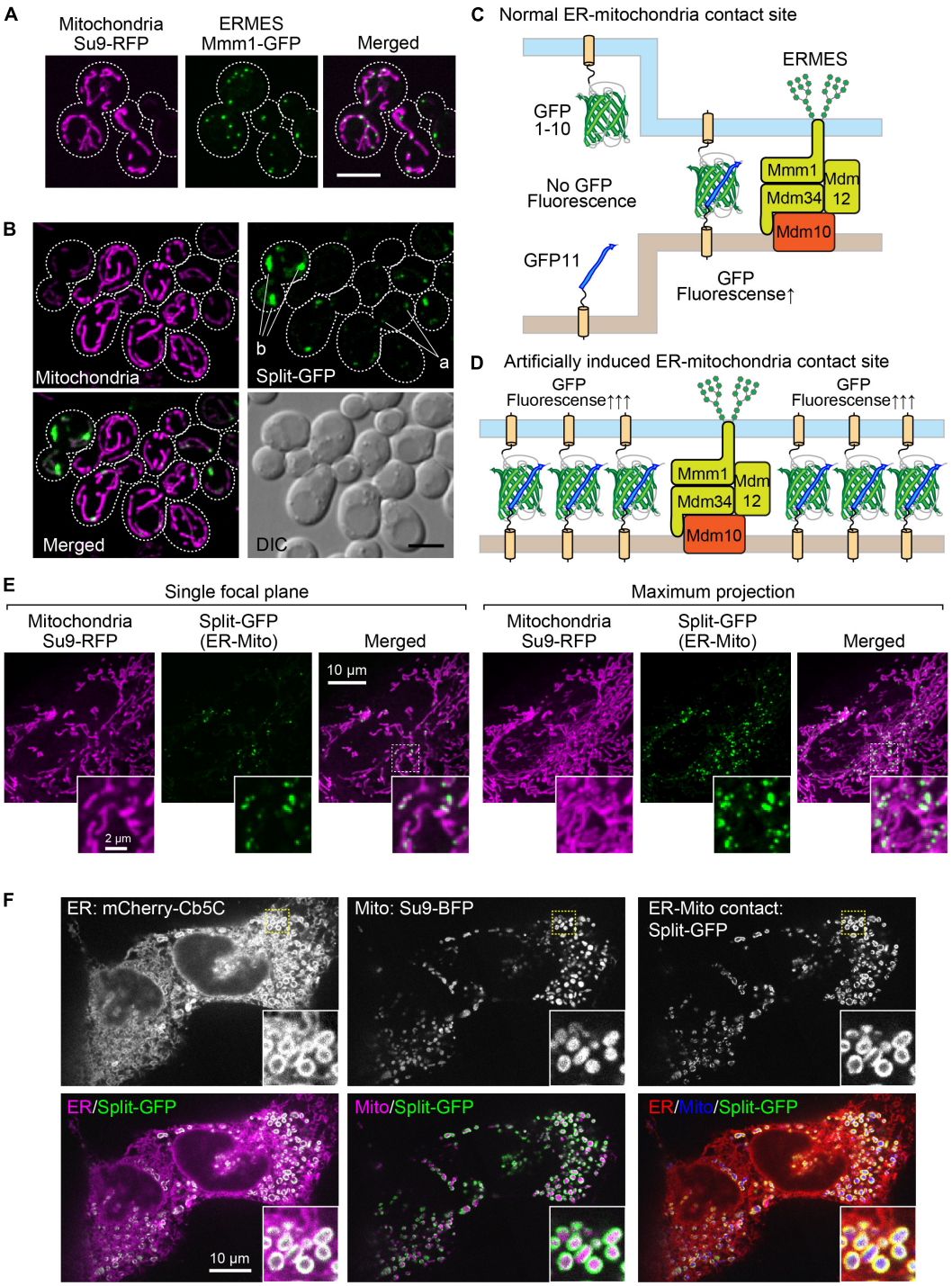

FIGURE 1 | The existing split-GFP systems for visualizing the ER-mitochondria contact sites in yeast and HeLa cells. **(A)** Yeast cells expressing Mmm1-GFP or **(B)** the split-GFP probes on the ER and MOM (Tom70N-GFP1-10 and Ifa38-V5-GFP11) and Su9-RFP were imaged by a confocal fluorescence microscope. Maximum projection images were shown. Scale bars represent 5 μm. "a" indicates GFP signals that resemble ERMES dots. "b" shows abnormal GFP signals that are much larger than ERMES dots. **(C)** Schematic diagrams of the ideal situation that the split-GFP probes work at the ER-mitochondria contact sites and **(D)** the artificial condition that overexpressed split-GFP probes induce undesired ER-mitochondria interactions. **(E)** HeLa cells transiently expressing Tom20N-FLAG-GFP1–10 and ERj1N-V5-GFP11 were stained with MitoTracker and imaged by a confocal fluorescence microscope. A single focal plane (left) and maximum projection image (right) were shown. **(F)** HeLa cells transiently expressing Tom70N-FLAG-GFP11, ERj1N-V5-GFP11, mCherry-Cb5C (ER marker), and Su9-BFP (Mitochondria marker), and were imaged by a confocal fluorescence microscope. A single focal plane was shown.

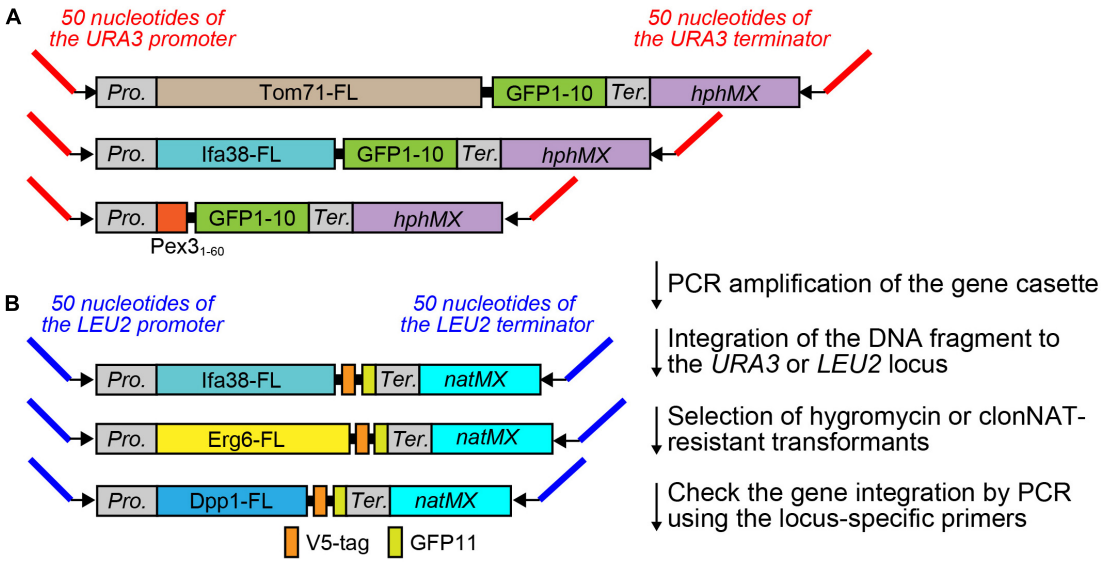

FIGURE 2 | PCR template modules for split-GFP gene integration. **(A)** PCR template modules for GFP1-10 and **(B)** GFP11-fusion genes were shown. Pro. And Ter. indicate the *GPD* promoter and *CYC1* terminator, respectively. FL means full length.

GFP signals with less variability in almost all yeast cells, making quantification of organelle-organelle contacts much easier.

We next tested if the expression levels of the split-GFP probes were indeed reduced in the present system as compared with those in the previous one. We performed immunoblotting using whole cell extracts prepared from yeast cells expressing the split-GFP probes such as Tom71-, Ifa38-, or Pex3N-GFP1-10 together with Ifa38-, Dpp1-, or Erg6-V5-GFP11 from the plasmids or genomic DNA. The results clearly showed that all the split proteins were expressed at lower levels when expressed from the genomic DNA (**Figure 4, g**) as compared those in the previous one (**Figure 4, p**). The overall expression levels were decreased to 30–50%. These results suggest that the genome-based split-GFP system in yeast is advantageous in terms of minimizing artificial organelle-contact sites, consequently improving the quantification of organelle-organelle interactions.

Validation of the Chromosomally Expressed Split-GFP Probes in Yeast Cells

We previously confirmed that the plasmid-based split-GFP system could visualize the ER-mitochondria contact sites using the ERMES complex labeled with RFP as a reference (Kakimoto et al., 2018). We thus examined if the genome-based system also properly worked as organelle contact site markers. For this purpose, we visualized the ER-mitochondria, nucleus-vacuole, mitochondria-vacuole, and ER-LDs contact sites by expressing red-fluorescent protein fused to known organelle tethering factors such as Mmm1, Nvj1, Vps39, and Sei1 (Pan et al., 2000; Kornmann et al., 2009; Elbaz-Alon et al., 2014; Hönscher et al., 2014; Grippa et al., 2015). Consistent with our previous study, the GFP signals arising from assembled Tom71-GFP1-10 and Ifa38-V5-GFP11 (MOM-ER), Ifa38-GFP1-10 and Dpp1-V5-GFP11 (ER-vacuole), Tom71-GFP1-10 and Dpp1-V5-GFP11 (MOM-vacuole), or Ifa38-GFP1-10 and Erg6-V5-GFP11 (ER-LDs) were well co-localized with Mmm1-mScarlet, Nvj1-mCherry, mCherry-Vps39, or Sei1-mCherry signals, which represent the ER-mitochondria, nuclear-vacuole, mitochondria-vacuole, or ER-LDs contact sites, respectively (**Figure 5**). Although Nvj1-mCherry exclusively stained the nuclear-vacuole contact sites (NVJ), the split-GFP signals arising from the ER-vacuole pair showed not only the NVJ signals but also granular GFP signals, which did not correspond to the NVJ regions. This is consistent with our previous observation and suggests the presence of contact sites between the peripheral ER and vacuole (Kakimoto et al., 2018).

Observations of Organelle Contact Sites in the Absence of the Known Organelle Tethering Factors

We next examined if the genome-based split-GFP system worked as quantitative indicators of dynamic changes in organelle contact sites. Firstly, we visualized the ER-mitochondria contact sites with Tom71-GFP1-10 and Ifa38-V5-GFP11 in the absence of Mdm34 and Mdm12, which are core subunits of the ERMES complex. To quantify the GFP signals that would reflect the ER-mitochondria contacts, we took advantage of FACS analysis. Intriguingly, we could detect *mdm34*Δ or *mdm12*Δ cells as a single peak that showed smaller GFP signals distinct from the one of wild-type cells (**Figure 6B**), suggesting that the formation of ER-mitochondrial contacts was impaired in the absence of Mdm34 or Mdm12. On the other hand, we noticed that the small populations of *mdm34*Δ and *mdm12*Δ cells exhibited stronger GFP signals than wild-type cells (**Figure 6B**). This suggests that the formation of ER-mitochondria contacts is restored or enhanced in a fraction

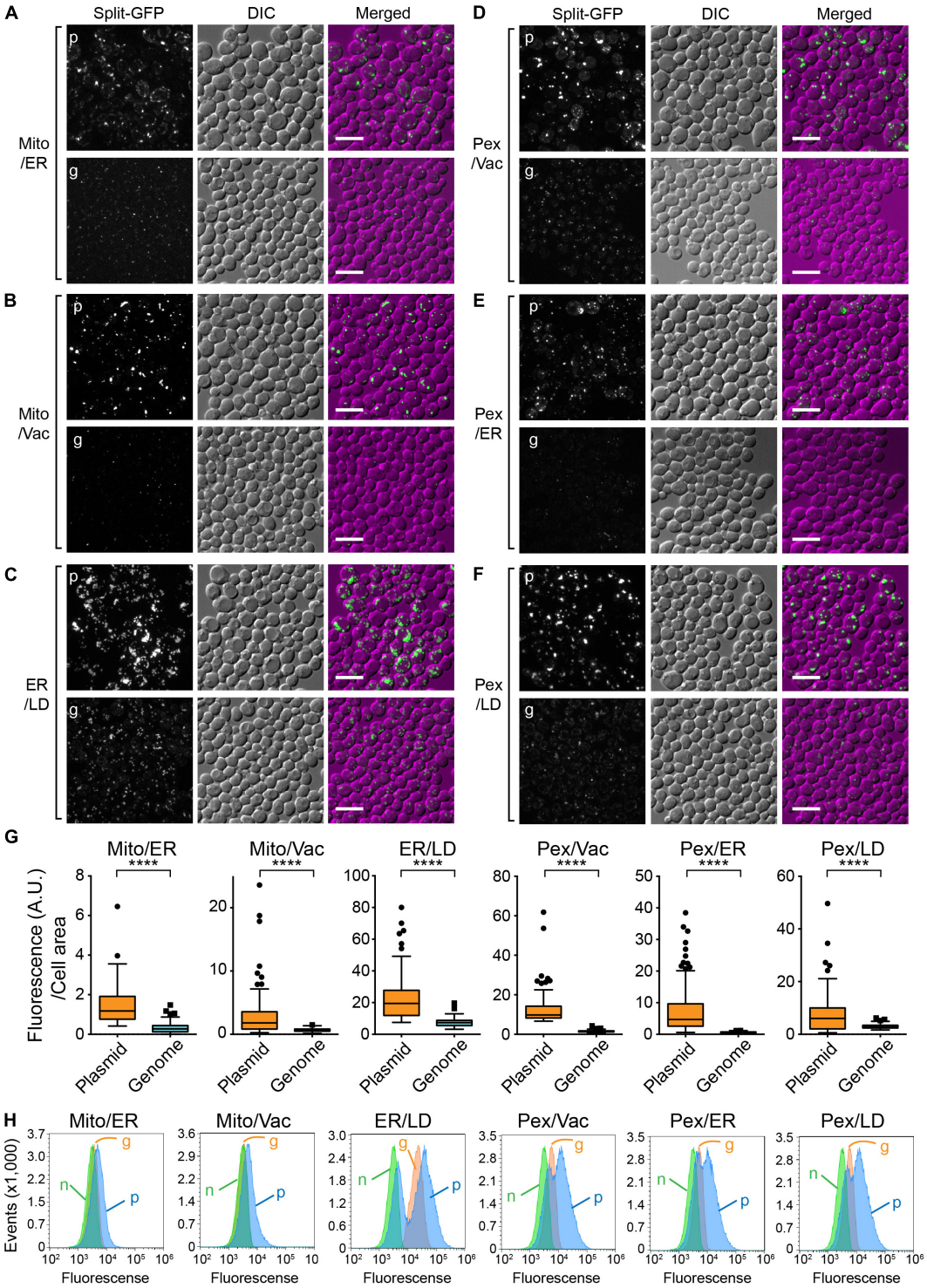

FIGURE 3 | Comparison between chromosomal and plasmid expressions of the split-GFP probes. Yeast cells expressing the split-GFP probes shown in **Figure 2** on **(A)** the MOM and the ER, **(B)** the MOM and vacuole, **(C)** the ER and LDs, **(D)** peroxisome and vacuole, **(E)** peroxisome and the ER, **(F)** peroxisome and LD were imaged by a fluorescence confocal microscope. Maximum projection images were shown. Scale bars represent 5 μm. p and g indicate the plasmid- and genome-based expressions of the split-GFP proteins, respectively. **(G)** Box and whisker plots showing the distribution of the fluorescence intensity of GFP signals normalized by the cell area. Over 100 cells were counted for each pair; ****$p < 0.0001$. **(H)** Logarithmically growing yeast cells expressing the split-GFP probes were subjected to FACS using GFP signal as an index. n, g, and p represent no expression, genome-, and plasmid-based expression of the split-GFP probes, respectively.

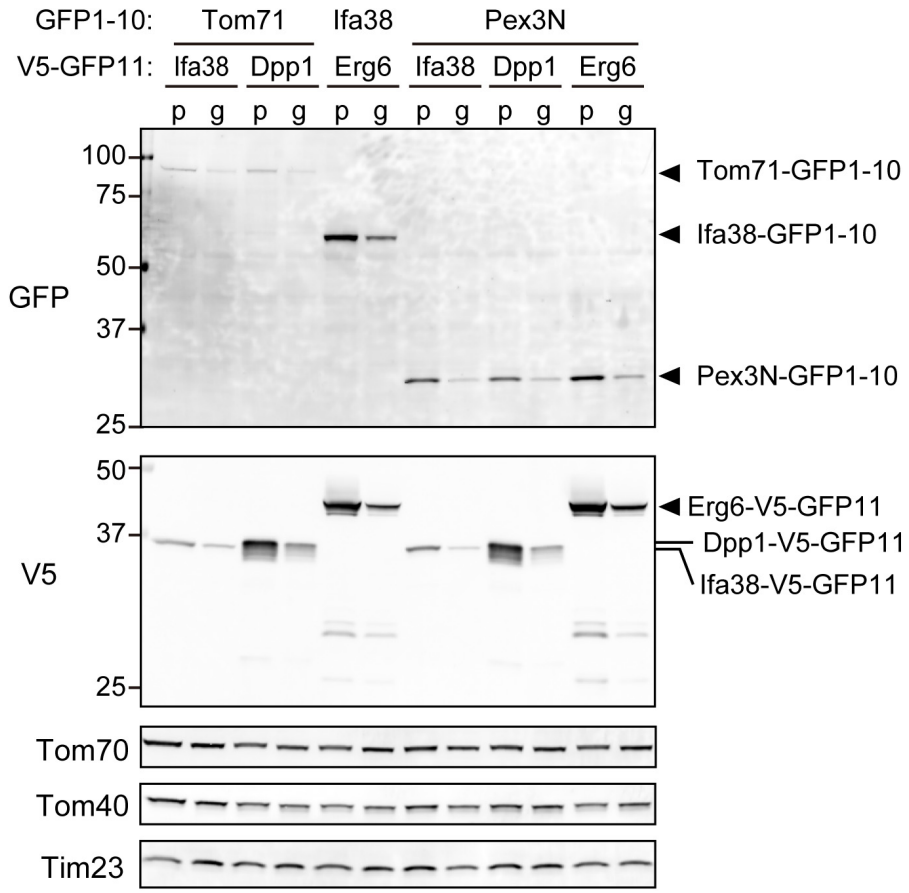

FIGURE 4 | The steady state levels of the split-GFP probes. Immunoblotting of total cell lysates prepared from yeast cells expressing the indicated split-GFP probes from the genomic DNA (g) or plasmid DNAs (p). Monoclonal anti-GFP and anti-V5 antibodies were used to detect the split-GFP proteins. Tom70, Tom40, and Tim23 were used as loading controls.

of *mdm34*Δ and *mdm12*Δ cells. Consistently, our microscopic analyses revealed that ∼10 or 20% of *mdm34*Δ or *mdm12*Δ cells showed large strong GFP signals whereas ∼40% of them exhibited no or small granular GFP signals (**Figures 6A,C**). These results suggest that although the ERMES complex is critical for the contact formation, alternative factors could compensate when the ERMES complex is inactive. The diminished GFP signals could be due to the decreases in the steady state levels of the split-GFP proteins (**Figure 6D**). However, we noticed that the decreased split-GFP protein levels did not necessarily diminish GFP signals. For example, when we observed the mitochondria-vacuole contact sites by expressing Tom71-GFP1-10 and Dpp1-V5-GFP11 from the genomic DNA in yeast cells lacking Vps39 or Ypt7, which are the vCLAMP components (Elbaz-Alon et al., 2014; Hönscher et al., 2014; González Montoro et al., 2018), we did not see decreases in the GFP signals and rather observed the slightly increased signals although the Dpp1-V5-GFP11 levels were decreased (**Figures 6E,F,H**). Our microscopic analyses showed that the number of GFP dots was increased in the absence of Vps39 or Ypt7 (**Figure 6G**). These results suggest that Vps39 and Ypt7 are not essential for the formation of mitochondria-vacuole contact sites.

Previous studies reported that NVJ regions expanded when yeast cells were subjected to starvation (Kvam and Goldfarb, 2006; Toulmay and Prinz, 2012; Hariri et al., 2018). Interestingly, despite the drastic decreases in the amounts of split-GFP proteins, Ifa38-GFP1-10 and Dpp1-V5-GFP11 under the nitrogen and carbon starvation conditions (**Figure 6K**), we observed clear increases in the GFP signals showing the ER-vacuole contact sites including NVJs (**Figures 6I,J**). These results indicate that the split-GFP system has the extra capacity to sense an increase in inter-organelle contacts even when the amount of split-GFP proteins is reduced.

To further validate the potency of this split-GFP system in quantifying organelle-organelle interactions, we visualized ER-LD contact sites by expressing Ifa38-GFP1-10 and Dpp1-V5-GFP11 in various mutant cells lacking Sei1, Ldb16, or Mdm1, which were reported to tether these two organelles (Wolinski et al., 2011; Grippa et al., 2015; Henne et al., 2015; Hariri et al., 2019). Strikingly, our FACS analyses showed that

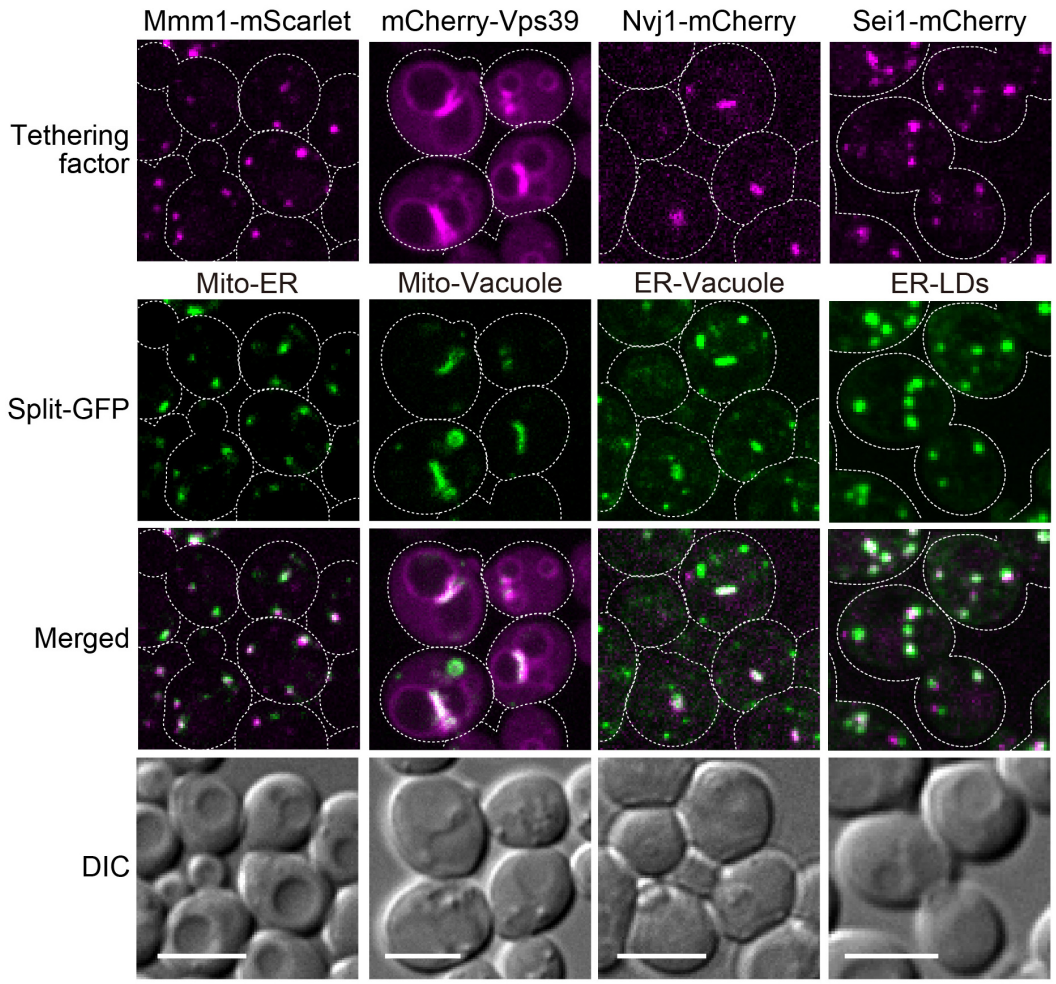

FIGURE 5 | Co-localizations of reconstituted split-GFP probes with ERMES, NVJ, vCLAMP, and ER-LD contact sites. Yeast cells expressing the split-GFP probes on mitochondria and the ER (Mito-ER), the MOM and vacuole (Mito-Vacuole), the ER and vacuole (ER-Vacuole), or the ER and LDs (ER-LDs) were imaged by a fluorescence confocal microscope. To visualize ERMES, NVJ and ER-LD contact sites, Mmm1-mScarlet, Nvj1-mCherry, and Sei1-mCherry were chromosomally expressed, respectively. mCherry-Vps39 was expressed under the *ADH1* promoter from a *CEN-URA3* plasmid to visualize vCLAMP regions. For MOM-ER, ER-vacuole, and ER-LD pairs, maximum projection images were shown. For the mitochondria-vacuole pair, a single focal plane was shown. Scale bars, 5 μm.

*sei1*Δ and *ldb16*Δ cells were sorted as distinct peaks that showed smaller GFP signals as compared with the one wild-type cells (**Figure 6M**). Consistent with the FACS results, we observed that the approximately 80% of *sei1*Δ and *ldb16*Δ cells showed the small and/or dim GFP signals while 90% of wild-type cells showed clear granular GFP signals that correspond to Sei1-mCherry (**Figures 5**, **6L,N**). On the other hand, *mdm1*Δ cells exhibited weaker GFP signals than that of wild-type cells (**Figure 6M**), although the GFP signal patterns looked quite similar to that of wild-type (**Figure 6N**), suggesting that Mdm1 plays a minor role in the ER-LD contact formation. We confirmed that the steady state levels of the split-GFP proteins were comparable among yeast cells tested here (**Figure 6O**). These observations consistently support the previous finding that the seipin complex Sei1/Ldb16 stabilizes ER-LD contact sites (Grippa et al., 2015). In summary, we conclude that the genome-base split-GFP system is useful tool to assess dynamic changes in the degree of organelle-organelle contacts.

The Inducible Split-GFP System in HeLa Cells

Previously, we transiently expressed the split-GFP probes on the ER and MOM to detect the ER-mitochondria-contact sites in HeLa cells (Kakimoto et al., 2018). However, in this transient method, it was difficult to control the expression levels of the split-GFP proteins (**Figures 1E,F**). We thus aimed to develop a more reliable split-GFP system in which the expression of the split-GFP probes could be controlled in HeLa cells. To achieve this, we utilized the Tet-One inducible expression system (Takara Bio USA, Inc.). In this system, we are able to induce the expression of a gene of interest, which is located downstream of the tetracycline-response element (TRE), by

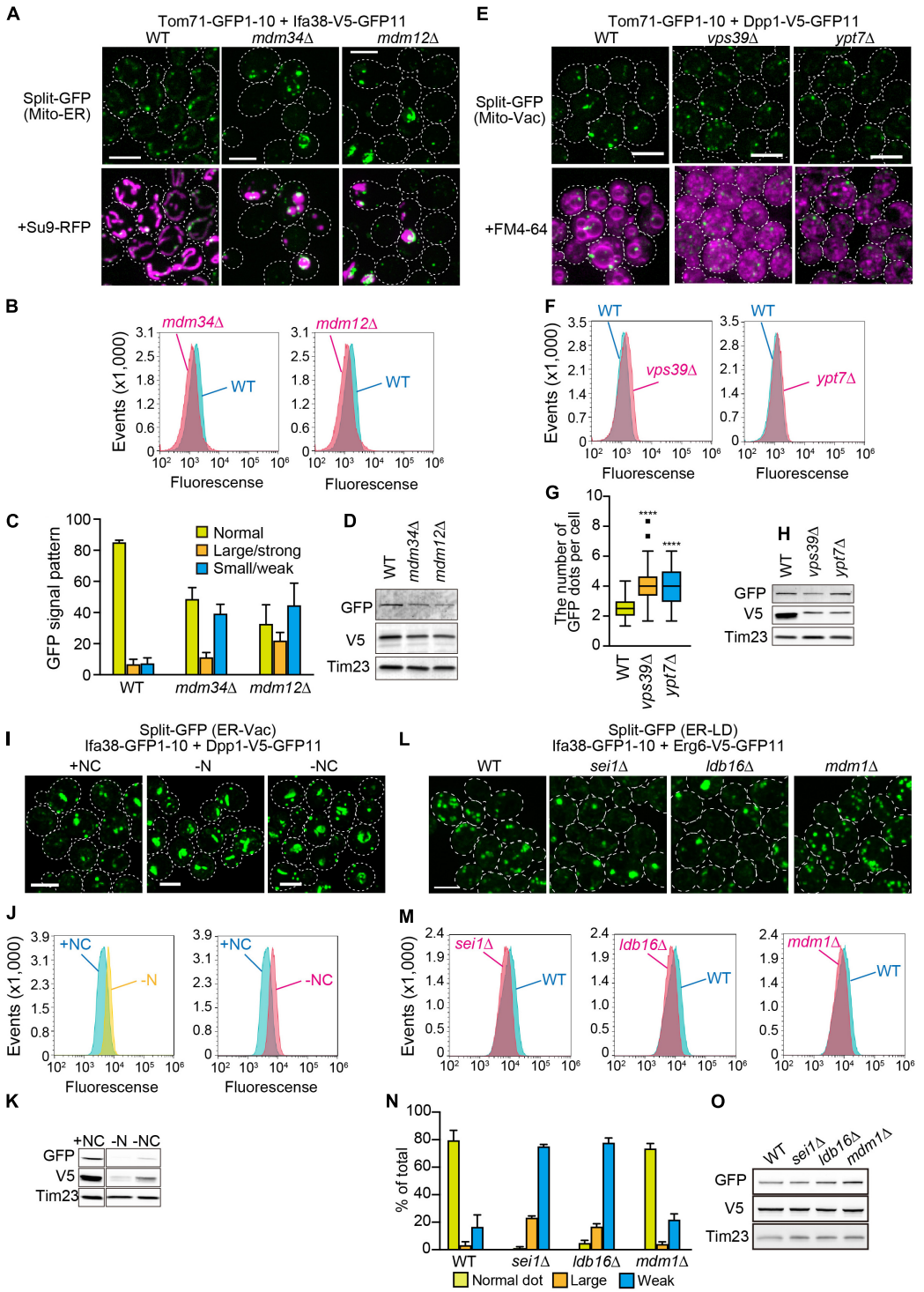

FIGURE 6 | Effects of the lack of known organelle-tethering factors on the organelle-organelle interactions. Logarithmically growing yeast cells expressing the split-GFP probes on **(A)** the ER and MOM (ER-Mito), **(E)** the MOM and vacuole (Mito-Vac), **(I)** the ER and vacuole (ER-Vac), or **(L)** the ER and LDs (ER-LD) were imaged by a fluorescence confocal microscope. To visualize mitochondria and the ER, we expressed Su9-RFP and BipN-mCherry-HDEL, respectively from plasmid DNAs. **(I)** For starvation experiments, yeast cells cultured in the SCD medium were further incubated in the SD-N or S-NC medium for 9 h, and then imaged. **(B,F,J,M)** Yeast cells were analyzed by FACS. **(C,N)** GFP signal patterns or **(G)** the number of GFP dots per cell were quantified. **(D,H,K,O)** Immunoblotting of whole cells extracts prepared from the indicated cells were performed. We detected the split-GFP proteins using anti-V5 and anti-GFP antibodies. Tim23 was used as a loading control. We performed three independent experiments for each condition. Error bars represent standard errors of three independent experiments. We counted total 223, 336, and 208 cells of wild-type, *mdm34*Δ, and *mdm12*Δ cells, respectively **(C)**, and total 217, 285, 259, or 389 cells of wild-type, *sei1*Δ, *ldb16*Δ, and *mdm1*Δ cells, respectively **(N)**. ****$p < 0.0001$. All images were maximum projections. Scale bars, 5 μm.

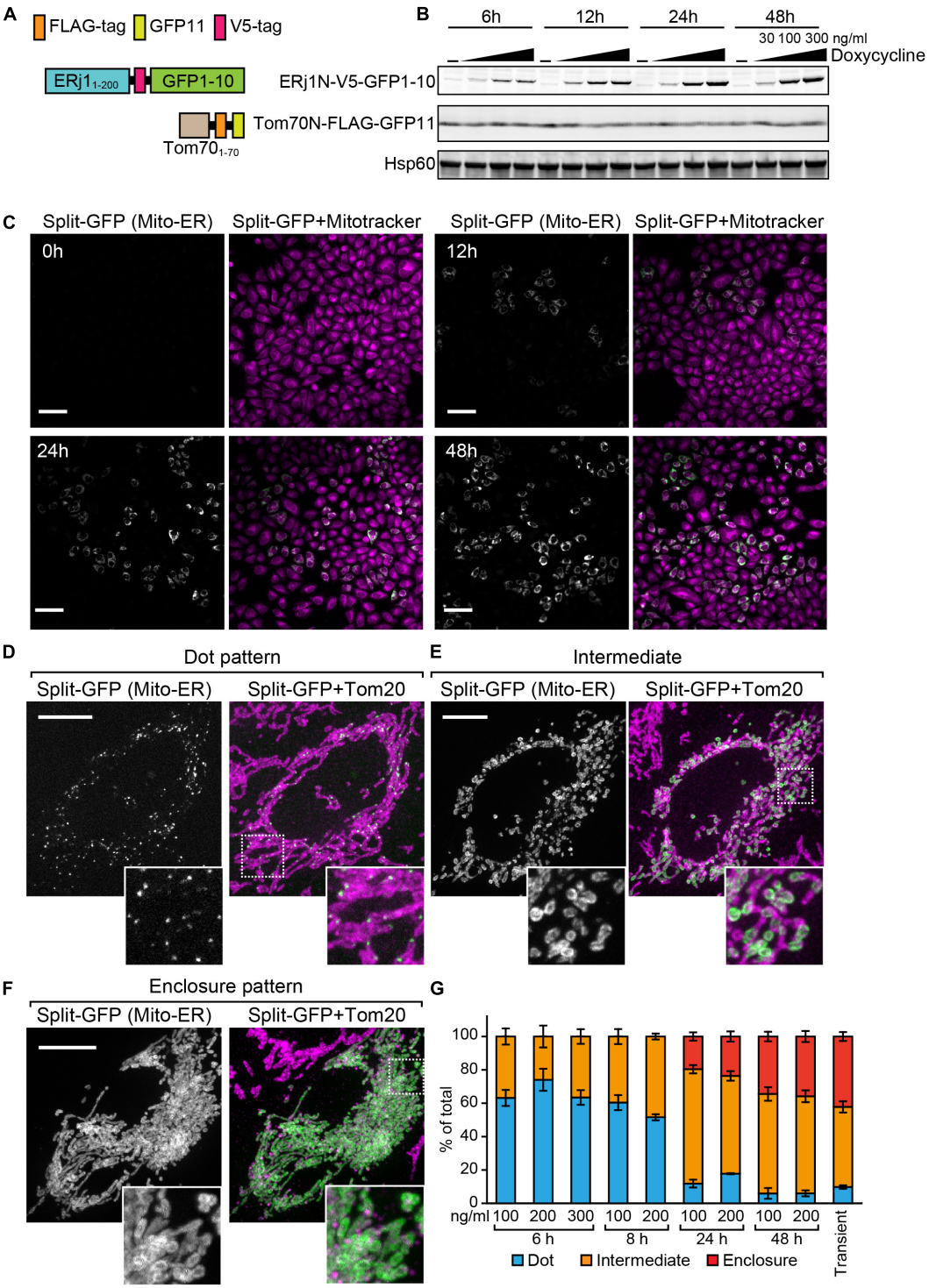

FIGURE 7 | Characterization of the HeLa cell line that enables inducible expression of the split-GFP probes in the presence of doxycycline. **(A)** Schematics of the split-GFP probes used in the HeLa cell line. **(B)** Western blotting of whole cell extracts prepared from the HeLa cells cultivated with different concentration (0, 30, 100, and 300 ng/ml) of doxycycline for the indicated time. Scale bars represent 100 μm. **(C)** The HeLa cells were imaged by fluorescence confocal microscopy 0, 12, 24, and 48 h after the addition of doxycycline. Mitochondria were stained with mitotracker. Scale bars, 10 μm. **(D,E)** Representative images of the HeLa cells after 6 h-induction of ERj1N-V5-GFP11 with 200 ng/ml doxycycline, or **(F)** transiently expressing the same probes were fixed and then imaged by a confocal fluorescence microscope. Mitochondria were stained by anti-Tom20 antibodies. Maximum projection images were shown. Scale bars represent 10 μm. **(G)** We performed 3 independent experiments and counted more than 60 cells showing GFP signals in total. Error bars represent standard errors (n = 3).

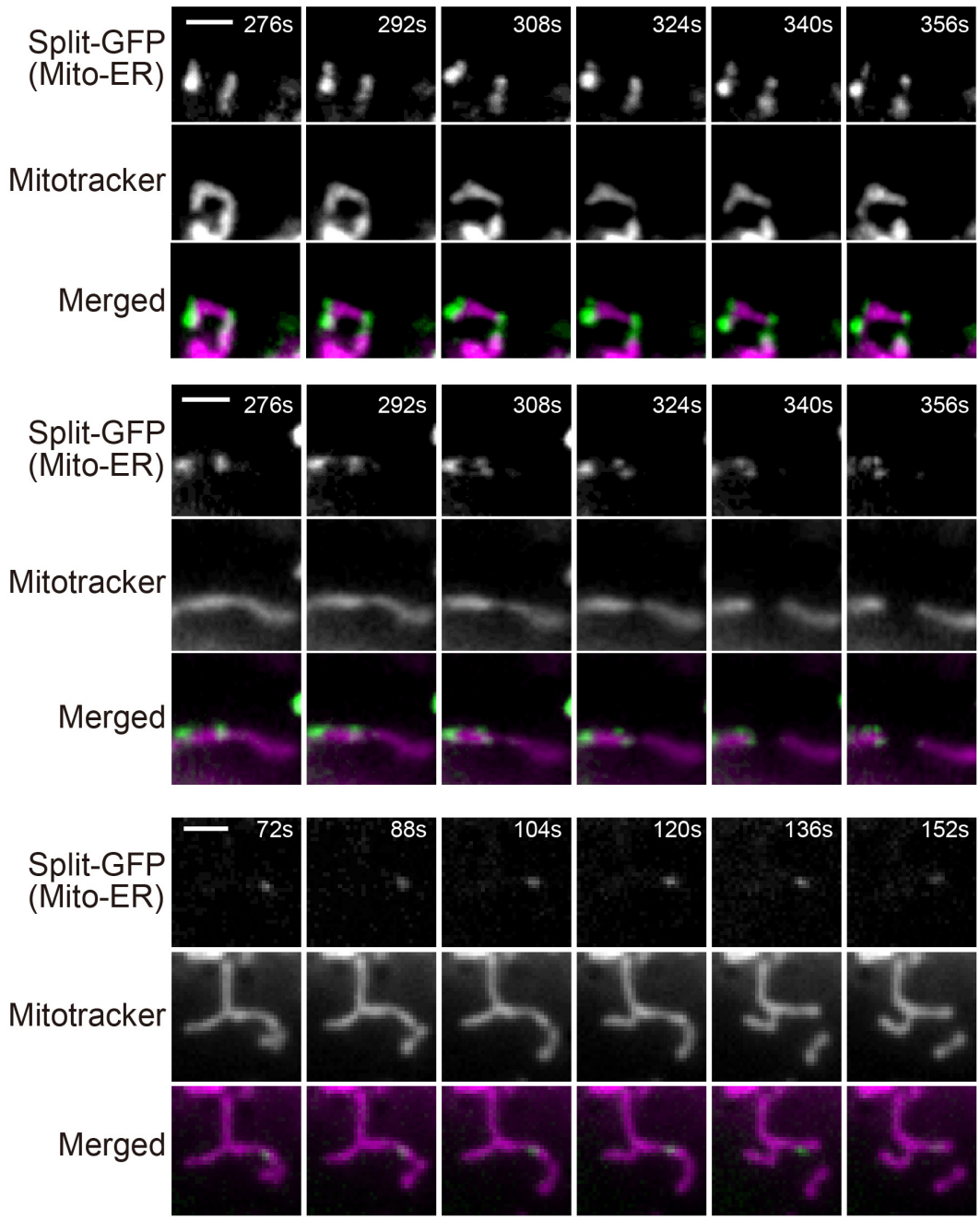

FIGURE 8 | Live-cell imaging of HeLa cells expressing the split-GFP probes on the ER and MOM. The HeLa cells were cultivated in the presence of 300 ng/ml doxycycline for 8 h and imaged by fluorescence microscopy. Mitochondria were stained with mitotracker. Three mitochondrial division events observed in **Supplementary Movies 1, 2**, were shown. Scale bars, 2 μm.

activating a transcription activator named rtTA with doxycycline (Gossen et al., 1995). First, we constructed a stable HeLa cell line expressing the MOM-targeted split-GFP protein Tom70N-FLAG-GFP11, comprising the first 70 N-terminal residues of Tomm70 followed by a 3xFLAG tag and GFP11 (**Figure 7A**). Subsequently, we cloned the gene encoding another split-GFP protein, ERj1N-V5-GFP1-10, which comprises the first 200 N-terminal residues of ERj1 followed by a V5 tag and GFP1-10, into the multi-cloning site downstream of the TRE of a pTet-One vector, which also expresses rtTA (**Figure 7A**). We then transfected the plasmid with a hygromycin marker into HeLa cells. To check the inducible expression of ERj1N-V5-GFP1-10, we prepared whole cell lysates from the resulting HeLa cells, which were cultured in the presence or absence

of different concentrations of doxycycline for different periods of time. Immunoblotting using the whole cell extracts showed that Tom70N-FLAG-GFP11 was stably expressed, while the expression of ERj1N-V5-GFP1-10 was induced by adding doxycycline. In particular, its expression was initially observed 6 h after the addition of doxycycline, and it was found that increased drug concentration or prolonged incubation time led to higher expression levels (**Figure 7B**). As the expression of the split-GFP protein was induced, we observed an increase in GFP signals (**Figure 7C**). These results indicated that we were able to control the expression levels of the split-GFP probes, which enabled us to minimize the undesired secondary effects caused by the excess reconstitution of the probes (**Figure 1F**). We further aimed to optimize the appropriate conditions required to observe small, dot-like GFP signals for the ER-mitochondria contact sites in HeLa cells. To this end, we tested various conditions with different concentrations of doxycycline and incubation time periods. Whereas the prolonged cultivation with doxycycline resulted in clear GFP signals (**Figure 7C**), relatively short-time induction (6 h) with 200 ng/ml doxycycline was the best condition to obtain dot-like GFP signals (**Figure 7D**). At the optimal condition, ∼70% of HeLa cells contained dot-like GFP signals (**Figure 7D**), while ∼30% of the cells showed ring-like GFP signals, which surrounded a part of mitochondria (**Figure 7E**, Intermediate pattern). The prolonged incubation led to an increase in the ratio of the HeLa cells showing the intermediate pattern as well as GFP signals that enclosed entire mitochondria (**Figure 7F**, Enclosure pattern). The previous transient expression system was comparable to the condition of the present inducible system with long cultivation (48 h) (**Figure 7G**). These results suggest that the present system offers a more accurate view of the ER-mitochondria contact sites as compared with the previous transient system.

Live Cell Imaging of HeLa Cells Expressing the Inducible Split-GFP Probes

Previous studies reported that ER tubules wrap around and constrict mitochondria to determine the sites of mitochondrial division (Friedman et al., 2011; Lewis et al., 2016). We therefore examined if mitochondrial fission occurs where granular GFP signals arising from the split-GFP proteins were present to confirm that the split-GFP probes really mark the ER-mitochondria contact sites in HeLa cells. To this end, we performed live-cell imaging of the HeLa cell after inducing the expression of ERj1N-V5-GFP1-10 and acquired time-lapse images every 4 s. The reconstituted time-lapse movies showed that mitochondrial fission occurred at or next to the sites that the GFP signal existed (**Supplementary Movies 1, 2** and **Figure 8**). These results suggest that the complete GFP molecules are reconstituted near authentic ER-mitochondria contact sites.

DISCUSSION

Previous studies have shown that split-fluorescent proteins are effective in visualizing inter-organelle-contact sites (Cieri et al., 2018; Kakimoto et al., 2018; Shai et al., 2018; Yang et al., 2018). However, a drawback of this method is the irreversible association of the split-fluorescent proteins, which induces artificial contact sites between different organelles and leads to an abnormality in the structure and function of the organelles (**Figure 1F**; Bishop et al., 2019). In this study, we found that the incorporation of the split-GFP genes into the yeast genome resulted in a decrease in the expression levels of the split-GFP proteins (**Figure 4**). Noteworthy, this decrease in expression levels successfully diminished the formation of unnecessary inter-organellar contacts (**Figure 3**). In addition, the variation in its expression levels among cells also decreased dramatically, which is advantageous in improving the quantitative evaluation of the organelle-contact sites. In fact, with the genome-based split-GFP system, we were able to detect changes in the organelle contacts, which had been difficult to judge by using the previous method. Specifically, we could observe clear differences in the GFP signal intensities and patterns when known organelle-tethering factors were absent (**Figure 6**).

Previously, a high-throughput microscopy system that makes use of the Yeast Knock-out deletion collection expressing the split-Venus probe successfully identified the tethering factors between the mitochondria and peroxisomes (Shai et al., 2018). However, such a large-scale microscope system is not commonly available and cannot be easily set up. With our improved split-GFP system, genetic screening experiments to search for factors involved in organelle-organelle contacts may be performed more easily. As mentioned above, our new split-GFP system resulted in lower GFP signals with small variation (**Figure 3G**), so that yeast cells expressing the split-GFP probes could be detected as a single sharp peak by flow cytometry using GFP fluorescence as an index (**Figure 3H**). It should be noted that almost all wild-type yeast cells showed the similar GFP signals when the split-GFP probes were expressed from the genomic DNA. This feature is advantageous for high-content screening by FACS as compared with the previous plasmid-based system in which yeast cells were detected as two wider peaks (**Figure 3H**). Therefore, this allows us to use fluorescence-activated cell sorting (FACS) to easily separate the subpopulation of cells in which the GFP signals are either diminished or enhanced after introducing random mutations or the yeast genome library cloned in a high copy number vector for the gene overexpression. This simple FACS study may help to perform comprehensive searches for the factors involved in inter-organelle-contact sites.

Genetic studies using mammalian cells may be performed by using the siRNA libraries and the CRISPR-Cas9 sgRNA libraries (Shalem et al., 2014). By using the HeLa cell line constructed in this study, it is possible to easily adjust the timing of the split-GFP expression. Expressing the split-GFP probes after introducing a siRNA or a CRISPR-Cas9 sgRNA library allows for a screening protocol wherein the secondary effects of split-GFP association are minimized. The application of this new split-GFP system to the study of various inter-organelle contact sites may lead to the discovery of novel factors involved in inter-organelle interactions in the future.

DATA AVAILABILITY STATEMENT

The raw data supporting the conclusions of this article will be made available by the authors, without undue reservation.

AUTHOR CONTRIBUTIONS

ST and YT designed the research and wrote the manuscript. ST performed experiments using HeLa cells. MS, YK, SF, and YT performed yeast experiments. All authors contributed to the article and approved the submitted version.

FUNDING

This work was supported by JSPS KAKENHI (Grant Numbers 17H06414 and 19H03174), AMED-Prime (JP20gm5910026), and the Naito Foundation to YT. ST was and YK is a Research Fellow of the JSPS.

ACKNOWLEDGMENTS

We thank the members of the Tamura Laboratory and Prof. Toshiya Endo (Kyoto Sangyo University) for discussions and critical comments on the manuscript.

SUPPLEMENTARY MATERIAL

The Supplementary Material for this article can be found online at: https://www.frontiersin.org/articles/10.3389/fcell.2020.571388/full#supplementary-material

REFERENCES

Bishop, A., Kamoshita, M., Passmore, J. B., Hacker, C., Schrader, T. A., Waterham, H. R., et al. (2019). Fluorescent tools to analyze peroxisome–endoplasmic reticulum interactions in mammalian cells. *Contact* 2:251525641984864. doi: 10.1177/2515256419848641

Cieri, D., Vicario, M., Giacomello, M., Vallese, F., Filadi, R., Wagner, T., et al. (2018). SPLICS: a split green fluorescent protein-based contact site sensor for narrow and wide heterotypic organelle juxtaposition. *Cell Death Differ.* 25, 1131–1145. doi: 10.1038/s41418-017-0033-z

Cohen, S., Valm, A. M., and Lippincott-Schwartz, J. (2018). Interacting organelles. *Curr. Opin. Cell Biol.* 53, 84–91. doi: 10.1016/j.ceb.2018.06.003

Eisenberg-Bord, M., Shai, N., Schuldiner, M., and Bohnert, M. (2016). A tether is a tether is a tether: tethering at membrane contact sites. *Dev. Cell* 39, 395–409. doi: 10.1016/j.devcel.2016.10.022

Elbaz-Alon, Y., Rosenfeld-Gur, E., Shinder, V., Futerman, A. H., Geiger, T., and Schuldiner, M. (2014). A dynamic interface between vacuoles and mitochondria in yeast. *Dev. Cell* 30, 95–102. doi: 10.1016/j.devcel.2014.06.007

Friedman, J. R., Lackner, L. L., West, M., DiBenedetto, J. R., Nunnari, J., and Voeltz, G. K. (2011). ER tubules mark sites of mitochondrial division. *Science* 334, 358–362. doi: 10.1126/science.1207385

Gietz, R. D., and Schiestl, R. H. (2007). High-efficiency yeast transformation using the LiAc/SS carrier DNA/PEG method. *Nat. Protoc.* 2, 31–34. doi: 10.1038/nprot.2007.13

González Montoro, A., Auffarth, K., Hönscher, C., Bohnert, M., Becker, T., Warscheid, B., et al. (2018). Vps39 interacts with Tom40 to establish one of two functionally distinct vacuole-mitochondria contact sites. *Dev. Cell* 45, 621–636.e7. doi: 10.1016/j.devcel.2018.05.011

Gossen, M., Freundlieb, S., Bender, G., Müller, G., Hillen, W., and Bujard, H. (1995). Transcriptional activation by tetracyclines in mammalian cells. *Science* 268, 1766–1769. doi: 10.1126/science.7792603

Grippa, A., Buxó, L., Mora, G., Funaya, C., Idrissi, F.-Z., Mancuso, F., et al. (2015). The seipin complex Fld1/Ldb16 stabilizes ER-lipid droplet contact sites. *J. Cell Biol.* 211, 829–844. doi: 10.1083/jcb.201502070

Hariri, H., Rogers, S., Ugrankar, R., Liu, Y. L., Feathers, J. R., and Henne, W. M. (2018). Lipid droplet biogenesis is spatially coordinated at ER–vacuole contacts under nutritional stress. *EMBO Rep.* 19, 57–72. doi: 10.15252/embr.201744815

Hariri, H., Speer, N., Bowerman, J., Rogers, S., Fu, G., Reetz, E., et al. (2019). Mdm1 maintains endoplasmic reticulum homeostasis by spatially regulating lipid droplet biogenesis. *J. Cell Biol.* 218, 1319–1334. doi: 10.1083/jcb.201808119

Henne, W. M., Zhu, L., Balogi, Z., Stefan, C., Pleiss, J. A., and Emr, S. D. (2015). Mdm1/Snx13 is a novel ER–endolysosomal interorganelle tethering protein. *J. Cell Biol.* 210, 541–551. doi: 10.1083/jcb.201503088

Hönscher, C., Mari, M., Auffarth, K., Bohnert, M., Griffith, J., Geerts, W., et al. (2014). Cellular metabolism regulates contact sites between vacuoles and mitochondria. *Dev. Cell* 30, 86–94. doi: 10.1016/j.devcel.2014.06.006

Kakimoto, Y., Tashiro, S., Kojima, R., Morozumi, Y., Endo, T., and Tamura, Y. (2018). Visualizing multiple inter-organelle contact sites using the organelle-targeted split-GFP system. *Sci. Rep.* 8:6175. doi: 10.1038/s41598-018-24466-0

Kawano, S., Tamura, Y., Kojima, R., Bala, S., Asai, E., Michel, A. H., et al. (2018). Structure–function insights into direct lipid transfer between membranes by Mmm1–Mdm12 of ERMES. *J. Cell Biol.* 217, 959–974. doi: 10.1083/jcb.201704119

Kojima, R., Endo, T., and Tamura, Y. (2016). A phospholipid transfer function of ER-mitochondria encounter structure revealed in vitro. *Sci. Rep.* 6:30777. doi: 10.1038/srep30777

Kojima, R., Kakimoto, Y., Furuta, S., Itoh, K., Sesaki, H., Endo, T., et al. (2019). Maintenance of cardiolipin and crista structure requires cooperative functions of mitochondrial dynamics and phospholipid transport. *Cell Rep.* 26, 518–528.e6. doi: 10.1016/j.celrep.2018.12.070

Kornmann, B. (2020). The endoplasmic reticulum-mitochondria encounter structure: coordinating lipid metabolism across membranes. *Biol. Chem.* 401, 811–820. doi: 10.1515/hsz-2020-0102

Kornmann, B., Currie, E., Collins, S. R., Schuldiner, M., Nunnari, J., Weissman, J. S., et al. (2009). An ER-mitochondria tethering complex revealed by a synthetic biology screen. *Science* 325, 477–481. doi: 10.1126/science.1175088

Kushnirov, V. V. (2000). Rapid and reliable protein extraction from yeast. *Yeast* 16, 857–860.

Kvam, E., and Goldfarb, D. S. (2006). Nucleus-vacuole junctions in yeast: anatomy of a membrane contact site. *Biochem. Soc. Trans.* 34, 340–342. doi: 10.1042/BST0340340

Lewis, S. C., Uchiyama, L. F., and Nunnari, J. (2016). ER-mitochondria contacts couple mtDNA synthesis with mitochondrial division in human cells. *Science* 353:aaf5549. doi: 10.1126/science.aaf5549

Murley, A., and Nunnari, J. (2016). The emerging network of mitochondria-organelle contacts. *Mol. Cell* 61, 648–653. doi: 10.1016/j.molcel.2016.01.031

Pan, X., Roberts, P., Chen, Y., Kvam, E., Shulga, N., Huang, K., et al. (2000). Nucleus-vacuole junctions in Saccharomyces cerevisiae are formed through the direct interaction of Vac8p with Nvj1p. *Mol. Biol. Cell* 11, 2445–2457. doi: 10.1091/mbc.11.7.2445

Prinz, W. A., Toulmay, A., and Balla, T. (2020). The functional universe of membrane contact sites. *Nat. Rev. Mol. Cell Biol.* 21, 7–24. doi: 10.1038/s41580-019-0180-9

Scorrano, L., De Matteis, M. A., Emr, S., Giordano, F., Hajnóczky, G., Kornmann, B., et al. (2019). Coming together to define membrane contact sites. *Nat. Commun.* 10:1287. doi: 10.1038/s41467-019-09253-3

Shai, N., Yifrach, E., van Roermund, C. W. T., Cohen, N., Bibi, C., IJlst, L., et al. (2018). Systematic mapping of contact sites reveals tethers and a function for the peroxisome-mitochondria contact. *Nat. Commun.* 9:1761. doi: 10.1038/s41467-018-03957-8

Shalem, O., Sanjana, N. E., Hartenian, E., Shi, X., Scott, D. A., Mikkelsen, T. S., et al. (2014). Genome-scale {CRISPR-Cas9} knockout screening in human cells. *Science* 343, 84–87. doi: 10.1126/science.1247005

Tamura, Y., Kawano, S., and Endo, T. (2019). Organelle contact zones as sites for lipid transfer. *J. Biochem.* 165, 115–123. doi: 10.1093/jb/mvy088

Toulmay, A., and Prinz, W. A. (2012). A conserved membrane-binding domain targets proteins to organelle contact sites. *J. Cell. Sci.* 125, 49–58. doi: 10.1242/jcs.085118

Williams, C. C., Jan, C. H., and Weissman, J. S. (2014). Targeting and plasticity of mitochondrial proteins revealed by proximity-specific ribosome profiling. *Science* 346, 748–751. doi: 10.1126/science.1257522

Wolinski, H., Kolb, D., Hermann, S., Koning, R. I., and Kohlwein, S. D. (2011). A role for seipin in lipid droplet dynamics and inheritance in yeast. *J. Cell Sci.* 124, 3894–3904. doi: 10.1242/jcs.091454

Wu, H., Carvalho, P., and Voeltz, G. K. (2018). Here, there, and everywhere: the importance of ER membrane contact sites. *Science* 361:eaan5835. doi: 10.1126/science.aan5835

Yang, Z., Zhao, X., Xu, J., Shang, W., and Tong, C. (2018). A novel fluorescent reporter detects plastic remodeling of mitochondria-ER contact sites. *J. Cell Sci.* 131:jcs208686. doi: 10.1242/jcs.208686

Conflict of Interest: The authors declare that the research was conducted in the absence of any commercial or financial relationships that could be construed as a potential conflict of interest.

frontiers in Cell and Developmental Biology

REVIEW
published: 15 December 2020
doi: 10.3389/fcell.2020.618322

Two Types of Contact Between Lipid Droplets and Mitochondria

Liujuan Cui[1] *and Pingsheng Liu*[1,2]*

[1] National Laboratory of Biomacromolecules, CAS Center for Excellence in Biomacromolecules, Institute of Biophysics, Chinese Academy of Sciences, Beijing, China, [2] University of Chinese Academy of Sciences, Beijing, China

Lipid droplets (LDs) and mitochondria are essential organelles involved in cellular lipid metabolism and energy homeostasis. Accumulated studies have revealed that the physical contact between these two organelles is important for their functions. Current understanding of the contact between cellular organelles is highly dynamic, fitting a "kiss-and-run" model. The same pattern of contact between LDs and mitochondria has been reported and several proteins are found to mediate this contact, such as perilipin1 (PLIN1) and PLIN5. Another format of the contact has also been found and termed anchoring. LD-anchored mitochondria (LDAM) are identified in oxidative tissues including brown adipose tissue (BAT), skeletal muscle, and heart muscle, and this anchoring between these two organelles is conserved from mouse to monkey. Moreover, this anchoring is generated during the brown/beige adipocyte differentiation. In this review, we will summarize previous studies on the interaction between LDs and mitochondria, categorize the types of the contacts into dynamic and stable/anchored, present their similarities and differences, discuss their potential distinct molecular mechanism, and finally propose a working hypothesis that may explain why and how cells use two patterns of contact between LDs and mitochondria.

Keywords: contact, lipid droplets, mitochondria, anchor, isolation, centrifugal force

OPEN ACCESS

Edited by:
Dan Zhang,
Temasek Life Sciences Laboratory, Singapore

Reviewed by:
Mark Christian,
Nottingham Trent University, United Kingdom
Wanzhu Jin,
Chinese Academy of Sciences (CAS), China

***Correspondence:**
Pingsheng Liu
pliu@ibp.ac.cn

Specialty section:
This article was submitted to Membrane Traffic, a section of the journal Frontiers in Cell and Developmental Biology

Received: *16 October 2020*
Accepted: *25 November 2020*
Published: *15 December 2020*

Citation:
Cui L and Liu P (2020) Two Types of Contact Between Lipid Droplets and Mitochondria. Front. Cell Dev. Biol. 8:618322. doi: 10.3389/fcell.2020.618322

INTRODUCTION

The lipid droplet (LD) is a specialized cellular organelle with a neutral lipid core covered by a monolayer phospholipid membrane and associated proteins (Murphy, 2001; Tauchi-Sato et al., 2002; Fujimoto et al., 2008; Thiam et al., 2013). Starting with the discovery by Antony van Leeuwenhoek in 1674, LD biology has taken a sweeping 300 year-long developmental path to the modern era. Our understanding has accelerated in the last two decades, importantly marked by the discovery of marker proteins, development of methods for purification, and the application of omics studies (Ding et al., 2013; Roberts and Olzmann, 2020).

The LD is an ancient organelle with a new face and a recent recognition of its importance has attracted great attention in the fields of biology and life science. The newly discovered fact that LDs exist in some bacteria extends our view of the origin of membrane-bound organelles. The finding that LDs contain not only triacylglycerol (TAG), but also cholesterol ester, retinal ester, and monoalk(en)yl diacylglycerol in animal cells (Bartz et al., 2007a) suggests many potential roles

for this organelle. In addition, the broad distribution of LDs from bacteria to humans implies its significance in all organisms (Murphy, 2012; Olzmann and Carvalho, 2019; Zhang and Liu, 2019).

The unique property of LDs in their sequestration of neutral lipids led to a perception of them merely as "a drop of oil," negatively impacting scientific interest and slowing down its research. However, the description of their proteome and lipidome and their linkage to metabolic syndromes impacting human health provoked a renaissance in research interest and activity (Brasaemle et al., 2004; Liu et al., 2004; Bartz et al., 2007a). The LD differs from other membrane-bound organelles by containing (1) a hydrophobic core compared with an aqueous phase lumen for other membranous organelles, (2) a monolayer phospholipid membrane in contrast with the bilayer or double bilayer membrane for others, (3) a distinct protein complements termed LD resident proteins. With these differences, the LD is a unique cellular organelle. The functions of the LD are lipid storage, lipid transportation, lipid synthesis, and lipid hydrolysis, a suite of functions far beyond their image as a static oil reservoir. According to recent proteomic and other experimental lines of evidence, LD functions are also thought to include membrane trafficking, protein storage and degradation, signal transduction, detoxification, and nucleic acid handling. The multifunctional property of the LD endows the organelle with an irreplaceable position in almost all cellular activities.

The LD is integrated with other organelles in maintaining lipid homeostasis (Walther and Farese, 2012; Schuldiner and Bohnert, 2017), which is responsible for the ectopic storage of lipids that has been linked to many metabolic disorders (Greenberg et al., 2011; Shulman, 2014; Xu et al., 2018). LDs possess the ability for directed movement on the cytoskeleton, likely supporting the movement of neutral lipids within the cell and between organelles. Biochemical studies previously revealed the interaction between LD and early endosome (Liu et al., 2007), mitochondria (Pu et al., 2011), endoplasmic reticulum (ER) (Martin et al., 2005; Ozeki et al., 2005), and peroxisomes (Binns et al., 2006). More interactions between LDs and other organelles have been developed in the past decade (Olzmann and Carvalho, 2019). Therefore, LD-governed cellular lipid homeostasis is driven by lipid metabolism on the LD as well as the interaction between LD and other organelles. For example, TAG sequestered in the LD is converted to fatty acids (FAs) via lipolysis and lipophagy (Zechner et al., 2017; Ogasawara et al., 2020). The FAs in turn, are transported from LD to mitochondria, where they are oxidized as an energy source to produce ATP or heat, and provide building blocks for synthesis of biological molecules. Thus, the LD and mitochondrion form a functional organelle pair, managing cellular energy homeostasis.

Mitochondria are the site of β-oxidation, converting hydrophobic substrates into usable cellular energy and reducing potential. The fuel for this reaction is stored in the hydrophobic interior of LDs, necessitating a mechanism for the transfer of FAs between these two organelles. Free transfer of FA (or coenzyme A ligated FA) is restricted by the hydrophobic character of the molecules. In fact, the accumulation of FA or acyl-CoA under certain stress conditions leads to cellular toxicity (lipotoxicity). To facilitate the transfer, cells developed a specific interaction between these two organelles. An understanding of this interaction was initiated by the visualization of the physical contact between LDs and mitochondria. The best images depicting this interaction were electron micrographs taken by George Palade, in which the physical contact was clearly shown between LDs and mitochondria in guinea pig pancreas (**Figure 1Aa**). Since then, the development of high resolution light microscopy techniques and the availability of dyes and marker proteins for both LDs and mitochondria have greatly facilitated the visualization of the association of the two organelles.

Despite early, clear visual evidence of the contact, it has been a long journey toward a biochemical understanding of the interaction. Investigations were hampered by underdeveloped techniques for biochemical isolation and a lack of molecular tools. The discovery of LD marker proteins perilipin (PLIN1) and adipocyte differentiation-related protein (ADRP/PLIN2) in the early 1990s (Greenberg et al., 1991; Jiang and Serrero, 1992; Brasaemle et al., 1997) permitted the development of purification techniques and an evaluation of the purity of isolated organelle (Wu et al., 2000; Ding et al., 2013). These techniques coupled with the blossoming of proteomics opened a window into the functions, interactions, and underlying molecular machinery governing LD dynamics. These advances permitted the discovery that other organelles, like ER and mitochondria, co-isolate with LDs. Morphological studies provided further evidence for inter-organelle contact while proteomic results identified likely protein candidates regulating the contact. Interestingly, it has been observed that some organelles which are co-purified with LDs when isolated with low speed centrifugation can be separated from the LDs in higher centrifugal force, while other remain firmly associated (Yu et al., 2015; Benador et al., 2018; Cui et al., 2019; Freyre et al., 2019). This distinction probably reflects underlying functional relationships. For example, LDs isolated from heart muscle (Li et al., 2016), skeletal muscle (Zhang et al., 2011), and brown adipocytes (Yu et al., 2015; Cui et al., 2019) always contain many mitochondrial proteins that were once considered contamination. On the other side of the co-isolation, some LD-associated proteins have also been identified on mitochondria, such as PLIN5 and PLIN3 (Bosma et al., 2012; Ramos et al., 2014). However, these proteins cannot be removed by ultracentrifugation. With morphological and biochemical evidence, these proteins reflect a stable contact between LDs and mitochondria in these highly oxidative cells.

This review summarizes the evidence supporting the contact between LDs and mitochondria using morphological, biochemical, and biophysical data and focuses on interactions which cannot be separated by ultracentrifugation. This review brings forward a new point of view, proposing a distinction between stable and dynamic contact which can describe and explain some recent experimental findings. We propose that the stable interaction between LDs and mitochondria is maintained by rivet-like protein structures that prevent the separation between them during ultracentrifugation.

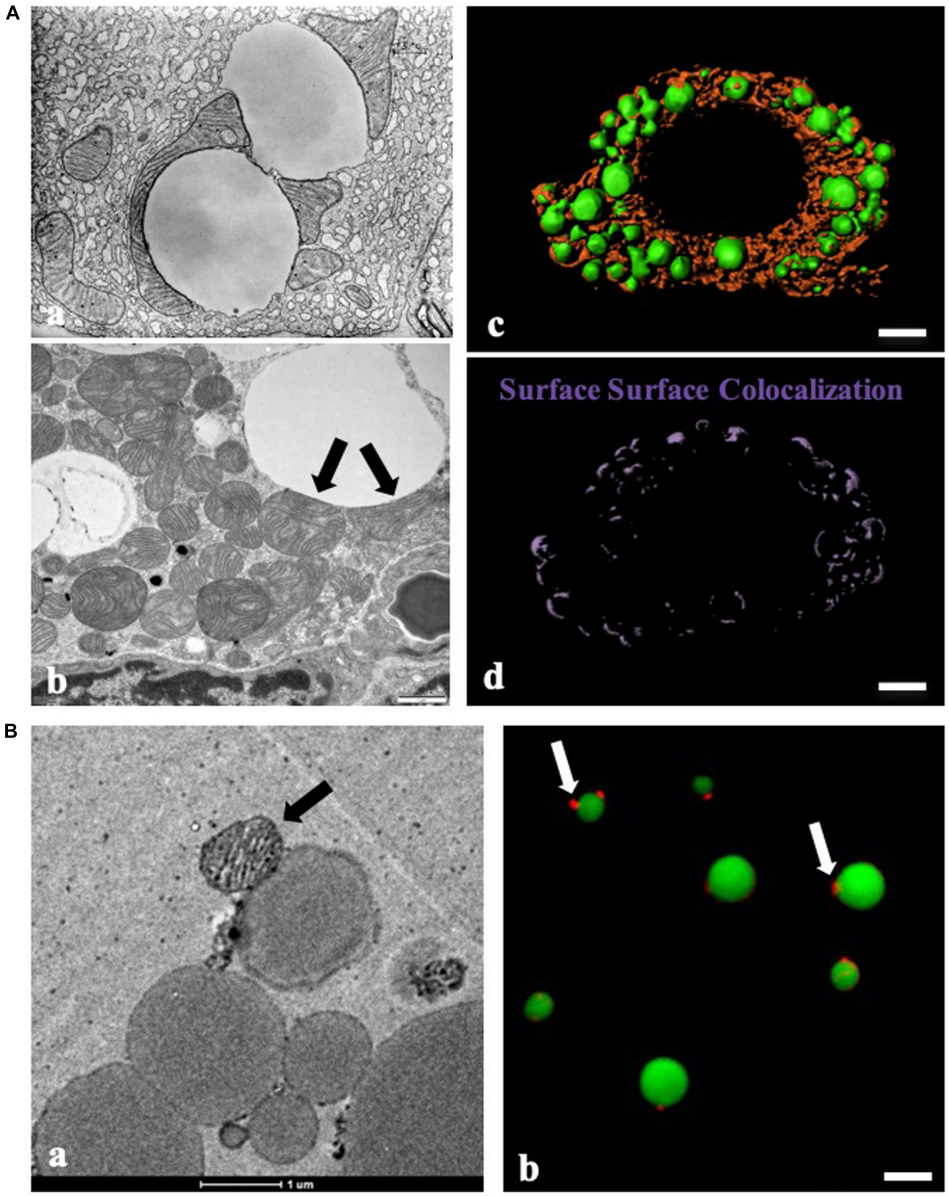

FIGURE 1 | Contact between LDs and mitochondria by morphological studies. **(A)** Morphological study of contact between lipid droplets (LDs) and mitochondria. **(a)** Physical contact between LDs and mitochondria in guinea pig pancreas imaged with transmission electron microscopy (TEM) by George E. Palade (Cite from http://www.microscopy.info/Gallery/Details/58). **(b)** Physical contact between LDs and mitochondria in mouse BAT using TEM. Arrows point to the physical contact between LDs and mitochondria. **(c,d)** LDs and mitochondria in differentiated brown adipocytes (day 8) were stained with LipidTOX Green for LDs and MitoTracker Red for mitochondria, respectively. The image was analyzed using three-dimensional structured illumination microscopy (3D-SIM), and Imaris analysis was applied to detect surface-surface colocalization. Bar = 5 μm. **(B)** Morphologic analysis of isolated BAT LDs from mice housed at 23°C. **(a)** TEM of isolated BAT LDs, Bar = 1 μm. **(b)** LipidTOX Green staining for LDs and MitoTracker Red staining for mitochondria in isolated BAT LDs. Bar = 5 μm. Arrows indicate LD-anchored mitochondrion (LDAM) in isolated BAT LDs (cite from Cui et al., 2019).

IDENTIFICATION OF MEMBRANE TRAFFICKING PROTEINS ON LIPID DROPLETS

The potential trafficking capability of LDs was revealed through the visualization of LDs moving along microtubules, mediated by the protein Klar (Welte et al., 1998) and other motor proteins (Xie et al., 2019). Proteomic studies of isolated LDs identified Rab and SNARE proteins (Fujimoto et al., 2004; Liu et al., 2004). The targeting of trafficking proteins to LDs has been studied through fluorescent fusion proteins and immunogold-labeled electron microscopy, providing further evidence that LDs are involved in membrane trafficking (Martin et al., 2005; Liu et al., 2007). In functional studies LD-associated Rabs have been demonstrated

to regulate interactions between LDs and ER (Rab 18) (Martin et al., 2005; Ozeki et al., 2005), LDs and mitochondria (Rabs and SNARE) (Jägerström et al., 2009; Pu et al., 2011), LDs and early endosomes (Rabs) (Liu et al., 2007), and to drive LD fusion (Rab8) (Wu et al., 2014). The movement of LDs throughout the cell with regulated interactions with other organelles hints at an active and important role for the LD in cellular lipid homeostasis.

The discovery of hormone-sensitive lipase (HSL) and PLIN1 on LDs, and the identification of the mechanism of activation and LD targeting of HSL via phosphorylation of both proteins, identified the catalytic function of this organelle. Additional proteomic studies found lipid synthetic enzymes on isolated LDs, pointing to an anabolic role (Fujimoto et al., 2004; Liu et al., 2004). In addition, some non-coding RNA-coded proteins are recently identified in isolated LDs (Huang et al., 2020). Functional studies of isolated LDs using *in vitro* assays confirmed that LD is a site for cellular lipid synthesis (Fujimoto et al., 2007; Zhang et al., 2016).

Thus, the LD is a site of neutral lipid storage, but is also metabolically active, can move rapidly throughout the cell, and possesses the molecular machinery to regulate interactions with other organelles. Collectively, these observations point to a central role for LDs in cellular lipid homeostasis.

THE MORPHOLOGICAL STUDIES OF CONTACT BETWEEN LIPID DROPLETS AND MITOCHONDRIA

The interaction between LDs and mitochondria was first observed more than a half-century ago. George E. Palade was one of the major contributors who visualized the physical contact between LDs and mitochondria in guinea pig pancreas using transmission electron microscopy (TEM) (**Figure 1Aa**). EM also revealed the contact between these two organelles in mammary gland cells (Stemberger et al., 1984) and brown adipose tissue (BAT) (**Figure 1Ab**). Since these discoveries, many biologists have contributed to this field, accumulated visual evidence documenting the interactions between LDs and mitochondria by EM (Peute et al., 1978; Pu et al., 2011; Yu et al., 2015; Cui et al., 2019).

Advances in biological dyes, such as JC-1 and MitoTracker for mitochondria and Nile red, Bodipy, Oil Red O, and LipidTOX for LDs, have permitted the application of fluorescence microscopy to the study of LD-mitochondrion interactions (**Figures 1Ac,d**). The discovery of LD marker proteins enabled the use of immunolabeling and fluorescent fusion proteins. Together these advances have greatly simplified the study of the organellar interactions. Furthermore, the recent development of high resolution light microscopy techniques has facilitated finer observations, significantly aiding functional studies of the interactions between LDs and mitochondria (Valm et al., 2017).

Morphological studies have described highly dynamic interactions between LDs and mitochondria. For example, it was observed by EM that endurance exercise training enhances the physical contact between LDs and mitochondria in muscle cells. This finding is fully consistent with the upregulation of FA β-oxidation in mitochondria to meet the energetic needs during exercise (Tarnopolsky et al., 2007). In another study using live-imaging light microscopy, the distance between LDs and mitochondria was found to change in response to various experimental manipulations with close co-localization interpreted as direct contact (Valm et al., 2017).

A wide range of terminology has been applied to direct the contact between LDs and mitochondria. These include, but are not limited to, approximation, association, interaction, targeting, tethering, contact, binding, and anchoring. In one instance, the interaction site was called recognition site (Zehmer et al., 2009). **Table 1** summarizes the most common terms used to describe inter-organelle interaction. Mainly based on morphologic observations, the current well-accepted term for the interaction between organelles, including LDs and mitochondria, is "contact" and the site for the interaction is termed as the "contact site." Contact is characterized by: (1) co-localization of organelles, (2) the distance between organelles approximately 10–70 nm, (3) a contact site composed of tethering proteins, and (4) the ability to transfer ions, lipids, and other molecules (Schuldiner and Bohnert, 2017).

The contact between LDs and mitochondria has been studied and visualized in many types of cells using a variety of technologies. However, molecular techniques are required to push our understanding further. As in other fields of biology, the powerful omics tools have been applied with great success. The first interactomic study screened LD and mitochondrial surface proteins, searching for interacting protein pairs using a bimolecular fluorescence complementation assay in *Saccharomyces cerevisiae* (Pu et al., 2011). In the same work an *in vitro* assay to study the interaction between isolated LDs and mitochondria was established, in which GTP was found to play a key role for this interaction (Pu et al., 2011). The most recent organelle-level interactomic study using high resolution microscopy visualized not only the interaction between LDs and mitochondria but also four other membranous organelles using a multispectral image acquisition method (Valm et al., 2017). Interactomic studies of this type provide a broad, system wide view of the network for interactions. However, insight into the mechanisms enabling these interactions requires other experimental techniques.

THE BIOCHEMICAL AND BIOPHYSICAL STUDIES OF CONTACT BETWEEN LIPID DROPLETS AND MITOCHONDRIA

Biochemical and biophysical studies have been used to probe the molecular basis of inter-organelle contact. Contact has been dissected into discrete phases: recognition/targeting, tethering, and binding/anchoring, with distinct proteins playing key roles in each step. While the Rab proteins previously described are key candidates for recognition and tethering, other proteins including PLIN1, PLIN5, MFN2, and MIGA2 have also been

TABLE 1 | Patterns of interaction between LDs and mitochondria.

Interaction terms	Organisms/tissues and cells	Methods	References
Interaction	Rat/skeletal muscle, L6	EM, LM, BpM, BcM, *In vitro* reconstitution	Pu et al., 2011
	Mouse/heart muscle	EM	Wang et al., 2013
	Monkey/kidney fibroblast cell	LM	Pribasnig et al., 2018
	Vero cell	EM	Herms et al., 2015
	Mouse/BAT	EM, LM, BpM, BcM	Yu et al., 2015
	Phaeodactylum tricornutum	EM	Lupette et al., 2019
Interaction (SNAP23)	NIH 3T3 cells	LM, BpM, BcM	Jägerström et al., 2009
Interaction (PLIN5)	CHO-K1 cell; AML12 cell; HL1 cell	BpM, BcM	Wang et al., 2011
	Human/skeletal muscle	EM, LM	Bosma et al., 2012; Gemmink et al., 2018
Interaction/contact (MFN2)	Human/BeWo cells	LM	Wasilewski et al., 2012
Interaction (RAB32)	Yellow catfish/hepatocytes	LM, BpM, BcM	Song et al., 2020
Interaction/association (MIGA2)	3T3-L1, COS7 cells	LM, EM, BpM, BcM	Freyre et al., 2019
Association	Mouse/BAT	LM	Benador et al., 2018
	Mouse/skeletal muscle, C2C12 cell	EM, LM, BpM, BcM	Zhang et al., 2011
	Mouse/Hepatocyte	EM	Shiozaki et al., 2011
	CHO Cell, 3T3-L1 fibroblasts	EM, LM	Murphy et al., 2009
Contact	Vero cell	EM	Barbosa et al., 2015
	MEF	LM	Rambold et al., 2015
	Dog/muscle cell (triceps)	EM	Vock et al., 1996
	Zebrafish/hepatocyte	EM	Peute et al., 1978
	Mouse /liver	EM	Krahmer et al., 2018
	Turtle/leydig cell	EM	Tarique et al., 2019
Contact (MFN2/PLIN1)	Mouse/BAT	EM, BpM, BcM	Boutant et al., 2017
Co-localization	Porcine/oocytes	LM	Sturmey et al., 2006; Milakovic et al., 2015
Adhere	Rat/mammary	EM	Stemberger et al., 1984
Close proximity	MEF	LM	Nguyen et al., 2017
Junction (PLIN5)	Mouse/cardiac tissue	EM	Varghese et al., 2019
Anchoring	Mouse/BAT	EM, LM, BpM, BcM	Cui et al., 2019

LM, light microscopy; EM, electron microscopy; BpM, biophysical methods; BcM, Biochemical methods.

implicated in these phases (Wasilewski et al., 2012; Boutant et al., 2017; Freyre et al., 2019; Varghese et al., 2019). Some proteins serve multiple functions. For example, VPS13C functions both as a binding component and plays a role in lipid transport (Kumar et al., 2018). Some proteins involved in LD-mitochondrion contact have been found to mediate the contact between other organelles as well. Studies using live-cell imaging have shown that these proteins are involved in highly dynamic contact, fitting a "kiss-and-run" model. Beyond morphologic observation, experiments using co-isolation (**Figures 1Ba,b**) and *in vitro* reconstitution have been used to further dissect the mechanisms of this contact (Pu et al., 2011).

Distinct from other membrane-bound organelles, the LD uniquely possesses a density less than 1 g/cm^3 due to the TAG forming its core. This enables the method of floatation in a centrifugal field for the isolation/purification of LDs (Ding et al., 2013). All other membrane-bound organelles with densities higher than 1 g/cm^3 are driven in the opposite direction into a pellet below the aqueous phase media. Therefore, a simple centrifugation can easily separate LDs from other membrane-bound organelles. Strong binding between LDs and other organelles could result in co-migration in the centrifugal field, either to the low-density region or the pellet.

In fact, other membranous organelles, such as ER and mitochondria, are commonly co-isolated with LDs and this co-fractionation historically was considered as contamination. Indeed, some membranous structures can be stripped from LDs through ultracentrifugation, but other structures remain tightly bound, suggesting that these co-fractionated organelles are bound physiologically in a type of organelle complex. The analysis of isolated and re-isolated LD fractions by EM and light microscopy provides visual evidence of intact membranous organelles bound to the surface of LDs, demonstrating the physiological and physical binding of LDs with other membranous organelles. The strength of the centrifugal field can be used to measure the binding strength, distinguishing weak contact (association/kiss-run) from strong contact (stable binding/anchoring). Therefore, this experimental approach can be used to classify types of contact.

This property of LDs can also be studied using *in vitro* assays (Pu et al., 2011). After incubation with controlled components, LDs can be re-isolated by floatation. Membranous structures induced to bind to the LDs in the *in vitro* system

are co-floated. Utilizing this unique property of LDs, isolated LDs were incubated with isolated early endosomes in the presence or absence of GTP, the reaction mixture was centrifuged, and the re-isolated LDs were analyzed. Through this experiment, the physiological binding of early endosomes to LDs was identified to be regulated by GTP. Stripping Rab proteins from both isolated LDs and early endosomes totally blocked the binding, demonstrating that Rab protein(s) are key players governing the physiological binding between early endosomes and LDs (Liu et al., 2007).

A similar experiment was conducted to investigate factors that govern the binding between LDs and mitochondria. The two organelles, isolated separately, were mixed and incubated in the presence or absence of GTP or cytosol, followed by the re-isolation of the LDs. Mitochondria were co-fractionated with the floating LD fraction under the GTP condition, identifying GTP as a key factor regulating the binding between these two organelles (Pu et al., 2011).

Many mitochondrial proteins were identified in LDs isolated from mouse skeletal muscle using ultracentrifugation, indicating the strong contact between these two organelles (Zhang et al., 2011). Another study of LDs isolated from rat heart with ultracentrifugation also found numerous mitochondrial proteins (Li et al., 2016). A summary of finding from proteomic studies of isolated LDs shows that mitochondrial proteins co-fractionate with LDs isolated from a broad range of cell types (**Table 2**). Most of these studies used ultracentrifugation conditions, demonstrating the tight contact between these two organelles. It is also quite interesting that this phenomenon primarily is present in cells from highly oxidative tissues (Cui et al., 2019). The LD-mitochondrion contact is especially easy to visualize in BAT, an observation that is consistent with the role of these cells in heat production and the resulting high energy demand of mitochondria (Géloën et al., 1990; Ohue and Makita, 1992). Therefore, brown adipocytes represent a uniquely suitable experimental system for these investigations.

Recent studies of isolated BAT LDs have suggested a distinction between two types of contact (Cui et al., 2019). The first is tight/stable contact (Cui et al., 2019), also called anchoring since it cannot be separated by ultracentrifugation, similar to the results from isolated LDs of muscle and heart (Zhang et al., 2011; Li et al., 2016). The other is dynamic contact that can be separated using high speed centrifugation (9,000*g*). The term peridroplet mitochondria (PDM) was proposed to describe these loosely associated mitochondria (Benador et al., 2018). After centrifugation with 9,000*g*, about 50% of LD-associated were still remained on re-isolated LD fraction. In addition, PDM are functionally different with cytosolic mitochondria and more toward to fatty acid synthesis (Benador et al., 2018). These differences can be understood physiologically due to the different demands placed on oxidative systems of the cell, depending on the role of the tissue.

DYNAMIC AND STABLE CONTACTS BETWEEN LIPID DROPLETS AND MITOCHONDRIA

The empirical distinction between weak and strong contact revealed by centrifugal force is likely to reflect important physiological complexity. The contact likely functions to permit efficient signaling and transport of hydrophobic molecules. For oxidative tissues such as heart muscle, skeletal muscle, and BAT, rapid delivery of FAs from LDs to mitochondria is an essential element for efficient ATP and heat production. The contact between these two organelles not only makes this delivery fast but also avoids insolubility and cytotoxicity of free FAs. Stable/anchoring contact found in these tissues (Cui et al., 2019) well represents the necessity for the constant production of ATP or heat with high efficiency (**Figure 3**). The term of LD-anchored mitochondria (LDAM) has been proposed for the mitochondria that stably associate with LDs (Cui et al., 2019). Both LDAM and PDM co-fractionate with LDs that are isolated with the low centrifugal force while only LDAM remain in the following centrifugation at speeds generating over 9,000*g*.

The current definition of contact is mainly based on morphological studies and includes four key characteristics that describe the dynamic contact well but seem to lack a criterion that defines the strength of contact. The nature of the molecules bridging these two organelles may explain the different strengths of contacts. Identifying the proteins mediating the different types of contact is important to understand the underlying physiology. Since LDAM are not affected in PLIN1 or PLIN5 deleted mouse BAT (Cui et al., 2019), the interaction between PLIN1 and MFN2 may be a good example of the protein pair involved in dynamic contact (Boutant et al., 2017; Olzmann and Carvalho, 2019). The proteins forming cellular tight junctions and the proteins with a nail (Havaux, 1998) or rivet-like (Iacovache et al., 2006) conformation may provide a useful model for understanding the stable contact (**Figure 3**). It is reasonable to include a

TABLE 2 | Mitochondrial proteins from previously published LD proteomes.

Model/cell line	Total proteins	Mitochondrial (%)	LD isolation	References
Mouse/skeletal muscle	324	29.63	300,000 *g* for 60 min at 4°C	Zhang et al., 2011
Rat/heart	752	31.38	256,000 *g* for 60 min at 4°C	Li et al., 2016
Mouse/BAT	169	66.87	2,000 *g* for 3 min at 4°C	Yu et al., 2015
A431	32	9.38	274,000 *g* for 60 min at 4°C	Kim et al., 2006
CHO K2	125	16.8	274,000 *g* for 60 min at 4°C	Bartz et al., 2007b
3T3-L1	39	17.95	26,000 *g* for 30 min at 4°C	Brasaemle et al., 2004

fifth criterion classifying the contact based on its stability in a centrifugal field.

The LDAM have also been identified in the oxidative tissues of Rhesus monkeys (*Macaca mulatta*), including BAT (BAT), heart (Heart), and muscles (MG and MS) (**Figure 2**, lanes 1–12), but not in liver (Liver) (**Figure 2**, lanes 13–15), suggesting that the LDAM are conserved from mice to monkeys. To further understand the physiological significance of this stable contact

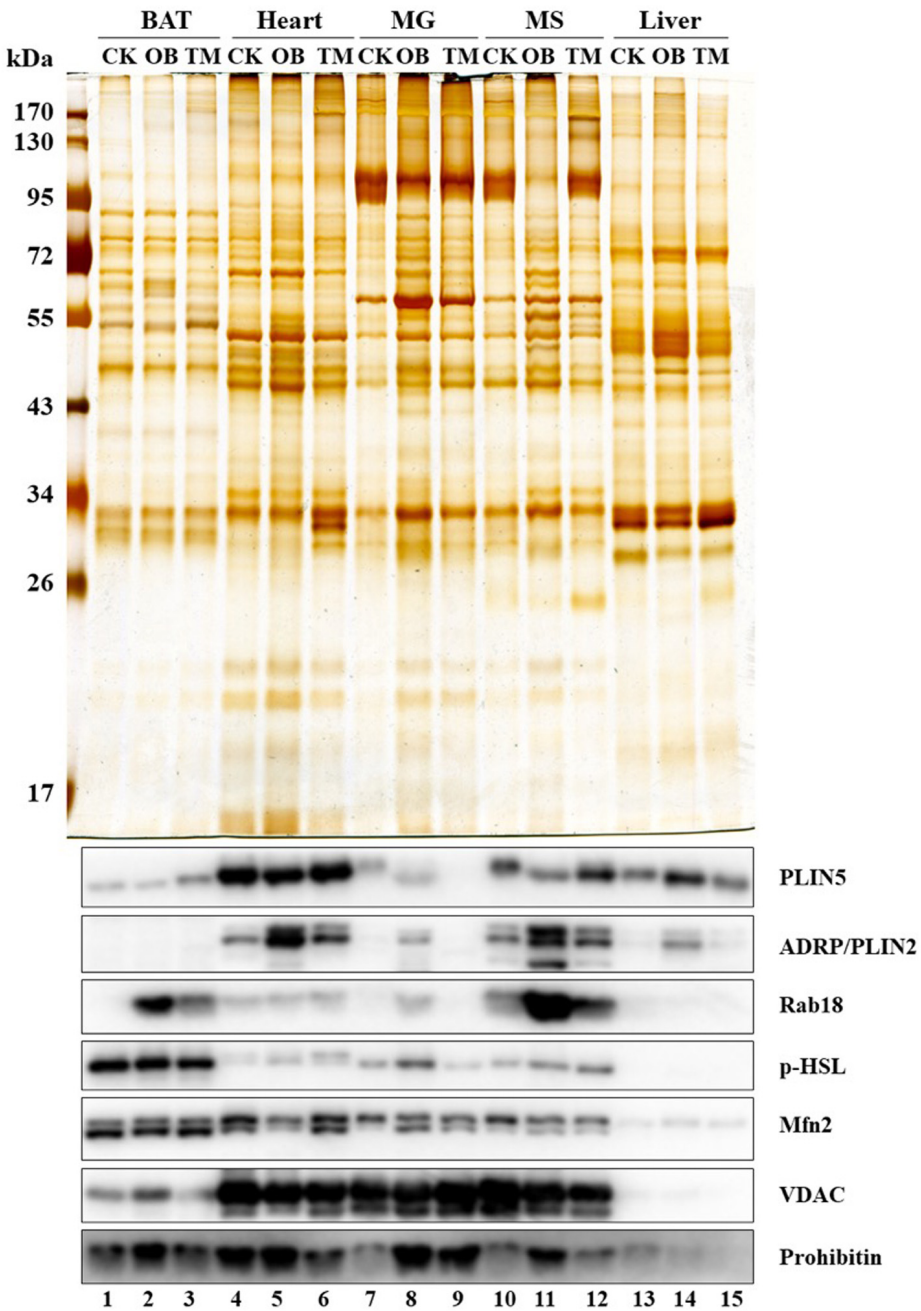

FIGURE 2 | Co-isolation of LDs and mitochondria. Rhesus monkeys (*Macaca mulatta*) including Normal (CK), Obese (OB), and Type 2 diabetes mellitus (TM) were obtained from Kunming Institute of Zoology, Chinese Academy of Sciences. The LDs from different tissues of these monkeys were isolated using indicated homogenization methods and centrifugal forces as following: (1) A dounce type glass-teflon homogenizer and a speed of 247,000*g* were used for heart, musculus gastrocnemius (MG), and musculus soleus (MS). (2) A dounce type loose-fitting potter-elvehjem tissue grinder and a speed of 247,000*g* were used for liver. (3) A 200-mesh screen with plastic syringe piston and speeds of 1,000*g* and 247,000*g* were used for BAT. The proteins from isolated LDs were separated by SDS-PAGE and visualized by silver staining (upper panel). The marker proteins for LDs (PLIN5, ADRP/PLIN2, Rab18, and p-HSL) and for mitochondria (Mfn2, VDAC, and Prohibitin) were determined by Western blots (lower panel) (cite from Cui et al., 2019).

(or LDAM), the monkeys with different metabolic conditions, such as normal (CK), obese (OB), and diabetes (TM), were utilized and the significant differences are found not only in LD-associated proteins but also in LDAM proteins (**Figure 2**).

Another fundamental question remaining to be answered for this anchoring hypothesis (**Figure 3**), is whether two types of contact are interchangeable based on physiological requirements. If this is possible, dynamic contact could transition to stable contact and back as energetic requirements fluctuate. Alternatively, if these are permanent states of association, there may be other important structural and functional differences between these two states. It is possible that mitochondria and LDs locked in stable contact coordinate in a manner similar to some protein complexes. In this case, it may be useful to think of LD and mitochondrion engaged in a stable contact as a distinct cellular structure, an organelle complex. Nevertheless, we suggest that both morphological and biochemical methods should be used together to study the contact between LDs and mitochondria as well as other organelle contacts.

To conduct the biochemical and biophysical study for the contact between LDs and mitochondria using isolation method, two critical factors should be addressed for isolation of LDs from BAT and brown adipocytes since they contain supersize LDs that are fragile and easy to be broken. These factors are (1) stringency of homogenization and (2) centrifugal force of floatation. Three homogenization methods that have been applied on BAT and brown adipocytes are listed by stringency (low to high): Nitrogen Cavitation technology (N_2 bomb) (Cui et al., 2019), grinding tissue on 200-mesh screen using plastic syringe piston (Yu et al., 2015; Cui et al., 2019), and dounce homogenization (Benador et al., 2018). The centrifugal force has been utilized for sample from BAT and brown adipocytes ranging from 500 to 100,000*g* depending on the processes of isolation, washing, and separation. The high homogenization stringency and high centrifugal force can remove nonspecific bound contaminations but result missing of supersize LDs. But low centrifugal force cannot float small LDs efficiently (Zhang et al., 2016). Therefore, homogenization methods and centrifugal forces should be selected properly to control the quality, the size, and the type of LDs isolated from different tissues and cells.

Finally, based on previous studies from ours and other laboratories, the working hypothesis is proposed that there are two types of contact (dynamic and stable) between LDs and mitochondria in oxidative cells (**Figure 3**). The co-isolation method is introduced to study the contact between LDs and mitochondria, as well as other bilayer membrane-bound organelles. Combined with morphological and biochemical approaches, the co-isolation study is going to uncover new

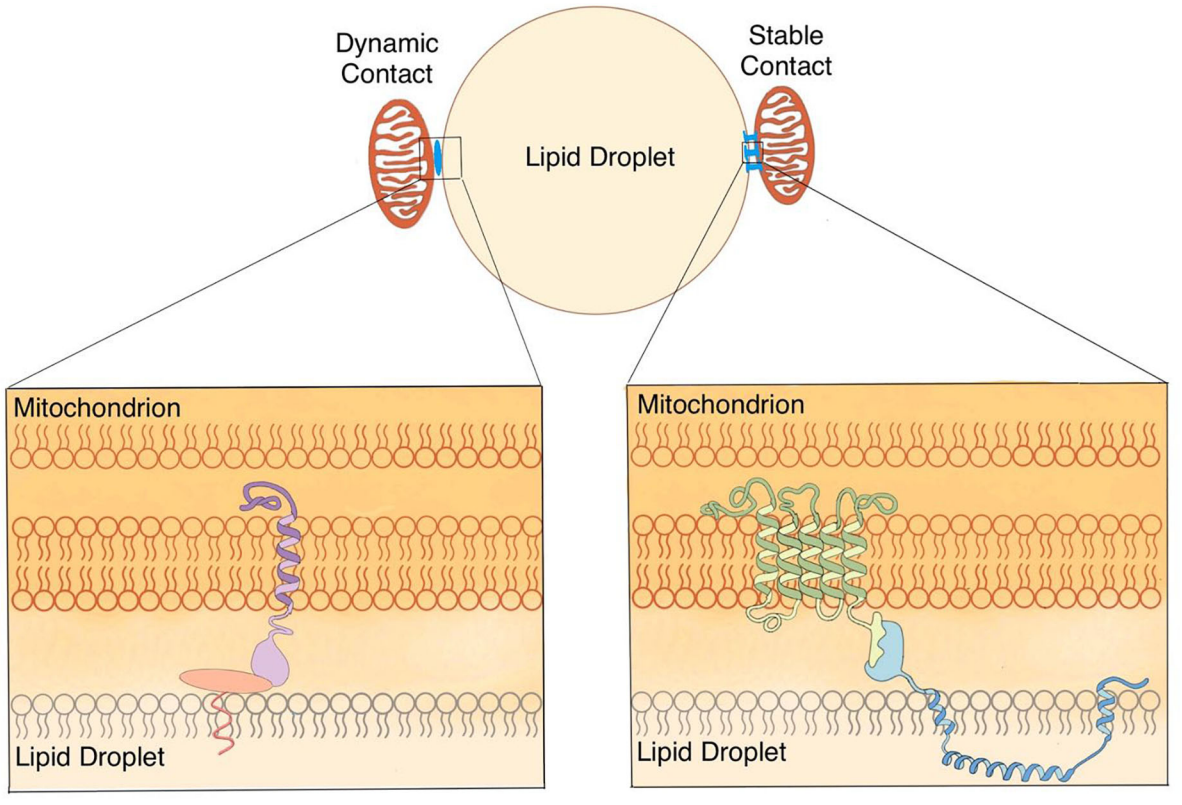

FIGURE 3 | Anchoring hypothesis of the contact between LDs and mitochondria. Based on previous studies from ours and other laboratories, the working hypothesis is proposed that there are two types of contact (dynamic and stable) between LDs and mitochondria in oxidative cells. Dynamic contact can tether LDs and mitochondria through protein complexes. Stable contact can anchor mitochondria on LDs by nail- or rivet-like proteins.

aspects toward to better dissect and understand the contact between these two organelles.

AUTHOR CONTRIBUTIONS

PL conceived the project. LC carried out the experiments and data analysis. LC and PL wrote the manuscript. Both authors contributed to the article and approved the submitted version.

FUNDING

This work was supported by the National Key R&D Program of China (Grant Nos. 2018YFA0800700, 2016YFA0500100, and 2018YFA0800900), National Natural Science Foundation of China (Grant Nos. 91857201, 91954108, 31671402, 31671233, 31701018, and U1702288). This work was also supported by the "Personalized Medicines-Molecular Signature-based Drug Discovery and Development," Strategic Priority Research Program of the Chinese Academy of Sciences, Grant No. XDA12040218.

ACKNOWLEDGMENTS

We thank Dr. John Zehmer for his critical reading and useful suggestions. We also thank Ms. Siyu Wang for her artwork of **Figure 3**.

REFERENCES

Barbosa, A. D., Savage, D. B., and Siniossoglou, S. (2015). Lipid droplet–organelle interactions: emerging roles in lipid metabolism. *Curr. Opin. Cell Biol.* 35, 91–97. doi: 10.1016/j.ceb.2015.04.017

Bartz, R., Li, W.-H., Venables, B., Zehmer, J. K., Roth, M. R., Welti, R., et al. (2007a). Lipidomics reveals that adiposomes store ether lipids and mediate phospholipid traffic. *J. Lipid Res.* 48, 837–847. doi: 10.1194/jlr.m600413-jlr200

Bartz, R., Zehmer, J. K., Zhu, M., Chen, Y., Serrero, G., Zhao, Y., and Liu, P. (2007b). Dynamic Activity of Lipid Droplets: Protein Phosphorylation and GTP-Mediated Protein Translocation. *J. Proteome. Res.* 6, 3256–3265. doi: 10.1021/pr070158j

Benador, I. Y., Veliova, M., Mahdaviani, K., Petcherski, A., Wikstrom, J. D., Assali, E. A., et al. (2018). Mitochondria bound to lipid droplets have unique bioenergetics, composition, and dynamics that support lipid droplet expansion. *Cell Metab.* 27, 869.e6–885.e6.

Binns, D., Januszewski, T., Chen, Y., Hill, J., Markin, V. S., Zhao, Y., et al. (2006). An intimate collaboration between peroxisomes and lipid bodies. *J. Cell Biol.* 173, 719–731. doi: 10.1083/jcb.200511125

Bosma, M., Minnaard, R., Sparks, L. M., Schaart, G., Losen, M., De Baets, M. H., et al. (2012). The lipid droplet coat protein perilipin 5 also localizes to muscle mitochondria. *Histochem. Cell Biol.* 137, 205–216. doi: 10.1007/s00418-011-0888-x

Boutant, M., Kulkarni, S. S., Joffraud, M., Ratajczak, J., Valera-Alberni, M., Combe, R., et al. (2017). Mfn2 is critical for brown adipose tissue thermogenic function. *EMBO J.* 36, 1543–1558. doi: 10.15252/embj.201694914

Brasaemle, D., Barber, T., Wolins, N. E., Serrero, G., Blanchette-Mackie, E. J., and Londos, C. (1997). Adipose differentiation-related protein is an ubiquitously expressed lipid storage droplet-associated protein. *J. Lipid Res.* 38, 2249–2263.

Brasaemle, D. L., Dolios, G., Shapiro, L., and Wang, R. (2004). Proteomic analysis of proteins associated with lipid droplets of basal and lipolytically stimulated 3T3-L1 adipocytes. *J. Biol. Chem.* 279, 46835–46842. doi: 10.1074/jbc.m409340200

Cui, L., Mirza, A. H., Zhang, S., Liang, B., and Liu, P. (2019). Lipid droplets and mitochondria are anchored during brown adipocyte differentiation. *Protein Cell* 10, 921–926. doi: 10.1007/s13238-019-00661-1

Ding, Y., Zhang, S., Yang, L., Na, H., Zhang, P., Zhang, H., et al. (2013). Isolating lipid droplets from multiple species. *Nat. Protoc.* 8:43. doi: 10.1038/nprot.2012.142

Freyre, C. A. C., Rauher, P. C., Ejsing, C. S., and Klemm, R. W. (2019). MIGA2 links mitochondria, the ER, and lipid droplets and promotes de novo Lipogenesis in Adipocytes. *Mol. Cell.* 76, 811.e4–825.e4.

Fujimoto, T., Ohsaki, Y., Cheng, J., Suzuki, M., and Shinohara, Y. (2008). Lipid droplets: a classic organelle with new outfits. *Histochem. Cell Biol.* 130, 263–279. doi: 10.1007/s00418-008-0449-0

Fujimoto, Y., Itabe, H., Kinoshita, T., Homma, K. J., Onoduka, J., Mori, M., et al. (2007). Involvement of ACSL in local synthesis of neutral lipids in cytoplasmic lipid droplets in human hepatocyte HuH7. *J. Lipid Res.* 48, 1280–1292. doi: 10.1194/jlr.m700050-jlr200

Fujimoto, Y., Itabe, H., Sakai, J., Makita, M., Noda, J., Mori, M., et al. (2004). Identification of major proteins in the lipid droplet-enriched fraction isolated from the human hepatocyte cell line HuH7. *Biochim. Biophys. Acta* 1644, 47–59. doi: 10.1016/j.bbamcr.2003.10.018

Géloën, A., Collet, A., Guay, G., and Bukowiecki, L. J. (1990). In vivo differentiation of brown adipocytes in adult mice: an electron microscopic study. *Am. J. Anat.* 188, 366–372. doi: 10.1002/aja.1001880404

Gemmink, A., Daemen, S., Kuijpers, H. J. H., Schaart, G., Duimel, H., Lopez-Iglesias, C., et al. (2018). Super-resolution microscopy localizes perilipin 5 at lipid droplet-mitochondria interaction sites and at lipid droplets juxtaposing to perilipin 2. *Biochim. Biophys. Acta Mol. Cell Biol. Lipids* 1863, 1423–1432. doi: 10.1016/j.bbalip.2018.08.016

Greenberg, A. S., Coleman, R. A., Kraemer, F. B., Mcmanaman, J. L., Obin, M. S., Puri, V., et al. (2011). The role of lipid droplets in metabolic disease in rodents and humans. *J. Clin. Investig.* 121, 2102–2110. doi: 10.1172/jci46069

Greenberg, A. S., Egan, J. J., Wek, S. A., Garty, N. B., Blanchette-Mackie, E., and Londos, C. (1991). Perilipin, a major hormonally regulated adipocyte-specific phosphoprotein associated with the periphery of lipid storage droplets. *J. Biol. Chem.* 266, 11341–11346.

Havaux, M. (1998). Carotenoids as membrane stabilizers in chloroplasts. *Trends Plant Sci.* 3, 147–151. doi: 10.1016/s1360-1385(98)01200-x

Herms, A., Bosch, M., Reddy, B. J. N., Schieber, N. L., Fajardo, A., Ruperez, C., et al. (2015). AMPK activation promotes lipid droplet dispersion on detyrosinated microtubules to increase mitochondrial fatty acid oxidation. *Nat. Commun.* 6:7176. doi: 10.1038/ncomms8176

Huang, T., Bamigbade, A. T., Xu, S., Deng, Y., Xie, K., Ogunsade, O. O., et al. (2020). Identification of noncoding RNA-encoded proteins on lipid droplets. *Sci. Bull.* doi: 10.1016/j.scib.2020.09.022 [Epub ahead of print].

Iacovache, I., Paumard, P., Scheib, H., Lesieur, C., Sakai, N., Matile, S., et al. (2006). A rivet model for channel formation by aerolysin-like pore-forming toxins. *EMBO J.* 25, 457–466. doi: 10.1038/sj.emboj.7600959

Jägerström, S., Polesie, S., Wickström, Y., Johansson, B. R., Schröder, H. D., Højlund, K., et al. (2009). Lipid droplets interact with mitochondria using SNAP23. *Cell Biol. Int.* 33, 934–940. doi: 10.1016/j.cellbi.2009.06.011

Jiang, H.-P., and Serrero, G. (1992). Isolation and characterization of a full-length cDNA coding for an adipose differentiation-related protein. *Proc. Natl. Acad. Sci. U.S.A.* 89, 7856–7860. doi: 10.1073/pnas.89.17.7856

Kim, S. C., Chen, Y., Mirza, S., Xu, Y., Lee, J., Liu, P., et al. (2006). A clean, more efficient method for in-solution digestion of protein mixtures without detergent or urea. *J. Proteome Res.* 5, 3446–3452. doi: 10.1021/pr0603396

Krahmer, N., Najafi, B., Schueder, F., Quagliarini, F., Steger, M., Seitz, S., et al. (2018). Organellar proteomics and phospho-proteomics reveal subcellular reorganization in diet-induced hepatic steatosis. *Dev. Cell* 47, 205–221.e207.

Kumar, N., Leonzino, M., Hancock-Cerutti, W., Horenkamp, F. A., Li, P., Lees, J. A., et al. (2018). VPS13A and VPS13C are lipid transport proteins differentially localized at ER contact sites. *J. Cell. Biol.* 217, 3625–3639. doi: 10.1083/jcb.201807019

Li, L., Zhang, H., Wang, W., Hong, Y., Wang, J., Zhang, S., et al. (2016). Comparative proteomics reveals abnormal binding of ATGL and dysferlin on

lipid droplets from pressure overload-induced dysfunctional rat hearts. *Sci. Rep.* 6:19782.

Liu, P., Bartz, R., Zehmer, J. K., Ying, Y.-S., Zhu, M., Serrero, G., et al. (2007). Rab-regulated interaction of early endosomes with lipid droplets. *Biochim. Biophys. Acta Mol. Cell Res.* 1773, 784–793. doi: 10.1016/j.bbamcr.2007.02.004

Liu, P., Ying, Y., Zhao, Y., Mundy, D. I., Zhu, M., and Anderson, R. G. (2004). Chinese hamster ovary K2 cell lipid droplets appear to be metabolic organelles involved in membrane traffic. *J. Biol. Chem.* 279, 3787–3792. doi: 10.1074/jbc.m311945200

Lupette, J., Jaussaud, A., Seddiki, K., Morabito, C., Brugiere, S., Schaller, H., et al. (2019). The architecture of lipid droplets in the diatom *Phaeodactylum tricornutum*. *Algal Res.* 38:101415. doi: 10.1016/j.algal.2019.101415

Martin, S., Driessen, K., Nixon, S. J., Zerial, M., and Parton, R. G. (2005). Regulated localization of Rab18 to lipid droplets: effects of lipolytic stimulation and inhibition of lipid droplet catabolism. *J. Biol. Chem.* 280, 42325–42335. doi: 10.1074/jbc.m506651200

Milakovic, I., Jeseta, M., Hanulakova, S., Knitlova, D., Hanzalova, K., Hulinska, P., et al. (2015). Energy status characteristics of porcine oocytes during *in vitro* maturation is influenced by their meiotic competence. *Reprod. Domest Anim.* 50, 812–819. doi: 10.1111/rda.12592

Murphy, D. J. (2001). The biogenesis and functions of lipid bodies in animals, plants and microorganisms. *Prog. Lipid Res.* 40, 325–438. doi: 10.1016/s0163-7827(01)00013-3

Murphy, D. J. (2012). The dynamic roles of intracellular lipid droplets: from archaea to mammals. *Protoplasma* 249, 541–585. doi: 10.1007/s00709-011-0329-7

Murphy, S., Martin, S., and Parton, R. G. (2009). Lipid droplet-organelle interactions; sharing the fats. *Biochim. Biophys. Acta Mol. Cell Biol. Lipids* 1791, 441–447. doi: 10.1016/j.bbalip.2008.07.004

Nguyen, T. B., Louie, S. M., Daniele, J. R., Tran, Q., Dillin, A., Zoncu, R., et al. (2017). DGAT1-dependent lipid droplet biogenesis protects mitochondrial function during starvation-induced autophagy. *Dev. Cell* 42, 9–21.e25. doi: 10.1016/Fj.devcel.2017.06.003

Ogasawara, Y., Tsuji, T., and Fujimoto, T. (2020). Multifarious roles of lipid droplets in autophagy – Target, product, and what else?. *Semin. Cell Dev. Biol.* [Epub ahead of print].

Ohue, M., and Makita, T. (1992). Interrelationship between lipid droplets and mitochondria in brown adipocytes of the hamster. *J. Vet. Med. Sci.* 54, 1131–1135. doi: 10.1292/jvms.54.1131

Olzmann, J. A., and Carvalho, P. (2019). Dynamics and functions of lipid droplets. *Nat. Rev. Mol. Cell Biol.* 20, 137–155. doi: 10.1038/s41580-018-0085-z

Ozeki, S., Cheng, J., Tauchi-Sato, K., Hatano, N., Taniguchi, H., and Fujimoto, T. (2005). Rab18 localizes to lipid droplets and induces their close apposition to the endoplasmic reticulum-derived membrane. *J. Cell Sci.* 118, 2601–2611. doi: 10.1242/jcs.02401

Peute, J., Van Der Gaag, M. A., and Lambert, J. G. D. (1978). Ultrastructure and lipid content of the liver of the zebrafish, Brachydanio rerio, related to vitellogenin synthesis. *Cell Tissue Res.* 186, 297–308. doi: 10.1007/bf00225539

Pribasnig, M., Kien, B., Pusch, L., Haemmerle, G., Zimmermann, R., and Wolinski, H. (2018). Extendedresolution imaging of the interaction of lipid droplets and mitochondria. *Biochim. Biophys. Acta Mol. Cell Biol. Lipids* 1863, 1285–1296.

Pu, J., Ha, C. W., Zhang, S., Jung, J. P., Huh, W.-K., and Liu, P. (2011). Interactomic study on interaction between lipid droplets and mitochondria. *Protein Cell* 2, 487–496. doi: 10.1007/s13238-011-1061-y

Rambold, A. S., Cohen, S., and Lippincott-Schwartz, J. (2015). Fatty acid trafficking in starved cells: regulation by lipid droplet lipolysis, autophagy, and mitochondrial fusion dynamics. *Dev. Cell* 32, 678–692. doi: 10.1016/j.devcel.2015.01.029

Ramos, S. V., Macpherson, R. E., Turnbull, P. C., Bott, K. N., Leblanc, P., Ward, W. E., et al. (2014). Higher PLIN5 but not PLIN3 content in isolated skeletal muscle mitochondria following acute in vivo contraction in rat hindlimb. *Physiol. Rep.* 2:e12154. doi: 10.14814/phy2.12154

Roberts, M. A., and Olzmann, J. A. (2020). Protein quality control and lipid droplet metabolism. *Annu. Rev. Cell Dev.Biol.* 36, 115–139. doi: 10.1146/annurev-cellbio-031320-101827

Schuldiner, M., and Bohnert, M. (2017). A different kind of love – lipid droplet contact sites. *Biochim. Biophys. Acta Mol. Cell Biol. Lipids* 1862, 1188–1196. doi: 10.1016/j.bbalip.2017.06.005

Shiozaki, M., Hayakawa, N., Shibata, M., Koike, M., Uchiyama, Y., and Gotow, T. (2011). Closer association of mitochondria with lipid droplets in hepatocytes and activation of Kupffer cells in resveratrol-treated senescence-accelerated mice. *Histochem. Cell Biol.* 136, 475–489.

Shulman, G. I. (2014). Ectopic fat in insulin resistance, dyslipidemia, and cardiometabolic disease. *N. Engl. J. Med.* 371, 1131–1141. doi: 10.1056/nejmra1011035

Stemberger, B. H., Walsh, R. M., and Patton, S. (1984). Morphometric evaluation of lipid droplet associations with secretory vesicles, mitochondria and other components in the lactating cell. *Cell Tissue Res.* 236, 471–475.

Song, Y.-F., Hogstrand, C., Ling, S.-C., Chen, G.-H., and Luo, Z. (2020). Creb-Pgc1α pathway modulates the interaction between lipid droplets and mitochondria and influences high fat diet-induced changes of lipid metabolism in the liver and isolated hepatocytes of yellow catfish. *J. Nutr. Biochem.* 80:108364. doi: 10.1016/j.jnutbio.2020.108364

Sturmey, R. G., O'toole, P. J., and Leese, H. J. (2006). Fluorescence resonance energy transfer analysis of mitochondrial:lipid association in the porcine oocyte. *Reproduction* 132, 829–837. doi: 10.1530/rep-06-0073

Tarique, I., Vistro, W. A., Bai, X., Yang, P., Hong, C., Huang, Y., et al. (2019). LIPOPHAGY: a novel form of steroidogenic activity within the LEYDIG cell during the reproductive cycle of turtle. *Reprod. Biol. Endocrinol.* 17:19. doi: 10.1186/s12958-019-0462-2

Tarnopolsky, M. A., Rennie, C. D., Robertshaw, H. A., Fedak-Tarnopolsky, S. N., Devries, M. C., and Hamadeh, M. J. (2007). Influence of endurance exercise training and sex on intramyocellular lipid and mitochondrial ultrastructure, substrate use, and mitochondrial enzyme activity. *Am. J. Physiol. Regul. Integr. Comp. Physiol.* 292, R1271–R1278.

Tauchi-Sato, K., Ozeki, S., Houjou, T., Taguchi, R., and Fujimoto, T. (2002). The surface of lipid droplets is a phospholipid monolayer with a unique fatty acid composition. *J. Biol. Chem.* 277, 44507–44512. doi: 10.1074/jbc.m207712200

Thiam, A. R., Farese, R. V. Jr., and Walther, T. C. (2013). The biophysics and cell biology of lipid droplets. *Nat. Rev. Mol. Cell Biol.* 14, 775–786. doi: 10.1038/nrm3699

Valm, A. M., Cohen, S., Legant, W. R., Melunis, J., Hershberg, U., Wait, E., et al. (2017). Applying systems-level spectral imaging and analysis to reveal the organelle interactome. *Nature* 546:162. doi: 10.1038/nature22369

Varghese, M., Kimler, V. A., Ghazi, F. R., Rathore, G. K., Perkins, G. A., Ellisman, M. H., et al. (2019). Adipocyte lipolysis affects Perilipin 5 and cristae organization at the cardiac lipid droplet-mitochondrial interface. *Sci. Rep.* 9:4734.

Vock, R., Hoppeler, H., Claassen, H., Wu, D. X., Billeter, R., Weber, J. M., et al. (1996). Design of the oxygen and substrate pathways. VI. structural basis of intracellular substrate supply to mitochondria in muscle cells. *J. Exp. Biol.* 199:1689.

Walther, T. C., and Farese, R. V. (2012). Lipid droplets and cellular lipid metabolism. *Annu. Rev. Biochem.* 81, 687–714. doi: 10.1146/annurev-biochem-061009-102430

Wang, H., Lei, M., Hsia, R.-C., and Sztalryd, C. (2013). "Chapter 8–analysis of lipid droplets in cardiac muscle," in *Methods in Cell Biology*, eds H. Yang and P. Li (Cambridge, MA: Academic Press), 129–149. doi: 10.1016/b978-0-12-408051-5.00008-5

Wang, H., Sreenivasan, U., Hu, H., Saladino, A., Polster, B. M., Lund, L. M., et al. (2011). Perilipin 5, a lipid droplet-associated protein, provides physical and metabolic linkage to mitochondria. *J. Lipid Res.* 52, 2159–2168. doi: 10.1194/jlr.m017939

Wasilewski, M., Semenzato, M., Rafelski, S. M., Robbins, J., Bakardjiev, A. I, and Scorrano, L. (2012). Optic atrophy 1-dependent mitochondrial remodeling controls steroidogenesis in trophoblasts. *Curr. Biol.* 22, 1228–1234. doi: 10.1016/j.cub.2012.04.054

Welte, M. A., Gross, S. P., Postner, M., Block, S. M., and Wieschaus, E. F. (1998). Developmental regulation of vesicle transport in *Drosophila* embryos: forces and kinetics. *Cell* 92, 547–557. doi: 10.1016/s0092-8674(00)80947-2

Wu, C. C., Howell, K. E., Neville, M. C., Yates Iii, J. R., and Mcmanaman, J. L. (2000). Proteomics reveal a link between the endoplasmic reticulum and lipid secretory mechanisms in mammary epithelial cells. *Electrophoresis Int. J.* 21, 3470–3482. doi: 10.1002/1522-2683(20001001)21:16<3470::aid-elps3470>3.0.co;2-g

Wu, L., Xu, D., Zhou, L., Xie, B., Yu, L., Yang, H., et al. (2014). Rab8a-AS160-MSS4 regulatory circuit controls lipid droplet fusion and growth. *Dev. Cell* 30, 378–393. doi: 10.1016/j.devcel.2014.07.005

Xie, K., Zhang, P., Na, H., Liu, Y., Zhang, H., and Liu, P. (2019). MDT-28/PLIN-1 mediates lipid droplet-microtubule interaction via DLC-1 in *Caenorhabditis elegans*. *Sci. Rep.* 9:14902.

Xu, S., Zhang, X., and Liu, P. (2018). Lipid droplet proteins and metabolic diseases. *Biochim. Biophys. Acta Mol. Basis Dis.* 1864, 1968–1983. doi: 10.1016/j.bbadis.2017.07.019

Yu, J., Zhang, S., Cui, L., Wang, W., Na, H., Zhu, X., et al. (2015). Lipid droplet remodeling and interaction with mitochondria in mouse brown adipose tissue during cold treatment. *Biochim. Biophys. Acta* 1853, 918–928. doi: 10.1016/j.bbamcr.2015.01.020

Zechner, R., Madeo, F., and Kratky, D. (2017). Cytosolic lipolysis and lipophagy: two sides of the same coin. *Nat. Rev. Mol. Cell Biol.* 18:671. doi: 10.1038/nrm.2017.76

Zehmer, J. K., Huang, Y., Peng, G., Pu, J., Anderson, R. G. W., and Liu, P. (2009). A role for lipid droplets in inter-membrane lipid traffic. *Proteomics* 9, 914–921. doi: 10.1002/pmic.200800584

Zhang, C., and Liu, P. (2019). The new face of the lipid droplet: lipid droplet proteins. *Proteomics* 19:1700223. doi: 10.1002/pmic.201700223

Zhang, H., Wang, Y., Li, J., Yu, J., Pu, J., Li, L., et al. (2011). Proteome of skeletal muscle lipid droplet reveals association with mitochondria and apolipoprotein a-I. *J. Proteome Res.* 10, 4757–4768. doi: 10.1021/pr200553c

Zhang, S., Wang, Y., Cui, L., Deng, Y., Xu, S., Yu, J., et al. (2016). Morphologically and functionally distinct lipid droplet subpopulations. *Sci. Rep.* 6:29539.

Conflict of Interest: The authors declare that the research was conducted in the absence of any commercial or financial relationships that could be construed as a potential conflict of interest.

frontiers in Cell and Developmental Biology

REVIEW
published: 15 December 2020
doi: 10.3389/fcell.2020.615600

Lipid Transfer–Dependent Endosome Maturation Mediated by Protrudin and PDZD8 in Neurons

*Michiko Shirane**

Department of Molecular Biology, Graduate School of Pharmaceutical Sciences, Nagoya City University, Nagoya, Japan

Endosome maturation refers to the conversion of early endosomes (EEs) to late endosomes (LEs) for subsequent fusion with lysosomes. It is an incremental process that involves a combination of endosome fusion and fission and which occurs at contact sites between endosomes and the endoplasmic reticulum (ER), with knowledge of the underlying mechanisms having increased greatly in recent years. Protrudin is an ER-resident protein that was originally shown to regulate neurite formation by promoting endosome trafficking, whereas PDZD8 is a mammalian paralog of a subunit of the yeast ERMES (ER-mitochondrial encounter structure) complex that possesses lipid transfer activity. A complex of protrudin and PDZD8 was recently found to promote endosome maturation by mediating lipid transfer at ER-endosome membrane contact sites. This review focuses on the roles of the protrudin-PDZD8 complex in tethering of endosomes to the ER, in mediating lipid transfer at such contact sites, and in regulating endosome dynamics, especially in neuronal cells. It also addresses the physiological contribution of endosome maturation mediated by this complex to neuronal polarity and integrity.

Keywords: organelle, endoplasmic reticulum, endosome, membrane contact site, neuron, PDZD8, protrudin, lipid transfer

OPEN ACCESS

Edited by:
Benoît Kornmann,
University of Oxford, United Kingdom

Reviewed by:
Harald Stenmark,
University of Oslo, Norway
Yusuke Hirabayashi,
The University of Tokyo, Japan
Andrés Guillén-Samander,
Yale University, United States

***Correspondence:**
Michiko Shirane
shiram@phar.nagoya-cu.ac.jp

Specialty section:
This article was submitted to Membrane Traffic, a section of the journal Frontiers in Cell and Developmental Biology

Received: *09 October 2020*
Accepted: *23 November 2020*
Published: *15 December 2020*

Citation:
Shirane M (2020) Lipid Transfer–Dependent Endosome Maturation Mediated by Protrudin and PDZD8 in Neurons. Front. Cell Dev. Biol. 8:615600. doi: 10.3389/fcell.2020.615600

INTRODUCTION

Most intracellular organelles of eukaryotic cells communicate with the endoplasmic reticulum (ER) network through membrane contact sites (MCSs), at which the membranes of the ER and the interacting organelle come into close proximity and are tethered. MCSs are thus thought to function as intracellular synapses, where molecular information is exchanged.

Neurons are polarized cells that consist of two distinct portions, the somatodendritic compartment and the axon. Trafficking of endosomes along the axon toward its terminus plays an important role in axonal outgrowth directed toward target cells as well as in neurotransmitter release. Protrudin was first identified as a protein that promotes neurite outgrowth through regulation of directional endosome trafficking (Shirane and Nakayama, 2006; Shirane, 2019). The protrudin binding proteins VAP [vesicle-associated membrane protein (VAMP)–associated protein] and KIF5 (kinesin heavy chain 5) also contribute to endosome trafficking (Saita et al., 2009; Matsuzaki et al., 2011), and protrudin-dependent regulation of such trafficking is mediated at MCSs between the ER and late endosomes (LEs) (Raiborg et al., 2015).

Axonopathy, a type of neurodegeneration, is caused by damage to the axon of neurons. The longest axons in the central nervous system of mammals are located in the corticospinal tract, which is the neural circuit responsible for voluntary movement. Hereditary spastic paraplegia (HSP) is an axonopathy in which upper motor neurons in the corticospinal tract undergo degeneration (Blackstone, 2012; Hubner and Kurth, 2014). Many HSP-related proteins—including spastin, REEPs (receptor expression–enhancing proteins), reticulons, atlastins, as well as protrudin—have been identified (Mannan et al., 2006; Hashimoto et al., 2014; Pyle et al., 2015; Connell et al., 2020). Most such proteins contain a hairpin domain, which is a key determinant of membrane structure and function in the ER. HSP-related proteins have recently been implicated in the regulation of endosome maturation at ER-endosome MCSs (Allison et al., 2017), although the physiological role and regulatory mechanisms of such maturation remain to be fully elucidated. A new study has now revealed that protrudin-dependent lipid transfer from the ER to endosomes promotes endosome maturation at ER-endosome MCSs (Shirane et al., 2020b). Protrudin-deficient mice show no signs of axonopathy, however, but instead manifest an abnormal behavioral phenotype (Shirane et al., 2020a), suggesting that protrudin might play an important role in normal neuronal development and behavior.

In this review, I summarize what is known of the mechanism responsible for regulation of endosome maturation by protrudin and its relation to the pathogenesis of neurological disease. We also address the role of PDZD8 (PDZ domain–containing protein 8), a protrudin-interacting protein, in the lipid transfer process underlying endosome maturation. Finally, we discuss the contribution of the protrudin-PDZD8 complex and its lipid transfer function to the maintenance of neuronal polarity and integrity.

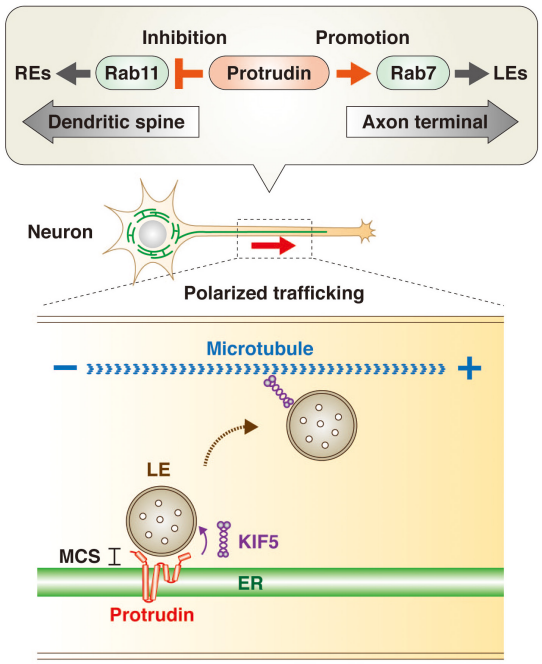

FIGURE 1 | Protrudin regulates endosome dynamics underlying directional endosome trafficking in neuronal cells through interaction with Rab GTPases and KIF5. Protrudin interacts with the GDP-bound (inactive) form of Rab11 and thereby inhibits RE trafficking toward dendritic spines. It also interacts with the GTP-bound (active) form of Rab7 and thereby promotes LE trafficking toward the axon terminal (upper insert). In addition, protrudin tethers LEs to the ER at MCSs, where it loads LEs with the microtubule-dependent motor protein KIF5. The subsequent release of the KIF5-loaded LEs to microtubules results in their transport from the minus end to the plus end of the microtubules in the direction of the axon terminal (lower insert).

PROTRUDIN REGULATES DIRECTIONAL ENDOSOME TRAFFICKING

Protrudin was originally discovered as a protein of unknown function that interacts with FK506 binding protein 38 (FKBP38) (Shirane and Nakayama, 2003; Shirane et al., 2008; Saita et al., 2013). Forced expression of protrudin in cultured cells resulted in pronounced membrane deformation followed by the formation of long protrusions, hence the designation "protrudin" (Shirane and Nakayama, 2006). Protrudin is an ER-resident protein that harbors various functional domains including a Rab11 binding domain (RBD11), two transmembrane (TM) domains, a hairpin (HP) domain, a low complexity region (LCR), a two phenylalanine in an acidic tract (FFAT) motif, a coiled-coil (CC) domain, and a Fab1, YOTB, Vac1, and EEA1 (FYVE) domain. These structural characteristics underlie the multiple functions of protrudin in the regulation of organelle dynamics including directional endosome trafficking and ER morphogenesis.

Rab GTPases are master regulators and markers of organelle identity in the endocytic pathway (Zerial and McBride, 2001; Stenmark, 2009; Wandinger-Ness and Zerial, 2014). The transformation of early endosomes (EEs) to LEs is accompanied by a switch in associated Rab protein from Rab5 to Rab7, whereas recycling endosomes (REs) are associated with Rab11. The GTP-bound (active) form of Rab11 promotes directional trafficking of REs from the apical to the basolateral domain of epithelial cells as well as from the axonal to the somatodendritic domain of neurons. In contrast, the GTP-bound form of Rab7 promotes LE trafficking toward the axon terminal in neuronal cells. Protrudin interacts with both the GDP-bound (inactive) form of Rab11 (Shirane and Nakayama, 2006) and the GTP-bound form of Rab7 (Raiborg et al., 2015) and appears to function as a hub for endosomal trafficking by inhibiting Rab11-dependent RE trafficking and promoting Rab7-dependent LE trafficking (**Figure 1**). Protrudin thus increases the supply of membrane to the tip of neurites by facilitating axonal transport of membrane-containing endosomes, resulting in polarized neurite outgrowth.

Protrudin also interacts with the microtubule-dependent motor protein KIF5, which mediates anterograde cargo trafficking along microtubules of axons in the plus-end direction (Saita et al., 2009; Matsuzaki et al., 2011; Ohnishi et al., 2014). Indeed, protrudin was recently shown to facilitate loading of the endosome membrane with KIF5 at ER-LE MCSs, with the KIF5-loaded endosomes then being released for interaction with microtubules (Raiborg et al., 2015; **Figure 1**).

VAP has also been identified as a protrudin binding protein (Saita et al., 2009), with the major sperm protein (MSP) domain of VAP mediating interaction with the FFAT motif of protrudin. VAP resides at MCSs and is implicated in lipid transfer processes (Helle et al., 2013; Phillips and Voeltz, 2016; Salvador-Gallego et al., 2017; Wu et al., 2018). Both the interaction of protrudin with VAP and the induction of process formation by protrudin were found to be attenuated by mutation of the FFAT motif of protrudin. Knockdown of VAP also resulted in mislocalization of protrudin and in inhibition of neurite outgrowth induced by nerve growth factor in PC12 pheochromocytoma cells, suggesting that binding to VAP is indispensable for the regulation of endosome trafficking by protrudin (Saita et al., 2009).

The precursor mRNA for protrudin is alternatively spliced, resulting in the generation of mature transcripts for two different isoforms of protrudin, designated L (long) and S (short) (Ohnishi et al., 2014). Protrudin-S appears to be ubiquitously expressed in mammalian tissues, whereas protrudin-L is expressed specifically in neuronal cells. Relative to protrudin-S, protrudin-L contains an additional seven amino acids encoded by exon L. These additional residues are located adjacent to the FFAT motif, which mediates binding to VAP, with the result that the binding affinity of protrudin-L for VAP is greater than that of protrudin-S. Protrudin-L is thus more effective at promoting neurite outgrowth than is protrudin-S. The neural-specific splicing regulator SRRM4 was found to promote the splicing of protrudin pre-mRNA to yield protrudin-L mRNA (Ohnishi et al., 2017).

ENDOSOME MATURATION AT ER-ENDOSOME MCSs

Endosomes play an important role in fundamental cellular activities. A subset of EEs formed by endocytosis through invagination of the plasma membrane undergoes conversion to LEs. LEs contain multiple intraluminal vesicles (ILVs) that are derived from luminal invaginations of the LE membrane, and so they are also known as multivesicular bodies (MVBs) (Huotari and Helenius, 2011). Endosome maturation is the process by which EEs are converted to LEs for fusion with lysosomes, which degrade endocytosed material for reutilization. It is an incremental process, with the vesicles on this continuum being collectively referred to as endolysosomes (LyLEs) (Hong et al., 2017). In addition to this degradation pathway dependent on the endocytic machinery, another subset of EEs is delivered to a recycling pathway, in which the EEs are converted to REs for recycling of material back to the plasma membrane. Some LEs also undergo exocytosis, resulting in the release of their ILVs as extracellular vesicles known as exosomes, which play a key role in intercellular communication (Colombo et al., 2014).

The membrane dynamics of endosome maturation are largely attributable to a combination of endosome fission and fusion (Rowland et al., 2014; Allison et al., 2017; Hoyer et al., 2018). Such fission and fusion as well as the transport of LEs are thought to depend on lipid transfer at ER-endosome MCSs (Johansson et al., 2005, 2007). However, the factors that tether endosomes to the ER at MCSs and the mechanism underlying such lipid transfer from the ER to endosomes had been mostly unknown until recently (Kobuna et al., 2010; Huotari and Helenius, 2011; van der Kant and Neefjes, 2014; Dong et al., 2016; Wong et al., 2018).

RELATION OF ER-ENDOSOME MCSs TO THE MECHANISM OF AXONOPATHY

Mutations of the protrudin gene (*ZFYVE27*) are responsible for a subset of cases of HSP (Mannan et al., 2006; Zhang et al., 2012; Hashimoto et al., 2014; Hubner and Kurth, 2014; Powers et al., 2017; Fowler et al., 2019). The genes mutated in different subsets of individuals with HSP are referred to as spastic paraplegia genes (SPGs), and protrudin is therefore also referred to as SPG33. The predominant clinical features of HSP are progressive spasticity and weakness of the lower limbs caused by degeneration of the long axons of motor neurons in the corticospinal tract. Proteomics analysis of the brain of neuron-specific protrudin transgenic mice showed that protrudin associates with multiple HSP-related proteins including myelin proteolipid protein 1 (SPG2), atlastin 1 (SPG3A), REEP1 (SPG31), REEP5, KIF5A (SPG10), KIF5B, KIF5C, and reticulons 1, 3, and 4 (which are similar to reticulon 2, or SPG12) (Hashimoto et al., 2014). Protrudin was also found to bind to spastin (SPG4) (Mannan et al., 2006). These various HSP-related proteins contain an HP domain, a hydrophobic wedge-shaped structure whose insertion into the cytosolic side of the ER membrane results in bending of the membrane bilayer and the formation of high-curvature tubules (Shibata et al., 2006; Voeltz et al., 2006; Hu et al., 2008, 2009). The axonopathy associated with HSP has therefore been suggested to result from an abnormal ER morphology that affects the smooth ER network and increases susceptibility to ER stress (Hashimoto et al., 2014; **Figure 2**). HSP caused by mutation of the protrudin gene may thus be attributable to a dominant negative effect resulting from accumulation of the mutant protein in the ER membrane and consequent ER stress.

Neurons with HSP-associated mutations of the genes for spastin or REEP1 were recently found to manifest abnormal enlargement of LEs and lysosomal dysfunction as a result of defects in ER-endosome MCSs and impaired endosomal homeostasis (Allison et al., 2017; Lee et al., 2020). As described in more detail below, disruption of the protrudin-PDZD8 complex has also been shown to result in the formation of abnormal LEs as well as in disturbance of neuronal polarity and axonal degeneration (Shirane et al., 2020b). These findings implicate the protrudin-PDZD8 complex in regulation of endosome maturation at ER-endosome MCSs.

A recent study has shed light on the physiological role of protrudin by subjecting protrudin-deficient mice to a comprehensive battery of behavioral tests (Shirane et al., 2020a). The protrudin-deficient mice showed no signs reminiscent of HSP, but instead manifested depression-like behavior with abnormalities in activity, attention, and cued fear-conditioning. Mutations of the protrudin gene therefore likely give rise to axonopathy as a result of a gain of toxic function, whereas

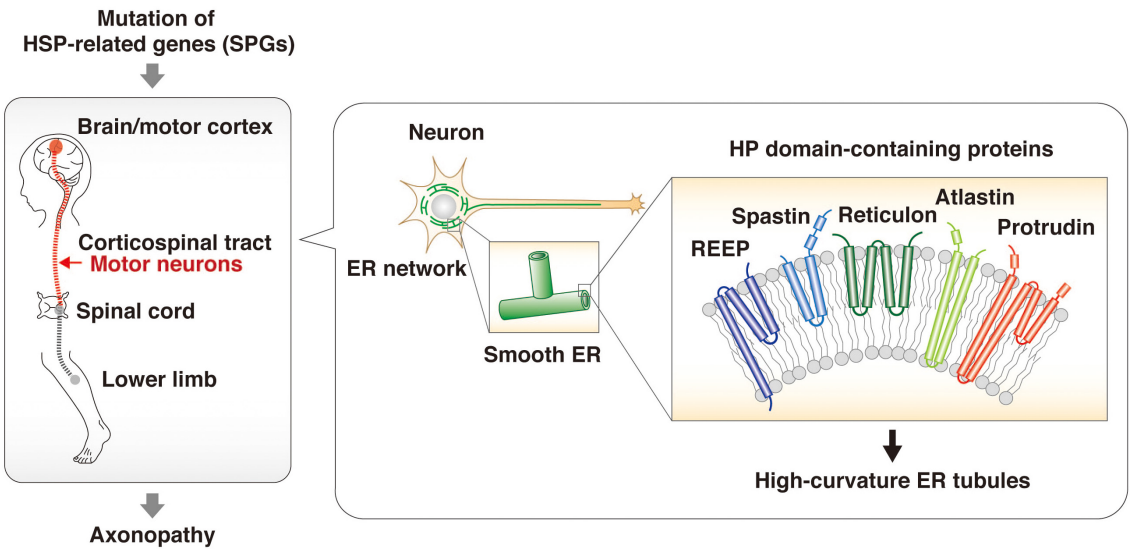

FIGURE 2 | HSP-related proteins regulate ER morphology through HP domains. HSP is an axonopathy that is caused by mutation of various genes and which is characterized by the degeneration of motor neurons in the corticospinal tract and consequent progressive spasticity and weakness of the lower limbs. The proteins encoded by such HSP-related genes—including spastin, REEPs, atlastins, and reticulons as well as protrudin—contain an HP domain. This hydrophobic wedge-shaped domain inserts into the cytosolic side of the ER membrane, resulting in bending of the membrane bilayer and the formation of high-curvature tubules. The HSP-associated mutant forms of these proteins give rise to structural defects in the smooth ER and an abnormal ER network.

protrudin nullizygosity gives rise to psychiatric-like disorders as a result of a loss of function. These findings suggest that protrudin might play an indispensable role in normal neuronal development and behavior (**Figure 3**).

THE PROTRUDIN-PDZD8 COMPLEX AT ER-ENDOSOME MCSs

A differential proteomics analysis of brain extracts from wild-type and protrudin-deficient mice was performed to identify proteins that might function cooperatively with protrudin at ER-endosome MCSs. This analysis uncovered PDZD8, in addition to VAP-A and VAP-B, as a key binding partner of protrudin (Elbaz-Alon et al., 2020; Shirane et al., 2020b). An independent study also identified protrudin as a binding partner of PDZD8 (Elbaz-Alon et al., 2020). PDZD8 is a mammalian paralog of yeast Mmm1, a subunit of the ER-mitochondrial encounter structure (ERMES) complex. This complex mediates interaction between the ER and mitochondria and contributes to the biosynthesis of phospholipids by mediating lipid transfer in a manner dependent on the synaptotagmin-like mitochondrial lipid–binding protein (SMP) domain of Mmm1 (**Figure 4**; Kornmann et al., 2009). Although PDZD8 was also known to tether the ER and mitochondria and to regulate Ca^{2+} dynamics in neurons (Hirabayashi et al., 2017), it was only shown to possess lipid transfer activity after its identification as a binding partner of protrudin (Shirane et al., 2020b). Protrudin and PDZD8 form a stable complex at the ER membrane, with the abundance of protrudin being greatly diminished in the brain of PDZD8-deficient mice. Knockdown of PDZD8 in PC12 cells also resulted in a loss of protrudin that was dependent on the proteasome (Shirane et al., 2020b).

Immunofluorescence analysis by super-resolution microscopy revealed that, like protrudin, PDZD8 is located at MCSs between the ER and endosomes (Shirane et al., 2020b). PDZD8 colocalized to a markedly greater extent with the ER than with endosomes at these MCSs, consistent with the notion that it is an ER-resident protein that makes contact with endosomes. The number of ER-endosome contacts was also found to be reduced in cells depleted of protrudin or PDZD8 by RNA interference. Although such depletion of protrudin or PDZD8 also attenuated MCS formation between the ER and mitochondria, this effect was less pronounced than that on ER-endosome contacts. Furthermore, protrudin and PDZD8 showed a synergistic effect on formation of ER-endosome contacts (Shirane et al., 2020b).

PDZD8 also contains a CC domain that interacts with the GTP-bound form of Rab7, which localizes to LEs (Chavrier et al., 1990; Raiborg et al., 2015; Guillen-Samander et al., 2019). In addition, a recent study suggested that the protrudin-PDZD8 complex resides at a microdomain at which three organelles—the ER, endosomes, and mitochondria—come into contact with each other (Elbaz-Alon et al., 2020). However, further studies are needed to reveal the physiological function of such ER-endosome-mitochondrion contacts mediated by the protrudin-PDZD8 complex.

PDZD8 POSSESSES LIPID TRANSFER ACTIVITY

MCSs mediate lipid transfer, Ca^{2+} homeostasis, and organelle dynamics. PDZD8 regulates Ca^{2+} dynamics in neurons, and it

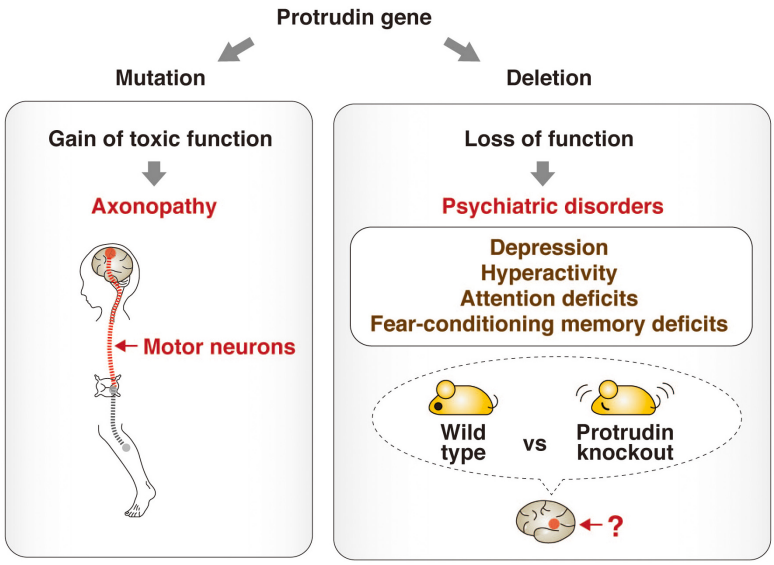

FIGURE 3 | Phenotypes associated with point mutation or deletion of the protrudin gene. Mutations of the protrudin gene (*ZFYVE27*) in humans give rise to axonopathy as a result of degeneration of motor neurons caused by a gain of toxic function (left). In contrast, deletion of the protrudin gene in mice gives rise to psychiatric-like disorders including depression-like behavior with abnormalities in activity, attention, and cued fear-conditioning as a result of a loss of function (right). The pathophysiologic mechanism, including the identity of the affected brain regions and neuronal circuits, underlying such behavioral defects in protrudin-deficient mice remains to be determined, but these deficits suggest that protrudin might play an indispensable role in the nervous system.

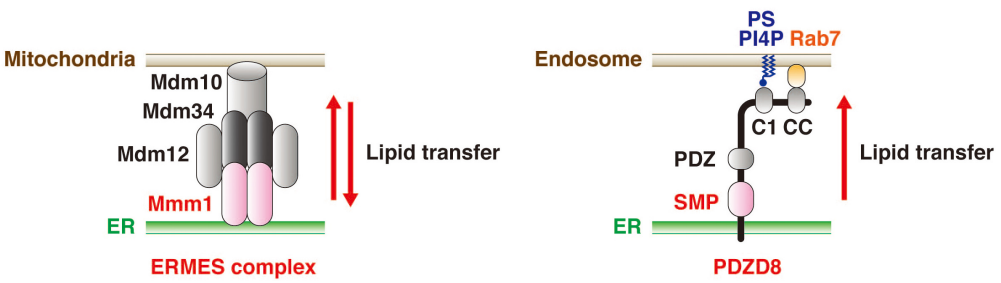

FIGURE 4 | PDZD8 mediates lipid transfer from the ER to endosomes. The yeast ERMES complex—which contains Mmm1, Mdm12, Mdm10, and Mdm34—mediates the transfer of phospholipids between the ER and mitochondria in both directions (left). On the other hand, PDZD8, a mammalian paralog of Mmm1, mediates the transfer of several types of lipid from the ER to endosomes in a manner dependent on its SMP domain (right). The C1 domain of PDZD8 contributes to tethering of endosomes to the ER through its interaction with PS or PI4P in the endosome membrane. The CC domain of PDZD8 also supports such tethering through its interaction with the GTP-bound form of Rab7.

contains a SMP domain characteristic of the TULIP (tubular lipid-binding protein) superfamily of proteins that possess lipid transfer activity (Kopec et al., 2010; Watanabe et al., 2015; Alva and Lupas, 2016). Furthermore, as mentioned above, the yeast PDZD8 paralog Mmm1 mediates lipid transfer by the ERMES complex (Kornmann et al., 2009). A liposome–FRET (fluorescence resonance energy transfer) assay was therefore applied to determine whether PDZD8 also possesses lipid transfer activity. For this assay, donor liposomes were prepared by mixing rhodamine-labeled lipid and nitrobenzoxadiazole (NBD)–labeled lipid, with the result that NBD fluorescence was quenched by FRET. Extraction of lipids from the donor liposomes and their dispersal by PDZD8 would abolish such quenching and thereby allow the detection of NBD fluorescence. This assay revealed that phospholipids—including phosphatidic acid, phosphatidylserine (PS), phosphatidylethanolamine, and phosphatidylcholine—as well as ceramide and cholesterol were extracted from the donor liposomes by PDZD8 (Shirane et al., 2020b).

Lipid transfer between membranes comprises two steps, lipid extraction from the donor membrane and lipid insertion into the acceptor membrane. These steps are distinguishable by performance of the liposome-FRET assay in the absence or presence of acceptor liposomes. Such analysis showed that PDZD8 possesses only lipid extraction activity, with this activity presumably being unidirectional from the ER to other organelles *in vivo*. In addition, both the SMP and PDZ domains of PDZD8 were found to contribute to this lipid extraction activity. As a result of the insolubility of full-length PDZD8, the

liposome-FRET assay was performed with a recombinant protein consisting of glutathione S-transferase (GST) fused to a form of PDZD8 lacking the TM domain [PDZD8(ΔTM)]. The mutant protein was thus unable to dock in the liposome membrane. This drawback was subsequently addressed by the addition of DGS-NTA(Ni), a conjugated phospholipid that binds the hexahistidine epitope tag, to the donor liposomes. Performance of the assay with His_6-PDZD8(ΔTM) thus allowed association of the tagged PDZD8 protein with the liposome membrane. Under these conditions, PDZD8 also showed lipid extraction activity (Shirane et al., 2020b).

Although the typical C1 domain binds to diacylglycerol, PDZD8 possesses a C1 domain that was found to preferentially interact with PS and phosphatidylinositol 4-phosphate (PI4P) but not with diacylglycerol (Shirane et al., 2020b). By analogy to extended synaptotagmin (E-Syt) proteins (Giordano et al., 2013; Schauder et al., 2014; Saheki et al., 2016; Bian et al., 2018), the C1 domain of PDZD8 might tether the ER and endosomes by interaction with PS and PI4P enriched in the endosome membrane. Such ER-endosome tethering might be regulated by an intracellular signal that induces a conformational change of PDZD8, resulting in an increase in lipid extraction activity mediated by its SMP domain. The tethering is also promoted by interaction between the CC domain of PDZD8 and the GTP-bound form of Rab7 (Raiborg et al., 2015; Guillen-Samander et al., 2019). PDZD8 likely promotes lipid transfer *in vivo* (**Figure 4**), given that depletion of PDZD8 results in a decrease in the abundance of PS in endosomes of neurons (Shirane et al., 2020b). However, further experiments will be required to demonstrate definitively the physiological lipid transfer activity of PDZD8.

LIPID TRANSFER PROTEINS AT ER-ENDOSOME MCSs

The mechanism underlying lipid transfer at MCSs has been extensively studied, with multiple tethering factors and lipid

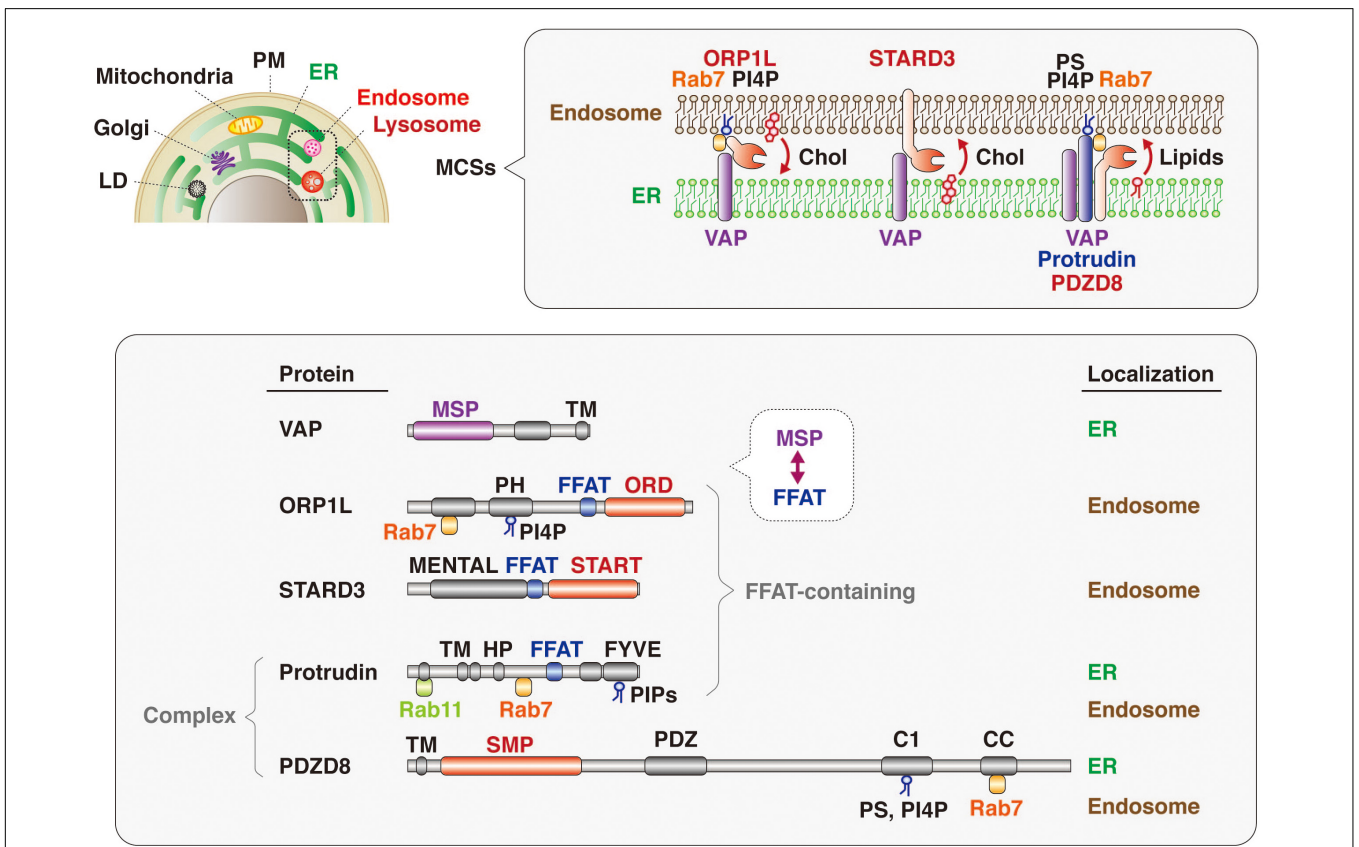

FIGURE 5 | Lipid transfer proteins at ER-endosome MCSs. Many intracellular compartments—including endosomes, lysosomes, the plasma membrane (PM), mitochondria, the Golgi apparatus, and lipid droplets (LD)—are tethered to the ER at MCSs (upper). Representative protein complexes that tether the ER and endosomes are shown (upper insert). ORP1L, which is recruited to endosomes through PI4P and Rab7, interacts with the ER-resident protein VAP and transfers cholesterol (Chol) from endosomes to the ER. The endosome-resident protein STARD3 binds to VAP and transports cholesterol from the ER to endosomes. The protrudin-PDZD8-VAP complex, which is localized at the ER and tethers endosomes through interaction with Rab7 and phosphoinositides (PIPs), transfers lipids from the ER to endosomes. The domain structure and subcellular localization of these various proteins are also shown (lower). The MSP domain of VAP interacts with the FFAT motifs of lipid transfer proteins such as ORP1L and STARD3. Both ORP1 and STARD3 possess lipid transfer domains: ORD and START, respectively. Protrudin also has an FFAT motif, and PDZD8 harbors a lipid transfer–related SMP domain. Both protrudin and PDZD8 interact with Rab7 and PIPs associated with the endosome membrane.

transfer proteins having been identified, including those that function at MCSs between the ER and endosomes (**Figure 5**). VAP (VAP-A and VAP-B) is an ER-resident protein that tethers other organelles to the ER and plays a key role in lipid transfer. VAP interacts via its MSP domain with multiple proteins that contain an FFAT motif (Kaiser et al., 2005; Loewen and Levine, 2005; Saita et al., 2009; Huttlin et al., 2015). Mutations in the MSP domain of VAP-B (also known as ALS8) are responsible for a dominant form of amyotrophic lateral sclerosis (ALS) (Nishimura et al., 2004). FFAT motif–containing proteins that contribute to tethering and lipid transfer at MCSs include oxysterol binding protein (OSBP)–related proteins (ORPs), steroidogenic acute regulatory protein (StAR)–related lipid transfer (START) domain–containing proteins, phosphatidylinositol transporter protein (PITP) domain–containing proteins, and Sec14-like proteins. With regard to lipid transfer at ER-endosome MCSs, OSBP and ORPs transport lipids such as sterol and phosphoinositides at MCSs (Olkkonen and Li, 2013); OSBP together with SNX2 and VAP regulates endosome budding through control of actin nucleation and retromer function at ER-endosome MCSs (Dong et al., 2016); ORP1L transports cholesterol from endosomes to the ER in cooperation with VAP and Rab7 (Zhao and Ridgway, 2017; Ma et al., 2018); and ORP5 together with NPC1 mediates the exit of cholesterol from LyLEs at MCSs (Du et al., 2011). The START domain–containing protein STARD3 is anchored to the membrane of LEs and mediates cholesterol transport from the ER to endosomes in concert with VAP (Alpy et al., 2013; Wilhelm et al., 2017). VPS13C, which is associated with early-onset Parkinson's disease, also tethers the ER and endosomes and transfers lipids at MCSs in cooperation with VAP and Rab7 (Lesage et al., 2016; Kumar et al., 2018; Gillingham et al., 2019).

It has also now been revealed that PDZD8, which harbors a lipid transfer–related SMP domain, interacts with the FFAT motif–containing protein protrudin as well as with Rab7. The protrudin-PDZD8 complex tethers the LyLE membrane to the ER and promotes lipid transfer from the ER to endosomes (**Figure 5**). The FYVE domain of protrudin is atypical in that the amino acid sequences responsible for binding to PI3P are not conserved and that it binds to several lipids such as PI(4,5)P_2, PI(3,4)P_2, and PI(3,4,5)P_3 (Gil et al., 2012). Furthermore, Rab7 interacts with both protrudin and PDZD8 (Raiborg et al., 2015; Guillen-Samander et al., 2019). However, it remains an open question and warrants further investigation whether both protrudin and PDZD8 are bound to the endosomal membrane simultaneously. Protrudin, PDZD8, and Rab7 are all related to neurological disorders, with mutations in the protrudin gene giving rise to the axonopathy HSP (Mannan et al., 2006; Hashimoto et al., 2014), protrudin-deficient mice manifesting psychiatric-like disorders (Shirane et al., 2020a), mutations in the PDZD8 gene being a risk factor for posttraumatic stress disorder (PTSD) (Bharadwaj et al., 2018), and mutations in the Rab7

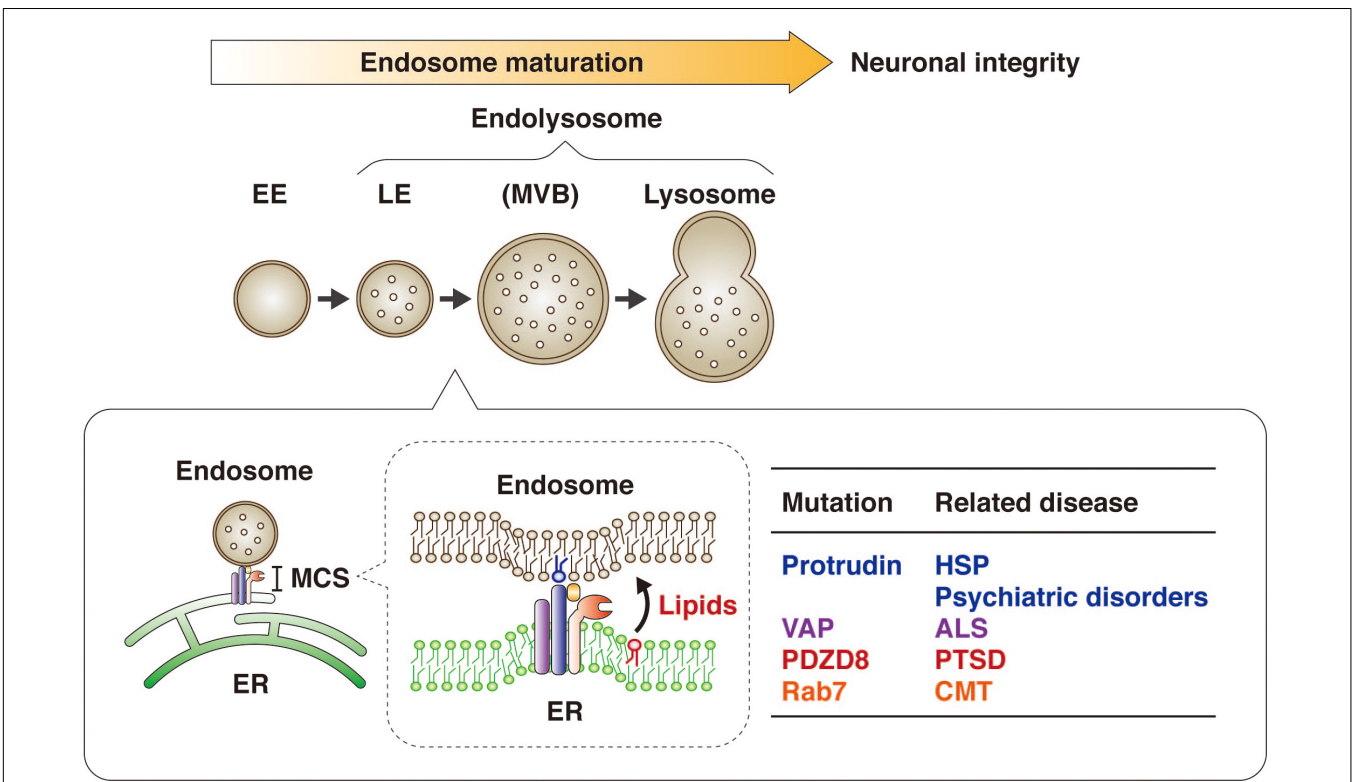

FIGURE 6 | Protrudin regulates endosome maturation at ER-endosome MCSs in neurons and thereby maintains neuronal integrity. Protrudin interacts with VAP, PDZD8, and Rab7 at ER-endosome MCSs, at which lipids are transferred from the ER to endosomes in a manner dependent on the SMP domain of PDZD8, resulting in endosome maturation. Mutations of protrudin, VAP, PDZD8, or Rab7 gene are related to neurological disorders.

gene causing another axonopathy, Charcot-Marie-Tooth disease (CMT) (Verhoeven et al., 2003; McCray et al., 2010).

ENDOSOME MATURATION INFLUENCES NEURONAL POLARITY AND INTEGRITY

The amounts of endogenous protrudin and PDZD8 are higher in the brain than in other tissues, suggesting that the protrudin-PDZD8 complex may function selectively in the nervous system. Depletion of protrudin or PDZD8 with the use of small interfering RNAs (siRNAs) in mouse primary neurons induced abnormal enlargement of LEs, with the resulting vesicles thus being designated abnormal large vacuoles (ALVs) (Shirane et al., 2020b). This phenotype caused by PDZD8 depletion was rescued by additional expression of an siRNA-resistant form of PDZD8 but not by that of a lipid extraction–deficient mutant [PDZD8(ΔSMP)]. The ALVs were also observed in neurons expressing PDZD8(ΔSMP) in the presence of endogenous PDZD8, likely as a result of a dominant negative effect of the mutant protein on the normal fission of LyLEs. The ALVs showed an aberrant multilamellar ultrastructure without ILVs. This phenotype was also highly reminiscent of that of neurons of spastin or REEP1 mutant mice (Allison et al., 2017).

Neurons depleted of PDZD8 showed a reduced axon length and increased somatodendritic area (Shirane et al., 2020b), reflecting impairment of cell polarity, and these abnormalities were similar to those of neurons derived from protrudin-deficient mice (Ohnishi et al., 2014; Shirane et al., 2020b). These observations thus suggested that the protrudin-PDZD8 complex is essential for the establishment of cell polarity in neurons.

Defects in ER-endosome contacts induced by HSP-associated mutations of spastin or REEP1 result in lysosomal abnormalities in neurons (Allison et al., 2017). The fact that mutations of the protrudin gene also cause HSP suggested that the protrudin-PDZD8 system might contribute to maintenance of neuronal integrity. Neurons depleted of protrudin or PDZD8 indeed manifested a morphology consistent with axonal degeneration (Shirane et al., 2020b), including axonal thinning as well as dissociation of Tau1 from microtubules (Morris et al., 2011). This phenotype thus suggested that the protrudin-PDZD8 system protects neurons from axonal degeneration and is essential for neuronal integrity (**Figure 6**). Given that mutations of the PDZD8 gene have been associated with PTSD (Bharadwaj et al., 2018), further study of the physiological role of PDZD8 by analysis of PDZD8-deficient mice is warranted.

CONCLUSION

I have here focused on the role of protrudin at ER-endosome MCSs in endosome maturation in neurons. Protrudin regulates endosome dynamics as well as ER structure, especially in neuronal cells. Mutations of the protrudin gene in humans give rise to the axonopathy HSP as a result of a gain of toxic function. Ablation of the protrudin gene in mice, however, gives rise to psychiatric-like disorders as a result of a loss of function, suggesting that protrudin might play an indispensable role in normal neuronal development and behavior. Protrudin forms a complex with PDZD8 as well as interacts with VAP and Rab7 at ER-endosome contacts. PDZD8 is a mammalian paralog of the ERMES subunit Mmm1, which mediates lipid transfer between the ER and mitochondria. PDZD8 in association with protrudin similarly mediates lipid transfer from the ER to endosomes and thereby contributes to endosome maturation and maintenance of neuronal integrity. The types of lipids transferred by the protrudin-PDZD8 complex *in vivo* remain to be determined. In addition, the detailed mechanism underlying lipid transfer mediated by the protrudin-PDZD8 complex at ER-endosome MCSs, including the identity of the factor or factors responsible for lipid insertion, awaits further investigation.

AUTHOR CONTRIBUTIONS

MS supervised the study and wrote the manuscript.

FUNDING

This work was supported in part by KAKENHI grants from Japan Society for the Promotion of Science (JSPS) and the Ministry of Education, Culture, Sports, Science, and Technology of Japan to MS (20H03255 and 20H04907).

REFERENCES

Allison, R., Edgar, J. R., Pearson, G., Rizo, T., Newton, T., Gunther, S., et al. (2017). Defects in ER-endosome contacts impact lysosome function in hereditary spastic paraplegia. *J. Cell Biol.* 216, 1337–1355. doi: 10.1083/jcb.201609033

Alpy, F., Rousseau, A., Schwab, Y., Legueux, F., Stoll, I., Wendling, C., et al. (2013). STARD3 or STARD3NL and VAP form a novel molecular tether between late endosomes and the ER. *J. Cell Sci.* 126(Pt 23), 5500–5512. doi: 10.1242/jcs.139295

Alva, V., and Lupas, A. N. (2016). The TULIP superfamily of eukaryotic lipid-binding proteins as a mediator of lipid sensing and transport. *Biochim. Biophys. Acta* 1861, 913–923. doi: 10.1016/j.bbalip.2016.01.016

Bharadwaj, R. A., Jaffe, A. E., Chen, Q., Deep-Soboslay, A., Goldman, A. L., Mighdoll, M. I., et al. (2018). Genetic risk mechanisms of posttraumatic stress disorder in the human brain. *J. Neurosci. Res.* 96, 21–30. doi: 10.1002/jnr.23957

Bian, X., Saheki, Y., and De Camilli, P. (2018). Ca(2+) releases E-Syt1 autoinhibition to couple ER-plasma membrane tethering with lipid transport. *EMBO J.* 37, 219–234. doi: 10.15252/embj.201797359

Blackstone, C. (2012). Cellular pathways of hereditary spastic paraplegia. *Annu. Rev. Neurosci.* 35, 25–47. doi: 10.1146/annurev-neuro-062111-150400

Chavrier, P., Parton, R. G., Hauri, H. P., Simons, K., and Zerial, M. (1990). Localization of low molecular weight GTP binding proteins to exocytic and endocytic compartments. *Cell* 62, 317–329. doi: 10.1016/0092-8674(90)90369-p

Colombo, M., Raposo, G., and Thery, C. (2014). Biogenesis, secretion, and intercellular interactions of exosomes and other extracellular vesicles. *Annu. Rev. Cell Dev. Biol.* 30, 255–289. doi: 10.1146/annurev-cellbio-101512-122326

Connell, J. W., Allison, R. J., Rodger, C. E., Pearson, G., Zlamalova, E., and Reid, E. (2020). ESCRT-III-associated proteins and spastin inhibit protrudin-dependent

polarised membrane traffic. *Cell Mol. Life Sci.* 77, 2641–2658. doi: 10.1007/s00018-019-03313-z

Dong, R., Saheki, Y., Swarup, S., Lucast, L., Harper, J. W., and De Camilli, P. (2016). Endosome-ER contacts control actin nucleation and retromer function through VAP-dependent regulation of PI4P. *Cell* 166, 408–423. doi: 10.1016/j.cell.2016.06.037

Du, X., Kumar, J., Ferguson, C., Schulz, T. A., Ong, Y. S., Hong, W., et al. (2011). A role for oxysterol-binding protein-related protein 5 in endosomal cholesterol trafficking. *J. Cell Biol.* 192, 121–135. doi: 10.1083/jcb.201004142

Elbaz-Alon, Y., Guo, Y., Segev, N., Harel, M., Quinnell, D. E., Geiger, T., et al. (2020). PDZD8 interacts with Protrudin and Rab7 at ER-late endosome membrane contact sites associated with mitochondria. *Nat. Commun.* 11:3645.

Fowler, P. C., Garcia-Pardo, M. E., Simpson, J. C., and O'Sullivan, N. C. (2019). NeurodegenERation: the central role for ER contacts in neuronal function and axonopathy, lessons from hereditary spastic paraplegias and related diseases. *Front. Neurosci.* 13:1051. doi: 10.3389/fnins.2019.01051

Gil, J. E., Kim, E., Kim, I. S., Ku, B., Park, W. S., Oh, B. H., et al. (2012). Phosphoinositides differentially regulate protrudin localization through the FYVE domain. *J. Biol. Chem.* 287, 41268–41276. doi: 10.1074/jbc.M112.419127

Gillingham, A. K., Bertram, J., Begum, F., and Munro, S. (2019). In vivo identification of GTPase interactors by mitochondrial relocalization and proximity biotinylation. *eLife* 8:e45916. doi: 10.7554/eLife.45916

Giordano, F., Saheki, Y., Idevall-Hagren, O., Colombo, S. F., Pirruccello, M., Milosevic, I., et al. (2013). PI(4,5)P(2)-dependent and Ca(2+)-regulated ER-PM interactions mediated by the extended synaptotagmins. *Cell* 153, 1494–1509. doi: 10.1016/j.cell.2013.05.026

Guillen-Samander, A., Bian, X., and De Camilli, P. (2019). PDZD8 mediates a Rab7-dependent interaction of the ER with late endosomes and lysosomes. *Proc. Natl. Acad. Sci. U.S.A.* 116, 22619–22623. doi: 10.1073/pnas.1913509116

Hashimoto, Y., Shirane, M., Matsuzaki, F., Saita, S., Ohnishi, T., and Nakayama, K. I. (2014). Protrudin regulates endoplasmic reticulum morphology and function associated with the pathogenesis of hereditary spastic paraplegia. *J. Biol. Chem.* 289, 12946–12961. doi: 10.1074/jbc.M113.528687

Helle, S. C., Kanfer, G., Kolar, K., Lang, A., Michel, A. H., and Kornmann, B. (2013). Organization and function of membrane contact sites. *Biochim. Biophys. Acta* 1833, 2526–2541. doi: 10.1016/j.bbamcr.2013.01.028

Hirabayashi, Y., Kwon, S. K., Paek, H., Pernice, W. M., Paul, M. A., Lee, J., et al. (2017). ER-mitochondria tethering by PDZD8 regulates Ca(2+) dynamics in mammalian neurons. *Science* 358, 623–630. doi: 10.1126/science.aan6009

Hong, Z., Pedersen, N. M., Wang, L., Torgersen, M. L., Stenmark, H., and Raiborg, C. (2017). PtdIns3P controls mTORC1 signaling through lysosomal positioning. *J. Cell Biol.* 216, 4217–4233. doi: 10.1083/jcb.201611073

Hoyer, M. J., Chitwood, P. J., Ebmeier, C. C., Striepen, J. F., Qi, R. Z., Old, W. M., et al. (2018). A novel class of ER membrane proteins regulates ER-associated endosome fission. *Cell* 175, 254–265.e14. doi: 10.1016/j.cell.2018.08.030

Hu, J., Shibata, Y., Voss, C., Shemesh, T., Li, Z., Coughlin, M., et al. (2008). Membrane proteins of the endoplasmic reticulum induce high-curvature tubules. *Science* 319, 1247–1250. doi: 10.1126/science.1153634

Hu, J., Shibata, Y., Zhu, P. P., Voss, C., Rismanchi, N., Prinz, W. A., et al. (2009). A class of dynamin-like GTPases involved in the generation of the tubular ER network. *Cell* 138, 549–561. doi: 10.1016/j.cell.2009.05.025

Hubner, C. A., and Kurth, I. (2014). Membrane-shaping disorders: a common pathway in axon degeneration. *Brain* 137(Pt 12), 3109–3121. doi: 10.1093/brain/awu287

Huotari, J., and Helenius, A. (2011). Endosome maturation. *EMBO J.* 30, 3481–3500. doi: 10.1038/emboj.2011.286

Huttlin, E. L., Ting, L., Bruckner, R. J., Gebreab, F., Gygi, M. P., Szpyt, J., et al. (2015). The BioPlex network: a systematic exploration of the human interactome. *Cell* 162, 425–440. doi: 10.1016/j.cell.2015.06.043

Johansson, M., Lehto, M., Tanhuanpaa, K., Cover, T. L., and Olkkonen, V. M. (2005). The oxysterol-binding protein homologue ORP1L interacts with Rab7 and alters functional properties of late endocytic compartments. *Mol. Biol. Cell* 16, 5480–5492. doi: 10.1091/mbc.e05-03-0189

Johansson, M., Rocha, N., Zwart, W., Jordens, I., Janssen, L., Kuijl, C., et al. (2007). Activation of endosomal dynein motors by stepwise assembly of Rab7-RILP-p150Glued, ORP1L, and the receptor betalll spectrin. *J. Cell Biol.* 176, 459–471. doi: 10.1083/jcb.200606077

Kaiser, S. E., Brickner, J. H., Reilein, A. R., Fenn, T. D., Walter, P., and Brunger, A. T. (2005). Structural basis of FFAT motif-mediated ER targeting. *Structure* 13, 1035–1045. doi: 10.1016/j.str.2005.04.010

Kobuna, H., Inoue, T., Shibata, M., Gengyo-Ando, K., Yamamoto, A., Mitani, S., et al. (2010). Multivesicular body formation requires OSBP-related proteins and cholesterol. *PLoS Genet.* 6:e1001055. doi: 10.1371/journal.pgen.1001055

Kopec, K. O., Alva, V., and Lupas, A. N. (2010). Homology of SMP domains to the TULIP superfamily of lipid-binding proteins provides a structural basis for lipid exchange between ER and mitochondria. *Bioinformatics* 26, 1927–1931. doi: 10.1093/bioinformatics/btq326

Kornmann, B., Currie, E., Collins, S. R., Schuldiner, M., Nunnari, J., Weissman, J. S., et al. (2009). An ER-mitochondria tethering complex revealed by a synthetic biology screen. *Science* 325, 477–481. doi: 10.1126/science.1175088

Kumar, N., Leonzino, M., Hancock-Cerutti, W., Horenkamp, F. A., Li, P., Lees, J. A., et al. (2018). VPS13A and VPS13C are lipid transport proteins differentially localized at ER contact sites. *J. Cell Biol.* 217, 3625–3639. doi: 10.1083/jcb.201807019

Lee, S., Park, H., Zhu, P. P., Jung, S. Y., Blackstone, C., and Chang, J. (2020). Hereditary spastic paraplegia SPG8 mutations impair CAV1-dependent, integrin-mediated cell adhesion. *Sci. Signal.* 13:eaau7500. doi: 10.1126/scisignal.aau7500

Lesage, S., Drouet, V., Majounie, E., Deramecourt, V., Jacoupy, M., Nicolas, A., et al. (2016). Loss of VPS13C function in autosomal-recessive parkinsonism causes mitochondrial dysfunction and increases PINK1/Parkin-dependent mitophagy. *Am. J. Hum. Genet.* 98, 500–513. doi: 10.1016/j.ajhg.2016.01.014

Loewen, C. J., and Levine, T. P. (2005). A highly conserved binding site in vesicle-associated membrane protein-associated protein (VAP) for the FFAT motif of lipid-binding proteins. *J. Biol. Chem.* 280, 14097–14104. doi: 10.1074/jbc.M500147200

Ma, X., Liu, K., Li, J., Li, H., Li, J., Liu, Y., et al. (2018). A non-canonical GTPase interaction enables ORP1L-Rab7-RILP complex formation and late endosome positioning. *J. Biol. Chem.* 293, 14155–14164. doi: 10.1074/jbc.RA118.001854

Mannan, A. U., Krawen, P., Sauter, S. M., Boehm, J., Chronowska, A., Paulus, W., et al. (2006). ZFYVE27 (SPG33), a novel spastin-binding protein, is mutated in hereditary spastic paraplegia. *Am. J. Hum. Genet.* 79, 351–357. doi: 10.1086/504927

Matsuzaki, F., Shirane, M., Matsumoto, M., and Nakayama, K. I (2011). Protrudin serves as an adaptor molecule that connects KIF5 and its cargoes in vesicular transport during process formation. *Mol. Biol. Cell* 22, 4602–4620. doi: 10.1091/mbc.e11-01-0068

McCray, B. A., Skordalakes, E., and Taylor, J. P. (2010). Disease mutations in Rab7 result in unregulated nucleotide exchange and inappropriate activation. *Hum. Mol. Genet.* 19, 1033–1047. doi: 10.1093/hmg/ddp567

Morris, M., Maeda, S., Vossel, K., and Mucke, L. (2011). The many faces of tau. *Neuron* 70, 410–426. doi: 10.1016/j.neuron.2011.04.009

Nishimura, A. L., Mitne-Neto, M., Silva, H. C., Richieri-Costa, A., Middleton, S., Cascio, D., et al. (2004). A mutation in the vesicle-trafficking protein VAPB causes late-onset spinal muscular atrophy and amyotrophic lateral sclerosis. *Am. J. Hum. Genet.* 75, 822–831. doi: 10.1086/425287

Ohnishi, T., Shirane, M., Hashimoto, Y., Saita, S., and Nakayama, K. I. (2014). Identification and characterization of a neuron-specific isoform of protrudin. *Genes Cells* 19, 97–111. doi: 10.1111/gtc.12109

Ohnishi, T., Shirane, M., and Nakayama, K. I. (2017). SRRM4-dependent neuron-specific alternative splicing of protrudin transcripts regulates neurite outgrowth. *Sci. Rep.* 7:41130. doi: 10.1038/srep41130

Olkkonen, V. M., and Li, S. (2013). Oxysterol-binding proteins: sterol and phosphoinositide sensors coordinating transport, signaling and metabolism. *Prog. Lipid Res.* 52, 529–538. doi: 10.1016/j.plipres.2013.06.004

Phillips, M. J., and Voeltz, G. K. (2016). Structure and function of ER membrane contact sites with other organelles. *Nat. Rev. Mol. Cell Biol.* 17, 69–82. doi: 10.1038/nrm.2015.8

Powers, R. E., Wang, S., Liu, T. Y., and Rapoport, T. A. (2017). Reconstitution of the tubular endoplasmic reticulum network with purified components. *Nature* 543, 257–260. doi: 10.1038/nature21387

Pyle, A., Smertenko, T., Bargiela, D., Griffin, H., Duff, J., Appleton, M., et al. (2015). Exome sequencing in undiagnosed inherited and sporadic ataxias. *Brain* 138(Pt 2), 276–283. doi: 10.1093/brain/awu348

Raiborg, C., Wenzel, E. M., Pedersen, N. M., Olsvik, H., Schink, K. O., Schultz, S. W., et al. (2015). Repeated ER-endosome contacts promote endosome translocation and neurite outgrowth. *Nature* 520, 234–238. doi: 10.1038/nature14359

Rowland, A. A., Chitwood, P. J., Phillips, M. J., and Voeltz, G. K. (2014). ER contact sites define the position and timing of endosome fission. *Cell* 159, 1027–1041. doi: 10.1016/j.cell.2014.10.023

Saheki, Y., Bian, X., Schauder, C. M., Sawaki, Y., Surma, M. A., Klose, C., et al. (2016). Control of plasma membrane lipid homeostasis by the extended synaptotagmins. *Nat. Cell Biol.* 18, 504–515. doi: 10.1038/ncb3339

Saita, S., Shirane, M., and Nakayama, K. I. (2013). Selective escape of proteins from the mitochondria during mitophagy. *Nat. Commun.* 4:1410. doi: 10.1038/ncomms2400

Saita, S., Shirane, M., Natume, T., Iemura, S., and Nakayama, K. I. (2009). Promotion of neurite extension by protrudin requires its interaction with vesicle-associated membrane protein-associated protein. *J. Biol. Chem.* 284, 13766–13777. doi: 10.1074/jbc.M807938200

Salvador-Gallego, R., Hoyer, M. J., and Voeltz, G. K. (2017). SnapShot: functions of endoplasmic reticulum membrane contact sites. *Cell* 171, 1224–1224.e1. doi: 10.1016/j.cell.2017.11.005

Schauder, C. M., Wu, X., Saheki, Y., Narayanaswamy, P., Torta, F., Wenk, M. R., et al. (2014). Structure of a lipid-bound extended synaptotagmin indicates a role in lipid transfer. *Nature* 510, 552–555. doi: 10.1038/nature13269

Shibata, Y., Voeltz, G. K., and Rapoport, T. A. (2006). Rough sheets and smooth tubules. *Cell* 126, 435–439. doi: 10.1016/j.cell.2006.07.019

Shirane, M. (2019). Roles of protrudin at interorganelle membrane contact sites. *Proc. Jpn. Acad. Ser. B Phys. Biol. Sci.* 95, 312–320. doi: 10.2183/pjab.95.023

Shirane, M., and Nakayama, K. I. (2003). Inherent calcineurin inhibitor FKBP38 targets Bcl-2 to mitochondria and inhibits apoptosis. *Nat. Cell Biol.* 5, 28–37. doi: 10.1038/ncb894

Shirane, M., and Nakayama, K. I. (2006). Protrudin induces neurite formation by directional membrane trafficking. *Science* 314, 818–821. doi: 10.1126/science.1134027

Shirane, M., Ogawa, M., Motoyama, J., and Nakayama, K. I. (2008). Regulation of apoptosis and neurite extension by FKBP38 is required for neural tube formation in the mouse. *Genes Cells* 13, 635–651. doi: 10.1111/j.1365-2443.2008.01194.x

Shirane, M., Shoji, H., Hashimoto, Y., Katagiri, H., Kobayashi, S., Manabe, T., et al. (2020a). Protrudin-deficient mice manifest depression-like behavior with abnormalities in activity, attention, and cued fear-conditioning. *Mol. Brain* 13, 146–163.

Shirane, M., Wada, M., Morita, K., Hayashi, N., Kunimatsu, R., Matsumoto, Y., et al. (2020b). Protrudin and PDZD8 contribute to neuronal integrity by promoting lipid extraction required for endosome maturation. *Nat. Commun.* 11:4576.

Stenmark, H. (2009). Rab GTPases as coordinators of vesicle traffic. *Nat. Rev. Mol. Cell Biol.* 10, 513–525. doi: 10.1038/nrm2728

van der Kant, R., and Neefjes, J. (2014). Small regulators, major consequences - Ca(2)(+) and cholesterol at the endosome-ER interface. *J. Cell Sci.* 127(Pt 5), 929–938. doi: 10.1242/jcs.137539

Verhoeven, K., De Jonghe, P., Coen, K., Verpoorten, N., Auer-Grumbach, M., Kwon, J. M., et al. (2003). Mutations in the small GTP-ase late endosomal protein RAB7 cause Charcot-Marie-Tooth type 2B neuropathy. *Am. J. Hum. Genet.* 72, 722–727. doi: 10.1086/367847

Voeltz, G. K., Prinz, W. A., Shibata, Y., Rist, J. M., and Rapoport, T. A. (2006). A class of membrane proteins shaping the tubular endoplasmic reticulum. *Cell* 124, 573–586. doi: 10.1016/j.cell.2005.11.047

Wandinger-Ness, A., and Zerial, M. (2014). Rab proteins and the compartmentalization of the endosomal system. *Cold Spring Harb. Perspect. Biol.* 6:a022616. doi: 10.1101/cshperspect.a022616

Watanabe, Y., Tamura, Y., Kawano, S., and Endo, T. (2015). Structural and mechanistic insights into phospholipid transfer by Ups1-Mdm35 in mitochondria. *Nat. Commun.* 6:7922. doi: 10.1038/ncomms8922

Wilhelm, L. P., Wendling, C., Vedie, B., Kobayashi, T., Chenard, M. P., Tomasetto, C., et al. (2017). STARD3 mediates endoplasmic reticulum-to-endosome cholesterol transport at membrane contact sites. *EMBO J.* 36, 1412–1433. doi: 10.15252/embj.201695917

Wong, Y. C., Ysselstein, D., and Krainc, D. (2018). Mitochondria-lysosome contacts regulate mitochondrial fission via RAB7 GTP hydrolysis. *Nature* 554, 382–386. doi: 10.1038/nature25486

Wu, H., Carvalho, P., and Voeltz, G. K. (2018). Here, there, and everywhere: the importance of ER membrane contact sites. *Science* 361:eaan5835. doi: 10.1126/science.aan5835

Zerial, M., and McBride, H. (2001). Rab proteins as membrane organizers. *Nat. Rev. Mol. Cell Biol.* 2, 107–117. doi: 10.1038/35052055

Zhang, C., Li, D., Ma, Y., Yan, J., Yang, B., Li, P., et al. (2012). Role of spastin and protrudin in neurite outgrowth. *J. Cell Biochem.* 113, 2296–2307. doi: 10.1002/jcb.24100

Zhao, K., and Ridgway, N. D. (2017). Oxysterol-binding protein-related protein 1L regulates cholesterol egress from the endo-lysosomal system. *Cell Rep.* 19, 1807–1818. doi: 10.1016/j.celrep.2017.05.028

Conflict of Interest: The author declares that the research was conducted in the absence of any commercial or financial relationships that could be construed as a potential conflict of interest.

frontiers in Cell and Developmental Biology

REVIEW
published: 21 December 2020
doi: 10.3389/fcell.2020.618733

Complex Interactions Between Membrane-Bound Organelles, Biomolecular Condensates and the Cytoskeleton

*Max Koppers†, Nazmiye Özkan† and Ginny G. Farías**

Cell Biology, Neurobiology and Biophysics, Department of Biology, Faculty of Science, Utrecht University, Utrecht, Netherlands

Membrane-bound and membraneless organelles/biomolecular condensates ensure compartmentalization into functionally distinct units enabling proper organization of cellular processes. Membrane-bound organelles form dynamic contacts with each other to enable the exchange of molecules and to regulate organelle division and positioning in coordination with the cytoskeleton. Crosstalk between the cytoskeleton and dynamic membrane-bound organelles has more recently also been found to regulate cytoskeletal organization. Interestingly, recent work has revealed that, in addition, the cytoskeleton and membrane-bound organelles interact with cytoplasmic biomolecular condensates. The extent and relevance of these complex interactions are just beginning to emerge but may be important for cytoskeletal organization and organelle transport and remodeling. In this review, we highlight these emerging functions and emphasize the complex interplay of the cytoskeleton with these organelles. The crosstalk between membrane-bound organelles, biomolecular condensates and the cytoskeleton in highly polarized cells such as neurons could play essential roles in neuronal development, function and maintenance.

Keywords: cytoskeleton, organelle contacts, organelle dynamics, ER, neurons, membraneless organelles, biomolecular condensates, membrane-bound organelles

OPEN ACCESS

Edited by:
Dan Zhang,
Temasek Life Sciences Laboratory, Singapore

Reviewed by:
Pravin Sehgal,
New York Medical College, United States
Luciana Bruno,
University of Buenos Aires, Argentina

***Correspondence:**
Ginny G. Farías
g.c.fariasgaldames@uu.nl

† These authors have contributed equally to this work

Specialty section:
This article was submitted to Membrane Traffic, a section of the journal Frontiers in Cell and Developmental Biology

Received: *18 October 2020*
Accepted: *03 December 2020*
Published: *21 December 2020*

Citation:
Koppers M, Özkan N and Farías GG (2020) Complex Interactions Between Membrane-Bound Organelles, Biomolecular Condensates and the Cytoskeleton. Front. Cell Dev. Biol. 8:618733. doi: 10.3389/fcell.2020.618733

INTRODUCTION

Cells execute numerous biochemical processes that need to be spatiotemporally regulated in the crowded cellular environment. This organization can be achieved by compartmentalization of the cell into functionally and morphologically distinct domains that include both membrane-bound organelles, such as the endoplasmic reticulum (ER), mitochondria and the endo-lysosomal system, and less well-characterized compartments that lack a lipid membrane called membraneless organelles or biomolecular condensates. These biomolecular condensates form by a process called phase separation that drives liquid-liquid demixing from the surrounding environment to create a local concentration of specific proteins and RNAs thereby promoting or inhibiting certain biochemical reactions (Banani et al., 2017; Boeynaems et al., 2018). Phase separation is driven by multivalent protein-protein, RNA-RNA and protein-RNA interactions (Boeynaems et al., 2018; Tauber et al., 2020). Biomolecular condensates have been identified in both the nucleus (e.g., the nucleolus, nuclear speckles, PML bodies and Cajal bodies) and the cytoplasm [e.g., germ granules, processing bodies (P-bodies), stress granules (SGs), and RNP transport granules] and a quickly

increasing amount of work is revealing that these condensates are involved in many different cellular processes such as cell division, ribosome biogenesis, regulation of RNA metabolism, and signal transduction (Banani et al., 2017; Boeynaems et al., 2018; Sabari et al., 2020).

Another essential component important for cellular organization is the cytoskeleton. The cytoskeleton consists of actin filaments, intermediate filaments, and microtubules (MTs) that form a dynamic and highly extensive network throughout the cell. The cytoskeleton determines cell shape, cell polarity, and mechanics and regulates cell division. In addition, it provides the tracks along which proteins, mRNAs and organelles can be transported driven by motor proteins, which is most prominent in highly polarized and morphologically complex cells such as neurons. This intracellular transport ensures the proper distribution, organization and dynamics of both membrane-bound organelles and biomolecular condensates. In animal cells, long-range organelle transport is mainly achieved on the microtubule cytoskeleton whereas the actin cytoskeleton regulates short-range cargo transport (Hirokawa et al., 2009; Burute and Kapitein, 2019). In plant cells, these roles are reversed with the actin cytoskeleton mainly driving the rapid motion of organelles called cytoplasmic streaming (Geitmann and Nebenfuhr, 2015).

The cytoskeleton, membrane-bound organelles and biomolecular condensates function together and are known to interact and communicate with each other. Contacts between membrane-bound organelles have been observed for many years. For instance, the ER can make extensive and dynamic contacts with other membrane-bound organelles such as mitochondria, the trans-Golgi network (TGN), the endo-lysosomal system, the plasma membrane and lipid droplets at so-called membrane contact sites (MCSs) (reviewed in Phillips and Voeltz, 2016; Fowler et al., 2019). MCSs, mediated by tethering proteins, provide an alternative to vesicle-dependent inter-organelle communication by allowing the exchange of small molecules and ions between organelles that is essential to maintain cellular homeostasis (Scorrano et al., 2019). More recent evidence has shown that these interactions play important roles in organelle positioning, dynamics and function. In addition to contacts between membrane-bound organelles, interactions between membrane-bound organelles and biomolecular condensates have emerged increasingly over the past few years (Zhao and Zhang, 2020). These discoveries have brought exciting new prospects to inter-organelle communication within the cell, but it remains largely unclear how these contacts are formed and regulated and what roles they play in cellular function. In addition, the role of the cytoskeleton in these contacts and the interplay of these organelles and condensates with the cytoskeleton are just beginning to emerge. Understanding the complex relationship and interplay between the cytoskeleton, membrane-bound organelles and biomolecular condensates is imperative since dysfunction of each of these components and the dysregulation of their interactions are known to be involved in several neurodegenerative diseases including hereditary spastic paraplegia (HSP) and amyotrophic lateral sclerosis (ALS) (Fowler et al., 2019; Sleigh et al., 2019; Zbinden et al., 2020).

In this review, we will discuss the current knowledge on the intricate interplay between the cytoskeleton, membrane-bound organelles and biomolecular condensates and expand the idea that this interplay is essential for many crucial cellular processes. In the first section, we will discuss how the cytoskeleton affects the organization and dynamics of membrane-bound organelles such as the ER and mitochondria; and conversely how dynamic membrane-bound organelles can affect cytoskeletal organization. Then we will explore complex interactions between membrane-bound organelles in conjunction with the cytoskeleton. In the second section, we will explore the role of the cytoskeleton in the transport and dynamics of biomolecular condensates and discuss how these condensates can influence the cytoskeleton. In the third section, we will discuss the interactions between membrane-bound organelles and biomolecular condensates and emphasize the intricate interplay of these contacts with the cytoskeleton. Finally, we will explore the link of these complex interactions with neurodegenerative diseases and point out open questions in this field.

THE INTERPLAY BETWEEN MEMBRANE-BOUND ORGANELLES AND THE CYTOSKELETON

The correct positioning of organelles, mediated by motor protein-driven intracellular transport along the microtubule and actin cytoskeleton, is essential for many cellular functions (reviewed in Rogers and Gelfand, 2000; Bonifacino and Neefjes, 2017; Burute and Kapitein, 2019). However, it has only recently become increasingly recognized that there is an intricate interplay between various membrane-bound organelles and the cytoskeleton that extends beyond single organelle movement. For instance, membrane-bound organelles are remodeled by the cytoskeleton and reciprocally, dynamic membrane-bound organelles contribute to cytoskeletal organization. Moreover, complex inter-organelle interactions have been found to play important roles in the transport, organization and dynamics of membrane-bound organelles in coordination with the cytoskeleton. In this section, we discuss this reciprocal crosstalk and their important cellular functions which are essential to maintain cellular homeostasis.

The Role of the Cytoskeleton in Membrane-Bound Organelle Organization

The Influence of the Cytoskeleton on the ER Network

The ER is the largest membrane-bound organelle and is involved in many crucial cellular functions including protein synthesis and processing, calcium storage and lipid metabolism (Rapoport, 2007; Fagone and Jackowski, 2009; Braakman and Hebert, 2013; Schwarz and Blower, 2016). The ER consists of dynamic tubules and sheets, which form a continuous interconnected network throughout the cell (English et al., 2009; Friedman and Voeltz, 2011; Goyal and Blackstone, 2013). In unpolarized cells, ER sheets are localized to the perinuclear area whereas the

interconnected tubules can extend throughout the periphery of the cell (Shibata et al., 2006; Chen et al., 2013). In polarized neurons, it has been shown that ER tubules can localize to both structurally and functionally different neuronal compartments, the somatodendritic and axonal domains; however, ER sheets are excluded from the axon (Wu et al., 2017; Farias et al., 2019).

The morphology of the ER is maintained by ER-shaping proteins. For instance, ER-resident proteins such as CLIMP63 generate the flattened structure of the sheets, Reticulons induce the high curvature of ER tubules, and the GTPase Atlastin-1 induces homo-fusion of tubules to generate a reticular network. The relative abundance of specific ER-shaping proteins regulates the sheet-to-tubule ratio and fusion between tubules, thus controlling the ER network (reviewed in Zhang and Hu, 2016; Wang and Rapoport, 2019). In addition, other factors may cooperate with these ER-shaping proteins to rearrange the ER network, as ER remodeling occurs in a timescale of milliseconds (Nixon-Abell et al., 2016; Guo et al., 2018).

Although a reticular ER network can be formed *in vitro* by ER-shaping proteins in absence of the cytoskeleton (Dreier and Rapoport, 2000), the ER can rearrange its network in response to cellular demands and this relies on its interaction with the cytoskeleton. First evidence for a role of MTs in ER organization came from experiments performed with the MT-depolymerizing drug nocodazole, which resulted in the retraction and interconversion of ER tubules into ER sheets (Terasaki et al., 1986). A similar phenotype has been observed in neurons, in which nocodazole induced the retraction of ER tubules from dendrites and the axon into the soma and their interconversion to somatic ER sheets (Farias et al., 2019).

ER network rearrangements can be mediated by the cytoskeleton via four different mechanisms. First, the ER can form contacts with polymerizing MTs at their growing plus ends through the interaction between the ER protein STIM1 and the MT-associated protein EB1 (**Figure 1A**). Through this "tip attachment complex" (TAC) growing ER tubules can be pulled out by the growing plus end of dynamic MTs (Waterman-Storer and Salmon, 1998; Grigoriev et al., 2008; Rodriguez-Garcia et al., 2020). This TAC mechanism is also involved the reshaping and positioning of the ER important for dendritic spine morphology in hippocampal neurons and for axonal growth cone dynamics in DRG sensory neurons (Pchitskaya et al., 2017; Pavez et al., 2019). A second mechanism that involves an interaction between the ER and MT cytoskeleton is the "sliding mechanism," in which newly produced ER tubules are coupled to MT-bound motor proteins such as kinesin-1 and dynein and are thereby extended along stable MTs (**Figure 1A**; Wozniak et al., 2009; Friedman et al., 2010). Knockdown of kinesin-1 and dynein was shown to impair anterograde and retrograde movement of ER tubules along the axon in rat hippocampal neurons, while knockdown of EBs 1–3 did not affect axonal ER distribution but does impair dendritic movement of the ER (Farias et al., 2019). In addition, a newly developed imaging technology called GI-SIM has revealed that newly extended ER tubules via TAC and sliding mechanisms meet and fuse with pre-existing tubules. This suggests a possible role of TAC and sliding mechanisms in maintaining a dynamic reticular ER network (Guo et al., 2018).

A third and recently identified mechanism for ER tubule rearrangement is a depolymerizing TAC (dTAC) mechanism in which newly formed ER tubules can be attached to the depolymerizing end of MTs and can be pulled out while MTs retract. It was suggested that molecules other than STIM1 and EB might play a role in this dTAC mechanism (Guo et al., 2018). However, recent evidence from *in vitro* assays revealed that at least the same EB protein might be involved in both TAC and dTAC mechanisms in which the amount of the forces applied are different (Rodriguez-Garcia et al., 2020).

Guo et al., also identified another way of MT-dependent ER network rearrangement, the so-called "hitchhiking" mechanism, in which an organelle takes advantage of the transport machinery of another organelle for their translocation. This will be further discussed in section "Complex Inter-Organelle Interactions in Coordination With the Cytoskeleton."

GI-SIM also revealed a remodeling mechanism in which ER tubules can be extended without any obvious direct or indirect MT involvement called *de novo* budding. These events were rare and it remains unknown whether the actin cytoskeleton, intermediate filaments or another unseen mediator could be involved in this *de novo* budding of the ER.

In addition to the involvement of MTs in ER rearrangement, the actin cytoskeleton might also contribute to the remodeling of the ER network. Actin filaments were observed to localize to polygons occupied by surrounding ER. Depolymerization of actin filaments with latrunculin treatment led to a fluctuation in the sheet-to-tubule ratio by increasing the transformation of sheets to tubules and it led to a change in size and morphology of ER sheets in mammalian cells (Joensuu et al., 2014). This suggests an interaction between actin and the ER that supports ER sheet formation.

The actin-based motor protein myosin Va has been shown to be involved in ER motility in animal cells and first evidence for this derived from the lack of ER tubules in dendritic spines in neurons of "dilute" mice and rats, which carry null mutations in the gene encoding for the heavy chain of myosin Va (Dekker-Ohno et al., 1996; Takagishi et al., 1996). Myosin-Va was later revealed to be involved in the translocation of ER into dendritic spines of Purkinje cells and experiments in wildtype and dilute mice support the model that myosin Va uses the actin cytoskeleton for short-range ER transport (Wagner et al., 2011). In a very recent study in CA1 pyramidal cells, expression of a dominant negative mutant for myosin Va reduced the number of spines that contain ER and enhanced mGluR-dependent LTD, which suggests that myosin Va is a key regulator of selective transport of ER tubules into highly active spines that regulates synaptic plasticity (Perez-Alvarez et al., 2020). Another recent study revealed that myosin Va-dependent ER transport into dendritic spines can be finely orchestrated by an intricate interaction between two Ca^{2+} binding proteins, calmodulin and caldendrin (Konietzny et al., 2020). However, how the actin-based myosin Va motor protein interacts with ER tubules remains to be elucidated. The ER can also dynamically move in and out of dendritic spines from hippocampal neurons and thereby regulate Ca^{2+} levels important for mGluR-dependent LTD (Toresson and Grant, 2005; Holbro et al., 2009). Treatment of Purkinje cells with

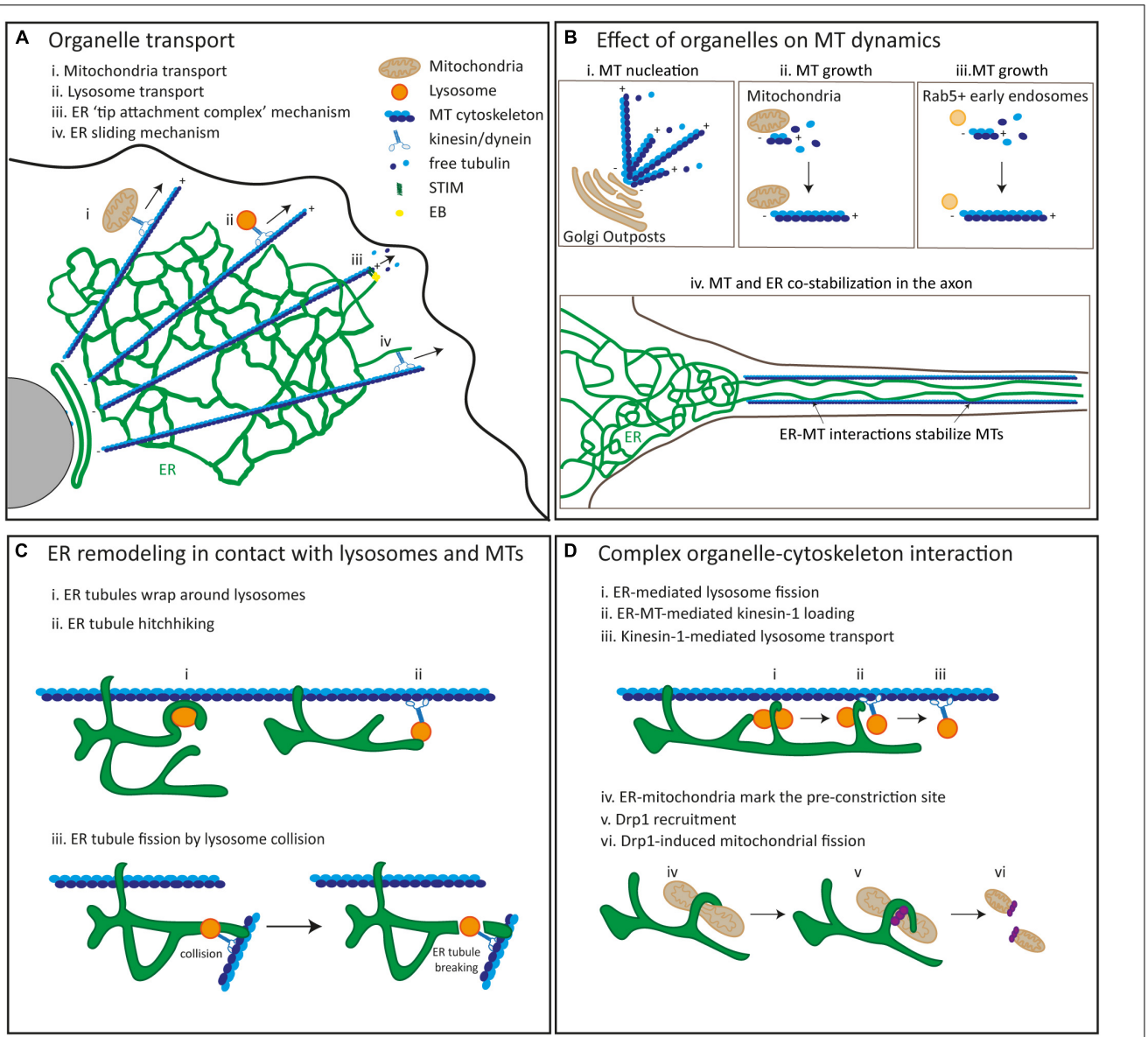

FIGURE 1 | The interplay and interactions between membrane-bound organelles and the cytoskeleton. **(A)** MT-dependent transport of membrane-bound organelles such as mitochondria (i), lysosomes (ii) and the ER (iii) and (iv) in mammalian cells. ER tubules and microtubules can elongate together at the tip of a growing MT (TAC; iii) or ER tubules can be pulled out by microtubules via motor-dependent sliding (iv). **(B)** MT dynamics is mediated by membrane-bound organelles. MT nucleation can be induced by Golgi outposts (i). MT growth can be regulated by mitochondria (ii) and Rab5 + early endosomes (iii). MTs and the ER colocalize and co-stabilize each other in axons via an interplay between MTs and the ER (iv). **(C)** ER remodeling is regulated by interactions between the ER and lysosomes in conjunction with the cytoskeleton. ER tubules wrap around lysosomes (i). ER tubules are pulled out by hitchhiking on moving lysosomes (ii). Fission of ER tubules is induced by lysosome collisions (iii). **(D)** Lysosome fission is regulated by an interaction between the ER and lysosomes in association with the cytoskeleton (i, ii, iii). ER tubules induce lysosome fission (i), ER-MT interactions promote kinesin-1 loading onto lysosomes (ii) and lysosome transport is driven by kinesin-1 along MTs. Mitochondrial fission is mediated by ER tubules (iv, v, vi). ER-mitochondria contacts mark the pre-constriction site (iv), Drp1 is recruited to this pre-constriction site (v) and promotes mitochondrial fission (vi).

low dose nocodazole suggested that the MT-dependency of ER transport into dendritic spines is minor (Wagner et al., 2011). The MT cytoskeleton is also known to transiently enter dendritic spines of hippocampal neurons (Hu et al., 2008; Jaworski et al., 2009). Although MTs are required for long-range transport of ER tubules into dendrites in hippocampal neurons (Farias et al., 2019), it remains unknown whether actin and MT crosstalk can coordinate the entrance of ER tubules into dendritic spines of these neurons.

The Influence of the Cytoskeleton on Mitochondria Dynamics

Mitochondria are the production house for meeting the energy demands of cells and can form a dynamic tubular network.

Mitochondria are also responsible for other cellular processes including calcium homeostasis, cell differentiation, apoptosis and metabolic signaling (Nunnari and Suomalainen, 2012). Mitochondrial morphology has to be maintained for its proper functioning and this is mediated by mitochondrial fusion, fission and motility. Whilst in simple eukaryotes such as budding yeast, actin can regulate the transport of mitochondria, in animal cells, mitochondria use motor protein-coupled transport along MTs for long-distance travels while actin filaments ensure short-distance transport of mitochondria (Wu et al., 2013). Transport of mitochondria is especially essential in neurons, where the proper distribution of proteins and organelles in the dendrites and long axon requires long-distance travels. The kinesin-1 motor protein can carry mitochondria along MTs toward MT plus ends whilst dynein and its partner dynactin can transport mitochondria along MTs toward MT minus ends (Pilling et al., 2006). The coupling of mitochondria to the MT-based motor proteins kinesin-1 and dynein is mediated by the TRAK/Miro motor adaptor complex (van Spronsen et al., 2013).

Besides motility, the cytoskeleton is also involved in mitochondrial anchoring. Mitochondria can be tethered to the actin cytoskeleton, which in neurons is crucial for mitochondrial anchoring at axonal presynaptic sites (Chada and Hollenbeck, 2004; Gutnick et al., 2019). In addition, the MT-binding protein syntaphilin was discovered as a regulator of mitochondrial anchoring at presynaptic sites (Chen and Sheng, 2013). This suggests there is likely a dual role for both the actin and MT cytoskeleton in mitochondrial anchoring at presynaptic sites. However, the proteins involved in tethering mitochondria to the actin cytoskeleton and the molecular mechanisms underlying this anchoring remain to be elucidated.

Studies performed in the amoeba *Dictyostelium discoideum* showed that MTs are highly involved in mitochondrial dynamics (Woods et al., 2016). Treatment with nocodazole to depolymerize MTs led to a reduction of motile mitochondria as well as a reduced number of mitochondrial fusion and fission events. Treatment with latrunculin, which depolymerizes actin filaments, did not affect the fusion, fission or motility of mitochondria but did decrease the number of motile mitochondria. This suggests that MTs are important for mitochondrial dynamics in *Dicytostelium discoideum* whilst actin is more important for determining the percentage of moving mitochondria (Woods et al., 2016).

Mehta et al. (2019) suggested that an interaction between dynamic MTs and mitochondria in budding yeast causes an increase in mitochondrial fission events. Deletion of several kinesin-like proteins to perturb MT dynamics revealed that long and stable MTs inhibit mitochondrial fission by hampering the ring assembly of GTPase dynamin-related protein Dnm1 (Drp1 in mammals) around mitochondria because long and stable MTs introduce a physical restriction. However, depolymerized and dynamic MTs led to an increase in mitochondrial fission events which are normally essential for independent segregation of mitochondria to daughter cells during mitosis and for eliminating damaged and fragmented mitochondrial content via mitophagy (Mehta et al., 2019).

In addition, intermediate filaments have been shown to associate with mitochondria and regulate their distribution and metabolic functions (Etienne-Manneville, 2018). Intermediate filaments may be involved in positioning of mitochondria to locations with high energy demand by providing an anchoring structure. In giant axonal neuropathy patient-derived fibroblasts, mitochondrial motility is inhibited, which is linked to abnormal organization and turnover of the intermediate filament protein vimentin (Lowery et al., 2016). On the other hand, Rac1 and its effector PAK1 can phosphorylate vimentin at mitochondrial binding sites which leads to the release of mitochondria, which then gain a higher motility and lower mitochondrial membrane potential (Matveeva et al., 2015). A recent study also revealed that mutations in another intermediate filament protein, desmin, causes mitochondrial dysfunction and alterations in mitochondrial network morphology although the underlying molecular mechanisms are still unclear (Smolina et al., 2020). It would be interesting to investigate how MTs, actin and intermediate filaments coordinate their functions to ensure proper mitochondria dynamics and positioning.

The Influence of Motile Membrane-Bound Organelles on Cytoskeletal Organization

Spatiotemporal regulation of cytoskeletal organization is essential for various cellular functions, such as the transport and dynamics of organelles and cell morphology. In the last 10 years, evidence has emerged supporting the notion of an intricate interplay between organelles and the cytoskeleton in which organelle dynamics can reciprocally regulate cytoskeletal organization. The simplest notion that motor-driven transport itself can act as an active force causing buckling and oscillation on MTs, highlights a complex mechanical interplay between cytoskeleton and motor-dependent organelle movement (Kulic et al., 2008; Man and Kanso, 2019). In addition to this mechanical interplay, organelles such as Golgi outposts, endosomes, mitochondria, and the ER, have all been implicated in cytoskeletal remodeling, specifically in MT dynamics.

Besides the perinuclear Golgi apparatus, well-known because of its role in acentrosomal MT nucleation (reviewed in Akhmanova and Steinmetz, 2019), small and more motile Golgi outposts (also referred to as satellite Golgi or Golgi vesicles) have also been found to nucleate MTs far from the nucleus in differentiated cells such as neurons, muscle cells and oligodendrocytes. In *Drosophila* and mammalian neurons, Golgi outposts distributed in dendrites can mark the main site of acentrosomal MT nucleation (**Figure 1B**). The Golgi structural protein GM130, as well as recruitment of γ-tubulin and CP309, the *Drosophila* homolog of AKAP450, to Golgi outpost, have been shown to be required for Golgi outpost-dependent acentrosomal MT growth and dendritic branch formation in *Drosophila* neurons (Ori-McKenney et al., 2012; Zhou et al., 2014). Golgi outposts in mouse skeletal muscle fibers were found to recruit γ-tubulin and pericentrin to sites of acentrosomal MT growth, but it remains largely unexplored whether Golgi outpost-dependent acentrosomal MT nucleation has a role in the complex MT grid-like network organization of muscle fibers (Oddoux et al., 2013). Golgi outpost have also recently been

found along primary, secondary and tertiary processes of mouse oligodendrocytes, far away from the perinuclear area. The protein TPPP, recently identified in oligodendrocyte Golgi outposts, nucleates MTs in *in vitro* assays, contributes to MT branching and mixed MT polarity in 3D microfiber cultures, and is required for myelin sheath elongation *in vivo* (Fu et al., 2019).

Although two studies have implicated Golgi outposts in dendritic MT nucleation (Ori-McKenney et al., 2012; Zhou et al., 2014), other reports have challenged these results, as dragging Golgi outpost away from dendrites using an activated kinesin, did not alter γ-tubulin distribution in *Drosophila* neurons and branching points lacking Golgi outposts still contained γ-tubulin (Nguyen et al., 2014). More recent work showed that these γ-tubulin nucleation sites in dendritic branches colocalize with and are regulated by components of the canonical *Wnt* signaling pathway. Puncta containing *Wnt* signaling components were found to colocalize with Rab5-positive early endosomes, from which new MT growth initiated (**Figure 1B**). This evidence suggests the involvement of early endosomes in dendritic acentrosomal MT nucleation (Weiner et al., 2020). However, more experiments are required to evaluate whether early endosome positioning in dendritic branching points are required for MT nucleation and branch formation. It would be interesting to evaluate whether the removal of early endosomes and other organelles from dendrites alters γ-tubulin distribution and local MT dynamics.

Mitochondria have also been implicated in MT growth (**Figure 1B**). In *Drosophila* spermatids, a non-centrosomal, testes-specific isoform of centrosomin is localized to giant mitochondria, and it is required to recruit the MT nucleator γ-tubulin ring complex (γ-TuRC) to regulate MT assembly and spermiogenesis (Chen et al., 2017).

Finally, an important role for ER – MT interactions in MT organization has been suggested for years. Mutations in the ER-associated proteins Spastin, Atlastin-1 and REEP1 cause the neurodegenerative disease HSP, which is characterized by progressive spasticity in lower motor neurons (Blackstone, 2012). The MT-severing protein Spastin, GTPase Atlastin-1 and MT-interacting protein REEP1 form a complex that interacts with MTs and has been shown to be enriched in the axonal ER in rat cortical neurons (Park et al., 2010). Although the role of these proteins in maintaining the ER tubule network has been shown (reviewed by Goyal and Blackstone, 2013), the exact role of axonal ER tubules in MT organization has been less explored. More recent experiments in rat hippocampal neurons have demonstrated an important role for ER tubules in MT stabilization and axon formation. ER tubules are preferentially distributed in the growing axon of developing neurons and interact with and stabilize MTs. Controlled removal of ER tubules from the axon, by coupling the ER to a minus-end directed motor, causes MT instability and prevents elongation of the developing axon (Farias et al., 2019). In addition, the Atlastin-1 ortholog, Atln-1, which is distributed in dendrites of *C. elegans* PVD sensory neurons, has been found to colocalize with and be required for MT entrance into secondary and tertiary dendritic branches (Liu et al., 2019). Although some evidence has started to emerge regarding the role of the ER in MT dynamics, it still remains unclear whether different domains of the ER play different roles in MT organization.

Complex Inter-Organelle Interactions in Coordination With the Cytoskeleton

It is now well-established that organelles interact with each other at MCSs and knowledge on the types and importance of MCSs has greatly increased in the past few years. Since the ER is the largest organelle and forms a continuous and interconnected network throughout a cell, it is not surprising that it participates in most MCSs (reviewed in Phillips and Voeltz, 2016). The ER can interact with several other organelles including mitochondria, late endosomes/lysosomes, Golgi, and the plasma membrane. These interactions are involved in organelle positioning and fission, and lipid and Ca^{2+} homeostasis (Phillips and Voeltz, 2016; Allison et al., 2017; Fowler et al., 2019). However, the interplay between inter-organelle contacts and the cytoskeleton is less well-studied. In this section, we highlight the current knowledge on the complex interactions between membrane-bound organelles in coordination with the cytoskeleton and emphasize the importance of this relationship in organelle dynamics including fission, fusion and transport.

Membrane-Bound Organelles Can "Hitchhike" for Transport

The concept of hitchhiking of membrane-bound organelles on other organelles for their transport emerged just recently. In the fungus *Ustilago Maydis,* movement of the ER, lipid droplets and peroxisomes is mediated by motile Rab5-positive early endosomes via kinesin-3 and dynein on MTs (Guimaraes et al., 2015; Salogiannis and Reck-Peterson, 2017). In mammals, several examples of this type of organelle hitchhiking have also been recently discovered. For instance, it was found that the ER can tether itself onto late endosomes/lysosomes for hitchhiking in cell lines and neurons (Guo et al., 2018; Lu et al., 2020). GI-SIM imaging also revealed that mitochondria can hitchhike on motile late endosomes/lysosomes for their translocation along MTs (Guo et al., 2018). This hitchhiking mechanism will be discussed in more detail below.

Complex Interactions Between the ER, Late Endosomes/Lysosomes and the MT Cytoskeleton

The ER can form extensive and dynamic contacts with late endosomes/lysosomes at MCSs. In fact, almost all late endosomes/lysosomes were found to be in contact with the ER (Friedman et al., 2013; Guo et al., 2018). MCSs between the ER and late endosome/lysosomes are involved in many essential cellular tasks including endosome fission and positioning. 3D reconstructions from electron microscopy serial tomography in COS7 cells and live-cell imaging revealed that MCSs between the ER and endosomes are tightly associated with MTs and this association can be maintained when endosomes are moving along MTs (Friedman et al., 2013). GI-SIM imaging revealed that the ER can rearrange its coral large tubular network into smaller structures that tightly wrap around late endosomes/lysosomes where they are close to MTs (**Figure 1C**). Late endosomes/lysosomes that are not in contact with the

ER were observed to undergo diffusive motion along MTs suggesting that the ER coordinates the stabilization of late endosomes/lysosomes (Guo et al., 2018). Interestingly, it has been previously shown that the ER can mediate kinesin-1 coupling to late endosomes/lysosomes for transport to the cell periphery via motor protein transfer (Raiborg et al., 2015). In this intriguing mechanism, the ER-resident protein Protrudin was shown to transfer kinesin-1 to the adaptor protein Rab7 and its effector FYCO1 localized on late endosomes/lysosomes for their anterograde transport along MTs in human and rat cell lines (Raiborg et al., 2015). This ER-mediated late endosome/lysosome translocation to the cell periphery was shown to promote neurite outgrowth in the neuroendocrine cell line PC12 (Raiborg et al., 2015). In a recent study, an interplay between the ER, lysosomes and MTs was proposed to play a role in lysosome translocation into the axon of rat hippocampal neurons (Özkan et al., 2020). Disruption of somatic, but not axonal ER tubules led to an accumulation of enlarged and less motile lysosomes in the soma, thus triggering a drastic reduction in the translocation of lysosomes into the axon. A similar phenotype was also observed after the knockdown of another ER-resident protein P180, which has binding domains for both MTs and kinesin-1. P180 was found to be particularly enriched in a region preceding the axon initial segment called the pre-axonal region. Serial z-stacking of this region revealed that P180-enriched ER can undergo ring rearrangements to tightly wrap around lysosomes. Lysosomes contacting the ER were observed in close proximity to stable MTs decorated by a rigor kinesin-1 motor mutant. Together, this raises the possibility that P180 stabilizes the interaction between MTs and ER-late endosome/lysosome contacts via its MT-binding domain and loads kinesin-1 onto late endosomes/lysosomes thereby facilitating their translocation into the axon (Özkan et al., 2020).

The first evidence revealing a role for ER-endosome contacts in endosomal fission came from studies in COS7 cells in which contacts between the ER and early endosomes or late endosomes/lysosomes defined the endosomal constriction and fission site (Rowland et al., 2014). More recent evidence showed that the ER-resident protein Spastin and the endosomal protein IST1 interact with each other at ER-endosome contact sites to promote endosomal tubule fission in mammalian cell lines (Allison et al., 2013, 2017). Primary cortical neurons from a Spastin-HSP mouse model and IPSC-derived HSP patient neurons contained abnormal enlarged lysosomes, which suggests that disruption of Spastin in ER-endosome contact sites impacts lysosome size in neurons (Allison et al., 2017). However, how the ER regulates lysosome size remained elusive. Interestingly, direct contacts between the ER and late endosomes/lysosomes have been observed in hippocampal neurons, and this interaction is required for late endosome/lysosome fission. Late endosomes/lysosomes undergo several fusion and fission events in control neurons, while ER tubule disruption causes enlarged lysosomes with reduced fission capacity (Özkan et al., 2020).

The role of the ER in late endosome/lysosome transport or fission has often been studied separately. Just recently, Özkan et al. (2020), proposed a model in which these events are connected through a complex interaction between MTs and ER-lysosome contacts that promotes lysosome fission and subsequent lysosome transport into the axon (**Figure 1D**).

Whilst the ER is now well-established as a prominent regulator of lysosome transport and fission, the effect of lysosome positioning on ER tubule rearrangement has remained unclear. With GI-SIM, the ER was observed to hitchhike on moving late endosomes/lysosomes along MTs for their transport (**Figure 1C**; Guo et al., 2018). In addition, ER fission was observed when moving late endosomes/lysosomes collided with and broke ER tubule network at junctions between fused tubules. Guo et al. suggested that Atlastin-1, an ER-shaping protein implicated in the formation of three-way junctions could be involved in this ER fission mechanism. However, the breaking of ER tubules was also observed along a single tubule (**Figure 1C**; Guo et al., 2018). It remains unknown which molecules are involved in this ER-breaking process, and further investigation is required. Dual-color single particle tracking in COS7 cells revealed that 98% of lysosomes are moving simultaneously with the ER and the growing tips of the ER associated with lysosomes are elongated and merged with the existing ER network to form three-way junctions whilst the ER growth tips that are not associated with lysosomes cannot maintain elongation and are retracted (Lu et al., 2020). In addition, manipulation of lysosome positioning by coupling lysosomes to dynein for retrograde movement to the perinuclear area or kinesins for anterograde movement to the cell periphery has been recently shown to cause a reduction in ER tubules or extension of ER tubules to the periphery of cells, respectively (Lu et al., 2020). Moreover, live-cell imaging in cultured *Xenopus laevis* retinal ganglion cell (RGC) axons showed that the ER can rearrange its structure into a ring arrangement that tightly wraps around lysosomes. These lysosomes then pull out the ER tubule for its extension. This suggests that ER tubule elongation is driven by lysosome positioning and is essential for ER tubule remodeling in axons to support axonal growth (Lu et al., 2020).

All this evidence indicates the importance of the interplay between the ER and lysosomes where the ER modulates lysosome fission and translocation, and lysosome motility mediates ER tubule transport and remodeling.

Defects in ER morphology and function as well as an impairment in the endolysosomal system are key pathological features of neurological diseases such as HSP. Therefore, it will be crucial to identify the regulators and molecular mechanisms underlying the crosstalk between these two organelles and further establish the link between these organelles and the cytoskeleton.

Complex Interactions Between Mitochondria, the ER and the Cytoskeleton

Friedman et al. (2011) revealed that ER-mitochondria contact sites are mainly formed at a pre-constriction site for mitochondrial fission, suggesting that contacts between the ER and mitochondria regulates mitochondrial fission (**Figure 1D**). The recruitment of Drp1 to the pre-constriction site is the key regulatory step in mitochondrial fission (Smirnova et al., 2001). However, other studies revealed that pre-constriction site formation can be mediated by Drp1-independent mechanisms

(Korobova et al., 2013). Hatch et al. suggested a possible mechanism in which the ER-driven interaction between mitochondria and the cytoskeleton regulates mitochondrial fission in mammalian cells by formation of a pre-constriction site and subsequent recruitment of Drp1 (Korobova et al., 2013; Hatch et al., 2014). ER-mitochondria contact sites marking the putative pre-constriction site can recruit formin-like protein INF2 which triggers actin polymerization on the ER. This actin polymerization then generates forces on the mitochondrial membrane that leads to the formation of a pre-constriction site to which Drp1 is recruited. The accumulation of Drp1 and subsequent GTP hydrolysis drives constriction and scission of the membrane leading to mitochondrial fission (Korobova et al., 2013; Hatch et al., 2014). Lee et al. (2016), proposed a model that includes a role for dynamin 2 (Dyn2) in the final step of mitochondrial fission. Drp1-mediated constriction of the mitochondrial membrane promotes Dyn2 assembly at the constriction site where it can promote membrane fission for successful mitochondrial division. Live-cell imaging and electron microcopy in different mammalian cells lines suggested Dyn2 and Drp1 work in harmony in sequential constriction steps to promote mitochondrial fission (Lee et al., 2016). By contrast, a recent study using human fibroblast cell lines showed that the knockout of Dyn1, 2, and 3 or knockdown of only Dyn2 did not alter mitochondrial fission. Similar results obtained in HeLa cells lacking Dyn1, 2, and 3 showed no effect on mitochondrial fission, eliminating the possibility of a cell-type specific effect of Dyn2 on mitochondrial fission (Fonseca et al., 2019). These controversial results request further studies to determine whether or not Dyn2 is dispensable for the scission of the mitochondrial membrane.

Recent studies revealed a more complex mechanism rather than simple Drp1-mediated mitochondrial fission. This mechanism involves an interplay between mitochondria, the ER, INF2-driven actin polymerization and calcium uptake by mitochondria (Chakrabarti et al., 2018; Steffen and Koehler, 2018). Extracellular calcium influx induces INF2-mediated actin polymerization on the ER that triggers subsequent calcium uptake by mitochondria from the ER. Calcium uptake by the inner membrane of mitochondria through the mitochondrial calcium uniporter drives inner membrane scission that precedes outer membrane fission, suggesting INF2-mediated actin polymerization on the ER regulates mitochondrial fission by affecting mitochondrial calcium uptake (Chakrabarti et al., 2018; Steffen and Koehler, 2018).

Another intriguing study investigating the role of ER morphology on mitochondria dynamics in *C. elegans* PVD neurons revealed an interaction between the ER network and mitochondria at dendritic branching points, which is crucial for mitochondrial fission (Liu et al., 2019). They showed that mitochondria are highly enriched at the dendritic branch points where the ER network is more complex in neurons expressing wildtype Atlastin-1. However, neurons expressing mutant Atlastin-1 had a less complex ER network and a reduced number of mitochondria at dendritic branch points (Liu et al., 2019). This suggests that the local ER network regulates mitochondrial distribution at dendritic branch points. Analysis of mitochondrial fission showed that the local ER network at branch points can attach to and promote the fission of mitochondria. Together with unpublished results indicating that ER tubule extension strongly relies on transient MT entry into dendrites, Liu et al. proposed a model in which the interaction between the complex ER network and mitochondria at dendritic branch points depends on MTs and is required for mitochondrial fission (Liu et al., 2019).

Surprisingly, a recent study revealed that ER-mitochondria contacts can also mark the mitochondrial fusion site (Abrisch et al., 2020) consistent with the observation that mitochondria fusion occurs in proximity to the ER (Guo et al., 2018). Abrisch et al. found that Mitofusin-1 (Mfn1), a regulator of mitochondrial fusion, is localized to ER-mitochondria contact sites and fluorescence loss in photobleaching (FLIP) experiments in U2OS and COS7 cells showed that Mfn1 and Drp1 colocalize and both fusion and fission events take place at the same site where the ER contacts mitochondria (Abrisch et al., 2020). This suggests a remarkable mechanism in which the ER can regulate both mitochondrial fusion and fission at the same position and provides a way to respond to cellular needs in a quick and coordinated manner. However, how switching between fusion and fission is achieved remains unclear.

Complex Interactions Between Mitochondria, Late Endosomes/Lysosomes, and the MT Cytoskeleton

Mitochondria can also hitchhike on motile late endosomes/lysosomes coupled to MT-bound motor proteins. Late endosomes/lysosomes that move in close proximity to mitochondria were reported to be important for mitochondrial morphology. Dynamic tubulation of mitochondria can be achieved during this hitchhiking, thus providing a mechanism for mitochondrial fusion (Guo et al., 2018). An indirect involvement of the MT cytoskeleton in the changes of mitochondrial morphology and corresponding functions can be speculated as mitochondrial hitchhiking along motile late endosomes/lysosomes requires MTs.

In summary, there is an outstanding communication between membrane-bound organelles in association with cytoskeleton, which is essential for organelle positioning, dynamics and morphology as well as cytoskeletal dynamics.

THE INTERPLAY BETWEEN THE CYTOSKELETON AND BIOMOLECULAR CONDENSATES

Biomolecular condensates form distinct compartments in the cell that lack a membrane boundary and are present in both the cytoplasm and nucleoplasm (Banani et al., 2017; Boeynaems et al., 2018; Sabari et al., 2020). In the cytoplasm, various biomolecular condensates have been identified of which some are cell-type specific (e.g., germ granules in germline cells) or stress condition-dependent (e.g., Sec bodies and stress granules) (Voronina et al., 2011; Decker and Parker, 2012; Zacharogianni et al., 2014; Banani et al., 2017). Liquid-liquid phase separation can also underlie the formation of neuronal synaptic densities and membrane clusters near the plasma membrane (Wu X. et al., 2020). In addition to

this, a fast-growing body of work shows that a number of viruses form cytosolic liquid-liquid phase separated condensates upon infection of cells, termed "viral factories" and viruses are known to induce changes in stress granule and P-body formation and composition (Alberti and Dormann, 2019).

Several cytosolic biomolecular condensates interact with the cytoskeleton, either directly or indirectly via "hitchhiking" (see section "Interactions Between Membrane-Bound Organelles and Biomolecular Condensates in Conjunction With the Cytoskeleton") and/or influence cytoskeletal remodeling. In this section we will focus on several of the best-studied cytoplasmic biomolecular condensates (P-bodies, stress granules and RNP transport granules) and discuss their direct interactions and interplay with the cytoskeleton as well as highlight the known functional roles of these interactions.

Direct Interactions Between Biomolecular Condensates and the Cytoskeleton

Regulation of Biomolecular Condensate Transport by the Cytoskeleton

Like membrane-bound organelles, biomolecular condensates can use the cytoskeleton for active, motor-driven transport throughout the cell (**Figure 2A**). One of these biomolecular condensates is the RNP transport granule, which consist of RNA-binding proteins (RBPs) and messenger RNAs (mRNAs). These granules can form by liquid-liquid phase separation and are well-known to be transported to ensure proper mRNA localization to specific subcellular locations for subsequent local mRNA translation (**Figure 2A**; Knowles et al., 1996; Buxbaum et al., 2015; Das et al., 2019). This RNP transport for mRNA localization is highly conserved and has been observed in many different model systems such as budding yeast (*Saccharomyces cerevisiae*), fibroblasts, *Drosophila* and *Xenopus* oocytes, oligodendrocytes and neurons where it plays a crucial role in biological processes such as cell division, migration, cell polarization, and axon guidance and neuronal synaptic plasticity (Holt and Bullock, 2009; Buxbaum et al., 2015). Extensive research in these different organisms and cell types has shown that mRNA/RNP transport depends on both the microtubule and actin cytoskeleton and is driven by kinesin, dynein and myosin motor proteins (**Figure 2A**; Kanai et al., 2004; Gopal et al., 2017; Mofatteh and Bullock, 2017; McClintock et al., 2018; Das et al., 2019; Baumann et al., 2020). RNA-binding proteins can interact with molecular motor proteins thereby enabling the transport of translationally repressed mRNAs in RNP granules along the cytoskeleton. During cell division of budding yeast, a well-characterized mRNP granule containing *Ash1* mRNA and several other mRNAs is transported to the tip of a daughter cell on the actin cytoskeleton mediated by the adaptor protein She3p, that couples the RNA-binding protein (RBP) She2P with the myosin motor protein Myo4p (Long et al., 1997; Takizawa et al., 1997; Edelmann et al., 2017). Other well-established examples include the transport of *Vg1* mRNA in *Xenopus* oocytes, that relies on overlapping functions of both kinesin-1 and kinesin-2 motors (Messitt et al., 2008) and the MT-based transport and actin-mediated anchoring of *oskar* and *bicoid* mRNAs in Drosophila oocytes (Trcek and Lehmann, 2019). In addition, several recent studies, both *in vitro* and in rat DRG neurons and mouse hippocampal neurons, have elucidated the interaction of the several RBPs (APC, SFPQ, and ZBP1) with specific adaptor and motor proteins, such as KAP3 with kinesin-2 and KLC1 or PAT1 with kinesin-1 (Baumann et al., 2020; Fukuda et al., 2020; Wu H. et al., 2020). Despite this progress in our understanding of RNP granule transport, many questions remain unanswered; for example, it is unclear how anchoring of RNP granules to specific subcellular locations is regulated and how mRNAs and RBPs are released from motor proteins.

In addition to RNP transport granules, the cytoplasm contains several other well-studied membraneless RNP granules such as P-bodies and stress granules (Buchan, 2014; Riggs et al., 2020). P-bodies are RNP granules that are highly conserved from yeast to humans (Eystathioy et al., 2002; Sheth and Parker, 2003; Riggs et al., 2020). In mammalian cells, P-bodies are present under basal conditions but can dynamically change in number, size and its components upon changes in the availability of non-translating mRNAs (Kedersha et al., 2005; Teixeira et al., 2005; Decker and Parker, 2012; Wang et al., 2018). Stress conditions that affect the amount of non-translating mRNAs therefore change P-body number and size. P-bodies are enriched in translationally inactive mRNAs and proteins involved in mRNA decapping, turnover and silencing, but lack ribosomal proteins and translation initiation factors (Hubstenberger et al., 2017; Luo et al., 2018). They have therefore been suggested to play a role in translational repression, microRNA-induced mRNA silencing, RNA storage and mRNA decay, although recent studies suggest that decay may not occur in P-bodies and they mainly serve as a repository for translationally repressed mRNAs that can reenter translation upon release (Brengues et al., 2005; Horvathova et al., 2017; Hubstenberger et al., 2017; Riggs et al., 2020).

P-bodies are able to perform directed movement in plant, yeast and mammalian cells (**Figure 2A**; Kedersha et al., 2005; Aizer et al., 2008; Cougot et al., 2008; Hamada et al., 2012; Garmendia-Torres et al., 2014; Rajgor et al., 2014). In plant cells (*Arabidopsis thaliana*), long-distance movement of P-bodies was dependent on the actin cytoskeleton and pausing behavior was observed at cortical microtubules (**Figure 2A**; Hamada et al., 2012; Steffens et al., 2014). In mammalian cells, live-cell imaging and single particle tracking experiments showed that P-bodies associate to both the actin and MT cytoskeleton (Aizer et al., 2008). Stationary P-bodies were associated with actin whereas P-bodies exhibited mainly confined movements and occasional long-range movements in association with MTs (**Figure 2A**; Aizer et al., 2008; Rajgor et al., 2014). MT depolymerization by nocodazole or vinblastine treatment severely reduced P-body movement (Aizer et al., 2008).

Several proteins have been implicated in the interaction between P-bodies and the cytoskeleton. Early studies in yeast showed that P-body markers Edc3p and Dcp1p can interact with tubulin proteins (Gavin et al., 2006). In addition, several P-body components, as well as mRNAs, were shown to co-precipitate and colocalize with the myosin motor protein Myo2p in budding yeast (Chang et al., 2008). During cell division in

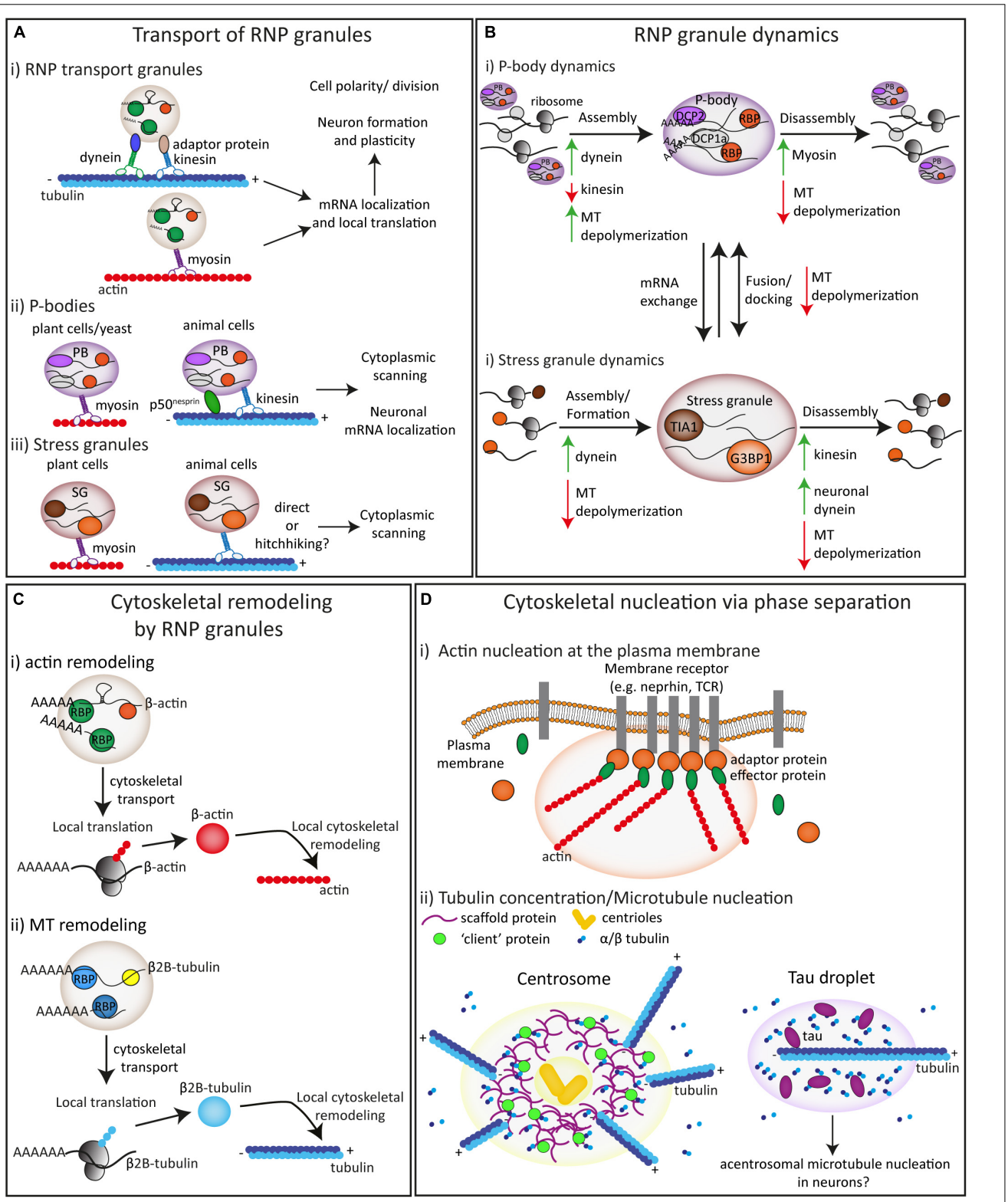

FIGURE 2 | The interplay and interactions between biomolecular condensates and the cytoskeleton. **(A)** The transport of RNP transport granules (i), P-bodies (ii) and stress granules (iii) is mediated by the actin and microtubule cytoskeleton driven by motor proteins. **(B)** The formation/assembly, disassembly and the fusion/docking of P-bodies (i) and stress granules (ii) is influenced by the cytoskeleton and motor proteins. **(C)** The local cytoskeleton can be remodeled by RNPs through mRNA supply and local translation of both actin (i) and microtubule (ii) proteins. **(D)** Both actin (i) and microtubule (ii) nucleation can be driven by concentration of specific proteins via phase separation at specific sub-cellular locations.

yeast, unidirectional transport of P-bodies, marked by Edc3p, was observed to be dependent on a complex of Myo4p and the She2P/She3P RBPs (**Figure 2A**; Garmendia-Torres et al., 2014). In HeLa cells, the expression of the dominant negative tail of another myosin protein, Myosin Va, reduced P-body motility although the authors suggested that this could be caused indirectly by reducing mRNP transport toward P-bodies (Lindsay and McCaffrey, 2011). Another study showed that interactions between DCP proteins and myosin proteins are likely conserved in yeast (Dcp1p with myo2p) and mammals (human Dcp1a and Dcp1b with mouse myosin Va) by performing yeast two-hybrid and coprecipitation experiments (Steffens et al., 2014). The presence of several myosin proteins in a large screen identification of P-body components further confirm the association between myosin motor proteins and P-bodies in mammalian cells (Hubstenberger et al., 2017). A more direct and functional link was found with the identification of an isoform of the MT-associated protein Nesprin, p50^{nesp1}. This protein was found to interact with and localize to P-bodies and anchor them to MTs, thereby facilitating P-body movement (**Figure 2A**; Rajgor et al., 2014). In neurons, several reports show that P-bodies or P-body-like structures that partly resemble neuronal transport granules undergo motor-driven transport on MTs in dendrites (Cougot et al., 2008; Zeitelhofer et al., 2008; Oh et al., 2013). These neuronal P-bodies increase their localization to dendritic synapses in response to neuronal activation, driven by the kinesin-1 motor (**Figure 2A**; Zeitelhofer et al., 2008; Cougot et al., 2008; Oh et al., 2013). Neuronal P-bodies have also been observed in axons of peripheral neurons but whether and how they are actively transported remains to be investigated (Melemedjian et al., 2014; Sahoo et al., 2018).

Stress granules are closely related to both P-bodies and RNP transport granules and can share many of the same components but appear only after stress conditions that inhibit translation (Kedersha et al., 2005; Khong et al., 2017; Markmiller et al., 2018; Youn et al., 2018; Matheny et al., 2019; Youn et al., 2019). Their exact composition differs between specific stress conditions and cell types (Markmiller et al., 2018). Stress granules sequester mRNAs and stalled initiation complexes and are therefore considered to be a storage site for certain non-translating mRNAs during stress that can re-enter translation when stress is relieved (Riggs et al., 2020). A recent study, however, partly challenged this notion and showed that stress granules also contain translating mRNAs that can shuttle between stress granules and the cytoplasm (Mateju et al., 2020).

Several studies have shown that stress granules can undergo directed transport although they appear to be less motile than P-bodies (**Figure 2A**; Kedersha et al., 2005). In plant cells, one study observed rapid and long-distance movement of stress granules marked by eIF42-GFP that decreased only upon actin, but not MT depolymerization (**Figure 2A**; Hamada et al., 2018). By contrast, another study in plant cells observed movement of stress granules (marked by Rbp47b) along MTs but the role of actin was not examined (Gutierrez-Beltran et al., 2015). In HeLa cells, it was shown that arsenite-induced stress granules move throughout the cytoplasm in a mostly diffusive manner (Chernov et al., 2009; Nadezhdina et al., 2010). However, a small percentage (±10%) of stress granules exhibited directed movement (**Figure 2A**; Nadezhdina et al., 2010). Both diffusive and directed stress granule movement was dependent on MTs, but not actin, as shown by colocalization experiments and treatment with cytoskeleton destabilizing drugs. It remains unknown which proteins drive stress granule movement, and it is unclear if movement can occur via direct interactions or whether it is mainly driven by indirect interactions with MTs via "hitchhiking" mechanisms (Liao et al., 2019), which will be further discussed in section "Interactions Between Membrane-Bound Organelles and Biomolecular Condensates in Conjunction With the Cytoskeleton.".

Regulation of Biomolecular Condensate Remodeling by the Cytoskeleton

Besides their movement throughout the cell, RNP granules (transport/neuronal granules, P-bodies and stress granules) are known to be highly dynamic structures that can assemble, disassemble and remodel by rapidly exchanging mRNAs and possibly proteins with each other and the cytoplasm (Kedersha et al., 2005; Aulas et al., 2017; Wang et al., 2018; Moon et al., 2019). Fluorescence recovery after photobleaching (FRAP) experiments have shown that RNP granules can exchange protein components with the cytoplasm (Tauber et al., 2020). Various molecular mechanisms such as extracellular cues, signaling, protein-protein interactions and posttranslational modifications as well as cellular states are known to influence these dynamics (Formicola et al., 2019; Tauber et al., 2020). In addition to this, the cytoskeleton plays an important role in the remodeling of biomolecular condensates (**Figure 2B**).

P-body formation and disassembly/dynamics are also affected by the cytoskeleton and motor-based transport. In budding yeast, U2OS and HeLa cells, depolymerization of MTs with different treatments led to an increase in P-body formation (**Figure 2B**; Sweet et al., 2007; Aizer et al., 2008; Carbonaro et al., 2011; Huang et al., 2011; Ayache et al., 2015). Interestingly, taxol-induced MT stabilization also increased P-body number (Carbonaro et al., 2011). The mechanisms that lead to increased P-body formation after MT depolymerization or stabilization are not entirely clear, but these MT disruptions likely lead to a decrease in mRNA translation and a release of mRNAs from polysomes. However, in yeast, benomyl-induced MT depolymerization did not seem to affect mRNA translation based on polysome profiles (Sweet et al., 2007). On the other hand, it has been shown that MT depolymerization with both nocodazole and vinblastine treatment decreases protein synthesis (Carbonaro et al., 2011; Coldwell et al., 2013; Ayache et al., 2015; Szaflarski et al., 2016). It is possible that both MT-depolymerization and stabilization (through impaired MT dynamics) lead to defective mRNA transport (Lifland et al., 2011; Pease-Raissi et al., 2017), either to sites of active translation or possibly into P-bodies themselves. In support of this, both MT stabilization with taxol or MT depolymerization with vinblastine or 2ME2 induced the release of HIF-1α mRNA from polysomes and subsequent incorporation into P-bodies. This effect was reversible after nocodazole washout and subsequent MT repolymerization (Carbonaro et al., 2011). In contrast to mRNAs, the depolymerization of MTs with

nocodazole did not change the dynamic exchange of Dcp proteins in and out of P-bodies based on FRAP experiments (Aizer et al., 2008).

The involvement of specific motor proteins on P-body formation has also been investigated (Loschi et al., 2009). Whilst under basal conditions P-body size or number was not affected by knockdown of the motor proteins dynein and kinesin, their increase in size was significantly affected after dynein, but not kinesin-1 knockdown under ER or oxidative stress conditions (Loschi et al., 2009). Interestingly, simultaneous knockdown of kinesin abrogated the effect of dynein knockdown on the stress-induced increase in P-body size. This led the authors to suggest that both anterograde and retrograde transport are important for the exchange of mRNAs from RNP granules into and out of P-bodies, at least under stress conditions (**Figure 2B**; Loschi et al., 2009). In addition to this, siRNA-mediated knockdown of the actin-based Myosin Va motor was found to decrease P-body assembly, but not stress granule formation in HeLa cells (**Figure 2B**; Lindsay and McCaffrey, 2011). The release of mRNAs from P-bodies may indeed also be regulated by the actin cytoskeleton, since P-body disassembly was found to be delayed in a yeast myosin motor mutant (Chang et al., 2008).

Under stress conditions, P-bodies often transiently dock in close proximity to stress granules and mRNAs are able to move bidirectionally between P-bodies and stress granules (Kedersha et al., 2005; Moon et al., 2019). When P-bodies and stress granules are docked together, they appear less motile (Kedersha et al., 2005) and the close docking of stress granules with P-bodies is dependent on intact microtubules (**Figure 2B**; Aizer et al., 2008; Rajgor et al., 2014). In cells with intact microtubules but where P-bodies were detached from microtubules by overexpression of a $p50^{nesp1}$ mutant the association between stress granules and P-bodies was also reduced (Rajgor et al., 2014). Together, this suggests that the cytoskeleton may provide a scaffold for P-body-stress granule docking. It would be interesting to determine if P-bodies and stress granules dock at specific locations on microtubules and how this could be mediated.

Stress granule formation is normally a reversible process that starts only under certain stress conditions (Wheeler et al., 2016; Riggs et al., 2020). After stress induction, granules start increasing in size by accumulating components or fusing with other stress granules (Kedersha et al., 2005; Nadezhdina et al., 2010; Wheeler et al., 2016). When stress is relieved, stress granules can disassemble or dissolve into the cytoplasm by releasing their contents into the cytoplasm. Splitting or fission of larger stress granules into smaller ones has been observed during disassembly (Kedersha et al., 2005; Nadezhdina et al., 2010; Wheeler et al., 2016; Lee et al., 2020). Both the formation and disassembly of stress granules have been shown to be dependent on the cytoskeleton and motor proteins (**Figure 2B**). Two initial studies first reported that MT depolymerization completely inhibited the formation of stress granules, but subsequent studies have shown it is more likely that MT disruption does not completely prevent stress granule formation but rather results in more numerous but smaller stress granules (Ivanov et al., 2003; Kwon et al., 2007; Chernov et al., 2009; Fujimura et al., 2009; Kolobova et al., 2009; Loschi et al., 2009). Interestingly, the addition of the MT-stabilizing drug taxol also resulted in smaller stress granules (Chernov et al., 2009). After stress relief, MT disruption impaired stress granule disassembly (Nadezhdina et al., 2010). The role of motor proteins in stress granule assembly and disassembly remains somewhat unclear as several studies have reported contradictory results. Whilst two studies reported a decreased formation of stress granules after treatment with dynein inhibitors (Kwon et al., 2007; Tsai et al., 2009), two other studies observed no effect (Chernov et al., 2009; Fujimura et al., 2009). In support of a role for dynein motors and retrograde transport in stress granules assembly, knockdown of dynein heavy chain 1 (DHC1) and the adaptor protein Bicaudal D1 in mammalian cells inhibits stress granule formation, and knockdown of dynein light chain subunit 2A in primary neurons impaired stress granule formation (Loschi et al., 2009; Tsai et al., 2009). Kinesin knockdown or kinesin inhibitors did not impair stress granule formation, but KIF5B or KLC knockdown did delay stress granule disassembly (**Figure 2B**; Loschi et al., 2009; Tsai et al., 2009). By contrast, inhibition of dynein, but not of kinesin motors in neurons, delayed stress granule disassembly (**Figure 2B**; Tsai et al., 2009). Interestingly, kinesin and dynein transport seemed to counterbalance each other as knockdown of KIF5B counteracted the effect of DHC1 knockdown in stress granule assembly and conversely, DHC1 knockdown partially rescued the delay in stress granule disassembly after KIF5B knockdown (Loschi et al., 2009).

Together, these results suggest microtubules are not crucial for the initial assembly of stress granules but are important for the formation of larger stress granules and for stress granule disassembly. This effect is likely mediated by facilitating transport of protein and mRNA components into and out of stress granules via motor proteins and/or increasing the chance of stress granule fusion.

Research on the role of the actin cytoskeleton on stress granule formation has yielded inconclusive results. One report observed an increase in stress granule size after Latrinculin B-mediated actin depolymerization in CV-1 cells (Ivanov et al., 2003), whilst another study found more numerous but smaller stress granules after cytochalasin B treatment in COS-7 cells (Loschi et al., 2009). Yet another study reported no change in stress granule formation after latrunculin B or cytochaslasin D treatment in HeLa cells, although stress granule size was not measured (Kwon et al., 2007). These discrepancies could be explained by differences in treatments and non-actin related side-effects (Ornelles et al., 1986). In addition, the actin-based Myosin Va motor was not required for stress granule formation, but this does not exclude the possibility that other actin-based motors are involved (Lindsay and McCaffrey, 2011).

Although understudied, several studies report an association of intermediate filaments with RNP condensates. A recent report showed that the intermediate filament protein vimentin associates with both P-bodies and stress granules and both stress granule formation and clearance is affected in vimentin knockout cells (Pattabiraman et al., 2020). Toxic ALS-associated poly-dipeptides were also found to bind along vimentin filaments (Lin et al., 2016). In addition to this, giantin-based

intermediate filaments have been suggested to serve as a scaffold for cytoplasmic condensates marked by myxovirus resistance proteins (reviewed in Sehgal et al., 2020). Together this shows that intermediate filaments may play an important role in the dynamics of various biomolecular condensates.

Biomolecular Condensates Can Influence the Cytoskeleton

Conversely, biomolecular condensates can influence the actin and microtubule cytoskeleton, either by supplying mRNAs encoding cytoskeletal proteins for local translation (**Figure 2C**) or by concentrating certain proteins that promote actin or microtubule nucleation (**Figure 2D**).

Early work has shown that mRNAs encoding cytoskeletal proteins such as Tau and β-actin are localized to specific subcellular locations in neurons, oocytes and other cell types (Jeffery et al., 1983; Litman et al., 1994). As mentioned above, these mRNAs travel together with RBPs in RNP granules along the cytoskeleton, in a translationally repressed state and are released for local translation upon stimulation with specific cues or signals. This local translation of mRNAs encoding cytoskeletal proteins is exemplified in axon guidance, where the steering of axonal growth cones in response to guidance cues relies on the local protein synthesis of specific cytoskeletal proteins (Buxbaum et al., 2015; Cioni et al., 2018). In addition, it was suggested that mRNAs encoding the actin cytoskeleton regulators Arp2 and Nd1 can be released from P-bodies in dendrites in response to neuronal activation, thereby influencing local F-actin dynamics at synapses (Oh et al., 2013). Intriguingly, it has been shown that both actin and microtubule regulators can act as RBPs in RNP granules containing mRNAs coding for cytoskeletal regulators (Preitner et al., 2014; Vidaki et al., 2017). This provides a possible self-regulatory mechanism in which certain cytoskeletal regulators coordinate the assembly of the actin or microtubule cytoskeleton by forming RNP granules that contain mRNAs encoding their components (**Figure 2C**).

As mentioned above, besides RNP granule formation, liquid-liquid phase separation can also underlie the formation of biomolecular condensates that enables the concentration of certain proteins to drive specific functions. In this manner, both actin and microtubule nucleation can be promoted by concentrating cytoskeletal proteins via phase separation mechanisms. For actin, this has been shown to occur near the plasma membrane, where clustering of transmembrane proteins with adaptor proteins can induce phase transitions forming a dense phase at the plasma membrane. This mechanism increases the dwell time of effector proteins that are recruited to these adaptor proteins and increase the likelihood of activation of signaling pathways (Case et al., 2019). In response to extracellular signals, the transmembrane protein Nephrin is phosphorylated and has been shown to subsequently trigger the formation of these phase-separated membrane clusters in combination with the adaptor protein Nck and the actin nucleation factors N-WASP and the ARP2/3 complex (Banjade and Rosen, 2014; Case et al., 2019; Kim et al., 2019). This promotes an increase in actin nucleation/assembly, thereby influencing the local organization of the cytoskeleton close to plasma membrane (**Figure 2D**). Similarly, T-cell receptors can form phase-separated clusters at the plasma membrane via phosphorylation-dependent association with the linker protein LAT (Su et al., 2016). These TCR-LAT clusters recruit specific adaptor and effector proteins whilst excluding others. In this manner, these clusters concentrate Nck, N-WASP and the ARP2/3 complex thereby enhancing actin filament assembly (Su et al., 2016). In addition, zona occludens proteins were shown to self-organize at tight junctions by phase separation and attract and concentrate cytoskeletal adaptor proteins and F-actin (Beutel et al., 2019). Together, this shows that phase separation at the plasma membrane creates membraneless compartments that influence the local actin cytoskeleton by enhancing actin polymerization. It is conceivable that other membrane proteins can drive the formation of phase-separated clusters and future research will have to determine how widespread this mechanism is. For example, it is interesting to speculate that this may be involved in axon guidance since extracellular cues are known to induce local changes in the actin cytoskeleton, thereby influencing growth cone steering (Dorskind and Kolodkin, 2020).

Microtubule nucleation can also be driven by phase separation. Several recent studies have shown that phase separation may be an important mechanism during cell division by promoting microtubule nucleation (Ong and Torres, 2020). *In vitro* work using *C. elegans* proteins revealed that tubulin concentration was increased approximately 4-fold by the formation of biomolecular condensates at the centrosome containing the scaffold protein SPD-5, which in turn recruits the microtubule effector protein homologs of XMAP215/CKAP5 and TPX2. This increase in tubulin concentration was sufficient to drive microtubule nucleation (**Figure 2D**; Woodruff et al., 2017). The microtubule-associated protein PLK4 was also shown to self-assemble into condensates and recruit and concentrate tubulin thereby promoting the formation of a microtubule organizing center (Montenegro Gouveia et al., 2018). In a similar manner, several other proteins have been shown to promote microtubule assembly by concentrating tubulin via phase separation at mitotic spindles (Jiang et al., 2015; So et al., 2019; King and Petry, 2020; Safari et al., 2020). In addition, it was shown that tubulin can be concentrated into liquid-like phase separated droplets *in vitro* formed by the microtubule-associated protein Tau (Hernandez-Vega et al., 2017). This concentrated tubulin polymerizes within these droplets and forms microtubule bundles (**Figure 2D**). Interestingly, tau droplets have been observed in neurons (Wegmann et al., 2018). This mechanism provides an interesting possibility for the formation of local, non-centrosomal microtubule nucleation (Kuijpers and Hoogenraad, 2011).

Finally, it has been suggested that the actin cytoskeleton itself can exhibit liquid-like behavior and form condensates (Weirich et al., 2017). In the presence of the crosslinker filamin, actin filaments can be condensed into a liquid droplet phase. This enables a mechanism to control the morphology and dynamics of the actin cytoskeleton.

Together, these recent studies provide compelling evidence that phase separation and the formation of condensates can

promote the nucleation and remodeling of the cytoskeleton at specific subcellular locations.

INTERACTIONS BETWEEN MEMBRANE-BOUND ORGANELLES AND BIOMOLECULAR CONDENSATES IN CONJUNCTION WITH THE CYTOSKELETON

As discussed in the previous two sections, it has become clear that both membrane-bound organelles and biomolecular condensates are directly or indirectly contacting the cytoskeleton. Increasing evidence shows that they also frequently form contacts with each other, often in conjunction with the cytoskeleton (Salogiannis and Reck-Peterson, 2017; Bethune et al., 2019; Zhao and Zhang, 2020). The functional roles of these contacts and their interplay with the cytoskeleton are just starting to emerge and recent advances will be discussed in this section.

Biomolecular Condensates Can Associate With Membrane-Bound Organelles

One of the first examples of an association between biomolecular condensates and membrane-bound organelles was shown when GW-bodies were found to associate with LAMP1- and CD63-positive lysosomes/multivesicular bodies (MVBs) (Gibbings et al., 2009; Lee et al., 2009). These GW-bodies, containing the miRNA processing proteins GW-182 and Ago2, are closely related to P-bodies and share several components but likely represent different condensates (Patel et al., 2016). The formation of MVBs was found to be important for miRNA-mediated gene silencing (Gibbings et al., 2009; Lee et al., 2009).

Huang et al. revealed that a large proportion of P-bodies can interact with mitochondria in various cell lines (Huang et al., 2011). Electron microscopy and live cell imaging analysis in HeLa cells showed that P-bodies can form close and dynamic contacts with mitochondria. The authors state they did not observe a close association of P-bodies with other organelles, such as the ER, endosomes or vacuoles, with electron microscopy. Depolymerization of the microtubule network by vinblastine treatment increased the number of P-bodies but decreased the association frequency with mitochondria, suggesting an intact microtubule network is required for these contacts. P-body depletion did not influence mitochondrial morphology and function and CCCP-induced mitochondrial uncoupling did not affect the size or number of P-bodies or their contact with mitochondria. By contrast, CCCP treatment drastically affected miRNA- and siRNA-mediated gene silencing, possibly by decreasing the accumulation of Ago2 in P-bodies (Huang et al., 2011).

In addition to mitochondria, a clear association between the ER and P-bodies has been established. In yeast, P-bodies only form under stress conditions and in this model system they were observed in close proximity to the ER with both co-localization analysis using fluorescence microscopy and by electron microscopy imaging (Kilchert et al., 2010). Differential centrifugation experiments to isolate ER membranes confirmed that P-bodies are physically associated to the ER (Kilchert et al., 2010; Weidner et al., 2014). Subsequently, the yeast ER proteins Scp160 and Brf1 (closest human homologs are vigilin and FMRP) were found to interact with several P-body components but deletion of these proteins did not impair P-body localization to the ER (Weidner et al., 2014). Although an association with the ER was not observed in HeLa cells (Huang et al., 2011), a very recent and elegant study used live-cell imaging methods to reveal that P-bodies, as well as stress granules can indeed form dynamic contacts with the ER in U2OS cells (Lee et al., 2020). The authors also investigated the relationship between ER shape and ER translational status with P-body formation and found that ER tubules and inhibition of translation promote P-body formation. Intriguingly, they revealed that fission of both P-bodies and stress granules occurs at ER contact sites (Lee et al., 2020). Two other recent studies also described associations of RNP or stress granules with the ER. In *Xenopus* RGC axons, a close association of RNA granules was observed with the ER (Cioni et al., 2019) and in U2OS cells a high colocalization of G3BP1-positive stress granules with the ER was found (Liao et al., 2019). The functional relevance of contacts between the ER and P-bodies or other RNP granules remains to be determined but possibly includes the exchange of mRNAs and regulation of RNP granule size. Although RNP granules do not contain a membrane, it is conceivable that the microtubule cytoskeleton is involved in RNP granule fission events analogous to the regulation of fission of membrane-bound organelles by the ER (Friedman et al., 2010; Rowland et al., 2014). In addition, since both P-bodies and stress granules interact with the ER and they all associate with microtubules, it is possible that the ER plays a role in the docking of P-bodies to stress granules. Moreover, it is unknown if the interaction of P-bodies and stress granules with the ER can reciprocally influence ER organization.

Two additional types of RNP granules have been shown to be associated with the ER; TIS granules and Sec bodies. TIS granules, containing the RBPs TIS11B and HuR as well as the chaperone protein HSPA8, are intertwined with ER sheets and concentrate specific mRNAs with AU-rich elements (Ma and Mayr, 2018). These gel-like granules are present under physiological conditions and have a tubular mesh-like morphology, driven by RNA-RNA interactions, that is different from the spherical morphology described for other RNP granules (Ma et al., 2020). The formation of TIS granules and its association to ER sheets enables the local translation of specific AU-rich mRNAs at the ER.

Sec bodies represent another stress-induced condensate and are also related to the ER since they are formed at ER exit sites (ERES) upon amino acid starvation in *Drosophila* S2 cells (Zacharogianni et al., 2014; Aguilera-Gomez et al., 2016). These condensates protect ERES components during stress and act as a reservoir to reinitiate secretory vesicle formation after stress relief. Thus far, it remains unknown if these Sec bodies also exist in mammalian cells and if their formation and disassembly require an intact cytoskeleton.

Together, these studies illustrate that interactions between biomolecular condensates and membrane-bound organelles occur frequently, but for most of these interactions the exact mechanisms and functions as well as their relationship with the cytoskeleton will require further investigation.

Biomolecular Condensates Can "Hitchhike" on Membrane-Bound Organelles for Transport

In recent years, it has become clear that both RNP transport granules and stress granules can also be transported via the cytoskeleton by "hitchhiking" on membrane-bound organelles. During asymmetric cell division in budding yeast, the cortical ER, a tubular ER structure which is in close contact with the plasma membrane, is transported by myosin motor proteins on the actin cytoskeleton to the daughter cell (Estrada et al., 2003). During this process, it has been shown that several mRNAs can be co-transported on the ER membrane via the adaptor RBP She2p to the yeast bud for local translation (Schmid et al., 2006; Aronov et al., 2007). This represents a first example of coordinated co-transport of biomolecular condensates (RNPs) with membrane-bound organelles on the cytoskeleton. Another clear and one of the best-studied examples of "hitchhiking" of RNP granules with membrane-bound organelles was found during the highly polarized growth of hyphae of the fungus *Ustilago Maydis*. In this organism, transport of several mRNAs by the RNA-binding protein Rrm4 is essential for this polarized growth (Konig et al., 2009; Bethune et al., 2019). It was found that Rrm4 colocalizes and co-moves only with motile but not static Rab5a-positive early endosomes that travel along MTs driven by kinesin-3 or dynein motors (Baumann et al., 2012, 2014). Several specific mRNAs, including mRNAs coding for all four septins (*cdc3, cdc10, cdc11,* and *cdc12*), co-transport together with ribosomes on these endosomes. These septin proteins can form heteromeric complexes on the cytoplasmic surface of endosomes in a Rrm4-dependent matter, indicating local translation occurs on these endosomes (Baumann et al., 2014; Higuchi et al., 2014). Since these findings, many components of this transport system in fungal hyphae, including adaptor proteins and additional mRNAs and RBPs have been identified (Pohlmann et al., 2015; Jankowski et al., 2019; Olgeiser et al., 2019).

In neurons, a similar hitchhiking mechanism involving RNP granules and endosomes was recently uncovered. Live-cell imaging of *Xenopus Laevis* RGC axons revealed that RNP granules often associate and co-transport with both Rab5-positive early endosomes and Rab7-positive late endosomes (Cioni et al., 2019). Another study found frequent associations and co-movement of heat shock-induced stress granules with LAMP1-positive lysosomes in a microtubule and motor-dependent fashion in U2OS cells and iPSC-derived cortical neurons (Liao et al., 2019). Interestingly, the authors utilized APEX2-mediated proximity labeling analysis in human iPSC-induced neurons to identify that Annexin 11 (ANXA11), a RNA granule–associated phosphoinositide binding protein also found in stress granules (Markmiller et al., 2018), tethers stress granules to actively transported lysosomes. Interestingly, stress granule-lysosome contacts were observed at the ER in U2OS cells (Liao et al., 2019). As described above, we recently found that ER-lysosome contacts in the soma of neurons are important for the axonal translocation of lysosomes (Özkan et al., 2020). Together, this raises the interesting possibility that neuronal somatic ER tubules provide a platform for mRNA localization or transfer to lysosomes and likely indirectly regulate RNP transport into axons by influencing lysosome distribution.

RNP granule hitchhiking provides a mechanism for neurons to localize mRNAs into axons for their local translation and indeed, the axonal translation of two mitochondrial mRNAs (*laminb2* and *vdac*) was shown to occur on Rab7a-positive late endosomes (Cioni et al., 2019). Interestingly, late endosomes that colocalized with RNA granules and stained positive for puromycin (indicating protein synthesis), were often observed in close proximity to mitochondria, suggesting newly synthesized proteins may be delivered to mitochondria by late endosomes.

An important role for endosomes in mRNA localization and translation is further supported by a recent study that showed both translation-dependent and -independent association of various mRNAs to early endosomes in HeLa cells (Popovic et al., 2020). This study provided important insights into which mRNAs localize to early endosomes and it will be interesting to determine if endosome-localized mRNAs are conserved across cell types and organisms or if there are cell-type specific or even context-dependent differences in endosomal mRNA localization and translation. In addition, future research will have to clarify why there seem to be cell-type specific differences in which type of endosome (early, late or lysosomes) is mainly responsible for mRNA transport and localized mRNA translation (Baumann et al., 2014; Cioni et al., 2019; Liao et al., 2019; Popovic et al., 2020).

Interestingly, two recent reports described a role for late endosomes/lysosomes in the transport of microRNAs in axons. Gershoni-Emek et al. (2018) showed that miRNAs and RNAi proteins colocalized and co-moved with acidic compartments marked by Lysotracker and frequently dock at mitochondria. The second report convincingly showed that pre-miRNAs are transported on CD63-positive late endosomes/lysosomes in RGC axons (Corradi et al., 2020). Since RNAi proteins and possibly miRNAs are known to reside in P-bodies or GW-bodies, these studies raise the interesting possibility that P-bodies or GW-bodies also utilize hitchhiking on endo-lysosomes for their co-transport. This possibility is supported by the aforementioned association of CD63- or LAMP1-positive multivesicular bodies/lysosomes with GW-bodies in *Drosophila* and human cells (Gibbings et al., 2009; Lee et al., 2009).

Finally, RNP granule hitchhiking on endosomal compartments can influence the local cytoskeleton by localizing and translating certain cytoskeletal mRNAs at specific subcellular locations. As mentioned above, all four mRNAs encoding the cytoskeletal septin proteins are localized to early endosomes in fungal hyphae and their translation on these endosomes is essential for correct septin filamentation and fungal growth (Baumann et al., 2014). In addition, β-actin mRNA was found to co-move on late endosomes/lysosomes in axons and several mRNAs coding for cytoskeletal proteins were identified on

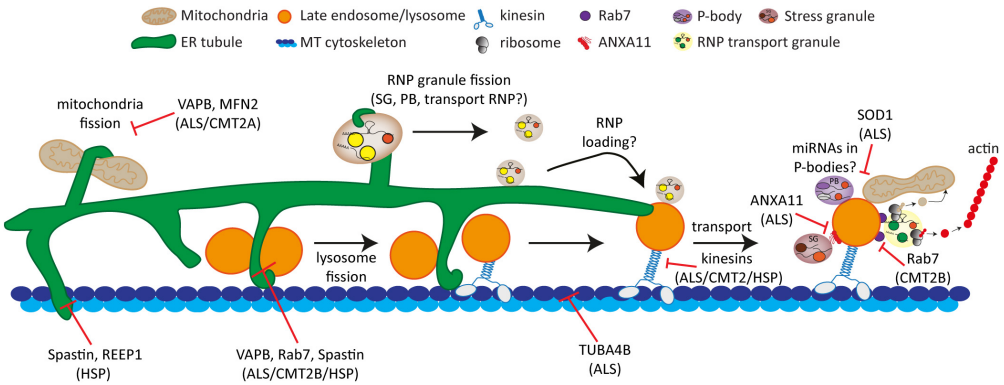

FIGURE 3 | Interplay between membrane-bound organelles, biomolecular condensates, and the cytoskeleton. A model depicting the complex interactions between membrane-bound organelles, biomolecular condensates and the cytoskeleton. Membrane-bound organelles (ER, mitochondria, endo-lysosomes) form contacts with each other and the microtubule cytoskeleton and can also form dynamic contacts with biomolecular condensates. For simplicity, transport granules, P-bodies and stress granules are depicted collectively as "RNP granules" for granule fission. These interactions and their complex interplay regulate the organization and remodeling of membrane-bound organelles, biomolecular condensates and the cytoskeleton. Mutations in various proteins influencing these complex interactions are linked to several neurodegenerative diseases and are indicated in the model.

EEA1-positive early endosomes in HeLa cells (Cioni et al., 2019; Liao et al., 2019; Popovic et al., 2020).

Together, these studies show that there is an intricate interplay between (multiple) membrane-bound organelles, biomolecular condensates and the cytoskeleton which is crucial for maintaining the proper distribution and function of both the organelles themselves as well as the cytoskeleton.

CONCLUDING REMARKS AND FUTURE PERSPECTIVES

It has long been clear that the distinct domains that organize a cell and allow the separation of cellular/biochemical processes, such as membrane-bound organelles, biomolecular condensates, and the cytoskeleton, do not merely perform their functions by themselves. Rather, they have to be well-coordinated by communicating with each other through frequent and dynamic interactions. The extent of complexity of these interactions is only recently becoming clear and has greatly advanced with the advent of new imaging and biochemical techniques. For example, the recent development of multispectral imaging approaches allowed the simultaneous imaging of six different membrane-bound organelles and revealed a complex organelle interactome that depends on an intact microtubule cytoskeleton (Valm et al., 2017). In addition, super-resolution imaging approaches that enable live-cell multi-color imaging at a high spatiotemporal resolution such as the above discussed GI-SIM imaging (Guo et al., 2018) revealed new types of inter-organelle interactions in conjunction with the cytoskeleton and their effect on organelle dynamics. These imaging techniques can be further applied in the future to study the dynamics of interactions between the cytoskeleton, (multiple) membrane-bound organelles and biomolecular condensates in different cell types and different cellular states and conditions. Moreover, the recent and continuing development of novel split reporter systems is improving the visualization of inter-organelle contacts (reviewed by Scorrano et al., 2019) and novel biochemical approaches such as proximity labeling will advance our understanding of the molecular makeup of each cellular compartment. The latter is especially important because it is often unknown which proteins mediate and regulate these contacts and these novel techniques will be able to identify possible tethering and regulatory proteins (Lam et al., 2015; Fazal et al., 2019; Gingras et al., 2019).

The highly complex interactions and interplay illustrated in this review may be especially important for the correct organization and functioning of morphologically complex and highly polarized cells such as neurons. Many studies have shown that dysfunction of the cytoskeleton, several membrane-bound organelles and biomolecular condensates is implicated in neuron dysfunction and neurological disorders (**Figure 3**; Fowler et al., 2019; Sleigh et al., 2019; Zbinden et al., 2020). However, the role of the complex interactions and interplay between them in disease pathogenesis is much less clear. Several lines of evidence support the notion that disruptions of this complex interplay may be an important causative factor in neurological disorders. For instance, mutations in ANXA11, the protein that was found to tether stress granules to lysosomes for their hitchhiking-based transport, cause ALS. These ALS-associated mutations in ANXA11 impair its tethering function and reduce RNA transport into the axon (**Figure 3**; Liao et al., 2019). Mutations in the late endosome/lysosome protein Rab7 that cause the neuropathy Charcot-Marie-Tooth Type 2B impair the axonal synthesis of mitochondrial proteins and led to reduced mitochondrial function and axonal viability (**Figure 3**). Although the exact mechanism leading to this phenotype is not entirely clear, it is conceivable that this is a consequence of impaired local translation of mitochondrial mRNAs on Rab7-positive endosomes that would normally be delivered to nearby mitochondria via the cytoskeleton to sustain their function (Cioni et al., 2019). In addition, the lysosome-associated axonal transport of a miRNA and RNAi proteins,

possibly contained in P-bodies (Gibbings et al., 2009; Lee et al., 2009), and their docking at mitochondria was altered in ALS-associated SOD1 mutant neurons (**Figure 3**; Gershoni-Emek et al., 2018). Finally, it is known that mutations in the ER-resident and MT-severing protein Spastin cause the neurodegenerative disease HSP (Blackstone, 2012). As mentioned above, Spastin interacts with IST1 at ER-late endosome/lysosome contact sites to promote endosomal fission (**Figure 3**; Allison et al., 2013). In both primary neurons from Spastin-HSP mice and HSP-patient-derived iPSC neurons enlarged lysosomes were observed, suggesting a disturbance of the complex interaction between the ER, late endosome/lysosomes and MTs although the exact mechanism that leads to the enlarged lysosomes in HSP patients remains to be determined (Allison et al., 2017).

In addition, several exciting recent studies have shown that there is crosstalk between cytoskeletal components. These components are inter-linked by proteins that directly or indirectly bind to the MT and actin cytoskeleton, and this crosstalk has been shown to play essential roles in cell division, migration, immune synapse and axonal growth (Rodriguez et al., 2003; Mohan and John, 2015; van de Willige et al., 2019; Biswas and Kalil, 2018; Martin-Cofreces and Sanchez-Madrid, 2018). The role of this cytoskeletal crosstalk on organelle dynamics remains largely unexplored.

The recent technical advances mentioned above open up the possibility to further investigate these complex interactions and study the consequence of disease mutations, which will likely increase our knowledge on disease pathogenesis.

AUTHOR CONTRIBUTIONS

MK and NÖ conceived and wrote the manuscript and designed the figures. GF contributed to manuscript writing, provided feedback, and proofread the manuscript. All authors read and approved the manuscript before submission.

FUNDING

This review was supported by funding from the Netherlands Organization for Scientific Research (NWO) through a VIDI grant (016.VIDI.189.019) to GF.

ACKNOWLEDGMENTS

We wish to apologize to colleagues whose work could not be cited due to space limitations.

REFERENCES

Abrisch, R. G., Gumbin, S. C., Wisniewski, B. T., Lackner, L. L., and Voeltz, G. K. (2020). Fission and fusion machineries converge at ER contact sites to regulate mitochondrial morphology. *J. Cell Biol.* 219:e201911122. doi: 10.1083/jcb.201911122

Aguilera-Gomez, A., Van Oorschot, M. M., Veenendaal, T., and Rabouille, C. (2016). In vivo vizualisation of mono-ADP-ribosylation by dPARP16 upon amino-acid starvation. *eLife* 5:e21475.

Aizer, A., Brody, Y., Ler, L. W., Sonenberg, N., Singer, R. H., and Shav-Tal, Y. (2008). The dynamics of mammalian P body transport, assembly, and disassembly in vivo. *Mol. Biol. Cell.* 19, 4154–4166. doi: 10.1091/mbc.e08-05-0513

Akhmanova, A., and Steinmetz, M. O. (2019). Microtubule minus-end regulation at a glance. *J. Cell. Sci.* 132:jcs227850. doi: 10.1242/jcs.227850

Alberti, S., and Dormann, D. (2019). Liquid-liquid phase separation in disease. *Annu. Rev. Genet.* 53, 171–194. doi: 10.1146/annurev-genet-112618-043527

Allison, R., Edgar, J. R., Pearson, G., Rizo, T., Newton, T., Gunther, S., et al. (2017). Defects in Er-endosome contacts impact lysosome function in hereditary spastic paraplegia. *J. Cell Biol.* 216, 1337–1355. doi: 10.1083/jcb.201609033

Allison, R., Lumb, J. H., Fassier, C., Connell, J. W., Ten Martin, D., Seaman, M. N., et al. (2013). An ESCRT-spastin interaction promotes fission of recycling tubules from the endosome. *J. Cell Biol.* 202, 527–543. doi: 10.1083/jcb.201211045

Aronov, S., Gelin-Licht, R., Zipor, G., Haim, L., Safran, E., and Gerst, J. E. (2007). mRNAs encoding polarity and exocytosis factors are cotransported with the cortical endoplasmic reticulum to the incipient bud in *Saccharomyces cerevisiae*. *Mol. Cell. Biol.* 27, 3441–3455. doi: 10.1128/mcb.01643-06

Aulas, A., Fay, M. M., Lyons, S. M., Achorn, C. A., Kedersha, N., Anderson, P., et al. (2017). Stress-specific differences in assembly and composition of stress granules and related foci. *J. Cell. Sci.* 130, 927–937. doi: 10.1242/jcs.199240

Ayache, J., Benard, M., Ernoult-Lange, M., Minshall, N., Standart, N., Kress, M., et al. (2015). P-body assembly requires DDX6 repression complexes rather than decay or Ataxin2/2L complexes. *Mol. Biol. Cell.* 26, 2579–2595. doi: 10.1091/mbc.e15-03-0136

Banani, S. F., Lee, H. O., Hyman, A. A., and Rosen, M. K. (2017). Biomolecular condensates: organizers of cellular biochemistry. *Nat. Rev. Mol. Cell. Biol.* 18, 285–298. doi: 10.1038/nrm.2017.7

Banjade, S., and Rosen, M. K. (2014). Phase transitions of multivalent proteins can promote clustering of membrane receptors. *eLife* 3:e04123.

Baumann, S., Komissarov, A., Gili, M., Ruprecht, V., Wieser, S., and Maurer, S. P. (2020). A reconstituted mammalian Apc-kinesin complex selectively transports defined packages of axonal mRNAs. *Sci. Adv.* 6:eaaz1588. doi: 10.1126/sciadv.aaz1588

Baumann, S., Konig, J., Koepke, J., and Feldbrugge, M. (2014). Endosomal transport of septin mrna and protein indicates local translation on endosomes and is required for correct septin filamentation. *EMBO Rep.* 15, 94–102. doi: 10.1002/embr.201338037

Baumann, S., Pohlmann, T., Jungbluth, M., Brachmann, A., and Feldbrugge, M. (2012). Kinesin-3 and dynein mediate microtubule-dependent co-transport of mRNPs and endosomes. *J. Cell. Sci.* 125, 2740–2752. doi: 10.1242/jcs.101212

Bethune, J., Jansen, R. P., Feldbrugge, M., and Zarnack, K. (2019). Membrane-associated RNA-binding proteins orchestrate organelle-coupled translation. *Trends Cell Biol.* 29, 178–188. doi: 10.1016/j.tcb.2018.10.005

Beutel, O., Maraspini, R., Pombo-Garcia, K., Martin-Lemaitre, C., and Honigmann, A. (2019). Phase separation of zonula occludens proteins drives formation of tight junctions. *Cell* 179, 923.e11–936.e11.

Biswas, S., and Kalil, K. (2018). The microtubule-associated protein tau mediates the organization of microtubules and their dynamic exploration of actin-rich lamellipodia and filopodia of cortical growth cones. *J. Neurosci.* 38, 291–307. doi: 10.1523/jneurosci.2281-17.2017

Blackstone, C. (2012). Cellular pathways of hereditary spastic paraplegia. *Annu. Rev. Neurosci.* 35, 25–47. doi: 10.1146/annurev-neuro-062111-150400

Boeynaems, S., Alberti, S., Fawzi, N. L., Mittag, T., Polymenidou, M., Rousseau, F., et al. (2018). Protein phase separation: a new phase in cell biology. *Trends Cell Biol.* 28, 420–435. doi: 10.1016/j.tcb.2018.02.004

Bonifacino, J. S., and Neefjes, J. (2017). Moving and positioning the endolysosomal system. *Curr. Opin. Cell Biol.* 47, 1–8. doi: 10.1016/j.ceb.2017.01.008

Braakman, I., and Hebert, D. N. (2013). Protein folding in the endoplasmic reticulum. *Cold Spring Harb. Perspect. Biol.* 5:a013201.

Brengues, M., Teixeira, D., and Parker, R. (2005). Movement of eukaryotic mrnas between polysomes and cytoplasmic processing bodies. *Science* 310, 486–489. doi: 10.1126/science.1115791

Buchan, J. R. (2014). mRNP granules. Assembly, function, and connections with disease. *RNA Biol.* 11, 1019–1030. doi: 10.4161/15476286.2014.972208

Burute, M., and Kapitein, L. C. (2019). Cellular logistics: unraveling the interplay between microtubule organization and intracellular transport. *Annu. Rev. Cell. Dev. Biol.* 35, 29–54. doi: 10.1146/annurev-cellbio-100818-125149

Buxbaum, A. R., Haimovich, G., and Singer, R. H. (2015). In the right place at the right time: visualizing and understanding mRNA localization. *Nat. Rev. Mol. Cell Biol.* 16, 95–109. doi: 10.1038/nrm3918

Carbonaro, M., O'brate, A., and Giannakakou, P. (2011). Microtubule disruption targets HIF-1alpha mRNA to cytoplasmic P-bodies for translational repression. *J. Cell Biol.* 192, 83–99. doi: 10.1083/jcb.201004145

Case, L. B., Zhang, X., Ditlev, J. A., and Rosen, M. K. (2019). Stoichiometry controls activity of phase-separated clusters of actin signaling proteins. *Science* 363, 1093–1097. doi: 10.1126/science.aau6313

Chada, S. R., and Hollenbeck, P. J. (2004). Nerve growth factor signaling regulates motility and docking of axonal mitochondria. *Curr. Biol.* 14, 1272–1276. doi: 10.1016/j.cub.2004.07.027

Chakrabarti, R., Ji, W. K., Stan, R. V., De juan sanz, J., Ryan, T. A., and Higgs, H. N. (2018). Inf2-mediated actin polymerization at the ER stimulates mitochondrial calcium uptake, inner membrane constriction, and division. *J. Cell. Biol.* 217, 251–268. doi: 10.1083/jcb.201709111

Chang, W., Zaarour, R. F., Reck-Peterson, S., Rinn, J., Singer, R. H., Snyder, M., et al. (2008). Myo2p, a class V myosin in budding yeast, associates with a large ribonucleic acid-protein complex that contains mRNAs and subunits of the RNA-processing body. *RNA* 14, 491–502. doi: 10.1261/rna.665008

Chen, J. V., Buchwalter, R. A., Kao, L. R., and Megraw, T. L. (2017). A splice variant of centrosomin converts mitochondria to microtubule-organizing centers. *Curr. Biol.* 27, 1928.e6–1940.e6.

Chen, S., Novick, P., and Ferro-Novick, S. (2013). ER structure and function. *Curr. Opin. Cell. Biol.* 25, 428–433.

Chen, Y., and Sheng, Z. H. (2013). Kinesin-1-syntaphilin coupling mediates activity-dependent regulation of axonal mitochondrial transport. *J. Cell Biol.* 202, 351–364. doi: 10.1083/jcb.201302040

Chernov, K. G., Barbet, A., Hamon, L., Ovchinnikov, L. P., Curmi, P. A., and Pastre, D. (2009). Role of microtubules in stress granule assembly: microtubule dynamical instability favors the formation of micrometric stress granules in cells. *J. Biol. Chem.* 284, 36569–36580. doi: 10.1074/jbc.m109.042879

Cioni, J. M., Koppers, M., and Holt, C. E. (2018). Molecular control of local translation in axon development and maintenance. *Curr. Opin. Neurobiol.* 51, 86–94. doi: 10.1016/j.conb.2018.02.025

Cioni, J. M., Lin, J. Q., Holtermann, A. V., Koppers, M., Jakobs, M. A. H., Azizi, A., et al. (2019). Late endosomes act as mrna translation platforms and sustain mitochondria in axons. *Cell* 176, 56.e15–72.e15.

Coldwell, M. J., Cowan, J. L., Vlasak, M., Mead, A., Willett, M., Perry, L. S., et al. (2013). Phosphorylation of eIF4GII and 4E-BP1 in response to nocodazole treatment: a reappraisal of translation initiation during mitosis. *Cell Cycle* 12, 3615–3628. doi: 10.4161/cc.26588

Corradi, E., Dalla Costa, I., Gavoci, A., Iyer, A., Roccuzzo, M., Otto, T. A., et al. (2020). Axonal precursor miRNAs hitchhike on endosomes and locally regulate the development of neural circuits. *EMBO J.* 39:e102513.

Cougot, N., Bhattacharyya, S. N., Tapia-Arancibia, L., Bordonne, R., Filipowicz, W., Bertrand, E., et al. (2008). Dendrites of mammalian neurons contain specialized P-body-like structures that respond to neuronal activation. *J. Neurosci.* 28, 13793–13804. doi: 10.1523/jneurosci.4155-08.2008

Das, S., Singer, R. H., and Yoon, Y. J. (2019). The travels of mRNAs in neurons: do they know where they are going? *Curr. Opin. Neurobiol.* 57, 110–116. doi: 10.1016/j.conb.2019.01.016

Decker, C. J., and Parker, R. (2012). P-bodies and stress granules: possible roles in the control of translation and mRNA degradation. *Cold Spring Harb. Perspect. Biol.* 4:a012286. doi: 10.1101/cshperspect.a012286

Dekker-Ohno, K., Hayasaka, S., Takagishi, Y., Oda, S., Wakasugi, N., Mikoshiba, K., et al. (1996). Endoplasmic reticulum is missing in dendritic spines of Purkinje cells of the ataxic mutant rat. *Brain Res.* 714, 226–230. doi: 10.1016/0006-8993(95)01560-4

Dorskind, J. M., and Kolodkin, A. L. (2020). Revisiting and refining roles of neural guidance cues in circuit assembly. *Curr. Opin. Neurobiol.* 66, 10–21. doi: 10.1016/j.conb.2020.07.005

Dreier, L., and Rapoport, T. A. (2000). In vitro formation of the endoplasmic reticulum occurs independently of microtubules by a controlled fusion reaction. *J. Cell. Biol.* 148, 883–898. doi: 10.1083/jcb.148.5.883

Edelmann, F. T., Schlundt, A., Heym, R. G., Jenner, A., Niedner-Boblenz, A., Syed, M. I., et al. (2017). Molecular architecture and dynamics of Ash1 mrna recognition by its mrna-transport complex. *Nat. Struct. Mol. Biol.* 24, 152–161. doi: 10.1038/nsmb.3351

English, A. R., Zurek, N., and Voeltz, G. K. (2009). Peripheral ER structure and function. *Curr. Opin. Cell. Biol.* 21, 596–602. doi: 10.1016/j.ceb.2009.04.004

Estrada, P., Kim, J., Coleman, J., Walker, L., Dunn, B., Takizawa, P., et al. (2003). Myo4p and She3p are required for cortical ER inheritance in *Saccharomyces cerevisiae*. *J. Cell. Biol.* 163, 1255–1266. doi: 10.1083/jcb.200304030

Etienne-Manneville, S. (2018). Cytoplasmic intermediate filaments in cell biology. *Annu. Rev. Cell. Dev. Biol.* 34, 1–28. doi: 10.1146/annurev-cellbio-100617-062534

Eystathioy, T., Chan, E. K., Tenenbaum, S. A., Keene, J. D., Griffith, K., and Fritzler, M. J. (2002). A phosphorylated cytoplasmic autoantigen, GW182, associates with a unique population of human mRNAs within novel cytoplasmic speckles. *Mol. Biol. Cell.* 13, 1338–1351. doi: 10.1091/mbc.01-11-0544

Fagone, P., and Jackowski, S. (2009). Membrane phospholipid synthesis and endoplasmic reticulum function. *J. Lipid Res.* 50(Suppl.), S311–S316.

Farias, G. G., Freal, A., Tortosa, E., Stucchi, R., Pan, X., Portegies, S., et al. (2019). Feedback-driven mechanisms between microtubules and the endoplasmic reticulum instruct neuronal polarity. *Neuron* 102, 184.e8–201.e8.

Fazal, F. M., Han, S., Parker, K. R., Kaewsapsak, P., Xu, J., Boettiger, A. N., et al. (2019). Atlas of Subcellular RNA localization revealed by APEX-Seq. *Cell* 178, 473.e26–490.e26.

Fonseca, T. B., Sanchez-Guerrero, A., Milosevic, I., and Raimundo, N. (2019). Mitochondrial fission requires Drp1 but not dynamins. *Nature* 570, E34–E42.

Formicola, N., Vijayakumar, J., and Besse, F. (2019). Neuronal ribonucleoprotein granules: dynamic sensors of localized signals. *Traffic* 20, 639–649.

Fowler, P. C., Garcia-Pardo, M. E., Simpson, J. C., and O'sullivan, N. C. (2019). Neurodegeneration: the central role for ER contacts in neuronal function and axonopathy, lessons from hereditary spastic paraplegias and related diseases. *Front. Neurosci.* 13:1051. doi: 10.3389/fnins.2019.01051

Friedman, J. R., Dibenedetto, J. R., West, M., Rowland, A. A., and Voeltz, G. K. (2013). Endoplasmic reticulum-endosome contact increases as endosomes traffic and mature. *Mol. Biol. Cell.* 24, 1030–1040. doi: 10.1091/mbc.e12-10-0733

Friedman, J. R., Lackner, L. L., West, M., Dibenedetto, J. R., Nunnari, J., and Voeltz, G. K. (2011). Er tubules mark sites of mitochondrial division. *Science* 334, 358–362. doi: 10.1126/science.1207385

Friedman, J. R., and Voeltz, G. K. (2011). The ER in 3D: a multifunctional dynamic membrane network. *Trends Cell Biol.* 21, 709–717. doi: 10.1016/j.tcb.2011.07.004

Friedman, J. R., Webster, B. M., Mastronarde, D. N., Verhey, K. J., and Voeltz, G. K. (2010). ER sliding dynamics and Er-mitochondrial contacts occur on acetylated microtubules. *J. Cell. Biol.* 190, 363–375. doi: 10.1083/jcb.200911024

Fu, M. M., Mcalear, T. S., Nguyen, H., Oses-Prieto, J. A., Valenzuela, A., Shi, R. D., et al. (2019). The golgi outpost protein TPPP nucleates microtubules and is critical for myelination. *Cell* 179, 132.e14–146.e14.

Fujimura, K., Katahira, J., Kano, F., Yoneda, Y., and Murata, M. (2009). Microscopic dissection of the process of stress granule assembly. *Biochim. Biophys. Acta* 1793, 1728–1737. doi: 10.1016/j.bbamcr.2009.08.010

Fukuda, Y., Pazyra-Murphy, M. F., Tasdemir-Yilmaz, O. E., Li, Y., Rose, L., Yeoh, Z. C., et al. (2020). Fast transport of RNA granules by direct interactions with KIF5A/KLC1 motors prevents axon degeneration. *BioRxiv* [Preprint]. doi: 10.1101/2020.02.02.931204

Garmendia-Torres, C., Skupin, A., Michael, S. A., Ruusuvuori, P., Kuwada, N. J., Falconnet, D., et al. (2014). Unidirectional P-body transport during the yeast cell cycle. *PLoS One* 9:e99428. doi: 10.1371/journal.pone.0099428

Gavin, A. C., Aloy, P., Grandi, P., Krause, R., Boesche, M., Marzioch, M., et al. (2006). Proteome survey reveals modularity of the yeast cell machinery. *Nature* 440, 631–636. doi: 10.1038/nature04532

Geitmann, A., and Nebenfuhr, A. (2015). Navigating the plant cell: intracellular transport logistics in the green kingdom. *Mol. Biol. Cell.* 26, 3373–3378. doi: 10.1091/mbc.e14-10-1482

Gershoni-Emek, N., Altman, T., Ionescu, A., Costa, C. J., Gradus-Pery, T., Willis, D. E., et al. (2018). Localization of RNAi machinery to axonal branch points and growth cones is facilitated by mitochondria and is disrupted in Als. *Front. Mol. Neurosci.* 11:311. doi: 10.3389/fnmol.2018.00311

Gibbings, D. J., Ciaudo, C., Erhardt, M., and Voinnet, O. (2009). Multivesicular bodies associate with components of mirna effector complexes and modulate miRNA activity. *Nat. Cell. Biol.* 11, 1143–1149. doi: 10.1038/ncb1929

Gingras, A. C., Abe, K. T., and Raught, B. (2019). Getting to know the neighborhood: using proximity-dependent biotinylation to characterize protein complexes and map organelles. *Curr. Opin. Chem. Biol.* 48, 44–54. doi: 10.1016/j.cbpa.2018.10.017

Gopal, P. P., Nirschl, J. J., Klinman, E., and Holzbaur, E. L. (2017). Amyotrophic lateral sclerosis-linked mutations increase the viscosity of liquid-like TDP-43 RNP granules in neurons. *Proc. Natl. Acad. Sci. U.S.A.* 114, E2466–E2475.

Goyal, U., and Blackstone, C. (2013). Untangling the web: mechanisms underlying ER network formation. *Biochim. Biophys. Acta* 1833, 2492–2498. doi: 10.1016/j.bbamcr.2013.04.009

Grigoriev, I., Gouveia, S. M., Van Der Vaart, B., Demmers, J., Smyth, J. T., Honnappa, S., et al. (2008). STIM1 is a MT-plus-end-tracking protein involved in remodeling of the ER. *Curr. Biol.* 18, 177–182. doi: 10.1016/j.cub.2007.12.050

Guimaraes, S. C., Schuster, M., Bielska, E., Dagdas, G., Kilaru, S., Meadows, B. R., et al. (2015). Peroxisomes, lipid droplets, and endoplasmic reticulum "hitchhike" on motile early endosomes. *J. Cell. Biol.* 211, 945–954. doi: 10.1083/jcb.201505086

Guo, Y., Li, D., Zhang, S., Yang, Y., Liu, J. J., Wang, X., et al. (2018). Visualizing intracellular organelle and cytoskeletal interactions at nanoscale resolution on millisecond timescales. *Cell* 175, 1430.e17–1442.e17.

Gutierrez-Beltran, E., Moschou, P. N., Smertenko, A. P., and Bozhkov, P. V. (2015). Tudor staphylococcal nuclease links formation of stress granules and processing bodies with mRNA catabolism in *Arabidopsis*. *Plant Cell* 27, 926–943. doi: 10.1105/tpc.114.134494

Gutnick, A., Banghart, M. R., West, E. R., and Schwarz, T. L. (2019). The light-sensitive dimerizer zapalog reveals distinct modes of immobilization for axonal mitochondria. *Nat. Cell. Biol.* 21, 768–777. doi: 10.1038/s41556-019-0317-2

Hamada, T., Tominaga, M., Fukaya, T., Nakamura, M., Nakano, A., Watanabe, Y., et al. (2012). Rna processing bodies, peroxisomes, Golgi bodies, mitochondria, and endoplasmic reticulum tubule junctions frequently pause at cortical microtubules. *Plant Cell Physiol.* 53, 699–708. doi: 10.1093/pcp/pcs025

Hamada, T., Yako, M., Minegishi, M., Sato, M., Kamei, Y., Yanagawa, Y., et al. (2018). Stress granule formation is induced by a threshold temperature rather than a temperature difference in *Arabidopsis*. *J. Cell. Sci.* 131:jcs216051. doi: 10.1242/jcs.216051

Hatch, A. L., Gurel, P. S., and Higgs, H. N. (2014). Novel roles for actin in mitochondrial fission. *J. Cell. Sci.* 127, 4549–4560. doi: 10.1242/jcs.153791

Hernandez-Vega, A., Braun, M., Scharrel, L., Jahnel, M., Wegmann, S., Hyman, B. T., et al. (2017). Local nucleation of microtubule bundles through tubulin concentration into a condensed tau phase. *Cell. Rep.* 20, 2304–2312. doi: 10.1016/j.celrep.2017.08.042

Higuchi, Y., Ashwin, P., Roger, Y., and Steinberg, G. (2014). Early endosome motility spatially organizes polysome distribution. *J. Cell. Biol.* 204, 343–357. doi: 10.1083/jcb.201307164

Hirokawa, N., Noda, Y., Tanaka, Y., and Niwa, S. (2009). Kinesin superfamily motor proteins and intracellular transport. *Nat. Rev. Mol. Cell. Biol.* 10, 682–696. doi: 10.1038/nrm2774

Holbro, N., Grunditz, A., and Oertner, T. G. (2009). Differential distribution of endoplasmic reticulum controls metabotropic signaling and plasticity at hippocampal synapses. *Proc. Natl. Acad. Sci. U.S.A.* 106, 15055–15060. doi: 10.1073/pnas.0905110106

Holt, C. E., and Bullock, S. L. (2009). Subcellular mRNA localization in animal cells and why it matters. *Science* 326, 1212–1216. doi: 10.1126/science.1176488

Horvathova, I., Voigt, F., Kotrys, A. V., Zhan, Y., Artus-Revel, C. G., Eglinger, J., et al. (2017). The dynamics of mRNA turnover revealed by single-molecule imaging in single cells. *Mol. Cell.* 68, 615.e9–625.e9.

Hu, X., Viesselmann, C., Nam, S., Merriam, E., and Dent, E. W. (2008). Activity-dependent dynamic microtubule invasion of dendritic spines. *J. Neurosci.* 28, 13094–13105. doi: 10.1523/jneurosci.3074-08.2008

Huang, L., Mollet, S., Souquere, S., Le Roy, F., Ernoult-Lange, M., Pierron, G., et al. (2011). Mitochondria associate with P-bodies and modulate MicroRNA-mediated RNA interference. *J. Biol. Chem.* 286, 24219–24230. doi: 10.1074/jbc.m111.240259

Hubstenberger, A., Courel, M., Bénard, M., Souquere, S., Ernoult-Lange, M., Chouaib, R., et al. (2017). P-body purification reveals the condensation of repressed mRNA regulons. *Mol. Cell.* 68, 144.e5–157.e5.

Ivanov, P. A., Chudinova, E. M., and Nadezhdina, E. S. (2003). Disruption of microtubules inhibits cytoplasmic ribonucleoprotein stress granule formation. *Exp. Cell Res.* 290, 227–233. doi: 10.1016/s0014-4827(03)00290-8

Jankowski, S., Pohlmann, T., Baumann, S., Muntjes, K., Devan, S. K., Zander, S., et al. (2019). The multi Pam2 protein Upa2 functions as novel core component of endosomal mRNA transport. *EMBO Rep.* 20:e47381.

Jaworski, J., Kapitein, L. C., Gouveia, S. M., Dortland, B. R., Wulf, P. S., Grigoriev, I., et al. (2009). Dynamic microtubules regulate dendritic spine morphology and synaptic plasticity. *Neuron* 61, 85–100. doi: 10.1016/j.neuron.2008.11.013

Jeffery, W. R., Tomlinson, C. R., and Brodeur, R. D. (1983). Localization of actin messenger RNA during early ascidian development. *Dev. Biol.* 99, 408–417. doi: 10.1016/0012-1606(83)90290-7

Jiang, H., Wang, S., Huang, Y., He, X., Cui, H., Zhu, X., et al. (2015). Phase transition of spindle-associated protein regulate spindle apparatus assembly. *Cell* 163, 108–122. doi: 10.1016/j.cell.2015.08.010

Joensuu, M., Belevich, I., Ramo, O., Nevzorov, I., Vihinen, H., Puhka, M., et al. (2014). Er sheet persistence is coupled to myosin 1c-regulated dynamic actin filament arrays. *Mol. Biol. Cell.* 25, 1111–1126. doi: 10.1091/mbc.e13-12-0712

Kanai, Y., Dohmae, N., and Hirokawa, N. (2004). Kinesin transports RNA: isolation and characterization of an Rna-transporting granule. *Neuron* 43, 513–525. doi: 10.1016/j.neuron.2004.07.022

Kedersha, N., Stoecklin, G., Ayodele, M., Yacono, P., Lykke-Andersen, J., Fritzler, M. J., et al. (2005). Stress granules and processing bodies are dynamically linked sites of mRNP remodeling. *J. Cell Biol.* 169, 871–884. doi: 10.1083/jcb.200502088

Khong, A., Matheny, T., Jain, S., Mitchell, S. F., Wheeler, J. R., and Parker, R. (2017). The stress granule transcriptome reveals principles of mRNA accumulation in stress granules. *Mol. Cell.* 68, 808.e5–820.e5.

Kilchert, C., Weidner, J., Prescianotto-Baschong, C., and Spang, A. (2010). Defects in the secretory pathway and high Ca2+ induce multiple P-bodies. *Mol. Biol. Cell.* 21, 2624–2638. doi: 10.1091/mbc.e10-02-0099

Kim, S., Kalappurakkal, J. M., Mayor, S., and Rosen, M. K. (2019). Phosphorylation of nephrin induces phase separated domains that move through actomyosin contraction. *Mol. Biol. Cell.* 30, 2996–3012. doi: 10.1091/mbc.e18-12-0823

King, M. R., and Petry, S. (2020). Phase separation of TPX2 enhances and spatially coordinates microtubule nucleation. *Nat. Commun.* 11:270.

Knowles, R. B., Sabry, J. H., Martone, M. E., Deerinck, T. J., Ellisman, M. H., Bassell, G. J., et al. (1996). Translocation of RNA granules in living neurons. *J. Neurosci.* 16, 7812–7820. doi: 10.1523/jneurosci.16-24-07812.1996

Kolobova, E., Efimov, A., Kaverina, I., Rishi, A. K., Schrader, J. W., Ham, A. J., et al. (2009). Microtubule-dependent association of AKAP350A and CCAR1 with RNA stress granules. *Exp. Cell Res.* 315, 542–555. doi: 10.1016/j.yexcr.2008.11.011

Konietzny, A., Grendel, J., Hertrich, N., Dekkers, D. H. W., Demmers, J. A. A., and Mikhaylova, M. (2020). Synaptic anchoring of the endoplasmic reticulum depends on myosin V and caldendrin activity. *bioRxiv* [Preprint]. doi: 10.1101/2020.08.14.250746

Konig, J., Baumann, S., Koepke, J., Pohlmann, T., Zarnack, K., and Feldbrugge, M. (2009). The fungal RNA-binding protein Rrm4 mediates long-distance transport of ubi1 and rho3 mRNAs. *EMBO J.* 28, 1855–1866. doi: 10.1038/emboj.2009.145

Korobova, F., Ramabhadran, V., and Higgs, H. N. (2013). An actin-dependent step in mitochondrial fission mediated by the ER-associated formin INF2. *Science* 339, 464–467. doi: 10.1126/science.1228360

Kuijpers, M., and Hoogenraad, C. C. (2011). Centrosomes, microtubules and neuronal development. *Mol. Cell. Neurosci.* 48, 349–358. doi: 10.1016/j.mcn.2011.05.004

Kulic, I. M., Brown, A. E., Kim, H., Kural, C., Blehm, B., Selvin, P. R., et al. (2008). The role of microtubule movement in bidirectional organelle transport. *Proc. Natl. Acad. Sci. U.S.A.* 105, 10011–10016. doi: 10.1073/pnas.0800031105

Kwon, S., Zhang, Y., and Matthias, P. (2007). The deacetylase HDAC6 is a novel critical component of stress granules involved in the stress response. *Genes Dev.* 21, 3381–3394. doi: 10.1101/gad.461107

Lam, S. S., Martell, J. D., Kamer, K. J., Deerinck, T. J., Ellisman, M. H., Mootha, V. K., et al. (2015). Directed evolution of APEX2 for electron microscopy and proximity labeling. *Nat. Methods* 12, 51–54. doi: 10.1038/nmeth.3179

Lee, J. E., Cathey, P. I., Wu, H., Parker, R., and Voeltz, G. K. (2020). Endoplasmic reticulum contact sites regulate the dynamics of membraneless organelles. *Science* 367:eaay7108. doi: 10.1126/science.aay7108

Lee, J. E., Westrate, L. M., Wu, H., Page, C., and Voeltz, G. K. (2016). Multiple dynamin family members collaborate to drive mitochondrial division. *Nature* 540, 139–143. doi: 10.1038/nature20555

Lee, Y. S., Pressman, S., Andress, A. P., Kim, K., White, J. L., Cassidy, J. J., et al. (2009). Silencing by small RNAs is linked to endosomal trafficking. *Nat. Cell. Biol.* 11, 1150–1156. doi: 10.1038/ncb1930

Liao, Y. C., Fernandopulle, M. S., Wang, G., Choi, H., Hao, L., Drerup, C. M., et al. (2019). RNA granules hitchhike on lysosomes for long-distance transport, using annexin A11 as a molecular tether. *Cell* 179, 147.e20–164.e20.

Lifland, A. W., Zurla, C., Yu, J., and Santangelo, P. J. (2011). Dynamics of native beta-actin mRNA transport in the cytoplasm. *Traffic* 12, 1000–1011. doi: 10.1111/j.1600-0854.2011.01209.x

Lin, Y., Mori, E., Kato, M., Xiang, S., Wu, L., Kwon, I., et al. (2016). Toxic PR poly-dipeptides encoded by the C9orf72 repeat expansion target LC domain polymers. *Cell* 167, 789.e12–802.e12.

Lindsay, A. J., and McCaffrey, M. W. (2011). Myosin Va is required for P body but not stress granule formation. *J. Biol. Chem.* 286, 11519–11528. doi: 10.1074/jbc.m110.182808

Litman, P., Barg, J., and Ginzburg, I. (1994). Microtubules are involved in the localization of tau mRNA in primary neuronal cell cultures. *Neuron* 13, 1463–1474. doi: 10.1016/0896-6273(94)90432-4

Liu, X., Guo, X., Niu, L., Li, X., Sun, F., Hu, J., et al. (2019). Atlastin-1 regulates morphology and function of endoplasmic reticulum in dendrites. *Nat. Commun.* 10:568.

Long, R. M., Singer, R. H., Meng, X., Gonzalez, I., Nasmyth, K., and Jansen, R. P. (1997). Mating type switching in yeast controlled by asymmetric localization of ASH1 mRNA. *Science* 277, 383–387. doi: 10.1126/science.277.5324.383

Loschi, M., Leishman, C. C., Berardone, N., and Boccaccio, G. L. (2009). Dynein and kinesin regulate stress-granule and P-body dynamics. *J. Cell. Sci.* 122, 3973–3982. doi: 10.1242/jcs.051383

Lowery, J., Jain, N., Kuczmarski, E. R., Mahammad, S., Goldman, A., Gelfand, V. I., et al. (2016). Abnormal intermediate filament organization alters mitochondrial motility in giant axonal neuropathy fibroblasts. *Mol. Biol. Cell.* 27, 608–616. doi: 10.1091/mbc.e15-09-0627

Lu, M., Van Tartwijk, F. W., Lin, J. Q., Nijenhuis, W., Parutto, P., Fantham, M., et al. (2020). The structure and global distribution of the endoplasmic reticulum network is actively regulated by lysosomes. *BioRxiv* [Preprint]. doi: 10.1101/2020.01.15.907444

Luo, Y., Na, Z., and Slavoff, S. A. (2018). P-bodies: composition. *Propert. Funct. Biochem.* 57, 2424–2431.

Ma, W., and Mayr, C. (2018). A membraneless organelle associated with the endoplasmic reticulum enables 3'utr-mediated protein-protein interactions. *Cell* 175, 1492.e19–1506.e19.

Ma, W., Zhen, G., Xie, W., and Mayr, C. (2020). Unstructured mRNAs form multivalent RNA-RNA interactions to generate TIS granule networks. *bioRxiv* [Preprint]. doi: 10.1101/2020.02.14.949503v1

Man, Y., and Kanso, E. (2019). Morphological transitions of axially-driven microfilaments. *Soft. Matter.* 15, 5163–5173. doi: 10.1039/c8sm02397b

Markmiller, S., Soltanieh, S., Server, K. L., Mak, R., Jin, W., Fang, M. Y., et al. (2018). Context-dependent and disease-specific diversity in protein interactions within stress granules. *Cell* 172, 590.e13–604.e13.

Martin-Cofreces, N. B., and Sanchez-Madrid, F. (2018). Sailing to and docking at the immune synapse: role of tubulin dynamics and molecular motors. *Front. Immunol.* 9:1174. doi: 10.3389/fimmu.2018.01174

Mateju, D., Eichenberger, B., Eglinger, J., Roth, G., and Chao, J. A. (2020). Single-molecule imaging reveals translation of mrnas localized to stress granules. *bioRxiv* [Preprint]. doi: 10.1101/2020.03.31.018093v1

Matheny, T., Rao, B. S., and Parker, R. (2019). Transcriptome-wide comparison of stress granules and P-bodies reveals that translation plays a major role in RNA partitioning. *Mol. Cell. Biol.* 39:e00313-19.

Matveeva, E. A., Venkova, L. S., Chernoivanenko, I. S., and Minin, A. A. (2015). Vimentin is involved in regulation of mitochondrial motility and membrane potential by Rac1. *Biol. Open* 4, 1290–1297. doi: 10.1242/bio.011874

McClintock, M. A., Dix, C. I., Johnson, C. M., Mclaughlin, S. H., Maizels, R. J., Hoang, H. T., et al. (2018). RNA-directed activation of cytoplasmic dynein-1 in reconstituted transport RNPs. *eLife* 7:e36312.

Mehta, K., Chacko, L. A., Chug, M. K., Jhunjhunwala, S., and Ananthanarayanan, V. (2019). Association of mitochondria with microtubules inhibits mitochondrial fission by precluding assembly of the fission protein Dnm1. *J. Biol. Chem.* 294, 3385–3396. doi: 10.1074/jbc.ra118.006799

Melemedjian, O. K., Mejia, G. L., Lepow, T. S., Zoph, O. K., and Price, T. J. (2014). Bidirectional regulation of P body formation mediated by eIF4F complex formation in sensory neurons. *Neurosci. Lett.* 563, 169–174. doi: 10.1016/j.neulet.2013.09.048

Messitt, T. J., Gagnon, J. A., Kreiling, J. A., Pratt, C. A., Yoon, Y. J., and Mowry, K. L. (2008). Multiple kinesin motors coordinate cytoplasmic RNA transport on a subpopulation of microtubules in *Xenopus oocytes*. *Dev. Cell.* 15, 426–436. doi: 10.1016/j.devcel.2008.06.014

Mofatteh, M., and Bullock, S. L. (2017). SnapShot: subcellular mRNA localization. *Cell* 169, 178.e–178.e.

Mohan, R., and John, A. (2015). Microtubule-associated proteins as direct crosslinkers of actin filaments and microtubules. *IUBMB Life* 67, 395–403. doi: 10.1002/iub.1384

Montenegro Gouveia, S., Zitouni, S., Kong, D., Duarte, P., Ferreira Gomes, B., Sousa, A. L., et al. (2018). Plk4 is a microtubule-associated protein that self-assembles promoting de novo MTOC formation. *J. Cell Sci.* 132:jcs219501. doi: 10.1242/jcs.219501

Moon, S. L., Morisaki, T., Khong, A., Lyon, K., Parker, R., and Stasevich, T. J. (2019). Multicolour single-molecule tracking of mRNA interactions with RNP granules. *Nat. Cell. Biol.* 21, 162–168. doi: 10.1038/s41556-018-0263-4

Nadezhdina, E. S., Lomakin, A. J., Shpilman, A. A., Chudinova, E. M., and Ivanov, P. A. (2010). Microtubules govern stress granule mobility and dynamics. *Biochim. Biophys. Acta* 1803, 361–371. doi: 10.1016/j.bbamcr.2009.12.004

Nguyen, M. M., Mccracken, C. J., Milner, E. S., Goetschius, D. J., Weiner, A. T., Long, M. K., et al. (2014). Gamma-tubulin controls neuronal microtubule polarity independently of Golgi outposts. *Mol. Biol. Cell.* 25, 2039–2050. doi: 10.1091/mbc.e13-09-0515

Nixon-Abell, J., Obara, C. J., Weigel, A. V., Li, D., Legant, W. R., Xu, C. S., et al. (2016). Increased spatiotemporal resolution reveals highly dynamic dense tubular matrices in the peripheral ER. *Science* 354:aaf3928. doi: 10.1126/science.aaf3928

Nunnari, J., and Suomalainen, A. (2012). Mitochondria: in sickness and in health. *Cell* 148, 1145–1159. doi: 10.1016/j.cell.2012.02.035

Oddoux, S., Zaal, K. J., Tate, V., Kenea, A., Nandkeolyar, S. A., Reid, E., et al. (2013). Microtubules that form the stationary lattice of muscle fibers are dynamic and nucleated at Golgi elements. *J. Cell. Biol.* 203, 205–213. doi: 10.1083/jcb.201304063

Oh, J. Y., Kwon, A., Jo, A., Kim, H., Goo, Y. S., Lee, J. A., et al. (2013). Activity-dependent synaptic localization of processing bodies and their role in dendritic structural plasticity. *J. Cell. Sci.* 126, 2114–2123. doi: 10.1242/jcs.125690

Olgeiser, L., Haag, C., Boerner, S., Ule, J., Busch, A., Koepke, J., et al. (2019). The key protein of endosomal mrnp transport Rrm4 binds translational landmark sites of cargo mRNAs. *EMBO Rep.* 20:e46588.

Ong, J. Y., and Torres, J. Z. (2020). Phase separation in cell division. *Mol. Cell.* 80, 9–20. doi: 10.1016/j.molcel.2020.08.007

Ori-McKenney, K. M., Jan, L. Y., and Jan, Y. N. (2012). Golgi outposts shape dendrite morphology by functioning as sites of acentrosomal microtubule nucleation in neurons. *Neuron* 76, 921–930. doi: 10.1016/j.neuron.2012.10.008

Ornelles, D. A., Fey, E. G., and Penman, S. (1986). Cytochalasin releases mRNA from the cytoskeletal framework and inhibits protein synthesis. *Mol. Cell. Biol.* 6, 1650–1662. doi: 10.1128/mcb.6.5.1650

Özkan, N., Koppers, M., Van Soest, I., Van Harten, A., Liv, N., Klumperman, J., et al. (2020). ER – lysosome contacts at a pre-axonal region regulate axonal lysosome availability. *bioRxiv* [Preprint]. doi: 10.1101/2020.06.16.153734

Park, S. H., Zhu, P. P., Parker, R. L., and Blackstone, C. (2010). Hereditary spastic paraplegia proteins Reep1, spastin, and atlastin-1 coordinate microtubule interactions with the tubular ER network. *J. Clin. Invest.* 120, 1097–1110. doi: 10.1172/jci40979

Patel, P. H., Barbee, S. A., and Blankenship, J. T. (2016). GW-bodies and P-bodies constitute two separate pools of sequestered non-translating RNAS. *PLoS One* 11:e0150291. doi: 10.1371/journal.pone.0150291

Pattabiraman, S., Azad, G. K., Amen, T., Brielle, S., Park, J. E., Sze, S. K., et al. (2020). Vimentin protects differentiating stem cells from stress. *Sci. Rep.* 10:19525.

Pavez, M., Thompson, A. C., Arnott, H. J., Mitchell, C. B., D'atri, I., Don, E. K., et al. (2019). STIM1 is required for remodeling of the endoplasmic reticulum and microtubule cytoskeleton in steering growth cones. *J. Neurosci.* 39, 5095–5114. doi: 10.1523/jneurosci.2496-18.2019

Pchitskaya, E., Kraskovskaya, N., Chernyuk, D., Popugaeva, E., Zhang, H., Vlasova, O., et al. (2017). Stim2-Eb3 association and morphology of dendritic spines in hippocampal neurons. *Sci. Rep.* 7:17625.

Pease-Raissi, S. E., Pazyra-Murphy, M. F., Li, Y., Wachter, F., Fukuda, Y., Fenstermacher, S. J., et al. (2017). Paclitaxel reduces axonal Bclw to initiate Ip3R1-dependent axon degeneration. *Neuron* 96, 373.e6–386.e6.

Perez-Alvarez, A., Yin, S., Schulze, C., Hammer, J. A., Wagner, W., and Oertner, T. G. (2020). Endoplasmic reticulum visits highly active spines and prevents runaway potentiation of synapses. *Nat. Commun.* 11:5083.

Phillips, M. J., and Voeltz, G. K. (2016). Structure and function of ER membrane contact sites with other organelles. *Nat. Rev. Mol. Cell. Biol.* 17, 69–82. doi: 10.1038/nrm.2015.8

Pilling, A. D., Horiuchi, D., Lively, C. M., and Saxton, W. M. (2006). Kinesin-1 and Dynein are the primary motors for fast transport of mitochondria in Drosophila motor axons. *Mol. Biol. Cell.* 17, 2057–2068. doi: 10.1091/mbc.e05-06-0526

Pohlmann, T., Baumann, S., Haag, C., Albrecht, M., and Feldbrugge, M. (2015). A FYVE zinc finger domain protein specifically links mrna transport to endosome trafficking. *eLife* 4:e06041.

Popovic, D., Nijenhuis, W., Kapitein, L. C., and Pelkmans, L. (2020). Co-translational targeting of transcripts to endosomes. *bioRxiv* [Preprint].

Preitner, N., Quan, J., Nowakowski, D. W., Hancock, M. L., Shi, J., Tcherkezian, J., et al. (2014). APC is an RNA-binding protein, and its interactome provides a link to neural development and microtubule assembly. *Cell* 158, 368–382. doi: 10.1016/j.cell.2014.05.042

Raiborg, C., Wenzel, E. M., Pedersen, N. M., Olsvik, H., Schink, K. O., Schultz, S. W., et al. (2015). Repeated ER-endosome contacts promote endosome translocation and neurite outgrowth. *Nature* 520, 234–238. doi: 10.1038/nature14359

Rajgor, D., Mellad, J. A., Soong, D., Rattner, J. B., Fritzler, M. J., and Shanahan, C. M. (2014). Mammalian microtubule P-body dynamics are mediated by nesprin-1. *J. Cell. Biol.* 205, 457–475. doi: 10.1083/jcb.201306076

Rapoport, T. A. (2007). Protein translocation across the eukaryotic endoplasmic reticulum and bacterial plasma membranes. *Nature* 450, 663–669. doi: 10.1038/nature06384

Riggs, C. L., Kedersha, N., Ivanov, P., and Anderson, P. (2020). Mammalian stress granules and P bodies at a glance. *J. Cell Sci.* 133:jcs242487. doi: 10.1242/jcs.242487

Rodriguez, O. C., Schaefer, A. W., Mandato, C. A., Forscher, P., Bement, W. M., and Waterman-Storer, C. M. (2003). Conserved microtubule-actin interactions in cell movement and morphogenesis. *Nat. Cell. Biol.* 5, 599–609. doi: 10.1038/ncb0703-599

Rodriguez-Garcia, R., Volkov, V. A., Chen, C. Y., Katrukha, E. A., Olieric, N., Aher, A., et al. (2020). Mechanisms of motor-independent membrane remodeling driven by dynamic microtubules. *Curr. Biol.* 30, 972.e12–987.e12.

Rogers, S. L., and Gelfand, V. I. (2000). Membrane trafficking, organelle transport, and the cytoskeleton. *Curr. Opin. Cell. Biol.* 12, 57–62. doi: 10.1016/s0955-0674(99)00057-5

Rowland, A. A., Chitwood, P. J., Phillips, M. J., and Voeltz, G. K. (2014). ER contact sites define the position and timing of endosome fission. *Cell* 159, 1027–1041. doi: 10.1016/j.cell.2014.10.023

Sabari, B. R., Dall'agnese, A., and Young, R. A. (2020). Biomolecular condensates in the nucleus. *Trends Biochem. Sci.* 45, 961–977. doi: 10.1016/j.tibs.2020.06.007

Safari, M. S., King, M. R., Brangwynne, C. P., and Petry, S. (2020). Branching microtubule nucleation is controlled by importin-mediated inhibition of TPX2 phase separation. *bioRxiv* [Preprint]. doi: 10.1101/2020.09.01.276469

Sahoo, P. K., Lee, S. J., Jaiswal, P. B., Alber, S., Kar, A. N., Miller-Randolph, S., et al. (2018). Axonal G3BP1 stress granule protein limits axonal mrna translation and nerve regeneration. *Nat. Commun.* 9:3358.

Salogiannis, J., and Reck-Peterson, S. L. (2017). Hitchhiking: a non-canonical mode of microtubule-based transport. *Trends Cell. Biol.* 27, 141–150. doi: 10.1016/j.tcb.2016.09.005

Schmid, M., Jaedicke, A., Du, T. G., and Jansen, R. P. (2006). Coordination of endoplasmic reticulum and mrna localization to the yeast bud. *Curr. Biol.* 16, 1538–1543. doi: 10.1016/j.cub.2006.06.025

Schwarz, D. S., and Blower, M. D. (2016). The endoplasmic reticulum: structure, function and response to cellular signaling. *Cell Mol. Life Sci.* 73, 79–94. doi: 10.1007/s00018-015-2052-6

Scorrano, L., De Matteis, M. A., Emr, S., Giordano, F., Hajnoczky, G., Kornmann, B., et al. (2019). Coming together to define membrane contact sites. *Nat. Commun.* 10:1287.

Sehgal, P. B., Westley, J., Lerea, K. M., Disenso-Browne, S., and Etlinger, J. D. (2020). Biomolecular condensates in cell biology and virology: phase-separated membraneless organelles (MLOS). *Anal. Biochem.* 597:113691. doi: 10.1016/j.ab.2020.113691

Sheth, U., and Parker, R. (2003). Decapping and decay of messenger RNA occur in cytoplasmic processing bodies. *Science* 300, 805–808. doi: 10.1126/science.1082320

Shibata, Y., Voeltz, G. K., and Rapoport, T. A. (2006). Rough sheets and smooth tubules. *Cell* 126, 435–439. doi: 10.1016/j.cell.2006.07.019

Sleigh, J. N., Rossor, A. M., Fellows, A. D., Tosolini, A. P., and Schiavo, G. (2019). Axonal transport and neurological disease. *Nat. Rev. Neurol.* 15, 691–703.

Smirnova, E., Griparic, L., Shurland, D. L., and van der Bliek, A. M. (2001). Dynamin-related protein Drp1 is required for mitochondrial division in mammalian cells. *Mol. Biol. Cell.* 12, 2245–2256. doi: 10.1091/mbc.12.8.2245

Smolina, N., Khudiakov, A., Knyazeva, A., Zlotina, A., Sukhareva, K., Kondratov, K., et al. (2020). Desmin mutations result in mitochondrial dysfunction regardless of their aggregation properties. *Biochim. Biophys. Acta Mol. Basis Dis.* 1866:165745. doi: 10.1016/j.bbadis.2020.165745

So, C., Seres, K. B., Steyer, A. M., Monnich, E., Clift, D., Pejkovska, A., et al. (2019). A liquid-like spindle domain promotes acentrosomal spindle assembly in mammalian oocytes. *Science* 364:eaat9557. doi: 10.1126/science.aat9557

Steffen, J., and Koehler, C. M. (2018). ER-mitochondria contacts: actin dynamics at the ER control mitochondrial fission via calcium release. *J. Cell. Biol.* 217, 15–17. doi: 10.1083/jcb.201711075

Steffens, A., Jaegle, B., Tresch, A., Hulskamp, M., and Jakoby, M. (2014). Processing-body movement in *Arabidopsis* depends on an interaction between myosins and Decapping Protein1. *Plant. Physiol.* 164, 1879–1892. doi: 10.1104/pp.113.233031

Su, X., Ditlev, J. A., Hui, E., Xing, W., Banjade, S., Okrut, J., et al. (2016). Phase separation of signaling molecules promotes T cell receptor signal transduction. *Science* 352, 595–599. doi: 10.1126/science.aad9964

Sweet, T. J., Boyer, B., Hu, W., Baker, K. E., and Coller, J. (2007). Microtubule disruption stimulates P-body formation. *RNA* 13, 493–502. doi: 10.1261/rna.355807

Szaflarski, W., Fay, M. M., Kedersha, N., Zabel, M., Anderson, P., and Ivanov, P. (2016). Vinca alkaloid drugs promote stress-induced translational repression and stress granule formation. *Oncotarget* 7, 30307–30322. doi: 10.18632/oncotarget.8728

Takagishi, Y., Oda, S., Hayasaka, S., Dekker-Ohno, K., Shikata, T., Inouye, M., et al. (1996). The dilute-lethal (dl) gene attacks a Ca2+ store in the dendritic spine of Purkinje cells in mice. *Neurosci. Lett.* 215, 169–172. doi: 10.1016/0304-3940(96)12967-0

Takizawa, P. A., Sil, A., Swedlow, J. R., Herskowitz, I., and Vale, R. D. (1997). Actin-dependent localization of an RNA encoding a cell-fate determinant in yeast. *Nature* 389, 90–93. doi: 10.1038/38015

Tauber, D., Tauber, G., and Parker, R. (2020). Mechanisms and regulation of RNA condensation in RNP granule formation. *Trends Biochem. Sci.* 45, 764–778. doi: 10.1016/j.tibs.2020.05.002

Teixeira, D., Sheth, U., Valencia-Sanchez, M. A., Brengues, M., and Parker, R. (2005). Processing bodies require RNA for assembly and contain nontranslating mRNAs. *RNA* 11, 371–382. doi: 10.1261/rna.7258505

Terasaki, M., Chen, L. B., and Fujiwara, K. (1986). Microtubules and the endoplasmic reticulum are highly interdependent structures. *J. Cell. Biol.* 103, 1557–1568. doi: 10.1083/jcb.103.4.1557

Toresson, H., and Grant, S. G. (2005). Dynamic distribution of endoplasmic reticulum in hippocampal neuron dendritic spines. *Eur. J. Neurosci.* 22, 1793–1798. doi: 10.1111/j.1460-9568.2005.04342.x

Trcek, T., and Lehmann, R. (2019). Germ granules in *Drosophila*. *Traffic* 20, 650–660. doi: 10.1111/tra.12674

Tsai, N. P., Tsui, Y. C., and Wei, L. N. (2009). Dynein motor contributes to stress granule dynamics in primary neurons. *Neuroscience* 159, 647–656. doi: 10.1016/j.neuroscience.2008.12.053

Valm, A. M., Cohen, S., Legant, W. R., Melunis, J., Hershberg, U., Wait, E., et al. (2017). Applying systems-level spectral imaging and analysis to reveal the organelle interactome. *Nature* 546, 162–167. doi: 10.1038/nature22369

van de Willige, D., Hummel, J. J., Alkemade, C., Kahn, O. I., Au, F. K., Qi, R. Z., et al. (2019). Cytolinker Gas2L1 regulates axon morphology through microtubule-modulated actin stabilization. *EMBO Rep.* 20:e47732.

van Spronsen, M., Mikhaylova, M., Lipka, J., Schlager, M. A., van den Heuvel, D. J., Kuijpers, M., et al. (2013). TRAK/Milton motor-adaptor proteins steer mitochondrial trafficking to axons and dendrites. *Neuron* 77, 485–502. doi: 10.1016/j.neuron.2012.11.027

Vidaki, M., Drees, F., Saxena, T., Lanslots, E., Taliaferro, M. J., Tatarakis, A., et al. (2017). A requirement for mena, an actin regulator, in local mRNA translation in developing neurons. *Neuron* 95, 608.e5–622.e5.

Voronina, E., Seydoux, G., Sassone-Corsi, P., and Nagamori, I. (2011). RNA granules in germ cells. *Cold Spring Harb. Perspect. Biol.* 3:a002774. doi: 10.1101/cshperspect.a002774

Wagner, W., Brenowitz, S. D., and Hammer, J. A. III (2011). Myosin-Va transports the endoplasmic reticulum into the dendritic spines of Purkinje neurons. *Nat. Cell. Biol.* 13, 40–48. doi: 10.1038/ncb2132

Wang, C., Schmich, F., Srivatsa, S., Weidner, J., Beerenwinkel, N., and Spang, A. (2018). Context-dependent deposition and regulation of mRNAs in P-bodies. *eLife* 7:e29815.

Wang, N., and Rapoport, T. A. (2019). Reconstituting the reticular ER network - mechanistic implications and open questions. *J. Cell. Sci.* 132:jcs227611. doi: 10.1242/jcs.227611

Waterman-Storer, C. M., and Salmon, E. D. (1998). Endoplasmic reticulum membrane tubules are distributed by microtubules in living cells using three distinct mechanisms. *Curr. Biol.* 8, 798–806. doi: 10.1016/s0960-9822(98)70321-5

Wegmann, S., Eftekharzadeh, B., Tepper, K., Zoltowska, K. M., Bennett, R. E., Dujardin, S., et al. (2018). Tau protein liquid-liquid phase separation can initiate tau aggregation. *EMBO J.* 37:e98049.

Weidner, J., Wang, C., Prescianotto-Baschong, C., Estrada, A. F., and Spang, A. (2014). The polysome-associated proteins Scp160 and Bfr1 prevent P body formation under normal growth conditions. *J. Cell. Sci.* 127, 1992–2004. doi: 10.1242/jcs.142083

Weiner, A. T., Seebold, D. Y., Torres-Gutierrez, P., Folker, C., Swope, R. D., Kothe, G. O., et al. (2020). Endosomal Wnt signaling proteins control microtubule nucleation in dendrites. *PLoS Biol.* 18:e3000647. doi: 10.1371/journal.pbio.3000647

Weirich, K. L., Banerjee, S., Dasbiswas, K., Witten, T. A., Vaikuntanathan, S., and Gardel, M. L. (2017). Liquid behavior of cross-linked actin bundles. *Proc. Natl. Acad. Sci. U.S.A.* 114, 2131–2136. doi: 10.1073/pnas.1616133114

Wheeler, J. R., Matheny, T., Jain, S., Abrisch, R., and Parker, R. (2016). Distinct stages in stress granule assembly and disassembly. *eLife* 5:e18413.

Woodruff, J. B., Ferreira Gomes, B., Widlund, P. O., Mahamid, J., Honigmann, A., and Hyman, A. A. (2017). The centrosome is a selective condensate that nucleates microtubules by concentrating tubulin. *Cell* 169, 1066.e10–1077.e10.

Woods, L. C., Berbusse, G. W., and Naylor, K. (2016). Microtubules are essential for mitochondrial dynamics-fission, fusion, and motility-in *Dictyostelium discoideum*. *Front. Cell. Dev. Biol.* 4:19. doi: 10.3389/fcell.2016.00019

Wozniak, M. J., Bola, B., Brownhill, K., Yang, Y. C., Levakova, V., and Allan, V. J. (2009). Role of kinesin-1 and cytoplasmic dynein in endoplasmic reticulum movement in Vero cells. *J. Cell. Sci.* 122, 1979–1989. doi: 10.1242/jcs.041962

Wu, H., Zhou, J., Zhu, T., Cohen, I., and Dictenberg, J. (2020). A kinesin adapter directly mediates dendritic mrna localization during neural development in mice. *J. Biol. Chem.* 295, 6605–6628. doi: 10.1074/jbc.ra118.005616

Wu, M., Kalyanasundaram, A., and Zhu, J. (2013). Structural and biomechanical basis of mitochondrial movement in eukaryotic cells. *Int. J. Nanomed.* 8, 4033–4042. doi: 10.2147/ijn.s52132

Wu, X., Cai, Q., Feng, Z., and Zhang, M. (2020). Liquid-liquid phase separation in neuronal development and synaptic signaling. *Dev. Cell.* 55, 18–29. doi: 10.1016/j.devcel.2020.06.012

Wu, Y., Whiteus, C., Xu, C. S., Hayworth, K. J., Weinberg, R. J., Hess, H. F., et al. (2017). Contacts between the endoplasmic reticulum and other membranes in neurons. *Proc. Natl. Acad. Sci. U.S.A.* 114, E4859–E4867.

Youn, J. Y., Dunham, W. H., Hong, S. J., Knight, J. D. R., Bashkurov, M., Chen, G. I., et al. (2018). High-density proximity mapping reveals the subcellular organization of mRNA-associated granules and bodies. *Mol. Cell.* 69, 517.e11–532.e11.

Youn, J. Y., Dyakov, B. J. A., Zhang, J., Knight, J. D. R., Vernon, R. M., Forman-Kay, J. D., et al. (2019). Properties of stress granule and P-body proteomes. *Mol. Cell.* 76, 286–294. doi: 10.1016/j.molcel.2019.09.014

Zacharogianni, M., Aguilera-Gomez, A., Veenendaal, T., Smout, J., and Rabouille, C. (2014). A stress assembly that confers cell viability by preserving ERES components during amino-acid starvation. *eLife* 3:e04132

Zbinden, A., Perez-Berlanga, M., De Rossi, P., and Polymenidou, M. (2020). Phase separation and neurodegenerative diseases: a disturbance in the force. *Dev. Cell.* 55, 45–68. doi: 10.1016/j.devcel.2020.09.014

Zeitelhofer, M., Karra, D., Macchi, P., Tolino, M., Thomas, S., Schwarz, M., et al. (2008). Dynamic interaction between P-bodies and transport ribonucleoprotein particles in dendrites of mature hippocampal neurons. *J. Neurosci.* 28, 7555–7562. doi: 10.1523/jneurosci.0104-08.2008

Zhang, H., and Hu, J. (2016). Shaping the endoplasmic reticulum into a social network. *Trends Cell. Biol.* 26, 934–943. doi: 10.1016/j.tcb.2016.06.002

Zhao, Y. G., and Zhang, H. (2020). Phase separation in membrane biology: the interplay between membrane-bound organelles and membraneless condensates. *Dev. Cell.* 55, 30–44. doi: 10.1016/j.devcel.2020.06.033

Zhou, W., Chang, J., Wang, X., Savelieff, M. G., Zhao, Y., Ke, S., et al. (2014). GM130 is required for compartmental organization of dendritic golgi outposts. *Curr. Biol.* 24, 1227–1233. doi: 10.1016/j.cub.2014.04.008

Conflict of Interest: The authors declare that the research was conducted in the absence of any commercial or financial relationships that could be construed as a potential conflict of interest.

frontiers in Cell and Developmental Biology

REVIEW
published: 23 December 2020
doi: 10.3389/fcell.2020.615856

Lipid Metabolism at Membrane Contacts: Dynamics and Functions Beyond Lipid Homeostasis

Jiesi Xu[1]* *and Xun Huang*[1,2]*

[1] State Key Laboratory of Molecular Developmental Biology, Institute of Genetics and Developmental Biology, Innovation Academy for Seed Design, Chinese Academy of Sciences, Beijing, China, [2] College of Advanced Agricultural Sciences, University of Chinese Academy of Sciences, Beijing, China

Membrane contact sites (MCSs), regions where the membranes of two organelles are closely apposed, play critical roles in inter-organelle communication, such as lipid trafficking, intracellular signaling, and organelle biogenesis and division. First identified as "fraction X" in the early 90s, MCSs are now widely recognized to facilitate local lipid synthesis and inter-organelle lipid transfer, which are important for maintaining cellular lipid homeostasis. In this review, we discuss lipid metabolism and related cellular and physiological functions in MCSs. We start with the characteristics of lipid synthesis and breakdown at MCSs. Then we focus on proteins involved in lipid synthesis and turnover at these sites. Lastly, we summarize the cellular function of lipid metabolism at MCSs beyond mere lipid homeostasis, including the physiological meaning and relevance of MCSs regarding systemic lipid metabolism. This article is part of an article collection entitled: Coupling and Uncoupling: Dynamic Control of Membrane Contacts.

Keywords: lipid biosynthesis, lipid degradation, membrane contact site, lipid functions, lipid composition

OPEN ACCESS

Edited by:
Dan Zhang,
Temasek Life Sciences Laboratory, Singapore

Reviewed by:
Yasushi Tamura,
Yamagata University, Japan
Alexandre Toulmay,
National Institutes of Health Clinical Center (NIH), United States

***Correspondence:**
Jiesi Xu
jxu@genetics.ac.cn
Xun Huang
xhuang@genetics.ac.cn

Specialty section:
This article was submitted to Membrane Traffic, a section of the journal Frontiers in Cell and Developmental Biology

Received: *10 October 2020*
Accepted: *30 November 2020*
Published: *23 December 2020*

Citation:
Xu J and Huang X (2020) Lipid Metabolism at Membrane Contacts: Dynamics and Functions Beyond Lipid Homeostasis. Front. Cell Dev. Biol. 8:615856. doi: 10.3389/fcell.2020.615856

INTRODUCTION

Compartmentalization is a basic organizational principle of cells. It can be achieved by intracellular membranes, which act as physical barriers to optimize the efficiency of cellular processes that occur within organelles (Aguzzi and Altmeyer, 2016). Lipids are fundamental components of cellular membranes. The lipid composition varies in different organelle membranes and/or subregions/domains within membranes. This heterogeneity of lipid distribution can be achieved by local lipid metabolism or by intracellular lipid trafficking, which delivers lipids from where they are synthesized (in most cases in the endoplasmic reticulum/ER) to their destination membranes and/or membrane domains in both vesicular and non-vesicular pathways.

Membrane contact sites (MCSs) are areas of close apposition between two organelles that mediate non-vesicular lipid trafficking, or between inner and outer membranes of the same organelle, such as mitochondria and chloroplast. It has been known for decades (Scorrano et al., 2019). However, the field of organelle interactions came into the spotlight only when the functional meaning of MCSs was revealed. Vance (1990) described the presence of "fraction X" in mitochondrial preparations, which harbored phospholipid synthetic activity and was later identified as mitochondrial-associated membranes (MAMs) (Vance, 1990). This is the first paper showing that a biochemical activity occurs specifically at contact sites. More recent studies have unveiled the functional significance of MCSs in regulating various cellular processes, such as Ca^{2+} transport, lipid exchange, apoptosis, and organelle biogenesis (Doghman-Bouguerra et al., 2016; Kannan et al., 2017; Wu et al., 2019; Schutter et al., 2020). It is now more evident that such close apposition between organelles facilitates inter-organelle communication and is essential

for the structure and function of eukaryotic cells including mammalian cells (**Figure 1**) and yeast (**Figure 2**).

Here, we will appraise the findings about the molecular basis, cellular functions, and physiological and pathological implications of lipid metabolism at MCSs. We will not focus on the molecular mechanism of lipid exchange at membrane contact sites, since many excellent reviews have touched on this subject already (Lahiri et al., 2015; Phillips and Voeltz, 2016; Muallem et al., 2017; Balla et al., 2019, 2020; Tamura et al., 2019; Prinz et al., 2020). We will discuss: (1) the characteristics of lipid synthesis and breakdown at MCSs, (2) proteins involved in lipid metabolism at MCSs, and (3) lipid function at MCSs beyond simple lipid homeostasis.

THE CHARACTERISTICS OF LIPID SYNTHESIS AND BREAKDOWN AT MCSs-PROTEINS AND LIPIDS

There is growing evidence that intimate physical contacts between the ER membrane and membranes of other organelles play major roles in lipid metabolism, including synthesis, breakdown, and transport (Scorrano et al., 2019). Mass spectrometry reveals that many proteins involved in lipid metabolism are detected in the MCS fractions (Sala-Vila et al., 2016; Ma et al., 2017; Wang et al., 2018). The MAM proteome has been analyzed in various cell lines and mouse tissues (Sala-Vila et al., 2016; Cho et al., 2017; Hung et al., 2017; Ma et al., 2017; Wang et al., 2018; Kwak et al., 2020). For example, using sequential centrifugation to isolate pure MAMs followed by mass spectrometry, over 1000 MAM proteins have been identified (Sala-Vila et al., 2016; Ma et al., 2017; Wang et al., 2018). It has been shown that approximately 10% of the MAM proteins from mouse liver are involved in lipid metabolism, including biosynthesis of cholesterol, fatty acids, steroids and phospholipids, and catabolism of fatty acids (Sala-Vila et al., 2016). Specific proteins at MCSs discussed in this review are listed in **Table 1**.

In recent years, the adoption of an alternative proteomic approach known as proximity-based labeling has advanced the mapping of MCS proteins (Cho et al., 2017; Hung et al., 2017; Antonicka et al., 2020; Kwak et al., 2020). In this approach, a bait protein is endowed with biotinylating activity via fusion with peroxidase (APEX), horseradish peroxidase (HRP), or promiscuous biotin ligase (pBirA); prey proteins near (<10 to 20 nm) the bait protein, or cellular regions enriched in the bait protein, are biotinylated and can then be purified and analyzed (Hung et al., 2017; Antonicka et al., 2020). Several studies have used this method to identify the MAM proteome, and they acquired a much smaller number of MAM proteins compared to conventional fractionation-based methods. One study demonstrated that proteins involved in triglyceride (TAG) synthesis [acyl-coA synthetase long chain family member 1 (ACSL1) and putative glycerol kinase 3 (GK3P) and fatty acid oxidation (carnitine palmitoyltransferase 1a (CPT1a)] are enriched in the MAM fraction of cells (Hung et al., 2017). However, this type of method also has a number of limitations, such as inducing changes in protein localization (toward or away from the membrane) in response to stimuli that are applied by this method, and failing to detect well-known MCS-resident proteins (Kwak et al., 2020).

Although certain lipid synthetic and catabolic enzymes have been identified at the contact sites, the immediate consequence of these enrichments, in particular on the lipid composition of membrane contacts, has scarcely been explored. This is probably due to the difficulty in separation and purification of intracellular membrane without contamination from other membranes (Schuiki et al., 2010; Horvath and Daum, 2013). Thus far, only three studies have analyzed the phospholipid composition of MCSs (Fischl and Carman, 1983; Vance, 1990; Pichler et al., 2001). In rat liver, the molar ratio of phosphatidylcholine (PC)/phosphatidylethanolamine (PE) of MAMs resembles that of the ER rather than the mitochondria (Vance, 1990), which suggests that the properties of MAMs are more similar to the ER in terms of biosynthesis of phospholipids (Vance, 1990). In yeast, analysis of the phospholipid composition of MAMs has revealed that the MAMs have a significantly higher phosphatidylinositol (PI) content and a lower phosphatidic acid (PA) content as compared to mitochondrial and other microsomal membranes (Gaigg et al., 1995). This is probably due to the fact that the highest level of PI synthase (Pis1) activity is found in the MAM fraction (Fischl and Carman, 1983; Gaigg et al., 1995). The lipid composition of ER-plasma membrane (PM) contacts is also more similar to the ER in yeast, with higher levels of PC, PE, and PI and a lower amount of phosphatidylserine (PS) compared to the PM (Pichler et al., 2001).

Similar to the PM, MAMs also contain microdomains, named lipid rafts. Lipid rafts are cholesterol and sphingolipids-rich microdomains in PM. The detergent-resistant lipid rafts in the MAMs from mammalian cells are rich in lipids, such as cholesterol, ceramides and glycosphingolipids, and proteins that are components of MAM-localized Ca^{2+} signaling complexes, such as sigma-1 receptor (Sigma 1R), IP3R, GRP75, and VDAC1 (Hayashi and Fujimoto, 2010; Poston et al., 2011). Of note, the lipid-protein interactions at this specific region play crucial roles in executing both cellular processes and organelle biogenesis. For instance, ceramides from the detergent-resistant membranes of MAMs are physically associated with Sigma 1R and anchor it to the MAMs (Hayashi and Fujimoto, 2010). Sigma 1R stabilizes IP3R3 at MAMs, therefore favoring Ca^{2+} transfer from the ER to the mitochondria (Hayashi and Su, 2007; **Figures 1A,B**). In mouse brain, GM1-ganglioside (GM1), one of the sialic acid-containing glycosphingolipids (GSLs), physically interacts with phosphorylated form of IP3R in glycosphingolipid-enriched microdomain (GEM) fractions of MAMs and influences Ca^{2+}-mediated apoptotic signaling (Sano et al., 2009; **Figure 1B**). Ganglioside (GD3) interacts with AMBRA1 and WIPI1, both of which are core-initiator proteins responsible for autophagosome formation (Garofalo et al., 2016).

The enrichment of a set of functionally linked lipid biosynthetic enzymes at MCSs also extends our understanding of the lipid composition at MCSs. For example, mammalian MAMs contain the PS synthases PSS1/2, which convert PE and PC to PS, PE methyltransferase (PEMT) which converts PE to

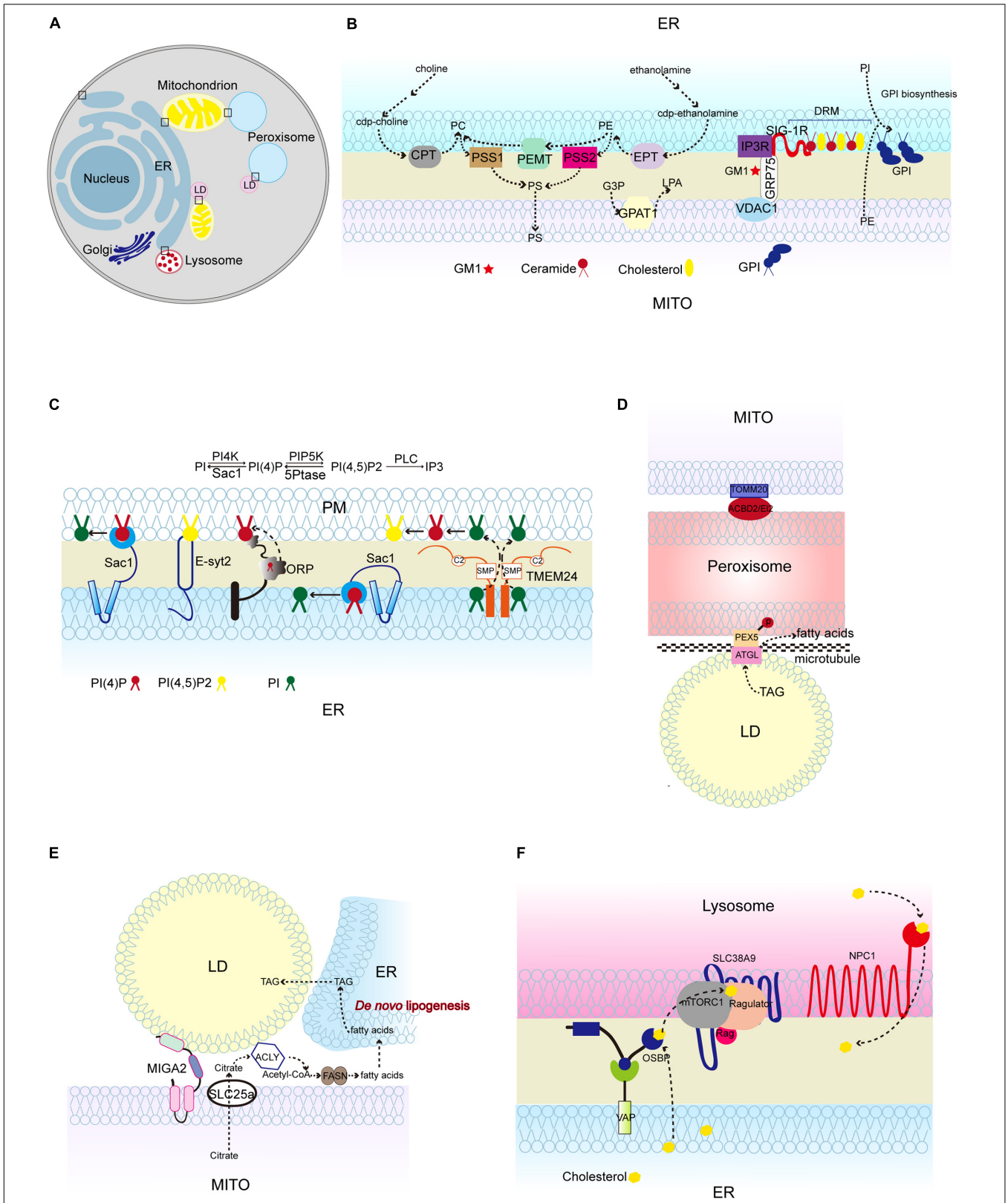

FIGURE 1 | Lipid synthesis and breakdown at MCSs in mammalian cells. **(A)** Schematic illustration of mammalian MCSs. The contact sites discussed in the text are boxed. **(B)** Lipid metabolism at the ER-mitochondrion contacts, highlighting the linked synthesis of PC, PE, and PS; the detergent-resistant membrane (DRM)

(Continued)

FIGURE 1 | Continued
domain enriched in ceramide, cholesterol, and associated proteins; and the biosynthesis of GPI using ER-derived PI and mitochondrion-derived PE. **(C)** Lipid metabolism at the ER-PM contacts, showing the Sac1-mediated conversion of phosphatidylinositol 4-phosphate (PI4P) to phosphatidylinositol (4,5)-bisphosphate (PIP2) *in trans* and *in cis*, and TMEM24-mediated PI transport. **(D)** Pex5 and ATGL interaction at peroxisome-LD contacts, and TOMM20 and ACBD2/EI2 interaction at mitochondrion-peroxisome contacts. **(E)** MIGA2-mediated LD-mitochondrion association to supply TAG from mitochondrially derived citrate. **(F)** The activation of mTORC1 by cholesterol delivered from the ER to the lysosome surface by OSBP, and the transport of cholesterol out of the lysosome lumen by NPC1. CPT, CDP-choline-1,2-diacylglycerol choline phosphotransferase (CPT); EPT, CDP-ethanolamine:1,2-diacylglycerol ethanolamine phosphotransferase; PSS1/2, phosphatidylserine synthase; PEMT, phosphatidylethanolamine methyltransferase; GPAT1, glycerophosphate acyltransferases; SIG-1R, Sigma 1R; PC, phosphatidylcholine; PE, phosphatidylethanolamine; PS, phosphatidylserine; G3P, glycerol-3-phosphatase; LPA, lysophosphatidic acid; GM1, GM1-ganglioside; GPI, glycosylphosphatidylinositol; TMEM24, transmembrane protein 24; PEX5, peroxisomal biogenesis factor 5; ATGL, triglyceride lipase; TOMM20, Translocase of outer mitochondrial membrane 20; ACBD2/EI2, acyl-coenzyme A-binding domain; ACLY, ATP citrate lyase; FASN, fatty acid synthase; NPC1, Niemann-Pick disease, type C1; OSBP, oxysterol-binding protein 1.

PC, and PS decarboxylase (PISD) which converts PS to PE. The linked synthesis of PS, PE, and PC segregates the pools of PS and PS-derived phospholipids from the bulk of the ER phospholipids (Vance, 1990). The segregation of these specific chemical reactions may increase the reaction efficiency and restrict the dissemination of reaction products, or may serve special functions. For instance, the cell uses the pool of PS-derived phospholipids for lipoprotein assembly (Vance, 1990).

Each subcellular compartment of the cell has a specific set of membrane lipids. PC and PE are the most abundant phospholipids in the membranes of mammalian and yeast cells (Horvath and Daum, 2013). PS is highly enriched in the PM of these cells (Horvath and Daum, 2013). PI is more enriched in the Golgi apparatus than in other subcellular compartments (Horvath and Daum, 2013). Sphingolipids are enriched in lysosomes (Horvath and Daum, 2013). To maintain the distinct membrane features and lipid composition of each subcellular compartment, coordinated regulation of lipid synthesis, degradation, and transport is required. The identification of lipid metabolic enzymes at MCSs and the lipid composition of MCSs lays the foundation of our understanding of lipid metabolism at MCSs. In the next part, we will discuss in detail the individual enzymes involved in lipid synthesis and breakdown at MCSs.

LIPID METABOLISM AT THE MEMBRANE CONTACTS

Phospholipid Synthesis and Breakdown at Membrane Contacts

Several lines of evidence suggest that non-vesicular lipid transport intersects with lipid biosynthetic and regulatory pathways at MCSs (Fernandez-Murray and McMaster, 2016; Phillips and Voeltz, 2016; Balla et al., 2019; **Figures 1A**, **2A**). In this part, we review studies of phospholipid metabolism at MCSs, with the emphasis on phospholipid biosynthesis and breakdown in mammalian system and yeast.

PS

Phosphatidylserine is transported from the ER to mitochondria and decarboxylated to synthesize PE, and PE is transferred in the reverse direction from mitochondria to the ER. The function of MAMs in PS import into mitochondria has been extensively studied in mammalian cells and yeast (Vance, 1990; Voelker, 1990; Gaigg et al., 1995; Shiao et al., 1995; Achleitner et al., 1999; Nguyen et al., 2012; Lahiri et al., 2014; Hernandez-Alvarez et al., 2019; Petrungaro and Kornmann, 2019). The best-studied ER-mitochondria tether that is responsible for PS transport is yeast ER-mitochondria encounter structure (ERMES) complex (Kawano et al., 2018; Petrungaro and Kornmann, 2019; **Figure 2B**). In addition to facilitating PS transport, MAMs also contains phospholipid synthetic activity. An excellent study performed by J. E. Vance demonstrated that the activities of phospholipid biosynthetic enzymes such as PS synthase (PSS), cholinephosphotransferase (CPT) and ethanolaminephosphotransferase (EPT) are present in MAMs (Vance, 1990) (**Figure 1B**). Later on, her group reported that both full-length PSS1 and PSS2 are located almost exclusively at MAMs and are largely excluded from the bulk of the ER (Stone and Vance, 2000; **Figure 1B**). The presence of phospholipid biosynthetic enzymes at the MAMs raises the following question: is the unique subcellular localization of these enzymes functionally significant in the regulation of metabolic processes? In fact, the newly synthesized PS is more readily transported from the ER to the mitochondria than the preexisting PS (Vance, 1991; Achleitner et al., 1995). Similarly, the newly synthesized PE is preferred for translocation from the mitochondria to the ER (Vance, 1991; Achleitner et al., 1995). Recently, Prinz et al. (2020) fused *E. coli* PS synthase with yeast Mmm1, which is specifically located to the MAMs, or with yeast Sec63, which is evenly distributed in all portions of the ER (Kannan et al., 2017). Their results showed that enrichment of PS synthase at the MAMs promotes more efficient PS transport than when PS synthase is located evenly in the ER (Kannan et al., 2017). This suggests that a MAM-localized phospholipid synthetic enzyme can increase phospholipid transport.

In mammalian cells, ER-derived PS is rapidly converted to PE by decarboxylation and this is thought to take place in mitochondria only. However, yeast has two PS decarboxylases: mitochondrial Psd1 and the *trans*-Golgi network/endosomal Psd2 (Wang et al., 2020). Psd2 is proposed to engage with MCSs for PS decarboxylation (Wang et al., 2020). Several proteins are known to be required in conjunction with Psd2 for PS transport to occur, such as the sec14-like phosphatidylinositol transfer protein (PITP) Sfh4, the phosphatidylinositol 4-kinase (PI4K) Stt4, the tether Scs2, and an uncharacterized protein Pbi1 (Wang et al., 2020; **Figure 2C**). A recent study demonstrated that Sfh4 affects Psd2 activity through direct physical interaction

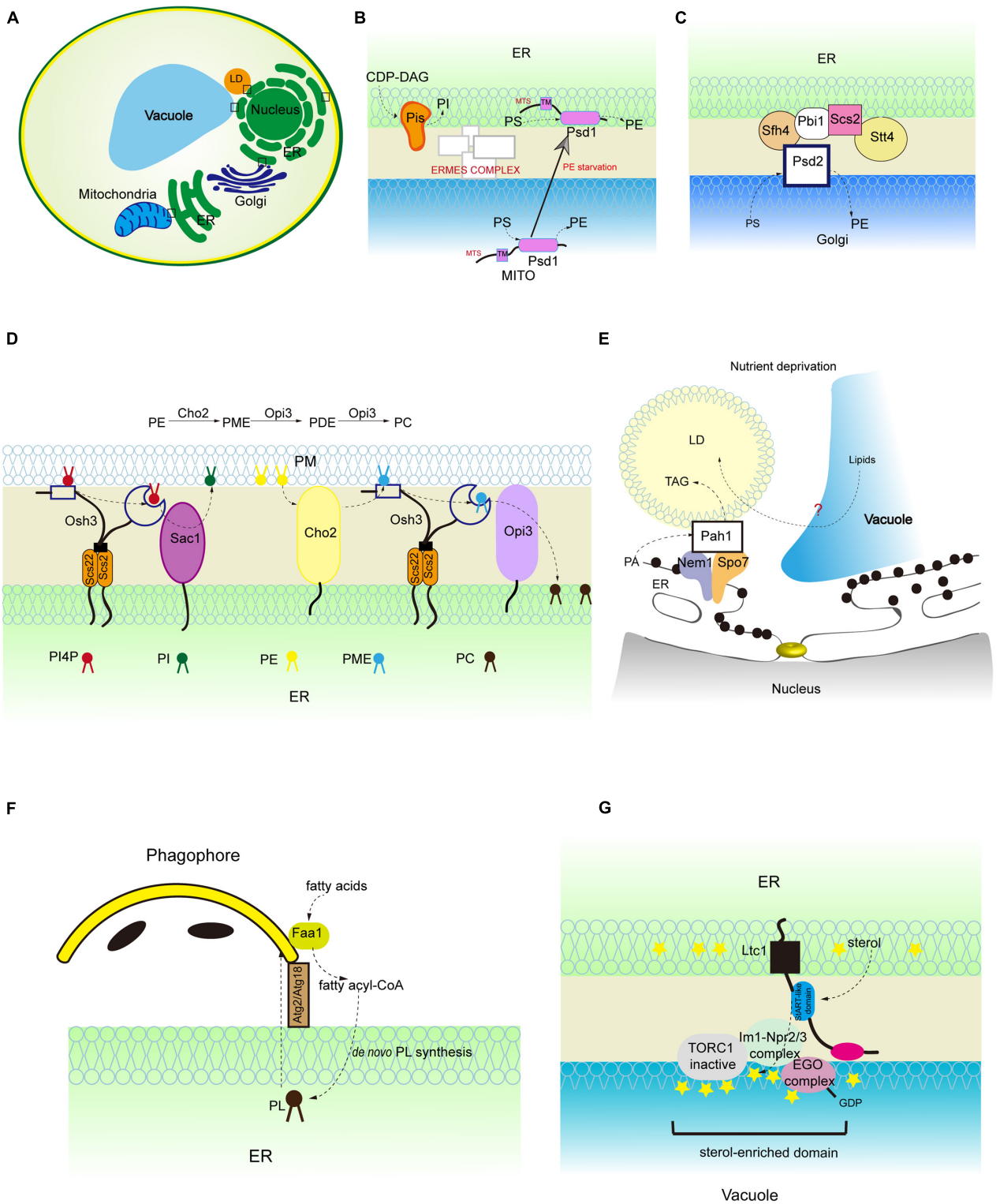

FIGURE 2 | Lipid synthesis and breakdown at MCSs in yeast. **(A)** Schematic illustration of yeast MCSs. The contact sites discussed in the text are boxed. **(B)** The mitochondrial and ER fractions of the PS decarboxylase Psd1, PI synthesis from CDP-DAG at MAMs, and PS transporter:ERMES complex. **(C)** The assembly of ER-Golgi contacts composed of the PS decarboxylase Psd2, Sfh4, the PI4P kinase Stt4, the tether Scs2 that binds Stt4, and Pbi1. **(D)** PI4P turnover at the ER-PM contact, and PC biosynthesis from PE. **(E)** LD-associated Pah1 at the nuclear vacuole junction. **(F)** Local phospholipid synthesis supports phagophore membrane expansion from the ER. **(G)** Concentration of the positive regulator of Torc1 (Ego complex) into sterol-enriched domains at ER-vacuole contacts. PME, phosphatidylmonomethylethanolamine; PDE, phosphatidyldimethylethanolamine.

TABLE 1 | Proteins involved in lipid metabolism at MCSs.

Protein	Related membrane contacts	System	References
Acyl-CoA synthetase long chain family member 1 (ACSL1)	MAM	mammalian cells	Hung et al., 2017
Carnitine palmitoyltransferase Ia (CPTIa)	MAM	mammalian cells	Hung et al., 2017
Glycerol kinase (GK)	MAM	mammalian cells	Hung et al., 2017
IP3R-GRP75-VDAC1 complex	MAM	mammalian cells	Poston et al., 2011
Sigma-1 receptor (Sigma 1R)	MAM	mammalian cells	Hayashi and Fujimoto, 2010
Sac1 PI phosphatase	ER-PM	mammalian cells	Dickson et al., 2016
Transmembrane protein 24 (TMEM24)	ER-PM	mammalian cells	Lees et al., 2017
Sorting nexin 14 (Snx14)	ER-LD	mammalian cells	Datta et al., 2019
Oxysterol binding protein (OSBP)	ER-lysosome	mammalian cells	Lim et al., 2019
Mitoguardin 2 (MIGA2)	mitochondrion-LD	mammalian cells	Freyre et al., 2019
Adipose triglyceride lipase (ATGL)	peroxisome-LD	mammalian cells	Kong et al., 2020
ACBD2/ECI2 isoform A	peroxisome-mitochondrion	mammalian cells	Fan et al., 2016
Cholinephosphotransferase (CPT)	MAM	rat liver	Vance, 1990
Ethanolaminephosphotransferase (EPT)	MAM	rat liver	Vance, 1990
Glycerophosphate acyltransferase 1 (GPAT1)	MAV	rat liver	Pellon-Malson et al., 2007
Mitofusion2 (MFN2)	MAM	mouse liver	Sebastian et al., 2012; Hernandez-Alvarez et al., 2019
PE methyltransferase (PEMT)	MAM	rat liver	Cui et al., 1993
PS synthases PSS1/2	MAM	rat liver	Vance, 1990
PS decarboxylase1 (Psd1)	MAM	yeast	Wang et al., 2020
PI synthase (Pis)	MAM, PAM	yeast	Gaigg et al., 1995; Pichler et al., 2001
Oxysterol-binding homology 3 (Osh3)	ER-PM	yeast	Stefan et al., 2011
Opi3	ER-PM	yeast	Tavassoli et al., 2013
Ltcl	ER-Vacuole	yeast	Murley et al., 2017
Faal	ER-autophagosome	yeast	Schutter et al., 2020
PS decarboxylase2 (Psd2)	ER-Golgi	yeast	Friedman et al., 2018
Pahl	NVJ associated LD	yeast	Karanasios et al., 2013
Mdml	NVJ associated LD	yeast	Hariri et al., 2018

with Psd2 and the functional effect of Sfh4 is independent of its PI-binding/exchange activity (Wang et al., 2020). This study challenges the general view of PITP as a PI transfer protein. Although Psd1 is considered as an inner mitochondrial membrane-anchored protein, a recent study showed that Psd1 has dual ER and mitochondrial localization with its transmembrane domain necessary and sufficient for its ER localization (Friedman et al., 2018; **Figure 2B**). Furthermore, the mitochondrial fraction of Psd1 is required for normal mitochondrial function and the ER-localized fraction of Psd1 is required for normal cellular PE homeostasis (Friedman et al., 2018). This finding implies that the mitochondrial-derived PE generated by mitochondrial Psd1 is not robust enough to provide cells with a sufficient PE pool. Thus, the different organelle-associated domains of a protein may play distinct but essential roles in organelle function.

PI AND PI4P

Phosphatidylinositol is synthesized in the ER and phosphorylated to PtdIns 4-phosphate (PI4P) at the PM and Golgi and PtdIns 4,5-biphosphate (PIP2) at the PM (Agranoff et al., 1958; Gaigg et al., 1995; **Figure 1C**). Mammalian phosphatidylinositol synthase (PIS), which catalyzes PI formation using CDP-DAG, is found at the ER. Interestingly, PIS has been detected in a highly mobile membrane compartment, which originates from the ER and provides PI to cellular membranes in mammalian cells (Kim et al., 2011). In addition, the autophagy initiation complex is located to the PIS-enriched ER subdomains of mammalian cells (Nishimura et al., 2017). In yeast, the specific activity of phosphatidylinositol synthase (Pis) is significantly higher in the MAM fraction than in the ER fractions (Gaigg et al., 1995; **Figure 2B**). The PI level in the MAMs is almost three times higher than that in ER fractions (Gaigg et al., 1995). The biosynthesis of PI is also enriched in the ER-associated plasma membrane (PAM) in yeast (Pichler et al., 2001).

PI4P, derived from PI by PI kinase, is an essential signaling molecule at the PM and Golgi with functions in signal transduction, lipid metabolism, and membrane trafficking (D'Angelo et al., 2008). Sac1 PI phosphatase is an important regulator of PI4P turnover and is located to the ER and Golgi (Nemoto et al., 2000; Foti et al., 2001; Faulhammer et al., 2007). *sac1* mutant yeast cells accumulate PI4P at the PM (Baird et al., 2008). Since Sac1 is not known to traffic to the PM, there must be factors that link Sac1 activity to PI4P at the PM (Stefan et al., 2011). Oxysterol-binding homology 3 (Osh3), a conserved pleckstrin-homology (PH)

domain-containing protein, is identified as linking Sac1 activity to PI4P homeostasis at the PM (Stefan et al., 2011). PI4P binds to the Osh3 PH domain and activates Osh3 at the ER-PM contact sites (Stefan et al., 2011). The association of PI4P with Osh3 facilitates the interaction between ORD, a lipid transfer domain in Osh3, and the downstream target protein Sac1, thus stimulating Sac1 PI phosphatase activity (Stefan et al., 2011; **Figure 2D**). Therefore, Osh proteins can act as sensors of PI4P at the PM and activators of Sac1 phosphatase at the ER. Although these findings support the notion that Sac1 controls the PI4P level at the PM *in trans*, some evidence suggests that it acts *in cis* (i.e., in the same membrane) (Mesmin et al., 2013). In fact, Sac1 dephosphorylates PI4P at the ER and creates a PI4P gradient. This process is accompanied by counter transport of cholesterol or PS by oxysterol-binding protein (OSBP) and Osh6, respectively, and is conserved in yeast and mammalian systems (von Filseck et al., 2015; Mesmin et al., 2017). In mammalian cells, Sac1 is reported to be located at the ER-PM junctions (Dickson et al., 2016). Depletion of PI(4,5)P2, the product from phosphorylation of PI4P, at the PM reduces the amount of Sac1 in contact with the PM, thus limiting PI4P dephosphorylation through a feedback mechanism (Dickson et al., 2016; **Figure 1C**). The above findings about the functions of lipid transfer proteins at the ER-PM contacts shed light on their roles in maintaining contact structures and the PM lipid composition. Indeed, elimination of lipid transfer proteins causes dysregulation of phospholipid biosynthesis and sterol transfer, which negatively impacts PM organization (Quon et al., 2018).

PA

Phosphatidic acid can be derived from lipid precursor: glycerol 3-phosphate (G3P). In this process, G3P is acylated by glycerophosphate acyltransferases (GPATs) to form lyso-PA which is further converted to PA by 1-acylglycerol 3-phosphate acyltransferases (AGPATs) (Gonzalez-Baro et al., 2007; Takeuchi and Reue, 2009). Thus far, four mammalian GPAT proteins have been identified. There are three N-ethylmaleimide (NEM)-sensitive microsomal and mitochondrial GPATs (GPAT2-4) and one NEM-resistant mitochondrial GPAT1 (Wang et al., 2007; Nagle et al., 2008). Because the enzymes that catalyze the final steps of TAG synthesis are localized to the ER, the mitochondrial localization of GPAT1 is unexpected. A study has shown that GPAT1 is highly enriched in the mitochondrial-associated vesicle (MAV) fraction, which is obtained from sedimentation of the upper band from Percoll density gradient centrifugation of crude mitochondria (Pellon-Malson et al., 2007; **Figure 1B**). MAVs share characteristics with both MAMs and crude mitochondrial fraction, which contains mitochondrial and MAM fractions. Many marker proteins present in above fractions are also recovered in the MAV fraction. The MAV fraction contains large vesicles, as viewed by electron microscopy (Pellon-Malson et al., 2007). Although the protein level of GPAT1 is highly enriched in this MAV fraction, GPAT1 activity is most enriched in pure mitochondria (Pellon-Malson et al., 2007). This suggests that GPAT1 is largely inactive in the MAV fraction. The discrepancy between GPAT1 protein expression and activity in the subcellular fraction suggests the possibility that GPAT1 in the MAV fraction may have novel roles beyond its enzymatic activity, and, as such, it has been postulated that GPAT1 from the MAV fraction is important for transporting its product, lyso-PA, from the mitochondria to the ER (Pellon-Malson et al., 2007).

PC

Phosphatidylcholine is the most abundant phospholipid in mammalian cells. PC is synthesized via either the CDP-choline pathway or the methylation of PE (Horvath and Daum, 2013). Liver-specific PEMT, which converts PE to PC, is specifically located at the MAMs (Cui et al., 1993; **Figure 1B**). Although PEMT is highly enriched in the MAMs, the PE methyltransferase activity in the MAMs is comparable with that in the ER, which indicates that other ER-localized enzymes may also have PE methyltransferase activity (Vance and Vance, 1988; Cui et al., 1993; Rusinol et al., 1994). In yeast, methylation of PE is the primary pathway for the biosynthesis of PC when cells are grown in the absence of choline, whereas the CDP-choline pathway is an auxiliary route since it requires exogenous choline (McDonough et al., 1995). Unlike the mammalian PEMT, which catalyzes all three transmethylation steps to form PC, yeast has two PEMT enzymes, designated Cho2 and Opi3, which catalyze the first and the last two consecutive transmethylation steps, respectively (Cui et al., 1993; **Figure 2D**). Of interest, a study showed that the ER-PM contacts are required for PC synthesis through the methylation of PE (Tavassoli et al., 2013). *SCS2* and *ICE2*, two ER-localized proteins, play important roles in ER biogenesis and the structure of ER-PM contacts (Tavassoli et al., 2013). Δ*scs2*Δ*ice2* mutant yeast exhibited disrupted ER-PM contacts, growth defects and reduced PC synthesis (Tavassoli et al., 2013). The reduced PC synthesis is due to the loss of function of Opi3 (Tavassoli et al., 2013). With disrupted ER-PM contacts, the access of lipid substrates such as phosphatidylmonomethylethanolamine (PME) and phosphatidyldimethylethanolamine (PDE) to Opi3 is compromised (**Figure 2D**). In addition, similar to the Sac1-Osh3 regulatory relationship at the ER-PM contacts, Osh3 also regulates Opi3 and facilitates its PC synthetic activity at these contacts (Stefan et al., 2011; Tavassoli et al., 2013; **Figure 2D**). The precise regulation of PC biosynthesis at the ER-PM contacts is crucial, because in yeast, Opi3 controls the ratio of PE:PC at the PM and decreased Opi3 activity results in an increased PE:PC ratio, therefore destabilizing the PM bilayer (Schueller et al., 2007).

Compelling evidence suggests that many phospholipid biosynthetic enzymes are enriched at MCSs. It is a paradox that their enzymatic activities are not always enriched at MCSs, which suggests that non-enzymatic roles/domains of these proteins may be important for their function at MCSs. The contact sites provide a confined environment for segregating phospholipid biosynthetic enzymes. Therefore, the pool of lipids generated by this segregation may serve special purposes, such as transport to other organelles or involvement in lipoprotein synthesis. Furthermore, the contact sites can spatially regulate

the accessibility of lipid substrates to their catalytic enzymes. Therefore, the fine regulation of chemical reactions can be accomplished at MCSs.

Neutral Lipid Synthesis and Degradation at Membrane Contacts

The ER synthesizes phospholipids for membrane growth and cell proliferation, and TAG to store energy in lipid droplets (LDs). LD biogenesis is generally considered to occur at the ER. In some cell types, LDs appear inside the nucleus (Layerenza et al., 2013; Uzbekov and Roingeard, 2013; Ohsaki et al., 2016). Yeast phosphatidate phosphatase, Pah1, catalyzes the conversion of PA to DAG, which channels PA toward TAG storage but away from phospholipid synthesis for membrane biogenesis and growth. Pah1 lacks transmembrane domains and requires translocation onto membranes to become functional (Karanasios et al., 2013). It has been shown that the acidic tail of Pah1 is required for both LD and nuclear membrane recruitment (Karanasios et al., 2013). It is likely that membrane-bound Pah1 and its regulation of lipid and membrane biogenesis are key metabolic adaptations when the cell requires drastic membrane remodeling (Karanasios et al., 2013). Indeed, during glucose exhaustion in yeast, Pah1 is targeted transiently to the nuclear membrane domain that contacts the vacuole, named the nuclear vacuole junction (NVJ) (Barbosa et al., 2015; **Figure 2E**). Subsequently, Pah1 is concentrated in two nuclear membrane puncta flanking the NVJ that are in contact with LDs (Barbosa et al., 2015; **Figure 2E**). The biological significance of this concentration of Pah1 and the associated LDs at the NVJ flanked by the nuclear envelope is not completely clear. Given that in nutrient-rich conditions in yeast, phospholipid synthesis is predominant, whereas during glucose exhaustion, lipid precursors are redirected to TAG storage, it is possible that Pah1 facilitates NVJ-mediated degradation of the nuclear membrane and LD biogenesis, both of which are lipid recycling processes during glucose exhaustion. Recent evidence suggests that yeast Mdm1 and its human homolog: sorting nexin protein (Snx14) are localized to NVJ-associated LD (ER-LD contact in mammalian cells) and regulate NVJ-associated LD production (Schuldiner and Bohnert, 2017; Eisenberg-Bord et al., 2018; Hariri et al., 2018; Datta et al., 2019).

It is clear that LD-organelle contacts are regulated by nutritional status. In mammalian system, the stored TAG undergoes lipolysis in adipocytes to release fatty acids and glycerol in response to starvation, and this process is mediated by TAG hydrolases including adipose triglyceride lipase (ATGL) and hormone-sensitive lipase (HSL). The released fatty acids are further oxidized in mitochondria or peroxisomes. Lipolysis coupled with fatty acid oxidation supplies energy during starvation. An interesting study revealed that fasting promotes the interaction between peroxisomes and LDs (Kong et al., 2020). Upon fasting, peroxisomal biogenesis factor 5 (PEX5) mediates the recruitment of ATGL at peroxisome-LD contact sites (Kong et al., 2020). Lipolysis is compromised if peroxisome-LD contacts are disrupted (Kong et al., 2020; **Figure 1D**). This study provides a clear example of how cells respond to environmental stress such as nutrient depletion by modulating organelle contacts (Zaman et al., 2008). In fact, cells can initiate various adaptations in response to cellular stress. For instance, during prolonged starvation in yeast, ER-mitochondria contact sites are lost, concomitant with sequestration of both cytosolic and ER lipid biosynthetic enzymes into deposits (Suresh et al., 2015). These two processes are considered as an adaptive response for yeast cells to regulate lipid flux when the supply of nutrients is limited (Suresh et al., 2015). The underlying mechanism is not completely clear. It might be that sequestration of enzymes permits regulation of lipid homeostasis without affecting the enzymatic activities and enables cells to quickly alter their lipid flux by simply relocalizing their enzymes when the nutritional status is favorable (Suresh et al., 2015).

Besides the aforementioned peroxisome-LD associations during starvation in cells, mitochondrion-LD associations have also been found in white and brown adipocytes (Benador et al., 2018). It is conceivable that there are factors that regulate mitochondrion-LD contacts. Through proteomic analysis of adipocyte LDs, a mitochondrial outer membrane protein, Mitoguardin 2 (MIGA2), was found to be associated with LDs in adipocytes or oleic acid-treated COS7 cells (Freyre et al., 2019; **Figure 1E**). MIGA2 is not only found at mitochondrion-LD contacts; it is also located to the ER, where *de novo* lipogenesis mainly takes place (Freyre et al., 2019; **Figure 1E**). It has been shown that MIGA2 promotes lipogenesis from non-lipid precursors such as citrate in the mitochondria, possibly leading to positive feedback to the adipogenic transcriptional program and driving adipogenesis and LD formation forward (Freyre et al., 2019). These results coincide with the finding that LD-associated mitochondria support LD expansion by increasing TAG synthesis (Benador et al., 2018).

Synthesis and Breakdown of Other Lipids at Contact Sites

In mammalian system, glycosylphosphatidylinositol (GPI) biosynthetic reactions are largely confined to MAMs (**Figure 1B**). GPIs are important for anchoring proteins to the cell membranes (Vidugiriene et al., 1999). It is likely that the localization of GPI biosynthetic activity at MAMs may allow the biosynthetic enzyme more accessibility to its substrate PE, which is mainly derived from decarboxylation of PS in mitochondria (Vidugiriene et al., 1999). Peroxisomes and mitochondria share some similarities in terms of their synergistic functioning in the metabolism of fatty acids, reactive oxygen species, and steroid biosynthesis (Fan et al., 2016). It has been demonstrated that peroxisomes are physically associated with mitochondria and that Pex34, a peroxisomal membrane protein, and Fzo1, the yeast mitofusion, serve as tethers of peroxisome-mitochondria contact (Fan et al., 2016; Shai et al., 2018). A family of acyl-CoA-binding domain (ACBD)-containing proteins regulates steroid biosynthesis in both peroxisomes and mitochondria (**Figure 1D**). Recent findings suggest that peroxisomal ACBD2/ECI2 isoform A, generated by alternative splicing, is also located to the mitochondria and mediates peroxisome-mitochondrion contact and steroid biosynthesis (Fan et al., 2016).

The autophagosome mediates the degradation of cytoplasmic materials by macroautophagy and is formed in close proximity to the ER (Zhao and Zhang, 2019). Autophagosome formation involves the nucleation of a single-membrane phagophore and its further expansion and closure of its membrane (Mari et al., 2010; Shima et al., 2019). This raises a question: what membranes or processes sustain autophagic membrane formation? It is considered that many organelles, such as ER, Golgi, endosomes, mitochondria, and plasma membrane, contribute to the formation of autophagosomes (Axe et al., 2008; Geng et al., 2010; Hailey et al., 2010; Puri et al., 2013; Nishimura et al., 2017). However, a study demonstrated that *de novo* phospholipid synthesis contributes to autophagosome membrane formation in yeast, which suggests a unique mechanism (Schutter et al., 2020). It has been shown that the long-chain acyl-CoA synthetase (Faa1), which catalyzes the formation of fatty acyl-CoA, is localized to nucleated phagophores. Faa1 channels activated FAs locally into *de novo* phospholipid synthesis at the ER, which forms stable contacts with nascent autophagosomes (Schutter et al., 2020; **Figure 2F**). Furthermore, the newly synthesized phospholipids at the ER promote the assembly and expansion of the phagophore membrane into an autophagosome (**Figure 2F**). The concentrated Faa1 activity specifically on nucleated phagophores allows spatiotemporal compartmentalization of *de novo* phospholipid synthesis, which readily facilitates autophagic membrane expansion under starvation conditions. This notion is conceptually similar to the idea discussed above, that the newly synthesized lipids at the contact sites support the local lipid flux between ER and tethered organelles (Kannan et al., 2017). Therefore, the fine spatial segregation of molecular components permits efficient organelle communication and is critical for cellular homeostasis.

In sum, based on the presence of many lipid biosynthetic enzymes at MCSs and their physiological significances in cellular processes, we may reconsider MCSs as being involved in both organizing lipid synthesis and facilitating intermembrane lipid transport. Newly synthesized lipids at MCSs may have distinct functions beyond simple lipid homeostasis, which will be discussed in the next part.

LIPID FUNCTIONS AT CONTACT SITES BEYOND SIMPLE LIPID HOMEOSTASIS

Distinct Functions of Lipids at MCSs

Lipids at contact sites are critical in maintaining lipid homeostasis and membrane organization. Furthermore, some lipids at membrane contact sites are capable of regulating enzyme activity or signal transduction. Here, we will review the findings about lipid function at contact sites beyond simple lipid metabolism.

As mentioned at the start of this review, compartmentalization is a key determinant of cellular function and biology. One type of compartmentalization is the specialized membrane domains that exist within membrane lipid bilayers (Rai et al., 2016). Membrane contact sites persist during harsh mechanical and chemical separation methods (Vance, 1990). It is possible that specific lipids and proteins are assembled and organized into membrane domains and tether contact sites which are of biophysical and physiological importance in living cells (King et al., 2020). Certain lipid species such as sterols and sphingolipids have greater propensity for membrane domain biogenesis (Harder and Simons, 1997; Simons and Ikonen, 1997). In addition, MCS-resident proteins can also facilitate membrane domain compartment formation. For instance, Osh proteins at ER-PM contact sites create a nanoscale membrane environment that facilitates the synergistic transport of unsaturated PS and sterol and stimulates phosphatidylinositol-4-phosphate 5-kinase (PIP5K) activity, thus affecting PIP2 generation and its related cellular events at the PM (Nishimura et al., 2019). Another example of how small-scale lipid organization controls an enzyme activity or signaling events is provided by the yeast sterol transport protein, Ltc1. It is found at ER-vacuole contact sites and facilitates the partitioning and concentration of the EGO complex, a positive regulator of TORC1, into sterol-enriched domains, thus inhibiting TORC1 activity during stress conditions in yeast (Murley et al., 2015, 2017; **Figure 2G**). These findings suggest that lipids together with membrane-associated proteins can be concentrated into membrane domains at MCSs and enable localized signal transduction.

In addition to being regulated by sterol-enriched membrane domains, mTORC1 activity can be activated by cholesterol on the surface of lysosomes in mammalian cells (Castellano et al., 2017). A study showed that oxysterol binding protein (OSBP), which is located to the ER-lysosome contacts, ensures ER-to-lysosome cholesterol transfer and mTORC1 activation (Lim et al., 2019; **Figure 1F**). Cholesterol from the ER-lysosome contact sites directly interacts with mTORC1 scaffolding proteins, leading to mTORC1 activation on the lysosomal surface (Lim et al., 2019; **Figure 1F**). NPC1 handles LDL-derived cholesterol and transfers cholesterol from the lysosomal lumen to other acceptor membranes (Gong et al., 2016; **Figure 1F**). NPC1-deficient cells have increased accumulation of cholesterol in lysosomes and hyperactive mTORC1. Inhibition of OSBP attenuates hyperactivity of mTORC1 signaling in NPC1-deficient cells by inhibiting the transfer of cholesterol from the ER to the lysosomal surface (Lim et al., 2019). This work uncovered the effect of cholesterol transfer at ER-lysosome contacts on the regulation of mTORC1 activity and shed light on the molecular mechanism underlying the pathogenesis of neurodegenerative diseases caused by inactivation of NPC1.

PIP2 at the PM controls insulin release from pancreatic beta cells (Xie et al., 2016). Transmembrane protein 24 (TMEM24) serves as a tether at ER-PM contact sites and has an SMP domain, which is capable of transporting PI, the precursor of PIP2, from its site of synthesis in the ER to the PM during glucose-induced insulin secretion (Lees et al., 2017; **Figure 1C**). TMEM24 also plays a critical role in calcium pulsatility, likely by replenishing PIP2 pools at the PM, which positively regulate IP3 receptors and the PM ion channels that control calcium influx by generating IP3 (Lees et al., 2017). This finding illuminates the elegant mechanism underlying the regulatory effect of an organelle contact-resident lipid-transfer protein on PI pools, Ca^{2+} oscillation and insulin secretion in beta cells (Lees et al., 2017). Together, these findings

reveal the function of lipids at MCSs in regulating MCS integrity and localized signal transduction.

Physiological Relevance of MCSs

Growing evidence suggests that MCS function is linked to neurodegenerative diseases, Alzheimer disease and metabolic diseases. Here, we will review the physiological function of MCSs in the development of metabolic diseases (**Table 2**).

Mitochondrial-associated membranes play crucial roles in regulating a variety of metabolic stresses, including virus infection, ER stress, hypoxia, nutrient deprivation, and excess glucose availability (Simmen and Herrera-Cruz, 2018). Since recent evidence suggests that MAMs are fundamentally important for hormonal and nutrient signaling, MAMs have come into the spotlight of research on metabolic diseases. MAM structure and function have been implicated in insulin sensing and glucose homeostasis in various tissues, such as liver, adipose tissue, and skeletal muscle. In the liver of diet-induced obese and diabetic mice, ER-mitochondrion contacts are increased, thus resulting in mitochondrial Ca^{2+} overload, oxidative stress and dysfunction, and insulin resistance (Arruda et al., 2014). This seems to be a paradox, because in hepatocytes, palmitate treatment reduces ER-mitochondrion contacts and insulin signaling, and induction of MAMs by overexpression of mitofusin 2 (Mfn2) or GRP75 can rescue the palmitate-induced aberrant insulin signaling (Tubbs et al., 2014; Shinjo et al., 2017). Moreover, loss of Mfn2 reduces ER-mitochondrion interactions and causes insulin resistance and altered glucose homeostasis (Sebastian et al., 2012). Accordingly, Tubbs et al. (2014) observed that MAM integrity is disrupted in the liver of obese and diabetic mouse models. In addition, MAM function has been linked to the pathogenesis of non-alcoholic fatty liver disease (NAFLD). For instance, deficiency of some MAM resident proteins involved in phospholipids biosynthesis, such as PEMT and phosphate cytidylyltransferase 1, choline, alpha (Pcyt1a), cause liver damage in mice (Fu et al., 2011; Jacobs et al., 2017). Furthermore, Recent evidence shows that liver-specific deletion of Mfn2 causes defected PS transport between the ER and mitochondria and leads to non-alcoholic fatty liver disease (Hernandez-Alvarez et al., 2019).

In skeletal muscle, it is found that obesity enhances MAM formation (Thoudam et al., 2019). Inactivation of PDK4 reduces MAM formation and improves insulin signaling in obese mice by disrupting the interaction between PDK4 and the IP3R1-GRP75-VDAC1 complex, which regulates Ca^{2+} transport and controls MAM stability (Thoudam et al., 2019). However, contradictory results showed that ER-mitochondrion contacts in skeletal muscle are disrupted in different mouse models of obesity and diabetes (Tubbs et al., 2018). Furthermore, experimental increase of the ER-mitochondrion contacts in human myotubes prevents palmitate-induced aberrant insulin sensitivity (Tubbs et al., 2018). The reason for the discrepancy between these studies is not clear, but is likely related to differences in the experimental systems and/or experimental analysis methods.

In adipose tissue, CDGSH iron sulfur domain 2 (Cisd2)-mediated loss of ER-mitochondrion contacts impairs mitochondrial Ca^{2+} uptake, decreases insulin-stimulated glucose transport and results in mitochondrial dysfunction (Chen et al., 2009; Wang et al., 2014). Furthermore, miscommunication between ER and mitochondria is an essential step in the pathogenesis of cardiac hypertrophy. Treatment of cardiomyocytes with norepinephrine increases the distance between ER and mitochondria and decreases insulin-induced mitochondrial Ca^{2+} uptake, thus resulting in insulin desensitization (Gutierrez et al., 2014). Glucose is identified as a novel regulator of MAMs and it reduces the ER-mitochondrion contacts, induces mitochondrial fission, and impairs mitochondrial respiration in hepatocytes (Theurey et al., 2016). In line with this, disruption of MAM integrity mimics the effects of glucose on mitochondrial dynamics and function (Theurey et al., 2016). Recently, it is suggested that genetic downregulation of FUN14 domain containing 1 (Fundc1) improved mitochondrial function in HG-treated cardiomyocytes (Wu et al., 2019). Based on recent studies, it is clear that MAMs are involved in metabolic diseases. However, studies on this topic are controversial. MAMs may be a target for treating metabolic diseases, but more studies on their physiological role and regulation are required.

TABLE 2 | Physiological function of MAMs in metabolic diseases.

Disease	Protein	References
Diabetes	Cyclophilin D (CypD)	Tubbs et al., 2014
Diabetes	MFN2	Sebastian et al., 2012; Shinjo et al., 2017
Diabetes	PDK4	Thoudam et al., 2019
Diabetes	FATE1	Tubbs et al., 2018
Diabetes	CISD2	Chen et al., 2009; Wang et al., 2014
Diabetic heart disease	FUNDC1	Wu et al., 2019
Obesity	IP3R-GRP75-VDAC1 complex, PACS2	Arruda et al., 2014
NAFLD	MFN2	Hernandez-Alvarez et al., 2019
NAFLD	PEMT	Jacobs et al., 2017
NAFLD	PCYTIa	Fu et al., 2011
Cardiac hypertrophy	IGF1	Gutierrez et al., 2014

CONCLUDING REMARKS

Membrane contact sites permit the speed and spatial confinement that are required for the intricate control of cellular processes and organelle biogenesis. It has been observed that MCSs are resistant to harsh separation methods, probably because of the biophysical properties of their resident membrane proteins and lipids. There is a general view that lipids allow particular proteins in membranes to aggregate, and others to disperse. In fact, lipids and associated membrane proteins can form nanoscale domains at MCSs. Furthermore, it is an emerging concept that the formation of membrane contacts depends on the lateral segregation of lipids into domains, where lipid and protein binding domains recognize and integrate signals between the

donor and/or acceptor membranes (van Meer et al., 2008). Therefore, lipid composition is essential for the biophysical, biochemical and physiological properties of MCSs. On the other hand, lipids synthesized at MCSs may serve special functions, such as ready transportation to an organelle, or acting as sensing molecules to transmit signals in transduction pathways, or stimulating local enzymatic activity. Accordingly, understanding the lipid composition of MCSs will be of great value to delineate their function. Currently, a comprehensive lipidomic analysis of MCSs has not been reported.

Another interesting phenomenon is that multiple phospholipid synthetic enzymes are enriched at MCSs. The segregation of these enzymes may allow generation of a local pool of phospholipids to support organelle membrane biogenesis or local signaling. Revealing the functions of distinct pools of lipids *in vivo* will be a great challenge. In addition, the discrepancy between the enriched enzymatic activities and their protein levels at MCSs may suggest that non-enzymatic functions of these proteins exist at contact sites. Furthermore, the regulation of the activity at MCSs may depend on specific actors or different local environment for activity such as lipid microdomains. The presence of these enzymes at MCSs may also permit more efficient access to their lipid substrates, or may generate a gradient of lipids (such as PI4P) between the donor and acceptor membranes to facilitate local lipid transport, or may regulate the phospholipid composition of adjacent organelles (such as PE levels in mitochondria and ER, controlled by Psd1).

In the last decade, MCSs have been implicated in metabolic diseases. However, the studies are sometimes controversial. Although a repertoire of methods has been applied to study MCSs, it still remains challenging to identify the contact sites, due to their transient nature and various abundance in different cell types. The current findings usually use knockout of an MCS-resident protein to study the link between MCSs and metabolic diseases. However, this approach may suffer from bias; for instance, the results may be caused by functions of the proteins other than their role at MCSs. Therefore, determining how lipid metabolism specifically at MCSs directly contributes to the pathogenesis of metabolic diseases will be an important future endeavor.

AUTHOR CONTRIBUTIONS

Both authors listed have made a substantial, direct and intellectual contribution to the work, and approved it for publication.

FUNDING

This research was performed in XH's laboratory was supported by grants 91954207, 31771305, 31630019, 2018YFA0506902, 2016YFA0500100, and XDA24030205 from the National Natural Science Foundation of China, National Key R&D Program of China, and Chinese Academy of Sciences.

REFERENCES

Achleitner, G., Gaigg, B., Krasser, A., Kainersdorfer, E., Kohlwein, S. D., Perktold, A., et al. (1999). Association between the endoplasmic reticulum and mitochondria of yeast facilitates interorganelle transport of phospholipids through membrane contact. *Eur. J. Biochem.* 264, 545–553. doi: 10.1046/j.1432-1327.1999.00658.x

Achleitner, G., Zweytick, D., Trotter, P. J., Voelker, D. R., and Daum, G. (1995). Synthesis and intracellular-transport of aminoglycerophospholipids in permeabilized cells of the yeast, *Saccharomyces cerevisiae*. *J. Biol. Chem.* 270, 29836–29842. doi: 10.1074/jbc.270.50.29836

Agranoff, B. W., Bradley, R. M., and Brady, R. O. (1958). The enzymatic synthesis of inositol phosphatide. *J. Biol. Chem.* 233, 1077–1083.

Aguzzi, A., and Altmeyer, M. (2016). Phase separation: linking cellular compartmentalization to disease. *Trends Cell Biol.* 26, 547–558. doi: 10.1016/j.tcb.2016.03.004

Antonicka, H., Lin, Z. Y., Janer, A., Aaltonen, M. J., Weraarpachai, W., Gingras, A. C., et al. (2020). A high-density human mitochondrial proximity interaction network. *Cell Metab.* 32, 479–497.e9.

Arruda, A. P., Pers, B. M., Parlakgul, G., Guney, E., Inouye, K., and Hotamisligil, G. S. (2014). Chronic enrichment of hepatic endoplasmic reticulum-mitochondria contact leads to mitochondrial dysfunction in obesity. *Nat. Med.* 20, 1427–1435. doi: 10.1038/nm.3735

Axe, E. L., Walker, S. A., Manifava, M., Chandra, P., Roderick, H. L., Habermann, A., et al. (2008). Autophagosome formation from membrane compartments enriched in phosphatidylinositol 3-phosphate and dynamically connected to the endoplasmic reticulum. *J. Cell Biol.* 182, 685–701. doi: 10.1083/jcb.200803137

Baird, D., Stefan, C., Audhya, A., Weys, S., and Emr, S. D. (2008). Assembly of the PtdIns 4-kinase Stt4 complex at the plasma membrane requires Ypp1 and Efr3. *J. Cell Biol.* 183, 1061–1074. doi: 10.1083/jcb.200804003

Balla, T., Kim, Y. J., Alvarez-Prats, A., and Pemberton, J. (2019). Lipid dynamics at contact sites between the endoplasmic reticulum and other organelles. *Annu. Rev. Cell Dev. Biol.* 35, 85–109. doi: 10.1146/annurev-cellbio-100818-125251

Balla, T., Sengupta, N., and Kim, Y. J. (2020). Lipid synthesis and transport are coupled to regulate membrane lipid dynamics in the endoplasmic reticulum. *Biochim. Biophys. Acta Mol. Cell Biol. Lipids* 1865, 158461. doi: 10.1016/j.bbalip.2019.05.005

Barbosa, A. D., Sembongi, H., Su, W. M., Abreu, S., Reggiori, F., Carman, G. M., et al. (2015). Lipid partitioning at the nuclear envelope controls membrane biogenesis. *Mol. Biol. Cell* 26, 3641–3657. doi: 10.1091/mbc.e15-03-0173

Benador, I. Y., Veliova, M., Mahdaviani, K., Petcherski, A., Wikstrom, J. D., Assali, E. A., et al. (2018). Mitochondria bound to lipid droplets have unique bioenergetics, composition, and dynamics that support lipid droplet expansion. *Cell Metab.* 27, 869–885.e6.

Castellano, B. M., Thelen, A. M., Moldavski, O., Feltes, M., van der Welle, R. E. N., Mydock-McGrane, L., et al. (2017). CHOLESTEROL SENSING Lysosomal cholesterol activates mTORC1 via an SLC38A9-Niemann-Pick C1 signaling complex. *Science* 355, 1306–1311. doi: 10.1126/science.aag1417

Chen, Y. F., Kao, C. H., Chen, Y. T., Wang, C. H., Wu, C. Y., Tsai, C. Y., et al. (2009). Cisd2 deficiency drives premature aging and causes mitochondria-mediated defects in mice. *Gene Dev.* 23, 1183–1194. doi: 10.1101/gad.1779509

Cho, I. T., Adelmant, G., Lim, Y., Marto, J. A., Cho, G., and Golden, J. A. (2017). Ascorbate peroxidase proximity labeling coupled with biochemical fractionation identifies promoters of endoplasmic reticulum-mitochondrial contacts. *J. Biol. Chem.* 292, 16382–16392. doi: 10.1074/jbc.m117.795286

Cui, Z., Vance, J. E., Chen, M. H., Voelker, D. R., and Vance, D. E. (1993). Cloning and expression of a novel phosphatidylethanolamine N-methyltransferase - a specific biochemical and cytological marker for a unique membrane-fraction in rat-liver. *J. Biol. Chem.* 268, 16655–16663.

D'Angelo, G., Vicinanza, M., Di Campli, A., and De Matteis, M. A. (2008). The multiple roles of PtdIns(4)P - not just the precursor of PtdIns(4,5)P-2. *J. Cell. Sci.* 121, 1955–1963. doi: 10.1242/jcs.023630

Datta, S., Liu, Y., Hariri, H., Bowerman, J., and Henne, W. M. (2019). Cerebellar ataxia disease-associated Snx14 promotes lipid droplet growth at ER-droplet contacts. *J. Cell Biol.* 218, 1335–1351. doi: 10.1083/jcb.201808133

Dickson, E. J., Jensen, J. B., Vivas, O., Kruse, M., Traynor-Kaplan, A. E., and Hille, B. (2016). Dynamic formation of ER-PM junctions presents a lipid phosphatase to regulate phosphoinositides. *J. Cell Biol.* 213, 33–48. doi: 10.1083/jcb.201508106

Doghman-Bouguerra, M., Granatiero, V., Sbiera, S., Sbiera, I., Lacas-Gervais, S., Brau, F., et al. (2016). FATE1 antagonizes calcium- and drug-induced apoptosis by uncoupling ER and mitochondria. *EMBO Rep.* 17, 1264–1280. doi: 10.15252/embr.201541504

Eisenberg-Bord, M., Mari, M., Weill, U., Rosenfeld-Gur, E., Moldavski, O., Castro, I. G., et al. (2018). Identification of seipin-linked factors that act as determinants of a lipid droplet subpopulation. *J. Cell Biol.* 217, 269–282. doi: 10.1083/jcb.201704122

Fan, J. J., Li, X. L., Issop, L., Culty, M., and Papadopoulos, V. (2016). ACBD2/ECI2-mediated peroxisome-mitochondria interactions in leydig cell steroid biosynthesis. *Mol. Endocrinol.* 30, 763–782. doi: 10.1210/me.2016-1008

Faulhammer, F., Kanjilal-Kolar, S., Knodler, A., Lo, J., Lee, Y., Konrad, G., et al. (2007). Growth control of golgi phosphoinositides by reciprocal localization of sac1 lipid phosphatase and pik1 4-kinase. *Traffic* 8, 1554–1567. doi: 10.1111/j.1600-0854.2007.00632.x

Fernandez-Murray, J. P., and McMaster, C. R. (2016). Lipid synthesis and membrane contact sites: a crossroads for cellular physiology. *J. Lipid Res.* 57, 1789–1805. doi: 10.1194/jlr.r070920

Fischl, A. S., and Carman, G. M. (1983). Phosphatidylinositol biosynthesis in *Saccharomyces cerevisiae*: purification and properties of microsome-associated phosphatidylinositol synthase. *J. Bacteriol.* 154, 304–311. doi: 10.1128/jb.154.1.304-311.1983

Foti, M., Audhya, A., and Emr, S. D. (2001). Sac1 lipid phosphatase and Stt4 phosphatidylinositol 4-kinase regulate a pool of phosphatidylinositol 4-phosphate that functions in the control of the actin cytoskeleton and vacuole morphology. *Mol. Biol. Cell* 12, 2396–2411. doi: 10.1091/mbc.12.8.2396

Freyre, C. A. C., Rauher, P. C., Ejsing, C. S., and Klemm, R. W. (2019). MIGA2 links mitochondria, the ER, and lipid droplets and promotes *de novo* lipogenesis in adipocytes. *Mol. Cell* 76, 811–825.e14.

Friedman, J. R., Kannan, M., Toulmay, A., Jan, C. H., Weissman, J. S., Prinz, W. A., et al. (2018). Lipid homeostasis is maintained by dual targeting of the mitochondrial PE biosynthesis enzyme to the ER. *Dev. Cell* 44, 261–270.e6.

Fu, S. N., Yang, L., Li, P., Hofmann, O., Dicker, L., Hide, W., et al. (2011). Aberrant lipid metabolism disrupts calcium homeostasis causing liver endoplasmic reticulum stress in obesity. *Nature* 473, 528–531. doi: 10.1038/nature09968

Gaigg, B., Simbeni, R., Hrastnik, C., Paltauf, F., and Daum, G. (1995). Characterization of a microsomal subfraction associated with mitochondria of the yeast, *Saccharomyces cerevisiae*. Involvement in synthesis and import of phospholipids into mitochondria. *Biochim. Biophys. Acta* 1234, 214–220. doi: 10.1016/0005-2736(94)00287-y

Garofalo, T., Matarrese, P., Manganelli, V., Marconi, M., Tinari, A., Gambardella, L., et al. (2016). Evidence for the involvement of lipid rafts localized at the ER-mitochondria associated membranes in autophagosome formation. *Autophagy* 12, 917–935. doi: 10.1080/15548627.2016.1160971

Geng, J. F., Nair, U., Yasumura-Yorimitsu, K., and Klionsky, D. J. (2010). Post-Golgi sec proteins are required for autophagy in *Saccharomyces cerevisiae*. *Mol. Biol. Cell* 21, 2257–2269. doi: 10.1091/mbc.e09-11-0969

Gong, X., Qian, H. W., Zhou, X. H., Wu, J. P., Wan, T., Cao, P. P., et al. (2016). Structural insights into the Niemann-Pick C1 (NPC1)-mediated cholesterol transfer and ebola infection. *Cell* 165, 1467–1478. doi: 10.1016/j.cell.2016.05.022

Gonzalez-Baro, M. R., Lewin, T. M., and Coleman, R. A. (2007). Regulation of triglyceride metabolism II. Function of mitochondrial GPAT1 in the regulation of triacylglycerol biosynthesis and insulin action. *Am. J. Physiol. Gastrointest. Liver Physiol.* 292, G1195–G1199.

Gutierrez, T., Parra, V., Troncoso, R., Pennanen, C., Contreras-Ferrat, A., Vasquez-Trincado, C., et al. (2014). Alteration in mitochondrial Ca2+ uptake disrupts insulin signaling in hypertrophic cardiomyocytes. *Cell Commun. Signal.* 12:68. doi: 10.1186/preaccept-1950166084128344

Hailey, D. W., Rambold, A. S., Satpute-Krishnan, P., Mitra, K., Sougrat, R., Kim, P. K., et al. (2010). Mitochondria supply membranes for autophagosome biogenesis during starvation. *Cell* 141, 656–667. doi: 10.1016/j.cell.2010.04.009

Harder, T., and Simons, K. (1997). Caveolae, DIGs, and the dynamics of sphingolipid-cholesterol microdomains. *Curr. Opin. Cell Biol.* 9, 534–542. doi: 10.1016/s0955-0674(97)80030-0

Hariri, H., Rogers, S., Ugrankar, R., Liu, Y. L., Feathers, J. R., and Henne, W. M. (2018). Lipid droplet biogenesis is spatially coordinated at ER-vacuole contacts under nutritional stress. *EMBO Rep.* 19, 57–72. doi: 10.15252/embr.201744815

Hayashi, T., and Fujimoto, M. (2010). Detergent-resistant microdomains determine the localization of sigma-1 receptors to the endoplasmic reticulum-mitochondria junction. *Mol. Pharmacol.* 77, 517–528. doi: 10.1124/mol.109.062539

Hayashi, T., and Su, T. P. (2007). Sigma-1 receptor chaperones at the ER-mitochondrion interface regulate Ca(2+) signaling and cell survival. *Cell* 131, 596–610. doi: 10.1016/j.cell.2007.08.036

Hernandez-Alvarez, M. I., Sebastian, D., Vives, S., Ivanova, S., Bartoccioni, P., Kakimoto, P., et al. (2019). Deficient endoplasmic reticulum-mitochondrial phosphatidylserine transfer causes liver disease. *Cell* 177, 881–895.e17.

Horvath, S. E., and Daum, G. (2013). Lipids of mitochondria. *Prog. Lipid Res.* 52, 590–614.

Hung, V., Lam, S. S., Udeshi, N. D., Svinkina, T., Guzman, G., Mootha, V. K., et al. (2017). Proteomic mapping of cytosol-facing outer mitochondrial and ER membranes in living human cells by proximity biotinylation. *eLife* 6:e24463.

Jacobs, R. L., Jiang, H., Kennelly, J. P., Orlicky, D. J., Allen, R. H., Stabler, S. P., et al. (2017). Cystathionine beta-synthase deficiency alters hepatic phospholipid and choline metabolism: post-translational repression of phosphatidylethanolamine N-methyltransferase is a consequence rather than a cause of liver injury in homocystinuria. *Mol. Genet. Metab.* 120, 325–336. doi: 10.1016/j.ymgme.2017.02.010

Kannan, M., Lahiri, S., Liu, L. K., Choudhary, V., and Prinz, W. A. (2017). Phosphatidylserine synthesis at membrane contact sites promotes its transport out of the ER. *J. Lipid Res.* 58, 553–562. doi: 10.1194/jlr.m072959

Karanasios, E., Barbosa, A. D., Sembongi, H., Mari, M., Han, G. S., Reggiori, F., et al. (2013). Regulation of lipid droplet and membrane biogenesis by the acidic tail of the phosphatidate phosphatase Pah1p. *Mol. Biol. Cell* 24, 2124–2133. doi: 10.1091/mbc.e13-01-0021

Kawano, S., Tamura, Y., Kojima, R., Bala, S., Asai, E., Michel, A. H., et al. (2018). Structure-function insights into direct lipid transfer between membranes by Mmm1-Mdm12 of ERMES. *J. Cell Biol.* 217, 959–974. doi: 10.1083/jcb.201704119

Kim, Y. J., Guzman-Hernandez, M. L., and Balla, T. (2011). A highly dynamic ER-derived phosphatidylinositol-synthesizing organelle supplies phosphoinositides to cellular membranes. *Dev. Cell* 21, 813–824. doi: 10.1016/j.devcel.2011.09.005

King, C., Sengupta, P., Seo, A. Y., and Lippincott-Schwartz, J. (2020). ER membranes exhibit phase behavior at sites of organelle contact. *Proc. Natl. Acad. Sci. U.S.A.* 117, 7225–7235. doi: 10.1073/pnas.1910854117

Kong, J., Ji, Y., Jeon, Y. G., Han, J. S., Han, K. H., Lee, J. H., et al. (2020). Spatiotemporal contact between peroxisomes and lipid droplets regulates fasting-induced lipolysis via PEX5. *Nat. Commun.* 11:578.

Kwak, C., Shin, S., Park, J. S., Jung, M., Nhung, T. T. M., Kang, M. G., et al. (2020). Contact-ID, a tool for profiling organelle contact sites, reveals regulatory proteins of mitochondrial-associated membrane formation. *Proc. Natl. Acad. Sci. U.S.A.* 117, 12109–12120. doi: 10.1073/pnas.1916584117

Lahiri, S., Chao, J. T., Tavassoli, S., Wong, A. K., Choudhary, V., Young, B. P., et al. (2014). A conserved endoplasmic reticulum membrane protein complex (EMC) facilitates phospholipid transfer from the ER to mitochondria. *PLoS Biol.* 12:e1001969. doi: 10.1371/journal.pbio.1001969

Lahiri, S., Toulmay, A., and Prinz, W. A. (2015). Membrane contact sites, gateways for lipid homeostasis. *Curr. Opin. Cell Biol.* 33, 82–87. doi: 10.1016/j.ceb.2014.12.004

Layerenza, J. P., Gonzalez, P., de Bravo, M. M. G., Polo, M. P., Sisti, M. S., and Ves-Losada, A. (2013). Nuclear lipid droplets: a novel nuclear domain. *Biochim. Biophys. Acta* 1831, 327–340. doi: 10.1016/j.bbalip.2012.10.005

Lees, J. A., Messa, M., Sun, E. W., Wheeler, H., Torta, F., Wenk, M. R., et al. (2017). Lipid transport by TMEM24 at ER-plasma membrane contacts regulates pulsatile insulin secretion. *Science* 355, eaah6171. doi: 10.1126/science.aah6171

Lim, C. Y., Davis, O. B., Shin, H. R., Zhang, J., Berdan, C. A., Jiang, X. T., et al. (2019). ER-lysosome contacts enable cholesterol sensing by mTORC1 and drive aberrant growth signalling in Niemann-Pick type C. *Nat. Cell Biol.* 21, 1206–1218. doi: 10.1038/s41556-019-0391-5

Ma, J. H. J., Shen, S. C., Wang, J. J., He, Z. W., Poon, A., Li, J., et al. (2017). Comparative proteomic analysis of the mitochondria-associated ER Membrane (MAM) in a Long-term Type 2 diabetic rodent model. *Sci. Rep.* 7:2062.

Mari, M., Griffith, J., Rieter, E., Krishnappa, L., Klionsky, D. J., and Reggiori, F. (2010). An Atg9-containing compartment that functions in the early steps of autophagosome biogenesis. *J. Cell Biol.* 190, 1005–1022. doi: 10.1083/jcb.200912089

McDonough, V. M., Buxeda, R. J., Bruno, M. E., Ozier-Kalogeropoulos, O., Adeline, M. T., McMaster, C. R., et al. (1995). Regulation of phospholipid biosynthesis in *Saccharomyces cerevisiae* by CTP. *J. Biol. Chem.* 270, 18774–18780.

Mesmin, B., Bigay, J., Moser von Filseck, J., Lacas-Gervais, S., Drin, G., and Antonny, B. (2013). A four-step cycle driven by PI(4)P hydrolysis directs sterol/PI(4)P exchange by the ER-Golgi tether OSBP. *Cell* 155, 830–843. doi: 10.1016/j.cell.2013.09.056

Mesmin, B., Bigay, J., Polidori, J., Jamecna, D., Lacas-Gervais, S., and Antonny, B. (2017). Sterol transfer, PI4P consumption, and control of membrane lipid order by endogenous OSBP. *EMBO J.* 36, 3156–3174. doi: 10.15252/embj.201796687

Muallem, S., Chung, W. Y., Jha, A., and Ahuja, M. (2017). Lipids at membrane contact sites: cell signaling and ion transport. *EMBO Rep.* 18, 1893–1904. doi: 10.15252/embr.201744331

Murley, A., Sarsam, R. D., Toulmay, A., Yamada, J., Prinz, W. A., and Nunnari, J. (2015). Ltc1 is an ER-localized sterol transporter and a component of ER-mitochondria and ER-vacuole contacts. *J. Cell Biol.* 209, 539–548. doi: 10.1083/jcb.201502033

Murley, A., Yamada, J., Niles, B. J., Toulmay, A., Prinz, W. A., Powers, T., et al. (2017). Sterol transporters at membrane contact sites regulate TORC1 and TORC2 signaling. *J. Cell Biol.* 216, 2679–2689. doi: 10.1083/jcb.201610032

Nagle, C. A., Vergnes, L., Dejong, H., Wang, S., Lewin, T. M., Reue, K., et al. (2008). Identification of a novel sn-glycerol-3-phosphate acyltransferase isoform, GPAT4, as the enzyme deficient in Agpat6-/- mice. *J. Lipid Res.* 49, 823–831. doi: 10.1194/jlr.m700592-jlr200

Nemoto, Y., Kearns, B. G., Wenk, M. R., Chen, H., Mori, K., Alb, J. G., et al. (2000). Functional characterization of a mammalian Sac1 and mutants exhibiting substrate-specific defects in phosphoinositide phosphatase activity. *J. Biol. Chem.* 275, 34293–34305. doi: 10.1074/jbc.m003923200

Nguyen, T. T., Lewandowska, A., Choi, J. Y., Markgraf, D. F., Junker, M., Bilgin, M., et al. (2012). Gem1 and ERMES do not directly affect phosphatidylserine transport from ER to mitochondria or mitochondrial inheritance. *Traffic* 13, 880–890. doi: 10.1111/j.1600-0854.2012.01352.x

Nishimura, T., Gecht, M., Covino, R., Hummer, G., Surma, M. A., Klose, C., et al. (2019). Osh proteins control nanoscale lipid organization necessary for PI(4,5)P-2 synthesis. *Mol. Cell* 75, 1043–1057.e8.

Nishimura, T., Tamura, N., Kono, N., Shimanaka, Y., Arai, H., Yamamoto, H., et al. (2017). Autophagosome formation is initiated at phosphatidylinositol synthase-enriched ER subdomains. *EMBO J.* 36, 1719–1735. doi: 10.15252/embj.201695189

Ohsaki, Y., Kawai, T., Yoshikawa, Y., Cheng, J., Jokitalo, E., and Fujimoto, T. (2016). PML isoform II plays a critical role in nuclear lipid droplet formation. *J. Cell Biol.* 212, 29–38. doi: 10.1083/jcb.201507122

Pellon-Malson, M., Montanaro, M. A., Coleman, R. A., and Gonzalez-Baro, M. R. (2007). Mitochondrial glycerol-3-P acyltransferase 1 is most active in outer mitochondrial membrane but not in mitochondrial associated vesicles (MAV). *Biochim. Biophys. Acta* 1771, 830–838. doi: 10.1016/j.bbalip.2007.04.001

Petrungaro, C., and Kornmann, B. (2019). Lipid exchange at ER-mitochondria contact sites: a puzzle falling into place with quite a few pieces missing. *Curr. Opin. Cell Biol.* 57, 71–76. doi: 10.1016/j.ceb.2018.11.005

Phillips, M. J., and Voeltz, G. K. (2016). Structure and function of ER membrane contact sites with other organelles. *Nat. Rev. Mol. Cell Biol.* 17, 69–82. doi: 10.1038/nrm.2015.8

Pichler, H., Gaigg, B., Hrastnik, C., Achleitner, G., Kohlwein, S. D., Zellnig, G., et al. (2001). A subfraction of the yeast endoplasmic reticulum associates with the plasma membrane and has a high capacity to synthesize lipids. *Eur. J. Biochem.* 268, 2351–2361. doi: 10.1046/j.1432-1327.2001.02116.x

Poston, C. N., Duong, E., Cao, Y., and Bazemore-Walker, C. R. (2011). Proteomic analysis of lipid raft-enriched membranes isolated from internal organelles. *Biochem. Biophys. Res. Commun.* 415, 355–360. doi: 10.1016/j.bbrc.2011.10.072

Prinz, W. A., Toulmay, A., and Balla, T. (2020). The functional universe of membrane contact sites. *Nat. Rev. Mol. Cell Biol.* 21, 7–24. doi: 10.1038/s41580-019-0180-9

Puri, C., Renna, M., Bento, C. F., Moreau, K., and Rubinsztein, D. C. (2013). Diverse autophagosome membrane sources coalesce in recycling endosomes. *Cell* 154, 1285–1299. doi: 10.1016/j.cell.2013.08.044

Quon, E., Sere, Y. Y., Chauhan, N., Johansen, J., Sullivan, D. P., Dittman, J. S., et al. (2018). Endoplasmic reticulum-plasma membrane contact sites integrate sterol and phospholipid regulation. *PLoS Biol.* 16:e2003864. doi: 10.1371/journal.pbio.2003864

Rai, A., Pathak, D., Thakur, S., Singh, S., Dubey, A. K., and Mallik, R. (2016). Dynein clusters into lipid microdomains on phagosomes to drive rapid transport toward lysosomes. *Cell* 164, 722–734. doi: 10.1016/j.cell.2015.12.054

Rusinol, A. E., Cui, Z., Chen, M. H., and Vance, J. E. (1994). A Unique mitochondria-associated membrane-fraction from rat-liver has a high-capacity for lipid-synthesis and contains pre-golgi secretory proteins including nascent lipoproteins. *J. Biol. Chem.* 269, 27494–27502.

Sala-Vila, A., Navarro-Lerida, I., Sanchez-Alvarez, M., Bosch, M., Calvo, C., Lopez, J. A., et al. (2016). Interplay between hepatic mitochondria-associated membranes, lipid metabolism and caveolin-1 in mice. *Sci. Rep.* 6:27351.

Sano, R., Annunziata, I., Patterson, A., Moshiach, S., Gomero, E., Opferman, J., et al. (2009). GM1-ganglioside accumulation at the mitochondria-associated ER membranes links ER stress to Ca2+-dependent mitochondrial apoptosis. *Mol. Cell* 36, 500–511. doi: 10.1016/j.molcel.2009.10.021

Schueller, C., Mamnun, Y. M., Wolfger, H., Rockwell, N., Thorner, J., and Kuchler, K. (2007). Membrane-active compounds activate the transcription factors Pdr1 and Pdr3 connecting pleiotropic drug resistance and membrane lipid homeostasis in *Saccharomyces cerevisiae*. *Mol. Biol. Cell* 18, 4932–4944. doi: 10.1091/mbc.e07-06-0610

Schuiki, I., Schnabl, M., Czabany, T., Hrastnik, C., and Daum, G. (2010). Phosphatidylethanolamine synthesized by four different pathways is supplied to the plasma membrane of the yeast *Saccharomyces cerevisiae*. *Biochim. Biophys. Acta* 1801, 480–486. doi: 10.1016/j.bbalip.2009.12.008

Schuldiner, M., and Bohnert, M. (2017). A different kind of love - lipid droplet contact sites. *Biochim. Biophys. Acta* 1862, 1188–1196. doi: 10.1016/j.bbalip.2017.06.005

Schutter, M., Giavalisco, P., Brodesser, S., and Graef, M. (2020). Local fatty acid channeling into phospholipid synthesis drives phagophore expansion during autophagy. *Cell* 180, 135–149.e14.

Scorrano, L., De Matteis, M. A., Emr, S., Giordano, F., Hajnoczky, G., Kornmann, B., et al. (2019). Coming together to define membrane contact sites. *Nat. Commun.* 10:1287.

Sebastian, D., Hernandez-Alvarez, M. I., Segales, J., Sorianello, E., Munoz, J. P., Sala, D., et al. (2012). Mitofusin 2 (Mfn2) links mitochondrial and endoplasmic reticulum function with insulin signaling and is essential for normal glucose homeostasis. *Proc. Natl. Acad. Sci. U.S.A.* 109, 5523–5528. doi: 10.1073/pnas.1108220109

Shai, N., Yifrach, E., van Roermund, C. W. T., Cohen, N., Bibi, C., Ijlst, L., et al. (2018). Systematic mapping of contact sites reveals tethers and a function for the peroxisome-mitochondria contact. *Nat. Commun.* 9:1761.

Shiao, Y. J., Lupo, G., and Vance, J. E. (1995). Evidence that phosphatidylserine is imported into mitochondria via a mitochondria-associated membrane and that the majority of mitochondrial phosphatidylethanolamine is derived from decarboxylation of phosphatidylserine. *J. Biol. Chem.* 270, 11190–11198. doi: 10.1074/jbc.270.19.11190

Shima, T., Kirisako, H., and Nakatogawa, H. (2019). COPII vesicles contribute to autophagosomal membranes. *J. Cell Biol.* 218, 1503–1510. doi: 10.1083/jcb.201809032

Shinjo, S., Jiang, S. Y., Nameta, M., Suzuki, T., Kanai, M., Nomura, Y., et al. (2017). Disruption of the mitochondria-associated ER membrane (MAM) plays a central role in palmitic acid induced insulin resistance. *Exp. Cell Res.* 359, 86–93. doi: 10.1016/j.yexcr.2017.08.006

Simmen, T., and Herrera-Cruz, M. S. (2018). Plastic mitochondria-endoplasmic reticulum (ER) contacts use chaperones and tethers to mould their structure and signaling. *Curr. Opin. Cell Biol.* 53, 61–69. doi: 10.1016/j.ceb.2018.04.014

Simons, K., and Ikonen, E. (1997). Functional rafts in cell membranes. *Nature* 387, 569–572. doi: 10.1038/42408

Stefan, C. J., Manford, A. G., Baird, D., Yamada-Hanff, J., Mao, Y. X., and Emr, S. D. (2011). Osh proteins regulate phosphoinositide metabolism at ER-plasma membrane contact sites. *Cell* 144, 389–401. doi: 10.1016/j.cell.2010.12.034

Stone, S. J., and Vance, J. E. (2000). Phosphatidylserine synthase-1 and-2 are localized to mitochondria-associated membranes. *J. Biol. Chem.* 275, 34534–34540. doi: 10.1074/jbc.m002865200

Suresh, H. G., dos Santos, A. X. D., Kukulski, W., Tyedmers, J., Riezman, H., Bukau, B., et al. (2015). Prolonged starvation drives reversible sequestration of lipid biosynthetic enzymes and organelle reorganization in *Saccharomyces cerevisiae*. *Mol. Biol. Cell* 26, 1601–1615. doi: 10.1091/mbc.e14-11-1559

Takeuchi, K., and Reue, K. (2009). Biochemistry, physiology, and genetics of GPAT, AGPAT, and lipin enzymes in triglyceride synthesis. *Am. J. Physiol. Endocrinol. Metab.* 296, E1195–E1209.

Tamura, Y., Kawano, S., and Endo, T. (2019). Organelle contact zones as sites for lipid transfer. *J. Biochem.* 165, 115–123. doi: 10.1093/jb/mvy088

Tavassoli, S., Chao, J. T., Young, B. P., Cox, R. C., Prinz, W. A., de Kroon, A. I. P. M., et al. (2013). Plasma membrane-endoplasmic reticulum contact sites regulate phosphatidylcholine synthesis. *EMBO Rep.* 14, 434–440. doi: 10.1038/embor.2013.36

Theurey, P., Tubbs, E., Vial, G., Jacquemetton, J., Bendridi, N., Chauvin, M. A., et al. (2016). Mitochondria-associated endoplasmic reticulum membranes allow adaptation of mitochondrial metabolism to glucose availability in the liver. *J. Mol. Cell. Biol.* 8, 129–143. doi: 10.1093/jmcb/mjw004

Thoudam, T., Ha, C. M., Leem, J., Chanda, D., Park, J. S., Kim, H. J., et al. (2019). PDK4 Augments ER-mitochondria contact to dampen skeletal muscle insulin signaling during obesity. *Diabetes* 68, 571–586. doi: 10.2337/db18-0363

Tubbs, E., Chanon, S., Robert, M., Bendridi, N., Bidaux, G., Chauvin, M. A., et al. (2018). Disruption of mitochondria-associated endoplasmic reticulum membrane (MAM) Integrity contributes to muscle insulin resistance in mice and humans. *Diabetes* 67, 636–650. doi: 10.2337/db17-0316

Tubbs, E., Theurey, P., Vial, G., Bendridi, N., Bravard, A., Chauvin, M. A., et al. (2014). Mitochondria-associated endoplasmic reticulum membrane (MAM) integrity is required for insulin signaling and is implicated in hepatic insulin resistance. *Diabetes* 63, 3279–3294. doi: 10.2337/db13-1751

Uzbekov, R., and Roingeard, P. (2013). Nuclear lipid droplets identified by electron microscopy of serial sections. *BMC Res. Notes* 6:386. doi: 10.1186/1756-0500-6-386

van Meer, G., Voelker, D. R., and Feigenson, G. W. (2008). Membrane lipids: where they are and how they behave. *Nat. Rev. Mol. Cell Biol.* 9, 112–124. doi: 10.1038/nrm2330

Vance, J. E. (1990). Phospholipid synthesis in a membrane fraction associated with mitochondria. *J. Biol. Chem.* 265, 7248–7256.

Vance, J. E. (1991). Newly made phosphatidylserine and phosphatidylethanolamine are preferentially translocated between rat liver mitochondria and endoplasmic reticulum. *J. Biol. Chem.* 266, 89–97.

Vance, J. E., and Vance, D. E. (1988). Does rat-liver golgi have the capacity to synthesize phospholipids for lipoprotein secretion. *J. Biol. Chem.* 263, 5898–5909.

Vidugiriene, J., Sharma, D. K., Smith, T. K., Baumann, N. A., and Menon, A. K. (1999). Segregation of glycosylphosphatidylinositol biosynthetic reactions in a subcompartment of the endoplasmic reticulum. *J. Biol. Chem.* 274, 15203–15212. doi: 10.1074/jbc.274.21.15203

Voelker, D. R. (1990). Characterization of phosphatidylserine synthesis and translocation in permeabilized animal-cells. *J. Biol. Chem.* 265, 14340–14346.

von Filseck, J. M., Copic, A., Delfosse, V., Vanni, S., Jackson, C. L., Bourguet, W., et al. (2015). Phosphatidylserine transport by ORP/Osh proteins is driven by phosphatidylinositol 4-phosphate. *Science* 349, 432–436. doi: 10.1126/science.aab1346

Wang, C. H., Chen, Y. F., Wu, C. Y., Wu, P. C., Huang, Y. L., Kao, C. H., et al. (2014). Cisd2 modulates the differentiation and functioning of adipocytes by regulating intracellular Ca2+ homeostasis. *Hum. Mol. Genet.* 23, 4770–4785. doi: 10.1093/hmg/ddu193

Wang, S., Lee, D. P., Gong, N., Schwerbrock, N. M., Mashek, D. G., Gonzalez-Baro, M. R., et al. (2007). Cloning and functional characterization of a novel mitochondrial N-ethylmaleimide-sensitive glycerol-3-phosphate acyltransferase (GPAT2). *Arch. Biochem. Biophys.* 465, 347–358. doi: 10.1016/j.abb.2007.06.033

Wang, X. L., Wen, Y. J., Dong, J., Cao, C. C., and Yuan, S. Q. (2018). Systematic in-depth proteomic analysis of mitochondria-associated endoplasmic reticulum membranes in mouse and human testes. *Proteomics* 18:e1700478.

Wang, Y., Yuan, P., Grabon, A., Tripathi, A., Lee, D., Rodriguez, M., et al. (2020). Noncanonical regulation of phosphatidylserine metabolism by a Sec14-like protein and a lipid kinase. *J. Cell Biol.* 219:e201907128.

Wu, S., Lu, Q., Ding, Y., Wu, Y., Qiu, Y., Wang, P., et al. (2019). Hyperglycemia-driven inhibition of AMP-activated protein kinase alpha2 induces diabetic cardiomyopathy by promoting mitochondria-associated endoplasmic reticulum membranes *in vivo*. *Circulation* 139, 1913–1936. doi: 10.1161/circulationaha.118.033552

Xie, B., Nguyen, P. M., Gucek, A., Thonig, A., Barg, S., and Idevall-Hagren, O. (2016). Plasma membrane phosphatidylinositol 4,5-bisphosphate regulates Ca(2+)-Influx and Insulin Secretion from Pancreatic beta Cells. *Cell Chem. Biol.* 23, 816–826. doi: 10.1016/j.chembiol.2016.06.009

Zaman, S., Lippman, S. I., Zhao, X., and Broach, J. R. (2008). How *Saccharomyces* responds to nutrients. *Annu. Rev. Genet.* 42, 27–81. doi: 10.14492/hokmj/1381758488

Zhao, Y. G., and Zhang, H. (2019). Autophagosome maturation: an epic journey from the ER to lysosomes. *J. Cell Biol.* 218, 757–770. doi: 10.1083/jcb.201810099

Conflict of Interest: The authors declare that the research was conducted in the absence of any commercial or financial relationships that could be construed as a potential conflict of interest.

frontiers in Cell and Developmental Biology

MINI REVIEW
published: 11 January 2021
doi: 10.3389/fcell.2020.619022

Tales of the ER-Golgi Frontier: *Drosophila*-Centric Considerations on Tango1 Function

Zhi Feng[1], *Ke Yang*[1] *and José C. Pastor-Pareja*[1,2]*

[1] School of Life Sciences, Tsinghua University, Beijing, China, [2] Tsinghua-Peking Center for Life Sciences, Beijing, China

In the secretory pathway, the transfer of cargo from the ER to the Golgi involves dozens of proteins that localize at specific regions of the ER called ER exit sites (ERES), where cargos are concentrated preceding vesicular transport to the Golgi. Despite many years of research, we are missing crucial details of how this highly dynamic ER-Golgi interface is defined, maintained and functions. Mechanisms allowing secretion of large cargos such as the very abundant collagens are also poorly understood. In this context, Tango1, discovered in the fruit fly *Drosophila* and widely conserved in animal evolution, has received a lot of attention in recent years. Tango1, an ERES-localized transmembrane protein, is the single fly member of the MIA/cTAGE family, consisting in humans of TANGO1 and at least 14 different related proteins. After its discovery in flies, a specific role of human TANGO1 in mediating secretion of collagens was reported. However, multiple studies in *Drosophila* have demonstrated that Tango1 is required for secretion of all cargos. At all ERES, through self-interaction and interactions with other proteins, Tango1 aids ERES maintenance and tethering of post-ER membranes. In this review, we discuss discoveries on *Drosophila* Tango1 and put them in relation with research on human MIA/cTAGE proteins. In doing so, we aim to offer an integrated view of Tango1 function and the nature of ER-Golgi transport from an evolutionary perspective.

Keywords: traffic, secretion, ER exit site, COPII, collagen, extracellular matrix

OPEN ACCESS

Edited by:
Yasunori Saheki, Nanyang Technological University, Singapore

Reviewed by:
Vivek Malhotra, Centre for Genomic Regulation (CRG), Spain
Jaakko Saraste, University of Bergen, Norway

***Correspondence:**
José C. Pastor-Pareja
josepastor@tsinghua.edu.cn

Specialty section:
This article was submitted to Membrane Traffic, a section of the journal Frontiers in Cell and Developmental Biology

Received: *19 October 2020*
Accepted: *14 December 2020*
Published: *11 January 2021*

Citation:
Feng Z, Yang K and Pastor-Pareja JC (2021) Tales of the ER-Golgi Frontier: Drosophila-Centric Considerations on Tango1 Function. Front. Cell Dev. Biol. 8:619022. doi: 10.3389/fcell.2020.619022

INTRODUCTION

The endoplasmic reticulum (ER) is the largest and most versatile organelle in eukaryotic cells, capable of generating, contacting and establishing coordinated relations with all other organelles and subcellular compartments. Among such relations, the one between the ER and the Golgi apparatus was the earliest to be recognized (Palade, 1975). ER-Golgi exchanges concentrate at ER exit sites (ERES): specialized ER regions where secretory cargos are collected prior to their trafficking to the Golgi (Bannykh et al., 1996). While dozens of proteins are required for exit of secretory cargo from the ER and entry into the Golgi, few are known to be involved in post-Golgi traffic (Lee et al., 2004; Barlowe and Miller, 2013), a clear indication that ER-to-Golgi cargo transfer at the ER-Golgi interface is the most critical step in secretion. In these same narrow ERES regions, in addition, traffic in the reverse Golgi-to-ER direction takes place as well (Roy Chowdhury et al., 2020). Despite their highly dynamic underlying nature, ERES are overall stable entities, raising the question of how they persist through time. Due to the high concentration of traffic regulators and proteins of the vesicle budding and fusion machineries, it has been postulated that

ERES may behave as membrane-less liquid droplets (Hanna et al., 2018). Against this background, Tango1 (Transport and Golgi Organization 1), an ERES-localized protein discovered in the fruit fly *Drosophila*, has captured a great deal of interest for its role in ERES-Golgi coordination.

Tango1 is a transmembrane protein of the MIA/cTAGE (Melanoma Inhibitory Activity/Cutaneous T-cell lymphoma-associated antiGEn) family (**Figure 1**; Usener et al., 2003; Malhotra and Erlmann, 2011). Members of this family were found to be upregulated in melanoma samples before a role in secretion had been described (Bosserhoff et al., 1997; Stoll et al., 2001). The ER-lumenal portions of Tango1 and human TANGO1, encoded by *MIA3*, contain an SH3 domain, typically mediating protein-protein interactions in the cytoplasm, but exceptional in an ER-resident or secreted protein (Stoll and Bosserhoff, 2008). Their cytoplasmic portions, in turn, display conserved regions with no recognizable domains, but presumed to organize as coiled coils, and a C-terminal region that is poorly conserved but proline-rich, with multiple occurrences of consecutive prolines (Saito et al., 2009). Apart from *MIA3*, the human genome possesses 10 additional genes encoding MIA/cTAGE proteins. Among these, TANGO1 and TANGO1-like (TALI), encoded by *MIA2*, most resemble *Drosophila* Tango1. The rest contain exclusively the SH3 domain and ER-lumenal portion, or the cytoplasmic portion, presumably membrane-anchored in most cases.

Yeast has provided for many years a genetically amenable system for studying secretion. Genetic screenings in *Saccharomyces cerevisiae* have identified many secretory genes (Schekman, 2010; Barlowe and Miller, 2013). *Drosophila*, however, is increasingly becoming an excellent alternative to investigate secretion in a higher eukaryote. Most proteins known to play roles in secretion have fly homologues, including COPI and COPII components, Rab GTPases, SNAREs, TRAPP complex, p24 and Golgins (Kondylis and Rabouille, 2009; Muschalik and Munro, 2018). Another advantage of *Drosophila* is the availability of sophisticated genetic tools allowing tagging of endogenous proteins, forward genetic screening and complex loss- and gain-of function experiments that can evaluate physiological readouts and functional significance in real tissue and whole-animal contexts. An apparent difference in secretory pathway organization between *Drosophila* and humans is that in vertebrates ERES-derived vesicles fuse to form an ER-Golgi intermediate compartment (ERGIC) where cargo transits to a single juxtanuclear Golgi ribbon. In flies, like in non-vertebrate animals and plants (Glick and Nakano, 2009; Brandizzi and Barlowe, 2013), Golgi elements remain dispersed throughout the cytoplasm in close proximity to ERES, forming ERES-Golgi units (Ripoche et al., 1994; Kondylis et al., 2011). In the reduced space between *Drosophila* ERES and cis-Golgi, nonetheless, electron microscopy studies have shown the existence of pleiomorphic elements (Kondylis et al., 2005), revealing high complexity of this interface and a possible relation with the vertebrate ERGIC. *Drosophila*, finally, provides a very distinct benefit when compared to mammals in the form of limited gene redundancy. For instance, and in contrast with the enormous complexity of the human family, only one MIA/cTAGE protein exists in *Drosophila*, making flies an ideal system to address its function.

DISCOVERY OF TANGO1 IN *DROSOPHILA*

A secretory function for *Drosophila* Tango1 (**Figure 2A**) was first uncovered in a genome-wide RNAi screening for genes required for secretion in *Drosophila* S2 cells (Bard et al., 2006), derived from embryonic macrophages. This screening selected genes for which depletion prevented secretion of ss-HRP (horseradish peroxidase with a signal sequence). A Tango1-V5 fusion, in addition, localized close to mid-Golgi marker ManII-GFP when expressed in S2 cells (Bard et al., 2006), consistent with ERES localization (**Figure 2B**). Gene hits in this screening that had not been characterized previously in *Drosophila* were named *Tango1* to *Tango14*, for *Transport and Golgi organization*, representing a hypothetical class of animal-specific secretory genes that screenings in yeast could not have uncovered. Most of them retain to this date this *Tango* denomination in their official names, although the only one for which a direct involvement in secretion has been established is *Tango1*. In a second S2 cell RNAi screening, *Tango1* was confirmed to be required for secretion, in this case of a secreted luciferase reporter, and ERES location of its product was observed again (Wendler et al., 2010). RNAi libraries used in the two screenings contained approximately 22,000 double stranded RNAs each and covered close to 100% of *Drosophila* protein-coding genes. Excluding hits nowadays mapping to non-coding or to multiple protein-coding genes, hit lists in the two screenings contained 240 (Bard et al., 2006) and 292 genes (Wendler et al., 2010). Of note, overlap of these two sets of genes, obtained using the same cell line and similar screening systems, was only 24 genes (Ke et al., 2018), which makes it the more remarkable that *Tango1* was selected in both.

A COLLAGEN SPECIFIC RECEPTOR?

After its discovery in flies, human TANGO1 was implicated in the transport of collagens from ERES to Golgi (Saito et al., 2009). At ERES, Golgi-bound, cargo-carrying vesicles are generated by the COPII complex, a set of proteins highly conserved in eukaryotes (Jensen and Schekman, 2011). Structural studies have shown that budding of COPII vesicles is mediated by the assembly of a vesicle-enclosing cage of 60–80 nm in diameter. In animals, many secreted proteins exceed these dimensions and, yet, they are efficiently secreted, raising questions on how this happens and whether specific mechanisms evolved in animals for secretion of large cargos (Fromme and Schekman, 2005). Examples of large secreted proteins include collagens, the main components of animal extracellular matrices, for which trimers assemble in the ER into 300–400 nm long semi-inflexible rods (Canty and Kadler, 2005), but also much larger proteins and protein complexes, such as lipoprotein particles and giant cuticular proteins of insects. Collagen-specific factors creating enlarged

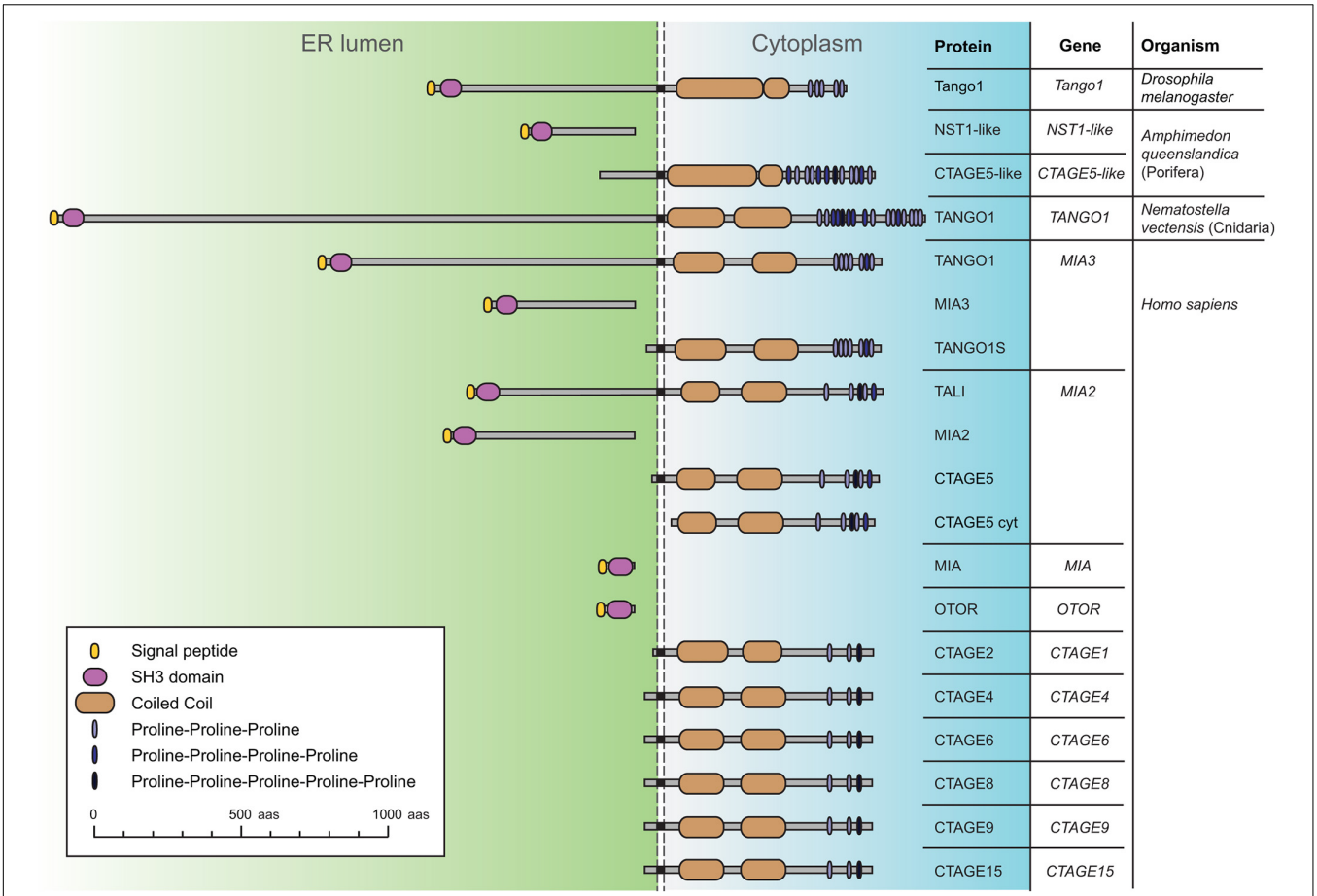

FIGURE 1 | Schematic representation of *Drosophila* Tango1 and proteins of the MIA/cTAGE family, found exclusively in animals. A single representative is found in flies, consisting of an ER-lumenal part, displaying a highly conserved SH3 domain, and a cytoplasmic part, containing coiled coils and a C-terminal proline-rich region. In the sponge *Amphimedon queenslandica*, a representative of the phylum Porifera, the most basal metazoans, ER lumenal and cytoplasmic parts are found as separate proteins. In the sea anemone *Nematostella vectensis*, a cnidarian, a complete TANGO1 protein is found. Human MIA/cTAGE family members include TANGO1 and TANGO1-like (TALI) as complete proteins, but also ER-lumenal and transmembrane cytoplasmic forms, and also at least one predicted completely cytoplasmic CTAGE5 isoform (CTAGE5 cyt). Sequences represented and corresponding RefSeq accession numbers are: Dmel Tango1 (NP_609058.2), Aque NST1-like (XP_019849291.1), Aque CTAGE5-like (XP_019849290.1), Nvec TANGO1 (XP_032221684.1), Hsap TANGO1 (NP_940953.2), Hsap_MIA3 (XP_937620.1), Hsap_TANGO1S (NP_001287796.1), Hsap TALI (NP_001316143.1), Hsap MIA2 (NP_473365.3), Hsap CTAGE5 (NP_976231.1), Hsap CTAGE5cyt (XP_011535087.1), Hsap MIA (NP_001189482.1), Hsap OTOR (NP_064542.1), Hsap CTAGE2 (NP_758441.2), Hsap CTAGE4 (NP_940897.2), Hsap CTAGE6 (NP_848656.2), Hsap CTAGE8 (NP_001265436.1), Hsap CTAGE9 (NP_001139131.1), and Hsap CTAGE15 (NP_001008747.1).

transporting vesicles have been postulated, TANGO1 among them (Malhotra and Erlmann, 2015).

TANGO1 silencing in human cells was reported to affect secretion of Collagen VII, but not of other types of collagen or other secreted proteins (Saito et al., 2009; Tanabe et al., 2016). The proline-rich region at the C-terminus of TANGO1 was shown to interact with the COPII coat, while its SH3 domain was described to bind specifically Collagen VII in the ER lumen (Saito et al., 2009). Soon after, however, *MIA3* knock-out mice were revealed to exhibit defects in secretion of multiple collagens (Wilson et al., 2011), while *Drosophila* Tango1 was required for secretion of basement membrane Collagen IV (Pastor-Pareja and Xu, 2011). Activities of TANGO1 in both retarding COPII coat assembly and recruiting ERGIC membranes to nascent vesicles have been proposed as mechanisms by which TANGO1 could mediate formation of enlarged vesicles capable of transporting collagens (Malhotra and Erlmann, 2015; Santos et al., 2015). In this way, TANGO1 would collect collagen at ERES as a specific receptor while at the same time ensuring that a large enough vesicle grows to package it. Additional studies described specific requirements of MIA/cTAGE proteins CTAGE5 and TANGO1S in collagen secretion, and of TALI for secretion of ApoB-containing lipoparticles (Saito et al., 2011, 2014; Maeda et al., 2016; Santos et al., 2016; Tanabe et al., 2016). Other factors reported to affect secretion of collagen specifically were TRAPP complex component Sedlin (Venditti et al., 2012), ubiquitination of Sec31 by ubiquitin ligase KLHL12 (Jin et al., 2012), Syntaxin 18 and SNARE regulator Sly1 (Nogueira et al., 2014). Together with TANGO1 and other MIA/cTAGE proteins, they would

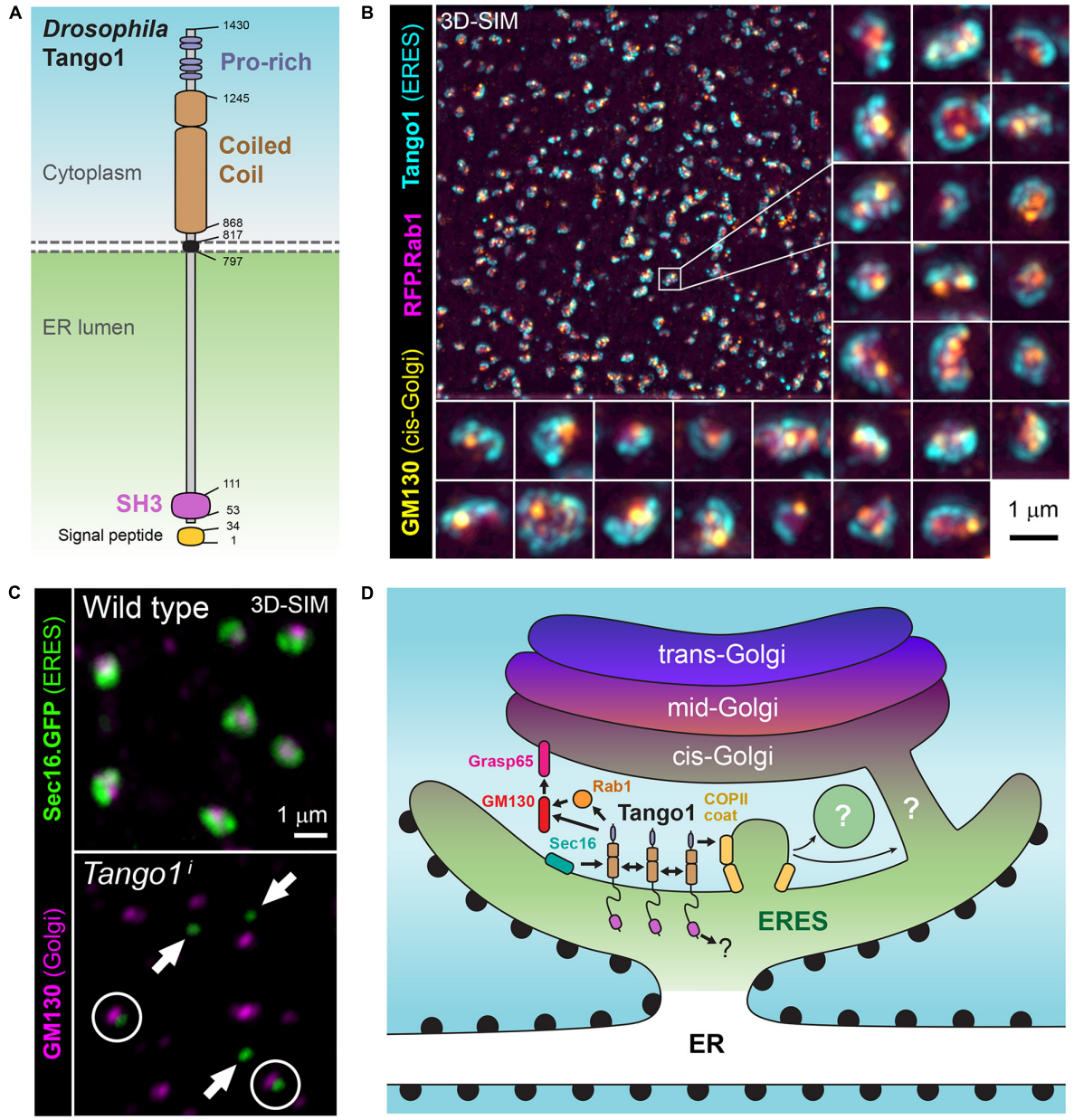

FIGURE 2 | (A) Schematic representation of *Drosophila* Tango1. **(B)** Superresolution micrograph (3D-SIM) showing the localization of Tango1 (antibody staining) at ER exit sites (ERES) in a *Drosophila* fat body cell. RFP.Rab1 and cis-Golgi marker GM130 are shown as well. **(C)** Tango1 preserves ERES size and connection ERES-Golgi. *Tango1* knock-down (*Tango1*^{i}) causes decrease in the size of ERES, marked with Sec16.GFP, and their uncoupling from Golgi (cis-Golgi marker GM130). **(D)** Role of *Drosophila* Tango1 in defining ERES, tethering Golgi membranes and stabilizing the ER-Golgi interface at ERES-Golgi units. Interactions with itself, Grasp65, GM130, Rab1 and Sar1 have been documented (Liu et al., 2017). Additionally, human TANGO1 and other MIA/cTAGE proteins have been collectively found to interact with multiple ERES proteins and ER-Golgi traffic regulators.

be at the core of a collagen-specific, or large protein-specific, secretion pathway.

NOT A COLLAGEN SPECIFIC RECEPTOR

Besides its advantages for secretion studies, *Drosophila* is a convenient model to investigate the biology of collagen and the extracellular matrix (Pastor-Pareja, 2020). Compared to the 28 types found in mammals, *Drosophila* possesses a reduced complement of collagens, consisting of basement membrane Collagen IV and Collagen XV/XVIII Multiplexin (Hynes and Zhao, 2000). Multiplexin expression, restricted to heart and nervous system, is dispensable for viability (Meyer and Moussian, 2009). Collagen IV, in contrast, is essential and abundantly present in most tissues. In flies, like in all animals, Collagen IV

is the main component of basement membranes: polymers of extracellular matrix proteins that underlie epithelia and provide structural tissue support (Yurchenco, 2011). *Drosophila* Collagen IV is a 450 nm-long heterotrimer composed of α1 chain Collagen at 25C (Cg25C) and α2 chain Viking (Vkg) (Natzle et al., 1982; Lunstrum et al., 1988; Fessler and Fessler, 1989). In the larva, the main source of Collagen IV is fat body adipocytes (Pastor-Pareja and Xu, 2011), known for their role in lipid storage, but also as a very active secretory tissue that produces the serum proteins and clotting factors present in the hemolymph (insect blood). Besides Collagen IV, the other main basement membranes components are Laminin, Nidogen and Perlecan, all conserved from flies to humans as well.

Drosophila Tango1 has been repeatedly shown to be required for Collagen IV secretion (Pastor-Pareja and Xu, 2011; Lerner et al., 2013; Isabella and Horne-Badovinac, 2015; Zang et al., 2015; Ke et al., 2018; Sun et al., 2019). However, it was also found that Tango1 loss causes retention of other matrix proteins, such as Perlecan in ovarian follicle cells (Lerner et al., 2013), Papilin in the proventriculus (Zhang et al., 2014), BM-40-SPARC in blood cells (Tiwari et al., 2015) and Laminin in glia (Petley-Ragan et al., 2016). Our laboratory, therefore, decided to carry out a comprehensive analysis of the requirement of Tango1 in secretion (Liu et al., 2017). In this study, Tango1 loss in fat body led to ER retention of not just Collagen IV, but all monitored cargos, including general secretion markers VSVG and secreted GFP (GFP with a signal sequence). Furthermore, Tango1 is expressed in all cell types of the larva and localizes to all ERES, inconsistent with a collagen-specific or large-protein specific role (Liu et al., 2017). Highest expression of Tango1 was found in the salivary gland, a dedicated secretory organ where Tango1 is required for glue secretion (Liu et al., 2017) and secretory genes are highly expressed as a group (Abrams and Andrew, 2005). In all assayed tissues, Tango1 maintains the size and integrity of ERES-Golgi units, as ERES decrease in size and uncouple from Golgi upon Tango1 loss (**Figure 2C**), whereas Tango1 overexpression, conversely, created more and larger ERES (Liu et al., 2017). Furthermore, supporting an organizing function of Tango1 at the ERES-Golgi interface, the cytoplasmic part of Tango1 could rescue Tango1 loss in the fat body (Liu et al., 2017). Consistent with a general secretion role, Tango1 is needed for secretion of both large and small cargos in terminal cells of the tracheal system (Rios-Barrera et al., 2017), and for secretion of mucins by the male accessory gland and female spermatheca (Reynolds et al., 2019). In all, multiple phenotypic studies demonstrate that Tango1 is not specifically needed for transport of collagens, matrix or large proteins. It is, in contrast, required for general secretion at all ERES, where it maintains ERES size and proximity to Golgi.

The lack of a collagen-specific secretion pathway is further hinted by the results of an RNAi screening in *Drosophila* larval fat body (Ke et al., 2018). This screening, targeting 6,200 genes (about 60% of the protein-coding genome), found 88 genes for which silencing caused intracellular Collagen IV accumulation. Secondary screenings with additional secretory markers revealed that enzymes Prolyl-4-hydroxylase PH4αEFB and Lysyl-oxidase Plod, known to modify collagen post-translationally (Bunt et al., 2011; Pastor-Pareja and Xu, 2011), were the only hits affecting Collagen IV secretion specifically. All other hits affected general secretion, suggesting that collagen secretion does not use devoted mechanisms of vesicular transport. Of the 88 hits in this screening, only 15 were found in the previous S2 cell screenings, with just 7 hits at the intersection of all three: *garz*, *Rab1*, *Use1*, *Slh*, *Syx18*, *Sec23,* and *Sec20* (Bard et al., 2006; Wendler et al., 2010; Ke et al., 2018). The little overlap between the two S2 cell screenings makes it difficult to draw conclusions. Nonetheless, a significant portion of hits in the fat body screening (32 out of 88) encode proteins known to be involved in traffic, including COPII and COPI proteins, SNAREs, TRAPP components, Grasp65, Rab1 and Rab-GTPase regulators (Ke et al., 2018). Remarkably, this screening was able to select known secretion components that neither of the two S2 cell screenings caught, such as Nsf2, Trs23, Trs33, Rep, Grasp65, and Loj (p24), as well as Zn transporter Catsup and SERCA, for which other studies have demonstrated secretory functions (Groth et al., 2013; Suisse and Treisman, 2019). By assaying secretion of an abundant endogenous protein in live animals, this screening may have led to the identification of novel secretory pathway components awaiting characterization. As for collagen secretion, the outcome of the screening points to the absence of a collagen-specific pathway. The requirement of *Drosophila* Tango1 in all secretory contexts, in turn, strongly suggests that human MIA/cTAGE5 proteins act redundantly to maintain ERES and facilitate general secretion. Nonetheless, the possibility remains that the general function of Tango1 in organizing ERES is separate from a specific function in mediating secretion of collagen or other cargos (Rios-Barrera et al., 2017). Indeed, *Drosophila* Tango1 loss seems to affect differentially secretion of Collagen IV when comparing its effects with those of Sec23 and Sar1 knock down on secretion of Collagen IV and secreted GFP (Liu et al., 2017). Whether these differential effects stem from true cargo binding specificity or from size-dependent quantitative differences in transport mode (vesicular vs. tubular carriers?) is currently one of the most pressing questions in the field.

MECHANISMS OF TANGO1 FUNCTION

The function of Tango1 as a stabilizer of the ER-Golgi interface is thought to involve interactions with multiple other proteins (**Figure 2D**). Through its cytoplasmic part, *Drosophila* Tango1 has been shown to self-interact (Liu et al., 2017). This interaction maps to one of the coiled coil motifs (Reynolds et al., 2019). Importantly, a fully cytoplasmic version of Tango1 correctly localizes to ERES, showing that this portion of the protein is sufficient for localization (Liu et al., 2017). The cytoplasmic portions of human CTAGE5 and TANGO1 had been shown to interact before (Saito et al., 2011), and it is known as well that, similar to *Drosophila* Tango1, human TANGO1 can self-interact (Raote et al., 2018, 2020). Besides self-interaction and interaction with other MIA/cTAGE family members, TANGO1 and related proteins have been shown to bind multiple other proteins present at ERES, such as COPII coat protein SEC23 (Saito et al., 2009; Ma and Goldberg, 2016), SNARE

regulator SLY (Nogueira et al., 2014), and ERES determinants SEC16 (Maeda et al., 2017) and SEC12 (Saito et al., 2014). Additionally, *Drosophila* Tango1 co-immunoprecipitates with Rab-GTPase Rab1 and cis-Golgi proteins Grasp65 and GM130 (Liu et al., 2017). Tango1, therefore, through its self-interaction and interaction with other proteins may act as a ER-Golgi interface stabilizer, contributing to concentrating and maintaining localization of all these proteins in a specific region of the ER and to tether post-ER membranes to ERES: Golgi directly in the case of *Drosophila* and ERGIC in vertebrates.

The role of the ER-lumenal part of Tango1, displaying a highly conserved SH3 domain, is still elusive. It has been shown that glycosylation of *Drosophila* Tango1 in the ER lumen prevents cleavage by Furin of this part of the protein (Zhang et al., 2014), suggestive of a proteolytic mechanism in the regulation of Tango1 function for which further details remain to be ascertained. Because Furin localizes to the trans-Golgi network and the endosomal compartments (Thomas, 2002), such cleavage is likely to occur there rather than at ERES, where most Tango1 is found due in part to recycling of the protein from the Golgi (Yuan et al., 2018). A role for the SH3 domain in binding cargos has been proposed. The SH3 domain in human TANGO1 was first reported to bind specifically Collagen VII, but not other collagens (Saito et al., 2009). Later, it was postulated that the SH3 domain could bind HSP47, a collagen chaperone, instead of collagens doing it directly (Ishikawa et al., 2016). Binding of TANGO1 to HSP47, containing an RDEL retrieval signal, would additionally ensure Golgi-to-ER recycling of TANGO1 via KDELR-mediated retrograde transport (Yuan et al., 2018). HSP47, also known as SERPINH1, is a Serpin rather than a typical chaperone. Serpin family members, of which 29 exist in *Drosophila* (Garrett et al., 2009), are highly specific protease inhibitors, some of them secreted proteins themselves, with diverse roles in the immune response. It has been claimed that Spn28F, lacking any RDEL or other putative ER retention motif, is the *Drosophila* homolog of HSP47/SERPINH1 (Sepulveda et al., 2018). However a phylogenetic analysis found no HSP47 orthologs outside of vertebrates (Kumar et al., 2017). A recent study, in addition, found HSP47 was absent from collagen carriers in human cells (Omari et al., 2020). Therefore, the relation between HSP47 and TANGO1, and, more generally, the role of the SH3 domain of Tango1, are still unclear.

WHAT WE STILL DO NOT KNOW ABOUT TANGO1 AND COLLAGEN SECRETION

Overwhelming evidence in *Drosophila* shows that Tango1 is required for general secretion. However, the question of whether collagen secretion requires any specific factors or uses a mode of ER-Golgi transport essentially different from the one other secreted proteins employ remains open. Besides TANGO1 and MIA/cTAGE proteins, loss of other factors of the general secretion machinery of eukaryotes have been linked to specific defects in collagen secretion in mammals (Boyadjiev et al., 2006; Jin et al., 2012; Venditti et al., 2012; Nogueira et al., 2014). An ER transmembrane protein, TMEM131, has been recently implicated in collagen secretion in *C. elegans*, *Drosophila* and human cells (Zhang et al., 2020), but a requirement for this protein in general secretion or ER homeostasis remains to be tested. It is possible that secretion of collagen and large cargo requires no specific factors, but imposes higher demands on the common secretory machinery. Because collagens are not just very large, but also very abundant (30% of the protein mass of the human body) mild general secretion defects may first become manifest in the form of intracellular collagen retention.

If not a collagen or large cargo receptor, what is the main role of Tango1? Tango1 could have evolved in animals to add stability to ERES, but it is unlikely to be the main upstream factor in an ERES determination cascade. A master role in ERES determination would correspond to Sec16 and Sec12, proteins that, unlike Tango1, are widely conserved from yeast to humans (Glick, 2014; Sprangers and Rabouille, 2015). Recently, it has been shown that phosphorylation of human TANGO1 at its C-terminus regulates ERES disassembly during mitosis (Maeda et al., 2020). However, the putative phosphorylation sites, conserved in vertebrates, do not seem conserved in *Drosophila*. TANGO1 and CTAGE5 have been shown to interact with both SEC16 and SEC12, and thus may cooperate with them in defining ERES through their multiple cytoplasmic interactions (Saito et al., 2014; Maeda et al., 2017). It remains to be seen if any of these interactions is a key high-affinity evolved interaction or rather Tango1 is a generally "sticky" protein ensuring tethering of post-ER membranes and concentration of many different factors at ERES. Interestingly, *C. elegans* has no Tango1 homolog (Erives, 2015), but contains TFG (Witte et al., 2011), absent in flies, which has been proposed to form oligomers that physically join ERES and ERGIC (Johnson et al., 2015; McCaughey et al., 2016). In this evolutionary context, therefore, alternative mechanisms may exist in animal cells to increase stability of ERES and capacity of ER-to-Golgi transport in terms of both cargo size and amount of cargo to be secreted. Unlike TFG, however, Tango1 is a transmembrane protein, and understanding the role of its ER-lumenal SH3 domain, its most conserved part, should be key for fully understanding its function.

Regardless of the specific role of Tango1 in maintaining ERES, the topology of the ER-Golgi interface and the nature of carrier membranes allowing efficient secretion of collagens and other large proteins are hotly debated (Mironov and Beznoussenko, 2019). Transport must involve COPII coated membranes, but these, logically, cannot be regular-sized COPII vesicles. Conflicting studies describe existence or absence of large vesicular carriers transporting collagen (Santos et al., 2015; Gorur et al., 2017; Raote et al., 2017; Yuan et al., 2018; McCaughey et al., 2019; Melville et al., 2019; Matsui et al., 2020; Omari et al., 2020). To be able to visualize collagen transport from ERES in cells, these studies prevent collagen trimerization through ascorbate depletion, followed by ascorbate readministration, which triggers resumption of transport. All these reports, consequently, should be taken with caution, as collagen monomers can still be secreted by cells (Pastor-Pareja and Xu, 2011). What is more, ER-phagy results in such situation (Omari et al., 2018), further complicating interpretation of structures formed under these conditions. The logical alternative to large vesicular carriers as mediators of

collagen transport is direct ER-Golgi connection, suggested to occur in yeast (Kurokawa et al., 2014) and plants (daSilva et al., 2004), where ERES and Golgi are closely juxtaposed like in *Drosophila* and, probably, attached physically (Sparkes et al., 2009). ERES-ERGIC contact has been proposed as a transport mechanism in mammals as well (Malhotra and Erlmann, 2015; Raote and Malhotra, 2019). Given the narrow space in which *Drosophila* ERES-Golgi transport takes place, COPII-coated buds may frequently start fusion with cis-Golgi before separating from ERES, thus creating intermittent tubular connections through which all large cargos and most other cargos could reach the Golgi in flies and the ERGIC in vertebrates. Confirmation of this may require electron microscopy analysis of the ER-Golgi frontier, as light microscopy has not been able so far to provide sufficient resolution to settle arguments.

AUTHOR CONTRIBUTIONS

All authors wrote the manuscript.

FUNDING

Work on secretion in our laboratory was supported by grants 91854207 and 31771600 from the Natural Science Foundation of China.

REFERENCES

Abrams, E. W., and Andrew, D. J. (2005). CrebA regulates secretory activity in the Drosophila salivary gland and epidermis. *Development* 132, 2743–2758. doi: 10.1242/dev.01863

Bannykh, S. I., Rowe, T., and Balch, W. E. (1996). The organization of endoplasmic reticulum export complexes. *J. Cell Biol.* 135, 19–35. doi: 10.1083/jcb.135.1.19

Bard, F., Casano, L., Mallabiabarrena, A., Wallace, E., Saito, K., Kitayama, H., et al. (2006). Functional genomics reveals genes involved in protein secretion and golgi organization. *Nature* 439, 604–607. doi: 10.1038/nature04377

Barlowe, C. K., and Miller, E. A. (2013). Secretory protein biogenesis and traffic in the early secretory pathway. *Genetics* 193, 383–410. doi: 10.1534/genetics.112.142810

Bosserhoff, A. K., Kondo, S., Moser, M., Dietz, U. H., Copeland, N. G., Gilbert, D. J., et al. (1997). Mouse CD-RAP/MIA gene: structure, chromosomal localization, and expression in cartilage and chondrosarcoma. *Dev. Dyn.* 208, 516–525. doi: 10.1002/(SICI)1097-0177(199704)208:4<516::AID-AJA7>3.0.CO;2-L

Boyadjiev, S. A., Fromme, J. C., Ben, J., Chong, S. S., Nauta, C., Hur, D. J., et al. (2006). Cranio-lenticulo-sutural dysplasia is caused by a SEC23A mutation leading to abnormal endoplasmic-reticulum-to-Golgi trafficking. *Nat. Genet.* 38, 1192–1197. doi: 10.1038/ng1876

Brandizzi, F., and Barlowe, C. (2013). Organization of the ER-Golgi interface for membrane traffic control. *Nat. Rev. Mol. Cell Biol.* 14, 382–392. doi: 10.1038/nrm3588

Bunt, S., Denholm, B., and Skaer, H. (2011). Characterisation of the drosophila procollagen lysyl hydroxylase, dPlod. *Gene. Expr. Patterns* 11, 72–78. doi: 10.1016/j.gep.2010.09.006

Canty, E. G., and Kadler, K. E. (2005). Procollagen trafficking, processing and fibrillogenesis. *J. Cell Sci.* 118(Pt 7), 1341–1353. doi: 10.1242/jcs.01731

daSilva, L. L., Snapp, E. L., Denecke, J., Lippincott-Schwartz, J., Hawes, C., and Brandizzi, F. (2004). Endoplasmic reticulum export sites and Golgi bodies behave as single mobile secretory units in plant cells. *Plant Cell.* 16, 1753–1771. doi: 10.1105/tpc.022673

Erives, A. J. (2015). Genes conserved in bilaterians but jointly lost with Myc during nematode evolution are enriched in cell proliferation and cell migration functions. *Dev. Genes Evol.* 225, 259–273. doi: 10.1007/s00427-015-0508-1

Fessler, J. H., and Fessler, L. I. (1989). Drosophila extracellular matrix. *Annu. Rev. Cell Biol.* 5, 309–339. doi: 10.1146/annurev.cb.05.110189.001521

Fromme, J. C., and Schekman, R. (2005). COPII-coated vesicles: flexible enough for large cargo? *Curr. Opin. Cell Biol.* 17, 345–352. doi: 10.1016/j.ceb.2005.06.004

Garrett, M., Fullaondo, A., Troxler, L., Micklem, G., and Gubb, D. (2009). Identification and analysis of serpin-family genes by homology and synteny across the 12 sequenced Drosophilid genomes. *BMC Genomics* 10:489. doi: 10.1186/1471-2164-10-489

Glick, B. S. (2014). Integrated self-organization of transitional ER and early Golgi compartments. *BioEssays* 36, 129–133. doi: 10.1002/bies.201300131

Glick, B. S., and Nakano, A. (2009). Membrane traffic within the Golgi apparatus. *Annu. Rev. Cell Dev. Biol.* 25, 113–132. doi: 10.1146/annurev.cellbio.24.110707.175421

Gorur, A., Yuan, L., Kenny, S. J., Baba, S., Xu, K., and Schekman, R. (2017). COPII-coated membranes function as transport carriers of intracellular procollagen I. *J. Cell Biol.* 216, 1745–1759. doi: 10.1083/jcb.201702135

Groth, C., Sasamura, T., Khanna, M. R., Whitley, M., and Fortini, M. E. (2013). Protein trafficking abnormalities in Drosophila tissues with impaired activity of the ZIP7 zinc transporter Catsup. *Development* 140, 3018–3027. doi: 10.1242/dev.088336

Hanna, M. G., Peotter, J. L., Frankel, E. B., and Audhya, A. (2018). Membrane transport at an organelle interface in the early secretory pathway: take your coat off and stay a while: evolution of the metazoan early secretory pathway. *Bioessays* 40:e1800004. doi: 10.1002/bies.201800004

Hynes, R. O., and Zhao, Q. (2000). The evolution of cell adhesion. *J. Cell Biol.* 150, F89–F96. doi: 10.1083/jcb.150.2.f89

Isabella, A. J., and Horne-Badovinac, S. (2015). Dynamic regulation of basement membrane protein levels promotes egg chamber elongation in Drosophila. *Dev. Biol.* 406, 212–221. doi: 10.1016/j.ydbio.2015.08.018

Ishikawa, Y., Ito, S., Nagata, K., Sakai, L. Y., and Bachinger, H. P. (2016). Intracellular mechanisms of molecular recognition and sorting for transport of large extracellular matrix molecules. *Proc. Natl. Acad. Sci. U S A.* 113, E6036–E6044. doi: 10.1073/pnas.1609571113

Jensen, D., and Schekman, R. (2011). COPII-mediated vesicle formation at a glance. *J. Cell Sci.* 124(Pt 1), 1–4. doi: 10.1242/jcs.069773

Jin, L., Pahuja, K. B., Wickliffe, K. E., Gorur, A., Baumgartel, C., Schekman, R., et al. (2012). Ubiquitin-dependent regulation of COPII coat size and function. *Nature* 482, 495–500. doi: 10.1038/nature10822

Johnson, A., Bhattacharya, N., Hanna, M., Pennington, J. G., Schuh, A. L., Wang, L., et al. (2015). TFG clusters COPII-coated transport carriers and promotes early secretory pathway organization. *EMBO J.* 34, 811–827. doi: 10.15252/embj.201489032

Ke, H., Feng, Z., Liu, M., Sun, T., Dai, J., Ma, M., et al. (2018). Collagen secretion screening in Drosophila supports a common secretory machinery and multiple Rab requirements. *J. Genet. Genomics* 45, 299–313. doi: 10.1016/j.jgg.2018.05.002

Kondylis, V., and Rabouille, C. (2009). The Golgi apparatus: lessons from drosophila. *FEBS Lett.* 583, 3827–3838. doi: 10.1016/j.febslet.2009.09.048

Kondylis, V., Spoorendonk, K. M., and Rabouille, C. (2005). dGRASP localization and function in the early exocytic pathway in Drosophila S2 cells. *Mol. Biol. Cell* 16, 4061–4072. doi: 10.1091/mbc.e04-10-0938

Kondylis, V., Tang, Y., Fuchs, F., Boutros, M., and Rabouille, C. (2011). Identification of ER Proteins Involved in the functional organisation of the early secretory pathway in drosophila cells by a targeted RNAi screen. *PLoS One* 6:e17173. doi: 10.1371/journal.pone.0017173

Kumar, A., Bhandari, A., Sarde, S. J., and Goswami, C. (2017). Ancestry & molecular evolutionary analyses of heat shock protein 47?kDa (HSP47/SERPINH1). *Sci. Rep.* 7:10394. doi: 10.1038/s41598-017-10740-0

Kurokawa, K., Okamoto, M., and Nakano, A. (2014). Contact of cis-Golgi with ER exit sites executes cargo capture and delivery from the ER. *Nat. Commun.* 5:3653. doi: 10.1038/ncomms4653

Lee, M. C. S., Miller, E. A., Goldberg, J., Orci, L., and Schekman, R. (2004). BI-directional protein transport between the er and golgi. *Ann. Rev. Cell Dev. Biol.* 20, 87–123. doi: 10.1146/annurev.cellbio.20.010403.105307

Lerner, D. W., McCoy, D., Isabella, A. J., Mahowald, A. P., Gerlach, G. F., Chaudhry, T. A., et al. (2013). A Rab10-dependent mechanism for polarized basement membrane secretion during organ morphogenesis. *Dev. Cell* 24, 159–168. doi: 10.1016/j.devcel.2012.12.005

Liu, M., Feng, Z., Ke, H., Liu, Y., Sun, T., Dai, J., et al. (2017). Tango1 spatially organizes ER exit sites to control ER export. *J. Cell Biol.* 216, 1035–1049. doi: 10.1083/jcb.201611088

Lunstrum, G. P., Bächinger, H. P., Fessler, L. I., Duncan, K. G., Nelson, R. E., and Fessler, J. H. (1988). Drosophila basement membrane procollagen IV. I. Protein characterization and distribution. *J. Biol. Chem.* 263, 18318–18327.

Ma, W., and Goldberg, J. (2016). TANGO1/cTAGE5 receptor as a polyvalent template for assembly of large COPII coats. *Proc. Natl. Acad. Sci. U S A.* 113, 10061–10066. doi: 10.1073/pnas.1605916113

Maeda, M., Katada, T., and Saito, K. (2017). TANGO1 recruits Sec16 to coordinately organize ER exit sites for efficient secretion. *J. Cell Biol.* 216, 1731–1743. doi: 10.1083/jcb.201703084

Maeda, M., Komatsu, Y., and Saito, K. (2020). Mitotic ER exit site disassembly and reassembly are regulated by the phosphorylation status of TANGO1. *Dev. Cell.* 55, 237–250. doi: 10.1016/j.devcel.2020.07.017

Maeda, M., Saito, K., and Katada, T. (2016). Distinct isoform-specific complexes of TANGO1 cooperatively facilitate collagen secretion from the endoplasmic reticulum. *Mol. Biol. Cell.* 27, 2688–2696. doi: 10.1091/mbc.E16-03-0196

Malhotra, V., and Erlmann, P. (2011). Protein export at the ER: loading big collagens into COPII carriers. *EMBO J.* 30, 3475–3480. doi: 10.1038/emboj.2011.255

Malhotra, V., and Erlmann, P. (2015). The pathway of collagen secretion. *Annu. Rev. Cell Dev. Biol.* 31, 109–124. doi: 10.1146/annurev-cellbio-100913-013002

Matsui, Y., Hirata, Y., Wada, I., and Hosokawa, N. (2020). Visualization of procollagen IV reveals ER-to-golgi transport by ERGIC-independent carriers. *Cell Struct. Funct.* 45, 107–119. doi: 10.1247/csf.20025

McCaughey, J., Miller, V. J., Stevenson, N. L., Brown, A. K., Budnik, A., Heesom, K. J., et al. (2016). TFG promotes organization of transitional er and efficient collagen secretion. *Cell Rep.* 15, 1648–1659. doi: 10.1016/j.celrep.2016.04.062

McCaughey, J., Stevenson, N. L., Cross, S., and Stephens, D. J. (2019). ER-to-Golgi trafficking of procollagen in the absence of large carriers. *J. Cell Biol.* 218, 929–948. doi: 10.1083/jcb.201806035

Melville, D., Gorur, A., and Schekman, R. (2019). Fatty-acid binding protein 5 modulates the SAR1 GTPase cycle and enhances budding of large COPII cargoes. *Mol. Biol. Cell* 30, 387–399. doi: 10.1091/mbc.E18-09-0548

Meyer, F., and Moussian, B. (2009). Drosophila multiplexin (Dmp) modulates motor axon pathfinding accuracy. *Dev. Growth Differ.* 51, 483–498. doi: 10.1111/j.1440-169X.2009.01111.x

Mironov, A. A., and Beznoussenko, G. V. (2019). Models of intracellular transport: pros and cons. *Front. Cell Dev. Biol.* 7:146. doi: 10.3389/fcell.2019.00146

Muschalik, N., and Munro, S. (2018). Golgins. *Curr. Biol.* 28, R374–R376. doi: 10.1016/j.cub.2018.01.006

Natzle, J. E., Monson, J. M., and McCarthy, B. J. (1982). Cytogenetic location and expression of collagen-like genes in Drosophila. *Nature* 296, 368–371. doi: 10.1038/296368a0

Nogueira, C., Erlmann, P., Villeneuve, J., Santos, A. J., Martinez-Alonso, E., Martinez-Menarguez, J. A., et al. (2014). SLY1 and Syntaxin 18 specify a distinct pathway for procollagen VII export from the endoplasmic reticulum. *Elife* 3:e02784. doi: 10.7554/eLife.02784

Omari, S., Makareeva, E., Gorrell, L., Jarnik, M., Lippincott-Schwartz, J., and Leikin, S. (2020). Mechanisms of procollagen and HSP47 sorting during ER-to-Golgi trafficking. *Matrix Biol.* 93, 79–94. doi: 10.1016/j.matbio.2020.06.002

Omari, S., Makareeva, E., Roberts-Pilgrim, A., Mirigian, L., Jarnik, M., Ott, C., et al. (2018). Noncanonical autophagy at ER exit sites regulates procollagen turnover. *Proc. Natl. Acad. Sci. U S A.* 115, E10099–E10108. doi: 10.1073/pnas.1814552115

Palade, G. (1975). Intracellular aspects of the process of protein synthesis. *Science* 189, 347–358. doi: 10.1126/science.1096303

Pastor-Pareja, J. C. (2020). Atypical basement membranes and basement membrane diversity - what is normal anyway? *J. Cell. Sci.* 133:jcs241794. doi: 10.1242/jcs.241794

Pastor-Pareja, J. C., and Xu, T. (2011). Shaping cells and organs in Drosophila by opposing roles of fat body-secreted Collagen IV and perlecan. *Dev. Cell.* 21, 245–256. doi: 10.1016/j.devcel.2011.06.026

Petley-Ragan, L. M., Ardiel, E. L., Rankin, C. H., and Auld, V. J. (2016). Accumulation of laminin monomers in drosophila glia leads to glial endoplasmic reticulum stress and disrupted larval locomotion. *J. Neurosci.* 36, 1151–1164. doi: 10.1523/JNEUROSCI.1797-15.2016

Raote, I., Ernst, A. M., Campelo, F., Rothman, J. E., Pincet, F., and Malhotra, V. (2020). TANGO1 membrane helices create a lipid diffusion barrier at curved membranes. *Elife* 9:e57822. doi: 10.7554/eLife.57822

Raote, I., and Malhotra, V. (2019). Protein transport by vesicles and tunnels. *J. Cell Biol.* 218, 737–739. doi: 10.1083/jcb.201811073

Raote, I., Ortega Bellido, M., Pirozzi, M., Zhang, C., Melville, D., Parashuraman, S., et al. (2017). TANGO1 assembles into rings around COPII coats at ER exit sites. *J. Cell Biol.* 216, 901–909. doi: 10.1083/jcb.201608080

Raote, I., Ortega-Bellido, M., Santos, A. J., Foresti, O., Zhang, C., Garcia-Parajo, M. F., et al. (2018). TANGO1 builds a machine for collagen export by recruiting and spatially organizing COPII, tethers and membranes. *Elife* 7:e32723. doi: 10.7554/eLife.32723

Reynolds, H. M., Zhang, L., Tran, D. T., and Ten Hagen, K. G. (2019). Tango1 coordinates the formation of endoplasmic reticulum/Golgi docking sites to mediate secretory granule formation. *J. Biol. Chem.* 294, 19498–19510. doi: 10.1074/jbc.RA119.011063

Rios-Barrera, L. D., Sigurbjornsdottir, S., Baer, M., and Leptin, M. (2017). Dual function for tango1 in secretion of bulky cargo and in ER-golgi morphology. *Proc. Natl. Acad. Sci. U S A.* 114, E10389–E10398. doi: 10.1073/pnas.1711408114

Ripoche, J., Link, B., Yucel, J. K., Tokuyasu, K., and Malhotra, V. (1994). Location of Golgi membranes with reference to dividing nuclei in syncytial drosophila embryos. *Proc. Natl. Acad. Sci. U S A.* 91, 1878–1882. doi: 10.1073/pnas.91.5.1878

Roy Chowdhury, S., Bhattacharjee, C., Casler, J. C., Jain, B. K., Glick, B. S., and Bhattacharyya, D. (2020). ER arrival sites associate with ER exit sites to create bidirectional transport portals. *J. Cell. Biol.* 219:e201902114. doi: 10.1083/jcb.201902114

Saito, K., Chen, M., Bard, F., Chen, S., Zhou, H., Woodley, D., et al. (2009). TANGO1 facilitates cargo loading at endoplasmic reticulum exit sites. *Cell* 136, 891–902. doi: 10.1016/j.cell.2008.12.025

Saito, K., Yamashiro, K., Ichikawa, Y., Erlmann, P., Kontani, K., Malhotra, V., et al. (2011). cTAGE5 mediates collagen secretion through interaction with TANGO1 at endoplasmic reticulum exit sites. *Mol. Biol. Cell* 22, 2301–2308. doi: 10.1091/mbc.E11-02-0143

Saito, K., Yamashiro, K., Shimazu, N., Tanabe, T., Kontani, K., and Katada, T. (2014). Concentration of Sec12 at ER exit sites via interaction with cTAGE5 is required for collagen export. *J. Cell Biol.* 206, 751–762. doi: 10.1083/jcb.201312062

Santos, A. J., Nogueira, C., Ortega-Bellido, M., and Malhotra, V. (2016). TANGO1 and Mia2/cTAGE5 (TALI) cooperate to export bulky pre-chylomicrons/VLDLs from the endoplasmic reticulum. *J. Cell. Biol.* 213, 343–354. doi: 10.1083/jcb.201603072

Santos, A. J., Raote, I., Scarpa, M., Brouwers, N., and Malhotra, V. (2015). TANGO1 recruits ERGIC membranes to the endoplasmic reticulum for procollagen export. *Elife* 4:e10982. doi: 10.7554/eLife.10982

Schekman, R. (2010). Charting the secretory pathway in a simple eukaryote. *Mol. Biol. Cell* 21, 3781–3784. doi: 10.1091/mbc.e10-05-0416

Sepulveda, D., Rojas-Rivera, D., Rodríguez, D. A., Groenendyk, J., Köhler, A., Lebeaupin, C., et al. (2018). Interactome screening identifies the ER luminal chaperone Hsp47 as a regulator of the unfolded protein response transducer IRE1α. *Mol. Cell* 69, 238–252. doi: 10.1016/j.molcel.2017.12.028

Sparkes, I. A., Ketelaar, T., de Ruijter, N. C., and Hawes, C. (2009). Grab a golgi: laser trapping of golgi bodies reveals in vivo interactions with the endoplasmic reticulum. *Traffic* 10, 567–571. doi: 10.1111/j.1600-0854.2009.00891.x

Sprangers, J., and Rabouille, C. (2015). SEC16 in COPII coat dynamics at ER exit sites. *Biochem. Soc. Transac.* 43, 97–103. doi: 10.1042/bst20140283

Stoll, R., and Bosserhoff, A. (2008). Extracellular SH3 domain containing proteins–features of a new protein family. *Curr. Protein Pept. Sci.* 9, 221–226. doi: 10.2174/138920308784534014

Stoll, R., Renner, C., Zweckstetter, M., Brüggert, M., Ambrosius, D., Palme, S., et al. (2001). The extracellular human melanoma inhibitory activity (MIA) protein adopts an SH3 domain-like fold. *Embo j.* 20, 340–349. doi: 10.1093/emboj/20.3.340

Suisse, A., and Treisman, J. E. (2019). Reduced SERCA function preferentially affects wnt signaling by retaining E-cadherin in the endoplasmic reticulum. *Cell Rep.* 26, 322–329. doi: 10.1016/j.celrep.2018.12.049

Sun, T., Song, Y., Dai, J., Mao, D., Ma, M., Ni, J. Q., et al. (2019). Spectraplakin shot maintains perinuclear microtubule organization in drosophila polyploid cells. *Dev. Cell* 49:e737. doi: 10.1016/j.devcel.2019.03.027

Tanabe, T., Maeda, M., Saito, K., and Katada, T. (2016). Dual function of cTAGE5 in collagen export from the endoplasmic reticulum. *Mol. Biol. Cell* 27, 2008–2013. doi: 10.1091/mbc.E16-03-0180

Thomas, G. (2002). Furin at the cutting edge: from protein traffic to embryogenesis and disease. *Nat. Rev. Mol. Cell Biol.* 3, 753–766. doi: 10.1038/nrm934

Tiwari, P., Kumar, A., Das, R. N., Malhotra, V., and VijayRaghavan, K. (2015). A tendon cell specific RNAi screen reveals novel candidates essential for muscle tendon interaction. *PLoS One* 10:e0140976. doi: 10.1371/journal.pone.0140976

Usener, D., Schadendorf, D., Koch, J., Dubel, S., and Eichmuller, S. (2003). cTAGE: a cutaneous T cell lymphoma associated antigen family with tumor-specific splicing. *J. Invest. Dermatol.* 121, 198–206. doi: 10.1046/j.1523-1747.2003.12318.x

Venditti, R., Scanu, T., Santoro, M., Di Tullio, G., Spaar, A., Gaibisso, R., et al. (2012). Sedlin controls the ER export of procollagen by regulating the Sar1 cycle. *Science* 337, 1668–1672. doi: 10.1126/science.1224947

Wendler, F., Gillingham, A. K., Sinka, R., Rosa-Ferreira, C., Gordon, D. E., Franch-Marro, X., et al. (2010). A genome-wide RNA interference screen identifies two novel components of the metazoan secretory pathway. *EMBO J.* 29, 304–314. doi: 10.1038/emboj.2009.350

Wilson, D. G., Phamluong, K., Li, L., Sun, M., Cao, T. C., Liu, P. S., et al. (2011). Global defects in collagen secretion in a Mia3/TANGO1 knockout mouse. *J. Cell Biol.* 193, 935–951. doi: 10.1083/jcb.201007162

Witte, K., Schuh, A. L., Hegermann, J., Sarkeshik, A., Mayers, J. R., Schwarze, K., et al. (2011). TFG-1 function in protein secretion and oncogenesis. *Nat. Cell Biol.* 13, 550–558. doi: 10.1038/ncb2225

Yuan, L., Kenny, S. J., Hemmati, J., Xu, K., and Schekman, R. (2018). TANGO1 and SEC12 are copackaged with procollagen I to facilitate the generation of large COPII carriers. *Proc. Natl. Acad. Sci. U S A.* 115, E12255–E12264. doi: 10.1073/pnas.1814810115

Yurchenco, P. D. (2011). Basement membranes: cell scaffoldings and signaling platforms. *Cold Spring Harb. Perspect. Biol.* 3:a004911. doi: 10.1101/cshperspect.a004911

Zang, Y., Wan, M., Liu, M., Ke, H., Ma, S., Liu, L. P., et al. (2015). Plasma membrane overgrowth causes fibrotic collagen accumulation and immune activation in Drosophila adipocytes. *Elife* 4:e07187. doi: 10.7554/eLife.07187

Zhang, L., Syed, Z. A., van Dijk Hard, I., Lim, J. M., Wells, L., and Ten Hagen, K. G. (2014). O-glycosylation regulates polarized secretion by modulating Tango1 stability. *Proc. Natl. Acad. Sci. U S A.* 111, 7296–7301. doi: 10.1073/pnas.1322264111

Zhang, Z., Bai, M., Barbosa, G. O., Chen, A., Wei, Y., Luo, S., et al. (2020). Broadly conserved roles of TMEM131 family proteins in intracellular collagen assembly and secretory cargo trafficking. *Sci. Adv.* 6:eaay7667. doi: 10.1126/sciadv.aay7667

Conflict of Interest: The authors declare that the research was conducted in the absence of any commercial or financial relationships that could be construed as a potential conflict of interest.

frontiers in Cell and Developmental Biology

REVIEW
published: 21 January 2021
doi: 10.3389/fcell.2020.615447

Secretory Vesicles Targeted to Plasma Membrane During Pollen Germination and Tube Growth

Huaqiang Ruan†, Jiang Li†, Ting Wang and Haiyun Ren**

Key Laboratory of Cell Proliferation and Regulation Biology of Ministry of Education, Center for Biological Science and Technology, Advanced Institute of Natural Science, Beijing Normal University, Zhuhai, China

Pollen germination and pollen tube growth are important biological events in the sexual reproduction of higher plants, during which a large number of vesicle trafficking and membrane fusion events occur. When secretory vesicles are transported via the F-actin network in proximity to the apex of the pollen tube, the secretory vesicles are tethered and fused to the plasma membrane by tethering factors and SNARE proteins, respectively. The coupling and uncoupling between the vesicle membrane and plasma membrane are also regulated by dynamic cytoskeleton, proteins, and signaling molecules, including small G proteins, calcium, and PIP2. In this review, we focus on the current knowledge regarding secretory vesicle delivery, tethering, and fusion during pollen germination and tube growth and summarize the progress in research on how regulators and signaling molecules participate in the above processes.

Keywords: secretory vesicles, plasma membrane, exocyst complex, SNAREs, regulation, pollen, F-actin

OPEN ACCESS

Edited by:
Junjie Hu,
Institute of Biophysics (CAS), China

Reviewed by:
Eyal Schejter,
Weizmann Institute of Science, Israel
Yusong Guo,
Hong Kong University of Science and Technology, Hong Kong

****Correspondence:***
Ting wang
twang@bnu.edu.cn
Haiyun Ren
hren@bnu.edu.cn

† These authors have contributed equally to this work and share first authorship

Specialty section:
This article was submitted to Membrane Traffic, a section of the journal Frontiers in Cell and Developmental Biology

Received: *09 October 2020*
Accepted: *14 December 2020*
Published: *21 January 2021*

Citation:
Ruan H, Li J, Wang T and Ren H (2021) Secretory Vesicles Targeted to Plasma Membrane During Pollen Germination and Tube Growth. Front. Cell Dev. Biol. 8:615447. doi: 10.3389/fcell.2020.615447

INTRODUCTION

In seed plants, the production of seeds depends on double fertilization. Mature pollen grains are tri-cellular and composed of two small sperm cells and a large vegetative cell in *Arabidopsis*. One of the two sperm cells fuses with an egg to form a diploid zygote that develops into an embryo, and the other fuses with the polar nucleus to form a primary endosperm nucleus; this process is called double fertilization (Shi and Yang, 2010). The developmental progression of plant double fertilization is well coordinated: it starts with pollen falling on the stigma; the pollen adheres, hydrates, and germinates on the stigma via specific recognition (Sprunck, 2020). Then, the pollen germinates to produce a tubular structure (the pollen tube) that rapidly elongates through polar growth, penetrates the stigma, and grows in style tissues to ultimately deliver the two immotile sperm cells into the ovule to complete double fertilization (Zheng et al., 2018). Since the proper pollen germination and tube growth are essential for two sperm cells transporting to female gametophyte, so exploring the molecular mechanism of pollen germination and pollen tube growth is of great interest in the field.

Pollen germination and pollen tube elongation form the whole process by which polarity is established and maintained. In this process, many cell wall materials, such as pectins and cellulose, are contained as cargo in vesicles with an average diameter of 0.182 μm (Ketelaar et al., 2008; Chebli et al., 2012). These vesicles arise from the Golgi and trans-Golgi network (TGN) and are directionally transported toward and fused with the plasma membrane (PM) at polar exocytosis sites to enable the membrane extension and sustained synthesis of new cell wall material (Wang et al., 2016; Zheng et al., 2018; Grebnev et al., 2020; Guo and Yang, 2020).

A better understanding of the molecular mechanisms of pollen germination and tube growth is key for successful sexual reproduction.

The process of pollen germination includes polarity establishment and site determination (Liu et al., 2018), after which the germinated pollen can continue membrane expansion for directional tube growth. Via membrane trafficking and integration, cell wall materials, proteins, and other components for germination and membrane expansion are transported and released; these processes are essential for pollen germination and tube growth (Chebli et al., 2012; Wang et al., 2016). It is generally thought that membrane contact between secretory vesicles and the PM is the most important cellular activity that coordinates pollen germination and pollen tube growth (Gu and Nielsen, 2013; Guo and Yang, 2020). If directional transport- and release-related processes are inhibited, pollen germination and subsequent tube growth and fertilization events will be strongly affected. In recent years, the progress in understanding the dynamic coordination between endocytosis and exocytosis in pollen tubes has been summarized and reviewed (Zhang et al., 2019; Guo and Yang, 2020). In this review, we focus on the process of secretory vesicle directional targeting the PM, which involves vesicle delivery, tethering, and fusion during pollen germination and tip growth, as well as on the different regulators involved, such as some key signaling proteins and other molecules.

VESICLE DELIVERY

It is generally thought that vesicles are transported by motor protein-mediated directed transport along microfilaments (MFs) toward the target membrane in plant cells, while in animal cells, the microtubule network serves as the track (Coudrier, 2007; Madison et al., 2015; Ueda et al., 2015; Duan and Tominaga, 2018). Experimental data also suggest that plant MFs maintain greater stability than animal MFs and can withstand long-distance vesicle transport (Ren et al., 2019).

Although massive dynamic vesicular transport is dependent on the MF network, the coordination between vesicles and their MF tracks shows quite different dynamic patterns during pollen germination and tube growth (Lan et al., 2018; Liu et al., 2018). Recent research has revealed that actin filaments rotate along the outer edges of pollen grains and then gather in future pollen germination sites, forming collar-like actin structures. Genetic and pharmacological evidence has further revealed an interdependent relationship between the mobility of vesicles and the polymerization of actin filaments. AtFH5, a highly expressed FORMIN protein in *Arabidopsis thaliana* pollen, is located in vesicles and promotes actin assembly; in turn, the force produced by MF polymerization pushes vesicles to the potential germination site (**Figure 1A**; Liu et al., 2018). In the pollen tube, the actin cytoskeleton shows a well-organized and highly dynamic structure that might correspond to the specific functions in different regions (**Figure 1B**; Xiang et al., 2007; Fu, 2015). In the shank region, the parallel F-actin cables are thought to serve as tracks for transporting organelles and vesicles to the pollen tube tip (Hepler and Cheung, 2001; Vidali et al., 2001). In the subapical region, the MFs are short and dense and form a collar-like zone, which might be used as a filter to prevent large organelles and other large membrane structures from entering the tip region (Kroeger et al., 2009; Dong et al., 2012; Diao et al., 2020). In the apical region of the pollen tube, actin filaments are highly dynamic and are thought to organize vesicle docking and fusion with the PM of the pollen tube tip (Vidali et al., 2001; Qu et al., 2013). Interestingly, there exist two alternative possible working patterns between F-actin and secretory vesicles during pollen germination and tube growth (**Figures 1A,B**). However, it is not yet clear how these two coordination patterns work and whether they equally contribute to pollen germination and tube growth. Furthermore, single molecular techniques and *in vitro* simulation assays are expected to be introduced that will help to reveal how single F-actin molecules function on vesicles and elucidate the underlying mechanism.

To ensure that secretory vesicles are delivered to the PM along the correct route, actin filaments need to be temporally and spatially coordinated and arranged in a highly dynamic manner. Different classes of actin-binding proteins (ABPs) are involved in this regulation. Among the ABPs, class I formins are very exciting candidate coordinators of actin and vesicle dynamics, since they can localize to secretory vesicles, bind to F-actin, and directly regulate F-actin dynamics (Deeks et al., 2005; Cvrckova et al., 2014; Li S. et al., 2017; Lan et al., 2018; Liu et al., 2018). Lan's et al. research showed that MF nucleation factor formins (FORMIN3 and FORMIN5) can localize to the PM at the tip of the pollen tube and initiate MF assembly (Lan et al., 2018). The pollen germination percentage is significantly reduced in *fh3-2 fh5-3* mutant plants. Loss of actin filaments in the pollen tubes of *fh3fh5* mutants reduces the velocity of tip-directed vesicle transport and alters the apical vesicle accumulation pattern, supporting the idea that apical actin filaments and their regulatory formin proteins can regulate vesicle trafficking (Ye et al., 2009; Lan et al., 2018). It would be very interesting to explore deeply whether and how these pollen-expressed formin proteins are involved in vesicle trafficking and integration processes. Another family of ABPs, the profilins, can interact with formins via the FH1–FH2 domain to enhance filament elongation rates and to thin and elongate actin bundles (Zhang et al., 2016; Li S. et al., 2017). Some actin depolymerization factors, such as ADF5 and actin-bundling proteins (i.e., VILLIN2 and VILLIN5), have been reported to affect actin dynamics, further influencing pollen germination and tube growth; however, there is no evidence showing an interaction with vesicle trafficking or vesicle integration (Qu et al., 2013; Zhu et al., 2017; Diao et al., 2020). Although it is known that the dynamic organization of MFs and their regulatory proteins are essential for targeting of vesicles to the PM for secretion, the underlying molecular mechanism is still unclear, especially regarding how actin organization interacts with secretory vesicles and directs vesicle targeting. Which protein families may be involved during this process still needs to be further explored.

Compared to the role of the MF cytoskeleton in vesicle delivery, the roles of microtubules in pollen tubes are less clear. Pollen tubes contain many microtubule motors of the kinesin family, and pollen-expressed kinesin proteins are believed

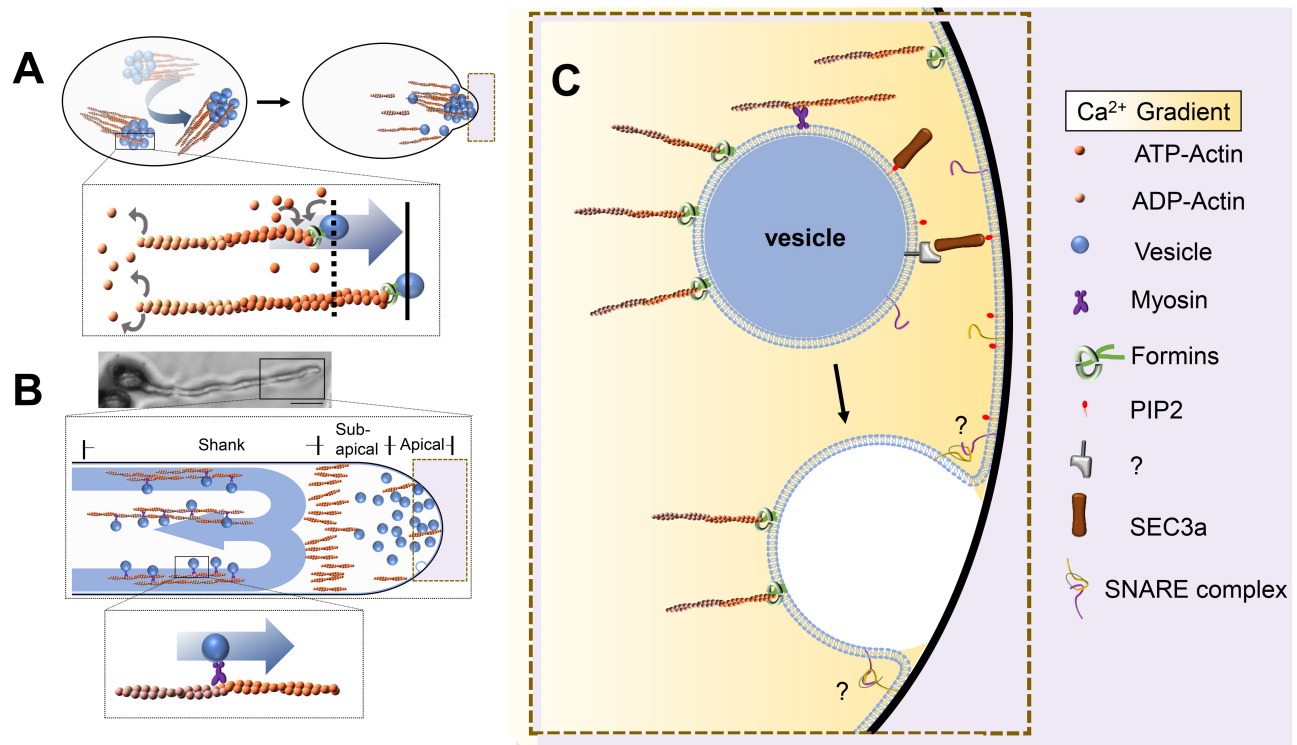

FIGURE 1 | Pattern of vesicle transport in pollen grains and pollen tubes. **(A)** AtFH5 is located to vesicles and promotes actin assembly, the force produced from microfilament polymerization push vesicles' rotational movement to the potential germination sites. Bottom: The box in the upper is enlarged. **(B)** Vesicles are transported along the microfilaments by moto proteins in the shank region, giving rise to a reverse-fountain cytoplasmic streaming pattern, the microfilaments are arranged into an actin fringe at the subapical region. Top: Pollen grains with pollen tubes. Bar is 20 μm. Middle: The box in the top is enlarged. Bottom: The box in the middle is enlarged. **(C)** An enlarged image of dotted frame in A and B. Vesicles are tethered and fused to the plasma membrane by tethering factors and SNAREs. Objects are not to scale.

to be involved in the distribution of organelles during pollen tube growth (Cai and Cresti, 2010). Further exploration of the function of the microtubule network, especially the role this network plays in vesicle trafficking during pollen germination and tube growth, would provide more information and help to comprehensively elucidate the role of the cytoskeleton.

Signaling molecules such as the small G protein Rho of plant GTPase (ROP), the second messenger Ca^{2+}, and the phospholipid molecule phosphatidylinositol-4,5-bisphosphate (PIP2) play important roles in pollen germination and vesicle transport in pollen tubes (Berken and Wittinghofer, 2008; Steinhorst and Kudla, 2013; Feiguelman et al., 2018). As molecular switches, small G proteins have two forms: an inactivated GDP-bound form and an active GTP-bound form. ROPs are regulated by ROPGEFs, ROPGAPs, and RHOGDIs (Berken, 2006). In *A. thaliana*, ROP1, ROP3, and ROP5 are expressed in pollen tubes. ROPs regulate cytoskeletal dynamics and endocytosis through their downstream effector proteins. The pollen-specific protein ROP1 accumulates in the PM of the top of the pollen tube to regulate the Ca^{2+} concentration gradient, activate the RIC3 pathway, and promote actin depolymerization (Gu et al., 2005; Zhou et al., 2015). Moreover, ROP1 also activates RIC4 to promote actin assembly, change the arrangement of the MF skeleton, and induce the accumulation and transport of vesicles to the tip region (Gu et al., 2005; Lee et al., 2008). These results indicate that ROP1 is involved in vesicle transport through regulation of MFs in pollen tubes. However, it is still unclear whether establishment of pollen polarity is also regulated by ROP during pollen germination.

PIP2 localizes at the pollen tube apical PM. The balance of its distribution and content is very important for maintenance of the normal growth of pollen tubes (Monteiro et al., 2005; Zhang and McCormick, 2010). PI(4,5)P2 is synthesized by PIP5K kinase, and the pollen germination and pollen tube polarity growth of the *pip5k4* homozygous mutant are significantly impaired (Sousa et al., 2008). Ischebeck et al. (2011) found that overexpression of PIP5K10 or PIP5K11 enlarged the tip of the pollen tube and caused abnormal arrangement of the MF cytoskeleton, indicating that PI(4,5)P2 regulates dynamic changes in the MF cytoskeleton. Phosphatidylserine (PS) is abundant in the inverted-cone zone of the apical pollen tube in *Arabidopsis*. Recent research has revealed that loss of apical localization of PS and significantly decreased distribution lead to obvious decreases in vesicle numbers and an obvious increase in pollen tube width, which indicates that tip-localized PS establishment is important for vesicle targeting/trafficking and polar growth of pollen tubes in *Arabidopsis* (Zhou et al., 2020).

Although the oscillation of $[Ca^{2+}]_{cyt}$ follows the growth rate pulse, the oscillation of the pollen tube growth rate is consistent with changes in vesicle dynamics (Holdaway-Clarke et al., 1997; Parton et al., 2001). When pollen tubes reach the growth peak, considerable exocytosis is observed at the top of the test tube. Ca^{2+}-dependent ABP LILIM1 binds F-actin bundles in lily pollen and protects them from depolymerization under low $[Ca^{2+}]_{cyt}$ (Wang et al., 2008). In contrast, with increases in $[Ca^{2+}]_{cyt}$, villin/gelsolin family members cut off actin filaments, decrease the activity of profilin, and reduce the polymerization of MFs (Zhang et al., 2010). The above data indicate that Ca^{2+} can indirectly affect vesicle transport in pollen tubes. Whether it can also directly affect cytoskeletal dynamics or intracellular vesicle transport remains to be further studied.

VESICLE TETHERING

After vesicles are delivered in proximity to the target membrane, contact is required between the vesicle and target membrane before fusion, and multisubunit tethering complexes are thought to enable this initial encounter (**Figure 1C**). The first contact between vesicles and the PM is mediated mainly by the exocyst complex (Yu and Hughson, 2010; Pleskot et al., 2015; Mei et al., 2018). The exocyst complex is composed of the subunits Sec3, Sec5, Sec6, Sec8, Sec10, Sec15, Exo70, and Exo84, which are highly conserved in eukaryotes (TerBush et al., 1996; Mei et al., 2018). There are two models for the mechanism by which the exocyst complex performs its tethering function in yeast and mammalian cells (Yu and Hughson, 2010). In the first model, Sec3 and Exo70 interact directly with P(4,5)P2 on the PM to mark secretion sites (He et al., 2007; Zhang et al., 2008). The remaining six subunits form a subcomplex, which is recruited to the vesicle membrane through interaction between Sec15 and the Rab GTPase Sec4p (Guo et al., 1999). In the other model, all eight subunits of the exocyst complex assemble into two different subcomplexes. One of them is composed of Sec3, Sec8, Sec5, and Sec6, which are anchored to the membrane through Sec3 and directly interact with P(4,5)P2. Another subcomplex consists of Sec10, Sec15, Exo70, and Exo84, which are located on the vesicle. Then, interaction between Sec8 and Sec10 assembles the two subcomplexes into a complete exocyst complex to complete the process of vesicle tethering to the PM (Katoh et al., 2015; Heider et al., 2016; Polgar and Fogelgren, 2018). However, the molecular mechanism of the exocyst complex in plants is still poorly understood. Mutations in plant exocyst subunits, such as *sec6*, *sec15a*, and *sec5a/sec5b* single and double mutations, cause defects in pollen germination and tube growth, while *sec8* and *sec3a* mutations have been reported to cause male-specific transmission defects (Cole et al., 2005; Bloch et al., 2016; Li Y. et al., 2017).

Pollen grain germination has been found to be defective in a *sec3a/SEC3A* heterozygous mutant (Li Y. et al., 2017), while in overexpression lines, multiple tips emerge from pollen grain surfaces, and GFP-SEC3A signals appear only in the PM at the tip of the growing pollen tube (Bloch et al., 2016). These results suggest that SEC3A plays an important role in establishing polarity during pollen germination and tube growth. In addition, in sec3a/GFP-SEC3A-overexpressing complementation lines, a strong positive correlation between the localization of GFP-SEC3A at the tips of growing pollen tubes and the secretion of esterified pectins suggests that GFP-SEC3A might work as an intracellular marker for exocytosis. It would be very interesting to explore how SEC3A and other components coordinate to participate in the vesicle secretion process and which other essential proteins/other molecules are secreted by the exocyst-related pathway. The localization and dynamics of SEC8 in pollen tubes are consistent with those of SEC3A, and the homozygous *sec8*-null mutant also shows defects in male-specific transmission, similar to the *sec3a* mutant (Cole et al., 2005; Hala et al., 2008), which indicates that SEC3A and SEC8 may function together to participate in polar transport and the release of key contents for germination and tube growth. There are 23 potential *EXO70* genes in *Arabidopsis*, and mutations in *EXO70* subunits cause different defects in pollen germination and tube growth (Elias, 2003; Synek et al., 2006, 2017; Li et al., 2010; Vukasinovic and Zarsky, 2016). The diversity of *EXO70* family genes implies that there is a large degree of functional redundancy among the subunits. EXO70C2 seems to play a dominant role together with EXO70C1, since the *exo70c1exo70c2* double mutation causes a complete pollen-specific transmission defect (Synek et al., 2017). The yeast two-hybrid system has identified interactions of *Arabidopsis* SEC3A with EXO70A1, SEC10 with SEC15b, and SEC6 with SEC8; these findings indicate that the plant exocyst complex might be structurally conserved and similar to that in animal and yeast cells (Hala et al., 2008). Given data from dynamic imaging analysis of exocyst components in other plant tissues and cells (e.g., root epidermal cells) and the molecular mechanisms of tethering in other cell types (Fendrych et al., 2013), it is reasonable to hypothesize that the exocyst complex also functions as a tethering complex for vesicle transport during pollen germination and tube growth. In the future, some alternative imaging methods could be developed and applied to pollen cells to track the dynamic pattern of each particle component. The results of such studies would offer us more details about how the exocyst complex functions in tethering secretory vesicles.

In yeast cells, sec3p and Exo70p can be recruited to the PM by binding directly with P(4,5)P2, and other subunits are assembled at the active secretion site by Sec4p (Novick et al., 2006). Similarly, the exocyst complex is also expressed in polar secretory active sites in animal cells (Anitei et al., 2006). Although the interaction of SEC3A and PIP2 in plant cells has been confirmed by *in vitro* assays, *in vivo* analysis of the truncated SEC3A protein with loss of the key PIP2 interaction domain has indicated that the interaction does not affect SEC3A apical PM localization and functionality in *Arabidopsis* (Bloch et al., 2016). However, different results from ectopic expression of the same truncated protein have been obtained in tobacco cells, so the interaction and functionality between PIP2 and exocyst components in plant cells still need to be explored (Bloch et al., 2016; Li Y. et al., 2017).

The Rho small G proteins Cdc42, RHO1, and RHO3 regulate the polar localization of sec3p and exo70p in yeast cells

(Finger et al., 1998; Zhang et al., 2008). In plant cells, it has been found that ICR/RIP, an effector protein of ROP, can form a complex with active ROP1 and SEC3A to regulate root cell polar growth (Lavy et al., 2007; Li Y. et al., 2017; Li et al., 2008). It would be very interesting to screen and identify whether some ROP effector or regulatory proteins interact with the exocyst complex and coordinate the tethering process during pollen germination and tube growth.

A general model of exocyst action suggests that most of the components that arrive at the PM and tether secretory vesicles cannot localize properly after disruption of the actin cytoskeleton (Synek et al., 2014). In budding yeast, gene mutations in *SEC10* and *SEC15* strongly affect the cytoskeleton, leading to significant defects in the actin cytoskeleton (Aronov and Gerst, 2004). Inhibition of the interaction between EXO70 and the Arp2/3 complex blocks the formation of actin-based membrane protrusions and affects cell motility in animal cells, which indicates the special role EXO70 might play in coordinating the cytoskeleton and membrane trafficking during cell migration (Zuo et al., 2006). Recent research has revealed that For1F is a fusion protein containing both the exocyst complex subunit (SEC10) domain and the conserved actin-nucleating factor (formin) domain and that this new fusion protein is essential for polar growth in *Physcomitrella patens* (van Gisbergen et al., 2018). This work suggests that both the exocyst complex and actin filaments are essential and cooperate in tethering secretory vesicles during exocytosis. Further exploration of exocyst–cytoskeleton interactions in different cell types would offer some very important clues and elucidate possible cooperative strategies in plant cells, which could help us to better understand the molecular mechanism of vesicle trafficking.

VESICLE FUSION

Membrane fusion occurs after the tethering of vesicles and target membranes; soluble *N*-ethylmaleimide-sensitive factor attachment receptors (SNAREs) play a major role in membrane fusion **Figure 1C** (Uemura et al., 2004; Lipka et al., 2007; Sanderfoot, 2007). SNAREs are classified as Qa-, Qb-, Qc-, and R-SNAREs based on their conserved residues, and all contain a hydrophobic SNARE domain. The SNARE proteins located in the PM and endosomes are listed in **Figure 2**. The Qa-SNARE family members AtSYP124, AtSYP125, and AtSYP131 are exclusively expressed in male gametophytes (Silva et al., 2010; Ichikawa et al., 2015; Slane et al., 2017). The *syp124syp125syp131* mutant shows more severe male gametophyte defects than the *syp124syp125* double mutant, and the pollen tube stops growing during passage through the style, suggesting functional redundancy (Silva et al., 2010; Ichikawa et al., 2015; Slane et al., 2017). SYP131 is mainly stably located in the PM, while SYP124/SYP125 seems to circulate between the PM and endosomes. Therefore, SYP124 and SYP125 may be responsible for membrane fusion in the recycling pathway, while SYP131 may preferentially mediate the membrane fusion of secretory vesicles and contribute to the growth of pollen tubes (Silva et al., 2010; Ichikawa et al., 2015; Slane et al., 2017). VAMP72 family proteins are plant-specific

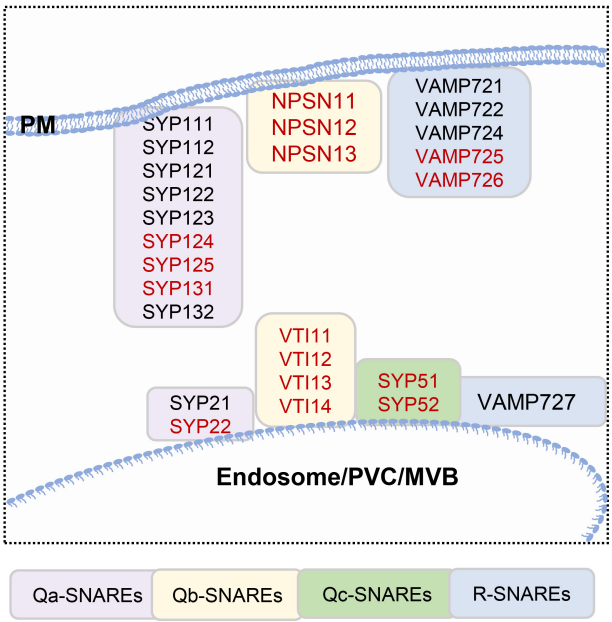

FIGURE 2 | SNAREs located in the plasma membrane and endosomes. Genes that are highly expressed in pollen, which are highlighted in red.

R-SNARE proteins that are located mainly in the PM (Lipka et al., 2007). It has been found that the pollen tubes of *vamp721*$^{+/-}$ *vamp722*$^{+/-}$ show a certain proportion of curly phenotypes, and half of them lack the Ca^{2+} channel AtCNGC18 on the PM (Meng et al., 2020). The N-terminal longin domains of AtVAMP721 and AtVAMP722 interact with AtMLO5, recruit AtCNGC18 to relocate to the PM, affect the local cytoplasmic Ca^{2+} concentration, and regulate the directional responses of pollen tubes to extracellular signals (Meng et al., 2020). However, research on SNAREs has been scarce; thus far, there have been no reports about Qb- and Qc-SNARE proteins in pollen. The specific members of the SNARE complex that are expressed in pollen and their functions in pollen germination and tube growth are unclear.

Many studies have shown that Ca^{2+} plays an important regulatory role in vesicle fusion (Konopka-Postupolska and Clark, 2017). In *Arabidopsis*, the localization of Qa-SNARE in pollen is also regulated by Ca^{2+} ions. The polarity establishment of SYP125 before germination seems to be related to the establishment of a Ca^{2+} gradient, and the location of SYP124 and SYP125 is also changed while Ca^{2+} flux is disturbed, suggesting that Ca^{2+} regulates vesicle fusion in many ways (Silva et al., 2010; Ichikawa et al., 2015). In addition, the distribution of SYP124 and SYP125 is closely related to MFs, MFs depolymerization destroys their localization (Silva et al., 2010; Ichikawa et al., 2015); and some actin or actin-related proteins have been identified in a interactome analysis of SNARE proteins (Fujiwara et al., 2014). In animal cells, synaptotagmin (SYT) proteins have been reported to regulate vesicle fusion (Kweon et al., 2019). There are seven SYTs in *Arabidopsis* (Ishikawa et al., 2020). In the plant SYT family, SYT1 is the

most extensively characterized protein; it acts as an endoplasmic reticulum (ER)–PM tethering factor and participates in biotic and abiotic stress responses in plants (Schapire et al., 2008; Siao et al., 2016). SYTs contain conserved C-terminal tandem C2A and C2B domains and interact with phosphatidylinositol, SNAREs, and Ca^{2+} channel proteins to regulate endocytosis/exocytosis (Wu et al., 2014). It will be interesting to study whether plant cells implement a similar regulatory mechanism in the processes of pollen germination and tube growth. SYT2 is expressed mainly in *Arabidopsis* pollen and is located in the Golgi and PM, and the SYT2-C2AB domain binds to the phospholipid membrane in a Ca^{2+}-dependent manner (Wang et al., 2015). The pollen germination rate of *syt2* mutants is decreased, and pollen tube elongation is restricted (Wang et al., 2015), but the relationship between SYT2 and vesicle fusion during pollen germination and pollen tube growth needs to be further confirmed. Annexin, a Ca^{2+} channel protein, can bind to membrane phospholipids in a Ca^{2+}-dependent manner and can also bind MFs. Thus, it may provide an important connection among intracellular Ca^{2+} signaling, the actin cytoskeleton, and the membrane and participate in intracellular vesicle trafficking (Konopka-Postupolska and Clark, 2017). Ann5 is a Ca^{2+} channel protein that is highly expressed in mature pollen grains and pollen tubes of *A. thaliana*, and a decrease in its expression leads to severe sterility (Lichocka et al., 2018). Ann5 seems to participate in pollen development, germination, and pollen tube elongation by promoting Ca^{2+}-regulated intimal transport, but the exact mechanism needs to be further studied (Zhu et al., 2014a,b; Lichocka et al., 2018).

PROSPECTS

Pollen germination and pollen tube growth are important biological processes in plant sexual reproduction. Many vesicle trafficking, tethering, and fusion events take place during polar pollen germination and tube elongation. In past years, some key tethered factors and SNARE family members have been identified and characterized. However, there are still some key issues that have not yet been resolved, such as the molecular mechanism of each subunit of the exocyst complex and each member of the SNARE family during pollen germination and pollen tube growth. Recent studies have revealed that actin filaments not only participate in intracellular vesicle transport as tracks but also provide the driving forces for vesicle trafficking. Further study is needed to determine whether and how MFs function in vesicle tethering and fusion with the PM and to reveal the interplay between these processes. In addition, Ca^{2+} is an important signaling molecule for pollen germination and tube growth (Iwano et al., 2004; Hepler et al., 2012; Steinhorst and Kudla, 2013); thus, it will be very meaningful to study which and how Ca^{2+} channels or calcium binding proteins are involved in the regulation of vesicle fusion during pollen germination and pollen tube growth. It is believed that the development of microscopic technologies and research methods will enable in-depth analysis of vesicle delivery, tethering, and fusion to the PM during pollen germination and pollen tube growth.

AUTHOR CONTRIBUTIONS

HR drew the figure and wrote the third part "vesicle fusion." JL wrote the first and second part of the manuscripts "vesicle delivery" and "vesicle tethering." TW wrote and revised the manuscript. HR designed and organized the concept of the manuscript and revised the manuscript. All authors contributed to the article and approved the submitted version.

ACKNOWLEDGMENTS

We are grateful for financial support from the National Natural Science Research Foundation of China (91854206 and 31770206 to HR).

REFERENCES

Anitei, M., Ifrim, M., Ewart, M. A., Cowan, A. E., Carson, J. H., Bansal, R., et al. (2006). A role for Sec8 in oligodendrocyte morphological differentiation. *J. Cell Sci.* 119, 807–818. doi: 10.1242/jcs.02785

Aronov, S., and Gerst, J. E. (2004). Involvement of the late secretory pathway in actin regulation and mRNA transport in yeast. *J. Biol. Chem.* 279, 36962–36971. doi: 10.1074/jbc.M402068200

Berken, A. (2006). ROPs in the spotlight of plant signal transduction. *Cell Mol. Life Sci.* 63, 2446–2459. doi: 10.1007/s00018-006-6197-1

Berken, A., and Wittinghofer, A. (2008). Structure and function of Rho-type molecular switches in plants. *Plant Physiol. Biochem.* 46, 380–393. doi: 10.1016/j.plaphy.2007.12.008

Bloch, D., Pleskot, R., Pejchar, P., Potocky, M., Trpkosova, P., Cwiklik, L., et al. (2016). Exocyst SEC3 and phosphoinositides define sites of exocytosis in pollen tube initiation and growth. *Plant Physiol.* 172, 980–1002. doi: 10.1104/pp.16.00690

Cai, G., and Cresti, M. (2010). Microtubule motors and pollen tube growth-still an open question. *Protoplasma* 247, 131–143. doi: 10.1007/s00709-010-0214-9

Chebli, Y., Kaneda, M., Zerzour, R., and Geitmann, A. (2012). The cell wall of the *Arabidopsis* pollen tube–spatial distribution, recycling, and network formation of polysaccharides. *Plant Physiol.* 160, 1940–1955. doi: 10.1104/pp.112.199729

Cole, R. A., Synek, L., Zarsky, V., and Fowler, J. E. (2005). SEC8, a subunit of the putative *Arabidopsis* exocyst complex, facilitates pollen germination and competitive pollen tube growth. *Plant Physiol.* 138, 2005–2018. doi: 10.1104/pp.105.062273

Coudrier, E. (2007). Myosins in melanocytes: to move or not to move? *Pigment Cell Res.* 20, 153–160. doi: 10.1111/j.1600-0749.2007.00376.x

Cvrckova, F., Oulehlova, D., and Zarsky, V. (2014). Formins: linking cytoskeleton and endomembranes in plant cells. *Int. J. Mol. Sci.* 16, 1–18. doi: 10.3390/ijms16010001

Deeks, M. J., Cvrckova, F., Machesky, L. M., Mikitova, V., Ketelaar, T., Zarsky, V., et al. (2005). *Arabidopsis* group le formins localize to specific cell membrane domains, interact with actin-binding proteins and cause defects in cell expansion upon aberrant expression. *New Phytol.* 168, 529–540. doi: 10.1111/j.1469-8137.2005.01582.x

Diao, M., Li, X., and Huang, S. (2020). *Arabidopsis* AIP1-1 regulates the organization of apical actin filaments by promoting their turnover in pollen tubes. *Sci. China Life Sci.* 63, 239–250. doi: 10.1007/s11427-019-9532-0

Dong, H., Pei, W., and an Ren, H. (2012). Actin fringe is correlated with tip growth velocity of pollen tubes. *Mol. Plant* 5, 1160–1162. doi: 10.1093/mp/sss073

Duan, Z., and Tominaga, M. (2018). Actin-myosin XI: an intracellular control network in plants. *Biochem. Biophys. Res. Commun.* 506, 403–408. doi: 10.1016/j.bbrc.2017.12.169

Elias, M. (2003). The exocyst complex in plants. *Cell Biol. Int.* 27, 199–201. doi: 10.1016/s1065-6995(02)00349-9

Feiguelman, G., Fu, Y., and Yalovsky, S. (2018). ROP GTPases structure-function and signaling pathways. *Plant Physiol.* 176, 57–79. doi: 10.1104/pp.17.01415

Fendrych, M., Synek, L., Pecenkova, T., Drdova, E. J., Sekeres, J., de Rycke, R., et al. (2013). Visualization of the exocyst complex dynamics at the plasma membrane of *Arabidopsis thaliana*. *Mol. Biol. Cell.* 24, 510–520. doi: 10.1091/mbc.E12-06-0492

Finger, F. P., Hughes, T. E., and Novick, P. (1998). Sec3p is a spatial landmark for polarized secretion in budding yeast. *Cell* 92, 559–571.

Fu, Y. (2015). The cytoskeleton in the pollen tube. *Curr. Opin. Plant Biol.* 28, 111–119. doi: 10.1016/j.pbi.2015.10.004

Fujiwara, M., Uemura, T., Ebine, K., Nishimori, Y., Ueda, T., Nakano, A., et al. (2014). Interactomics of Qa-SNARE in *Arabidopsis thaliana*. *Plant Cell Physiol.* 55, 781–789. doi: 10.1093/pcp/pcu038

Grebnev, G., Cvitkovic, M., Fritz, C., Cai, G., Smith, A. S., and Kost, B. (2020). Quantitative structural organization of bulk apical membrane traffic in pollen tubes. *Plant Physiol.* 183, 1559–1585.

Gu, F., and Nielsen, E. (2013). Targeting and regulation of cell wall synthesis during tip growth in plants. *J. Integr. Plant Biol.* 55, 835–846. doi: 10.1111/jipb.12077

Gu, Y., Fu, Y., Dowd, P., Li, S., Vernoud, V., Gilroy, S., et al. (2005). A Rho family GTPase controls actin dynamics and tip growth via two counteracting downstream pathways in pollen tubes. *J. Cell Biol.* 169, 127–138. doi: 10.1083/jcb.200409140

Guo, J., and Yang, Z. (2020). Exocytosis and endocytosis: coordinating and fine-tuning the polar tip growth domain in pollen tubes. *J. Exp. Bot.* 71, 2428–2438. doi: 10.1093/jxb/eraa134

Guo, W., Roth, D., Walch-Solimena, C., and Novick, P. (1999). The exocyst is an effector for Sec4p, targeting secretory vesicles to sites of exocytosis. *The EMBO J.* 18, 1071–1080.

Hala, M., Cole, R., Synek, L., Drdova, E., Pecenkova, T., Nordheim, A., et al. (2008). An exocyst complex functions in plant cell growth in *Arabidopsis* and tobacco. *Plant Cell* 20, 1330–1345. doi: 10.1105/tpc.108.059105

He, B., Xi, F., Zhang, J., TerBush, D., Zhang, X., and Guo, W. (2007). Exo70p mediates the secretion of specific exocytic vesicles at early stages of the cell cycle for polarized cell growth. *J. Cell Biol.* 176, 771–777.

Heider, M. R., Gu, M., Duffy, C. M., Mirza, A. M., Marcotte, L. L., Walls, A. C., et al. (2016). Subunit connectivity, assembly determinants and architecture of the yeast exocyst complex. *Nat. Struct. Mol. Biol.* 23, 59–66.

Hepler, P. K., and Cheung, A. (2001). Polarized cell growth in higher plants. *Annu. Rev. Cell Dev. Bio.* 17, 159–187.

Hepler, P. K., Kunkel, J. G., Rounds, C. M., and Winship, L. J. (2012). Calcium entry into pollen tubes. *Trends Plant Sci.* 17, 32–38. doi: 10.1016/j.tplants.2011.10.007

Holdaway-Clarke, T. L., Feijo, J. A., Hackett, G. R., Kunkel, J. G., and Hepler, P. K. (1997). Pollen tube growth and the intracellular cytosolic calcium gradient oscillate in phase while extracellular calcium influx is delayed. *Plant Cell.* 9, 1999–2010. doi: 10.1105/tpc.9.11.1999

Ichikawa, M., Iwano, M., and Sato, M. H. (2015). Nuclear membrane localization during pollen development and apex-focused polarity establishment of SYP124/125 during pollen germination in *Arabidopsis thaliana*. *Plant Reprod.* 28, 143–151. doi: 10.1007/s00497-015-0265-3

Ischebeck, T., Stenzel, I., Hempel, F., Jin, X., Mosblech, A., and Heilmann, I. (2011). Phosphatidylinositol-4,5-bisphosphate influences Nt-Rac5-mediated cell expansion in pollen tubes of Nicotiana tabacum. *Plant J.* 65, 453–468. doi: 10.1111/j.1365-313X.2010.04435.x

Ishikawa, K., Tamura, K., Fukao, Y., and Shimada, T. (2020). Structural and functional relationships between plasmodesmata and plant endoplasmic reticulum-plasma membrane contact sites consisting of three synaptotagmins. *New Phytol.* 226, 798–808.

Iwano, M., Shiba, H., Miwa, T., Che, F. S., Takayama, S., Nagai, T., et al. (2004). Ca^{2+} dynamics in a pollen grain and papilla cell during pollination of Arabidopsis. *Plant Physiol.* 136, 3562–3571. doi: 10.1104/pp.104.046961

Katoh, Y., Nozaki, S., Hartanto, D., Miyano, R., and Nakayama, K. (2015). Architectures of multisubunit complexes revealed by a visible immunoprecipitation assay using fluorescent fusion proteins. *J. Cell Sci.* 128, 2351–2362.

Ketelaar, T., Galway, M. E., Mulder, B. M., and Emons, A. M. (2008). Rates of exocytosis and endocytosis in *Arabidopsis* root hairs and pollen tubes. *J. Microscopy* 231, 265–273.

Konopka-Postupolska, D., and Clark, G. (2017). Annexins as overlooked regulators of membrane trafficking in plant cells. *Int. J. Mol. Sci.* 18:863. doi: 10.3390/ijms18040863

Kroeger, J. H., Daher, F. B., Grant, M., and Geitmann, A. (2009). Microfilament orientation constrains vesicle flow and spatial distribution in growing pollen tubes. *Biophys. J.* 97, 1822–1831. doi: 10.1016/j.bpj.2009.07.038

Kweon, D. H., Kong, B., and Shin, Y. K. (2019). Search for a minimal machinery for Ca^{2+}-triggered millisecond neuroexocytosis. *Neuroscience* 420, 4–11. doi: 10.1016/j.neuroscience.2018.07.031

Lan, Y., Liu, X., Fu, Y., and Huang, S. (2018). *Arabidopsis* class I formins control membrane-originated actin polymerization at pollen tube tips. *PLoS Genet.* 14:e1007789. doi: 10.1371/journal.pgen.1007789

Lavy, M., Bloch, D., Hazak, O., Gutman, I., Poraty, L., Sorek, N., et al. (2007). A novel ROP/RAC effector links cell polarity, root-meristem maintenance, and vesicle trafficking. *Cur. Biol.* 17, 947–952. doi: 10.1016/j.cub.2007.04.038

Lee, Y. J., Szumlanski, A., Nielsen, E., and Yang, Z. (2008). Rho-GTPase-dependent filamentous actin dynamics coordinate vesicle targeting and exocytosis during tip growth. *J. Cell Biol.* 181, 1155–1168. doi: 10.1083/jcb.200801086

Li, S., Dong, H., Pei, W., Liu, C., Zhang, S., Sun, T., et al. (2017). LlFH1-mediated interaction between actin fringe and exocytic vesicles is involved in pollen tube tip growth. *New Phytol.* 214, 745–761. doi: 10.1111/nph.14395

Li, Y., Tan, X., Wang, M., Li, B., Zhao, Y., Wu, C., et al. (2017). Exocyst subunit SEC3A marks the germination site and is essential for pollen germination in *Arabidopsis thaliana*. *Sci. Rep.* 7:40279. doi: 10.1038/srep40279

Li, S., Gu, Y., Yan, A., Lord, E., and Yang, Z. (2008). RIP1 (ROP Interactive Partner 1)/ICR1 marks pollen germination sites and may act in the ROP1 pathway in the control of polarized pollen growth. *Mol. Plant* 1, 1021–1035. doi: 10.1093/mp/ssn051

Li, S., van Os, G. M., Ren, S., Yu, D., Ketelaar, T., Emons, A. M., et al. (2010). Expression and functional analyses of EXO70 genes in *Arabidopsis* implicate their roles in regulating cell type-specific exocytosis. *Plant Physiol.* 154, 1819–1830. doi: 10.1104/pp.110.164178

Lichocka, M., Rymaszewski, W., Morgiewicz, K., Barymow-Filoniuk, I., Chlebowski, A., Sobczak, M., et al. (2018). Nucleus- and plastid-targeted annexin 5 promotes reproductive development in *Arabidopsis* and is essential for pollen and embryo formation. *BMC Plant Biol.* 18:183. doi: 10.1186/s12870-018-1405-3

Lipka, V., Kwon, C., and Panstruga, R. (2007). SNARE-ware: the role of SNARE-domain proteins in plant biology. *Annu. Rev. Cell Dev. Biol.* 23, 147–174. doi: 10.1146/annurev.cellbio.23.090506.123529

Liu, C., Zhang, Y., and Ren, H. (2018). Actin polymerization mediated by AtFH5 directs the polarity establishment and vesicle trafficking for pollen germination in *Arabidopsis*. *Mol. Plant.* 11, 1389–1399. doi: 10.1016/j.molp.2018.09.004

Madison, S. L., Buchanan, M. L., Glass, J. D., McClain, T. F., Park, E., and Nebenfuhr, A. (2015). Class XI myosins move specific organelles in pollen tubes and are required for normal fertility and pollen tube growth in *arabidopsis*. *Plant Physiol.* 169, 1946–1960. doi: 10.1104/pp.15.01161

Mei, K., Li, Y., Wang, S., Shao, G., Wang, J., Ding, Y., et al. (2018). Cryo-EM structure of the exocyst complex. *Nat. Struct. Mol. Biol.* 25, 139–146. doi: 10.1038/s41594-017-0016-2

Meng, J., Liang, L., Jia, P., Wang, Y., Li, H., and Yang, W. (2020). Integration of ovular signals and exocytosis of a Ca^{2+} channel by MLOs in pollen tube guidance. *Nat. Plants.* 6, 143–153. doi: 10.1038/s41477-020-0599-1

Monteiro, D., Liu, Q., Lisboa, S., Scherer, G. E., Quader, H., and Malho, R. (2005). Phosphoinositides and phosphatidic acid regulate pollen tube growth and reorientation through modulation of $[Ca^{2+}]c$ and membrane secretion. *J. Exp. Bot.* 56, 1665–1674. doi: 10.1093/jxb/eri163

Novick, P., Medkova, M., Dong, G., Hutagalung, A., Reinisch, K., and Grosshans, B. (2006). Interactions between Rabs, tethers, SNAREs and their regulators in exocytosis. *Biochem. Soc. Trans.* 34, 683–686. doi: 10.1042/BST0340683

Parton, R. M., Fischer-Parton, S., Watahiki, M. K., and Trewavas, A. J. (2001). Dynamics of the apical vesicle accumulation and the rate of growth are related in individual pollen tubes. *J. Cell Sci.* 114, 2685–2695.

Pleskot, R., Cwiklik, L., Jungwirth, P., Zarsky, V., and Potocky, M. (2015). Membrane targeting of the yeast exocyst complex. *Biochim Biophys. Acta* 1848, 1481–1489. doi: 10.1016/j.bbamem.2015.03.026

Polgar, N., and Fogelgren, B. (2018). Regulation of cell polarity by exocyst-mediated trafficking. *Cold Spring Harb. Perspect. Biol.* 10:a031401.

Qu, X., Zhang, H., Xie, Y., Wang, J., Chen, N., and Huang, S. (2013). *Arabidopsis villins* promote actin turnover at pollen tube tips and facilitate the construction of actin collars. *Plant Cell* 25, 1803–1817. doi: 10.1105/tpc.113.110940

Ren, Z., Zhang, Y., Zhang, Y., He, Y., Du, P., Wang, Z., et al. (2019). Cryo-EM structure of actin filaments from zea mays pollen. *Plant Cell* 31, 2855–2867. doi: 10.1105/tpc.18.00973

Sanderfoot, A. (2007). Increases in the number of SNARE genes parallels the rise of multicellularity among the green plants. *Plant Physiol.* 144, 6–17. doi: 10.1104/pp.106.092973

Schapire, A. L., Voigt, B., Jasik, J., Rosado, A., Lopez-Cobollo, R., Menzel, D., et al. (2008). *Arabidopsis* synaptotagmin 1 is required for the maintenance of plasma membrane integrity and cell viability. *Plant Cell* 12, 3374–3388. doi: 10.1105/tpc.108.063859

Shi, D. Q., and Yang, W. C. (2010). Pollen germination and tube growth. *Plant Dev. Biol. Biotechnol. Perspect.* 1, 245–282.

Siao, W., Wang, P., Voigt, B., Hussey, P. J., and Baluska, F. (2016). *Arabidopsis* SYT1 maintains stability of cortical endoplasmic reticulum networks and VAP27-1-enriched endoplasmic reticulum-plasma membrane contact sites. *J. Exp. Bot.* 67, 6161–6171. doi: 10.1093/jxb/erw381

Silva, P. A., Ul-Rehman, R., Rato, C., Sansebastiano, G. P. D., and Malho, R. (2010). Asymmetric localization of *Arabidopsis* SYP124 syntaxin at the pollen tube apical and sub-apical zones is involved in tip growth. *BMC Plant Biol.* 10:179. doi: 10.1186/1471-2229-10-179

Slane, D., Reichardt, I., El Kasmi, F., Bayer, M., and Jurgens, G. (2017). Evolutionarily diverse SYP1 Qa-SNAREs jointly sustain pollen tube growth in *Arabidopsis*. *Plant J.* 92, 375–385. doi: 10.1111/tpj.13659

Sousa, E., Kost, B., and Malho, R. (2008). *Arabidopsis* phosphatidylinositol-4-monophosphate 5-kinase 4 regulates pollen tube growth and polarity by modulating membrane recycling. *Plant Cell* 20, 3050–3064. doi: 10.1105/tpc.108.058826

Sprunck, S. (2020). Twice the fun, double the trouble: gamete interactions in flowering plants. *Curr. Opin. Plant Biol.* 53, 106–116. doi: 10.1016/j.pbi.2019.11.003

Steinhorst, L., and Kudla, J. (2013). Calcium - a central regulator of pollen germination and tube growth. *Biochim Biophys Acta.* 1833, 1573–1581. doi: 10.1016/j.bbamcr.2012.10.009

Synek, L., Schlager, N., Elias, M., Quentin, M., Hauser, M. T., and Zarsky, V. (2006). AtEXO70A1, a member of a family of putative exocyst subunits specifically expanded in land plants, is important for polar growth and plant development. *Plant J.* 48, 54–72. doi: 10.1111/j.1365-313X.2006.02854.x

Synek, L., Sekeres, J., and Zarsky, V. (2014). The exocyst at the interface between cytoskeleton and membranes in eukaryotic cells. *Front. Plant Sci.* 4:543. doi: 10.3389/fpls.2013.00543

Synek, L., Vukasinovic, N., Kulich, I., Hala, M., Aldorfova, K., Fendrych, M., et al. (2017). EXO70C2 is a key regulatory factor for optimal tip growth of pollen. *Plant Physiol.* 174, 223–240. doi: 10.1104/pp.16.01282

TerBush, D. R., Maurice, T., Roth, D., and Novick, P. (1996). The Exocyst is a multiprotein complex required for exocytosis in Saccharomyces cerevisiae. *The EMBO Journal* 15, 6483–6494. doi: 10.1002/j.1460-2075.1996.tb01039.x

Ueda, H., Tamura, K., and Hara-Nishimura, I. (2015). Functions of plant-specific myosin XI: from intracellular motility to plant postures. *Curr. Opin. Plant Biol.* 28, 30–38. doi: 10.1016/j.pbi.2015.08.006

Uemura, T., Ueda, T., Ohniwa, R. L., Nakano, A., Takeyasu, K., and Sato, M. H. (2004). Systematic analysis of SNARE molecules in *Arabidopsis*: dissection of the post-Golgi network in plant cells. *Cell Struct. Funct.* 29, 49–65. doi: 10.1247/csf.29.49

van Gisbergen, P. A. C., Wu, S., Chang, M., Pattavina, K. A., Bartlett, M. E., and Bezanilla, M. (2018). An ancient Sec10-formin fusion provides insights into actin-mediated regulation of exocytosis. *J. Cell Biol.* 217, 945–957. doi: 10.1083/jcb.201705084

Vidali, L., McKenna, S. T., and Hepler, P. K. (2001). Actin polymerization is essential for pollen tube growth. *Mol. Biol. Cell* 12, 2534–2545. doi: 10.1091/mbc.12.8.2534

Vukasinovic, N., and Zarsky, V. (2016). Tethering complexes in the *Arabidopsis* endomembrane system. *Front. Cell Dev. Biol.* 4:46. doi: 10.3389/fcell.2016.00046

Wang, H., Han, S., Siao, W., Song, C., Xiang, Y., Wu, X., et al. (2015). *Arabidopsis* synaptotagmin 2 participates in pollen germination and tube growth and is delivered to plasma membrane via conventional secretion. *Mol. Plant* 8, 1737–1750. doi: 10.1016/j.molp.2015.09.003

Wang, H., Wan, A., and Jauh, G. Y. (2008). An actin-binding protein, LlLIM1, mediates calcium and hydrogen regulation of actin dynamics in pollen tubes. *Plant Physiol.* 147, 1619–1636. doi: 10.1104/pp.108.118604

Wang, H., Zhuang, X., Wang, X., Law, A. H., Zhao, T., Du, S., et al. (2016). A Distinct pathway for polar exocytosis in plant cell wall formation. *Plant Physiol.* 172, 1003–1018. doi: 10.1104/pp.16.00754

Wu, L., Hamid, E., Shin, W., and Chiang, H. (2014). Exocytosis and endocytosis: modes, functions, and coupling mechanisms. *Annu. Rev. Physiol.* 76, 301–331. doi: 10.1146/annurev-physiol-021113-170305

Xiang, Y., Huang, X., Wang, T., Zhang, Y., Liu, Q., Hussey, P. J., et al. (2007). Actin binding protein 29 from lilium pollen plays an important role in dynamic actin remodeling. *Plant Cell* 19, 1930–1946. doi: 10.1105/tpc.106.048413

Ye, J., Zheng, Y., Yan, A., Chen, N., Wang, Z., Huang, S., et al. (2009). *Arabidopsis* formin3 directs the formation of actin cables and polarized growth in pollen tubes. *Plant Cell* 21, 3868–3884. doi: 10.1105/tpc.109.068700

Yu, I. M., and Hughson, F. M. (2010). Tethering factors as organizers of intracellular vesicular traffic. *Annu. Rev. Cell Dev. Biol.* 26, 137–156. doi: 10.1146/annurev.cellbio.042308.113327

Zhang, H., Qu, X., Bao, C., Khurana, P., Wang, Q., Xie, Y., et al. (2010). *Arabidopsis* VILLIN5, an actin filament bundling and severing protein, is necessary for normal pollen tube growth. *Plant Cell* 22, 2749–2767. doi: 10.1105/tpc.110.076257

Zhang, L., Xing, J., and Lin, J. (2019). At the intersection of exocytosis and endocytosis in plants. *New Phytologist* 224, 1479–1489. doi: 10.1111/nph.16018

Zhang, S., Liu, C., Wang, J., Ren, Z., Staiger, C. J., and Ren, H. (2016). A processive *arabidopsis* formin modulates actin filament dynamics in association with profilin. *Mol. Plant* 9, 900–910. doi: 10.1016/j.molp.2016.03.006

Zhang, X., Orlando, K., He, B., Xi, F., Zhang, J., Zajac, A., et al. (2008). Membrane association and functional regulation of Sec3 by phospholipids and Cdc42. *J. Cell Biol.* 180, 145–158. doi: 10.1083/jcb.200704128

Zhang, Y., and McCormick, S. (2010). The regulation of vesicle trafficking by small GTPases and phospholipids during pollen tube growth. *Sex Plant Reprod.* 23, 87–93. doi: 10.1007/s00497-009-0118-z

Zheng, Y., Lin, X., Liang, H., Wang, F., and Chen, L. (2018). The long journey of pollen tube in the pistil. *Int. J. Mol. Sci.* 19:3529. doi: 10.3390/ijms19113529

Zhou, Y., Yang, Y., Niu, Y., Fan, T., Qian, D., Luo, C., et al. (2020). The tip-localized phosphatidylserine established by *arabidopsis* ala3 is crucial for rab gtpase-mediated vesicle trafficking and pollen tube growth. *Plant Cell* 32, 3170–3187. doi: 10.1105/tpc.19.00844

Zhou, Z., Shi, H., Chen, B., Zhang, R., Huang, S., and Fu, Y. (2015). *Arabidopsis* RIC1 severs actin filaments at the apex to regulate pollen tube growth. *Plant Cell* 27, 1140–1161. doi: 10.1105/tpc.114.135400

Zhu, J., Nan, Q., Qin, T., Qian, D., Mao, T., Yuan, S., et al. (2017). Higher-ordered actin structures remodeled by *arabidopsis* actin-depolymerizing factor5 are important for pollen germination and pollen tube growth. *Mol. Plant* 10, 1065–1081. doi: 10.1016/j.molp.2017.06.001

Zhu, J., Wu, X., Yuan, S., Qian, D., Nan, Q., An, L., et al. (2014a). Annexin5 plays a vital role in *Arabidopsis* pollen development via Ca^{2+}-dependent membrane trafficking. *PLoS One* 9:e102407. doi: 10.1371/journal.pone.0102407

Zhu, J., Yuan, S., Wei, G., Qian, D., Wu, X., Jia, H., et al. (2014b). Annexin5 is essential for pollen development in *Arabidopsis*. *Mol. Plant* 7, 751–754. doi: 10.1093/mp/sst171

Zuo, X., Zhang, J., Zhang, Y., Hsu, S. C., Zhou, D., and Guo, W. (2006). Exo70 interacts with the Arp2/3 complex and regulates cell migration. *Nat. Cell Biol.* 8, 1383–1388. doi: 10.1038/ncb1505

Conflict of Interest: The authors declare that the research was conducted in the absence of any commercial or financial relationships that could be construed as a potential conflict of interest.

frontiers in Cell and Developmental Biology

REVIEW
published: 04 February 2021
doi: 10.3389/fcell.2021.627700

Endoplasmic Reticulum–Plasma Membrane Contact Sites: Regulators, Mechanisms, and Physiological Functions

Chenlu Li[1], *Tiantian Qian*[1], *Ruyue He*[1], *Chun Wan*[2], *Yinghui Liu*[1]* *and Haijia Yu*[1]*

[1] *Jiangsu Key Laboratory for Molecular and Medical Biotechnology, College of Life Sciences, Nanjing Normal University, Nanjing, China,* [2] *Department of Molecular, Cellular and Developmental Biology, University of Colorado, Boulder, CO, United States*

The endoplasmic reticulum (ER) forms direct membrane contact sites with the plasma membrane (PM) in eukaryotic cells. These ER-PM contact sites play essential roles in lipid homeostasis, ion dynamics, and cell signaling, which are carried out by protein-protein or protein-lipid interactions. Distinct tethering factors dynamically control the architecture of ER-PM junctions in response to intracellular signals or external stimuli. The physiological roles of ER-PM contact sites are dependent on a variety of regulators that individually or cooperatively perform functions in diverse cellular processes. This review focuses on proteins functioning at ER-PM contact sites and highlights the recent progress in their mechanisms and physiological roles.

Keywords: membrane contact sites (MCSs), endoplasmic reticulum (ER), plasma membrane, tether, lipid transfer, enzyme

OPEN ACCESS

Edited by:
Dan Zhang,
Temasek Life Sciences Laboratory, Singapore

Reviewed by:
Tito Cali',
University of Padua, Italy
Chi-Lun Chang,
Janelia Research Campus, United States

***Correspondence:**
Yinghui Liu
yinghuiliu@njnu.edu.cn
Haijia Yu
yuhaijia@njnu.edu.cn

Specialty section:
This article was submitted to Membrane Traffic, a section of the journal Frontiers in Cell and Developmental Biology

Received: *10 November 2020*
Accepted: *13 January 2021*
Published: *04 February 2021*

Citation:
Li C, Qian T, He R, Wan C, Liu Y and Yu H (2021) Endoplasmic Reticulum–Plasma Membrane Contact Sites: Regulators, Mechanisms, and Physiological Functions. Front. Cell Dev. Biol. 9:627700. doi: 10.3389/fcell.2021.627700

INTRODUCTION

Intracellular trafficking between membrane-bound organelles is divided into two types, vesicular trafficking and non-vesicular trafficking. Vesicular trafficking is the predominant pathway to transport macromolecular substances and exchange information between organelles. The cargo is wrapped by or integrated into the membrane to form a vesicle, and exchange proteins or lipids between organelles through membrane fusion (Bonifacino and Glick, 2004; Südhof and Rothman, 2009). However, recent studies demonstrated that non-vesicular trafficking is another critical trafficking approach among intracellular membranous organelles, directly communicating through a close gap (typically within 10–30 nm) formed by two opposed membranes (Wong et al., 2019). This kind of intracellular communication is ensured by particular regions within the cell, defined as membrane contact sites (MCSs), structures mediated by protein-protein or protein-lipid interactions.

The largest membrane-bound organelle in eukaryotic cells is the endoplasmic reticulum (ER). It is the primary place for the synthesis of proteins and lipids, which are needed to maintain and propagate other membranous organelles and plasma membrane (PM) (Bonifacino and Glick, 2004). The ER extends throughout the whole cell and engages in broad communications with PM and other organelles by MCSs. ER-PM contact sites were first observed in muscle cells in the 1950s (Porter and Palade, 1957), and later were demonstrated as a general feature in eukaryotes. The MCSs formed between the ER and the PM provide an ideal platform for non-vesicular transport

of lipids, ions, and many other signaling molecules (Gallo et al., 2016; Saheki and De Camilli, 2017a; Stefan, 2020). The architecture of ER-PM junctions is dynamically controlled by distinct tethering factors, and the cellular functions of ER-PM contact sites are highly dependent on those regulators located in these regions (Gallo et al., 2016). However, a variety of proteins localized at the crowded ER-PM junctions, frequently resulting in the co-existence of multiple regulators with similar or partially similar functions (Manford et al., 2012; Hoffmann et al., 2019; Johnson et al., 2019; Kang et al., 2019). They act synergistically to maintain the local microenvironment, which largely increases the difficulties of identifying their individual functions and mechanisms. Therefore, it is important to clarify how these proteins act in concert to play roles in the MCSs, especially under physiological or pathological conditions. This review focuses on the representative regulators localized at ER-PM contact sites, highlighting their physiological functions, molecular mechanisms as well as conservations in eukaryotes.

TETHERING MECHANISMS OF PROTEINS AT ER-PM CONTACT SITES

The extensive cortical ER network is highly dynamic in eukaryotic cells. The tethering factors build and maintain the ER-PM contact sites demanded by diverse biological processes. Most proteins localized at the ER-PM contact sites can span and tether the two opposed membranes. It often happens that multiple proteins coordinate to tether the same MCSs and perform more than one physiological functions (Manford et al., 2012; Fernandez-Busnadiego et al., 2015; Kang et al., 2019). While some protein tethers are constitutively localized at ER-PM contact sites, the locations of others are dynamically regulated by stimuli such as calcium ions and phosphoinositides (**Figure 1A**) (Gallo et al., 2016; Okeke et al., 2016; Saheki and De Camilli, 2017a; Stefan, 2020). How these protein tethers accurately modulate the structure and plasticity of ER-PM contact sites has not been completely understood. Comprehensive understanding of the tethering mechanisms will shed important light on the dynamical control of the cortical ER network. In this section, we summarized the major ER-PM tethering proteins and discussed their membrane-targeting mechanisms.

VAPs

Vesicle-associated membrane protein (VAMP)-associated protein (VAP) is an evolutionarily conserved ER membrane protein in all eukaryotes. It plays a vital role in many ER processes, especially in maintaining ER-PM contact sites. Loss of VAP by mutations leads to neurodegeneration, such as sporadic ALS or Parkinson's disease (Anagnostou et al., 2010; Kun-Rodrigues et al., 2015). There are mainly 2 VAPs (VAP-A and VAP-B) in mammals, 2 homologs (Scs2p and Scs22p) in yeast, and 10 homologs (VAP27-1 to VAP27-10) in *Arabidopsis*. VAP contains a major sperm protein (MSP) domain, a coiled-coil linker domain, and a C-terminal transmembrane domain required for ER surface location (**Figure 1B**) (Lev et al., 2008).

Although named by interaction with VAMP, VAP's primary function is not as a soluble *N*-ethylmaleimide-sensitive factor attachment protein receptor (SNARE) regulator. It binds more than 100 peripheral proteins, including those anchored into other organelles (Murphy and Levine, 2016). By interacting with those partners, VAP dynamically controls the junctions formed between the ER and other organelles such as Golgi, lipid droplets, mitochondria, endosomes, and PM (Murphy and Levine, 2016). By localization at particular contact sites, VAPs and their binding partners coordinate to mediate diverse cellular processes (Lev et al., 2008). However, the distribution of VAP in mammals is not limited to the MCSs but throughout the ER, suggesting it has other functions than membrane tethering. For example, VAP interacts with secernin-1 at the ER membrane to regulate dynamic ER remodeling (Lindhout et al., 2019).

Unlike in mammals, the homologs of VAPs in fission yeast and *Arabidopsis* are more concentrated at MCSs (Zhang et al., 2012; Wang et al., 2014). Scs2p and Scs22p were discovered as two major tethering factors at the ER-PM contact sites (Manford et al., 2012; Zhang et al., 2012). Scs2p was reported as an inositol binding protein that responds to phospholipid composition (Kagiwada and Hashimoto, 2007). However, there is no direct evidence showing Scs2p connects the ER to the PM through the interaction with phosphoinositides. In *Arabidopsis*, the tethering function of VAP27s at ER-PM contact sites was also identified. VAP27 co-localizes with NET3C and forms a tetra complex with microtubules and actin filaments to tether the ER to the PM (Wang et al., 2014). Recent studies suggested VAP27s-mediated ER-PM contact sites regulate plant endocytosis (Stefano et al., 2018; Wang et al., 2019). However, the detailed tethering mechanisms of VAP27s remain largely unknown.

The location of VAP largely relies on its binding partners. It is generally accepted that most of the VAP-mediated ER-PM tethering requires at least one PM-targeting partner. One primary class of the VAP-binding partners are cytoplasmic proteins containing an FFAT motif, which binds specifically to the MSP domain (Kamemura and Chihara, 2019). At MCSs, these FFAT-containing proteins interact with the PM through a membrane-targeting domain, for example, the pleckstrin homology domain (PHD). The lipid-transfer proteins (LTPs) are the most well-studied FFAT-containing proteins at MCSs. For instance, as an Scs2p/Scs22p-binding partner, yeast LTP Osh3p dynamically targets the PM by its PHD under the regulation of PM PI(4)P levels (Jansen et al., 2011; Kamemura and Chihara, 2019). Nir2, another type of FFAT-containing LTP, connects the PM by its C-terminal LNS2 domain binding to phosphatidic acid (PA) (Kim et al., 2013; Balla, 2018). The mechanisms of how these LTPs coordinate with VAP to regulate lipid metabolism will be discussed in the following corresponding section.

Kv2 Channels

Voltage-gated potassium (Kv) channel is a tetramer composed of 4α subunits (70 kDa), and each subunit monomer contains six transmembrane helix segments (**Figure 1B**) (Christie, 1995; Yellen, 1998; Shah and Aizenman, 2014; Fu et al., 2017;

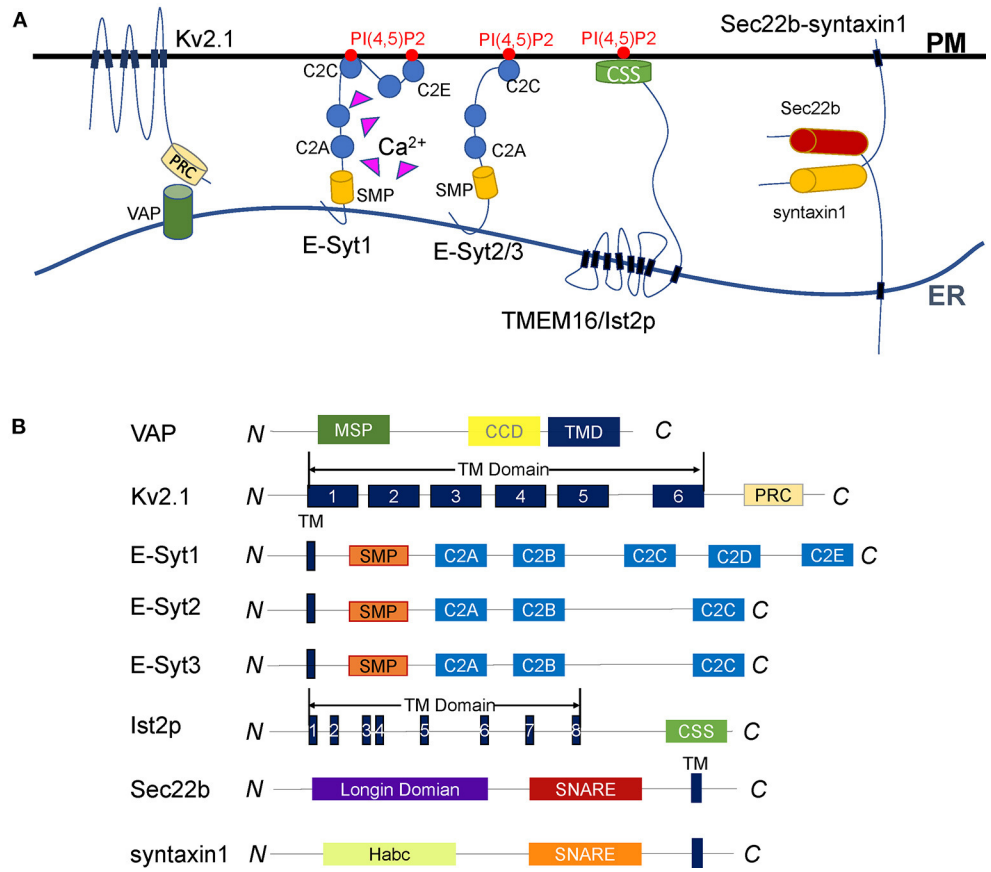

FIGURE 1 | Diverse tethering mechanisms of proteins at ER-PM contact sites. **(A)** Representative illustration of the proteins that tether the ER and the PM. VAP anchors to the ER surface through the transmembrane domain and interacts with its binding partners to tether the ER and PM. The Kv2.1 channel is a VAP-binding partner. It anchors to the PM by six transmembrane domains and interacts with VAP through the C-terminal PRC domain. The Kv2.1-VAP interaction bridges the ER-PM junctions regulated by PRC domain phosphorylation. E-Syts are ER membrane proteins anchored to the ER *via* an N-terminal hydrophobic hairpin. E-Syt1 dynamically tethers the ER to the PM through a Ca^{2+}-dependent interaction between the C2C domain and PI(4,5)P2. E-Syt2/3 constitutively maintains ER-PM junctions regardless of Ca^{2+}. TMEM16/Ist2p is an eight-span integrin protein in the ER and connects the ER to the PM by its C-terminal CSS domain binding to PI(4,5)P2. The ER SNARE protein Sec22b forms an incomplete trans-SNARE complex with syntaxin1 on the PM that does not mediate membrane fusion but promotes the ER and PM tethering. **(B)** Diagrams of the membrane tethering proteins described in (A). The major functional domains are shown in each of the proteins.

Jedrychowska and Korzh, 2019). Kv2 channels Kv2.1 and Kv2.2, also named KCNB1 and KCNB2, are abundantly expressed in the brain and present in other tissues like muscle and pancreatic islets. The central part of the Kv2 channel is cytosolic, which forms large clusters in the ER-PM interface. The Kv2 is a delayed rectifier potassium channel, participates in the repolarization of neural action potentials (Murakoshi and Trimmer, 1999; Bishop et al., 2015). However, the clustered Kv2 channels do not readily conduct potassium (Lim et al., 2000; O'Connell et al., 2010), but involved in reshaping the ER-PM connections (Fox et al., 2015; Kirmiz et al., 2018a).

Kv2 channels are VAP-binding partners. They interact with VAPs through the C-terminal proximal restriction and clustering (PRC) domain (Lim et al., 2000; Johnson et al., 2019). This Kv2-VAP interaction mediates the ER-PM junctions responsible for Kv2 clustering (Johnson et al., 2018, 2019). The phosphorylation of serine residues in the PRC domain produces negative charges to enable VAP binding and control the clustering of Kv2 channels, which is the prerequisites for Kv2 channels-mediated ER-PM connections (Redman et al., 2007; Cobb et al., 2015; Johnson et al., 2018, 2019; Kirmiz et al., 2018b).

The clustering enables Kv2 channels to play a structural role in forming ER-PM junctions, and the non-conductive state is essential for avoiding electrically silencing neuronal activity (Fox et al., 2015). Hence, Kv2 clusters-induced ER-PM junctions could serve as a scaffold for other cell activities such as Ca^{2+} signaling and membrane trafficking. It has been reported Kv2.1 cluster promotes the coupling of PM L-type Ca^{2+} channels (LTCCs) and ER ryanodine receptor (RyR) Ca^{2+} release channels to generate partial Ca^{2+} release without the requirement of action potentials (Vierra et al., 2019). Recent studies revealed the Kv2.1 channels facilitate insulin exocytosis in pancreatic beta cells by their structural role of the clustering rather than the ability to conduct K^+. Kv2.1 clusters could be applied as a target for insulin secretion (Fu et al., 2017; Greitzer-Antes et al., 2018). Currently, the localization mechanism of Kv2 channels at ER-PM junctions has been primarily uncovered, but the physiological function is still unclear.

Extended Synaptotagmins (E-Syts)

E-Syts are integral membrane proteins anchored on the ER membrane. They are named by the similarity with synaptotagmins, key regulators in calcium-dependent vesicle fusion (Min et al., 2007). E-Syts are identified as a conserved family of tethering proteins at ER-PM contact sites. All E-Syts contain an N-terminal membrane anchor, followed by a synaptotagmin-like mitochondrial lipid-binding protein (SMP) domain and multiple C2 domains (**Figure 1B**) (Lee and Hong, 2006; Manford et al., 2012; Yu et al., 2016). While they are anchored to the ER membrane by the hydrophobic hairpin region, E-Syts can associate with the inner leaflet of the PM through their C-terminal C2 domains. The SMP domain is capable of harboring lipids, which we will discuss separately in the lipid exchange section.

The C2 domains are membrane-binding molecules representing a family of proteins with diverse functions (Rizo and Südhof, 1998). As for E-Syts, the C2 domains are connected in series to interact with acidic phospholipids on PM to mediate the ER-PM tethering. In mammals, E-Syt1 has five C2 domains, while E-Syt2 and E-Syt3 have three. The difference in numbers and characteristics of C2 domains among E-Syts leads to their distinct subcellular localization and tethering functions. E-Syt2 and E-Syt3 are located mainly at cortical ER. E-Syt1, by contrast, is broadly localized to the ER but migrate to ER-PM MCSs in response to elevated cytosolic Ca^{2+} (Min et al., 2007; Chang et al., 2013; Giordano et al., 2013; Idevall-Hagren et al., 2015). Cryo-ET studies indicated ER-PM contact sites mediated by E-Syts are structurally different from those bridged by STIM1 (Fernandez-Busnadiego et al., 2015). The average ER-PM distance at E-Syt3-mediated junctions is shorter than that observed at E-Syt1-mediated contact sites, although the latter could be shortened about 30% when cytosolic Ca^{2+} increases (Fernandez-Busnadiego et al., 2015). The C2C domain of E-Syt2/3 binds to PI(4,5)P2 through a conserved basic patch to constitutively maintain ER-PM contact sites. In contrast, the C2C domain of E-Syt1 interacts with PI(4,5)P2 upon Ca^{2+} binding to dynamically control the MCSs (Giordano et al., 2013; Idevall-Hagren et al., 2015; Saheki et al., 2016; Yu et al., 2016). In addition to ER-PM connections, E-Syts are also involved in the tethering of peroxisome-ER membrane contacts. They regulate cholesterol transport employing a similar C2C domain-PI(4,5)P2-binding mechanism (Xiao et al., 2019).

In yeast, the homologs of E-Syts are called tricalbins (Tcb1, Tcb2, and Tcb3) (Creutz et al., 2004; Schulz and Creutz, 2004; Lee and Hong, 2006). All the three tricalbins are major tethering contributors for ER-PM contact sites (Manford et al., 2012; Toulmay and Prinz, 2012). Recent studies showed tricalbins form curved cortical ER membrane with a requirement of C2 domains (Collado et al., 2019; Hoffmann et al., 2019). However, the detailed molecular mechanism of tricalbins in maintaining MCSs is still missing.

Plant SYT1 (synaptotagmin 1), the homolog of E-Syts in *Arabidopsis*, is enriched at ER-PM contact sites, especially the MCSs between immobile ER tubules and the PM (Yamazaki et al., 2010; Perez-Sancho et al., 2015; Ishikawa et al., 2018). The cortical ER network maintained by SYT1 correlates with the C2 domains, identical to E-Syts in mammals and tricalbins in yeast (Yamazaki et al., 2010). A recent study discovered that ionic stress could increase SYT1-mediated ER-PM connectivity by promoting the accumulation of PI(4,5)P2 on PM (Lee et al., 2019). These data suggest that the interaction between negatively charged lipids on PM and the C2 domains represents an evolutionarily conserved mechanism for E-Syt family proteins.

Ist2p

Ist2p is the yeast homolog of the TMEM16, an eight-span integrin in the ER. The structure of Ist2p contains a specific ion channel followed by a long cytoplasmic C-terminal region riches in lysine and histidine residues (**Figure 1B**) (Juschke et al., 2005; Maass et al., 2009; Brach et al., 2011). The cortical localization of Ist2p relies on its C-terminal region, which was defined as the cortical sorting signal (CSS) (Brach et al., 2011). The CSS fragment regulates Ist2p expression and transports the protein to the PM, where it interacts with PI(4,5)P2 to bring the cortical ER and the PM closer to 15–50 nm (Juschke et al., 2005; Fischer et al., 2009; Maass et al., 2009; Wolf et al., 2012). The loss of Ist2p leads to an increase in the distance between the ER and the PM, suggesting Ist2p is a determinant for the span of ER-PM connections (Ercan et al., 2009).

The sorting mechanism of Ist2p from the ER to PM-associated domains is somewhat similar to the recruitment of STIM. They both bind to phospholipids on PM through the C-terminal domain, suggesting the recruitment of integral membrane proteins to PM through specific protein-lipid interactions represents a common mechanism. Ist2p was reported to be associated with the H^+ pump Pma1 in the PM, allowing cells to adapt to different growth stages (Wolf et al., 2012). A recent study showed Ist2p and the LTP Osh6p are co-localized at ER-PM connections. Ist2p interacts with Osh6p to target the latter to the ER-PM contact sites, and they jointly participate in the lipid transport between the ER and the PM (D'Ambrosio et al., 2020).

While the function of Ist2p in yeast has been extensively studied, we currently still know little about its mammalian homolog TMEM16 (Hartzell et al., 2009). The two isoforms TMEM16A and TMEM16B, have recently been identified as calcium-activated chloride channels (Ercan et al., 2009; Xiao et al., 2011). However, whether TMEM16 and Ist2p have conserved functions at ER-PM contact sites remains to be clarified (Kunzelmann et al., 2016).

Sec22b-Syntaxin1

SNARE proteins represent a superfamily in which the members share a conserved SNARE motif with about 60–70 residues. They are the core engine of intracellular vesicle fusion. SNAREs can be classified as Q-SNAREs and R-SNAREs. Membrane fusion is initiated when one R-SNARE on the vesicle pairs with three t-SNAREs on the target membrane to form a four-helix trans-SNARE complex (Sutton et al., 1998; Weber et al., 1998). Sec22 has three isoforms in mammals as Sec22a, Sec22b, and Sec22c. Only Sec22b has a SNARE motif and is conserved in yeast (Sun et al., 2020). Sec22b belongs to the R-SNARE family. It anchored

to ER through a C-terminal transmembrane domain right after the SNARE motif. In addition to the coiled-coil SNARE motif and transmembrane domain, Sec22b contains an N-terminal longin domain conserved with a profilin-like folded structure (**Figure 1B**) (Fasshauer, 2003; Hong, 2005; Jahn and Scheller, 2006). The SNARE motif and longin domain of Sec22b may play essential roles in vesicular transport between the ER and the Golgi apparatus. While the SNARE motif forms four helixes with its cognate t-SNAREs, the longin domain regulates the membrane fusion by interaction with the SNARE motif (Daste et al., 2015).

Distinct to its traditional function on membrane fusion, Sec22b has another non-fusogenic role in PM expansion (Petkovic et al., 2014). It can interact with syntaxin1 to form a partial but tight SNARE complex, which could not drive the membrane fusion due to the absence of SNAP25. However, this kind of non-fusogenic SNARE bridge tethers the ER to the PM, and more interesting, this tethering function is conserved in yeast. The yeast Sec22p and Sso1p (the homolog of syntaxin1) interact with Osh2p and Osh3p to regulate non-vesicular lipid transport between the ER and the PM. The existence of these SNARE-mediated junctions can shorten the distances and improve the efficiency of lipid transport (Prinz, 2010; Petkovic et al., 2014). In the mammalian nervous system, one latest research found the Sec22b-syntaxin1 complex can interact with E-Syts and form a ternary complex that plays a vital role in PM expansion and axon growth (Gallo et al., 2020). Together, the Sec22b-syntaxin1 complex plays a role in the tethering of the ER to the PM, from which it indirectly participate in the regulation of lipid metabolism and contribute to PM extension and other physiological processes (Petkovic et al., 2014; Gallo et al., 2016).

Versatile Tethering Regulators

Besides these representative tethering factors, there are many other versatile regulators at ER-PM contact sites. These regulators tether the ER and the PM when they perform their critical cellular functions, for example, the Ca^{2+} dynamics regulator stromal interaction molecule 1 (STIM1). Interestingly, STIM1-mediated membrane tethering is Ca^{2+}-dependent. In response to the low concentration of Ca^{2+}, The ER-anchored STIM1 oligomerizes and recognizes the PM polyphosphoinositides and Orai1 (Liou et al., 2007; Zhou et al., 2013). This action coordinatively regulates the membrane tethering and Ca^{2+} homeostasis. Another type of versatile-tethering protein is LTPs, which couple the membrane tethering and lipid metabolisms. Most LTPs anchor the ER through the transmembrane domain or VAP interactions while target the PM using protein-lipid interactions (Kim et al., 2015; Ghai et al., 2017; Naito et al., 2019). The mechanisms of these regulators will be discussed in the following sections.

Together, a variety of regulators have the ability of membrane tethering at ER-PM contact sites. They bridge the two membranes *via* diverse connections. Some connections are constant to maintain the primary cortical ER network, while the others are dynamically regulated to perform demanded functions. As the foundation of ER-PM contacts, all these tethering molecules coordinate to modulate the cellular processes through the fine tune of MCSs.

REGULATION OF Ca^{2+} DYNAMICS AT ER-PM CONTACT SITES

As an important second messenger, Ca^{2+} is essential for many cellular and physiological processes, including gene transcription, protein modification, lipid metabolism, cell growth, and apoptosis (Stathopulos et al., 2006; Soboloff et al., 2012). So that precise and dynamic controls are needed to ensure calcium ions play proper functions at a specific time or place (Stathopulos et al., 2006). The cytoplasmic Ca^{2+} signals are generated by releasing Ca^{2+} from the calcium pool or the extracellular Ca^{2+} influx. The store-operated calcium entry (SOCE), a concept proposed in the 1990s, is a ubiquitous Ca^{2+} influx pathway at the ER-PM contact sites (Putney, 1986, 1990; Patterson et al., 1999; Yao et al., 1999). The Ca^{2+} entry is triggered when Ca^{2+} stores in the ER lumen depleted and the cytosolic Ca^{2+} concentration is at a low level. STIM proteins and Orai channels (**Figure 2A**) are the foundation proteins in the regulation of SOCE and Ca^{2+} signals (Liou et al., 2005; Roos et al., 2005; Feske et al., 2006; Vig et al., 2006; Zhang et al., 2006).

STIM-Orai Complexes

STIM crosses the ER membrane and senses Ca^{2+} in the cavity of the ER (Williams et al., 2001; Zhang et al., 2005; Feske et al., 2006). Orai is a Ca^{2+} release-activated Ca^{2+} channel on PM (Chakrabarti and Chakrabarti, 2006; Prakriya et al., 2006; Soboloff et al., 2006a). Upon Ca^{2+} depletion, STIM protein interacts with Orai and initiates SOCE (Carrasco and Meyer, 2011; Zhou et al., 2013; Balla, 2018). There are two STIM proteins in mammals: STIM1 and STIM2. Both of them are mainly located at the ER with a similar structure (Hogan and Rao, 2015). STIM is anchored to the ER *via* a transmembrane domain, with an N-terminal domain in the ER lumen and a C-terminal domain in the cytoplasm (**Figure 2B**). The expression pattern of STIM1 and STIM2 are different. In most tissues, the expression level of STIM1 is higher than STIM2 in support that STIM1 is the predominant STIM protein that regulates the influx of Ca^{2+} in non-excitable cells (Soboloff et al., 2006b; Collins and Meyer, 2011; Hogan and Rao, 2015; Prakriya and Lewis, 2015).

STIM has the EF-hand and stereo alpha motif (SAM) domains in the lumen of the ER. Its cytoplasmic side contains several coiled-coil domains and a CRAC activation domain (CAD, also known as the STIM-Orai activation region, Or SOAR) (Manji et al., 2000; Yang et al., 2012; Prakriya and Lewis, 2015). In the presence of Ca^{2+}, the EF-hand domains are tightly bound to the SAM domain. Therefore, the STIM protein exists as a monomer and in an inactive state, in which the nearby coiled-coil domain blocks CAD/SOAR. When the ER calcium pool is exhausted, the STIM protein senses Ca^{2+} change (Yuan et al., 2009). The structure of the EF-SAM domain becomes loose and stretched. STIM proteins dimerize from the ER lumen side to the cytoplasm and further form oligomers. These activated STIM1 oligomers interact with PI(4,5)P2 and the Orai channel through the released CAD/SOAR domain to accurately mediate the Ca^{2+} influx (Park et al., 2009; Ma et al., 2015; Prakriya and Lewis, 2015).

Although occupying a similar structure, the EF-SAM domains from STIM1 and STIM2 show different affinity to Ca^{2+}. STIM1

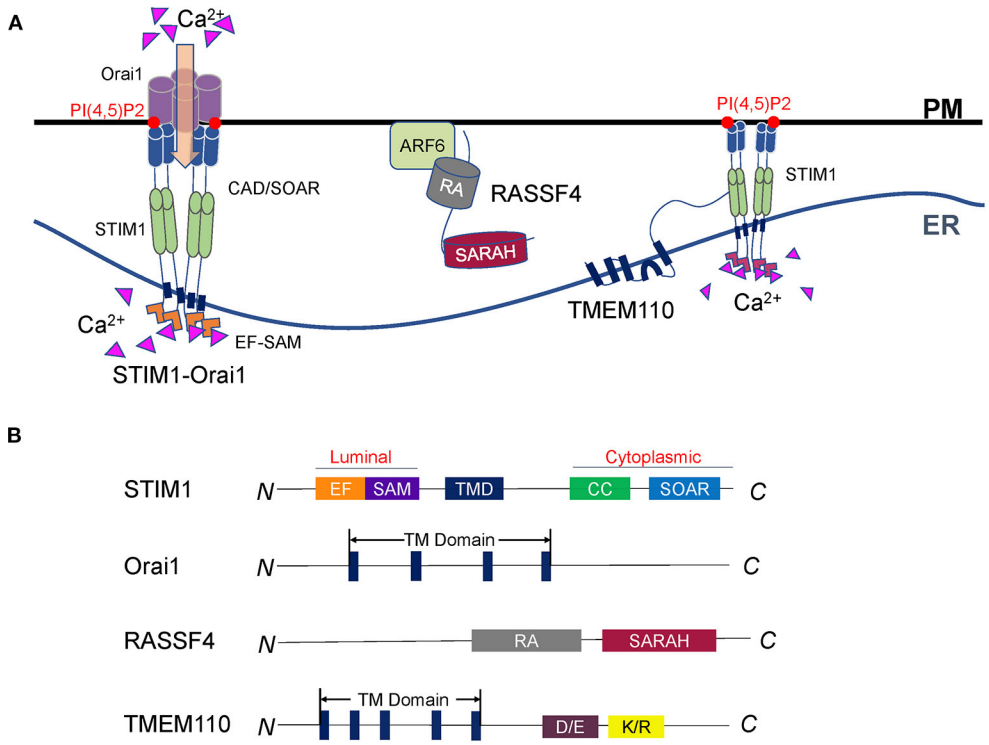

FIGURE 2 | Regulation of Ca^{2+} dynamics at ER-PM contact sites. **(A)** Representative illustration of the STIM-Orai complex and its regulators. STIM1 in the ER and Orai1 on the PM compose the core machinery of SOCE. STIM1 senses the Ca^{2+} change in the ER lumen and forms oligomers. The STIM1 oligomers bind to polyphosphoinositides and activate Orai1 to import extracellular Ca^{2+}. RASSF4 regulates SOCE and ER-PM junction through the control of the PM PI(4,5)P2 level, which is essential for the localization of STIM1. TMEM110 is an ER membrane protein that physically interacts with STIM1 to reshape ER-PM connections and facilitate STIM1 conformational conversion. Future studies are required to discover more STIM interacting partners, which is important to understand STIM proteins' sensing and coupling mechanisms. **(B)** Diagrams of the SOCE regulators described in A. The major functional domains are shown in each of the proteins.

is in a state of autoinhibition at rest but highly active upon Ca^{2+} depletion. STIM2 is more sensitive to tiny changes in the ER calcium store due to its low Ca^{2+} affinity, thus could be activated in response to less Ca^{2+} change (Zheng et al., 2011; Soboloff et al., 2012; Hogan and Rao, 2015). The different biophysical characteristics of STIM1 and STIM2 enable cells to sense changes in intracellular Ca^{2+} concentration accurately and take further actions (Brandman et al., 2007; Prakriya and Lewis, 2015). It seems reasonable that the basal Ca^{2+} homeostasis maintenance at rest is the primary responsibility of STIM2 (Wang et al., 2009; Kar et al., 2012). However, no significant change of Ca^{2+} level was observed in the calcium store of STIM2 KO cells at rest. In some tissues, for example, the neuronal cells and dendritic cells, the expression of STIM2 is significantly higher than STIM1, suggesting STIM2 may have other functions than the regulation of basal Ca^{2+} homeostasis (Williams et al., 2001; Oh-Hora et al., 2008; Prakriya and Lewis, 2015).

Many proteins around the STIM-Orai complex participate in SOCE. It is worth noted that SOCE recruits E-Syt1 to ER-PM junctions and rearranges adjacent ER structures into circular MCSs, which in turn stabilizes STIM-Orai clusters and accelerates Ca^{2+} replenishment (Kang et al., 2019). Another recent study showed ER protein Anoctamin 8 (ANO8) is translocated to STIM1-Orai1-mediated contact sites in a PI(4,5)P2-dependent manner. ANO8 further recruits the ER-localized SERCA (Sarco/endoplasmic reticulum Ca^{2+}-ATPase) Ca^{2+} pump to replenish the Ca^{2+} reservoir, which may inactivate SOCE and regulate the receptor-stimulated Ca^{2+} signaling (Jha et al., 2019; Stefan, 2020).

RASSF4

The RAS association domain family (RASSF) consists of 10 members (RASSF1-10) localized at the cytoplasmic side of the PM. RASSF4 contains a C-terminal RAS association (RA) domain linked to a Sav-RASSF-Hpo (SARAH) domain (**Figure 2B**) (Chan et al., 2013; Iwasa et al., 2013). While the RA domain mediates the interactions with RAS GTPases, the SARAH domain was reported to facilitate dimerization between SARAH domain-containing proteins (Chan et al., 2013).

At ER-PM contact sites, RASSF4 acts in concert with ARF6, the upstream regulator of type I phosphatidylinositol phosphokinase (PIP5K), to regulate PI(4,5)P2 levels on the PM (Chen et al., 2017). Since PI(4,5)P2 is essential to position STIM1 and E-Syts, RASSF4 participates in the regulation of SOCE and ER-PM junctions indirectly through the regulation of PI(4,5)P2 homeostasis (Dickson, 2017).

TMEM110

ER-resident transmembrane protein 110 (TMEM110) is a STIM-activating enhancer (STIMATE). It contains 4–5 transmembrane domains, co-localized with STIM (**Figure 2B**). TMEM110 can remodel the short-term physiological junctions and relocate STIM1. Overexpression of TMEM110 leads to the formation of large STIM aggregates, while knockdown of this gene reduces STIM1 puncta at the ER-PM junctions (Jing et al., 2015; Quintana et al., 2015).

Furthermore, TMEM110 could physically interact with STIM1 and interfere with the autoinhibition of CAD/SOAR. When the Ca^{2+} storage is exhausted, STIM1 converts its conformation, facilitating the TMEM110 C-terminus interaction with the coiled-coil domain of STIM1. It releases the autoinhibition of CAD/SOAR and activates Ca^{2+} channel Orai (Hooper and Soboloff, 2015; Jing et al., 2015). Overall, TMEM110 is an ER protein that cooperates with STIM to reshape ER-PM connections and regulate calcium signaling dynamically. These studies indicate the STIM-Orai signaling heavily relies on proteins that regulate the ER-PM connections or the STIM conformation.

ENZYMES AT ER-PM CONTACT SITES

MCSs are ideal platforms to exchange molecules and local signals between organelles, dependent on their carriers or enzymes. Many protein enzymes, especially the phosphatases, play critical regulatory roles in ER-PM contact sites (**Figure 3A**) (Saheki and De Camilli, 2017a). They can catalyze substrates either in *cis* or in *trans* to participate in the regulatory network of many cellular processes such as cyclic adenosine 3′,5′-adenosine monophosphate (cAMP) signaling, calcium dynamics, and lipid metabolism.

AC3/8

Adenylate cyclase (AC) is an important signaling molecule downstream of G protein-coupled receptors. It is located on the PM *via* two multi-transmembrane domains and contains two catalytic domains (**Figure 3B**) (Cooper et al., 1995; Cooper and Crossthwaite, 2006; Dessauer et al., 2017). AC regulates cAMP, thereby participating in various physiological processes. Nine AC subtypes have been identified in mammals. Among them, the AC3 and AC8 are located at ER-PM junctions, and both of their activities are regulated by Ca^{2+}. AC3 regulates blood glucose homeostasis, which makes it a new target for the development of anti-obesity drugs. However, AC8 plays a crucial role in neuroplasticity rather than in glucose regulation (Zachariou et al., 2008; Bogard et al., 2014; Wu et al., 2016).

Inside the cell, many signals transmit between the ER and the PM. In addition to the SOCE-regulated Ca^{2+} signal, cAMP is another vital signal which usually functions as a second messenger. At the ER-PM junctions, AC3 is an enzyme that relies on STIM1. STIM1 interacts with AC3 and generates cAMP, and this process is called storage operational cAMP signaling (SOcAMPS) (Lefkimmiatis et al., 2009; Maiellaro et al., 2012; Willoughby et al., 2012). AC8 directly interacts with Orai1 to alter the Ca^{2+} microenvironment under the PM, which in turn activates AC8 and produces cAMP (Willoughby et al., 2010, 2012). The dynamic interaction between Ca^{2+} and cAMP signals at the ER-PM junctions represents an important scenario of cell homeostasis and plays vital roles in physiology and pathology (Lefkimmiatis et al., 2009; Maiellaro et al., 2012; Willoughby et al., 2012; Okeke et al., 2016).

Sac1

Localized on the ER and Golgi apparatus, suppressor of actin 1 (Sac1) is a phosphoinositide phosphatase whose protein sequence and function are both highly conserved in yeast and mammals. In mammals, Sac1 protein commonly expresses in adult and embryonic tissues (Del Bel and Brill, 2018). The C-terminal region anchored Sac1 to the ER. A conserved catalytic CX5R (T/S) motif in the N-terminal domain enables Sac1 to have a catalytic function (**Figure 3B**) (Manford et al., 2010; Saheki and De Camilli, 2017a). The role of Sac1 is to remove phosphoric acid from the inositol ring to balance the level of PI(4)P (Del Bel and Brill, 2018).

Primarily as a PI(4)P phosphatase between the ER and the PM, Sac1 was proposed to either act in *trans* on the opposed PM PI(4)P or act in *cis* on the ER PI(4)P (Manford et al., 2010; Stefan et al., 2011; Mesmin et al., 2013). In the latter, ORP5/8 (Osh6p/7p in yeast) transfers PM PI(4)P to the ER, where Sac1 dephosphorylates the lipid on the same ER membrane. Sac1-catalyzed PI(4)P hydrolysis is essential to maintain PI(4)P concentration gradient, which facilitates the continuous exchange of PI(4)P/PS between the ER and the PM (Chung et al., 2015; Moser von Filseck et al., 2015b; Del Bel and Brill, 2018). Therefore, Sac1 indirectly controls the lipid metabolism where the ER and the PM are in close contact.

However, PI(4)P alone is insufficient to localize Sac1 to the ER-PM contact sites. Other proteins that connect the ER and the PM may jointly participate in the Sac1 localization. For example, the activated SOCE increases the amount of Sac1 in contact with the PM, while disruption of E-Syt2-mediated ER-PM junctions reduces the access of Sac1 on the PM (Dickson et al., 2016). Sac1 was found co-localized with E-Syt2 at ER-PM contact sites. E-Syt2 narrows ER and PM distance, which may restrict Sac1 to the right position. Sac1 consumes PI(4)P in this microdomain and thus produces the PI(4)P gradient (Dickson et al., 2016). However, it is still uncertain whether E-Syt2 directly interacts with Sac1.

PTP1B

Protein tyrosine phosphatase 1B (PTP1B) is a non-receptor phosphatase and belongs to the PTP family. First isolated from the human placenta, PTP1B is anchored to the surface of the ER membrane *via* a C-terminal fragment composed of 35 proline-rich residues (Frangioni et al., 1992). The N-terminus of PTP1B protein contains the catalytic domain with two proline-rich motifs (**Figure 3B**). PTP1B plays a catalytic function at ER-PM junctions by dephosphorylation of its substrates located on the PM through the cytosolic catalytic domain (Anderie et al., 2007).

PTP1B has several identified substrates. These substrates have diverse functions that make PTP1B play various roles in cellular physiology. For example, ER-bound PTP1B dynamically interacts

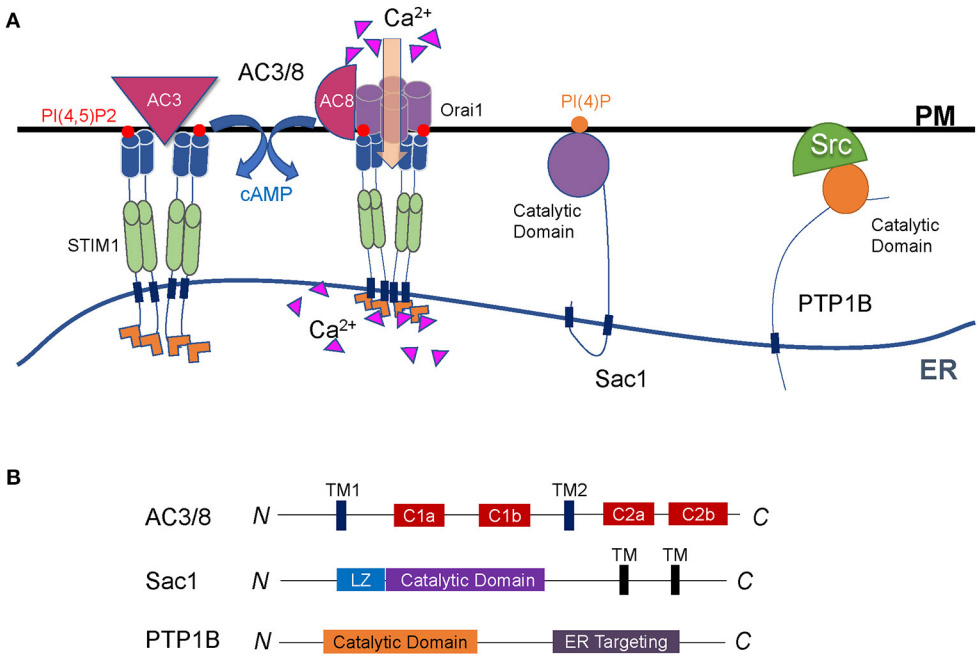

FIGURE 3 | Regulation of cell signaling by enzymes at ER-PM contact sites. **(A)** Representative illustration of enzymes functioning at the interface between the ER and the PM. Both AC3 and AC8 are located on the PM through multiple transmembrane domains. AC3 interacts with STIM1, and AC8 binds directly to Orai1. They are both regulated by Ca^{2+} signals to produce cAMP. Sac1 is a conserved PI(4)P phosphatase anchored to the ER and can dephosphorylate PI(4)P both on the PM and in the ER membrane. PTP1B is anchored to the ER membrane *via* a C-terminal fragment and dephosphorylates its substrates on the PM through the cytosolic catalytic domain. **(B)** Diagrams of the enzymes described in A. The major functional domains are shown in each of the proteins.

with the protein tyrosine kinase Src on the PM, controls Src activation, and recruits adhesion complexes (Monteleone et al., 2012). PTP1B also plays roles in tumor growth, metastasis, and metabolism. It has double-sided effects with either promoting or suppressing cancer in tumor tissues, depending on the active substrate and cell environment (Lessard et al., 2010). Exploring the roles of PTP1B in individual tumors will provide new ideas for the diagnosis and treatment of tumors. The insulin signaling pathway and glucose metabolism is another process that PTP1B negatively regulates. The tyrosine-phosphorylated insulin receptor, insulin receptor substrate-1, and AKT are all possible targets of PTP1B (Abdelsalam et al., 2019). Targeting PTP1B is considered a strategy to treat insulin resistance and type 2 diabetes by improving insulin sensitivity (Hussain et al., 2019).

LIPID EXCHANGES AT ER-PM CONTACT SITES

The ER is the central organelle that synthesizes various lipids such as phospholipids and cholesterol, which need to be transported to or exchanged with other organelles and PM. Unlike the bulk lipid transports mediated by vesicle fusion, LTPs are able to sense and transport particular lipids between organelles that are mostly happened within a short distance like at the MCS regions (Wong et al., 2019). The ER forms extensive membrane junctions with the PM where LTPs play vital roles in the regulation of lipid metabolism as well as other physiological processes (**Figures 4A,B**) (Kentala et al., 2016; Saheki and De Camilli, 2017a; Cockcroft and Raghu, 2018; Jeyasimman and Saheki, 2019; Stefan, 2020).

SMP Domain Proteins

SMP domain proteins are evolutionarily conserved in eukaryotes. The SMP domain was first discovered in 2006 by the sequence analysis of a mitochondrial integral membrane protein. Later it was identified as a member of the superfamily of tubular Lipid-binding (TULIP) domain-containing proteins that have the ability to harbor lipids in the hydrophobic cavity (Kopec et al., 2010; Alva and Lupas, 2016). SMP domain proteins are commonly localized at MCSs formed by organelles and play versatile functions such as lipid transport, Ca^{2+} homeostasis, and signaling (Saheki and De Camilli, 2017a).

Benefited from the SMP domain, E-Syts are considered as LTPs at ER-PM contact sites (Giordano et al., 2013; Saheki and De Camilli, 2017b). The crystal structure of E-Syt2 showed SMP domain forms a dimer of approximately nine nm-long cylinders that harbors glycerolipids without selectivity (Schauder et al., 2014). E-Syt1, E-Syt-2, and E-Syt-3 have been demonstrated to form homo- and heterodimers inside the cell (Giordano et al., 2013). By the *in vitro* reconstituted system, E-Syt1 was identified as a Ca^{2+} dependent LTP, which directly transfers glycerophospholipids and DAG between the ER and the PM (Saheki et al., 2016; Yu et al., 2016). The SMP dimer is indispensable for E-Syt1 to transfer lipids. Considering the length of SMP dimer is far less than the average distance between

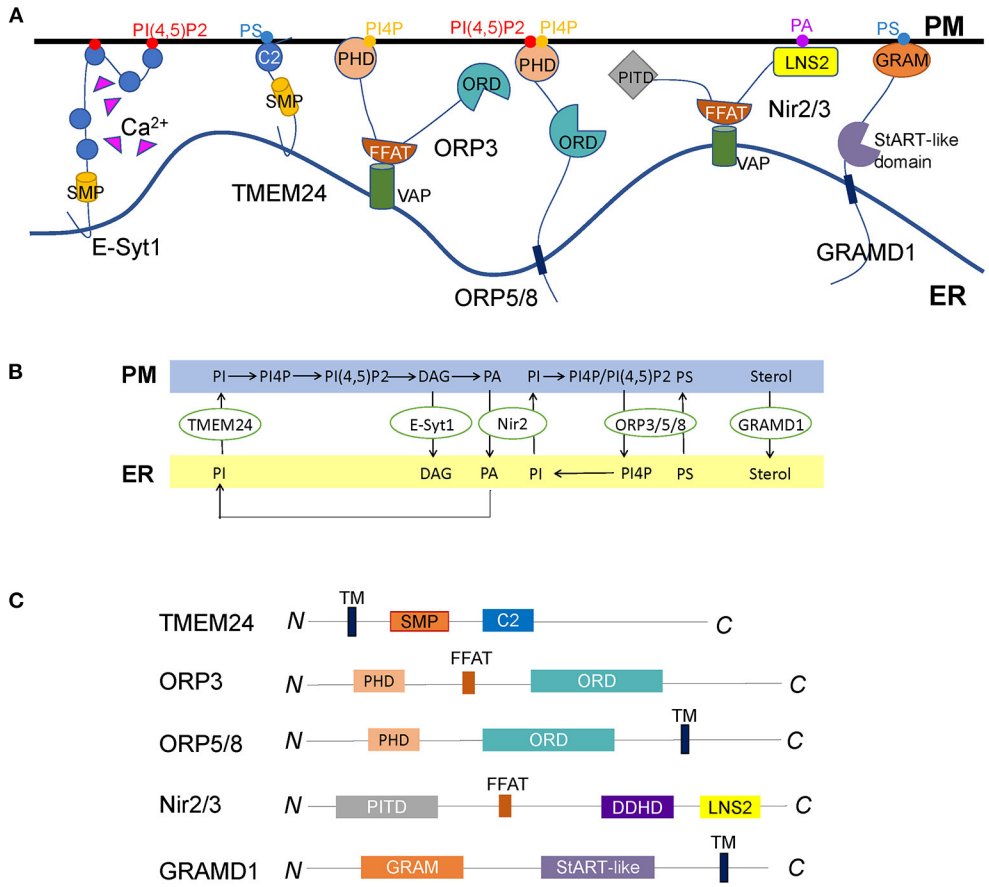

FIGURE 4 | Diverse LTPs functioning at the ER-PM contact sites. **(A)** Representative illustration of LTPs located at the ER-PM junctions. E-Syt1 transfers phospholipids and DAG directly through the SMP domain between the ER and the PM, regulated by interactions of the C2 domains with Ca^{2+}. TMEM24 is another SMP domain protein localized to the ER through a transmembrane domain. It transfers PI from the ER to the PM controlled by the dephosphorylation of the C-terminal polybasic region. Whether other SMP domain proteins, for example, E-Syt2/3 and tricalbins, mediate lipid transport at ER-PM contact sites remains unknown. ORP3, ORP5, and ORP8 are so far discovered ORPs at ER-PM contact sites. While ORP5 and ORP8 are ER membrane proteins, ORP3 is anchored to the ER through the interaction of its FFAT motif with VAP. All the three ORPs contain a PHD to interact with the PM lipids and an ORD to exchange PI(4)P/PI(4,5)P2 and PS between the ER and the PM. It remains elusive why the cell has three ORPs at ER-PM contact sites to mediate the same lipids. The discovery of the initial triggers of these LTPs might solve this problem. Nir2 and Nir3 are anchored to the ER *via* interactions of FFAT motifs with VAPs and connect to the PM by LNS2 domains, facilitating the PI and PA exchange between the two membranes. How other tethering molecules, such as E-Syts and Kv2s, couple with Nir2/3 to mediate PA/PI exchange need to be further explored. GRAMD1s are anchored to the ER *via* a C-terminal transmembrane domain and interact with cholesterol and PS on the PM through the N-terminal GRAM domain to connect the two opposed membranes. Thus, the accessible cholesterol is transported from the PM to the ER by StART-like domains. Whether there are other sterol transfer proteins transporting PM cholesterol to the ER or other organelles remains to be discovered. **(B)** The summary of LTPs-mediated lipid exchange at ER-PM contact sites. **(C)** Diagrams of the lipid transfer proteins described in A, except E-Syt1, are shown in **Figure 1B**. The major functional domains are shown in each of the proteins.

the ER and the PM, the "shuttle model" in which SMP dimer shuttles between the ER and the PM to transport lipids is more acceptable. This shuttle model was further supported by an artificially designed assay using the DNA-origami nanostructures to define precise distances between membranes (Bian et al., 2019).

In addition to the SMP domain, the C2 domains in E-Syt1 are also essential to regulate lipid transfer (Saheki et al., 2016; Yu et al., 2016; Bian et al., 2018). At least, both the C2A and C2C domains are indispensable in E-Syt1-mediated lipid transport (Saheki et al., 2016; Yu et al., 2016; Bian et al., 2018). The C2C domain is the predominant region for membrane tethering, facilitating lipid transport by shortening the distance. The C2A domain was proposed as an autoinhibitory domain that inactivates the SMP domain. Ca^{2+} releases this autoinhibition to enable lipid transport (Bian et al., 2018). Recent studies in yeast demonstrated SMP domain and C2 domains of tricalbins act in concert to form highly curved ER peaks on the cortical ER membrane facing the PM, raising a possibility that the C2A domain involves in the interaction with the ER membrane to facilitate the lipid transport (Collado et al., 2019; Hoffmann et al., 2019).

Although the membrane tethering function of the E-Syt family is conserved in eukaryotes, it was unclear whether all family members are capable of transporting lipids between the ER and

PM. Only E-Syt1 in mammalian cells was identified to mediate lipid exchange directly. Although the locations of E-Syt2 and E-Syt3 at ER-PM contact sites are not affected by Ca^{2+}, Ca^{2+} does bind to their C2A domains and induce a local protein conformational transition (Xu et al., 2014). Whether E-Syt2 and E-Syt3 directly mediate lipid exchange are still open questions to the field.

As a highly conserved protein family, E-Syts likely play essential roles in cell physiology. Unexpectedly, they're non-essential proteins. No obvious defects were observed in E-Syts triple knockout mice (Sclip et al., 2016; Tremblay and Moss, 2016). Neither mammalian cells lacking E-Syts nor yeast cells lacking tricalbins showed significant abnormalities (Manford et al., 2012; Toulmay and Prinz, 2012; Saheki et al., 2016). Given that many factors coordinate at ER-PM junctions, one possible explanation could be the functional redundancy. Other factors may replace the function of E-Syts once the latter is omitted (Saheki, 2017). However, E-Syts and tricalbins do have physiological effects. For example, E-Syts can maintain PM lipid homeostasis, promote nerve transmission and synaptic growth, modulate virus-induced membrane fusion, mediate the endocytosis of FGFR, and play roles in insulin secretion and diet-induced obesity development (Saheki et al., 2016; Tremblay et al., 2016; Kikuma et al., 2017; El Kasmi et al., 2018; Xie et al., 2019; Nath et al., 2020; Zhang et al., 2020). Tricalbins act in maintaining PM integrity (Toulmay and Prinz, 2012; Collado et al., 2019). More interesting, plant SYT1 is required for withstanding mechanical stress, maintaining cell membrane integrity and virus movement, suggesting this protein family is of importance to cell physiology (Min et al., 2007; Chang et al., 2013; Giordano et al., 2013; Idevall-Hagren et al., 2015).

Transmembrane protein 24 (TMEM24) is another SMP domain protein localized at ER-PM contact sites. It is anchored to the ER membrane through an N-terminal transmembrane domain, followed by an SMP domain, a C2 domain, and a polybasic C-terminal region (**Figure 4C**). TMEM24 is involved in regulating insulin secretion and neuronal excitability (Pottekat et al., 2013; Lees et al., 2017; Sun et al., 2019). Like E-Syts, the SMP domain forms a dimer in TMEM24, and each SMP domain binds one lipid molecule, one less than that in E-Syt2 (Schauder et al., 2014; Lees et al., 2017). TMEM24 selectively transports PI from the ER to the PM, supplying PM with PI(4,5)P2 during signal transductions. This process is regulated by protein kinase C (PKC)-dependent phosphorylation of the C-terminal PM binding regions in response to cytosolic Ca^{2+} (Lees et al., 2017).

Glucose-stimulated insulin secretion is regulated by the inositol phosphate signaling pathway and Ca^{2+}. While TMEM24 transfers the PI(4,5)P2 precursor PI from the ER to the PM, E-Syt1 clears the PI(4,5)P2 metabolite DAG on PM. Since the dissociation of TMEM24 from PM is controlled by PKC-mediated phosphorylation, and E-Syt1 regulates PKC activity, E-Syt1 is considered an indirect regulator of TMEM24 (Xie et al., 2019). Both of them play a role in phosphoinositide metabolism and Ca^{2+} homeostasis, thus indirectly regulate insulin secretion in pancreatic β cells (Xie et al., 2019).

ORPs

The oxysterol-binding protein (OSBP) and its related proteins (ORPs) compose a conserved family that mediates non-vesicular lipid transports at the MCSs (Im et al., 2005; de Saint-Jean et al., 2011; Olkkonen and Li, 2013; Du et al., 2015). There are two conserved domains in this protein family, the PHD and OSBP-related domain (ORD). The PHD plays a role in membrane docking by interactions with anionic lipids such as phosphatidylserine (PS), PI(4)P, and PI(4,5)P2. The ORD is a ligand binding and lipid exchange domain (Kentala et al., 2016; Cockcroft and Raghu, 2018). Besides, ORPs have either an FFAT domain or a transmembrane domain through which they are located on the surface of membranous organelles, including the ER (Mesmin et al., 2013; Pulli et al., 2018).

ORP3, ORP5, and ORP8 are ORPs mainly localized at ER-PM contact sites in mammals. ORP5 and ORP8 possess a single C-terminal transmembrane domain that anchors them on the ER surface and a PHD to interact with the PM (**Figure 4C**). They were reported to mediate the PI(4)P/PS exchange cycle that transfers PS from the ER to the PM and move PI(4)P from the PM to the ER. Sac1 depletes PI(4)P and generates a PI(4)P gradient to drive this exchange (Chung et al., 2015; Moser von Filseck et al., 2015b; Dickson et al., 2016). However, another study showed PI(4,5)P2, rather than PI(4)P is the critical lipid for the targeting of ORP5 and ORP8 to the PM (Ghai et al., 2017). Besides ER-PM contact sites, ORP5 and ORP8 are also localized at other MCSs such as ER-mitochondria and ER-lipid droplet contact sites (Galmes et al., 2016; Du et al., 2020). Unlike ORP5 and ORP8, ORP3 is anchored to the ER *via* its FFAT motif that interacts with VAP protein (**Figure 4C**). Recent studies uncovered that ORP3 is capable of regulating PI(4)P homeostasis and Ca^{2+} dynamics by activating PKC (Dong et al., 2020; D'Souza et al., 2020; Gulyás et al., 2020).

In yeast, the conserved ORP family is called oxysterol-binding homology (Osh) protein. At ER-PM contact sites, Osh6p and Osh7p mediate the exchange of PI(4)P and PS fueled by PI(4)P metabolism, similar to the ORP5 and ORP8 in mammals (Maeda et al., 2013; Moser von Filseck et al., 2015a). Osh3p is more like ORP3 in mammals, which binds PI(4)P and recruits the Sac1p to ER-PM contact sites to regulate the PM PI(4)P levels (Stefan et al., 2011; Tong et al., 2013; Omnus et al., 2020). These studies demonstrated that phosphoinositides, mainly the PI(4)P and PI(4,5)P2, are common lipid ligands for the ORP family localized at ER-PM contact sites. Although 12 conserved members have been identified in *Arabidopsis*, the functions of ORPs in plant lipid metabolism are still poorly understood (Skirpan et al., 2006). Whether the functions and mechanisms of ORPs discovered in mammals and yeast are conserved in plants remain to be determined.

ORPs localized at ER-PM contact sites play multiple roles in cell physiology. For example, Osh2p and Osh3p interact with Myo5p and Scs2p to bridge the ER contact with endocytic areas and facilitate actin polymerization (Encinar Del Dedo et al., 2017). ORP3 participates in Ca^{2+} homeostasis and cell adhesion (Lehto et al., 2008). ORP5 and ORP8 can regulate cancer growth, making them potential drug targets for cancer therapy (Ishikawa et al., 2010; Guo et al., 2017).

TABLE 1 | Summary of the proteins functioned at ER-PM contact sites.

Proteins			Locations	Comments
Mammalians	Yeast	Plants		
VAP-A VAP-B	Scs2p Scs22p	VAP27-1 to-10	ER	VAPs are ER membrane proteins that dynamically tether the PM through its binding partners
Kv2	—	—	PM	The clustered Kv2 channels reshape the ER-PM connections by the interaction with VAPs
E-Syt1 E-Syt2 E-Syt3	Tcb1 Tcb2 Tcb3	SYT1	ER	The C2 domains play essential roles in the tethering function of E-Syt protein family. E-Syt1 bidirectionally transfers phospholipids and DAG. Whether other E-Syt proteins directly transfer lipids remain unknown
TMEM16	Ist2p	—	ER	The interaction of Ist2p with PI(4,5)P2 brings the ER and the PM closer to 15-50 nm. Whether TMEM16 has similar functions remains unknown
Sec22b-syntaxin1	Sec22p-Sso1p	—	ER-PM	The two proteins form a non-fusogenic SNARE bridge between the opposed membranes
STIM1-Orai1	—	—	ER-PM	In SOCE, STIM1 senses the Ca^{2+} level and acts as a switch for Orai1 to import external Ca^{2+}. The mechanism and physiological function of STIM1-Orai1 needs a further study
RASSF4	—	—	PM	RASSF4 is a regulator of PI(4,5)P2 homeostasis that further regulates SOCE
TMEM110	—	—	ER	TMEM110 is a STIM-activating enhancer
AC3/8	—	—	PM	AC3 and AC8 interact with STIM1 and Orai1 separately to produce cAMP
Sac1	—	—	ER	Sac1 dephosphorylates PI(4)P to regulate phosphoinositide metabolism
PTP1B	—	—	ER	PTP1B dephosphorylates its substrates on the PM, and plays roles in glucose metabolism, and other physiological processes
ORP3 ORP5 ORP8	Osh2p Osh3p Osh6p Osh7p	ORPs	ER	ORPs located at ER-PM contact sites mediate the exchange of PI(4)P/PI(4,5)P2 with PS, their individual mechanism needs to be further studied. The functions of ORPs in plants are still not clear
TMEM24	—	—	ER	TMEM24 transfers PI from the ER to the PM
Nir2 Nir3	—	—	ER	Nir2 and Nir3 exchange PI and PA between the ER and the PM
GRAMD1s	—	—	ER	GRAMD1s contribute to PM sterol homeostasis

Nir2/3

Nir2 and Nir3 belong to the PI transfer protein (PITP) family, a class of central players involved in phospholipid homeostasis at ER-PM contact sites. They are the mammalian ortholog proteins of Drosophila retinal degeneration B (rdgB), which was proven to transfer PI and phosphatidylcholine (PC) between membrane bilayers (Amarilio et al., 2005). The structure of Nir2/3 contains a PI-transfer domain at the very N-terminus, then followed by an FFAT motif, six hydrophobic stretches, and a C-terminal LNS2 domain (**Figure 4C**). Nir2/3 is anchored to the ER through the binding of the FFAT sequence to the VAP protein and connects with PM by the interaction of the LNS2 domain with phosphatidic acid (PA) (Kim et al., 2013; Balla, 2018).

PA and PI are interconverted lipid second messengers that play roles in many signaling pathways, coupled by the Nir2/rdgB family. Phospholipase C (PLC) hydrolyses PI(4,5)P2 to generate DAG and its phosphorylated lipid PA. After binding PA, Nir2/rdgB is translocated to ER-PM contact sites to exchange PI and PA between the two opposed membranes (Chang et al., 2013; Kim et al., 2013, 2015; Balla, 2018). This process coordinates local lipid metabolism with downstream signaling at ER-PM contact sites (Kim et al., 2013). A recent study found that Nir2 and Kv2.1 are co-localized at ER-PM contact sites in neuronal cells, indicating Kv2-VAP tethers may regulate Nir2 localization and PI homeostasis (Kirmiz et al., 2019). Different from Nir2, the ability of Nir3 is to sense subtle PA production and sustain basal PM PI(4,5)P2 levels (Chang and Liou, 2015). They cooperatively regulate PI(4,5)P2 homeostasis at ER-PM contact sites.

GRAMD

The protein containing the Glucosyltransferases, Rab-like GTPase activators, and myotubularins (GRAM) domain was named GRAMD, a recently discovered class of conserved ER proteins. Bioinformatics studies identified six GRAMD proteins (Ysp1p, Sip3p, Ysp2p, Lam4p, Lam5p, and Lam6p) in yeast and five members (GRAMD1a, GRAMD1b, GRAMD1c, GRAMD2, and GRAMD3) in mammals (Gatta et al., 2015). However, only three GRAMD1s in mammals contain StART-like lipid transfer domains. GRAMD2 and GRAMD3 are supposed not to mediate lipid transport (Naito et al., 2019). GRAMD proteins are anchored to ER *via* its C-terminal transmembrane domain and target the PM using the N-terminal GRAM domain (**Figure 4C**) (Stefan et al., 2011; Chu et al., 2015; Besprozvannaya et al., 2018).

The existence of the StART-like domain makes GRAMD1 proteins contribute to PM sterol homeostasis by recognizing accessible PM cholesterol and transporting it to the ER (Holthuis and Levine, 2005; van Meer et al., 2008; Sandhu et al., 2018). A recent study showed GRAMD1s form homo- and heteromeric complexes that interact with the free cholesterol and PS on the PM by the GRAM domain. Thus, the accessible cholesterol is transported to the ER through StART-like domains. Loss of the three GRAMD1s leads to a significant expansion of the available PM cholesterol pool, suggesting GRAMD1s are major cholesterol transporters between the ER and the PM (Sandhu et al., 2018; Naito et al., 2019). Different from GRAMD1, GRAMD2 co-localizes with E-Syts and help to maintain the ER-PM contacts. Based on this tethering function, GRAMD2 may play a role in SOCE and Ca^{2+} homeostasis by the recruitment of STIM1 (Besprozvannaya et al., 2018).

The trafficking of low-density-lipoprotein (LDL)-cholesterol is essential in cholesterol metabolism. Imbalance in this process could cause diseases, for example, the Niemann-Pick type C (NPC). The ER is the central organelle senses and synthesizes endogenous cholesterol. After endocytosis, the vast majority of LDL-cholesterol is transported to the PM (Pfisterer et al., 2016). The PM cholesterol could then supply the ER by GRAMD1s (Sandhu et al., 2018). However, about 30% of LDL-cholesterol is directly transported from endosomes/lysosomes to the ER, mediated by ORP1L and STARD3. When ER cholesterol is excessive, these sterol-transfer proteins can act in the opposite direction, transporting the cholesterol to the endosomes (Eden et al., 2016; Wilhelm et al., 2017). Recent studies indicate NPC1 tethers the ER to the endocytic organelles and facilitates cholesterol egress through ORP5 and GRAMD1s. Both of the LTPs localized at the ER-endocytic organelles MCSs in response to the cholesterol levels (Du et al., 2011; Höglinger et al., 2019).

CERT (ceramide transport protein) is another LTP containing a StART-like domain. In addition to glycerophospholipids and sterols, ceramide is also synthesized in the ER. CERT anchors to the ER *via* the FFAT motif-VAP interaction. It contains a PHD that interacts with PI(4)P to build the ER-Golgi contacts. Through the StART-like domain, CERT transports ceramide to the Golgi apparatus, where glucosylceramide and sphingomyelin are synthesized (Hanada et al., 2003). Glycolipid-transfer protein, another VAP-interacting LTP, transports glucosylceramide from *cis*-Golgi to *trans*-Golgi or the ER (Smith et al., 2006; Halter et al., 2007; Backman et al., 2018). These processes are indispensable for sphingomyelin and glycosphingolipid homeostasis (Breslow, 2013; Hanada, 2018).

Coordination of Ca^{2+} Signaling and Phospholipid Metabolism

Many regulators coordinate to form an extensive protein network at ER-PM contact sites, regulating intracellular signal transductions coupled with Ca^{2+} and phospholipid signaling. The elevated cytoplasmic Ca^{2+} triggers the enrichment of E-Syt1 at ER-PM contact sites (Giordano et al., 2013). In another way, the ER-Ca^{2+} depletion induces STIM1 translocation to ER-PM contact sites (Liou et al., 2007). Both the Ca^{2+}-regulated processes enhance the ER-PM connections, which subsequently promotes the recruitment of Nir2 to the ER-PM interface (Chang et al., 2013). Nir2 binds and transfers PA from the PM to the ER (Kim et al., 2015). In turn, it moves PI from the ER to the PM and generates PI(4)P and PI(4,5)P2, in which step RASSF4 and ARF6 participate (Stathopulos et al., 2006; Chen et al., 2017; Dickson, 2017). PI(4,5)P2 reinforces relocations of E-Syts and STIM1 at the contact sites and further regulates Ca^{2+} dynamics. The consumption of excess PI(4,5)P2 generates DAG and PA, which facilitate Nir2 enter the next circle. Overall, this network combines SOCE regulators with LTPs to develop a synergistic effect between Ca^{2+} signaling and PI(4,5)P2 metabolism at the ER-PM junctions and extend the duration of signal transductions (Dickson, 2017; Ong and Ambudkar, 2020).

CONCLUSIONS

The ER communicates with the PM through direct physical contacts, which are regulated by various proteins. These key players cooperatively mediate the reactions between the opposed membranes and drive diverse fundamental cellular processes. ER-PM contact sites are involved in the regulation of ion and lipid transports, signal transductions, ER morphology and remodeling, membrane trafficking, and yeast polarized growth (Encinar Del Dedo et al., 2017; Ng et al., 2018, 2020; Kang et al., 2019; Kirmiz et al., 2019; Weber-Boyvat et al., 2020). Substantial progress has been made toward understanding their functions and mechanisms (**Table 1**) (Saheki and De Camilli, 2017a; Wang et al., 2017; Ong and Ambudkar, 2020; Stefan, 2020). However, all proteins located at the MCSs seem to tether the membranes. Multiple regulators perform the same functions at the ER-PM contact sites in some cellular processes (Manford et al., 2012; Collado et al., 2019). The unique significance of these proteins needs to be further explored. For example, why are three E-Syts in yeast and mammals but only one in plants and flies?

Given that most of the regulators at ER-PM contact sites are highly conserved, it seems unlikely the cell keeps redundant proteins at this narrow and crowded place during evolution. These proteins are more likely of great significance to the cell. However, the general functional redundancy gives us trouble understanding their exact physiological functions. One speculation is each of these functional redundant proteins still has its features. Take tethering as an example. Although all protein tethers are capable of bridging the ER and the PM, the ER-PM junctions formed by distinct tethers have variable architectures and different mechanisms (Petkovic et al., 2014; Fernandez-Busnadiego et al., 2015; Johnson et al., 2018). These differences make them feasible to regulate the diverse cellular processes or play roles in specific conditions such as ER stress or cell damage. The same situation also happens in LTPs. It remains unclear why multiple LTPs transfer one specific lipid at MCSs. Perhaps the future discovery of their regulation and triggering mechanisms will give us the answer.

Tissue specificity is another possibility. Proteins with similar functions at ER-PM contact sites may individually play a

predominant role in the specific type of cells, depending on their expression enrichments or stimuli. Studies of those proteins in specific tissues will be a way to identify their physiological roles. Recent studies have already confirmed this possibility (Guo et al., 2017; Kirmiz et al., 2018a; Zhang et al., 2020). On the other hand, some regulators' functions are not related to ER-PM contact sites (Tremblay et al., 2016; El Kasmi et al., 2018). Further efforts are needed to study their correlations.

To better understand the functions and mechanisms of ER-PM contact sites, high-resolution structures of protein-membrane complexes mimicking MCSs or partially mimicking MCSs will be expected. The development of advanced Cryo-EM and live-cell imaging technology will enable us to comprehensively understand the protein network-mediated ER-PM contact sites. Many regulators at these sites are implicated in disease pathologies. Studies of these proteins for their physiological and pathological functions will be of great significance for understanding the disease occurrence, new drug developments, and clinical applications.

AUTHOR CONTRIBUTIONS

CL, TQ, RH, CW, YL, and HY wrote the manuscript. All authors contributed to the article and approved the submitted version.

FUNDING

This work was supported by the National Natural Science Foundation of China (NSFC) grants (Nos. 91854117 and 31871425), Natural Science Foundation of Jiangsu Province (BK20200036), the Priority Academic Program Development of Jiangsu Higher Education Institutions (PAPD), Six talent peaks project in Jiangsu Province, and Jiangsu Distinguished Professor Funding.

ACKNOWLEDGMENTS

We thank Dr. Jingshi Shen for the Comments and critically reading of the manuscript and all Yu lab members for helpful discussions.

REFERENCES

Abdelsalam, S. S., Korashy, H. M., Zeidan, A., and Agouni, A. (2019). The role of protein tyrosine phosphatase (PTP)-1B in cardiovascular disease and its interplay with insulin resistance. *Biomolecules* 9:9070286. doi: 10.3390/biom9070286

Alva, V., and Lupas, A. N. (2016). The TULIP superfamily of eukaryotic lipid-binding proteins as a mediator of lipid sensing and transport. *Biochim. Biophys. Acta* 1861, 913–923. doi: 10.1016/j.bbalip.2016.01.016

Amarilio, R., Ramachandran, S., Sabanay, H., and Lev, S. (2005). Differential regulation of endoplasmic reticulum structure through VAP-Nir protein interaction. *J. Biol. Chem.* 280, 5934–5944. doi: 10.1074/jbc.M409566200

Anagnostou, G., Akbar, M. T., Paul, P., Angelinetta, C., Steiner, T. J., and de Belleroche, J. (2010). Vesicle associated membrane protein B (VAPB) is decreased in ALS spinal cord. *Neurobiol. Aging* 31, 969–985. doi: 10.1016/j.neurobiolaging.2008.07.005

Anderie, I., Schulz, I., and Schmid, A. (2007). Direct interaction between ER membrane-bound PTP1B and its plasma membrane-anchored targets. *Cell Signal.* 19, 582–592. doi: 10.1016/j.cellsig.2006.08.007

Backman, A. P. E., Halin, J., Nurmi, H., Möuts, A., Kjellberg, M. A., and Mattjus, P. (2018). Glucosylceramide acyl chain length is sensed by the glycolipid transfer protein. *PLoS ONE* 13:0209230. doi: 10.1371/journal.pone.0209230

Balla, T. (2018). Ca(2+) and lipid signals hold hands at endoplasmic reticulum-plasma membrane contact sites. *J. Physiol.* 596, 2709–2716. doi: 10.1113/JP274957

Besprozvannaya, M., Dickson, E., Li, H., Ginburg, K. S., Bers, D. M., Auwerx, J., et al. (2018). GRAM domain proteins specialize functionally distinct ER-PM contact sites in human cells. *Elife* 7:31019. doi: 10.7554/eLife.31019

Bian, X., Saheki, Y., and De Camilli, P. (2018). Ca(2+) releases E-Syt1 autoinhibition to couple ER-plasma membrane tethering with lipid transport. *EMBO J.* 37, 219–234. doi: 10.15252/embj.201797359

Bian, X., Zhang, Z., Xiong, Q., De Camilli, P., and Lin, C. (2019). A programmable DNA-origami platform for studying lipid transfer between bilayers. *Nat. Chem. Biol.* 15, 830–837. doi: 10.1038/s41589-019-0325-3

Bishop, H. I., Guan, D., Bocksteins, E., Parajuli, L. K., Murray, K. D., Cobb, M. M., et al. (2015). Distinct cell- and layer-specific expression patterns and independent regulation of Kv2 channel subtypes in cortical pyramidal neurons. *J. Neurosci.* 35, 14922–14942. doi: 10.1523/JNEUROSCI.1897-15.2015

Bogard, A. S., Birg, A. V., and Ostrom, R. S. (2014). Non-raft adenylyl cyclase 2 defines a cAMP signaling compartment that selectively regulates IL-6 expression in airway smooth muscle cells: differential regulation of gene expression by AC isoforms. *Naunyn. Schmiedebergs. Arch. Pharmacol.* 387, 329–339. doi: 10.1007/s00210-013-0950-4

Bonifacino, J. S., and Glick, B. S. (2004). The mechanisms of vesicle budding and fusion. *Cell* 116, 153–166. doi: 10.1016/S0092-8674(03)01079-1

Brach, T., Specht, T., and Kaksonen, M. (2011). Reassessment of the role of plasma membrane domains in the regulation of vesicular traffic in yeast. *J. Cell Sci.* 124, 328–337. doi: 10.1242/jcs.078519

Brandman, O., Liou, J., Park, W. S., and Meyer, T. (2007). STIM2 is a feedback regulator that stabilizes basal cytosolic and endoplasmic reticulum Ca^2+ levels. *Cell* 131, 1327–1339. doi: 10.1016/j.cell.2007.11.039

Breslow, D. K. (2013). Sphingolipid homeostasis in the endoplasmic reticulum and beyond. *Cold Spring Harb. Perspect. Biol.* 5:a013326. doi: 10.1101/cshperspect.a013326

Carrasco, S., and Meyer, T. (2011). STIM proteins and the endoplasmic reticulum-plasma membrane junctions. *Annu. Rev. Biochem.* 80, 973–1000. doi: 10.1146/annurev-biochem-061609-165311

Chakrabarti, R., and Chakrabarti, R. (2006). Calcium signaling in non-excitable cells: Ca^2+ release and influx are independent events linked to two plasma membrane Ca^{2+} entry channels. *J. Cell Biochem.* 99, 1503–1516. doi: 10.1002/jcb.21102

Chan, J. J., Flatters, D., Rodrigues-Lima, F., Yan, J., Thalassinos, K., and Katan, M. (2013). Comparative analysis of interactions of RASSF1-10. *Adv. Biol. Regul.* 53, 190–201. doi: 10.1016/j.jbior.2012.12.001

Chang, C. L., Hsieh, T. S., Yang, T. T., Rothberg, K. G., Azizoglu, D. B., Volk, E., et al. (2013). Feedback regulation of receptor-induced Ca^{2+} signaling mediated by E-Syt1 and Nir2 at endoplasmic reticulum-plasma membrane junctions. *Cell Rep.* 5, 813–825. doi: 10.1016/j.celrep.2013.09.038

Chang, C. L., and Liou, J. (2015). Phosphatidylinositol 4,5-bisphosphate homeostasis regulated by Nir2 and Nir3 proteins at endoplasmic reticulum-plasma membrane junctions. *J. Biol. Chem.* 290, 14289–14301. doi: 10.1074/jbc.M114.621375

Chen, Y. J., Chang, C. L., Lee, W. R., and Liou, J. (2017). RASSF4 controls SOCE and ER-PM junctions through regulation of PI(4,5)P2. *J. Cell Biol.* 216, 2011–2025. doi: 10.1083/jcb.201606047

Christie, M. J. (1995). Molecular and functional diversity of K+ channels. *Clin. Exp. Pharmacol. Physiol.* 22, 944–951. doi: 10.1111/j.1440-1681.1995.tb02331.x

Chu, B. B., Liao, Y. C., Qi, W., Xie, C., Du, X., Wang, J., et al. (2015). Cholesterol transport through lysosome-peroxisome membrane contacts. *Cell* 161, 291–306. doi: 10.1016/j.cell.2015.02.019

Chung, J., Torta, F., Masai, K., Lucast, L., Czapla, H., Tanner, L. B., et al. (2015). PI4P/phosphatidylserine countertransport at ORP5- and

ORP8-mediated ER–plasma membrane contacts. *Science* 349, 428–432. doi: 10.1126/science.aab1370

Cobb, M. M., Austin, D. C., Sack, J. T., and Trimmer, J. S. (2015). Cell cycle-dependent changes in localization and phosphorylation of the plasma membrane Kv2.1 K+ channel impact endoplasmic reticulum membrane contact sites in COS-1 cells. *J. Biol. Chem.* 290, 29189–29201. doi: 10.1074/jbc.M115.690198

Cockcroft, S., and Raghu, P. (2018). Phospholipid transport protein function at organelle contact sites. *Curr. Opin. Cell Biol.* 53, 52–60. doi: 10.1016/j.ceb.2018.04.011

Collado, J., Kalemanov, M., Campelo, F., Bourgoint, C., Thomas, F., Loewith, R., et al. (2019). Tricalbin-mediated contact sites control ER curvature to maintain plasma membrane integrity. *Dev. Cell.* 51, 476–487 e477. doi: 10.1016/j.devcel.2019.10.018

Collins, S. R., and Meyer, T. (2011). Evolutionary origins of STIM1 and STIM2 within ancient Ca2+ signaling systems. *Trends Cell Biol.* 21, 202–211. doi: 10.1016/j.tcb.2011.01.002

Cooper, D. M., and Crossthwaite, A. J. (2006). Higher-order organization and regulation of adenylyl cyclases. *Trends Pharmacol. Sci.* 27, 426–431. doi: 10.1016/j.tips.2006.06.002

Cooper, D. M., Mons, N., and Karpen, J. W. (1995). Adenylyl cyclases and the interaction between calcium and cAMP signalling. *Nature* 374, 421–424. doi: 10.1038/374421a0

Creutz, C. E., Snyder, S. L., and Schulz, T. A. (2004). Characterization of the yeast tricalbins: membrane-bound multi-C2-domain proteins that form complexes involved in membrane trafficking. *Cell Mol. Life Sci.* 61, 1208–1220. doi: 10.1007/s00018-004-4029-8

D'Ambrosio, J. M., Albanèse, V., Lipp, N. F., Fleuriot, L., Debayle, D., Drin, G., et al. (2020). Osh6 requires Ist2 for localization to ER-PM contacts and efficient phosphatidylserine transport in budding yeast. *J. Cell Sci.* 133:243733. doi: 10.1242/jcs.243733

Daste, F., Galli, T., and Tareste, D. (2015). Structure and function of longin SNAREs. *J. Cell Sci.* 128, 4263–4272. doi: 10.1242/jcs.178574

de Saint-Jean, M., Delfosse, V., Douguet, D., Chicanne, G., Payrastre, B., Bourguet, W., et al. (2011). Osh4p exchanges sterols for phosphatidylinositol 4-phosphate between lipid bilayers. *J. Cell Biol.* 195, 965–978. doi: 10.1083/jcb.201104062

Del Bel, L. M., and Brill, J. A. (2018). Sac1, a lipid phosphatase at the interface of vesicular and nonvesicular transport. *Traffic* 19, 301–318. doi: 10.1111/tra.12554

Dessauer, C. W., Watts, V. J., Ostrom, R. S., Conti, M., Dove, S., and Seifert, R. (2017). International union of basic and clinical pharmacology. CI. structures and small molecule modulators of mammalian adenylyl cyclases. *Pharmacol. Rev.* 69, 93–139. doi: 10.1124/pr.116.013078

Dickson, E. J. (2017). RASSF4: Regulator of plasma membrane PI(4,5)P2. *J. Cell Biol.* 216, 1879–1881. doi: 10.1083/jcb.201706042

Dickson, E. J., Jensen, J. B., Vivas, O., Kruse, M., Traynor-Kaplan, A. E., and Hille, B. (2016). Dynamic formation of ER-PM junctions presents a lipid phosphatase to regulate phosphoinositides. *J. Cell Biol.* 213, 33–48. doi: 10.1083/jcb.201508106

Dong, X., Wang, Z., Ye, S., and Zhang, R. (2020). The crystal structure of ORP3 reveals the conservative PI4P binding pattern. *Biochem. Biophys. Res. Commun.* 529, 1005–1010. doi: 10.1016/j.bbrc.2020.06.090

D'Souza, R. S., Lim, J. Y., Turgut, A., Servage, K., Zhang, J., Orth, K., et al. (2020). Calcium-stimulated disassembly of focal adhesions mediated by an ORP3/IQSec1 complex. *Elife* 9:e54113. doi: 10.7554/eLife.54113.sa2

Du, X., Brown, A. J., and Yang, H. (2015). Novel mechanisms of intracellular cholesterol transport: oxysterol-binding proteins and membrane contact sites. *Curr. Opin. Cell Biol.* 35, 37–42. doi: 10.1016/j.ceb.2015.04.002

Du, X., Kumar, J., Ferguson, C., Schulz, T. A., Ong, Y. S., Hong, W., et al. (2011). A role for oxysterol-binding protein-related protein 5 in endosomal cholesterol trafficking. *J. Cell Biol.* 192, 121–135. doi: 10.1083/jcb.201004142

Du, X., Zhou, L., Aw, Y. C., Mak, H. Y., Xu, Y., Rae, J., et al. (2020). ORP5 localizes to ER-lipid droplet contacts and regulates the level of PI(4)P on lipid droplets. *J. Cell Biol,* 219: 201905162. doi: 10.1083/jcb.201905162

Eden, E. R., Sanchez-Heras, E., Tsapara, A., Sobota, A., Levine, T. P., and Futter, C. E. (2016). Annexin A1 tethers membrane contact sites that mediate ER to endosome cholesterol transport. *Dev. Cell.* 37, 473–483. doi: 10.1016/j.devcel.2016.05.005

El Kasmi, I., Khadivjam, B., Lackman, M., Duron, J., Bonneil, E., Thibault, P., et al. (2018). Extended synaptotagmin 1 interacts with herpes simplex virus 1 glycoprotein M and negatively modulates virus-induced membrane fusion. *J. Virol.* 92:17. doi: 10.1128/JVI.01281-17

Encinar Del Dedo, J., Idrissi, F. Z., Fernandez-Golbano, I. M., Garcia, P., Rebollo, E., Krzyzanowski, M. K., et al. (2017). ORP-Mediated ER contact with endocytic sites facilitates actin polymerization. *Dev. Cell* 43, 588–602.e586. doi: 10.1016/j.devcel.2017.10.031

Ercan, E., Momburg, F., Engel, U., Temmerman, K., Nickel, W., and Seedorf, M. (2009). A conserved, lipid-mediated sorting mechanism of yeast Ist2 and mammalian STIM proteins to the peripheral ER. *Traffic* 10, 1802–1818. doi: 10.1111/j.1600-0854.2009.00995.x

Fasshauer, D. (2003). Structural insights into the SNARE mechanism. *Biochim. Biophys. Acta* 1641, 87–97. doi: 10.1016/S0167-4889(03)00090-9

Fernandez-Busnadiego, R., Saheki, Y., and De Camilli, P. (2015). Three-dimensional architecture of extended synaptotagmin-mediated endoplasmic reticulum-plasma membrane contact sites. *Proc. Natl. Acad. Sci. U.S.A.* 112, E2004–2013. doi: 10.1073/pnas.1503191112

Feske, S., Gwack, Y., Prakriya, M., Srikanth, S., Puppel, S. H., Tanasa, B., et al. (2006). A mutation in Orai1 causes immune deficiency by abrogating CRAC channel function. *Nature* 441, 179–185. doi: 10.1038/nature04702

Fischer, M. A., Temmerman, K., Ercan, E., Nickel, W., and Seedorf, M. (2009). Binding of plasma membrane lipids recruits the yeast integral membrane protein Ist2 to the cortical ER. *Traffic* 10, 1084–1097. doi: 10.1111/j.1600-0854.2009.00926.x

Fox, P. D., Haberkorn, C. J., Akin, E. J., Seel, P. J., Krapf, D., and Tamkun, M. M. (2015). Induction of stable ER-plasma-membrane junctions by Kv2.1 potassium channels. *J. Cell Sci.* 128, 2096–2105. doi: 10.1242/jcs.166009

Frangioni, J. V., Beahm, P. H., Shifrin, V., Jost, C. A., and Neel, B. G. (1992). The nontransmembrane tyrosine phosphatase PTP-1B localizes to the endoplasmic reticulum via its 35 amino acid C-terminal sequence. *Cell* 68, 545–560. doi: 10.1016/0092-8674(92)90190-N

Fu, J., Dai, X., Plummer, G., Suzuki, K., Bautista, A., Githaka, J. M., et al. (2017). Kv2.1 Clustering contributes to insulin exocytosis and rescues human beta-cell dysfunction. *Diabetes* 66, 1890–1900. doi: 10.2337/db16-1170

Gallo, A., Danglot, L., Giordano, F., Hewlett, B., Binz, T., Vannier, C., et al. (2020). Role of the Sec22b–E-Syt complex in neurite growth and ramification. *J. Cell Sci.* 133:jcs247148. doi: 10.1242/jcs.247148

Gallo, A., Vannier, C., and Galli, T. (2016). Endoplasmic reticulum-plasma membrane associations:structures and functions. *Annu. Rev. Cell Dev. Biol.* 32, 279–301. doi: 10.1146/annurev-cellbio-111315-125024,

Galmes, R., Houcine, A., van Vliet, A. R., Agostinis, P., Jackson, C. L., and Giordano, F. (2016). ORP5/ORP8 localize to endoplasmic reticulum-mitochondria contacts and are involved in mitochondrial function. *EMBO Rep.* 17, 800–810. doi: 10.15252/embr.201541108

Gatta, A. T., Wong, L. H., Sere, Y. Y., Calderon-Norena, D. M., Cockcroft, S., Menon, A. K., et al. (2015). A new family of StART domain proteins at membrane contact sites has a role in ER-PM sterol transport. *Elife* 4:253. doi: 10.7554/eLife.07253.024

Ghai, R., Du, X., Wang, H., Dong, J., Ferguson, C., Brown, A. J., et al. (2017). ORP5 and ORP8 bind phosphatidylinositol-4, 5-biphosphate (PtdIns(4,5)P 2) and regulate its level at the plasma membrane. *Nat. Commun.* 8:757. doi: 10.1038/s41467-017-00861-5

Giordano, F., Saheki, Y., Idevall-Hagren, O., Colombo, S. F., Pirruccello, M., Milosevic, I., et al. (2013). PI(4,5)P(2)-dependent and Ca(2+)-regulated ER-PM interactions mediated by the extended synaptotagmins. *Cell* 153, 1494–1509. doi: 10.1016/j.cell.2013.05.026

Greitzer-Antes, D., Xie, L., Qin, T., Xie, H., Zhu, D., Dolai, S., et al. (2018). Kv2.1 clusters on beta-cell plasma membrane act as reservoirs that replenish pools of newcomer insulin granule through their interaction with syntaxin-3. *J. Biol. Chem.* 293, 6893–6904. doi: 10.1074/jbc.RA118.002703

Gulyás, G., Sohn, M., Kim, Y. J., Várnai, P., and Balla, T. (2020). ORP3 phosphorylation regulates phosphatidylinositol 4-phosphate and Ca(2+) dynamics at plasma membrane-ER contact sites. *J. Cell Sci.* 133:jcs.237388. doi: 10.1242/jcs.237388

Guo, X., Zhang, L., Fan, Y., Zhang, D., Qin, L., Dong, S., et al. (2017). Oxysterol-binding protein-related protein 8 inhibits gastric cancer growth through

induction of ER stress, inhibition of Wnt signaling, and activation of apoptosis. *Oncol. Res.* 25, 799–808. doi: 10.3727/096504016X14783691306605

Halter, D., Neumann, S., van Dijk, S. M., Wolthoorn, J., de Maziere, A. M., Vieira, O. V., et al. (2007). Pre- and post-Golgi translocation of glucosylceramide in glycosphingolipid synthesis. *J. Cell. Biol.* 179, 101–115. doi: 10.1083/jcb.200704091

Hanada, K. (2018). Lipid transfer proteins rectify inter-organelle flux and accurately deliver lipids at membrane contact sites. *J. Lipid Res.* 59, 1341–1366. doi: 10.1194/jlr.R085324

Hanada, K., Kumagai, K., Yasuda, S., Miura, Y., Kawano, M., Fukasawa, M., et al. (2003). Molecular machinery for non-vesicular trafficking of ceramide. *Nature* 426, 803–809. doi: 10.1038/nature02188

Hartzell, H. C., Yu, K., Xiao, Q., Chien, L.-T., and Qu, Z. (2009). Anoctamin/TMEM16 family members are Ca2+-activated Cl–channels. *J. Physiol.* 587, 2127–2139. doi: 10.1113/jphysiol.2008.163709

Hoffmann, P. C., Bharat, T. A. M., Wozny, M. R., Boulanger, J., Miller, E. A., and Kukulski, W. (2019). Tricalbins contribute to cellular lipid flux and form curved ER-PM contacts that are bridged by rod-shaped structures. *Dev. Cell* 51, 488–502.e488. doi: 10.1016/j.devcel.2019.09.019

Hogan, P. G., and Rao, A. (2015). Store-operated calcium entry: mechanisms and modulation. *Biochem. Biophys. Res. Commun.* 460, 40–49. doi: 10.1016/j.bbrc.2015.02.110

Höglinger, D., Burgoyne, T., Sanchez-Heras, E., Hartwig, P., Colaco, A., Newton, J., et al. (2019). NPC1 regulates ER contacts with endocytic organelles to mediate cholesterol egress. *Nat. Commun.* 10:4276. doi: 10.1038/s41467-019-12152-2

Holthuis, J. C. M., and Levine, T. P. (2005). Lipid traffic: floppy drives and a superhighway. *Nat. Rev. Mol. Cell Biol.* 6, 209–220. doi: 10.1038/nrm1591

Hong, W. (2005). SNAREs and traffic. *Biochim. Biophys. Acta* 1744, 120–144. doi: 10.1016/j.bbamcr.2005.03.014

Hooper, R., and Soboloff, J. (2015). STIMATE reveals a STIM1 transitional state. *Nat. Cell Biol.* 17, 1232–1234. doi: 10.1038/ncb3245

Hussain, H., Green, I. R., Abbas, G., Adekenov, S. M., Hussain, W., and Ali, I. (2019). Protein tyrosine phosphatase 1B (PTP1B) inhibitors as potential anti-diabetes agents: patent review (2015-2018). *Exp. Opin. Ther. Pat.* 29, 689–702. doi: 10.1080/13543776.2019.1655542

Idevall-Hagren, O., Lu, A., Xie, B., and De Camilli, P. (2015). Triggered Ca2+ influx is required for extended synaptotagmin 1-induced ER-plasma membrane tethering. *EMBO J.* 34, 2291–2305. doi: 10.15252/embj.201591565

Im, Y. J., Raychaudhuri, S., Prinz, W. A., and Hurley, J. H. (2005). Structural mechanism for sterol sensing and transport by OSBP-related proteins. *Nature* 437, 154–158. doi: 10.1038/nature03923

Ishikawa, K., Tamura, K., Ueda, H., Ito, Y., Nakano, A., Hara-Nishimura, I., et al. (2018). Synaptotagmin-associated endoplasmic reticulum-plasma membrane contact sites are localized to immobile ER tubules. *Plant Physiol.* 178, 641–653. doi: 10.1104/pp.18.00498

Ishikawa, S., Nagai, Y., Masuda, T., Koga, Y., Nakamura, T., Imamura, Y., et al. (2010). The role of oxysterol binding protein-related protein 5 in pancreatic cancer. *Cancer Sci.* 101, 898–905. doi: 10.1111/j.1349-7006.2009.01475.x

Iwasa, H., Kuroyanagi, H., Maimaiti, S., Ikeda, M., Nakagawa, K., and Hata, Y. (2013). Characterization of RSF-1, the Caenorhabditis elegans homolog of the Ras-association domain family protein 1. *Exp. Cell Res.* 319, 1–11. doi: 10.1016/j.yexcr.2012.10.008

Jahn, R., and Scheller, R. H. (2006). SNAREs—engines for membrane fusion. *Nat. Rev. Mol. Cell Biol.* 7, 631–643. doi: 10.1038/nrm2002

Jansen, M., Ohsaki, Y., Rega, L. R., Bittman, R., Olkkonen, V. M., and Ikonen, E. (2011). Role of ORPs in sterol transport from plasma membrane to ER and lipid droplets in mammalian cells. *Traffic* 12, 218–231. doi: 10.1111/j.1600-0854.2010.01142.x

Jedrychowska, J., and Korzh, V. (2019). Kv2.1 voltage-gated potassium channels in developmental perspective. *Dev. Dyn.* 248, 1180–1194. doi: 10.1002/dvdy.114

Jeyasimman, D., and Saheki, Y. (2019). SMP domain proteins in membrane lipid dynamics. *Biochim. Biophys. Acta Mol. Cell. Biol. Lipids* 1865:158447. doi: 10.1016/j.bbalip.2019.04.007

Jha, A., Chung, W. Y., Vachel, L., Maleth, J., Lake, S., Zhang, G., et al. (2019). Anoctamin 8 tethers endoplasmic reticulum and plasma membrane for assembly of Ca(2+) signaling complexes at the ER/PM compartment. *EMBO J.* 38:e101452. doi: 10.15252/embj.2018101452

Jing, J., He, L., Sun, A., Quintana, A., Ding, Y., Ma, G., et al. (2015). Proteomic mapping of ER-PM junctions identifies STIMATE as a regulator of Ca(2)(+) influx. *Nat. Cell Biol.* 17, 1339–1347. doi: 10.1038/ncb3234

Johnson, B., Leek, A. N., Sole, L., Maverick, E. E., Levine, T. P., and Tamkun, M. M. (2018). Kv2 potassium channels form endoplasmic reticulum/plasma membrane junctions via interaction with VAPA and VAPB. *Proc. Natl. Acad. Sci. U.S.A.* 115, E7331–E7340. doi: 10.1073/pnas.1805757115

Johnson, B., Leek, A. N., and Tamkun, M. M. (2019). Kv2 channels create endoplasmic reticulum/plasma membrane junctions: a brief history of Kv2 channel subcellular localization. *Channels (Austin)* 13, 88–101. doi: 10.1080/19336950.2019.1568824

Juschke, C., Wachter, A., Schwappach, B., and Seedorf, M. (2005). SEC18/NSF-independent, protein-sorting pathway from the yeast cortical ER to the plasma membrane. *J. Cell Biol.* 169, 613–622. doi: 10.1083/jcb.200503033

Kagiwada, S., and Hashimoto, M. (2007). The yeast VAP homolog Scs2p has a phosphoinositide-binding ability that is correlated with its activity. *Biochem. Biophys. Res. Commun.* 364, 870–876. doi: 10.1016/j.bbrc.2007.10.079

Kamemura, K., and Chihara, T. (2019). Multiple functions of the ER-resident VAP and its extracellular role in neural development and disease. *J. Biochem.* 165, 391–400. doi: 10.1093/jb/mvz011

Kang, F., Zhou, M., Huang, X., Fan, J., Wei, L., Boulanger, J., et al. (2019). E-syt1 re-arranges STIM1 clusters to stabilize ring-shaped ER-PM contact sites and accelerate Ca(2+) store replenishment. *Sci. Rep.* 9:3975. doi: 10.1038/s41598-019-40331-0

Kar, P., Bakowski, D., Di Capite, J., Nelson, C., and Parekh, A. B. (2012). Different agonists recruit different stromal interaction molecule proteins to support cytoplasmic Ca^{2+} oscillations and gene expression. *Proc. Natl. Acad. Sci. U.S.A.* 109, 6969–6974. doi: 10.1073/pnas.1201204109

Kentala, H., Weber-Boyvat, M., and Olkkonen, V. M. (2016). OSBP-related protein family: mediators of lipid transport and signaling at membrane contact sites. *Int. Rev. Cell Mol. Biol.* 321, 299–340. doi: 10.1016/bs.ircmb.2015.09.006

Kikuma, K., Li, X., Kim, D., Sutter, D., and Dickman, D. K. (2017). Extended synaptotagmin localizes to presynaptic ER and promotes neurotransmission and synaptic growth in *Drosophila*. *Genetics* 207, 993–1006. doi: 10.1534/genetics.117.300261

Kim, S., Kedan, A., Marom, M., Gavert, N., Keinan, O., Selitrennik, M., et al. (2013). The phosphatidylinositol-transfer protein Nir2 binds phosphatidic acid and positively regulates phosphoinositide signalling. *EMBO Rep.* 14, 891–899. doi: 10.1038/embor.2013.113

Kim, Y. J., Guzman-Hernandez, M. L., Wisniewski, E., and Balla, T. (2015). Phosphatidylinositol-phosphatidic acid exchange by Nir2 at ER-PM contact sites maintains phosphoinositide signaling competence. *Dev. Cell* 33, 549–561. doi: 10.1016/j.devcel.2015.04.028

Kirmiz, M., Gillies, T. E., Dickson, E. J., and Trimmer, J. S. (2019). Neuronal ER-plasma membrane junctions organized by Kv2-VAP pairing recruit Nir proteins and affect phosphoinositide homeostasis. *J. Biol. Chem.* 294, 17735–17757. doi: 10.1074/jbc.RA119.007635

Kirmiz, M., Palacio, S., Thapa, P., King, A. N., Sack, J. T., and Trimmer, J. S. (2018a). Remodeling neuronal ER-PM junctions is a conserved nonconducting function of Kv2 plasma membrane ion channels. *Mol. Biol. Cell* 29, 2410–2432. doi: 10.1091/mbc.E18-05-0337

Kirmiz, M., Vierra, N. C., Palacio, S., and Trimmer, J. S. (2018b). Identification of VAPA and VAPB as Kv2 channel-interacting proteins defining endoplasmic reticulum-plasma membrane junctions in mammalian brain neurons. *J. Neurosci.* 38, 7562–7584. doi: 10.1523/JNEUROSCI.0893-18.2018

Kopec, K. O., Alva, V., and Lupas, A. N. (2010). Homology of SMP domains to the TULIP superfamily of lipid-binding proteins provides a structural basis for lipid exchange between ER and mitochondria. *Bioinformatics* 26, 1927–1931. doi: 10.1093/bioinformatics/btq326

Kun-Rodrigues, C., Ganos, C., Guerreiro, R., Schneider, S. A., Schulte, C., Lesage, S., et al. (2015). A systematic screening to identify *de novo* mutations causing sporadic early-onset Parkinson's disease. *Hum. Mol. Genet.* 24, 6711–6720. doi: 10.1093/hmg/ddv376

Kunzelmann, K., Cabrita, I., Wanitchakool, P., Ousingsawat, J., Sirianant, L., Benedetto, R., et al. (2016). Modulating Ca(2)(+) signals: a common theme for TMEM16, Ist2, and TMC. *Pflugers Arch.* 468, 475–490. doi: 10.1007/s00424-015-1767-4

Lee, E., Vanneste, S., Perez-Sancho, J., Benitez-Fuente, F., Strelau, M., Macho, A. P., et al. (2019). Ionic stress enhances ER-PM connectivity via phosphoinositide-associated SYT1 contact site expansion in Arabidopsis. *Proc. Natl. Acad. Sci. U.S.A.* 116, 1420–1429. doi: 10.1073/pnas.1818099116

Lee, I., and Hong, W. (2006). Diverse membrane-associated proteins contain a novel SMP domain. *FASEB J.* 20, 202–206. doi: 10.1096/fj.05-4581hyp

Lees, J. A., Messa, M., Sun, E. W., Wheeler, H., Torta, F., Wenk, M. R., et al. (2017). Lipid transport by TMEM24 at ER-plasma membrane contacts regulates pulsatile insulin secretion. *Science* 355:aah6171. doi: 10.1126/science.aah6171

Lefkimmiatis, K., Srikanthan, M., Maiellaro, I., Moyer, M. P., Curci, S., and Hofer, A. M. (2009). Store-operated cyclic AMP signalling mediated by STIM1. *Nat. Cell Biol.* 11, 433–442. doi: 10.1038/ncb1850

Lehto, M., Mäyränpää, M. I., Pellinen, T., Ihalmo, P., Lehtonen, S., Kovanen, P. T., et al. (2008). The R-Ras interaction partner ORP3 regulates cell adhesion. *J. Cell Sci.* 121, 695–705. doi: 10.1242/jcs.016964

Lessard, L., Stuible, M., and Tremblay, M. L. (2010). The two faces of PTP1B in cancer. *Biochim. Biophys. Acta* 1804, 613–619. doi: 10.1016/j.bbapap.2009.09.018

Lev, S., Ben Halevy, D., Peretti, D., and Dahan, N. (2008). The VAP protein family: from cellular functions to motor neuron disease. *Trends Cell Biol.* 18, 282–290. doi: 10.1016/j.tcb.2008.03.006

Lim, S. T., Antonucci, D. E., Scannevin, R. H., and Trimmer, J. S. (2000). A novel targeting signal for proximal clustering of the Kv2.1 K+ channel in hippocampal neurons. *Neuron* 25, 385–397. doi: 10.1016/S0896-6273(00)80902-2

Lindhout, F. W., Cao, Y., Kevenaar, J. T., Bodzeta, A., Stucchi, R., Boumpoutsari, M. M., et al. (2019). VAP-SCRN1 interaction regulates dynamic endoplasmic reticulum remodeling and presynaptic function. *EMBO J.* 38:e101345. doi: 10.15252/embj.2018101345

Liou, J., Fivaz, M., Inoue, T., and Meyer, T. (2007). Live-cell imaging reveals sequential oligomerization and local plasma membrane targeting of stromal interaction molecule 1 after Ca2+ store depletion. *Proc. Natl. Acad. Sci. U.S.A.* 104, 9301–9306. doi: 10.1073/pnas.0702866104

Liou, J., Kim, M. L., Heo, W. D., Jones, J. T., Myers, J. W., Ferrell, J. E. Jr., et al. (2005). STIM is a Ca^{2+} sensor essential for Ca^{2+}-store-depletion-triggered Ca^{2+} influx. *Curr. Biol.* 15, 1235–1241. doi: 10.1016/j.cub.2005.05.055

Ma, G., Wei, M., He, L., Liu, C., Wu, B., Zhang, S. L., et al. (2015). Inside-out Ca(2+) signalling prompted by STIM1 conformational switch. *Nat. Commun.* 6:7826. doi: 10.1038/ncomms8826

Maass, K., Fischer, M. A., Seiler, M., Temmerman, K., Nickel, W., and Seedorf, M. (2009). A signal comprising a basic cluster and an amphipathic alpha-helix interacts with lipids and is required for the transport of Ist2 to the yeast cortical ER. *J. Cell Sci.* 122, 625–635. doi: 10.1242/jcs.036012

Maeda, K., Anand, K., Chiapparino, A., Kumar, A., Poletto, M., Kaksonen, M., et al. (2013). Interactome map uncovers phosphatidylserine transport by oxysterol-binding proteins. *Nature* 501, 257–261. doi: 10.1038/nature12430

Maiellaro, I., Lefkimmiatis, K., Moyer, M. P., Curci, S., and Hofer, A. M. (2012). Termination and activation of store-operated cyclic AMP production. *J. Cell Mol. Med.* 16, 2715–2725. doi: 10.1111/j.1582-4934.2012.01592.x

Manford, A., Xia, T., Saxena, A. K., Stefan, C., Hu, F., Emr, S. D., et al. (2010). Crystal structure of the yeast Sac1: implications for its phosphoinositide phosphatase function. *EMBO J.* 29, 1489–1498. doi: 10.1038/emboj.2010.57

Manford, A. G., Stefan, C. J., Yuan, H. L., Macgurn, J. A., and Emr, S. D. (2012). ER-to-plasma membrane tethering proteins regulate cell signaling and ER morphology. *Dev. Cell* 23, 1129–1140. doi: 10.1016/j.devcel.2012.11.004

Manji, S. S., Parker, N. J., Williams, R. T., van Stekelenburg, L., Pearson, R. B., Dziadek, M., et al. (2000). STIM1: a novel phosphoprotein located at the cell surface. *Biochim. Biophys. Acta* 1481, 147–155. doi: 10.1016/S0167-4838(00)00105-9

Mesmin, B., Bigay, J., Moser von Filseck, J., Lacas-Gervais, S., Drin, G., and Antonny, B. (2013). A four-step cycle driven by PI(4)P hydrolysis directs sterol/PI(4)P exchange by the ER-Golgi tether OSBP. *Cell* 155, 830–843. doi: 10.1016/j.cell.2013.09.056

Min, S. W., Chang, W. P., and Südhof, T. C. (2007). E-Syts, a family of membranous Ca^{2+}-sensor proteins with multiple C2 domains. *Proc. Natl. Acad. Sci. U.S.A.* 104, 3823–3828. doi: 10.1073/pnas.0611725104

Monteleone, M. C., Gonzalez Wusener, A. E., Burdisso, J. E., Conde, C., Caceres, A., and Arregui, C. O. (2012). ER-bound protein tyrosine phosphatase PTP1B interacts with Src at the plasma membrane/substrate interface. *PLoS ONE* 7:e38948. doi: 10.1371/journal.pone.0038948

Moser von Filseck, J., Copič, A., Delfosse, V., Vanni, S., Jackson, C. L., Bourguet, W., et al. (2015a). Phosphatidylserine transport by ORP/Osh proteins is driven by phosphatidylinositol 4-phosphate. *Science* 349:aab1346. doi: 10.1126/science.aab1346

Moser von Filseck, J., Vanni, S., Mesmin, B., Antonny, B., and Drin, G. (2015b). A phosphatidylinositol-4-phosphate powered exchange mechanism to create a lipid gradient between membranes. *Nat. Commun.* 6:6671. doi: 10.1038/ncomms7671

Murakoshi, H., and Trimmer, J. S. (1999). Identification of the Kv2.1 K+ channel as a major component of the delayed rectifier K+ current in rat hippocampal neurons. *J. Neurosci.* 19, 1728–1735. doi: 10.1523/JNEUROSCI.19-05-01728.1999

Murphy, S. E., and Levine, T. P. (2016). VAP, a versatile access point for the endoplasmic reticulum: review and analysis of FFAT-like motifs in the VAPome. *Biochim. Biophys. Acta* 1861, 952–961. doi: 10.1016/j.bbalip.2016.02.009

Naito, T., Ercan, B., Krshnan, L., Triebl, A., Koh, D. H. Z., Wei, F. Y., et al. (2019). Movement of accessible plasma membrane cholesterol by the GRAMD1 lipid transfer protein complex. *Elife* 8:e51401. doi: 10.7554/eLife.51401.sa2

Nath, V. R., Mishra, S., Basak, B., Trivedi, D., and Raghu, P. (2020). Extended synaptotagmin regulates membrane contact site structure and lipid transfer function *in vivo*. *EMBO Rep.* 21:e50264. doi: 10.15252/embr.202050264

Ng, A. Q. E., Ng, A. Y. E., and Zhang, D. (2020). Plasma membrane furrows control plasticity of ER-PM contacts. *Cell Rep.* 30, 1434–1446.e1437. doi: 10.1016/j.celrep.2019.12.098

Ng, A. Y. E., Ng, A. Q. E., and Zhang, D. (2018). ER-PM contacts restrict exocytic sites for polarized morphogenesis. *Curr. Biol.* 28, 146–153.e145. doi: 10.1016/j.cub.2017.11.055

O'Connell, K. M., Loftus, R., and Tamkun, M. M. (2010). Localization-dependent activity of the Kv2.1 delayed-rectifier K+ channel. *Proc. Natl. Acad. Sci. U.S.A.* 107, 12351–12356. doi: 10.1073/pnas.1003028107

Oh-Hora, M., Yamashita, M., Hogan, P. G., Sharma, S., Lamperti, E., Chung, W., et al. (2008). Dual functions for the endoplasmic reticulum calcium sensors STIM1 and STIM2 in T cell activation and tolerance. *Nat. Immunol.* 9, 432–443. doi: 10.1038/ni1574

Okeke, E., Dingsdale, H., Parker, T., Voronina, S., and Tepikin, A. V. (2016). Endoplasmic reticulum-plasma membrane junctions: structure, function and dynamics. *J. Physiol.* 594, 2837–2847. doi: 10.1113/JP271142

Olkkonen, V. M., and Li, S. (2013). Oxysterol-binding proteins: sterol and phosphoinositide sensors coordinating transport, signaling and metabolism. *Prog. Lipid Res.* 52, 529–538. doi: 10.1016/j.plipres.2013.06.004

Omnus, D. J., Cadou, A., Thomas, F. B., Bader, J. M., Soh, N., Chung, G. H. C., et al. (2020). A heat-sensitive Osh protein controls PI4P polarity. *BMC Biol.* 18:28. doi: 10.1186/s12915-020-0758-x

Ong, H. L., and Ambudkar, I. S. (2020). The endoplasmic reticulum-plasma membrane junction: a hub for agonist regulation of Ca(2+) entry. *Cold Spring Harb. Perspect. Biol.* 12:a035253. doi: 10.1101/cshperspect.a035253

Park, C. Y., Hoover, P. J., Mullins, F. M., Bachhawat, P., Covington, E. D., Raunser, S., et al. (2009). STIM1 clusters and activates CRAC channels via direct binding of a cytosolic domain to Orai1. *Cell* 136, 876–890. doi: 10.1016/j.cell.2009.02.014

Patterson, R. L., van Rossum, D. B., and Gill, D. L. (1999). Store-operated Ca^{2+} entry: evidence for a secretion-like coupling model. *Cell* 98, 487–499. doi: 10.1016/S0092-8674(00)81977-7

Perez-Sancho, J., Vanneste, S., Lee, E., McFarlane, H. E., Esteban Del Valle, A., Valpuesta, V., et al. (2015). The *Arabidopsis* synaptotagmin1 is enriched in endoplasmic reticulum-plasma membrane contact sites and confers cellular resistance to mechanical stresses. *Plant Physiol.* 168, 132–143. doi: 10.1104/pp.15.00260

Petkovic, M., Jemaiel, A., Daste, F., Specht, C. G., Izeddin, I., Vorkel, D., et al. (2014). The SNARE Sec22b has a non-fusogenic function in plasma membrane expansion. *Nat. Cell Biol.* 16, 434–444. doi: 10.1038/ncb2937

Pfisterer, S. G., Peränen, J., and Ikonen, E. (2016). LDL-cholesterol transport to the endoplasmic reticulum: current concepts. *Curr. Opin. Lipidol.* 27, 282–287. doi: 10.1097/MOL.0000000000000292

Porter, K. R., and Palade, G. E. (1957). Studies on the endoplasmic reticulum. III. Its form and distribution in striated muscle cells. *J. Biophys. Biochem. Cytol.* 3, 269–300. doi: 10.1083/jcb.3.2.269

Pottekat, A., Becker, S., Spencer, K. R., Yates, J. R. III, Manning, G., Itkin-Ansari, P., et al. (2013). Insulin biosynthetic interaction network component, TMEM24, facilitates insulin reserve pool release. *Cell Rep.* 4, 921–930. doi: 10.1016/j.celrep.2013.07.050

Prakriya, M., Feske, S., Gwack, Y., Srikanth, S., Rao, A., and Hogan, P. G. (2006). Orai1 is an essential pore subunit of the CRAC channel. *Nature* 443, 230–233. doi: 10.1038/nature05122

Prakriya, M., and Lewis, R. S. (2015). Store-operated calcium channels. *Physiol. Rev.* 95, 1383–1436. doi: 10.1152/physrev.00020.2014

Prinz, W. A. (2010). Lipid trafficking sans vesicles: where, why, how? *Cell.* 143, 870–874. doi: 10.1016/j.cell.2010.11.031

Pulli, I., Lassila, T., Pan, G., Yan, D., Olkkonen, V. M., and Tornquist, K. (2018). Oxysterol-binding protein related-proteins (ORPs) 5 and 8 regulate calcium signaling at specific cell compartments. *Cell Calcium.* 72, 62–69. doi: 10.1016/j.ceca.2018.03.001

Putney, J. W. Jr. (1986). A model for receptor-regulated calcium entry. *Cell Calcium.* 7, 1–12. doi: 10.1016/0143-4160(86)90026-6

Putney, J. W. Jr. (1990). Capacitative calcium entry revisited. *Cell Calcium.* 11, 611–624. doi: 10.1016/0143-4160(90)90016-N

Quintana, A., Rajanikanth, V., Farber-Katz, S., Gudlur, A., Zhang, C., Jing, J., et al. (2015). TMEM110 regulates the maintenance and remodeling of mammalian ER-plasma membrane junctions competent for STIM-ORAI signaling. *Proc. Natl. Acad. Sci. U.S.A.* 112, E7083–7092. doi: 10.1073/pnas.1521924112

Redman, P. T., He, K., Hartnett, K. A., Jefferson, B. S., Hu, L., Rosenberg, P. A., et al. (2007). Apoptotic surge of potassium currents is mediated by p38 phosphorylation of Kv2.1. *Proc. Natl. Acad. Sci. U.S.A.* 104, 3568–3573. doi: 10.1073/pnas.0610159104

Rizo, J., and Südhof, T. C. (1998). C2-domains, structure and function of a universal Ca2+-binding domain. *J. Biol. Chem.* 273, 15879–15882. doi: 10.1074/jbc.273.26.15879

Roos, J., DiGregorio, P. J., Yeromin, A. V., Ohlsen, K., Lioudyno, M., Zhang, S., et al. (2005). STIM1, an essential and conserved component of store-operated Ca^{2+} channel function. *J. Cell Biol.* 169, 435–445. doi: 10.1083/jcb.200502019

Saheki, Y. (2017). Endoplasmic reticulum—plasma membrane crosstalk mediated by the extended synaptotagmins. *Adv. Exp. Med. Biol.* 997, 83–93. doi: 10.1007/978-981-10-4567-7_6

Saheki, Y., Bian, X., Schauder, C. M., Sawaki, Y., Surma, M. A., Klose, C., et al. (2016). Control of plasma membrane lipid homeostasis by the extended synaptotagmins. *Nat. Cell Biol.* 18, 504–515. doi: 10.1038/ncb3339

Saheki, Y., and De Camilli, P. (2017a). Endoplasmic reticulum-plasma membrane contact sites. *Annu. Rev. Biochem.* 86, 659–684. doi: 10.1146/annurev-biochem-061516-044932

Saheki, Y., and De Camilli, P. (2017b). The extended-synaptotagmins. *Biochim. Biophys. Acta Mol. Cell Res.* 1864, 1490–1493. doi: 10.1016/j.bbamcr.2017.03.013

Sandhu, J., Li, S., Fairall, L., Pfisterer, S. G., Gurnett, J. E., Xiao, X., et al. (2018). Aster proteins facilitate nonvesicular plasma membrane to ER cholesterol transport in mammalian cells. *Cell* 175, 514–529.e520. doi: 10.1016/j.cell.2018.08.033

Schauder, C. M., Wu, X., Saheki, Y., Narayanaswamy, P., Torta, F., Wenk, M. R., et al. (2014). Structure of a lipid-bound extended synaptotagmin indicates a role in lipid transfer. *Nature* 510, 552–555. doi: 10.1038/nature13269

Schulz, T. A., and Creutz, C. E. (2004). The tricalbin C2 domains: lipid-binding properties of a novel, synaptotagmin-like yeast protein family. *Biochemistry* 43, 3987–3995. doi: 10.1021/bi036082w

Sclip, A., Bacaj, T., Giam, L. R., and Sudhof, T. C. (2016). Extended synaptotagmin (ESyt) triple knock-out mice are viable and fertile without obvious endoplasmic reticulum dysfunction. *PLoS ONE* 11:e0158295. doi: 10.1371/journal.pone.0158295

Shah, N. H., and Aizenman, E. (2014). Voltage-gated potassium channels at the crossroads of neuronal function, ischemic tolerance, and neurodegeneration. *Transl. Stroke Res.* 5, 38–58. doi: 10.1007/s12975-013-0297-7

Skirpan, A. L., Dowd, P. E., Sijacic, P., Jaworski, C. J., Gilroy, S., and Kao, T. H. (2006). Identification and characterization of PiORP1, a Petunia oxysterol-binding-protein related protein involved in receptor-kinase mediated signaling in pollen, and analysis of the ORP gene family in Arabidopsis. *Plant Mol. Biol.* 61, 553–565. doi: 10.1007/s11103-006-0030-y

Smith, D. C., Sillence, D. J., Falguières, T., Jarvis, R. M., Johannes, L., Lord, J. M., et al. (2006). The association of shiga-like toxin with detergent-resistant membranes is modulated by glucosylceramide and is an essential requirement in the endoplasmic reticulum for a cytotoxic effect. *Mol. Biol. Cell.* 17, 1375–1387. doi: 10.1091/mbc.e05-11-1035

Soboloff, J., Rothberg, B. S., Madesh, M., and Gill, D. L. (2012). STIM proteins: dynamic calcium signal transducers. *Nat. Rev. Mol. Cell Biol.* 13, 549–565. doi: 10.1038/nrm3414

Soboloff, J., Spassova, M. A., Dziadek, M. A., and Gill, D. L. (2006a). Calcium signals mediated by STIM and Orai proteins—a new paradigm in inter-organelle communication. *Biochim. Biophys. Acta* 1763, 1161–1168. doi: 10.1016/j.bbamcr.2006.09.023

Soboloff, J., Spassova, M. A., Hewavitharana, T., He, L. P., Xu, W., Johnstone, L. S., et al. (2006b). STIM2 is an inhibitor of STIM1-mediated store-operated Ca^{2+} entry. *Curr. Biol.* 16, 1465–1470. doi: 10.1016/j.cub.2006.05.051

Stathopulos, P. B., Li, G. Y., Plevin, M. J., Ames, J. B., and Ikura, M. (2006). Stored Ca2+ depletion-induced oligomerization of stromal interaction molecule 1 (STIM1) *via* the EF-SAM region: an initiation mechanism for capacitive Ca^{2+} entry. *J. Biol. Chem.* 281, 35855–35862. doi: 10.1074/jbc.M608247200

Stefan, C. J. (2020). Endoplasmic reticulum-plasma membrane contacts: principals of phosphoinositide and calcium signaling. *Curr. Opin. Cell Biol.* 63, 125–134. doi: 10.1016/j.ceb.2020.01.010

Stefan, C. J., Manford, A. G., Baird, D., Yamada-Hanff, J., Mao, Y., and Emr, S. D. (2011). Osh proteins regulate phosphoinositide metabolism at ER-plasma membrane contact sites. *Cell* 144, 389–401. doi: 10.1016/j.cell.2010.12.034

Stefano, G., Renna, L., Wormsbaecher, C., Gamble, J., Zienkiewicz, K., and Brandizzi, F. (2018). Plant endocytosis requires the ER membrane-anchored proteins VAP27-1 and VAP27-3. *Cell Rep.* 23, 2299–2307. doi: 10.1016/j.celrep.2018.04.091

Südhof, T. C., and Rothman, J. E. (2009). Membrane fusion: grappling with SNARE and SM proteins. *Science* 323, 474–477. doi: 10.1126/science.1161748

Sun, E. W., Guillen-Samander, A., Bian, X., Wu, Y., Cai, Y., Messa, M., et al. (2019). Lipid transporter TMEM24/C2CD2L is a Ca(2+)-regulated component of ER-plasma membrane contacts in mammalian neurons. *Proc. Natl. Acad. Sci. U.S.A.* 116, 5775–5784. doi: 10.1073/pnas.1820156116

Sun, W., Tian, B. X., Wang, S. H., Liu, P. J., and Wang, Y. C. (2020). The function of SEC22B and its role in human diseases. *Cytoskeleton (Hoboken)* 77, 303–312. doi: 10.1002/cm.21628

Sutton, R. B., Fasshauer, D., Jahn, R., and Brunger, A. T. (1998). Crystal structure of a SNARE complex involved in synaptic exocytosis at 2.4 A resolution. *Nature* 395, 347–353. doi: 10.1038/26412

Tong, J., Yang, H., Yang, H., Eom, S. H., and Im, Y. J. (2013). Structure of Osh3 reveals a conserved mode of phosphoinositide binding in oxysterol-binding proteins. *Structure* 21, 1203–1213. doi: 10.1016/j.str.2013.05.007

Toulmay, A., and Prinz, W. A. (2012). A conserved membrane-binding domain targets proteins to organelle contact sites. *J. Cell Sci.* 125, 49–58. doi: 10.1242/jcs.085118

Tremblay, M. G., Herdman, C., Guillou, F., Mishra, P. K., Baril, J., Bellenfant, S., et al. (2016). Extended synaptotagmin interaction with the fibroblast growth factor receptor depends on receptor conformation, not catalytic activity. *J. Biol. Chem.* 291:3173. doi: 10.1074/jbc.A115.656918

Tremblay, M. G., and Moss, T. (2016). Loss of all 3 extended synaptotagmins does not affect normal mouse development, viability or fertility. *Cell Cycle* 15, 2360–2366. doi: 10.1080/15384101.2016.1203494

van Meer, G., Voelker, D. R., and Feigenson, G. W. (2008). Membrane lipids: where they are and how they behave. *Nat. Rev. Mol. Cell Biol.* 9, 112–124. doi: 10.1038/nrm2330

Vierra, N. C., Kirmiz, M., van der List, D., Santana, L. F., and Trimmer, J. S. (2019). Kv2.1 mediates spatial and functional coupling of L-type calcium channels and ryanodine receptors in mammalian neurons. *Elife* 8:49953. doi: 10.7554/eLife.49953

Vig, M., Peinelt, C., Beck, A., Koomoa, D. L., Rabah, D., Koblan-Huberson, M., et al. (2006). CRACM1 is a plasma membrane protein essential for store-operated Ca^{2+} entry. *Science* 312, 1220–1223. doi: 10.1126/science.1127883

Wang, P., Hawes, C., and Hussey, P. J. (2017). Plant endoplasmic reticulum-plasma membrane contact sites. *Trends Plant Sci.* 22, 289–297. doi: 10.1016/j.tplants.2016.11.008

Wang, P., Hawkins, T. J., Richardson, C., Cummins, I., Deeks, M. J., Sparkes, I., et al. (2014). The plant cytoskeleton, NET3C, and VAP27 mediate the link between the plasma membrane and endoplasmic reticulum. *Curr. Biol.* 24, 1397–1405. doi: 10.1016/j.cub.2014.05.003

Wang, P., Pleskot, R., Zang, J., Winkler, J., Wang, J., Yperman, K., et al. (2019). Plant AtEH/Pan1 proteins drive autophagosome formation at ER-PM contact sites with actin and endocytic machinery. *Nat. Commun.* 10:5132. doi: 10.1038/s41467-019-12782-6

Wang, Y., Deng, X., Zhou, Y., Hendron, E., Mancarella, S., Ritchie, M. F., et al. (2009). STIM protein coupling in the activation of Orai channels. *Proc. Natl. Acad. Sci. U.S.A.* 106, 7391–7396. doi: 10.1073/pnas.0900293106

Weber, T., Zemelman, B. V., McNew, J. A., Westermann, B., Gmachl, M., Parlati, F., et al. (1998). SNAREpins: minimal machinery for membrane fusion. *Cell* 92, 759–772. doi: 10.1016/S0092-8674(00)81404-X

Weber-Boyvat, M., Trimbuch, T., Shah, S., Jäntti, J., Olkkonen, V. M., and Rosenmund, C. (2020). ORP/Osh mediate cross-talk between ER-plasma membrane contact site components and plasma membrane SNAREs. *Cell Mol. Life Sci*. doi: 10.1007/s00018-020-03604-w. [Epub ahead of print].

Wilhelm, L. P., Wendling, C., Védie, B., Kobayashi, T., Chenard, M. P., Tomasetto, C., et al. (2017). STARD3 mediates endoplasmic reticulum-to-endosome cholesterol transport at membrane contact sites. *EMBO J.* 36, 1412–1433. doi: 10.15252/embj.201695917

Williams, R. T., Manji, S. S., Parker, N. J., Hancock, M. S., Van Stekelenburg, L., Eid, J. P., et al. (2001). Identification and characterization of the STIM (stromal interaction molecule) gene family: coding for a novel class of transmembrane proteins. *Biochem. J.* 357, 673–685. doi: 10.1042/bj3570673

Willoughby, D., Everett, K. L., Halls, M. L., Pacheco, J., Skroblin, P., Vaca, L., et al. (2012). Direct binding between Orai1 and AC8 mediates dynamic interplay between Ca^{2+} and cAMP signaling. *Sci. Signal.* 5:ra29. doi: 10.1126/scisignal.2002299

Willoughby, D., Wachten, S., Masada, N., and Cooper, D. M. (2010). Direct demonstration of discrete Ca2+ microdomains associated with different isoforms of adenylyl cyclase. *J. Cell Sci.* 123, 107–117. doi: 10.1242/jcs.062067

Wolf, W., Kilic, A., Schrul, B., Lorenz, H., Schwappach, B., and Seedorf, M. (2012). Yeast Ist2 recruits the endoplasmic reticulum to the plasma membrane and creates a ribosome-free membrane microcompartment. *PLoS ONE* 7:e39703. doi: 10.1371/journal.pone.0039703

Wong, L. H., Gatta, A. T., and Levine, T. P. (2019). Lipid transfer proteins: the lipid commute via shuttles, bridges and tubes. *Nat. Rev. Mol. Cell Biol.* 20, 85–101. doi: 10.1038/s41580-018-0071-5

Wu, L., Shen, C., Seed Ahmed, M., Östenson, C. G., and Gu, H. F. (2016). Adenylate cyclase 3: a new target for anti-obesity drug development. *Obes. Rev.* 17, 907–914. doi: 10.1111/obr.12430

Xiao, J., Luo, J., Hu, A., Xiao, T., Li, M., Kong, Z., et al. (2019). Cholesterol transport through the peroxisome-ER membrane contacts tethered by PI(4,5)P(2) and extended synaptotagmins. *Sci. China Life Sci.* 62, 1117–1135. doi: 10.1007/s11427-019-9569-9

Xiao, Q., Yu, K., Perez-Cornejo, P., Cui, Y., Arreola, J., and Hartzell, H. C. (2011). Voltage- and calcium-dependent gating of TMEM16A/Ano1 chloride channels are physically coupled by the first intracellular loop. *Proc. Natl. Acad. Sci. U.S.A.* 108, 8891–8896. doi: 10.1073/pnas.1102147108

Xie, B., Nguyen, P. M., and Idevall-Hagren, O. (2019). Feedback regulation of insulin secretion by extended synaptotagmin-1. *FASEB J.* 33, 4716–4728. doi: 10.1096/fj.201801878R

Xu, J., Bacaj, T., Zhou, A., Tomchick, D. R., Sudhof, T. C., and Rizo, J. (2014). Structure and Ca(2)(+)-binding properties of the tandem C(2) domains of E-Syt2. *Structure* 22, 269–280. doi: 10.1016/j.str.2013.11.011

Yamazaki, T., Takata, N., Uemura, M., and Kawamura, Y. (2010). Arabidopsis synaptotagmin SYT1, a type I signal-anchor protein, requires tandem C2 domains for delivery to the plasma membrane. *J. Biol. Chem.* 285, 23165–23176. doi: 10.1074/jbc.M109.084046

Yang, X., Jin, H., Cai, X., Li, S., and Shen, Y. (2012). Structural and mechanistic insights into the activation of Stromal interaction molecule 1 (STIM1). *Proc. Natl. Acad. Sci. U.S.A.* 109, 5657–5662. doi: 10.1073/pnas.1118947109

Yao, Y., Ferrer-Montiel, A. V., Montal, M., and Tsien, R. Y. (1999). Activation of store-operated Ca^{2+} current in Xenopus oocytes requires SNAP-25 but not a diffusible messenger. *Cell* 98, 475–485. doi: 10.1016/S0092-8674(00)81976-5

Yellen, G. (1998). The moving parts of voltage-gated ion channels. *Q. Rev. Biophys.* 31, 239–295. doi: 10.1017/S0033583598003448

Yu, H., Liu, Y., Gulbranson, D. R., Paine, A., Rathore, S. S., and Shen, J. (2016). Extended synaptotagmins are Ca2+-dependent lipid transfer proteins at membrane contact sites. *Proc. Natl. Acad. Sci.* 113, 4362–4367. doi: 10.1073/pnas.1517259113

Yuan, J. P., Zeng, W., Dorwart, M. R., Choi, Y. J., Worley, P. F., and Muallem, S. (2009). SOAR and the polybasic STIM1 domains gate and regulate Orai channels. *Nat. Cell Biol.* 11, 337–343. doi: 10.1038/ncb1842

Zachariou, V., Liu, R., LaPlant, Q., Xiao, G., Renthal, W., Chan, G. C., et al. (2008). Distinct roles of adenylyl cyclases 1 and 8 in opiate dependence: behavioral, electrophysiological, and molecular studies. *Biol. Psychiatry.* 63, 1013–1021. doi: 10.1016/j.biopsych.2007.11.021

Zhang, D., Vjestica, A., and Oliferenko, S. (2012). Plasma membrane tethering of the cortical ER necessitates its finely reticulated architecture. *Curr. Biol.* 22, 2048–2052. doi: 10.1016/j.cub.2012.08.047

Zhang, S. L., Yeromin, A. V., Zhang, X. H., Yu, Y., Safrina, O., Penna, A., et al. (2006). Genome-wide RNAi screen of Ca(2+) influx identifies genes that regulate Ca(2+) release-activated Ca(2+) channel activity. *Proc. Natl. Acad. Sci. U.S.A.* 103, 9357–9362. doi: 10.1073/pnas.0603161103

Zhang, S. L., Yu, Y., Roos, J., Kozak, J. A., Deerinck, T. J., Ellisman, M. H., et al. (2005). STIM1 is a Ca^{2+} sensor that activates CRAC channels and migrates from the Ca^{2+} store to the plasma membrane. *Nature* 437, 902–905. doi: 10.1038/nature04147

Zhang, Y., Guan, Y., Pan, S., Yan, L., Wang, P., Chen, Z., et al. (2020). Hypothalamic extended synaptotagmin-3 contributes to the development of dietary obesity and related metabolic disorders. *Proc. Natl. Acad. Sci. U.S.A.* 117, 20149–20158. doi: 10.1073/pnas.2004392117

Zheng, L., Stathopulos, P. B., Schindl, R., Li, G. Y., Romanin, C., and Ikura, M. (2011). Auto-inhibitory role of the EF-SAM domain of STIM proteins in store-operated calcium entry. *Proc. Natl. Acad. Sci. U.S.A.* 108, 1337–1342. doi: 10.1073/pnas.1015125108

Zhou, Y., Srinivasan, P., Razavi, S., Seymour, S., Meraner, P., Gudlur, A., et al. (2013). Initial activation of STIM1, the regulator of store-operated calcium entry. *Nat. Struct. Mol. Biol.* 20, 973–981. doi: 10.1038/nsmb.2625

Conflict of Interest: The authors declare that the research was conducted in the absence of any commercial or financial relationships that could be construed as a potential conflict of interest.

frontiers in Cell and Developmental Biology

REVIEW
published: 11 February 2021
doi: 10.3389/fcell.2021.635518

ER-PM Contact Sites – SNARING Actors in Emerging Functions

Bailey Hewlett[1†], Neha Pratap Singh[1], Christian Vannier[1] and Thierry Galli[1,2]*

[1] INSERM U1266, Institut de Psychiatrie et Neurosciences de Paris, Université de Paris, Paris, France, [2] GHU PARIS Psychiatrie and Neurosciences, Paris, France

The compartmentalisation achieved by confining cytoplasm into membrane-enclosed organelles in eukaryotic cells is essential for maintaining vital functions including ATP production, synthetic and degradative pathways. While intracellular organelles are highly specialised in these functions, the restricting membranes also impede exchange of molecules responsible for the synchronised and responsive cellular activities. The initial identification of contact sites between the ER and plasma membrane (PM) provided a potential candidate structure for communication between organelles without mixing by fusion. Over the past decades, research has revealed a far broader picture of the events. Membrane contact sites (MCSs) have been recognized as increasingly important actors in cell differentiation, plasticity and maintenance, and, upon dysfunction, responsible for pathological conditions such as cancer and neurodegenerative diseases. Present in multiple organelles and cell types, MCSs promote transport of lipids and Ca^{2+} homoeostasis, with a range of associated protein families. Interestingly, each MCS displays a unique molecular signature, adapted to organelle functions. This review will explore the literature describing the molecular components and interactions taking place at ER-PM contact sites, their functions, and implications in eukaryotic cells, particularly neurons, with emphasis on lipid transfer proteins and emerging function of SNAREs.

Keywords: membrane contact sites, tethers, lipid transfer, SNAREs, neurons

OPEN ACCESS

Edited by:
Yasunori Saheki,
Lee Kong Chian School of Medicine, Nanyang Technological University, Singapore

Reviewed by:
Raghu Padinjat,
National Centre for Biological Sciences, India
Christopher Stroupe,
University of Virginia, United States

****Correspondence:***
Thierry Galli
thierry.galli@inserm.fr

†Present address:
Bailey Hewlett,
MRC-LMCB, University College London, London, United Kingdom

Specialty section:
This article was submitted to Membrane Traffic, a section of the journal Frontiers in Cell and Developmental Biology

Received: *30 November 2020*
Accepted: *21 January 2021*
Published: *11 February 2021*

Citation:
Hewlett B, Singh NP, Vannier C and Galli T (2021) ER-PM Contact Sites – SNARING Actors in Emerging Functions. Front. Cell Dev. Biol. 9:635518. doi: 10.3389/fcell.2021.635518

INTRODUCTION

A distinctive property of eukaryotic cells is the compartmentaliasation of the cytoplasm by intracellular membranes. In addition to the plasma membrane (PM), phospholipid bilayers and monolayers form complex internal networks, defining individual organelles specialised for specific functions. While this is useful for separating incompatible biochemical reactions and restricting specific conditions such as low pH, and/or redox potential, compartmentalisation can impede the transfer of molecules which instead relies on vesicular trafficking (Helle et al., 2013; Scorrano et al., 2019). Recent studies however have shown that long known specialised regions of membrane in close proximity to each other, called membrane contact sites (MCSs), could also be involved in communication (Gallo et al., 2016; Kang et al., 2019; Bohnert, 2020). Early research identified closely apposed domains of the endoplasmic reticulum (ER) and mitochondria in hepatocytes (Bernhard and Rouiller, 1956) and of ER with T-tubule invaginations of the PM in muscle cells (Porter and Palade, 1957). However, the physiological significance of many MCSs was poorly understood. The first insights only arrived in the 1990s, with observations suggesting that phosphoserine-derivatives in the mitochondrial membranes are synthesised by the ER, and that

contact between the organelles was involved in lipid transfer (Vance, 1990; Stefan et al., 2017). Since, MCSs have been identified in a range of organisms, cell types and between different organelles, the structure and function of many are still yet to be fully understood. MCSs are defined as domains of organelles in close apposition to each other, in general via biochemically defined interactions. They involve most organelles and can be homotypic (contacts between distal regions of an organelle or organelles of the same type) or heterotypic (between organelles of different nature) (Gatta and Levine, 2017; Scorrano et al., 2019). Due to its extensive and dynamic network throughout the cell (Nixon-Abell et al., 2016), the ER is engaged as a partner in almost all heterotypic connections and mitochondria have also been shown to form contacts with multiple organelles (Gatta and Levine, 2017).

The diversity of interactions observed suggests a variety of functions and processes that MCSs are involved in. For example, ER contacts with mitochondria are important in lipid transport and metabolism (Dimmer and Rapaport, 2017). Additionally, the ER can wrap around mitochondrial tubules and facilitate fission (Tilokani et al., 2018). Remarkably, numerous cellular processes depend on ER contacts beside organelle dynamics. ER-mediated contacts sites have been shown to facilitate Ca^{2+} homoeostasis (Wu et al., 2006) lipid transport (Tavassoli et al., 2013), modulate autophagic biogenesis (Nascimbeni et al., 2017), organelle morphology (Manford et al., 2012), and excitability in neurons and muscle cells (Ito et al., 2001; Sahu et al., 2019). Incidentally, several protein families of no obvious similarity have been identified at MCSs. Specific isoforms or even entirely separate families are allocated to MCSs depending on the membranes involved and the cell type, raising questions regarding their functionality and expression patterns. This review will summarize the literature describing the nature and molecular composition of ER-PM MCSs, presenting the roles of various populating protein families, emphasising MCSs in neurons and among related functions, the emerging role of SNAREs at MCSs.

ER-PM CONTACT SITES IN NEURONS

Main Features and Morphology

The ER forms an extensive network of tubules and cisternae throughout the cell and has a range of roles integral to cell survival and function including lipid synthesis, protein synthesis, and Ca^{2+} regulation. The network projects to all parts of the cell and is functionally connected to other organelles (Nixon-Abell et al., 2016). ER-mediated contact sites typically present the following characteristics: 1) the two membranes involved are tethered within 7 – 30 nm of each other, 2) despite this close proximity, membrane composition is maintained and there are no reports of fusion between organelles, and 3) specific proteins and lipids are enriched at MCSs, creating microdomains (Prinz, 2014; Eisenberg-Bord et al., 2016; Gallo et al., 2016). Depending on their type, MCSs can be transient or stable over time, according to their role in cellular structure and physiology, as noted in Orai–Stim (Helle et al., 2013) and Kv2.1 (Fox et al., 2015) induced tethering respectively. Importantly, the interactions at MCSs influence the function of either or both the participating organelles.

Endoplasmic reticulum-mediated MCSs also show specific characteristics. Studies in *Saccharomyces cerevisiae* indicate that tethering another membrane excludes ribosomes from the cytoplasmic face of the ER (Wolf et al., 2012) and controls membrane curvature, vital for maintaining membrane integrity (Collado et al., 2019). The ER MCSs with other organelles, including mitochondria and peroxisomes (Elbaz and Schuldiner, 2011), are some of the best characterized examples of MCSs and have been described in multiple cell types and organisms, mediating additional processes at each contact site.

Initial evidence for ER-PM MCSs in neurons and muscle cells came from observation by electron microscopy, identifying subsurface cisternae "closely opposed" to the PM, maintaining a separation of 5–8 nm between the membranes (Porter and Palade, 1957; Rosenbluth, 1962). The high concentration of proteins in the membrane at these sites, as observed by freeze-fracture techniques, opened the possibility that these junctions had functions related to cell excitability (Henkart et al., 1976). Much later, this hypothesis was reinforced in rat hippocampal neurons (Spacek and Harris, 1997) with subsequent characterisation of novel tethers such as Kv2.1 K^+ channels (Fox et al., 2015; Kirmiz et al., 2018) along with several SNARE proteins (Petkovic et al., 2014). 3D reconstructions show that the percentage of cell body PM engaged in MCSs with the ER as approximately 12.5% in the *Nucleus accumbens*, but varies in other brain regions (Wu et al., 2017). In agreement with earlier studies, the authors also found that, while the ER extends throughout neuronal cells, ER-PM MCSs are far less frequent in dendrites, only at the periphery of the post-synaptic densities and not at all in spines (Spacek and Harris, 1997; Wu et al., 2017). In contrast, yeast ER MCSs can cover 25–40% of the PM while separation reports have varied between studies, averaging 33 nm (West et al., 2011) but also reported lower at 21 nm (Collado et al., 2019). Several studies have also distinguished the morphology of ER associated with the PM in various models (West et al., 2011; Manford et al., 2012; Nixon-Abell et al., 2016; Wu et al., 2017). While the ER network surrounds the nucleus to form the nuclear envelope (Helle et al., 2013), tubules extend throughout the cell into the periphery, referred to as cortical ER (cER). Here the ER presents highly variable morphology, with "flattened sheets" with lumen width >25 nm (in neurons) (Orci et al., 2009; Wu et al., 2017) separated by thin tubules (Fernández-Busnadiego et al., 2015; Wu et al., 2017; Collado et al., 2019). Consistent with the dynamic nature of the ER, the larger sheets observed can quickly assemble and disassemble, likely due to interactions with motor proteins on microtubules (Nixon-Abell et al., 2016), which are frequently found in alignment with the cER (Orci et al., 2009). Extending into dendrites, the ER predominantly forms tubules and is less frequently in contact with the PM (Wu et al., 2017). ER-PM MCSs in the axons and dendrites of neurons are smaller and less frequent than in the cell body, and while the ER can enter the necks of large spines, they do not seem to form contacts (Spacek and Harris, 1997; Wu et al., 2017).

Molecular Composition of ER-PM MCSs

Membrane contact sites could be viewed as microenvironments where selected proteins, namely tethering proteins, first establish physical bridge(s) between membranes, then recruit partner proteins which perform contact specific functions (Helle et al., 2013). In MCSs, membrane-associated tethering proteins maintain two distinct membranes in close apposition, under conditions where no membrane fusion occurs. Tethering proteins are often ER integral membrane proteins able to directly bind to either PM lipids or soluble lipid-binding proteins (Prinz, 2014; Eisenberg-Bord et al., 2016). Alternatively, trans-interactions involve integral membrane proteins that can project from each membrane into the cytoplasm. Broadly, tethers are defined as proteins or protein complexes that a) are physically present at the MCS, b) contribute a tethering force between the participating membranes, c) affect the processes taking place at the MCS, and d) modulate the degree of proximity and number of MCSs (Helle et al., 2013; Eisenberg-Bord et al., 2016).

Multiple protein families have been indicated at ER-PM junctions, hosting unusual molecular compositions including selected proteomes and potentially lipidomes (Phillips and Voeltz, 2016). No single-family appears to solely perform as a tether. More commonly, tethers are involved in additional functions either by themselves or together with binding partners, identified in model systems and translated to human homologues by sequencing and proteomics. Accordingly, studies presenting ablation of a tethering family generally show reduced numbers of contact sites rather than complete abolition, as exemplified in ER-endolysosomal contacts (Henne et al., 2015) and ER-PM contacts (Manford et al., 2012), further indicating functional redundancy. Loss of all the aforementioned proteins leads to ER-PM dissociation, together with the accumulation of cytoplasmic ER, resulting in misregulation of phosphoinositide (at PM) and Ca^{2+} signalling; compromising cellular integrity, and activating ER unfolded response (Manford et al., 2012; Stefan, 2018; Wang and Dehesh, 2018). The role played by ER-PM MCS in maintaining membrane homoeostasis remains to be investigated. So far, several families of proteins have been identified for their functions in lipid modification and/or transfer between membranes; the TMEM16 family, E-Syt (Extended Synaptotagmins), VAPs (VAMP-associated proteins), Junctophilins, and more recently, SNAREs (**Figure 1**), as described below.

Anoctamin/TMEM16 Family

Ist2 is an integral membrane protein predominantly found in the cER in yeast. Studies of the Ist2 family have shown its members can bind to phosphatidylinositol-4,5-bisphosphate ($PI(4,5)P_2$) in the PM, via a *C*-terminal basic stretch of 69 amino acids (Ercan et al., 2009; Fischer et al., 2009; Maass et al., 2009). This interaction not only contributes to the localisation of Ist2 to cER but also recruits ER to the PM, creating a compartment devoid of ribosomes (Wolf et al., 2012). Furthermore, deletion of Ist2 increased the distance between ER-PM associations, while overexpression dramatically increased the percentage of cER associated with the yeast PM (Wolf et al., 2012).

The first identified mammalian orthologues, TMEM16A/Ano1 and TMEM16B/Ano2 are Ca^{2+} activated Cl^- channels (Yang et al., 2008; Caputo et al., 2008). Other Anoctamins of the 10-member family include TMEM16C (ANO3), TMEM16D (ANO4), TMEM16F (ANO6), TMEM16G (ANO7), and TMEM16J (ANO9) and although some of which can be found localised to ER-PM MCSs (Duran et al., 2012; Bushell et al., 2019), their functions are not fully understood (Picollo et al., 2015). The family members display substantial functional diversity (Milenkovic et al., 2010) and different tissue localisation (Schreiber et al., 2010), though their structural analysis shows a conserved topology including eight *N*-terminal transmembrane domains (TMDs) and stretches of basic amino acids at the *C*-terminus (Pedemonte and Galietta, 2014). As TMEM family members are tethers with an intrinsic activity in lipid transfer (for example, that of phosphatidylserine, i.e., PS) (Lees et al., 2017), it was unexpected to discover that, in yeast, efficient transport of PS to the PM by the cytosolic lipid transfer protein (LTP) Osh6, requires its association with Ist2 (D'Ambrosio et al., 2020). This functionally distinct contribution to PS homoeostasis illustrates the complexity of TMEM16 biology at MCSs. Besides delineating the regulatory role of Ca^{2+} channels, the structural bases of the family members' functional diversity remain to be elucidated (Picollo et al., 2015). The TMEM16F interactome includes Munc18-1, a partner of the PM SNARE Syntaxin1 (Stx1) (Brooks et al., 2015). TMEM16K, an ER lipid scramblase involved in spinocerebellar ataxia, was found at ER-endosome MCSs further emphasising the importance of this family of proteins. Several ER and endosomal SNAREs were found in close proximity to TMEM16K (Petkovic et al., 2020) but the potential functional relationship is unknown.

VAPs (VAMP-Associated Proteins)

VAMP-associated proteins or VAPs are another family suggested to act as tethers at MCSs, with orthologues identified in plants (Siao et al., 2016) and yeast (Loewen et al., 2003). VAP's acronym refer to the initial interaction of VAP-A with the SNARE VAMP in *Aplysia* (Skehel et al., 1995) but the functional relevance of VAP-SNARE interactions is not yet well defined (Weir et al., 2001). VAPs are highly conserved type II integral ER membrane proteins and interact with a wide variety of intracellular proteins (Nishimura et al., 1999; Murphy and Levine, 2016), regulating several cellular processes (Soussan et al., 1999; Kagiwada and Zen, 2003). Structurally, VAPs consist of an *N*-terminal MSP (major sperm protein) domain, a coiled-coil domain involved in dimerisation (Kim et al., 2010) and finally a *C*-terminal TMD, responsible for anchoring in the ER membrane (Murphy and Levine, 2016; Sun and De Camilli, 2018). VAPs are prominently present at several ER-mediated contact sites including with the PM, Golgi, and mitochondria (Eisenberg-Bord et al., 2016). Deletion of the yeast homologues Scs2 and Scs22 result in a loss of cER associated with the PM (Manford et al., 2012). VAPs can also recruit proteins containing an FFAT motif, which consists of two phenylalanine residues flanked by an acidic tract which binds to a positively charged binding motif on the face of the MSP domain (Murphy and Levine, 2016). FFAT motifs have been found in the oxysterol-binding protein (OSBP) related

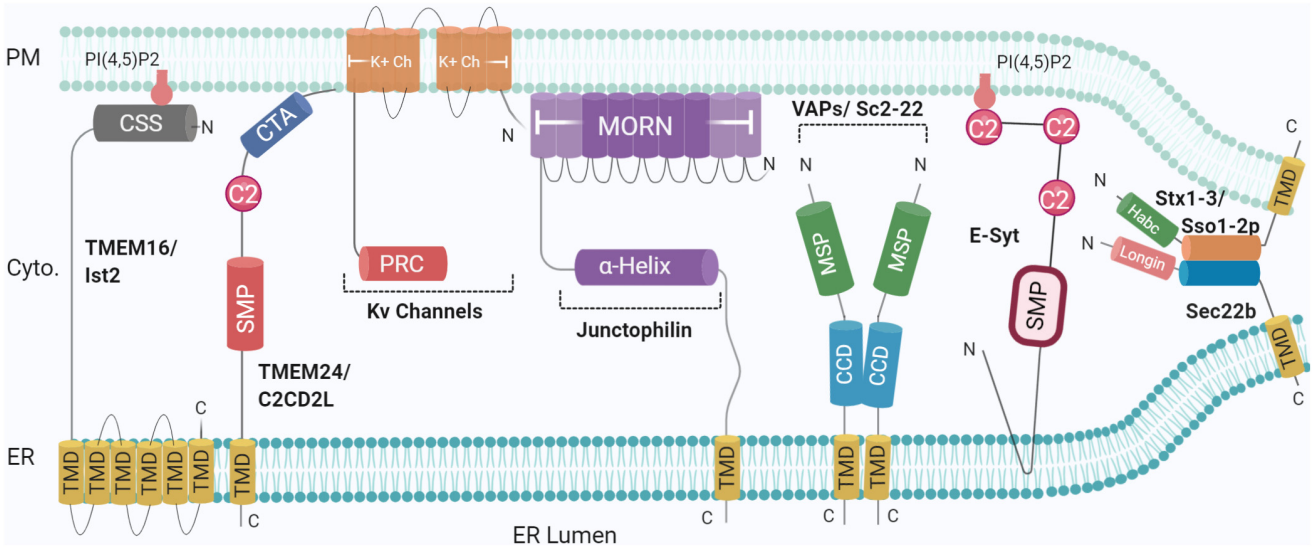

FIGURE 1 | Schematic illustration of the organization and topology of ER-PM tethering proteins. Shown are the so-far identified protein complexes acting in ER to PM membrane recruitment, in yeast and mammals: Sec22b-Syntaxin1/3 (Sso1/2p in yeast) complex, TMEM16 (Ist2 in Yeast), TMEM24 (C2CD2L in Yeast), Kv Channels, Junctophillins, VAPs (Sc2-22 in Yeast), Extended Synaptotagmin (E-Syt). SNARE complexes generate short-range (~10 nm) MCS whereas other tethers generate longer range (~20–30 nm). Created with BioRender.com.

protein family (ORPs), Ceramide transfer protein and *N*-terminal domain-interacting receptor 1–3 (Loewen et al., 2003; Murphy and Levine, 2016). The versatility of this structure gives VAP an opening to interact with multiple proteins, divided into three categories, 1) SNAREs, 2) Viral proteins, and 3) FFAT-motif-containing proteins (Loewen et al., 2003). VAPs, therefore, have a diverse catalogue of binding partners, including LTPs such as oxysterol-binding homology (Osh) proteins and Nir2, located at ER-PM contact sites. Accordingly, the presence of VAP-A and VAP-B is paramount for lipid transport at ER-Golgi contact sites, with knockdown experiments showing detrimental effects on Golgi conformation and distorted composition of phosphatidylinositol-4-phosphate (PI4P), sphingomyelin, and diacylglycerol (DAG) in the Golgi membrane (Peretti et al., 2008).

Two groups independently identified an unexpected VAP binding partner in hippocampal neurons. Despite lacking a typical FFAT motif, PM-localised Kv2 channels form ER-PM MCSs via the recruitment of the ER-resident VAPs. This interaction is thought to be regulated by Kv2 phosphorylation (Kirmiz et al., 2018; Johnson et al., 2019), thus involving negative charges acting like the acidic amino acid residues of the FFAT motif of ORPs/Oshs (Sun and De Camilli, 2018) (see below). Incidentally, VAP-A and VAP-B knockdown reduces Kv2 clustering (Kirmiz et al., 2018; Johnson et al., 2019). Finally, VAP-B in particular is associated with the progressive neurodegenerative diseases Amyotrophic Lateral Sclerosis and Parkinson's disease. Mutations in the MSP domain result in conformational changes that promote oligomerisation and degradation (Kim et al., 2010; Murphy and Levine, 2016), altering ER morphology (Yamanaka et al., 2020). This leads to a range of mechanistic dysfunctions including the different extent of MCS tethering, cytoskeletal coordination, and lipid homoeostasis (Murphy and Levine, 2016) as shown in *Drosophila* (Forrest et al., 2013), highlighting the role of VAPs as an important mediator in ER-PM contact formation (**Figures 1**, **2**).

JPH (Junctophilins)

Junctophilins were originally identified as junction components in muscle cells, with JPH-2 knockouts presenting reduced associations between the sarcoplasmic reticulum (SR) and PM (Takeshima et al., 2000). While invertebrates have one genomic copy, mammals have four, all identified in excitable cells (Landstrom et al., 2014). Subtypes 1 and 2 are expressed in skeletal and cardiac muscle respectively, while 3 and 4 have been shown to be expressed in hippocampal pyramidal neurons (Nishi et al., 2003). JPHs are embedded in the ER/SR via a C-terminal TMD (Nishi et al., 2000; Takeshima et al., 2000), following a defining feature of the family; eight *N*-terminal MORN (membrane and recognition nexus) motifs, the final two of which are separated by a joining region (Landstrom et al., 2014). These MORN motifs are hypothesised to bind phospholipids, specifically phosphatidylinositol phosphates (PIPs) such as PI4P and PIP_2 (Landstrom et al., 2014), mediating attachment to the PM according to the number and sequence present, as removal of specific MORN motifs in JPH-1 leads to localisation in the nucleus and cytoplasm rather than PM (Takeshima et al., 2000). There is evidence that the *N*-terminal region (containing the MORN repeats) mediates PM targeting, though the direct involvement of MORN repeats has not been demonstrated (Nakada et al., 2018; Rossi et al., 2019). Between the MORN motifs and *C*-terminal TMD sits an alpha helix, which modulates the distance between the ER/SR and PM, followed by a divergent region of unknown function, so named due to limited sequence conservation between isoforms (Garbino et al., 2009) (**Figure 1**).

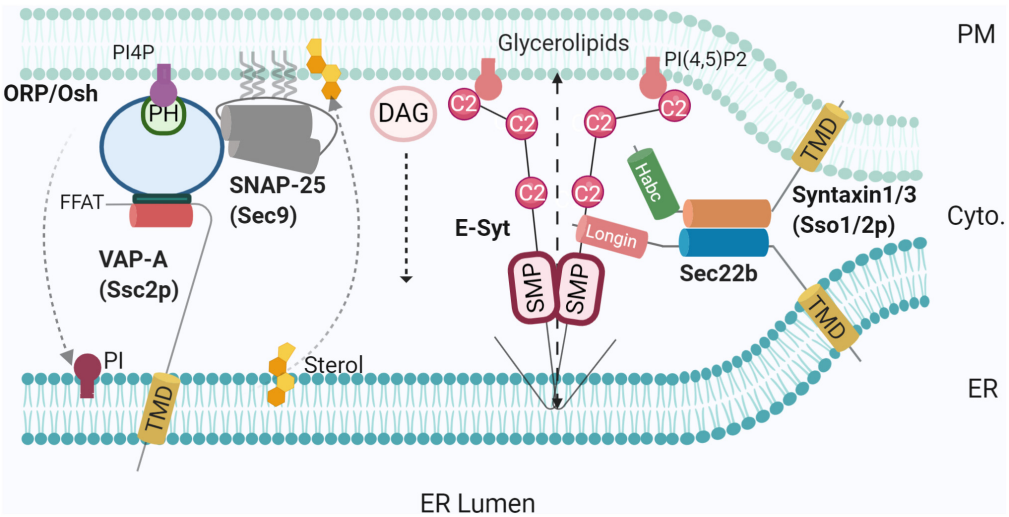

FIGURE 2 | SNAREs and lipid transfer proteins at the MCS. Using varying mechanisms such as FFAT to bridge SNAP25-OSH/ORP-VAP-A, and non-fusogenic Sec22b-Stx1- E-Syt complex, LTPs promote MCS tethering and mediate lipid transfer [PI4P, sterol, glycerolipids, and diacylglycerol (DAG)]. PI4P phosphatase at the ER membrane Sac1 was not represented for simplicity. Created with BioRender.com.

Initially thought to be primarily structural components, Ito et al. (2001) highlights roles for JPHs mediating Ca^{2+} regulation in muscle cells by stabilising a complex of Ryanodine receptor and DHPR Ca^{2+} channels in the SR and PM, respectively. More recently, this has also been observed in T cells (Woo et al., 2016) and several neuronal populations. For example, JPH-3 and -4 double knockouts result in behavioural and physiological defects in mice in addition to dysfunctional Ca^{2+} release and impaired plasticity in hippocampal neurons (Moriguchi et al., 2006). Loss of JPH isoforms prevents the after hyperpolarisation necessary to form Ca^{2+} microdomains (Kakizawa et al., 2008; Takeshima et al., 2015) as JPH-3 and/or -4 are needed to tether and stabilise a Cav1-RyR2-KCa3.1 Tripartite Complex necessary for neuronal excitability regulation (Sahu et al., 2019). Aside from functional studies, JPH-3 has been implicated in neurodegenerative disorders, notably in Huntington's disease-like (HDL) syndrome. Up to 15% of patients lacking pathological mutations in Huntingtin, the canonical cause of Huntington's disease, show CAG/CTG repeats in JPH-3 (Holmes et al., 2001) which generate toxic RNA foci and protein aggregation. Loss of JPH-3 in mouse models presents progressive motor abnormalities, consistent with JPH-3 as an, albeit rare, cause of HDL syndrome (Seixas et al., 2012). JPHs have not been connected to SNAREs yet.

E-Syts (Extended Synaptotagmins)

Extended synaptogamins (E-Syts) are evolutionarily conserved proteins shown to function at ER-PM membrane contact sites in multicellular organisms. Sequence and domain analysis revealed homology with the yeast Tricalbins family, also identified at ER-PM MCSs. The deletion of all three known Tricalbin isoforms in combination with deletion of other associated tethers reduces the number of contact sites (Manford et al., 2012). Tricalbins consist of an *N*-terminal TMD, followed by a synaptotagmin-like mitochondrial lipid-binding protein (SMP) domain and three to five C2 domains (Toulmay and Prinz, 2012), which bind to membranes in a Ca^{2+}-dependent manner (Schulz and Creutz, 2004). Indeed, of the three mammalian E-Syt isoforms, E-Syts differs from the yeast orthologues in the number of C2 domains; E-Syt1 has five, while E-Syts2/3 have three C2 domains (Saheki and De Camilli, 2017), enabling recruitment to ER-PM interfaces by membrane-binding of C2 domains upon an increase of cytosolic Ca^{2+} level (Chang et al., 2013; Giordano et al., 2013; Saheki et al., 2016).

In yeast, the Tricalbins are involved in lipid transfer and maintenance of ER curvature, specifically in the formation of cER peaks which are essential for lipid transfer to maintain PM integrity (Collado et al., 2019; Hoffmann et al., 2019). As such, all E-Syts have been shown to perform similar roles under Ca^{2+} regulation. E-Syts2/3 bind $PI(4,5)P_2$ at the PM via the C2C domain (**Figure 1**), but E-Syt1, which is distributed over the whole ER surface area under resting conditions, binds at low Ca^{2+} concentrations via C2E (Giordano et al., 2013). Upon micromolar changes in cytosolic Ca^{2+}, E-Syt1 is recruited to ER-PM sites where it can control the distance between the membranes, after Ca^{2+}-binding to the C2C domain (Fernández-Busnadiego et al., 2015; Idevall-Hagren et al., 2015). Additionally, hetero- or homodimerisation of SMP domains forms a hydrophobic channel that can facilitate lipid transfer *in vitro* (Schauder et al., 2014; Yu et al., 2016) (**Figures 1**, **2**). Finally, the single E-Syt orthologue in *Drosophila*, catalysing lipid transfer in photoreceptors at the submicrovillar cisternae and the growth of the organism (Nath et al., 2020), was also suggested to modulate synaptogenesis (Kikuma et al., 2017). E-Syts have since been identified in mammalian neuronal cells but, while it is plausible that they can perform these functions

(Giordano et al., 2013; Fernández-Busnadiego et al., 2015) their physiological significance in neurons is so far unclear and may only be noticeable under specific conditions. Indeed, hippocampal neurons from E-Syt triple knockout mice exhibited no change in ER morphology or protein composition, and neuronal survival under stress was not impaired, suggesting that other tethers may provide compensation for their loss (Sclip et al., 2016). ESyts have recently been connected to SNAREs as discussed below.

SNAREs

Soluble *N*-ethylmaleimide-sensitive factor attachment protein receptors (SNAREs) constitute the basic molecular machinery of intracellular membrane fusion. Positioned on opposite membranes, vesicular SNAREs on one side and target SNAREs on the other assemble in a ternary complex which allows for close docking and subsequent fusion as exemplified in the case of synaptic vesicle fusion with the presynaptic PM (Galli and Haucke, 2004). ER-localised vesicular SNARE Sec22b contains an *N*-terminal Longin domain, followed by the characteristic SNARE domain and finally a C-terminal TMD (Petkovic et al., 2014) (**Figure 1**). Previously shown to be involved in trafficking between the ER and Golgi via its interaction with t-SNAREs Syntaxin 5, membrin, and rbet1 (Williams et al., 2004), Sec22b was shown to associate with Stx1 at ER-PM contact sites in the growth cones of developing neurons (Petkovic et al., 2014). This complex does not include SNAP23/25/29/47. However, liposome assays, while confirming a fusogenic activity of Sec22b in a tripartite assembly with Stx1 and SNAP-25, did not elicit the fusion of membranes in the absence of SNAP25. Additionally, Sec22b was not found at the cell surface. Altogether, this evidence suggest that Sec22b/Stx1 association does not lead to membrane fusion. This assembly represents a new short range (∼10 nm) tether between ER and the PM (Petkovic et al., 2014) able to determine MCS distance, as elongating the linker between the SNARE and TMD domains of Sec22b with polyproline motifs increased the distance between the ER and PM.

Meanwhile, Sec22b was also essential for neuronal development, as RNAi-mediated knockdown of Sec22b inhibited axonal and dendritic growth. Altogether this supports the notion that the complex is not involved in membrane fusion but instead acts as a tether and facilitates additional functions such as lipid transfer. Indeed, in the brain, E-Syts were recently found in complexes containing Stx1 or Stx3 and Sec22b but not SNAP25 (Gallo et al., 2020). Notably, the interaction between the ER-resident ESyts and Sec22b depends on the latter's Longin domain. Removal of the Longin domain induces recovery of SNAP25 in Sec22b immunoprecipitates. Therefore, Sec22b Longin domain likely excludes SNAP25 allowing the occurrence of a non-fusogenic Sec22b-Stx1 complex. Super-resolution imaging of growth cones in developing neurons demonstrated the very close proximity of E-Syt2 and Sec22b beneath the PM, plausibly populating ER-PM contact sites. Moreover, the interaction between E-Syt and Sec22b seems to promote and/or stabilize the association of Sec22b with Stx1/3. E-Syt overexpression is responsible for neuronal membrane expansion in the form of filopodia leading to protuberant hyper-ramified axons, an effect which depends on Stx1 and Sec22b as shown using clostridial toxins and expression of Sec22b extended by a polyproline spacer and the Longin domain. Brought together, these observations allow postulating E-Syt engagement in a tripartite complex with Sec22b and Stx1/3, regulating lipid transfer to the PM within ER-PM contact sites (Gallo et al., 2020). This situation provides the first example of a SNARE-containing MCS where an aborted formation of a fusogenic SNARE complex contributes to the function of an LTP, namely E-Syts. It further emphasises the importance of Longin domains conserved molecular functions in SNARE regulation via promoting and inhibiting membrane fusion by folding back onto the fusion-inducing SNARE coiled-coil domain, along with managing Longin SNAREs interactions with proteins controlling intracellular sorting (Daste et al., 2015; Gallo et al., 2020; Singh et al., 2020).

Other ER-PM Tethers

In addition to the above tethering proteins, which appear to be ubiquitously expressed among mammalian cells, there is recent evidence for tethering candidates exclusive to neuronal populations. For example, TMEM24/C2CD2L is an ER-localised protein shown to transport phosphatidylinositol between the ER and the PM via its SMP domain, binding to the PM in a Ca^{2+}-dependent manner (Lees et al., 2017). TMEM24 is also enriched at ER-PM MCSs in neurons and acts as a tether. TMEM24 is redistributed throughout the ER at high cytosolic Ca^{2+} levels and may interact with other potential tethers including VAPs and Kv2 channels, indicating a regulatory loop related to neuronal activity (Sun et al., 2019) (**Table 1**).

Widely expressed throughout mammalian brain Kv2 K+ channels are distinguished for their neuronal surface localisation pattern divided into a) freely diffusive channels in PM and b) micron-sized clusters present on the soma, dendrites, and axon initial segment (Johnson et al., 2019). Kv2 voltage-gated K^+ channels are frequently identified as interactor partners with known tethers. However, several lines of evidence have recently implicated Kv2 channels as tethers in their own right. Multiple studies identified Kv2 (Kv2.1 and Kv2.2) channel clustering at the PM in hippocampal neurons (Antonucci et al., 2001), cerebellar Purkinje cells (Kaufmann et al., 2009), and even Aplysia neurons (Zhang et al., 2008) due to a 26-amino acid long targeting sequence called the Proximal Restriction and Clustering domain (Lim et al., 2000). While early studies recognised clusters at close appositions, more recent studies have shown that Kv2 clustering remodels the ER, initiating the formation of ER-PM contact sites (Fox et al., 2015; Kirmiz et al., 2018), where L-type Ca^{2+} channels and Ryanodine receptors are recruited to mediate burst firing (Mandikian et al., 2014; Irie and Trussell, 2017; Kirmiz et al., 2018). Further investigation conducted by Kirmiz et al. (2019) has shown that Kv2.1 knockout mice have significantly reduced PI4P and PI(4,5)P2, suggesting their integral involvement in PI4P and PI(4,5)P2 regulation; components crucial for generating secondary messengers inositol trisphosphate (IP3) and DAG (Balla et al., 2020; Jing et al., 2020). However, clustering at close appositions was not equal in all cells; Kv2.1 (also called BK channels) expression differed between pyramidal neurons and

TABLE 1 | Summary of the structural and functional actors at ER-PM membrane contact sites.

Protein	Structure	Cell type	Organelle	Binding pattern	Interactions	References
TMEM16	Evolutionary conserved eight TMDs and C-terminal stretch of basic amino acids	Yeast – Mammal	Cortical ER	Contacts PM via highly basic COOH terminus	IP3R1, Osh6, Munc18-1	Pedemonte and Galietta, 2014; Brooks et al., 2015
VAMP-associated proteins (VAPs)	N-terminal MSP domain, a coiled-coil domain and a C-terminal TMD	Yeast and plant	ER-mediated contact sites including with the PM, Golgi, and mitochondria	Binds via MSP domain to a FFAT motif located on the binding partner	Osh, Nir2, Kv2	Murphy and Levine, 2016; Johnson et al., 2019
Junctophilins (JPH)	Eight N-terminal MORN motifs with C-terminal TMD sits and alpha helix between them	Mammal – Muscle (skeletal and cardiac) + Pyramidal neurons	ER residents	Binds PM via MORN domains	PIPs – PI4P and PIP_2	Nishi et al., 2000; Landstrom et al., 2014
Extended synaptotagmins (E-Syt)	SMP-domain-containing tethers with N-terminal TMD and three to five C2 domains	Yeast, and mammal	ER residents	Ca^{2+} dependent dynamic tether. E-Syt1 binds at low Ca^{2+} concentrations via C2E E-Syts2/3 bind PI(4,5)P2 at the PM via the C2C domain	Sec22b-Stx1; SNAP25	Giordano et al., 2013; Gallo et al., 2020
SNARE Sec22b	N-terminal Longin domain, SNARE domain and a C-terminal TMD	Yeast and mammal	ER-localised	Hypothesized to recruit E-Syt via its Longin domain, involved in non-fusogenic Sec22b-Stx1 complex.	Stx1/3, SNAP-25, E-Syt	Petkovic et al., 2014; Gallo et al., 2020
Kv2 channels	C-terminus with proximal restriction and clustering (PRC) domain	Mammal (Brain), plants	PM -localised	Clusters opposite to astrocytic processes, mediating intercellular communication with non-neuronal cells, in addition to regulating synaptic firing	Ryanodine receptor, VAPs, Stx1, SNAP-25	Du et al., 1998; Fili et al., 2001; Leung et al., 2003; Johnson et al., 2019
TMEM24	Anchored to the ER membrane via an N-terminal transmembrane span, followed by the SMP domain, a C2 domain, and C-terminal region (CTR)	Mammal- neuronal property i.e., pancreatic β-cells, fibroblasts	ER-localised	Binding to the PM in a Ca^{2+}-dependent manner	VAPs and Kv2 channels	Sun et al., 2019
Oxysterol-binding protein (OSBP) related proteins (ORPs)	FFAT motif or C-terminal TMD and membrane-binding domains such as PH domain	Yeast – Mammal	Anchored to PM tethering to ER	Binding to the ER transmembrane protein via the FFAT motif	VAP, Scs2p, Sec9p	Lehto et al., 2001
Steroidogenic acute regulatory protein-related lipid transfer (StARt)	210 conserved amino acid sequence, folding into an α/β helix-grip structure with hydrophobic binding pocket	Yeast – Mammal	Anchored to ER, tethering to PM	Bridging is enabled through phospholipid – GRAM domain and shuttle sterols present through START-like domain	Binds with Cholesterol and interacts with VAP	Besprozvannaya et al., 2018; Sandhu et al., 2018; Naito et al., 2019

interneurons of the hippocampus, potentially in reference to their different functions (Antonucci et al., 2001). Furthermore, Kv2.1 channels in the soma are commonly found clustering opposite to astrocytic processes, so may mediate a method of intercellular communication with non-neuronal cells, not just by regulating synaptic firing (Du et al., 1998).

Interestingly, disrupting the phosphorylation-dependent interaction between Kv2.1 and VAP-A (Kirmiz et al., 2019) is neuroprotective and prevents pro-apoptotic K^+ entry upon ischaemic injury (Schulien et al., 2020). It is particularly interesting that Kv1.1 and Kv2.1 channels were also found to interact with Stx1 (Fili et al., 2001) and SNAP-25 (MacDonald et al., 2002; Leung et al., 2003). These interactions appear conserved in plants where they were shown to regulate membrane expansion for cell growth independently of vesicle traffic (Honsbein et al., 2009). Future studies should address the potential role of Kv-SNARE interactions in regulating MCSs' protein complexes and lipid transfer.

Functions Mediated at ER-PM MCSs

The characterisation of the molecular composition of MCSs has aided the evaluation of their physiological significance, with most tethering proteins seemingly mediating functions such as Ca^{2+} homoeostasis or lipid transport. We will thereafter go on to review the recognised functions occurring at MCSs and their significance in neurons.

Lipid Transfer at ER-PM MCSs

The translocation of lipids between membranes has been shown since some of the earliest studies (Vance, 1990). More recent evidence has begun to shed light on the potential mechanisms and the components involved. LTPs are able to bind lipids in one membrane and deliver them to another, closely situated membrane. Consequently, it is logical that LTPs function at MCSs (Toulmay and Prinz, 2012). While the mechanisms of translocation are still contested, there are two prevailing theories related to their mechanism of action. The tunnel model proposes that lipid-binding domains form a tunnel bridging the intermembrane space, with a small channel open along the length of the domain, such that the polar head group is exposed to the hydrophilic environment as it traverses the channel (Schauder et al., 2014). Hydrophobic residues line the inside of the tunnel stabilising the tails, with conformational changes revealing lipid-binding sites at the tunnel entrance, permitting lipid binding and translocation to the opposing membrane (Schauder et al., 2014; Lees and Reinisch, 2020). Alternatively, the shuttle model suggests that LTPs specifically deliver lipids from the donor membrane, particularly across short distances (under ∼200Å). A series of conformational changes extract the lipid from the single entry point along the closed hydrophobic environment and insert the lipid into the acceptor membrane (Schauder et al., 2014; Wong et al., 2019). Some LTPs have been shown to dimerise to form the tunnel, while others utilise β-barrels (Im et al., 2005), α-helices (Tong et al., 2018), or a mix to form the bridge (Wong et al., 2019). In concert with this, it has been suggested some LTPs (e.g., E-Syt2) may necessarily interact with partners, including other LTPs, to discriminate and transport specific lipids (Schauder et al., 2014). The channel model of E-Syts action clearly fits well with the notion that lipid transfer would work best at the closest contacts such as those involving SNAREs (<10 nm) (Gallo et al., 2020) (**Figure 2**).

Sequence analysis of SMP domains, identified in proteins of the ERMES complex in yeast ER-mitochondrial MCSs (Lee and Hong, 2006), showed homology with the TULIP superfamily, confirming lipid-binding interactions (Kopec et al., 2010; Alva and Lupas, 2016). SMP domains have been shown to dimerise in order to facilitate lipid transport. A shuttle mechanism, as described above, likely operates in E-Syt as the 90Å-long SMP dimer is too short to span the distance between membranes (Schauder et al., 2014). E-Syts were found to mediate the transport of glycerophospholipids in a bidirectional manner using *in vitro* assays (Saheki et al., 2016; Yu et al., 2016; Bian et al., 2018; Bian and De Camilli, 2019). E-Syts might also participate in mechanisms altering lipid composition. For example, $PI(4,5)P_2$ hydrolysis following phospholipase C (PLC) activation by mediated via G-protein coupled receptor (GPCR) (**Figure 3**) led to the release and accumulation of DAG in E-Syt knockout cells (Saheki et al., 2016). In addition, Ca^{2+} influx is needed to relieve autoinhibition of the SMP domain in E-Syt1 by the C2A domain (Yu et al., 2016; Bian et al., 2018). Furthermore, a study in human embryonic kidney cells and rat superior cervical ganglia neurons has shown that E-Syt2 stabilises Sac1, an ER-localised lipid phosphatase, at ER-PM MCSs (Dickson et al., 2016). Here, Sac1 dephosphorylates phosphatidylinositol monophosphates; overexpression of Sac1 increased PI levels approximately two-fold, while PI4P and PIP_2 levels decreased. In accordance with this role, Sac1 and E-Syt2 were shown to co-localise while E-Syt2 knockdown significantly reduced Sac1 puncta at MCSs coinciding with accumulation of PI4P and PIP_2 (Dickson et al., 2016). A role of E-Syt2 in PM PI regulation fits well with the observation that E-Syts regulates growth as shown in *Drosophila* (Nath et al., 2020) and mammalian neurons (Gallo et al., 2020) because of the role of PIP_2 in PM dynamics (Scholze et al., 2018). Furthermore, E-Syts were found to interact with FGFR1 (Tremblay et al., 2015), a receptor that regulates PM PIP_2 (Herdman and Moss, 2016).

Another major class of LTPs are ORPs (**Table 1**). There are 12 members of the ORP family in humans and seven in yeast (homologue Osh proteins), each containing a conserved OSBP-related domain (ORD). In addition, members usually contain ER-targeting sequences (e.g., FFAT motif or *C*-terminal TMD) and membrane-binding domains, most commonly a Pleckstrin homology (PH) domain (Lehto et al., 2001). Recently, studies have shown that ORPs facilitate lipid transport at several MCSs, including ER-lipid droplets (Du et al., 2020) and ER-PM MCSs (Chung et al., 2015; Mochizuki et al., 2018). The function of ORPs (and Oshs) relies on their binding to the ER transmembrane protein, VAP (Scs2p in yeast) via the FFAT motif (Loewen et al., 2003). In yeast, Osh2/3p-Scs2p complexes are located at ER-PM MCSs (Weber-Boyvat et al., 2015) where they are thought to be responsible for the extensive tethering of the cortical ER and PM (**Figure 2**). Although being topologically adapted to this function through selective Scs2p binding, Osh were also shown to be highly integrated in an intriguing interplay with SNARE proteins (Weber-Boyvat et al., 2020). This later study demonstrated the direct interaction of Osh and the SNARE domain of Sec9p (SNAP25 homologue), along with the previously defined Sec9p interaction with Sso1 (Stx homologue). Furthermore, this crosstalk was conserved in hippocampal neurons. Knocking down ORP2 in neurons reduced both neurite

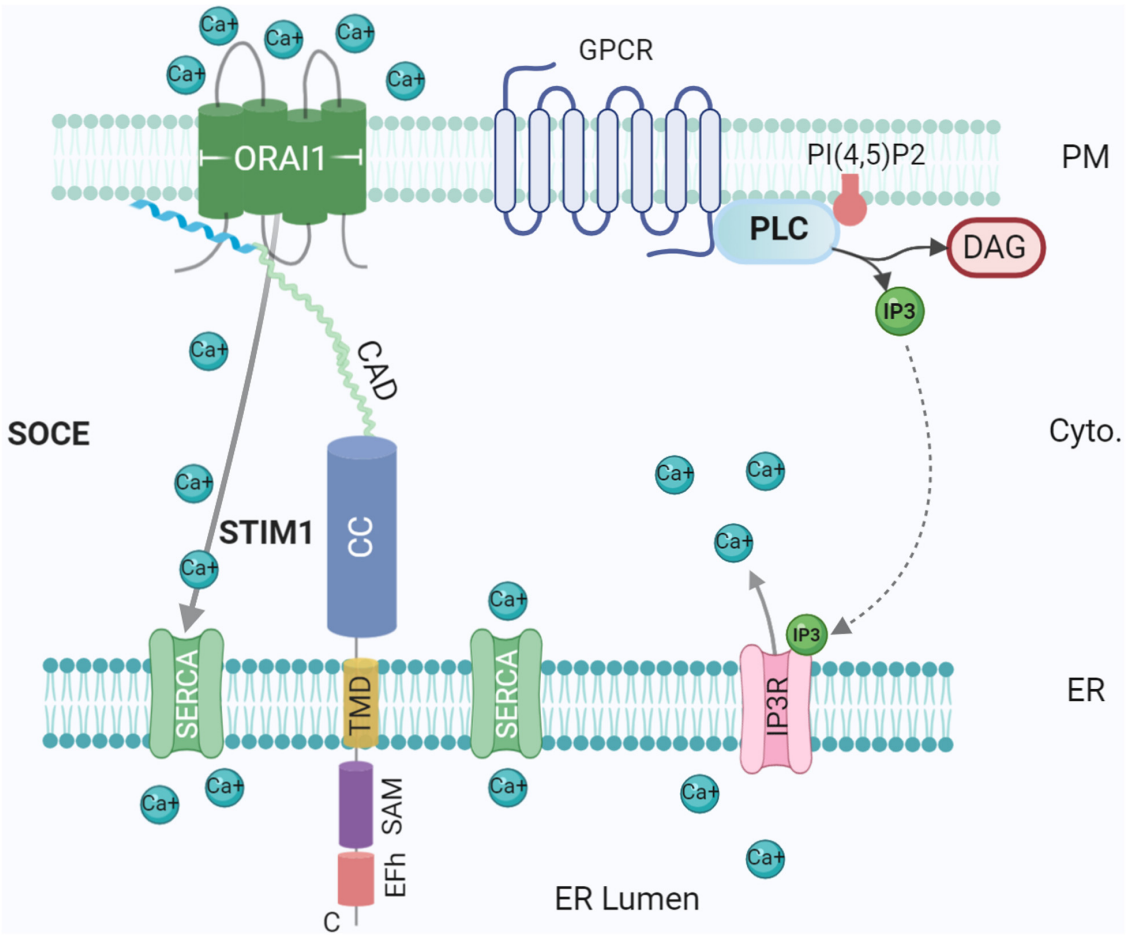

FIGURE 3 | Ca^{2+} influx at the ER-PM contact site. Tethering proteins involved in the control of the Ca^{2+} ions fluxes between the ER lumen, the cytosol and the extracellular medium: ORA1, STIM1, SERCA, and IP3 Receptor (IP3R). IP3R is activated by IP3 generated by Phospholipase C (PLC) upon activation of G-protein coupled receptor (GPCR). The G protein subunits ware not represented for simplicity. Created with BioRender.com.

growth and synaptogenesis, further emphasising the importance of lipid transfer. In this situation, a plausible hypothesis is the recruitment of Sec9p (SNAP25) by an Osh-Scs2p complex reinforcing tethering between ER and PM (**Figure 2**). In the absence of an ER-resident v-SNARE and thus membrane fusion, negative regulation of exocytosis by Osh overexpression (Weber-Boyvat et al., 2020) could be due to a re-routing of Sec9p (SNAP25) by Osh towards a ternary Osh-Scs2p-Sec9p complex, allowing only lipid transfer/modification.

Additional sterol transporters were identified as StARt (steroidogenic acute regulatory protein-related lipid transfer) domain (StARD) proteins (**Table 1**), also known as the StARkin superfamily (Jentsch et al., 2018). Following, LAM/Ltc proteins were identified in yeast to contain StART-like domains, structurally similar to the StART domains (Gatta et al., 2015). LAM/Ltcs are localised to the ER via a C-terminal TMD and can be found at ER-PM MCSs. A hydrophobic cavity the StARt domain accommodates sterols, supported by slowed sterol transport upon deletion (Horenkamp et al., 2018; Tong et al., 2018). LAM isoforms also contain a PH-like domain, *N*-terminal to the StARt domain, thought to be involved in targeting, although unable to bind lipids (Jentsch et al., 2018; Tong et al., 2018). In mammals, several StART (e.g., StARDs) and StART-like domain-containing proteins have been suggested to transport cholesterol to the PM and between intracellular organelles (Horenkamp et al., 2018; Clark, 2020). For example, mammalian homologues of yeast LAM proteins GRAMD1s/ASTERs contain a C-terminal TMD localising the protein at the ER, an *N*-terminal GRAM domain associating with the PM and a StART-like domain (also called VaST domain) to facilitate lipid transfer (Sandhu et al., 2018; Naito et al., 2019). While consistent with a role in sterol homoeostasis at MCSs, the potential physiological function in neurons remains to be investigated.

While much of the mechanistic detail describing lipid transfer remains elusive, the diversity among the identified molecular components (and potential for unidentified members) indicates extensive functional redundancy, highlighting the significance of lipid homoeostasis in biological membranes. Enhancement of ER-PM MCSs by E-Syt recruitment also

induces translocation of Nir2 to ER-PM MCSs, potentially via interactions with VAP isoforms (Amarilio et al., 2005). Here, Nir2, a phosphatidylinositol transfer protein, replenishes PIP_2 in the PM by promoting transfer from the ER, offering a feedback loop for receptor-induced Ca^{2+} signalling (Chang et al., 2013). Abnormal localisation and disproportionate lipid concentrations can have dire effects on organelle function and downstream signalling pathways. In this manner, it has been suggested LTPs do not simply move lipids between compartments, but they also present them to metabolising enzymes to maintain specific compositions (e.g., Sac1 and E-Syt2 localisation). For example, studies in yeast show that the lipid transporter Osh3 is needed not only for PI4P transport, but is independently necessary for the localisation of Opi3, a phosphatidylethanolamine *N*-methyltransferase involved in phosphatidylcholine synthesis (Tavassoli et al., 2013). In accordance with roles in signalling pathways, temperature stress in yeast induces recruitment of phosphoinositide-dependent kinase orthologues by PI4P and PIP_2, modulating the PDK-TORC2-Akt cascade thus activating sphingolipid synthesis in the ER. A key component of the PM, sphingolipid transfer from the ER is essential in maintaining PM integrity under stress (Omnus et al., 2016). Following, the same study showed that deletion of ER-PM tethers resulting in dysfunctional Ca^{2+} signalling and subsequent impaired sphingolipid synthesis, manifesting in PM integrity defects.

Ca^{2+} HOMOEOSTASIS AND SIGNALLING

Ca^{2+} is an essential second messenger utilised ubiquitously in eukaryotes. Early work by Michell (1975) suggested an integral role played by ER-PM contacts in Ca^{2+} signaling. A prerequisite for Ca^{2+} signaling is a low baseline Ca^{2+} concentration in the cytosol; in resting cells, Ca^{2+} levels are actively maintained in the nanomolar range, several orders of magnitude below typical extracellular concentrations (Carrasco and Meyer, 2011). With low intracellular concentrations, Ca^{2+} is acquired from the extracellular milieu and/or from specific stores in ER, Golgi, and mitochondria (Giorgi et al., 2018). When low, these stocks must be replenished from the extracellular milieu, requiring signalling between organelles, thus MCSs are obvious candidate hubs for signal transduction (Wu et al., 2006). Post ER Ca^{2+} depletion, mediated by GPCR, PLC and IP3, Ca^{2+} is replenished through a process called store-operated Ca^{2+} entry (SOCE) (**Figure 3**), directly mediated by ER-PM junctions through ER Ca^{2+} sensor STIM1 and PM Ca^{2+} channel Orai1 (Michell, 1975; Chang et al., 2013). These form an elementary unit upon Ca^{2+} depletion, sensed by the lumenal EF domain of STIM1 protein, generating cytoplasmic Ca^{2+} signals and refilling ER Ca^{2+} (Balla et al., 2020; Stefan, 2020) (**Figure 3**). Defects in this mechanism could contribute to degenerative diseases such as Alzheimer's disease (Popugaeva and Bezprozvanny, 2014).

At rest, STIM1 and Orai1 are evenly distributed across ER/PM, however, post ER Ca^{2+} depletion, STIM1 is activated and releases Ca^{2+} from the lumenal EF-hand, eventually enabling oligomerization and translocation. STIM1 in activated state directly interacts and gates Orai1 Ca^{2+} channel (Jing et al., 2020). Orai1 permits the entry of Ca^{2+} into the cytosol, where repletion of the ER as a Ca^{2+} store is facilitated by SERCA channels (Luik et al., 2008; Chang and Liou, 2016). Mammals express two STIM isoforms, which share high sequence homology (Berna-Erro et al., 2009). Both isoforms are widely expressed in the brain, although show differential patterns with STIM1 more common in Purkinje neurons of the cerebellar cortex (Hartmann et al., 2014) while STIM2 is the predominant isoform expressed in the hippocampus (Berna-Erro et al., 2009) and cortex (Gruszczynska-Biegala et al., 2011). Further research has revealed additional regulatory and stabilising partners. Receptor-induced PIP_2 hydrolysis results in Ca^{2+} influx due to the generation of IP3 and subsequent opening of IP3 receptors, Ca^{2+} channels in the ER. Additionally, E-Syts are Ca^{2+}-activated, transferring PLC generated DAG from the PM to ER (Saheki et al., 2016). Recruitment of E-Syt1 to ER-PM junctions (Chang et al., 2013; Idevall-Hagren et al., 2015) modifies ER which form a ring around the site of Ca^{2+} entry, thereby stabilising MCSs and accelerating Ca^{2+} replenishment (Kang et al., 2019). Furthermore, localisation at $PI(4,5)P_2$-rich microdomains tethered by E-Syt1 seems to be necessary for binding and inactivation of STIM by SARAF (Maléth et al., 2014). Interestingly, knockdown of Sec22b does not impair SOCE but increasing the length of Sec22b strongly affects SOCE (Petkovic et al., 2014), suggesting that different tethering mechanisms could operate in an independent manner at ER-PM MCSs to a limited extent. In addition, an essential role of α-SNAP, a SNARE interactor, was found in binding to and mediating functional coupling of Stim1 and Orai1. This function for α-SNAP is direct and independent of its known activity in NSF dependent SNARE complex disassembly (Miao et al., 2013).

Another intriguing protein family playing a critical role in modulating Ca^{2+} at ER-PM MCSs is GRAMD1/Aster. GRAMD1 and GRAMD2 localise to separate MCSs, suggesting different physiological functions. For example, GRAMD2 localisation at ER-PM MCSs is $PI(4,5)P_2$-dependent, highlighting the MCS for recruitment and translocation of STIM1 post depletion of Ca^{2+} (Besprozvannaya et al., 2018).

RISING MATTER: ER-PM MCSs AND AUTOPHAGY

Lipid transfer is essential to maintain cell homoeostasis and simultaneously mediate dynamic changes upon stimulus. Indeed, transfer can modulate lipid synthesis, cell growth and is also vital for organelle biogenesis and function, as each membrane possesses specific lipid compositions, including asymmetric distributions between leaflets. This requires targeted and often large-scale transport of lipids throughout the cell (Prinz, 2014). Lipid transfer operates complementarily to vesicular transport and membrane fusion. Contrary to the latter, lipid transfer does

not imply full lipid mixing between organelles, nor co-transfer of proteins and can operate for amounts of molecules not defined by quantal size of organelles. This complementarity between vesicular transport and lipid transfer at contact sites is illustrated by the formation of the phagophore, the initial step of autophagy. For instance, macroautophagy is dependent on the formation of the phosphatidylinositol-3,4,5-trisphosphate (PIP_3)-enriched phagophore, which requires progressive vesicular fusion to form the maturing structure (Rubinsztein et al., 2012; Wang et al., 2016) and also lipid transfer by ATG2 (Maeda et al., 2019; Sawa-Makarska et al., 2020). Further evidence suggests that ER-PM contact sites can be directly involved in autophagy. Induction of autophagy by nutrient deprivation results in upregulated and stabilised E-Syt-mediated MCSs in mammalian cells. Co-localisation of phagophore markers such as LC3 and DCFP1 with E-Syt2 or 3 suggests that about 30% of all autophagosome assembly occurs at ER-PM MCSs (Nascimbeni et al., 2017). SiRNA-mediated knockdown of E-Syt2 and 3 resulted in decreased expression of some members of the PI3KC3 complex, such as Beclin1 and VMP1. Both precipitated with E-Syt2, suggesting E-Syts stabilise the PI3KC3 complex, needed for local PI3P synthesis, therefore making E-Syt-mediated ER-PM MCSs ideal locations for autophagosome assembly. The extent of this mechanism in neurons and how this may contribute to a disease characterised by deficiencies in the autophagy-lysosomal pathway has yet to be investigated. Sec22b was suggested to mediate the fusion of autophagosome with the PM via interaction with syntaxin 3/4 and SNAP-23/29 in on neuronal cells (Kimura et al., 2017). It is tempting to speculate that autophagosome Sec22b might differ from ER Sec22b in a regulatory process, maybe related to the Longin domain, which would allow for fusion with the PM in the case of the autophagosome but not the ER.

CONCLUSION

The study of MCSs has grown tremendously in the last 20 years, however, our understanding of their structure and functions still shows many gaps. Much of this difficulty arises from the inherent features of MCSs; they are minute, dynamic structures with diverse molecular compositions between organelles and organisms and thus can be difficult to study. ER-PM MCSs, while relatively well characterised, exemplify the complexity surrounding MCSs, with multiple tethering complexes and binding partners defining the structure's performance as a signalling hub and as key homeostatic regulators, responsive to physiological and stressful conditions. What remains a major question in the field is the relationship between MCS and particularly their lipid transfer activity with membrane fusion events. The fact that SNAREs, which constitute the basic membrane fusion machinery, would interact with LTPs and be found both at MCSs suggest that their regulation might be key to either generate a contact or fuse. In such scenario, we propose an important function for the Longin domain of Sec22b. In other words, could membrane contact correspond to a membrane docking with frustrated fusion? An evolutionary view of these processes would certainly solve this question.

AUTHOR CONTRIBUTIONS

BH wrote initial version and revised last version. NS and CV extensively rewrote and completed. NS designed the figures using BioRender. TG supervised and wrote final draft.

FUNDING

Work in our group was funded by grants from the French National Research Agency (MetDePaDi ANR-16-CE16-0012), the Institut National du Cancer (PLBIO 2018-149), the Fondation pour la Recherche Médicale (FRM), and Fondation Bettencourt-Schueller to TG. NS is recipient of a fellowship from the University de Paris – CD4Impact international program (ANR-18-IDEX-0001).

REFERENCES

Alva, V., and Lupas, A. N. (2016). The TULIP superfamily of eukaryotic lipid-binding proteins as a mediator of lipid sensing and transport. *Biochim. Biophys. Acta* 1861, 913–923. doi: 10.1016/j.bbalip.2016.01.016

Amarilio, R., Ramachandran, S., Sabanay, H., and Lev, S. (2005). Differential regulation of endoplasmic reticulum structure through VAP-Nir interactions. *J. Bio. Chem.* 280, 5934–5944. doi: 10.1074/jbc.m409566200

Antonucci, D. E., Lim, S. T., Vassanelli, S., and Trimmer, J. S. (2001). Dynamic localization and clustering of dendritic Kv2.1 voltage-dependent potassium channels in developing hippocampal neurons. *Neuroscience* 108, 69–81. doi: 10.1016/s0306-4522(01)00476-476

Balla, T., Gulyas, G., Kim, Y. J., and Pemberton, J. (2020). Phosphoinositides and calcium signaling. a marriage arranged in er-pm contact sites. *Curr. Opin. Physiol.* 17, 149–157. doi: 10.1016/j.cophys.2020.08.007

Berna-Erro, A., Braun, A., Kraft, R., Kleinschnitz, C., Schuhmann, M. K., Stegner, D., et al. (2009). STIM2 regulates capacitive Ca2+ entry in neurons and plays a key role in hypoxic neuronal cell death. *Sci. Signal.* 2:ra67. doi: 10.1126/scisignal.2000522

Bernhard, W., and Rouiller, C. (1956). Close topographical relationship between mitochondria and ergastoplasm of liver cells in a definite phase of cellular activity. *J. Biophys. Biochem. Cytol.* 2, 73–78. doi: 10.1083/jcb.2.4.73

Besprozvannaya, M., Dickson, E., Li, H., Ginburg, K. S., Bers, D. M., Auwerx, J., et al. (2018). GRAM domain proteins specialize functionally distinct ER-PM contact sites in human cells. *eLife* 7:e31019. doi: 10.7554/eLife.31019

Bian, X., and De Camilli, P. (2019). In vitro assays to measure the membrane tethering and lipid transport activities of the extended synaptotagmins. *Methods Mol. Biol.* 1949, 201–212. doi: 10.1007/978-1-4939-9136-5_15

Bian, X., Saheki, Y., and De Camilli, P. (2018). Ca 2+ releases E-Syt1 autoinhibition to couple ER -plasma membrane tethering with lipid transport. *EMBO J.* 37, 219–234. doi: 10.15252/embj.201797359

Bohnert, M. (2020). Tether me, tether me not-dynamic organelle contact sites in metabolic rewiring. *Dev. Cell* 54, 212–225. doi: 10.1016/j.devcel.2020.06.026

Brooks, M. B., Catalfamo, J. L., MacNguyen, R., Tim, D., Fancher, S., and McCardle, J. A. (2015). A TMEM16F point mutation causes an absence of canine platelet TMEM16F and ineffective activation and death-induced phospholipid scrambling. *J. Thromb. Haemost.* 13, 2240–2252. doi: 10.1111/jth.13157

Bushell, S. R., Pike, A. C. W., Falzone, M. E., Rorsman, N. J. G., Ta, C. M., Corey, R. A., et al. (2019). The structural basis of lipid scrambling and inactivation

in the endoplasmic reticulum scramblase TMEM16K. *Nat. Commun.* 10:3956. doi: 10.1038/s41467-019-11753-11751

Caputo, A., Caci, E., Ferrera, L., Pedemonte, N., Barsanti, C., Sondo, E., et al. (2008). TMEM16A, a membrane protein associated with calcium-dependent chloride channel activity. *Science* 322, 590–594. doi: 10.1126/science.1163518

Carrasco, S., and Meyer, T. (2011). STIM proteins and the endoplasmic reticulum-plasma membrane junctions. *Annu. Rev. Biochem.* 80, 973–1000. doi: 10.1146/annurev-biochem-061609-165311

Chang, C.-L., Hsieh, T.-S., Yang, T. T., Rothberg, K. G., Azizoglu, D. B., Volk, E., et al. (2013). Feedback regulation of receptor-induced Ca2+ signaling mediated by E-Syt1 and Nir2 at endoplasmic reticulum-plasma membrane junctions. *Cell Rep.* 5, 813–825. doi: 10.1016/j.celrep.2013.09.038

Chang, C.-L., and Liou, J. (2016). Homeostatic regulation of the PI(4,5)P2-Ca(2+) signaling system at ER-PM junctions. *Biochim. Biophys. Acta* 1861, 862–873. doi: 10.1016/j.bbalip.2016.02.015

Chung, J., Torta, F., Masai, K., Lucast, L., Czapla, H., Tanner, L. B., et al. (2015). Intracellular transport. PI4P/phosphatidylserine countertransport at ORP5- and ORP8-mediated ER-plasma membrane contacts. *Science* 349, 428–432. doi: 10.1126/science.aab1370

Clark, B. J. (2020). The START-domain proteins in intracellular lipid transport and beyond. *Mol. Cell. Endocrinol.* 54:110704. doi: 10.1016/j.mce.2020.110704

Collado, J., Kalemanov, M., Campelo, F., Bourgoint, C., Thomas, F., Loewith, R., et al. (2019). Tricalbin-Mediated contact sites control ER curvature to maintain plasma membrane integrity. *Dev. Cell* 51, 476–487.e7. doi: 10.1016/j.devcel.2019.10.018

D'Ambrosio, J. M., Albanèse, V., Lipp, N.-F., Fleuriot, L., Debayle, D., Drin, G., et al. (2020). Osh6 requires Ist2 for localization to ER-PM contacts and efficient phosphatidylserine transport in budding yeast. *J. Cell Sci.* 133:jcs243733. doi: 10.1242/jcs.243733

Daste, F., Galli, T., and Tareste, D. (2015). Structure and function of longin SNAREs. *J. Cell Sci.* 128, 4263–4272. doi: 10.1242/jcs.178574

Dickson, E. J., Jensen, J. B., Vivas, O., Kruse, M., Traynor-Kaplan, A. E., and Hille, B. (2016). Dynamic formation of ER-PM junctions presents a lipid phosphatase to regulate phosphoinositides. *J. Cell Biol.* 213, 33–48. doi: 10.1083/jcb.201508106

Dimmer, K. S., and Rapaport, D. (2017). Mitochondrial contact sites as platforms for phospholipid exchange. *Biochim. Biophys. Acta Mol. Cell Biol. Lipids* 1862, 69–80. doi: 10.1016/j.bbalip.2016.07.010

Du, J., Tao-Cheng, J. H., Zerfas, P., and McBain, C. J. (1998). The K+ channel, Kv2.1, is apposed to astrocytic processes and is associated with inhibitory postsynaptic membranes in hippocampal and cortical principal neurons and inhibitory interneurons. *Neuroscience* 84, 37–48. doi: 10.1016/s0306-4522(97)00519-518

Du, X., Zhou, L., Aw, Y. C., Mak, H. Y., Xu, Y., Rae, J., et al. (2020). ORP5 localizes to ER-lipid droplet contacts and regulates the level of PI(4)P on lipid droplets. *J. Cell Biol.* 219:e201905162. doi: 10.1083/jcb.201905162

Duran, C., Qu, Z., Osunkoya, A. O., Cui, Y., and Hartzell, H. C. (2012). ANOs 3-7 in the anoctamin/Tmem16 Cl- channel family are intracellular proteins. *Am. J. Physiol. Cell Physiol.* 302, C482–C493. doi: 10.1152/ajpcell.00140.2011

Eisenberg-Bord, M., Shai, N., Schuldiner, M., and Bohnert, M. (2016). A tether is a tether is a tether: tethering at membrane contact sites. *Dev. Cell* 39, 395–409. doi: 10.1016/j.devcel.2016.10.022

Elbaz, Y., and Schuldiner, M. (2011). Staying in touch: the molecular era of organelle contact sites. *Trends Biochem. Sci.* 36, 616–623. doi: 10.1016/j.tibs.2011.08.004

Ercan, E., Momburg, F., Engel, U., Temmerman, K., Nickel, W., and Seedorf, M. (2009). A conserved, lipid-mediated sorting mechanism of yeast Ist2 and mammalian STIM proteins to the peripheral ER. *Traffic* 10, 1802–1818. doi: 10.1111/j.1600-0854.2009.00995

Fernández-Busnadiego, R., Saheki, Y., and De Camilli, P. (2015). Three-dimensional architecture of extended synaptotagmin-mediated endoplasmic reticulum-plasma membrane contact sites. *Proc. Natl. Acad. Sci. U S A.* 112, E2004–E2013. doi: 10.1073/pnas.1503191112

Fili, O., Michaelevski, I., Bledi, Y., Chikvashvili, D., Singer-Lahat, D., Boshwitz, H., et al. (2001). Direct interaction of a brain voltage-gated K+ channel with syntaxin 1A: functional impact on channel gating. *J. Neurosci.* 21, 1964–1974. doi: 10.1523/jneurosci.21-06-01964.2001

Fischer, M. A., Temmerman, K., Ercan, E., Nickel, W., and Seedorf, M. (2009). Binding of plasma membrane lipids recruits the yeast integral membrane protein Ist2 to the cortical ER. *Traffic* 10, 1084–1097. doi: 10.1111/j.1600-0854.2009.00926.x

Forrest, S., Chai, A., Sanhueza, M., Marescotti, M., Parry, K., Georgiev, A., et al. (2013). Increased levels of phosphoinositides cause neurodegeneration in a *Drosophila* model of amyotrophic lateral sclerosis. *Hum. Mol. Genet.* 22, 2689–2704. doi: 10.1093/hmg/ddt118

Fox, P. D., Haberkorn, C. J., Akin, E. J., Seel, P. J., Krapf, D., and Tamkun, M. M. (2015). Induction of stable ER-plasma-membrane junctions by Kv2.1 potassium channels. *J. Cell Sci.* 128, 2096–2105. doi: 10.1242/jcs.166009

Galli, T., and Haucke, V. (2004). Cycling of synaptic vesicles: how far? How fast! *Sci. STKE* 2004:re19. doi: 10.1126/stke.2642004re19

Gallo, A., Danglot, L., Giordano, F., Hewlett, B., Binz, T., Vannier, C., et al. (2020). Role of the Sec22b-E-Syt complex in neurite growth and ramification. *J. Cell Sci.* 133:jcs247148. doi: 10.1242/jcs.247148

Gallo, A., Vannier, C., and Galli, T. (2016). Endoplasmic reticulum-plasma membrane associations:structures and functions. *Annu. Rev. Cell Dev. Biol.* 32, 279–301. doi: 10.1146/annurev-cellbio-111315-125024

Garbino, A., van Oort, R. J., Dixit, S. S., Landstrom, A. P., Ackerman, M. J., and Wehrens, X. H. T. (2009). Molecular evolution of the junctophilin gene family. *Physiol. Genom.* 37, 175–186. doi: 10.1152/physiolgenomics.00017.2009

Gatta, A. T., and Levine, T. P. (2017). Piecing together the patchwork of contact sites. *Trends Cell Biol.* 27, 214–229. doi: 10.1016/j.tcb.2016.08.010

Gatta, A. T., Wong, L. H., Sere, Y. Y., Calderón-Noreña, D. M., Cockcroft, S., Menon, A. K., et al. (2015). A new family of StART domain proteins at membrane contact sites has a role in ER-PM sterol transport. *eLife* 4:e07253. doi: 10.7554/eLife.07253

Giordano, F., Saheki, Y., Idevall-hagren, O., Colombo, S. F., Pirruccello, M., Milosevic, I., et al. (2013). PI(4,5)P2-Dependent and Ca2+-Regulated ER-PM interactions mediated by the extended synaptotagmins. *Cell* 153, 1494–1509. doi: 10.1016/j.cell.2013.05.026

Giorgi, C., Danese, A., Missiroli, S., Patergnani, S., and Pinton, P. (2018). Calcium dynamics as a machine for decoding signals. *Trends Cell Biol.* 28, 258–273. doi: 10.1016/j.tcb.2018.01.002

Gruszczynska-Biegala, J., Pomorski, P., Wisniewska, M. B., and Kuznicki, J. (2011). Differential roles for STIM1 and STIM2 in store-operated calcium entry in rat neurons. *PLoS One* 6:e19285. doi: 10.1371/journal.pone.0019285

Hartmann, J., Karl, R. M., Alexander, R. P. D., Adelsberger, H., Brill, M. S., Rühlmann, C., et al. (2014). STIM1 controls neuronal Ca2+ signaling, mGluR1-dependent synaptic transmission, and cerebellar motor behavior. *Neuron* 82, 635–644. doi: 10.1016/j.neuron.2014.03.027

Helle, S. C. J., Kanfer, G., Kolar, K., Lang, A., Michel, A. H., and Kornmann, B. (2013). Organization and function of membrane contact sites. *Biochim. Biophys. Acta* 1833, 2526–2541. doi: 10.1016/j.bbamcr.2013.01.028

Henkart, M., Landis, D. M., and Reese, T. S. (1976). Similarity of junctions between plasma membranes and endoplasmic reticulum in muscle and neurons. *J. Cell Biol.* 70, 338–347. doi: 10.1083/jcb.70.2.338

Henne, W. M., Zhu, L., Balogi, Z., Stefan, C., Pleiss, J. A., and Emr, S. D. (2015). Mdm1/Snx13 is a novel ER-endolysosomal interorganelle tethering protein. *J. Cell Biol.* 210, 541–551. doi: 10.1083/jcb.201503088

Herdman, C., and Moss, T. (2016). Extended-Synaptotagmins (E-Syts); the extended story. *Pharmacol. Res.* 107, 48–56. doi: 10.1016/j.phrs.2016.01.034

Hoffmann, P. C., Bharat, T. A. M., Wozny, M. R., Boulanger, J., Miller, E. A., and Kukulski, W. (2019). Tricalbins contribute to cellular lipid flux and form curved ER-PM contacts that are bridged by rod-shaped structures. *Dev. Cell* 51, 488–502.e8. doi: 10.1016/j.devcel.2019.09.019

Holmes, S. E., O'Hearn, E., Rosenblatt, A., Callahan, C., Hwang, H. S., Ingersoll-Ashworth, R. G., et al. (2001). A repeat expansion in the gene encoding junctophilin-3 is associated with Huntington disease-like 2. *Nat. Genet.* 29, 377–378. doi: 10.1038/ng760

Honsbein, A., Sokolovski, S., Grefen, C., Campanoni, P., Pratelli, R., Paneque, M., et al. (2009). A tripartite SNARE-K+ channel complex mediates in channel-dependent K+ nutrition in Arabidopsis. *Plant Cell* 21, 2859–2877. doi: 10.1105/tpc.109.066118

Horenkamp, F. A., Valverde, D. P., Nunnari, J., and Reinisch, K. M. (2018). Molecular basis for sterol transport by StART-like lipid transfer domains. *EMBO J.* 37:e98002. doi: 10.15252/embj.201798002

Idevall-Hagren, O., Lü, A., Xie, B., and De Camilli, P. (2015). Triggered Ca2+ influx is required for extended synaptotagmin 1-induced ER-plasma membrane tethering. *EMBO J.* 34, 2291–2305. doi: 10.15252/embj.201591565

Im, Y. J., Raychaudhuri, S., Prinz, W. A., and Hurley, J. H. (2005). Structural mechanism for sterol sensing and transport by OSBP-related proteins. *Nature* 437, 154–158. doi: 10.1038/nature03923

Irie, T., and Trussell, L. O. (2017). Double-Nanodomain coupling of calcium channels, ryanodine receptors, and BK channels controls the generation of burst firing. *Neuron* 96, 856–870.e4. doi: 10.1016/j.neuron.2017.10.014

Ito, K., Komazaki, S., Sasamoto, K., Yoshida, M., Nishi, M., Kitamura, K., et al. (2001). Deficiency of triad junction and contraction in mutant skeletal muscle lacking junctophilin type 1. *J. Cell Biol.* 154, 1059–1067. doi: 10.1083/jcb.200105040

Jentsch, J.-A., Kiburu, I., Pandey, K., Timme, M., Ramlall, T., Levkau, B., et al. (2018). Structural basis of sterol binding and transport by a yeast StARkin domain. *J. Biol. Chem.* 293, 5522–5531. doi: 10.1074/jbc.RA118.001881

Jing, J., Liu, G., Huang, Y., and Zhou, Y. (2020). A molecular toolbox for interrogation of membrane contact sites. *J. Physiol. (Lond.)* 598, 1725–1739. doi: 10.1113/JP277761

Johnson, B., Leek, A. N., and Tamkun, M. M. (2019). Kv2 channels create endoplasmic reticulum / plasma membrane junctions: a brief history of Kv2 channel subcellular localization. *Channels* 13, 88–101. doi: 10.1080/19336950.2019.1568824

Kagiwada, S., and Zen, R. (2003). Role of the yeast VAP homolog, Scs2p, in INO1 expression and phospholipid metabolism. *J. Biochem.* 133, 515–522. doi: 10.1093/jb/mvg068

Kakizawa, S., Moriguchi, S., Ikeda, A., Iino, M., and Takeshima, H. (2008). Functional crosstalk between cell-surface and intracellular channels mediated by junctophilins essential for neuronal functions. *Cerebellum* 7, 385–391. doi: 10.1007/s12311-008-0040-41

Kang, F., Zhou, M., Huang, X., Fan, J., Wei, L., Boulanger, J., et al. (2019). E-syt1 Re-arranges STIM1 Clusters to stabilize ring-shaped ER-PM contact sites and accelerate Ca2+ store replenishment. *Sci. Rep.* 9:3975. doi: 10.1038/s41598-019-40331-40330

Kaufmann, W. A., Ferraguti, F., Fukazawa, Y., Kasugai, Y., Shigemoto, R., Laake, P., et al. (2009). Large-conductance calcium-activated potassium channels in purkinje cell plasma membranes are clustered at sites of hypolemmal microdomains. *J. Comp. Neurol.* 515, 215–230. doi: 10.1002/cne.22066

Kikuma, K., Li, X., Kim, D., Sutter, D., and Dickman, D. K. (2017). Extended synaptotagmin localizes to presynaptic er and promotes neurotransmission and synaptic growth in *Drosophila*. *Genetics* 207, 993–1006. doi: 10.1534/genetics.117.300261

Kim, S., Leal, S. S., Ben Halevy, D., Gomes, C. M., and Lev, S. (2010). Structural requirements for VAP-B oligomerization and their implication in amyotrophic lateral sclerosis-associated VAP-B(P56S) neurotoxicity. *J. Biol. Chem.* 285, 13839–13849. doi: 10.1074/jbc.M109.097345

Kimura, T., Jia, J., Kumar, S., Choi, S. W., Gu, Y., Mudd, M., et al. (2017). Dedicated SNAREs and specialized TRIM cargo receptors mediate secretory autophagy. *EMBO J.* 36, 42–60. doi: 10.15252/embj.201695081

Kirmiz, M., Gillies, T. E., Dickson, E. J., and Trimmer, J. S. (2019). Neuronal ER-plasma membrane junctions organized by Kv2-VAP pairing recruit Nir proteins and affect phosphoinositide homeostasis. *J. Biol. Chem.* 294, 17735–17757. doi: 10.1074/jbc.RA119.007635

Kirmiz, M., Palacio, S., Thapa, P., King, A. N., Sack, J. T., and Trimmer, J. S. (2018). Remodeling neuronal ER-PM junctions is a conserved nonconducting function of Kv2 plasma membrane ion channels. *Mol. Biol. Cell* 29, 2410–2432. doi: 10.1091/mbc.E18-05-0337

Kopec, K. O., Alva, V., and Lupas, A. N. (2010). Homology of SMP domains to the TULIP superfamily of lipid-binding proteins provides a structural basis for lipid exchange between ER and mitochondria. *Bioinformatics* 26, 1927–1931. doi: 10.1093/bioinformatics/btq326

Landstrom, A. P., Beavers, D. L., and Wehrens, X. H. T. (2014). The junctophilin family of proteins: from bench to bedside. *Trends Mol. Med.* 20, 353–362. doi: 10.1016/j.molmed.2014.02.004

Lee, I., and Hong, W. (2006). Diverse membrane-associated proteins contain a novel SMP domain. *FASEB J.* 20, 202–206. doi: 10.1096/fj.05-4581hyp

Lees, J. A., Messa, M., Sun, E. W., Wheeler, H., Torta, F., Wenk, M. R., et al. (2017). Lipid transport by TMEM24 at ER-plasma membrane contacts regulates pulsatile insulin secretion. *Science* 355:eaah6171. doi: 10.1126/science.aah6171

Lees, J. A., and Reinisch, K. M. (2020). Inter-organelle lipid transfer: a channel model for Vps13 and chorein-N motif proteins. *Curr. Opin. Cell Biol.* 65, 66–71. doi: 10.1016/j.ceb.2020.02.008

Lehto, M., Laitinen, S., Chinetti, G., Johansson, M., Ehnholm, C., Staels, B., et al. (2001). The OSBP-related protein family in humans. *J. Lipid Res.* 42, 1203–1213. doi: 10.1016/s0022-2275(20)31570-4

Leung, Y. M., Kang, Y., Gao, X., Xia, F., Xie, H., Sheu, L., et al. (2003). Syntaxin 1A binds to the cytoplasmic C terminus of Kv2.1 to regulate channel gating and trafficking. *J. Biol. Chem.* 278, 17532–17538. doi: 10.1074/jbc.M213088200

Lim, S. T., Antonucci, D. E., Scannevin, R. H., and Trimmer, J. S. (2000). A novel targeting signal for proximal clustering of the Kv2.1 K+ channel in hippocampal neurons. *Neuron* 25, 385–397. doi: 10.1016/s0896-6273(00)80902-80902

Loewen, C. J. R., Roy, A., and Levine, T. P. (2003). A conserved ER targeting motif in three families of lipid binding proteins and in Opi1p binds VAP. *EMBO J.* 22, 2025–2035. doi: 10.1093/emboj/cdg201

Luik, R. M., Wang, B., Prakriya, M., Wu, M. M., and Lewis, R. S. (2008). Oligomerization of STIM1 couples ER calcium depletion to CRAC channel activation. *Nature* 454, 538–542. doi: 10.1038/nature07065

Maass, K., Fischer, M. A., Seiler, M., Temmerman, K., Nickel, W., and Seedorf, M. (2009). A signal comprising a basic cluster and an amphipathic alpha-helix interacts with lipids and is required for the transport of Ist2 to the yeast cortical ER. *J. Cell Sci.* 122, 625–635. doi: 10.1242/jcs.036012

MacDonald, P. E., Wang, G., Tsuk, S., Dodo, C., Kang, Y., Tang, L., et al. (2002). Synaptosome-associated protein of 25 kilodaltons modulates Kv2.1 voltage-dependent K(+) channels in neuroendocrine islet beta-cells through an interaction with the channel N terminus. *Mol. Endocrinol.* 16, 2452–2461. doi: 10.1210/me.2002-2058

Maeda, S., Otomo, C., and Otomo, T. (2019). The autophagic membrane tether ATG2A transfers lipids between membranes. *eLife* 8:e45777. doi: 10.7554/eLife.45777

Maléth, J., Choi, S., Muallem, S., and Ahuja, M. (2014). Translocation between PI(4,5)P2-poor and PI(4,5)P2-rich microdomains during store depletion determines STIM1 conformation and Orai1 gating. *Nat. Commun.* 5:5843. doi: 10.1038/ncomms6843

Mandikian, D., Bocksteins, E., Parajuli, L. K., Bishop, H. I., Cerda, O., Shigemoto, R., et al. (2014). Cell type-specific spatial and functional coupling between mammalian brain Kv2.1 K+ channels and ryanodine receptors. *J. Comp. Neurol.* 522, 3555–3574. doi: 10.1002/cne.23641

Manford, A. G., Stefan, C. J., Yuan, H. L., Macgurn, J. A., and Emr, S. D. (2012). ER-to-plasma membrane tethering proteins regulate cell signaling and ER morphology. *Dev. Cell* 23, 1129–1140. doi: 10.1016/j.devcel.2012.11.004

Miao, Y., Miner, C., Zhang, L., Hanson, P. I., Dani, A., and Vig, M. (2013). An essential and NSF independent role for α-SNAP in store-operated calcium entry. *eLife* 2:e00802. doi: 10.7554/eLife.00802

Michell, R. H. (1975). Inositol phospholipids and cell surface receptor function. *Biochim. Biophys. Acta* 415, 81–47. doi: 10.1016/0304-4157(75)90017-90019

Milenkovic, V. M., Brockmann, M., Stöhr, H., Weber, B. H., and Strauss, O. (2010). Evolution and functional divergence of the anoctamin family of membrane proteins. *BMC Evol. Biol.* 10:319. doi: 10.1186/1471-2148-10-319

Mochizuki, S., Miki, H., Zhou, R., Kido, Y., Nishimura, W., Kikuchi, M., et al. (2018). Oxysterol-binding protein-related protein (ORP) 6 localizes to the ER and ER-plasma membrane contact sites and is involved in the turnover of PI4P in cerebellar granule neurons. *Exp. Cell Res.* 370, 601–612. doi: 10.1016/j.yexcr.2018.07.025

Moriguchi, S., Nishi, M., Komazaki, S., Sakagami, H., Miyazaki, T., Masumiya, H., et al. (2006). Functional uncoupling between Ca2+ release and afterhyperpolarization in mutant hippocampal neurons lacking junctophilins. *Proc. Natl. Acad. Sci. U S A.* 103, 10811–10816. doi: 10.1073/pnas.0509863103

Murphy, S. E., and Levine, T. P. (2016). VAP, a versatile access point for the endoplasmic reticulum: review and analysis of FFAT-like motifs in the VAPome. *Biochim. Biophys. Acta* 1861, 952–961. doi: 10.1016/j.bbalip.2016.02.009

Naito, T., Ercan, B., Krshnan, L., Triebl, A., Koh, D. H. Z., Wei, F. Y., et al. (2019). Movement of accessible plasma membrane cholesterol by GRAMD1 lipid transfer protein complex. *eLife* 8:e51401. doi: : 10.7554/eLife.51401

Nakada, T., Kashihara, T., Komatsu, M., Kojima, K., Takeshita, T., and Yamada, M. (2018). Physical interaction of junctophilin and the CaV1.1 C terminus is crucial for skeletal muscle contraction. *Proc. Natl. Acad. Sci. U S A.* 115, 4507–4512. doi: 10.1073/pnas.1716649115

Nascimbeni, A. C., Giordano, F., Dupont, N., Grasso, D., Vaccaro, M. I., Codogno, P., et al. (2017). ER-plasma membrane contact sites contribute to autophagosome biogenesis by regulation of local PI3P synthesis. *EMBO J.* 36, 2018–2033. doi: 10.15252/embj.201797006

Nath, V. R., Mishra, S., Basak, B., Trivedi, D., and Raghu, P. (2020). Extended synaptotagmin regulates membrane contact site structure and lipid transfer function in vivo. *EMBO Rep.* 21:e50264. doi: 10.15252/embr.202050264

Nishi, M., Mizushima, A., Nakagawara, K. I., and Takeshima, H. (2000). Characterization of human junctophilin subtype genes. *Biochem. Biophys. Res. Commun.* 273, 920–927. doi: 10.1006/bbrc.2000.3011

Nishi, M., Sakagami, H., Komazaki, S., Kondo, H., and Takeshima, H. (2003). Coexpression of junctophilin type 3 and type 4 in brain. *Brain Res. Mol. Brain Res.* 118, 102–110. doi: 10.1016/s0169-328x(03)00341-343

Nishimura, Y., Hayashi, M., Inada, H., and Tanaka, T. (1999). Molecular cloning and characterization of mammalian homologues of vesicle-associated membrane protein-associated (VAMP-associated) proteins. *Biochem. Biophys. Res. Commun.* 254, 21–26. doi: 10.1006/bbrc.1998.9876

Nixon-Abell, J., Obara, C. J., Weigel, A. V., Li, D., Legant, W. R., Xu, C. S., et al. (2016). Increased spatiotemporal resolution reveals highly dynamic dense tubular matrices in the peripheral ER. *Science* 354:aaf3928. doi: 10.1126/science.aaf3928

Omnus, D. J., Manford, A. G., Bader, J. M., Emr, S. D., and Stefan, C. J. (2016). Phosphoinositide kinase signaling controls ER-PM cross-talk. *Mol. Biol. Cell* 27, 1170–1180. doi: 10.1091/mbc.E16-01-0002

Orci, L., Ravazzola, M., Le Coadic, M., Shen, W.-W., Demaurex, N., and Cosson, P. (2009). From the cover: STIM1-induced precortical and cortical subdomains of the endoplasmic reticulum. *Proc. Natl. Acad. Sci. U S A.* 106, 19358–19362. doi: 10.1073/pnas.0911280106

Pedemonte, N., and Galietta, L. J. V. (2014). Structure and function of tmem16 proteins (anoctamins). *Physiol. Rev.* 94, 419–459. doi: 10.1152/physrev.00039.2011

Peretti, D., Dahan, N., Shimoni, E., Hirschberg, K., and Lev, S. (2008). Coordinated lipid transfer between the endoplasmic reticulum and the golgi complex requires the VAP proteins and is essential for Golgi-mediated transport. *Mol. Biol. Cell* 19, 3871–3884. doi: 10.1091/mbc.E08-05-0498

Petkovic, M., Jemaiel, A., Daste, F., Specht, C. G., Izeddin, I., Vorkel, D., et al. (2014). The SNARE Sec22b has a non-fusogenic function in plasma membrane expansion. *Nat. Cell Biol.* 16, 434–444. doi: 10.1038/ncb2937

Petkovic, M., Oses-Prieto, J., Burlingame, A., Jan, L. Y., and Jan, Y. N. (2020). TMEM16K is an interorganelle regulator of endosomal sorting. *Nat. Commun.* 11, 3298. doi: 10.1038/s41467-020-17016-17018

Phillips, M. J., and Voeltz, G. K. (2016). Structure and function of ER membrane contact sites with other organelles. *Nat. Rev. Mol. Cell Biol.* 17, 69–82. doi: 10.1038/nrm.2015.8

Picollo, A., Malvezzi, M., and Accardi, A. (2015). TMEM16 proteins: unknown structure and confusing functions. *J. Mol. Biol.* 427, 94–105. doi: 10.1016/j.jmb.2014.09.028

Popugaeva, E., and Bezprozvanny, I. (2014). Can the calcium hypothesis explain synaptic loss in Alzheimer's disease? *Neurodegener. Dis.* 13, 139–141. doi: 10.1159/000354778

Porter, K. R., and Palade, G. E. (1957). Studies on the endoplasmic reticulum. III. Its form and distribution in striated muscle cells. *J. Biophys. Biochem. Cytol.* 3, 269–300.

Prinz, W. A. (2014). Bridging the gap: membrane contact sites in signaling, metabolism, and organelle dynamics. *J. Cell Biol.* 205, 759–769. doi: 10.1083/jcb.201401126

Rosenbluth, J. (1962). Subsurface cisterns and their relationship to the neuronal plasma membrane. *J. Cell Biol.* 13, 405–421. doi: 10.1083/jcb.13.3.405

Rossi, D., Scarcella, A. M., Liguori, E., Lorenzini, S., Pierantozzi, E., Kutchukian, C., et al. (2019). Molecular determinants of homo- and heteromeric interactions of Junctophilin-1 at triads in adult skeletal muscle fibers. *Proc. Natl. Acad. Sci. U S A.* 116, 15716–15724. doi: 10.1073/pnas.1820980116

Rubinsztein, D. C., Shpilka, T., and Elazar, Z. (2012). Mechanisms of autophagosome biogenesis. *Curr. Biol.* 22, R29–R34. doi: 10.1016/j.cub.2011.11.034

Saheki, Y., Bian, X., Schauder, C. M., Sawaki, Y., Surma, M. A., Klose, C., et al. (2016). Control of plasma membrane lipid homeostasis by the extended synaptotagmins. *Nat. Cell Biol.* 18, 504–515. doi: 10.1038/ncb3339

Saheki, Y., and De Camilli, P. (2017). The Extended-Synaptotagmins. *Biochim. et Biophys. Acta - Mol. Cell Res.* 1864, 1490–1493. doi: 10.1016/j.bbamcr.2017.03.013

Sahu, G., Wazen, R.-M., Colarusso, P., Chen, S. R. W., Zamponi, G. W., and Turner, R. W. (2019). Junctophilin proteins tether a Cav1-RyR2-KCa3.1 tripartite complex to regulate neuronal excitability. *Cell Rep.* 28, 2427–2442.e6. doi: 10.1016/j.celrep.2019.07.075

Sandhu, J., Li, S., Fairall, L., Pfisterer, S. G., Gurnett, J. E., Xiao, X., et al. (2018). Aster proteins facilitate nonvesicular plasma membrane to ER cholesterol transport in mammalian cells. *Cell* 175, 514–529.e20. doi: 10.1016/j.cell.2018.08.033

Sawa-Makarska, J., Baumann, V., Coudevylle, N., von Bülow, S., Nogellova, V., Abert, C., et al. (2020). Reconstitution of autophagosome nucleation defines Atg9 vesicles as seeds for membrane formation. *Science* 369:eaaz7714. doi: 10.1126/science.aaz7714

Schauder, C. M., Wu, X., Saheki, Y., Narayanaswamy, P., Torta, F., Wenk, M. R., et al. (2014). Structure of a lipid-bound extended synaptotagmin indicates a role in lipid transfer. *Nature* 510, 552–555. doi: 10.1038/nature13269

Scholze, M. J., Barbieux, K. S., De Simone, A., Boumasmoud, M., Süess, C. C. N., Wang, R., et al. (2018). PI(4,5)P2 forms dynamic cortical structures and directs actin distribution as well as polarity in *Caenorhabditis elegans* embryos. *Development* 145:dev164988. doi: 10.1242/dev.164988

Schreiber, R., Uliyakina, I., Kongsuphol, P., Warth, R., Mirza, M., Martins, J. R., et al. (2010). Expression and function of epithelial anoctamins. *J. Biol. Chem.* 285, 7838–7845. doi: 10.1074/jbc.M109.065367

Schulien, A. J., Yeh, C., Orange, B. N., Pav, O. J., Hopkins, M. P., Moutal, A., et al. (2020). Targeted disruption of Kv2 . 1-VAPA association provides neuroprotection against ischemic stroke in mice by declustering Kv2 . 1 channels. *Cell. Neurosci.* 6:eaaz8110. doi: 10.1126/sciadv.aaz8110

Schulz, T. A., and Creutz, C. E. (2004). The tricalbin C2 domains: lipid-binding properties of a novel, synaptotagmin-like yeast protein family. *Biochemistry* 43, 3987–3995. doi: 10.1021/bi036082w

Sclip, A., Bacaj, T., Giam, L. R., and Südhof, T. C. (2016). Extended Synaptotagmin (ESyt) triple knock-out mice are viable and fertile without obvious endoplasmic reticulum dysfunction. *PLoS One* 11:e0158295. doi: 10.1371/journal.pone.0158295

Scorrano, L., De Matteis, M. A., Emr, S., Giordano, F., Hajnóczky, G., Kornmann, B., et al. (2019). Coming together to define membrane contact sites. *Nat. Commun.* 10:1287. doi: 10.1038/s41467-019-09253-9253

Seixas, A. I., Holmes, S. E., Takeshima, H., Pavlovich, A., Sachs, N., Pruitt, J. L., et al. (2012). Loss of junctophilin-3 contributes to Huntington disease-like 2 pathogenesis. *Ann. Neurol.* 71, 245–257. doi: 10.1002/ana.22598

Siao, W., Wang, P., Voigt, B., Hussey, P. J., and Baluska, F. (2016). Arabidopsis SYT1 maintains stability of cortical endoplasmic reticulum networks and VAP27-1-enriched endoplasmic reticulum-plasma membrane contact sites. *J. Exp. Bot.* 67, 6161–6171. doi: 10.1093/jxb/erw381

Singh, N. P., Vannier, C., and Galli, T. (2020). SNAP iN, SNAP oUT—SNAREs at ER-PM contact sites. *Contact* 3:251525642097958. doi: 10.1177/2515256420979586

Skehel, P. A., Martin, K. C., Kandel, E. R., and Bartsch, D. (1995). A VAMP-binding protein from Aplysia required for neurotransmitter release. *Science* 269, 1580–1583. doi: 10.1126/science.7667638

Soussan, L., Burakov, D., Daniels, M. P., Toister-Achituv, M., Porat, A., Yarden, Y., et al. (1999). ERG30, a VAP-33-related protein, functions in protein transport mediated by COPI vesicles. *J. Cell Biol.* 146, 301–311. doi: 10.1083/jcb.146.2.301

Spacek, J., and Harris, K. M. (1997). Three-dimensional organization of smooth endoplasmic reticulum in hippocampal CA1 dendrites and dendritic spines of the immature and mature rat. *J. Neurosci.* 17, 190–203. doi: 10.1523/jneurosci.17-01-00190.1997

Stefan, C. J. (2018). Building ER-PM contacts: keeping calm and ready on alarm. *Curr. Opin. Cell Biol.* 53, 1–8. doi: 10.1016/j.ceb.2018.03.008

Stefan, C. J. (2020). Endoplasmic reticulum-plasma membrane contacts: principals of phosphoinositide and calcium signaling. *Curr. Opin. Cell Biol.* 63, 125–134. doi: 10.1016/j.ceb.2020.01.010

Stefan, C. J., Trimble, W. S., Grinstein, S., Drin, G., Reinisch, K., De Camilli, P., et al. (2017). Membrane dynamics and organelle biogenesis-lipid pipelines and vesicular carriers. *BMC Biol.* 15:102. doi: 10.1186/s12915-017-0432-430

Sun, E. W., and De Camilli, P. (2018). Kv2 potassium channels meet VAP. *Proc. Natl. Acad. Sci. U S A.* 115, 7849–7851. doi: 10.1073/pnas.1810059115

Sun, E. W., Guillén-Samander, A., Bian, X., Wu, Y., Cai, Y., Messa, M., et al. (2019). Lipid transporter TMEM24/C2CD2L is a Ca2+-regulated component of ER-plasma membrane contacts in mammalian neurons. *Proc. Natl. Acad. Sci. U S A.* 116, 5775–5784. doi: 10.1073/pnas.1820156116

Takeshima, H., Hoshijima, M., and Song, L.-S. (2015). Ca2+ microdomains organized by junctophilins. *Cell Calcium* 58, 349–356. doi: 10.1016/j.ceca.2015.01.007

Takeshima, H., Komazaki, S., Nishi, M., Iino, M., and Kangawa, K. (2000). Junctophilins: a novel family of junctional membrane complex proteins. *Mol. Cell* 6, 11–22. doi: 10.1016/s1097-2765(00)00003-4

Tavassoli, S., Chao, J. T., Young, B. P., Cox, R. C., Prinz, W. A., de Kroon, A. I. P. M., et al. (2013). Plasma membrane–endoplasmic reticulum contact sites regulate phosphatidylcholine synthesis. *EMBO Rep.* 14, 434–440. doi: 10.1038/embor.2013.36

Tilokani, L., Nagashima, S., Paupe, V., and Prudent, J. (2018). Mitochondrial dynamics: overview of molecular mechanisms. *Essays Biochem.* 62, 341–360. doi: 10.1042/EBC20170104

Tong, J., Manik, M. K., and Im, Y. J. (2018). Structural basis of sterol recognition and nonvesicular transport by lipid transfer proteins anchored at membrane contact sites. *Proc. Natl. Acad. Sci. U S A.* 115, E856–E865. doi: 10.1073/pnas.1719709115

Toulmay, A., and Prinz, W. A. (2012). A conserved membrane-binding domain targets proteins to organelle contact sites. *J. Cell Sci.* 125, 49–58. doi: 10.1242/jcs.085118

Tremblay, M. G., Herdman, C., Guillou, F., Mishra, P. K., Baril, J., Bellenfant, S., et al. (2015). Extended synaptotagmin interaction with the fibroblast growth factor receptor depends on receptor conformation, not catalytic activity. *J. Biol. Chem.* 290, 16142–16156. doi: 10.1074/jbc.M115.656918

Vance, J. E. (1990). Phospholipid synthesis in a membrane fraction associated with mitochondria. *J. Biol. Chem.* 265, 7248–7256. doi: 10.1016/s0021-9258(19)39106-9

Wang, J.-Z., and Dehesh, K. (2018). ER: the silk road of interorganellar communication. *Curr. Opin. Plant Biol.* 45, 171–177. doi: 10.1016/j.pbi.2018.07.012

Wang, Y., Li, L., Hou, C., Lai, Y., Long, J., Liu, J., et al. (2016). SNARE-mediated membrane fusion in autophagy. *Semin. Cell Dev. Biol.* 60, 97–104. doi: 10.1016/j.semcdb.2016.07.009

Weber-Boyvat, M., Kentala, H., Peränen, J., and Olkkonen, V. M. (2015). Ligand-dependent localization and function of ORP-VAP complexes at membrane contact sites. *Cell Mol. Life Sci.* 72, 1967–1987. doi: 10.1007/s00018-014-1786-x

Weber-Boyvat, M., Trimbuch, T., Shah, S., Jäntti, J., Olkkonen, V. M., and Rosenmund, C. (2020). ORP/Osh mediate cross-talk between ER-plasma membrane contact site components and plasma membrane SNAREs. *Cell Mol. Life Sci.* doi: 10.1007/s00018-020-03604-w Online ahead of print.

Weir, M. L., Xie, H., Klip, A., and Trimble, W. S. (2001). VAP-A binds promiscuously to both v- and tSNAREs. *Biochem. Biophys. Res. Commun.* 286, 616–621. doi: 10.1006/bbrc.2001.5437

West, M., Zurek, N., Hoenger, A., and Voeltz, G. K. (2011). A 3D analysis of yeast ER structure reveals how ER domains are organized by membrane curvature. *J. Cell Biol.* 193, 333–346. doi: 10.1083/jcb.201011039

Williams, A. L., Ehm, S., Jacobson, N. C., Xu, D., and Hay, J. C. (2004). rsly1 binding to syntaxin 5 is required for endoplasmic reticulum-to-golgi transport but does not promote SNARE motif accessibility. *Mol. Biol. Cell.* 15, 162–175. doi: 10.1091/mbc.E03-07-0535

Wolf, W., Kilic, A., Schrul, B., Lorenz, H., Schwappach, B., and Seedorf, M. (2012). Yeast Ist2 recruits the endoplasmic reticulum to the plasma membrane and creates a ribosome-free membrane microcompartment. *PLoS One* 7:e39703. doi: 10.1371/journal.pone.0039703

Wong, L. H., Gatta, A. T., and Levine, T. P. (2019). Lipid transfer proteins: the lipid commute via shuttles, bridges and tubes. *Nat. Rev. Mol. Cell Biol.* 20, 85–101. doi: 10.1038/s41580-018-0071-75

Woo, J. S., Srikanth, S., Nishi, M., Ping, P., Takeshima, H., and Gwack, Y. (2016). Junctophilin-4, a component of the endoplasmic reticulum-plasma membrane junctions, regulates Ca2+ dynamics in T cells. *Proc. Natl. Acad. Sci. U S A.* 113, 2762–2767. doi: 10.1073/pnas.1524229113

Wu, M. M., Buchanan, J., Luik, R. M., and Lewis, R. S. (2006). Ca2+ store depletion causes STIM1 to accumulate in ER regions closely associated with the plasma membrane. *J. Cell Biol.* 174, 803–813. doi: 10.1083/jcb.200604014

Wu, Y., Whiteus, C., Xu, C. S., Hayworth, K. J., Weinberg, R. J., Hess, H. F., et al. (2017). Contacts between the endoplasmic reticulum and other membranes in neurons. *Proc. Natl. Acad. Sci. U S A.* 114, E4859–E4867. doi: 10.1073/pnas.1701078114

Yamanaka, T., Nishiyama, R., Shimogori, T., and Nukina, N. (2020). Proteomics-Based approach identifies altered ER domain properties by ALS-linked VAPB mutation. *Sci. Rep.* 10:7610. doi: 10.1038/s41598-020-64517-z

Yang, Y. D., Cho, H., Koo, J. Y., Tak, M. H., Cho, Y., Shim, W.-S., et al. (2008). TMEM16A confers receptor-activated calcium-dependent chloride conductance. *Nature* 455, 1210–1215. doi: 10.1038/nature07313

Yu, H., Liu, Y., Gulbranson, D. R., Paine, A., Rathore, S. S., and Shen, J. (2016). Extended synaptotagmins are Ca2+-dependent lipid transfer proteins at membrane contact sites. *Proc. Natl. Acad. Sci. U S A.* 113, 4362–4367. doi: 10.1073/pnas.1517259113

Zhang, Y., McKay, S. E., Bewley, B., and Kaczmarek, L. K. (2008). Repetitive firing triggers clustering of Kv2.1 potassium channels in *Aplysia neurons*. *J. Biol. Chem.* 283, 10632–10641. doi: 10.1074/jbc.M800253200

Conflict of Interest: The authors declare that the research was conducted in the absence of any commercial or financial relationships that could be construed as a potential conflict of interest.

frontiers in Cell and Developmental Biology

PERSPECTIVE
published: 18 March 2021
doi: 10.3389/fcell.2021.640456

Exploiting Connections for Viral Replication

*Louise H. Wong[1], James R. Edgar[2], Andrea Martello[1], Brian J. Ferguson[2] and Emily R. Eden[1]**

[1] UCL Institute of Ophthalmology, London, United Kingdom, [2] Department of Pathology, University of Cambridge, Cambridge, United Kingdom

Severe acute respiratory syndrome coronavirus 2 (SARS-CoV-2), the cause of the COVID-19 (coronavirus disease 2019) pandemic, is a positive strand RNA (+RNA) virus. Like other +RNA viruses, SARS-CoV-2 is dependent on host cell metabolic machinery to survive and replicate, remodeling cellular membranes to generate sites of viral replication. Viral RNA-containing double-membrane vesicles (DMVs) are a striking feature of +RNA viral replication and are abundant in SARS-CoV-2–infected cells. Their generation involves rewiring of host lipid metabolism, including lipid biosynthetic pathways. Viruses can also redirect lipids from host cell organelles; lipid exchange at membrane contact sites, where the membranes of adjacent organelles are in close apposition, has been implicated in the replication of several +RNA viruses. Here we review current understanding of DMV biogenesis. With a focus on the exploitation of contact site machinery by +RNA viruses to generate replication organelles, we discuss evidence that similar mechanisms support SARS-CoV-2 replication, protecting its RNA from the host cell immune response.

Keywords: Membrane contact sites (MCS), double membrane vesicles (DMVs), SARS-CoV-2, viral replication, lipid transport

OPEN ACCESS

Edited by:
Benoît Kornmann, University of Oxford, United Kingdom

Reviewed by:
Graca Raposo, Institut Curie, France
Thomas Simmen, University of Alberta, Canada

****Correspondence:***
Emily R. Eden
e.eden@ucl.ac.uk

Specialty section:
This article was submitted to Membrane Traffic, a section of the journal Frontiers in Cell and Developmental Biology

Received: *11 December 2020*
Accepted: *01 February 2021*
Published: *18 March 2021*

Citation:
Wong LH, Edgar JR, Martello A, Ferguson BJ and Eden ER (2021) Exploiting Connections for Viral Replication. Front. Cell Dev. Biol. 9:640456. doi: 10.3389/fcell.2021.640456

INTRODUCTION

On entry into the host cell, the viral genome is released, and replication–transcription complexes (RTCs) are assembled that drive viral genome replication and expression of viral proteins. Replication of +RNA virus takes place in the cytoplasm, potentially exposing viral RNA to host cell defense mechanisms. However, viruses have developed creative ways to circumvent the host's defensive response. RTCs assemble in association with cytoplasmic membranes, and +RNA viruses co-opt host factors to induce extensive membrane remodeling including the formation of double-membrane vesicles (DMVs) (Wolff et al., 2020b). This rearrangement of cellular membranes provides structural scaffolding for viral RTCs, as well as protection from antiviral host responses. DMVs are clearly visible in cells infected with a variety of +RNA viruses, including severe acute respiratory syndrome coronavirus 2 (SARS-CoV-2) (**Figure 1**). As the name suggests, DMVs are small vesicles, of approximately 100–300 nm in diameter, surrounded by two membranes, often clustered together. DMVs are major replication organelles (ROs), housing viral RNA that is enriched in the DMV core (Knoops et al., 2008; Klein et al., 2020). A molecular pore has been described spanning both membranes, providing a transport route for viral RNA out of the DMVs to be translated and packaged (Wolff et al., 2020a).

The primary targets for SARS-CoV-2 infection are cells of the nasal and respiratory epithelium, which form polarized monolayers, with distinct apical and basolateral domains. The polarized distribution of receptors and proteases may impact mechanistically on viral replication. Primary respiratory epithelial cells offer the most accurate reflection of SARS-CoV-2 target tissues, but epithelial cell lines have proved extremely valuable in informing current understanding of

coronavirus cell biology. For example, much has been learned from viral infection of the widely used African green monkey kidney epithelial cell line, Vero-E6. However, although Vero-E6 cells express the SARS-CoV-2 receptor ACE2 on their apical surface, they do not express the serine protease TMPRSS2 that activates viral spike protein (Hoffmann M. et al., 2020). The human lung adenocarcinoma Calu-3 cells are perhaps a more relevant cell line, expressing both ACE2 and TMPRSS2, all be it at higher and lower levels, respectively, than human lung tissue (Kawase et al., 2012), but the influence of cell type on viral behavior, or the relationship between viral entry and biogenesis of the RO, is not yet clear.

DMV BIOGENESIS

Although our understanding of the SARS-CoV-2 DMV molecular architecture is incomplete, studies on other coronaviruses, SARS-CoV and Middle East respiratory syndrome–related coronavirus (MERS), have shown that viral non-structural protein (nsp)s play a key role in DMV formation. Interaction between the luminal loops of SARS-CoV nsp3 and nsp4 was shown to drive membrane rearrangements (Hagemeijer et al., 2014), and expression of these two nsps is sufficient to induce DMV formation (Angelini et al., 2013; Oudshoorn et al., 2017). DMVs have an interesting topology; studies in Vero-E6 cells have revealed a cytosolic core, whereas the lumen of the endoplasmic reticulum (ER) appears continuous with the material between the inner and outer DMV membranes, indicating that DMVs are derived from host ER membrane (Knoops et al., 2008). However, markers from other organelles, including Golgi, have also been identified on ROs (Schlegel et al., 1996). Coxsackie B virus 3 forms their ROs from both ER and Golgi membranes. The earliest ROs formed are single-membrane tubules, which are transformed into DMVs and multilamellar vesicles as infection progresses (Limpens et al., 2011). By electron tomography, early viral ROs, which later transform into DMVs, appear to originate from *cis*-Golgi membranes (Belov et al., 2012). Moreover, newly synthesized viral RNA was detected at the *trans*-Golgi network (TGN) in coxsackievirus B3–infected cells, and later-stage ROs remained positive for the GTPase Arf1, which in uninfected cells, localizes to the TGN (Hsu et al., 2010).

Machine learning models indicate that SARS-CoV-2 viral RNA also localizes to the mitochondria (Wu et al., 2020), raising the possibility that SARS-CoV-2 may also manipulate mitochondrial membrane to generate mitochondrial-derived DMVs. Interestingly, point mutations in murine coronavirus that decrease the number of ER-derived DMVs also resulted in relocalization of nsp3 and nsp4 to the mitochondria (Clementz et al., 2008). RNA replication of other +RNA viruses, such as alphanodavirus flock house virus, has been shown to occur on the outer mitochondrial membranes of infected cells (Miller et al., 2001). Mitochondrial-derived vesicles (MDVs), of approximately 70–150 nm, can extrude from mitochondrial membranes to transport mitochondrial protein and lipids to other organelles (Sugiura et al., 2014). Although the contribution of MDVs to RO formation has not yet been established, it has been suggested that mitochondrial damage by SARS-CoV-2 could induce the generation of double-membrane, viral RNA-containing MDVs (Singh et al., 2020).

Like mitochondria, autophagosomes are enclosed by a characteristic double-membrane and have also been implicated in coronavirus RO biogenesis. In SARS-CoV–infected Vero-E6 cells, the viral replicase protein, nsp8, colocalized with the autophagosome marker LC3 (Prentice et al., 2004b). Similarly, in cells infected with mouse hepatitis virus (MHV), two replication complex–localized viral proteins (p22 and N) also colocalized with LC3, as well as ATG12, which with ATG5 promotes LC3 lipidation, an important step in autophagosome formation. MHV replication was impaired in autophagy-deficient cells and rescued by ATG5 re-expression (Prentice et al., 2004a). In contrast, although confirming the overlap between SARS-CoV viral replicase proteins and LC3, another study found that neither ATG5 nor LC3 lipidation was required for MHV replication (Zhao et al., 2007). Likewise, viral titers did not differ between SARS-CoV–infected wild-type or $ATG5^{-/-}$ mouse embryonic fibroblasts (Schneider et al., 2012). Careful analysis of LC3-positive DMVs revealed that only the endogenous non-lipidated LC3-I associates with MHV-induced DMVs, and while the LC3 lipidation machinery was dispensable for MHV replication, decreased LC3 impaired MHV replication (Reggiori et al., 2010). Consistent with viral RO assembly being facilitated by autophagosome formation, but not lysosomal targeting and fusion, a recent study reported an incomplete autophagy response to SARS-CoV-2 infection (Qu et al., 2020). Expression of SARS-CoV-2, but not SARS-CoV, ORF3a, was sufficient to trigger incomplete autophagy, where autophagosome formation is increased, but maturation impaired. Importantly, inhibition of autophagosome formation reduced viral replication. Similarly, MERS-CoV infection increased the number of phagocytic vesicles, but impaired autophagosome–lysosome fusion. However, induction of the complete autophagy process severely impaired MERS-CoV replication (Gassen et al., 2019). A genome-wide study performed in a human hepatoma cell line (Huh-7.5) expressing ACE2/TMPRSS2 and validated in human pulmonary epithelial A549 cells expressing ACE2/TMPRSS2 identified TMEM41B as an essential host factor for SARS-CoV-2 and three seasonal CoVs (HCoV-OC43, HCoV-NL63, and HCoV-229E) (Schneider et al., 2020). Similarly, TMEM41B was also recently found to be essential for flavivirus replication (Hoffmann et al., 2021). TMEM41B is an ER resident protein with known roles in phagophore maturation (Morita et al., 2018; Shoemaker et al., 2019) and lipid mobilization (Moretti et al., 2018). As in both studies no other autophagy-related proteins scored as positive regulators of viral infection, it is possible that TMEM41B's role in lipid mobilization and membrane remodeling, rather than phagophore maturation, is more relevant for virus infectivity. Taken together, these findings suggest that coronaviruses can exploit autophagosome formation machinery to support DMV biogenesis, while stalling lysosome fusion to evade autophagy-mediated degradation.

DMV formation occurs early in infection. Within 2 h postinfection (hpi) with SARS-CoV, DMVs are found throughout the cytoplasm, occasionally connected to ER membrane,

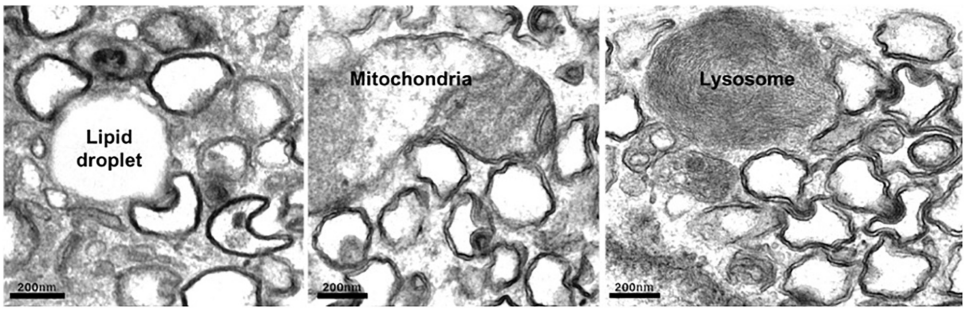

FIGURE 1 | Human lung carcinoma epithelial cell (A549) infected with SARS-Co-V-2 were fixed and prepared for electron microscopy. Abundant DMVs are visible, often in contact with host cell organelles. Scale bar, 200 nm.

consistent with the ER being the source of DMV membranes. At the start of infection, the inner and outer DMV membranes are tightly apposed, but the distance between the two membranes becomes less uniform, with wider gaps evident at later stages. Within 4 hpi, DMVs are dramatically increased in number, often in clusters of up to 300 vesicles at 7 hpi. At late stages, membranous vesicle "packets" arise that appear as a single membrane surrounding one or several single-membrane vesicles, possibly as a result of DMV outer membranes fusing together (Harak and Lohmann, 2015).

HIJACKING LIPID BIOSYNTHETIC PATHWAYS

Lipid composition has a strong influence on the physical properties of cellular membranes, including fluidity and curvature, as well as the activity of membrane proteins. As such, different organelles have a specialized lipid composition according to their specific needs. Cholesterol is an essential membrane lipid that maintains membrane integrity but is heterogeneously distributed throughout cellular membranes (Maxfield and Menon, 2006). As cholesterol levels are relatively low at its site of synthesis (the ER), cholesterol transport to other membranes tends to occur against its concentration gradient and utilizes a lipid counter-exchange mechanism at sites of contact between the ER and other organelles (see Box 1).

Interesting differences in lipid composition between viral DMVs and the ER membranes from which they are derived have been uncovered. Hepatitis C virus (HCV)–induced DMVs contain nine times more cholesterol than the host ER membranes (Paul et al., 2013) and are also enriched in the phospholipid PI4P (Reiss et al., 2011). Thus, viral induction of host lipid synthesis is likely required to supply the lipids necessary for the membrane rearrangements associated with viral replication (Li et al., 2007). Recently, a focused interactome CRISPR screen identified a dependency for host factors involved in cholesterol biosynthesis for coronaviruses including SARS-CoV-2 (Hoffmann H.-H. et al., 2020). Host lipid biosynthetic pathways are largely regulated by sterol regulatory element binding proteins (SREBPs). Inhibition of SREBP-mediated transcription was found to suppress viral replication in a variety of MERS-CoV–infected cells including primary small epithelial cells, as well as increasing survival rates/reducing alveolar damage in infected mice (Yuan et al., 2019). A lipodomics study on human coronavirus 229E-infected cells found that total cellular lipid composition is also altered, with a global increase in fatty acids and glycerophospholipid (Yan et al., 2019). It is likely that these lipids supply membrane for the generation of viral ROs. Enrichment of phosphatidyl choline at viral DMV is also observed in other +RNA viruses such as HCV (Zhang et al., 2016).

HIJACKING CELLULAR LIPID SOURCES

As well as upregulating lipogenesis, viral infection can also redirect host lipids from other organelles for viral replication and connections with host organelles at membrane contact sites (MCSs) have been implicated in the formation of the RO (**Table 1**). A recent BioID study has identified several putative interactions between viral proteins and host MCS-localizing proteins, including lipid transfer proteins (St-Germain et al., 2020) (LTPs, see Box 1).

ER to DMV Lipid Transport

Golgi-localized oxysterol-binding protein (OSBP) mediates transport of newly synthesized cholesterol from the ER to the Golgi at MCS, in a counter-exchange mechanism whereby the phospholipid PI4P is transferred from the Golgi to the ER (Mesmin et al., 2013) (see **Box 1**). This PI4P-cholesterol counter flux mechanism can be usurped to support viral replication. Several diverse (+)RNA viruses including poliovirus (Arita, 2014), HCV (Wang et al., 2014), rhinovirus (Roulin et al., 2014), Aichi virus (Ishikawa-Sasaki et al., 2018), and encephalomyocarditis virus (Dorobantu et al., 2015) hijack OSBP by recruiting PI4-kinase (PI4K) to their RO. Viral PI4K recruitment enriches the RO with PI4P, increasing OSBP recruitment and therefore PI4P-cholesterol counter-exchange at ER contacts to supply cholesterol for viral replication.

PI4Ks include four isoforms in human cells. Enteroviruses such as coxsackievirus recruit PI4KIIIβ to their RO (Hsu et al., 2010) to generate PI4P and recruit OSBP. This exploitation of MCS machinery to drive OSBP/PI4P-dependent cholesterol transport from the ER to the viral ROs plays an important

BOX 1 | Lipid transport at membrane contact sites.

Membrane contact sites (MCSs) are formed when membranes of different organelles are tethered (Eisenberg-Bord et al., 2016) in very close proximity (typically < 30 nm) but without membrane fusion (Scorrano et al., 2019). MCSs occur between most pairings of cellular organelles and have a range of functions important for the regulation of cellular physiology. MCSs provide sites of interorganellar communication, including lipid and calcium exchange, as well as regulating organelle dynamics and positioning (Bohnert, 2020; Prinz et al., 2020; Silva et al., 2020). As such, MCSs are dynamic, with their extent finely tuned to meet the needs of the cell or organelle. An example of this is the expansion of ER–endosome MCSs during maturation of the endosome (Friedman et al., 2013), coordinating endocytic fission events for recycling/retrograde transport (Rowland et al., 2014; Allison et al., 2017; Hoyer et al., 2018), with endosome positioning (Raiborg et al., 2016; Cabukusta and Neefjes, 2018; Di Mattia et al., 2019), signaling regulation (Eden et al., 2010; Palande et al., 2011; Jongsma et al., 2016; Hong et al., 2017), and lipid and calcium exchange (van der Kant and Neefjes, 2014; Atakpa et al., 2018; Lee and Blackstone, 2020; Martello et al., 2020).

Specific proteins, or more commonly protein complexes, can bridge the two opposing membranes and populate and regulate MCSs (Scorrano et al., 2019). One type of protein enriched at MCSs are LTPs, which facilitate non-vesicular lipid transport between the two membranes (Wong et al., 2019). These proteins have domains with a hydrophobic cavity or groove that can accommodate one or more lipid monomers, protecting the hydrophobic element from the cytosol. Many LTPs undergo rapid conformational changes in response to the lipid environment and often reside on more than one organelle, with the ability to bridge MCSs and transport lipids against their concentration gradient according to the needs of the cell. Recent developments in the field have identified lipid counter-exchange as a common way in which LTPs operate at MCSs.

OSBP is a soluble mammalian LTP that usually localizes to ER–Golgi MCSs. This localization is a result of simultaneous recruitment to the ER membrane via interaction with ER-residing VAP proteins and to the Golgi membrane by the enrichment of PI4P lipids at the membrane by Golgi-specific PI4KIIIβ. At ER–Golgi MCSs, OSBP mediates transport of newly synthesized cholesterol from the ER to the Golgi. This cholesterol transfer occurs against its concentration gradient, driven by a counter-exchange mechanism with the phospholipid (Mesmin et al., 2013). The generation of PI4P at the Golgi by PI4KIIIβ at the Golgi membrane and the consumption of PI4P at the ER membrane by the phosphatase Sac1 maintain a high concentration gradient of PI4P, allowing the transport of PI4P down its gradient from Golgi to the ER and the counter-transport of cholesterol from ER to Golgi.

A mechanism of regulation of plasma membrane phospholipids by MCS has also been proposed. Phosphorylation of PI4P increases the $PI(4,5)P_2$ composition of the plasma membrane. When $PI(4,5)P_2$ is elevated, an integral ER membrane protein, ORP8, is recruited to ER–plasma membrane MCSs. Together with another ER-resident OSBP, ORP5, ORP8 at MCSs mediates transport of ER-derived PS to the plasma membrane in exchange for plasma membrane-derived PI4P to limit $PI(4,5)P_2$ production and maintain homeostatic levels of phospholipids at the plasma membrane (Sohn et al., 2018).

role in efficient viral replication as PI4KIIIβ kinase inhibition or OSBP depletion significantly reduced viral RNA synthesis (reviewed in Altan-Bonnet, 2017). Alternatively, other viruses, including cardiovirus and HCV, recruit OSBP using PI4KIIIα (usually found at ER-PM contact sites) (Dorobantu et al., 2015). Viral protein NS5A was found to bind and activate PI4KIIIα, raising PI4P levels on the viral DMVs (Berger et al., 2011; Reiss et al., 2011), and depletion of PI4KIIIα or PI4P inhibited HCV replication. Interestingly, for HCV and cardiovirus, the normal RO structure was also altered with OSBP/PI4K depletion, suggesting that the action of OSBP is important for the structural characteristics of DMVs. SARS-CoV-2 nsp4 was recently found to interact with OSBP and PI4KIIIβ in a BioID study (St-Germain et al., 2020), suggesting that SARS-Cov-2 may also utilize OSBP-mediated lipid exchange for cholesterol enrichment.

Golgi to DMV Lipid Transport

+RNA viruses can also utilize other PI4P-binding proteins. The PI4P effector, four-phosphate adaptor protein 2 (FAPP2), a Golgi-localizing LTP, is also involved in HCV replication and is speculated to transport glycosphingolipids to the RO (Khan et al., 2014). Depletion of FAPP2 caused massive inhibition (>100-fold) of viral RNA replication. Both the PI4P-binding PH domain, which is thought to localize FAPP2 to the Golgi, and its glycolipid transport domain were found to be important for HCV replication. Similarly, depletion of another Golgi PI4P-binding protein, GOLPH3, also inhibited HCV secretion (Bishe et al., 2012).

Lipid Droplets (LDs)

In addition to activation and hijacking of host lipid transport mechanisms, it is also in the virus's interests to simultaneously downregulate lipid storage. Cholesterol is esterified in the ER prior to transport for storage in LDs, which are dynamic organelles where neutral lipids are stored, synthesized, and mobilized according to cellular requirements. Enteroviruses inhibit cholesterol esterification, preventing its transport to LDs, thereby increasing the availability of cellular cholesterol for use in viral ROs. This corresponds with reduced LDs (Ilnytska et al., 2013). Congruent with viral exploitation of cellular lipid stores, enterovirus infection induces MCS formation between ROs and existing LDs that provide platforms for transport of fatty acids to the RO. Electron microscopy (EM) studies have shown that ROs of rhinovirus, poliovirus, and coxsackievirus form MCSs with LDs (Roulin et al., 2014; Laufman et al., 2019; Melia et al., 2019), and similarly, we have observed DMV:LD contacts in cells infected with SARS-CoV-2 (**Figure 1**). In contrast to enterovirus infection, however, LDs and lipolysosomes were increased in SARS-CoV-2–infected cells, but not following SARS-CoV infection (Nardacci et al., 2020). Another intriguing observation was an increase in MCSs between mitochondria and LDs, possibly in response to dysregulation of host organelles by viral infection.

Importantly, inhibition of LD lipolysis was found to disrupt both RO formation and enterovirus replication, suggesting an important role for these LDs in the provision of lipids for RO biogenesis (Laufman et al., 2019). Indeed, a number of studies have implicated LD-derived lipid transport to ROs as a mechanism to support poliovirus replication. Fluorescently labeled fatty acids from LDs were transported to polioviral ROs (Laufman et al., 2019), and LD-derived phospholipids are required for poliovirus replication (Viktorova et al., 2018; Laufman et al., 2019). Lipases are recruited to LDs in poliovirus-infected cells to mobilize and release free fatty acids, and the poliovirus protein 3A, which localizes to ROs, was found to

TABLE 1 | Viral DMVs with known host organelle MCSs or lipid transport mechanisms.

Virus	RO[f] (primary membrane source)	RO:host organelle contacts[g]	Host MCS/lipid transfer proteins[h]	Lipids[i]
Hepatitis C virus[a]	DMV (ER) (Romero-Brey et al., 2012)	ER and lipid droplets (Romero-Brey et al., 2012) and endosomes (Stoeck et al., 2018)	PI4KIIIβ/PI4KIIIα (Berger et al., 2009), OSBP (Wang et al., 2014), VAP (Paul et al., 2013), STARD3, PITPNM1/Nir2 and NPC1 (Stoeck et al., 2018), ORP1 and CERT (Stoeck et al., 2018)	PIP (Reiss et al., 2011), Cholesterol (Stoeck et al., 2018), PIP2 (Cho et al., 2015), PA (Mingorance et al., 2018), SL (Sakamoto et al., 2005; Hirata et al., 2012), FA (Khan et al., 2014)
Poliovirus[b]	Single-membrane tubules/DMV (Golgi) (Belov et al., 2012)	ER and lipid droplets (Laufman et al., 2019), mitochondria (Belov et al., 2012)	PI4KIIIβ (Belov et al., 2012; Arita, 2014), OSBP (Arita, 2014)	PIP cholesterol (Ilnytska et al., 2013), PL (Banerjee et al., 2018; Viktorova et al., 2018), FA (Viktorova et al., 2018)
Coxsackievirus B3[b]	Single-membrane tubules/DMV (ER/Golgi) (Limpens et al., 2011)	Lipid droplets (Melia et al., 2019)	PI4KIIIβ, OSBP (Lanke et al., 2009)	Cholesterol (Albulescu et al., 2015)
Aichi virus[b]	Unknown	ER (Ishikawa-Sasaki et al., 2018)	OSBP, PITPNB, VAP, PI4KIIIβ (Ishikawa-Sasaki et al., 2018)	PIP (Ishikawa-Sasaki et al., 2014), Cholesterol (Ishikawa-Sasaki et al., 2018)
Rhinovirus[b]	Multimembrane vesicles (Golgi) (Roulin et al., 2014)	Lipid droplets and ER (Roulin et al., 2014)	PI4KIIIβ (Roulin et al., 2014), OSBP, PITPβ, VAP (Roulin et al., 2014)	PI4P, Cholesterol (Roulin et al., 2014)
Encephalomyocarditis virus[b]	Single membrane tubules/DMV (ER) (Gazina et al., 2002; Melia et al., 2019)	ER	PI4KIIIα, OSBP (Dorobantu et al., 2015)	PIP (Dorobantu et al., 2015), cholesterol (Ilnytska et al., 2013; Albulescu et al., 2015; Dorobantu et al., 2015)
Norovirus[b]	DMV (ER) (Doerflinger et al., 2017)	Lipid droplets and endosomes (Doerflinger et al., 2017)	VAP (McCune et al., 2017)	Unknown
SARS CoV[c]	DMV (ER) (Snijder et al., 2006; Knoops et al., 2008)	Mitochondria (Snijder et al., 2006; Knoops et al., 2008; Snijder et al., 2020)	Unknown	Unknown
MERS-CoV[c]	DMV/CMs (ER?) (de Wilde et al., 2013)	Mitochondria (Snijder et al., 2020)	Unknown	LPL (Muller et al., 2018)
Human coronavirus-229E[c]	DMV (ER?) (Snijder et al., 2020)	(ER)	Unknown	LPL and ceramide (Muller et al., 2018)
SARS-CoV2[c]	DMV (ER?) (Wolff et al., 2020a)	Peroxisomes and mitochondria (Cortese et al., 2020), LDs, and lysosomes (**Figure 1**)	Unknown	Unknown
Porcine reproductive and respiratory syndrome virus[d]	DMV (ER) (Zhang et al., 2018)	Unknown	Unknown	FA (Long et al., 2019), Cholesterol (Jeon and Lee, 2017)
Berne virus[e]	DMV (?) (vila-Perez et al., 2016)	ER and mitochondria (vila-Perez et al., 2016)	Unknown	Unknown

Viruses from the families: [a]Flaviviridae, [b]Picornaviridae, [c]Coronaviridae, [d]Arteriviridae, and [e]Tobaniviridae. [f]Viral replication organelle structures. [g]Observed contacts between viral replication organelles and host organelles. [h]Host factors localizing to membrane contact sites or involved in lipid transfer that appears to be involved in viral replication. [i]Host lipid species implicated in viral replication. CM, Convoluted membrane; DMV, double-membrane vesicle; ER, endoplasmic reticulum; FA, fatty acids; LPL, lysophospholipids; MERS-CoV, Middle East respiratory syndrome-related coronavirus; PA, phosphatidic acid; PIP, phosphatidylinositol-phosphate; PIP2, phosphatidylinositol bisphosphate; PLs, phospholipids; SARS-CoV, severe acute respiratory syndrome coronavirus; SL, sphingolipids.

interact with LD-associated lipases, inhibition of which prevented the development of ROs (Laufman et al., 2019).

HCV infection also causes membrane rearrangements around LDs, increasing contacts between LDs and cisternae membranes (Miyanari et al., 2007). HCV capsid protein associates with LDs and recruits non-structural proteins and replication complexes to LD-associated membrane (Miyanari et al., 2007).

While the molecular architecture of DMV:LD contact sites has not been characterized, similar mechanisms to those operating at the ER:LD interface likely tether these contacts and provide sites for lipid transport to the DMV. The integral ER protein seipin facilitates ER to LD trigyceride flow at lipidic bridges that form between the two organelles, where the LD phospholipid monolayer is continuous with the outer leaflet of the ER membrane (Salo et al., 2019). Several other proteins have been implicated in tethering LD contact sites, including the triglyceride synthesis enzyme DAG acyl transferase 2 (DGAT2) (Xu et al., 2012), Rab18 (Xu et al., 2018), and Snx14 (Datta et al., 2019). Interestingly, an interaction between the LD tethering protein Rab18 and viral nsp7 was identified in a SARS-CoV-2 virus–host protein interactome (Gordon et al., 2020). When viewed together with the known role of LDs in

viral replication and the extensive contact between DMVs and LDs in SARS-CoV-2–infected cells, these findings collectively provide compelling evidence of coronavirus appropriation of LD contact sites machinery for the biogenesis/maturation of its RO.

Endosome to DMV Lipid Transport

Dietary cholesterol, packaged into lipoproteins, enters the cell through the endocytic pathway, which can be targeted by viruses as an alternative source of lipids. Several viruses enrich their RO with PI4P by PI4K recruitment. However, PI4K also directly interacts with endosomal Rab11 (Burke et al., 2014) and can recruit Rab11-positive recycling endosomes to ROs for cholesterol exchange (Ilnytska et al., 2013; Albulescu et al., 2015).

Reasoning that DMV cholesterol enrichment likely depends on host LTPs, one study set out to establish whether any known LTPs are required for HCV replication. Several HCV dependency late endosomal sterol-binding proteins were identified, including STARD3, OSBP1, and NPC1, all of which have roles at MCSs (Salvador-Gallego et al., 2017). A follow-up study provided further evidence that viruses sequester endocytic organelles to provide the sterols necessary for viral replication. A role for the late endosomal sterol-binding protein NPC1 in mediating recruitment of endosomal cholesterol to ROs via MCSs with late endosomes/lysosomes in cells infected with HCV was demonstrated (Stoeck et al., 2018). A recent proximity labeling BioID study identified SARS-CoV-2 protein crosstalk with several lipid transport and MCS proteins, including NPC1, StARD3, and MOSPD2 (St-Germain et al., 2020). However, while NPC1 mediates transport of low-density lipoprotein (LDL)–derived cholesterol from late endosomes/lysosomes to the ER, STARD3 transports newly synthesized cholesterol in the opposite direction, from the ER to the endosome (Wilhelm et al., 2017). It is, therefore, hard to envisage a role for STARD3 as an LTP that enriches DMVs with endosomal sterol, and a recent study screening a CRISPR library for proteins required for SARS-CoV-2 infection found that neither endosomal STARD3 nor one of its ER-localized binding partners, MOSPD2 (Di Mattia et al., 2018), mediates viral infection or virus-induced cell death (Schneider et al., 2020). Indeed, a second genome-wide CRISPR screen identified STARD3 STARD3NL and MOSPD2 as negative regulators of SARS-CoV2 infection (Schneider et al., 2020). However, consistent with a role for DMV:endosome MCSs in viral replication, a study mapping SARS-CoV-2 virus–host protein interactions identified several Rabs interacting with a viral protein (nsp7) (Gordon et al., 2020), including Rab7, which is important for endocytic traffic and ER–endosome contact site formation (Martello et al., 2020). Rab8, which promotes recycling of cholesterol-rich endosomes to the plasma membrane (Kanerva et al., 2013), was also found to interact with nsp7, suggesting that Rab8-dependent cholesterol transport may be diverted away from the plasma membrane in infected cells to contribute to the DMV cholesterol supply. That MCSs form between DMVs. and endocytic organelles (e.g., DMV:lysosome MCSs in **Figure 1**) further support the notion that SARS-CoV-2 can exploit MCS machinery to sequester LDL-derived lipids for its ROs.

MANIPULATION OF MITOCHONDRIA TO EVADE THE IMMUNE RESPONSE

In order to proliferate, viruses must survive the host's immune response. Coronaviruses, including SARS-CoV-2, have evolved extensive measures to dampen the mechanism of innate sensing that cells use to sound the infection alarm. Multiple coronavirus proteins inhibit the production of interferons (IFNs) and cytokines from infected cells, thereby aiding viral replication. As discussed above, DMV formation offers protection for viral RNA replication, but viruses take further immune evasion measures, to actively disrupt the host innate immunity.

One intriguing aspect of innate immune sensing is the use of membrane surfaces for construction and regulation of many of the protein complexes responsible for determining signaling outputs. Mitochondria, in addition to their key role in cellular metabolism, are also important in the regulation of innate immunity in this context as they provide a platform for signaling complexes that drive IFN production and cell death. During infection, recognition of viral RNA by cytosolic pattern recognition receptors (PRRs) initiates oligomerization of the signaling adaptor mitochondrial antiviral signaling (MAVS), which in turn stimulates recruitment and activation of transcription factors that induce type I and type III IFN and proinflammatory cytokine production. There is a growing body of evidence that membrane reorganization and interactions help to orchestrate these events to promote appropriate antiviral responses. Sensing of intracellular RNA by PRRs results in extensive mitochondrional remodeling via regulation of mitochondrial fission through dynamin-like protein 1 (Drp1) (Chen et al., 2020) and fusion through mitofusin 1 (Mfn1) (Castanier et al., 2010). In non-infected cells, both fission and fusion events are defined by ER–mitochondria MCSs (Abrisch et al., 2020): interaction between mitochondrial Drp1 and ER-localized syntaxin 17 at MCSs promotes Drp1-mediated mitochondrial fission (Arasaki et al., 2015), whereas Mfn2 localizes to ER:mitochondria MCSs at sites of mitochondrial fusion (Abrisch et al., 2020). As discussed below, as both Drp1 and Mfn2 can be depleted by viral proteins, MCS disruption may contribute to mitochondrial remodeling in infected cells. Equally, virus infection can result in extensive mitochondrial damage, release of mtDNA, and subsequent activation of stimulator of IFN genes (STING)–dependent DNA sensing PRRs that also drive IFN-I transcription (Schoggins et al., 2014). MAVS and STING are both membrane-associated adaptor proteins that accumulate large signaling complexes on organelle surfaces and potentially at MCSs.

Extensive crosstalk between mitochondria and the ER at mitochondria-associated membranes (MAMs) is important for the regulation of mitochondrial function and signaling pathways involved in numerous cellular processes including inflammation and apoptosis (reviewed in Missiroli et al., 2018) and can be targeted by +RNA viruses to promote viral replication. Using time-lapse microscopy, the HIV-1 viral protein R (Vpr) was shown to be transported from the ER to mitochondria at MAMs (Huang et al., 2012). Vpr expression resulted in reduced levels of both Mfn2 and Drp1 and increased OMM permeability.

Similarly, infection with dengue virus also resulted in reduced mitochondrial Mfn2 and Drp1, as well as elongated mitochondria due to a loss of Drp1-mediated fission. Reduced fission may advantage the virus through the associated impaired clearance of dysfunctional mitochondria potentially containing viral RNA or protein. Interestingly, dengue virus infection induced the formation of nsp4-containing ROs that were in close contact with mitochondria, possibly at the expense of MAM formation, as ER–mitochondria interactions appeared to be reduced. Thus, it seems likely that viral proteins targeted to the ER, where the RO originates, may also hijack interactions with mitochondria to enable disruption of MAVS immune signaling pathways. Indeed, dengue Ns4A/B proteins inhibit viral RNA sensing, blocking activation of Tank-binding kinase 1 (TBK1) downstream of MAVS (Dalrymple et al., 2015).

Loss of Drp1 was also observed in cells infected with coronavirus. A SARS-CoV protein, open reading frame-9b (ORF9b), was found to localize to mitochondria and promote ubiquination and proteosomal degradation of both Drp1 and MAVS protein, resulting in elongated mitochondria, increased viral replication and inhibition of immune activation. Mitochondrial ORF9b mediates recruitment of the E3 ligase AIP4, to promote MAVS polyubiquitination. Reducing MAVS degradation through AIP4 depletion or disruption of AIP4 mitochondrial recruitment reversed the Orf9b-mediated suppression of antiviral immune response (Shi et al., 2014). DMV:mitochondria MCSs are common to Vero-E6 cells infected with SARS-CoV (Snijder et al., 2006) or A549 lung carcinoma epithelial cells infected with SARS-CoV-2 (**Figure 1**), and a recently published interactome suggests that SARS-CoV-2 also targets mitochondria, identifying interactions between viral Nsp4 and host mitochondrial TIMM complex, Nsp8, and mitochondrial ribosome proteins, and ORF9C and mitochondrial electron transport proteins (Gordon et al., 2020). Indeed, SARS-CoV-2 ORF9b also localizes to mitochondria and suppresses type I IFN responses by targeting mitochondrial TOM70 (Jiang et al., 2020). Interestingly, TOM70 overexpression can overcome type I IFN inhibition. Moreover, STING has also been implicated in SARS-CoV-2 innate sensing (Neufeldt et al., 2020), suggesting mtDNA release following SARS-CoV-2–induced mitochondrial damage.

Despite the nomenclature, MAVS can be found on peroxisomes, as well as mitochondria, with peroxisome-targeted MAVS producing a rapid transient response to influenza virus infection, complementing the delayed and stable response produced by mitochondria-targeted MAVS (Dixit et al., 2010). The influenza nsp, NS1, plays important roles in resisting host cell immune responses. NS1 was found to interact with a peroxisome-targeted host protein NS1-interactor (NS1-I) (Wolff et al., 1996), implicating peroxisome crosstalk in viral immune evasion. Crosstalk between HIV and peroxisomes was also found to contribute to dampening of the immune response, with interaction between HIV Nef and a peroxisomal thioesterase associated with CD4 downregulation and enhanced viral infectivity (Cohen et al., 2000). Roles for peroxisome proteins contributing to SARS-CoV-2 immune evasion have not yet been established, but clustering of peroxisomes in close proximity to DMVs was identified in cells infected with SARS-CoV-2 (Cortese et al., 2020). Moreover, a recent proximity labeling BioID study identified SARS-CoV-2 nsp4 association with VAP and ACBD5 (St-Germain et al., 2020), putative ER:peroxisome MCS proteins (Costello et al., 2017). The functional significance of this peroxisome association with DMVs is not yet known, but mechanisms for the prevention of oxidative damage to viral RNA or for peroxisome-mediated lipid metabolism in viral replication were proposed (Cortese et al., 2020).

DISCUSSION

The morphology of enterovirus ROs develops and changes during the course of viral infection, suggesting that ROs are dynamic and undergo a form of maturation. Polio and coxsackie ROs start as tubules that transform into DMVs, which are then enwrapped with more tubules to form multilamellar structures at later stages of infection (Limpens et al., 2011; Belov et al., 2012). For coronaviruses, the exact mechanism for DMV formation is as yet unconfirmed, but the number of DMVs, as well as the extent of surrounding convoluted membranes, increases during infection, and vesicle packs form late in the infection. The distribution and morphology of the RO change over the course of infection, which could in itself induce changes in its interaction with other organelles. Depletion of lipids from host organelles such as LDs could also be a factor in changes in MCS occurrence. Taken together, evidence suggests that MCSs between ROs and host cell organelles are regulated for the provision of specific lipids to the RO during infection, as required for replication of +RNA viruses. The importance of viral exploitation of host MCS machinery for biogenesis of the RO is further substantiated by a recent BioID proximity labeling study identifying an association between SARS-CoV-2 proteins and proteins functioning at ER contact sites with a variety of cellular organelles, including the plasma membrane (Gramd1a/b, eSyt, STIM1, ORP8), endo/lysosomes (NPC1, ORP1L, STARD3, PDZD8, ORP8, VAP, MOSPD2, Gramd1b), LDs (ORP2, VPS13A), mitochondria (ORP8, VPS13A, PDZD8), Golgi (VAP, ORP9/10), and peroxisomes (VAP, ABCD5) (St-Germain et al., 2020). As well as physically protecting viral RNA from host immune responses, host membrane rearrangements, often exploiting MCS machinery, can also compromise innate sensing to evade mitochondrial mediated immune response and safeguard viral replication.

DATA AVAILABILITY STATEMENT

The raw data supporting the conclusions of this article will be made available by the authors, without undue reservation.

AUTHOR CONTRIBUTIONS

All authors listed have made a substantial, direct and intellectual contribution to the work, and approved it for publication. Images for **Figure 1** were provided by JE.

FUNDING

LW was supported by MRC funding to Clare Futter and EE (Grant No. MRC/P010091/1). AM was supported by BBSRC funding to Andrew Peden and EE (Grant No. BB/S009566/1). JE was a Sir Henry Dale Fellow. Sir Henry Dale Fellowship jointly funded by the Wellcome Trust and the Royal Society (Grant No. 216370/Z/19/Z). BF is supported by BBSRC grant BB/S001336/1.

REFERENCES

Abrisch, R. G., Gumbin, S. C., Wisniewski, B. T., Lackner, L. L., and Voeltz, G. K. (2020). Fission and fusion machineries converge at ER contact sites to regulate mitochondrial morphology. *J. Cell Biol.* 219:e201911122.

Albulescu, L., Wubbolts, R., van Kuppeveld, F. J., and Strating, J. R. (2015). Cholesterol shuttling is important for RNA replication of coxsackievirus B3 and encephalomyocarditis virus. *Cell Microbiol.* 17, 1144–1156. doi: 10.1111/cmi.12425

Allison, R., Edgar, J. R., Pearson, G., Rizo, T., Newton, T., Gunther, S., et al. (2017). Defects in ER-endosome contacts impact lysosome function in hereditary spastic paraplegia. *J. Cell Biol.* 216, 1337–1355. doi: 10.1083/jcb.201609033

Altan-Bonnet, N. (2017). Lipid tales of viral replication and transmission. *Trends Cell Biol.* 27, 201–213. doi: 10.1016/j.tcb.2016.09.011

Angelini, M. M., Akhlaghpour, M., Neuman, B. W., and Buchmeier, M. J. (2013). Severe acute respiratory syndrome coronavirus nonstructural proteins 3, 4, and 6 induce double-membrane vesicles. *mBio* 4:e00524-13.

Arasaki, K., Shimizu, H., Mogari, H., Nishida, N., Hirota, N., Furuno, A., et al. (2015). A role for the ancient SNARE syntaxin 17 in regulating mitochondrial division. *Dev. Cell* 32, 304–317. doi: 10.1016/j.devcel.2014.12.011

Arita, M. (2014). Phosphatidylinositol-4 kinase III beta and oxysterol-binding protein accumulate unesterified cholesterol on poliovirus-induced membrane structure. *Microbiol. Immunol.* 58, 239–256. doi: 10.1111/1348-0421.12144

Atakpa, P., Thillaiappan, N. B., Mataragka, S., Prole, D. L., and Taylor, C. W. (2018). IP3 receptors preferentially associate with ER-lysosome contact sites and selectively Deliver Ca(2+) to lysosomes. *Cell Rep.* 25, 3180–3193. doi: 10.1016/j.celrep.2018.11.064

Banerjee, S., Aponte-Diaz, D., Yeager, C., Sharma, S. D., Ning, G., Oh, H. S., et al. (2018). Hijacking of multiple phospholipid biosynthetic pathways and induction of membrane biogenesis by a picornaviral 3CD protein. *PLoS Pathog.* 14:e1007086. doi: 10.1371/journal.ppat.1007086

Belov, G. A., Nair, V., Hansen, B. T., Hoyt, F. H., Fischer, E. R., and Ehrenfeld, E. (2012). Complex dynamic development of poliovirus membranous replication complexes. *J. Virol.* 86, 302–312. doi: 10.1128/jvi.05937-11

Berger, K. L., Kelly, S. M., Jordan, T. X., Tartell, M. A., and Randall, G. (2011). Hepatitis C virus stimulates the phosphatidylinositol 4-kinase III alpha-dependent phosphatidylinositol 4-phosphate production that is essential for its replication. *J. Virol.* 85, 8870–8883. doi: 10.1128/jvi.00059-11

Berger, L., Cooper, J. D., Heaton, N. S., Yoon, R., Oakland, T. E., Jordan, T. X., et al. (2009). Roles for endocytic trafficking and phosphatidylinositol 4-kinase III alpha in hepatitis C virus replication. *Proc. Natl. Acad. Sci. U.S.A.* 106, 7577–7582. doi: 10.1073/pnas.0902693106

Bishe, B., Syed, G. H., Field, S. J., and Siddiqui, A. (2012). Role of phosphatidylinositol 4-phosphate (PI4P) and its binding protein GOLPH3 in hepatitis C virus secretion. *J. Biol. Chem.* 287, 27637–27647. doi: 10.1074/jbc.m112.346569

Bohnert, M. (2020). Tether Me, Tether Me Not-dynamic organelle contact sites in metabolic rewiring. *Dev. Cell* 54, 212–225. doi: 10.1016/j.devcel.2020.06.026

Burke, E., Inglis, A. J., Perisic, O., Masson, G. R., McLaughlin, S. H., Rutaganira, F., et al. (2014). Structures of PI4KIIIbeta complexes show simultaneous recruitment of Rab11 and its effectors. *Science* 344, 1035–1038. doi: 10.1126/science.1253397

Cabukusta, B., and Neefjes, J. (2018). Mechanisms of lysosomal positioning and movement. *Traffic* 19, 761–769. doi: 10.1111/tra.12587

Castanier, C., Garcin, D., Vazquez, A., and Arnoult, D. (2010). Mitochondrial dynamics regulate the RIG-I-like receptor antiviral pathway. *EMBO Rep.* 11, 133–138. doi: 10.1038/embor.2009.258

Chen, S., Liu, S., Wang, J., Wu, Q., Wang, A., Guan, H., et al. (2020). TBK1-mediated DRP1 targeting confers nucleic acid sensing to reprogram mitochondrial dynamics and physiology. *Mol. Cell* 80, 810–827.e817.

Cho, J., Lee, C., Pang, P. S., Pham, E. A., Fram, B., Nguyen, K., et al. (2015). Phosphatidylinositol 4,5-bisphosphate is an HCV NS5A ligand and mediates replication of the viral genome. *Gastroenterology* 148, 616–625. doi: 10.1053/j.gastro.2014.11.043

Clementz, M. A., Kanjanahaluethai, A., O'Brien, T. E., and Baker, S. C. (2008). Mutation in murine coronavirus replication protein nsp4 alters assembly of double membrane vesicles. *Virology* 375, 118–129. doi: 10.1016/j.virol.2008.01.018

Cohen, G. B., Rangan, V. S., Chen, B. K., Smith, S., and Baltimore, D. (2000). The human thioesterase II protein binds to a site on HIV-1 Nef critical for CD4 down-regulation. *J. Biol. Chem.* 275, 23097–23105. doi: 10.1074/jbc.m000536200

Cortese, M., Lee, J. Y., Cerikan, B., Neufeldt, C. J., Oorschot, V. M. J., Kohrer, S., et al. (2020). Integrative imaging reveals SARS-CoV-2-Induced Reshaping of Subcellular Morphologies. *Cell Host Microb.* 28, 853–866.e5.

Costello, J. L., Castro, I. G., Hacker, C., Schrader, T. A., Metz, J., Zeuschner, D., et al. (2017). ACBD5 and VAPB mediate membrane associations between peroxisomes and the ER. *J. Cell Biol.* 216, 331–342. doi: 10.1083/jcb.201607055

Dalrymple, N. A., Cimica, V., and Mackow, E. R. (2015). Dengue virus NS proteins inhibit RIG-I/MAVS signaling by blocking TBK1/IRF3 phosphorylation: dengue virus serotype 1 NS4A is a unique interferon-regulating virulence determinant. *mBio* 6:e00553-15.

Datta, S., Liu, Y., Hariri, H., Bowerman, J., and Henne, W. M. (2019). Cerebellar ataxia disease-associated Snx14 promotes lipid droplet growth at ER-droplet contacts. *J. Cell Biol.* 218, 1335–1351. doi: 10.1083/jcb.201808133

de Wilde, H., Raj, V. S., Oudshoorn, D., Bestebroer, T. M., van Nieuwkoop, S., Limpens, R., et al. (2013). MERS-coronavirus replication induces severe in vitro cytopathology and is strongly inhibited by cyclosporin A or interferon-alpha treatment. *J. Gen. Virol.* 94, 1749–1760. doi: 10.1099/vir.0.052910-0

Di Mattia, T., Tomasetto, C., and Alpy, F. (2019). Faraway, so close! Functions of endoplasmic reticulum-Endosome contacts. *Biochim. Biophys. Acta Mol. Cell Biol. Lipids* 1865:158490. doi: 10.1016/j.bbalip.2019.06.016

Di Mattia, T., Wilhelm, L. P., Ikhlef, S., Wendling, C., Spehner, D., Nomine, Y., et al. (2018). Identification of MOSPD2, a novel scaffold for endoplasmic reticulum membrane contact sites. *EMBO Rep.* 19:e45453.

Dixit, E., Boulant, S., Zhang, Y., Lee, A. S., Odendall, C., Shum, B., et al. (2010). Peroxisomes are signaling platforms for antiviral innate immunity. *Cell* 141, 668–681. doi: 10.1016/j.cell.2010.04.018

Doerflinger, S. Y., Cortese, M., Romero-Brey, I., Menne, Z., Tubiana, T., Schenk, C., et al. (2017). Membrane alterations induced by nonstructural proteins of human norovirus. *PLoS Pathog.* 13:e1006705. doi: 10.1371/journal.ppat.1006705

Dorobantu, C. M., Albulescu, L., Harak, C., Feng, Q., van Kampen, M., Strating, J. R., et al. (2015). Modulation of the host lipid landscape to promote RNA virus replication: the picornavirus encephalomyocarditis virus converges on the pathway used by hepatitis C virus. *PLoS Pathog.* 11:e1005185. doi: 10.1371/journal.ppat.1005185

Eden, E. R., White, I. J., Tsapara, A., and Futter, C. E. (2010). Membrane contacts between endosomes and ER provide sites for PTP1B-epidermal growth factor receptor interaction. *Nat. Cell Biol.* 12, 267–272. doi: 10.1038/ncb2026

Eisenberg-Bord, M., Shai, N., Schuldiner, M., Bohnert, M., and Tether, A. (2016). Is a tether is a tether: tethering at membrane contact sites. *Dev. Cell* 39, 395–409. doi: 10.1016/j.devcel.2016.10.022

Friedman, J. R., Dibenedetto, J. R., West, M., Rowland, A. A., and Voeltz, G. K. (2013). Endoplasmic reticulum-endosome contact increases as endosomes traffic and mature. *Mol. Biol. Cell* 24, 1030–1040. doi: 10.1091/mbc.e12-10-0733

Gassen, N. C., Niemeyer, D., Muth, D., Corman, V. M., Martinelli, S., Gassen, A., et al. (2019). SKP2 attenuates autophagy through Beclin1-ubiquitination and its inhibition reduces MERS-Coronavirus infection. *Nat. Commun.* 10:5770.

Gazina, E. V., Mackenzie, J. M., Gorrell, R. J., and Anderson, D. A. (2002). Differential requirements for COPI coats in formation of replication complexes among three genera of Picornaviridae. *J. Virol.* 76, 11113–11122. doi: 10.1128/jvi.76.21.11113-11122.2002

Gordon, D. E., Jang, G. M., Bouhaddou, M., Xu, J., Obernier, K., White, K. M., et al. (2020). A SARS-CoV-2 protein interaction map reveals targets for drug repurposing. *Nature* 583, 459–468.

Hagemeijer, M. C., Monastyrska, I., Griffith, J., van der Sluijs, P., Voortman, J., van Bergen en Henegouwen, P. M., et al. (2014). Membrane rearrangements mediated by coronavirus nonstructural proteins 3 and 4. *Virology* 458–459, 125–135. doi: 10.1016/j.virol.2014.04.027

Harak, C., and Lohmann, V. (2015). Ultrastructure of the replication sites of positive-strand RNA viruses. *Virology* 479–480, 418–433. doi: 10.1016/j.virol.2015.02.029

Hirata, Y., Ikeda, K., Sudoh, M., Tokunaga, Y., Suzuki, A., Weng, L., et al. (2012). Self-enhancement of hepatitis C virus replication by promotion of specific sphingolipid biosynthesis. *PLoS Pathog.* 8:e1002860. doi: 10.1371/journal.ppat.1002860

Hoffmann, H. H., Schneider, W. M., Rozen-Gagnon, K., Miles, L. A., Schuster, F., Razooky, B., et al. (2021). TMEM41B is a Pan-flavivirus host factor. *Cell* 184, 133–148.e120.

Hoffmann, H.-H., Schneider, W. M., Sánchez-Rivera, F. J., Luna, J. L., Ashbrook, A. W., Soto-Feliciano, Y. M., et al. (2020). Functional interrogation of a SARS-CoV-2 host protein interactome identifies unique and shared coronavirus host factors. *bioRxiv* [Preprint]. doi: 10.1101/2020.09.11.291716v1

Hoffmann, M., Kleine-Weber, H., Schroeder, S., Kruger, N., Herrler, T., Erichsen, S., et al. (2020). SARS-CoV-2 cell entry depends on ACE2 and TMPRSS2 and is blocked by a clinically proven protease inhibitor. *Cell* 181, 271–280.e278.

Hong, Z., Pedersen, N. M., Wang, L., Torgersen, M. L., Stenmark, H., and Raiborg, C. (2017). PtdIns3P controls mTORC1 signaling through lysosomal positioning. *J. Cell Biol.* 216, 4217–4233. doi: 10.1083/jcb.201611073

Hoyer, M. J., Chitwood, P. J., Ebmeier, C. C., Striepen, J. F., Qi, R. Z., Old, W. M., et al. (2018). of ER membrane proteins regulates ER-associated endosome fission. *Cell* 175, 254–265.e214.

Hsu, N. Y., Ilnytska, O., Belov, G., Santiana, M., Chen, Y. H., Takvorian, P. M., et al. (2010). Viral reorganization of the secretory pathway generates distinct organelles for RNA replication. *Cell* 141, 799–811. doi: 10.1016/j.cell.2010.03.050

Huang, C. Y., Chiang, S. F., Lin, T. Y., Chiou, S. H., and Chow, K. C. (2012). HIV-1 Vpr triggers mitochondrial destruction by impairing Mfn2-mediated ER-mitochondria interaction. *PLoS One* 7:e33657. doi: 10.1371/journal.pone.0033657

Ilnytska, O., Santiana, M., Hsu, N. Y., Du, W. L., Chen, Y. H., Viktorova, E. G., et al. (2013). Enteroviruses harness the cellular endocytic machinery to remodel the host cell cholesterol landscape for effective viral replication. *Cell Host Microb.* 14, 281–293. doi: 10.1016/j.chom.2013.08.002

Ishikawa-Sasaki, K., Nagashima, S., Taniguchi, K., and Sasaki, J. (2018). Model of OSBP-mediated cholesterol supply to aichi Virus RNA replication sites involving protein-protein interactions among viral proteins, ACBD3, OSBP, VAP-A/B, and SAC1. *J. Virol.* 92:e01952-17.

Ishikawa-Sasaki, K., Sasaki, J., and Taniguchi, K. (2014). A complex comprising phosphatidylinositol 4-kinase IIIbeta, ACBD3, and Aichi virus proteins enhances phosphatidylinositol 4-phosphate synthesis and is critical for formation of the viral replication complex. *J. Virol.* 88, 6586–6598. doi: 10.1128/jvi.00208-14

Jeon, J. H., and Lee, C. (2017). Cellular cholesterol is required for porcine nidovirus infection. *Arch. Virol.* 162, 3753–3767. doi: 10.1007/s00705-017-3545-4

Jiang, H. W., Zhang, H. N., Meng, Q. F., Xie, J., Li, Y., Chen, H., et al. (2020). 2 Orf9b suppresses type I interferon responses by targeting TOM70. *Cell Mol. Immunol.* 17, 998–1000. doi: 10.1038/s41423-020-0514-8

Jongsma, M. L., Berlin, I., Wijdeven, R. H., Janssen, L., Janssen, G. M., Garstka, M. A., et al. (2016). An ER-associated pathway defines endosomal architecture for controlled cargo transport. *Cell* 166, 152–166. doi: 10.1016/j.cell.2016.05.078

Kanerva, K., Uronen, R. L., Blom, T., Li, S., Bittman, R., Lappalainen, P., et al. (2013). LDL cholesterol recycles to the plasma membrane via a Rab8a-Myosin5b-actin-dependent membrane transport route. *Dev. Cell* 27, 249–262. doi: 10.1016/j.devcel.2013.09.016

Kawase, M., Shirato, K., van der Hoek, L., Taguchi, F., and Matsuyama, S. (2012). Simultaneous treatment of human bronchial epithelial cells with serine and cysteine protease inhibitors prevents severe acute respiratory syndrome coronavirus entry. *J. Virol.* 86, 6537–6545. doi: 10.1128/jvi.00094-12

Khan, I., Katikaneni, D. S., Han, Q., Sanchez-Felipe, L., Hanada, K., Ambrose, R. L., et al. (2014). Modulation of hepatitis C virus genome replication by glycosphingolipids and four-phosphate adaptor protein 2. *J. Virol.* 88, 12276–12295. doi: 10.1128/jvi.00970-14

Klein, S., Cortese, M., Winter, S. L., Wachsmuth-Melm, M., Neufeldt, C. J., Cerikan, B., et al. (2020). SARS-CoV-2 structure and replication characterized by in situ cryo-electron tomography. *Nat. Commun.* 11:5885.

Knoops, K., Kikkert, M., Worm, S. H., Zevenhoven-Dobbe, J. C., van der Meer, Y., Koster, A. J., et al. (2008). SARS-coronavirus replication is supported by a reticulovesicular network of modified endoplasmic reticulum. *PLoS Biol.* 6:e226. doi: 10.1371/journal.pbio.0060226

Lanke, H., van der Schaar, H. M., Belov, G. A., Feng, Q., Duijsings, D., Jackson, C. L., et al. (2009). GBF1, a guanine nucleotide exchange factor for Arf, is crucial for coxsackievirus B3 RNA replication. *J. Virol.* 83, 11940–11949. doi: 10.1128/jvi.01244-09

Laufman, O., Perrino, J., and Andino, R. (2019). Viral generated inter-organelle contacts redirect lipid flux for genome replication. *Cell* 178, 275–289. doi: 10.1016/j.cell.2019.05.030

Lee, C. A., and Blackstone, C. (2020). ER morphology and endo-lysosomal crosstalk: Functions and disease implications. *Biochim. Biophys. Acta Mol. Cell Biol. Lipids* 1865:158544. doi: 10.1016/j.bbalip.2019.158544

Li, G. M., Li, Y. G., Yamate, M., Li, S. M., and Ikuta, K. (2007). Lipid rafts play an important role in the early stage of severe acute respiratory syndrome-coronavirus life cycle. *Microb. Infect.* 9, 96–102. doi: 10.1016/j.micinf.2006.10.015

Limpens, R. W., van der Schaar, H. M., Kumar, D., Koster, A. J., Snijder, E. J., van Kuppeveld, F. J., et al. (2011). The transformation of enterovirus replication structures: a three-dimensional study of single- and double-membrane compartments. *mBio* 2:e0166-11.

Long, S., Zhou, Y., Bai, D., Hao, W., Zheng, B., Xiao, S., et al. (2019). Fatty acids regulate porcine reproductive and respiratory syndrome virus infection via the AMPK-ACC1 signaling pathway. *Viruses* 11:1145. doi: 10.3390/v11121145

Martello, A., Platt, F. M., and Eden, E. R. (2020). Staying in touch with the endocytic network: the importance of contacts for cholesterol transport. *Traffic* 21, 354–363. doi: 10.1111/tra.12726

Maxfield, F. R., and Menon, A. K. (2006). Intracellular sterol transport and distribution. *Curr. Opin. Cell Biol.* 18, 379–385. doi: 10.1016/j.ceb.2006.06.012

McCune, B. T., Tang, W., Lu, J., Eaglesham, J. B., Thorne, L., Mayer, A. E., et al. (2017). Noroviruses Co-opt the function of host proteins VAPA and VAPB for replication via a phenylalanine-phenylalanine-acidic-tract-motif mimic in nonstructural viral protein NS1/2. *mBio* 8:e0668-17.

Melia, C. E., Peddie, C. J., de Jong, A. W. M., Snijder, E. J., Collinson, L. M., Koster, A. J., et al. (2019). Origins of enterovirus replication organelles established by whole-cell electron microscopy. *mBio* 10:e0951-19.

Mesmin, B., Bigay, J., Moser von Filseck, J., Lacas-Gervais, S., Drin, G., and Antonny, B. (2013). A four-step cycle driven by PI(4)P hydrolysis directs sterol/PI(4)P exchange by the ER-Golgi tether OSBP. *Cell* 155, 830–843. doi: 10.1016/j.cell.2013.09.056

Miller, D. J., Schwartz, M. D., and Ahlquist, P. (2001). Flock house virus RNA replicates on outer mitochondrial membranes in *Drosophila* cells. *J. Virol.* 75, 11664–11676. doi: 10.1128/jvi.75.23.11664-11676.2001

Mingorance, L., Castro, V., Avila-Perez, G., Calvo, G., Rodriguez, M. J., Carrascosa, J. L., et al. (2018). Host phosphatidic acid phosphatase lipin1 is rate limiting for functional hepatitis C virus replicase complex formation. *PLoS Pathog.* 14:e1007284. doi: 10.1371/journal.ppat.1007284

Missiroli, S., Patergnani, S., Caroccia, N., Pedriali, G., Perrone, M., Previati, M., et al. (2018). Mitochondria-associated membranes (MAMs) and inflammation. *Cell Death Dis.* 9, 329.

Miyanari, Y., Atsuzawa, K., Usuda, N., Watashi, K., Hishiki, T., Zayas, M., et al. (2007). The lipid droplet is an important organelle for hepatitis C virus production. *Nat. Cell Biol.* 9, 1089–1097. doi: 10.1038/ncb1631

Moretti, F., Bergman, P., Dodgson, S., Marcellin, D., Claerr, I., Goodwin, J. M., et al. (2018). TMEM41B is a novel regulator of autophagy and lipid mobilization. *EMBO Rep.* 19:e45889.

Morita, K., Hama, Y., Izume, T., Tamura, N., Ueno, T., Yamashita, Y., et al. (2018). Genome-wide CRISPR screen identifies TMEM41B as a gene required for autophagosome formation. *J. Cell Biol.* 217, 3817–3828. doi: 10.1083/jcb.201804132

Muller, C., Hardt, M., Schwudke, D., Neuman, B. W., Pleschka, S., and Ziebuhr, J. (2018). Inhibition of cytosolic phospholipase A2alpha impairs an early step of coronavirus replication in cell culture. *J. Virol.* 92:e001463-17.

Nardacci, R., Colavita, F., Castilletti, C., Lapa, D., Matusali, G., Meschi, S., et al. (2020). SARS-CoV-2 cytopathogenesis in cultured cells and in COVID-19 autoptic lung, evidences of lipid involvement. *Research Square* [Preprint]. doi: 10.21203/rs.3.rs-39274/v1

Neufeldt, C. J., Cerikan, B., Cortese, M., Frankish, J., Lee, J.-Y., Plociennikowska, A., et al. (2020). SARS-CoV-2 infection induces a pro-inflammatory cytokine response through cGAS-STING and NF-κB. *bioRxiv* [Preprint]. doi: 10.1101/2020.07.21.212639

Oudshoorn, D., Rijs, K., Limpens, R., Groen, K., Koster, A. J., Snijder, E. J., et al. (2017). Expression and cleavage of middle east respiratory syndrome coronavirus nsp3-4 Polyprotein induce the formation of double-membrane vesicles that mimic those associated with coronaviral RNA replication. *mBio* 8:e01658-17.

Palande, K., Roovers, O., Gits, J., Verwijmeren, C., Iuchi, Y., Fujii, J., et al. (2011). Peroxiredoxin-controlled G-CSF signalling at the endoplasmic reticulum-early endosome interface. *J. Cell Sci.* 124, 3695–3705. doi: 10.1242/jcs.089656

Paul, D., Hoppe, S., Saher, G., Krijnse-Locker, J., and Bartenschlager, R. (2013). Morphological and biochemical characterization of the membranous hepatitis C virus replication compartment. *J. Virol.* 87, 10612–10627. doi: 10.1128/jvi.01370-13

Prentice, E., Jerome, W. G., Yoshimori, T., Mizushima, N., and Denison, M. R. (2004a). Coronavirus replication complex formation utilizes components of cellular autophagy. *J. Biol. Chem.* 279, 10136–10141. doi: 10.1074/jbc.m306124200

Prentice, E., McAuliffe, J., Lu, X., Subbarao, K., and Denison, M. R. (2004b). Identification and characterization of severe acute respiratory syndrome coronavirus replicase proteins. *J. Virol.* 78, 9977–9986. doi: 10.1128/jvi.78.18.9977-9986.2004

Prinz, W. A., Toulmay, A., and Balla, T. (2020). The functional universe of membrane contact sites. *Nat. Rev. Mol. Cell Biol.* 21, 7–24. doi: 10.1038/s41580-019-0180-9

Qu, Y., Xin, W., Zhu, Y., Wang, Y., Yang, X., Hu, G., et al. (2020). ORF3a mediated-incomplete autophagy facilitates SARS-CoV-2 replication. *bioRxiv* [Preprint]. doi: 10.1101/2020.11.12.380709

Raiborg, C., Wenzel, E. M., Pedersen, N. M., and Stenmark, H. (2016). ER-endosome contact sites in endosome positioning and protrusion outgrowth. *Biochem. Soc. Trans.* 44, 441–446. doi: 10.1042/bst20150246

Reggiori, F., Monastyrska, I., Verheije, M. H., Cali, T., Ulasli, M., Bianchi, S., et al. (2010). Coronaviruses Hijack the LC3-I-positive EDEMosomes, ER-derived vesicles exporting short-lived ERAD regulators, for replication. *Cell Host Microb.* 7, 500–508. doi: 10.1016/j.chom.2010.05.013

Reiss, S., Rebhan, I., Backes, P., Romero-Brey, I., Erfle, H., Matula, P., et al. (2011). Recruitment and activation of a lipid kinase by hepatitis C virus NS5A is essential for integrity of the membranous replication compartment. *Cell Host Microb.* 9, 32–45. doi: 10.1016/j.chom.2010.12.002

Romero-Brey, I., Merz, A., Chiramel, A., Lee, J. Y., Chlanda, P., Haselman, U., et al. (2012). Three-dimensional architecture and biogenesis of membrane structures associated with hepatitis C virus replication. *PLoS Pathog.* 8:e1003056. doi: 10.1371/journal.ppat.1003056

Roulin, P. S., Lotzerich, M., Torta, F., Tanner, L. B., van Kuppeveld, F. J., Wenk, M. R., et al. (2014). Rhinovirus uses a phosphatidylinositol 4-phosphate/cholesterol counter-current for the formation of replication compartments at the ER-Golgi interface. *Cell Host Microb.* 16, 677–690. doi: 10.1016/j.chom.2014.10.003

Rowland, A. A., Chitwood, P. J., Phillips, M. J., and Voeltz, G. K. (2014). ER contact sites define the position and timing of endosome fission. *Cell* 159, 1027–1041. doi: 10.1016/j.cell.2014.10.023

Sakamoto, H., Okamoto, K., Aoki, M., Kato, H., Katsume, A., Ohta, A., et al. (2005). Host sphingolipid biosynthesis as a target for hepatitis C virus therapy. *Nat. Chem. Biol.* 1, 333–337. doi: 10.1038/nchembio742

Salo, V. T., Li, S., Vihinen, H., Holtta-Vuori, M., Szkalisity, A., Horvath, P., et al. (2019). Seipin facilitates triglyceride flow to lipid droplet and counteracts droplet ripening via endoplasmic reticulum contact. *Dev. Cell* 50, 478–493.e479.

Salvador-Gallego, R., Hoyer, M. J., and Voeltz, G. K. (2017). SnapShot: functions of endoplasmic reticulum membrane contact sites. *Cell* 171, 1224–1224.e1221. doi: 10.1016/j.cell.2017.11.005

Schlegel, A., Giddings, T. H. Jr., Ladinsky, M. S., and Kirkegaard, K. (1996). Cellular origin and ultrastructure of membranes induced during poliovirus infection. *J. Virol.* 70, 6576–6588. doi: 10.1128/jvi.70.10.6576-6588.1996

Schneider, M., Ackermann, K., Stuart, M., Wex, C., Protzer, U., Schatzl, H. M., et al. (2012). Severe acute respiratory syndrome coronavirus replication is severely impaired by MG132 due to proteasome-independent inhibition of M-calpain. *J. Virol.* 86, 10112–10122. doi: 10.1128/jvi.01001-12

Schneider, W. M., Luna, J. M., Hoffmann, H.-H., Sánchez-Rivera, F. J., Leal, A. A., Ashbrook, A. W., et al. (2020). Genome-scale identification of SARS-CoV-2 and pan-coronavirus host factor networks. *bioRxiv* [Preprint]. doi: 10.1101/2020.10.07.326462v1

Schoggins, J. W., MacDuff, D. A., Imanaka, N., Gainey, M. D., Shrestha, B., Eitson, J. L., et al. (2014). Rice, Pan-viral specificity of IFN-induced genes reveals new roles for cGAS in innate immunity. *Nature* 505, 691–695. doi: 10.1038/nature12862

Scorrano, L., De Matteis, M. A., Emr, S., Giordano, F., Hajnoczky, G., Kornmann, B., et al. (2019). Coming together to define membrane contact sites. *Nat. Commun.* 10:1287.

Shi, S., Qi, H. Y., Boularan, C., Huang, N. N., Abu-Asab, M., Shelhamer, J. H., et al. (2014). SARS-coronavirus open reading frame-9b suppresses innate immunity by targeting mitochondria and the MAVS/TRAF3/TRAF6 signalosome. *J. Immunol.* 193, 3080–3089. doi: 10.4049/jimmunol.1303196

Shoemaker, C. J., Huang, T. Q., Weir, N. R., Polyakov, N. J., Schultz, S. W., and Denic, V. (2019). CRISPR screening using an expanded toolkit of autophagy reporters identifies TMEM41B as a novel autophagy factor. *PLoS Biol.* 17:e2007044. doi: 10.1371/journal.pbio.2007044

Silva, B. S. C., DiGiovanni, L., Kumar, R., Carmichael, R. E., Kim, P. K., and Schrader, M. (2020). Maintaining social contacts: the physiological relevance of organelle interactions. *Biochim. Biophys. Acta Mol. Cell Res.* 1867:118800. doi: 10.1016/j.bbamcr.2020.118800

Singh, K. K., Chaubey, G., Chen, J. Y., and Suravajhala, P. (2020). Decoding SARS-CoV-2 hijacking of host mitochondria in COVID-19 pathogenesis. *Am. J. Physiol. Cell Physiol.* 319, C258–C267.

Snijder, E. J., Limpens, R., de Wilde, A. H., de Jong, A. W. M., Zevenhoven-Dobbe, J. C., Maier, H. J., et al. (2020). A unifying structural and functional model of the coronavirus replication organelle: tracking down RNA synthesis. *PLoS Biol.* 18:e3000715. doi: 10.1371/journal.pbio.3000715

Snijder, E. J., van der Meer, Y., Zevenhoven-Dobbe, J., Onderwater, J. J., van der Meulen, J., Koerten, H. K., et al. (2006). Ultrastructure and origin of membrane vesicles associated with the severe acute respiratory syndrome coronavirus replication complex. *J. Virol.* 80, 5927–5940. doi: 10.1128/jvi.02501-05

Sohn, M., Korzeniowski, M., Zewe, J. P., Wills, R. C., Hammond, G. R. V., Humpolickova, J., et al. (2018). PI(4,5)P2 controls plasma membrane PI4P and PS levels via ORP5/8 recruitment to ER-PM contact sites. *J. Cell Biol.* 217, 1797–1813. doi: 10.1083/jcb.201710095

St-Germain, J. R., Astori, A., Samavarchi-Tehrani, P., Abdouni, H., Macwan, V., Kim, D.-K., et al. (2020). SARS-CoV-2 BioID-based virus-host membrane protein interactome and virus peptide compendium: new proteomics resources for COVID-19 research. *bioRxiv* [Preprint]. doi: 10.1101/2020.08.28.269175v1

Stoeck, K., Lee, J. Y., Tabata, K., Romero-Brey, I., Paul, D., Schult, P., et al. (2018). Hepatitis C Virus replication depends on endosomal cholesterol homeostasis. *J. Virol.* 92:JVI.1196-1117.

Sugiura, A., McLelland, G. L., Fon, E. A., and McBride, H. M. (2014). A new pathway for mitochondrial quality control: mitochondrial-derived vesicles. *EMBO J.* 33, 2142–2156. doi: 10.15252/embj.201488104

van der Kant, R., and Neefjes, J. (2014). Small regulators, major consequences – Ca2+ and cholesterol at the endosome-ER interface. *J. Cell Sci.* 127, 929–938. doi: 10.1242/jcs.137539

Viktorova, E. G., Nchoutmboube, J. A., Ford-Siltz, L. A., Iverson, E., and Belov, G. A. (2018). Phospholipid synthesis fueled by lipid droplets drives

the structural development of poliovirus replication organelles. *PLoS Pathog.* 14:e1007280. doi: 10.1371/journal.ppat.1007280

vila-Perez, G. A., Rejas, M. T., and Rodriguez, D. (2016). Ultrastructural characterization of membranous torovirus replication factories. *Cell Microbiol.* 18, 1691–1708. doi: 10.1111/cmi.12620

Wang, H., Perry, J. W., Lauring, A. S., Neddermann, P., De Francesco, R., and Tai, A. W. (2014). Oxysterol-binding protein is a phosphatidylinositol 4-kinase effector required for HCV replication membrane integrity and cholesterol trafficking. *Gastroenterology* 146, 1373–1385.e1371–e1311.

Wilhelm, P., Wendling, C., Vedie, B., Kobayashi, T., Chenard, M. P., Tomasetto, C., et al. (2017). STARD3 mediates endoplasmic reticulum-to-endosome cholesterol transport at membrane contact sites. *EMBO J.* 36, 1412–1433. doi: 10.15252/embj.201695917

Wolff, G., Limpens, R., Zevenhoven-Dobbe, J. C., Laugks, U., Zheng, S., de Jong, A. W. M., et al. (2020a). A molecular pore spans the double membrane of the coronavirus replication organelle. *Science* 369, 1395–1398. doi: 10.1126/science.abd3629

Wolff, G., Melia, C. E., Snijder, E. J., and Barcena, M. (2020b). Double-membrane vesicles as platforms for viral replication. *Trends Microbiol.* 28, 1022–1033. doi: 10.1016/j.tim.2020.05.009

Wolff, T., O'Neill, R. E., and Palese, P. (1996). Interaction cloning of NS1-I, a human protein that binds to the nonstructural NS1 proteins of influenza A and B viruses. *J. Virol.* 70, 5363–5372. doi: 10.1128/jvi.70.8.5363-5372.1996

Wong, L. H., Gatta, A. T., and Levine, T. P. (2019). Lipid transfer proteins: the lipid commute via shuttles, bridges and tubes. *Nat. Rev. Mol. Cell Biol.* 20, 85–101. doi: 10.1038/s41580-018-0071-5

Wu, K. E., Fazal, F. M., Parker, K. R., Zou, J., Chang, H. Y., and Predicts, R. N. A.-G. P. S. (2020). SARS-CoV-2 RNA residency to host mitochondria and nucleolus. *Cell Syst.* 11, 102–108.e103.

Xu, D., Li, Y., Wu, L., Li, Y., Zhao, D., Yu, J., et al. (2018). Rab18 promotes lipid droplet (LD) growth by tethering the ER to LDs through SNARE and NRZ interactions. *J. Cell Biol.* 217, 975–995. doi: 10.1083/jcb.201704184

Xu, N., Zhang, S. O., Cole, R. A., McKinney, S. A., Guo, F., Haas, J. T., et al. (2012). The FATP1-DGAT2 complex facilitates lipid droplet expansion at the ER-lipid droplet interface. *J. Cell Biol.* 198, 895–911. doi: 10.1083/jcb.201201139

Yan, B., Chu, H., Yang, D., Sze, K. H., Lai, P. M., Yuan, S., et al. (2019). Characterization of the Lipidomic profile of human coronavirus-infected cells: implications for lipid metabolism remodeling upon coronavirus replication. *Viruses* 11:73. doi: 10.3390/v11010073

Yuan, S., Chu, H., Chan, J. F., Ye, Z. W., Wen, L., Yan, B., et al. (2019). SREBP-dependent lipidomic reprogramming as a broad-spectrum antiviral target. *Nat. Commun.* 10:120.

Zhang, J., Zhang, Z., Chukkapalli, V., Nchoutmboube, J. A., Li, J., Randall, G., et al. (2016). Positive-strand RNA viruses stimulate host phosphatidylcholine synthesis at viral replication sites. *Proc. Natl. Acad. Sci. U.S.A.* 113, E1064–E1073.

Zhang, W., Chen, K., Zhang, X., Guo, C., Chen, Y., and Liu, X. (2018). An integrated analysis of membrane remodeling during porcine reproductive and respiratory syndrome virus replication and assembly. *PLoS One* 13:e0200919. doi: 10.1371/journal.pone.0200919

Zhao, Z., Thackray, L. B., Miller, B. C., Lynn, T. M., Becker, M. M., Ward, E., et al. (2007). Coronavirus replication does not require the autophagy gene ATG5. *Autophagy* 3, 581–585. doi: 10.4161/auto.4782

Conflict of Interest: The authors declare that the research was conducted in the absence of any commercial or financial relationships that could be construed as a potential conflict of interest.

frontiers in Cell and Developmental Biology

REVIEW
published: 20 May 2021
doi: 10.3389/fcell.2021.653828

Endoplasmic Reticulum–Mitochondria Contact Sites—Emerging Intracellular Signaling Hubs

*Saeko Aoyama-Ishiwatari[1] and Yusuke Hirabayashi[2]**

[1] Graduate School of Pharmaceutical Sciences, The University of Tokyo, Tokyo, Japan, [2] Department of Chemistry and Biotechnology, School of Engineering, The University of Tokyo, Tokyo, Japan

It has become apparent that our textbook illustration of singular isolated organelles is obsolete. In reality, organelles form complex cooperative networks involving various types of organelles. Light microscopic and ultrastructural studies have revealed that mitochondria–endoplasmic reticulum (ER) contact sites (MERCSs) are abundant in various tissues and cell types. Indeed, MERCSs have been proposed to play critical roles in various biochemical and signaling functions such as Ca^{2+} homeostasis, lipid transfer, and regulation of organelle dynamics. While numerous proteins involved in these MERCS-dependent functions have been reported, how they coordinate and cooperate with each other has not yet been elucidated. In this review, we summarize the functions of mammalian proteins that localize at MERCSs and regulate their formation. We also discuss potential roles of the MERCS proteins in regulating multiple organelle contacts.

Keywords: mitochondria, ER, organelle contact sites, mammalian protein, tether

OPEN ACCESS

Edited by:
Yasunori Saheki,
Nanyang Technological University, Singapore

Reviewed by:
Julien Prudent,
University of Cambridge, United Kingdom
Jaakko Saraste,
University of Bergen, Norway

****Correspondence:***
Yusuke Hirabayashi
hirabayashi@chembio.t.u-tokyo.ac.jp

Specialty section:
This article was submitted to Membrane Traffic, a section of the journal Frontiers in Cell and Developmental Biology

Received: *15 January 2021*
Accepted: *06 April 2021*
Published: *20 May 2021*

Citation:
Aoyama-Ishiwatari S and Hirabayashi Y (2021) Endoplasmic Reticulum–Mitochondria Contact Sites—Emerging Intracellular Signaling Hubs. Front. Cell Dev. Biol. 9:653828. doi: 10.3389/fcell.2021.653828

INTRODUCTION

Electron microscopy (EM) studies have revealed that a significant portion of membranes from a variety of organelles are closely apposed but do not fuse. Among the membrane appositions within the range of 10–30 nm, membrane contact sites (MCSs) have been defined by the presence of proteins tethering two organelles (Scorrano et al., 2019). In recent years, it has become rapidly apparent that MCSs serve as unique intracellular platforms regulating a wide range of biochemical reactions. The mitochondria–endoplasmic reticulum (ER) contact sites (MERCSs) are the most frequently observed MCSs in many cell types, and extensive studies have revealed that MERCSs are hubs for the exchange of metabolites (Valm et al., 2017). For instance, the mitochondrial calcium uniporter (MCU) protein is activated only when the MCU complex is exposed to a high concentration of Ca^{2+} rarely reached in the cytoplasm of most cell types (1–5 μM depending on the components of the MCU complex) (Csordás et al., 2013; Patron et al., 2014; Petrungaro et al., 2015). These channel properties necessitate that the mitochondrial surface be very closely apposed to the ER surface, where Ca^{2+} is released from either inositol 1,4,5-trisphosphate (IP3) receptors (IP3Rs) and/or ryanodine receptors (RyRs) (Rizzuto et al., 1993; Cremer et al., 2020). Furthermore, lipid exchange between the ER and mitochondria is required for the coordinated synthesis of glycerophospholipids by lipid biosynthetic enzymes that localize at either the ER membrane (ERM) or the mitochondrial matrix. In the absence of vesicular transport between these organelles, transfer of intermediate lipid molecules relies on non-vesicular lipid transfer at

contact sites (Vance, 1990; Petrungaro and Kornmann, 2019). In addition, MERCSs have been suggested to define sites of mitochondrial division and mitochondrial DNA (mtDNA) replication (Friedman et al., 2011; Murley et al., 2013; Lewis et al., 2016) as well as mitochondrial fusion (Guo et al., 2018; Abrisch et al., 2020). They also provide a platform for autophagosome biogenesis (Hailey et al., 2010; Hamasaki et al., 2013; Garofalo et al., 2016; Böckler and Westermann, 2014; Wu et al., 2016; Gomez-Suaga et al., 2017). In order to regulate this wide variety of functions at MERCSs, various protein complexes are specifically recruited and dynamically maintained at these unique contact sites.

In yeast, a protein complex called the ER–mitochondria encounter structure (ERMES) was identified as a molecular zipper bridging the ER and mitochondria (Kornmann et al., 2009). The ERMES complex consists of four core proteins: an ER-anchored maintenance of mitochondrial morphology 1 (Mmm1), mitochondrial distribution and morphology 10 (Mdm10) localized to the outer membrane of mitochondria (OMM), Mdm34 (Mmm2), and cytosolic Mdm12. The protein–protein interactions among these core components generate the tethering force between these two organelles. A few ERMES complex binding proteins such as a Ca^{2+}-binding GTPase Gem1 (Kornmann et al., 2011; Stroud et al., 2011; Nguyen et al., 2012) and Mdm10 binding translocase of outer membrane 7 (Tom7) (Meisinger et al., 2006; Yamano et al., 2010; Becker et al., 2011; Ellenrieder et al., 2016) have been identified as the auxiliary subunits of ERMES complex. Gem1 is required for MERCS formation (Kornmann et al., 2011), whereas the function of Tom7 in regulating MERCSs is unclear.

Like Tom7, the sorting and assembly machinery (SAM) complex, which is responsible for the membrane insertion of mitochondrial outer membrane proteins, interacts with the β-barrel structure of Mdm10 at the opposite side of Mdm12 binding site (Ellenrieder et al., 2016). Given the competition between the ERMES and SAM complexes for Mdm10 binding, it is possible that MERCS formation and mitochondrial protein import are interrelated. Mmm1, Mdm12, and Mdm34 contain synaptotagmin-like mitochondrial lipid-binding protein (SMP) domains, which are homologous to the structurally well-characterized tubular lipid binding protein (TULIP) domain present in many lipid-binding proteins (I. Lee and Hong, 2006; Kopec et al., 2010). Structural analyses have shown that the SMP domain-containing proteins interact with a wide variety of glycerophospholipids (Schauder et al., 2014; AhYoung et al., 2015; Jeong et al., 2016, 2017). Thus, it has been hypothesized that ERMES might be a candidate in non-vesicular transfer of lipids between ER and mitochondria.

Likewise, characterizing the molecules responsible for MERCS formation in other eukaryotic cell types including multicellular organisms has been of great interest for a decade, which leads to the identification of proteins regulating this contact formation (**Figure 1** and **Table 1**). The large variety of proteins identified indicates that the regulation of MERCSs in mammals is more complicated than in yeast. However, the coordination and dynamics of these protein complexes remain unclear and sometimes debated.

MITOCHONDRIA-ENDOPLASMIC RETICULUM CONTACT SITE-RESIDENT PROTEINS INVOLVED IN THE CONTACT FORMATION

Yeast Endoplasmic Reticulum–Mitochondria Encounter Structure Complex and Functional Mammalian Homologs

Several orthologs of the ERMES complex proteins have been identified in metazoans, although until recently, only those of regulatory subunits of the complex were known. In mammals, mitochondria-localized GTPase family members Ras homolog family member T1 (RHOT1, also known as Miro1) and RHOT2 (Miro2) are identified as orthologs of Gem1. Confocal microscopy analysis in mouse embryonic fibroblasts (MEFs) showed that RHOT1 and RHOT2 double-knockout (DKO) resulted in the reduction of Mander's coefficient between ER- and mitochondria-localized fluorescent proteins, as well as a slight decrease in the number of MERCSs identified by transmission EM (TEM) (Modi et al., 2019). Recruitment of RHOT1 to MERCS is promoted by its phosphorylation. Blocking the phosphorylation *via* a polo-like kinase 1 (PLK1) inhibitor reduced the interaction between voltage-dependent anion channel (VDAC) and IP3R, which tether the ER and mitochondria (see below) (S. Lee et al., 2016). It seems that the Tom7–SAM complex is conserved in mammals as a mitochondrial protein transport machinery; however, it remains unknown whether it is involved in MERCS formation.

Compared to the auxiliary subunits, orthologs of the core ERMES complex proteins had not been identified in metazoans because of low levels of conservation in the primary amino acid sequences. However, we recently identified the SMP domain-containing ER-resident protein called PDZ domain-containing protein 8 (PDZD8) as a functional homolog of yeast Mmm1 (Hirabayashi et al., 2017).

Mammalian Regulators of Mitochondria–Endoplasmic Reticulum Contact Sites

The recent development of the automatic Serial Scanning EM (SSEM) enabled us to visualize the three-dimensional (3D) structures of MERCSs. This technique unequivocally demonstrated that the aforementioned MMM1 homolog PDZD8 is required for MERCS formation in human HeLa cells without any effects on the 3D architecture of ER and mitochondria. Furthermore, dual-color Ca^{2+} imaging showed that ER–mitochondria tethering mediated by PDZD8 is essential for Ca^{2+} flux from the ER to the mitochondria in NIH3T3 cells and in mouse cortical pyramidal neurons (Hirabayashi et al., 2017). A recent *in vitro* assay suggested that SMP and PDZ domains of PDZD8 extract glycerophospholipids and ceramides, as well as cholesterol, albeit with low efficiency (Shirane et al., 2020). Thus, PDZD8 is potentially capable of transferring lipids in MCSs.

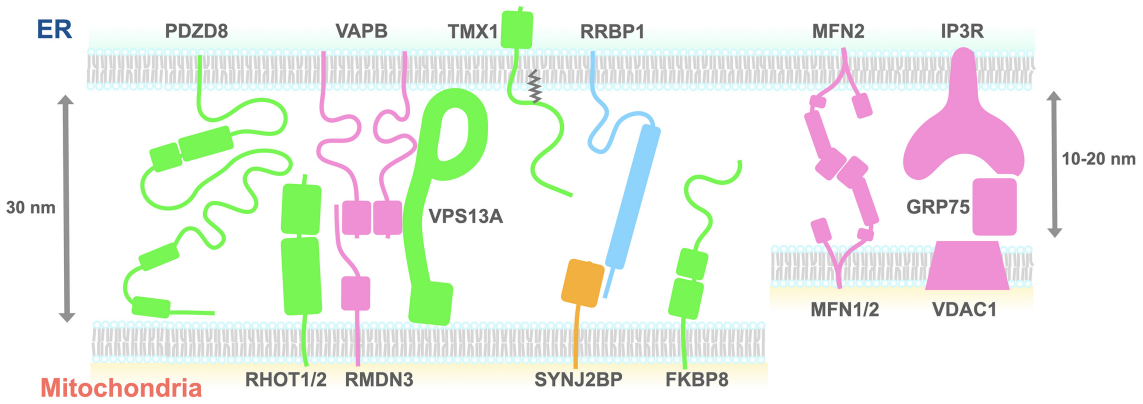

FIGURE 1 | A schematic diagram of the proteins proposed to tether the ER and mitochondria. The size of each domain structure was either calculated from the structures deposited on the Protein Data Bank or estimated using the Phyre2 protein structure prediction tool. Proteins shown to be necessary (green, pink) or sufficient (yellow) for tethering the ER and mitochondria are depicted. Green indicates that tethering partners of the proteins remain to be determined. Light blue indicates that roles of the proteins need to be determined. ER, endoplasmic reticulum; FKBP8, FK506-binding protein 8; IP3R, inositol 1,4,5-trisphosphate receptor; Mfn2, mitofusin 2; PDZD8, PDZ domain-containing protein 8; RHOT1, Ras homolog family member T1; GRP75, glucose-regulated protein 75; RMDN3, regulator of microtubule dynamics protein 3; RRBP1, ribosome-binding protein 1; SYNJ2BP, synaptojanin-2-binding protein; TMX1, thioredoxin-related transmembrane protein 1; VAPB, VAMP-associated protein B; VPS13A, vacuolar protein sorting-associated protein 13 A; VDAC, voltage-dependent anion channel.

Further studies are required to reveal the mitochondrial binding partner of PDZD8.

Mitochondria fusion protein mitofusin 2 (Mfn2) is the most intensively studied yet controversial ER–mitochondria tethering protein. It has been proposed that ER-localized Mfn2 engages in homotypic and heterotypic complexes with OMM localizing Mfn2 or Mnf1, respectively (De Brito and Scorrano, 2008). However, the role of Mfn2 complex in MERCS formation has been under intense debate (Filadi et al., 2018). Indeed, a recent study using split green fluorescent protein (GFP)-based contact site sensors (SPLICSs) showed that Mfn2 depletion increased and decreased the number of ER–mitochondria contact sites detected by SPLICS having spacers corresponding to short (8–10 nm) and long (40–50 nm) membrane distances, respectively (Cieri et al., 2018). Considering that the loss of Mfn1/2 complex increased the average distance between the two membranes at MERCSs only to 18 nm (De Brito and Scorrano, 2008), it is possible that the Mfn complex fine-tunes the membrane distance at MERCSs. It remains to be elucidated in what context and how Mfn2 controls MERCSs, as well as if it is related to its role in OMM fusion.

Consistent with the observation that mitochondrial fission occurs at MERCSs, the mitochondrial fission protein 1 (Fis1) is proposed to reside at MERCSs *via* the interaction with an ER-resident protein B-cell receptor-associated protein 31 (BAP31) (Iwasawa et al., 2011), although it remains uninvestigated whether the complex impacts MERCS formation. Also, the mitochondrial fission GTPase dynamin-related protein 1 (Drp1) has been shown to functionally stabilize MERCSs through mitochondrial E3 ubiquitin protein ligase 1 (Mul1, also known as MAPL)-dependent SUMOylation (Prudent et al., 2015).

The OMM-localized protein Spire1C, one of the splicing isoforms of Spire1, is yet another protein regulating mitochondrial fission at MERCSs. Spire1C interacts with the ER-localized isoform of Inverted formin 2 (INF2) *via* its kinase non-catalytic C-lobe domain (KIND) (Manor et al., 2015). The overexpression of KIND-deleted Spire1C decreased the overlap between the ER and mitochondria as identified by immunofluorescence imaging in light microscopy.

The yeast two-hybrid screening identified VDAC1–glucose-regulated protein (GRP)75–IP3R complex as a linker between the ER and mitochondria (Szabadkai et al., 2006). The OMM channel VDAC1 mediates Ca^{2+} channeling from microdomains with high Ca^{2+} concentration generated by the opening of the ER-resident Ca^{2+}-release channel IP3Rs to the intermembrane space (Gincel et al., 2001; Rapizzi et al., 2002). IP3R2 is reported to interact not only with VDAC but also with the OMM-localized protein FUN14 domain-containing protein 1 (FUNDC1) at least in cardiac myocytes (S. Wu et al., 2017). Grp75 is a cytosolic regulator of the IP3R–VDAC complex that promotes the interaction between the channels to increase the efficiency of mitochondrial Ca^{2+} uptake (Szabadkai et al., 2006). The interaction between Grp75 and a MERCS-localized protein transglutaminase type 2 (TG2) has also been suggested to contribute to MERCS formation (D'Eletto et al., 2018). Inferred from the 3D structure of each protein, the size of VDAC1–GRP75–IP3R complex is around 15 nm. Given that the triple-KO (TKO) of IP3R isoforms decreased more specifically the tight contact sites where the two membranes are less than 20 nm apart (Bartok et al., 2019), it is likely that this complex brings the ER and mitochondria in particularly close proximity. Tom70 was also reported to interact with IP3R3 to recruit it to the proximity of mitochondria, which results in promoting Ca^{2+} transfer from the ER to mitochondria (Filadi et al., 2018).

Another protein complex identified by the yeast two-hybrid screening is the VAMP-associated protein B (VAPB)–regulator of microtubule dynamics protein 3 (RMDN3, also called PTPIP51) complex (De vos et al., 2012). The quantification of the single-plane TEM images revealed that depletion of either VAPB

TABLE 1 | List of MERCS-Regulating Proteins.

Gene Name	Localization	How to assess the roles in MERCS formation	Interactors	Other Roles	Evolutionary conservation	References
ATAD3A	Mitochondria (IMM, OMM)		-	Steroidogenesis, Cholesterol homeostasis, Cristae structure maintenance		Baudier, 2018; Issop et al., 2015
BAP31	ER		Fis1	Proapoptotic		Iwasawa et al., 2011
CISD2	Mitochondria (OMM), ER	TEM, Immunofluorescence, Ca^{2+} transfer (in WFS2-patient-derived cells) (Rouzier et al., 2017)	GIMAP5	Wolfram syndrome type 2 (WFS2)-related gene		Wang et al., 2014; Rouzier et al., 2017
CKAP4	ER	TEM, Split-GFP, Ca^{2+} transfer	VDAC2			Harada et al., 2020
Drp1	Cytoplasm, Mitochondria (OMM)	Immunofluorescence, Ca^{2+} transfer (in Mul1-deficient cells) (Prudent et al., 2015)		Mitochondrial fission		Prudent et al., 2015
EMC	ER	TEM (in yeast)	SLC25A46?	Transmembrane helix insertase	Conserved from yeast	Lahiri et al., 2014
EMD (Emerin)	Nucleus, ER		FATE1	Causal gene of Emery–Dreifuss muscular dystrophy		Doghman-Bouguerra et al., 2016
FATE1	Mitochondria (OMM), Mitochondria-associated membrane (MAM)	TEM, Immunofluorescence, Ca^{2+} transfer	EMD/Emerin?	Antiapoptotic		Doghman-Bouguerra et al., 2016
Fis1	Mitochondria (OMM)		BAP31	Mitochondrial fission, Proapoptotic		Iwasawa et al., 2011
FKBP8	Mitochondria (OMM), ER	TEM, Ca^{2+} transfer	Unknown	Antiapoptotic, Mitophagy		Kwak et al., 2020
FUNDC1	Mitochondria (OMM)	TEM (Wu et al., 2017)	IP3R2, Calnexin (under hypoxia)	Mitophagy, Mitochondrial fission, Ca^{2+} regulation		Wu et al., 2016; Wu et al., 2017
GIMAP5	MAM, ER?		CISD2			Wang et al., 2014
Gp78 (AMFR)	ER	TEM, Immunofluorescence	Mfn1/2 (ubiquitination)	E3 ubiquitin ligase, ER-associated protein degradation		Wang et al., 2015
GRP75	Cytoplasm (MAM)	Ca^{2+} transfer	IP3R, VDAC1			Szabadkai et al., 2006
INF2	ER	Immunofluorescence	Spire1C	Actin polymerization		Manor et al., 2015
IP3R	ER	TEM (Bartok et al., 2019)	Grp75	Ca^{2+} transport		Szabadkai et al., 2006; Bartok et al., 2019
Mfn1	Mitochondria (OMM)		Mfn2	Mitochondrial fusion		De Brito and Scorrano, 2008
Mfn2	Mitochondria (OMM), ER	Ca^{2+} transfer (De Brito and Scorrano, 2008) TEM (Cosson et al., 2012; Filadi et al., 2015; Naon et al., 2016)	Mfn2, Mfn1	Mitochondrial fusion		De Brito and Scorrano, 2008; Cosson et al., 2012; Filadi et al., 2018
Miga2	Mitochondria (OMM)	TEM (in fly) (Xu et al., 2020)	VAPA, VAPB	Mitochondrial fusion		Freyre et al., 2019; Xu et al., 2020
MITOL (MARCH5)	MAM, Mitochondria	Immunofluorescence, *In vitro* ER-mitochondria binding assay, Ca^{2+} transfer (Sugiura et al., 2013) SBF-SEM (Nagashima et al., 2019)	Mfn2 (ubiquitination)	E3 ubiquitin ligase		Sugiura et al., 2013; Nagashima et al., 2019
Mul1 (MAPL)	Mitochondria	Immunofluorescence, Ca^{2+} transfer (Prudent et al., 2015) TEM, Immunofluorescence in stimulated emission depletion microscopy (STED) (Puri et al., 2019)	Mfn2 (ubiquitination), Drp1 (SUMOlylation)	E3 ubiquitin ligase		Prudent et al., 2015; Puri et al., 2019
PDZD8	ER (partially MAM)	Serial SEM, Ca^{2+} transfer,	Unknown	Resident in ER-late endosome/lysosome contacts	Potential Ortholog (Paralog) of MMM1	Hirabayashi et al., 2017
PS2	ER	Immunofluorescence, Ca^{2+} transfer	Mfn2	Causally linked to familial Alzheimer's disease (FAD)		Filadi et al., 2016
Reep1	ER, Mitochondria	Split-RLuc8 assay (in Reep1-overexpressing cells)	Unknown	Hereditary spastic paraplegias (HSPs)-associated gene		Lim et al., 2015

(Continued)

TABLE 1 | Continued

Gene Name	Localization	How to assess the roles in MERCS formation	Interactors	Other Roles	Evolutionary conservation	References
RHOT1/2 (MIRO1/2)	Mitochondria (OMM)	TEM, Immunofluorescence, Ca^{2+} transfer (Modi et al., 2019)	IP3R?	Mitochondrial motility (Microtubule binding)	GEM1 in yeast	Kornmann et al., 2011; S. Lee et al., 2016; Modi et al., 2019;
RMDN3 (PTPIP51)	Mitochondria (OMM)	Ca^{2+} transfer (De vos et al., 2012) TEM, Immunofluorescence (Stoica et al., 2014)	VAPB			De vos et al., 2012; Stoica et al., 2014; Gomez-Suaga et al., 2017; Fecher et al., 2019
RRBP1	ER	TEM (Anastasia et al., 2021)	SYNJ2BP	Kinesin binding		Hung et al., 2017; Anastasia et al., 2021
SLC25A46	Mitochondria (OMM)		EMC component?	Phospholipid exchange		Janer et al., 2016
Spire1C	Mitochondria (OMM)	Immunofluorescence	INF2	Actin nucleation		Manor et al., 2015
SYNJ2BP	Mitochondria (OMM)	TEM (in SYNJ2BP-overexpressing cells)	RRBP1	Negative regulator of angiogenesis, tumor growth and metastasis		Hung et al., 2017
Tom70	Mitochondria (OMM)	SPLICS, Immunofluorescence, Ca^{2+} transfer	IP3R3	Translocase of OMM		Filadi et al., 2018
VAPB	ER	Ca^{2+} transfer (De vos et al., 2012) TEM, Immunofluorescence (Stoica et al., 2014)	RMDN3	Resident in ER–endosome contacts, ER–golgi contacts and ER–PM contacts		De vos et al., 2012; Stoica et al., 2014; Freyre et al., 2019; Xu et al., 2020
VDAC1	Mitochondria (OMM)	TEM (Bosc et al., 2020)	GRP75	Ca^{2+} transport		Szabadkai et al., 2006; Bosc et al., 2020
VDAC2	Mitochondria (OMM)		CKAP4	Ca^{2+} transport		Harada et al., 2020
VPS13A	MAM	TEM (Muñoz-Braceras et al., 2019) Immunofluorescence (Kumar et al., 2018) SPLICS (Yeshaw et al., 2019)	VAPA, VAPB	Autophagy regulation, Lipid droplet motility		Kumar et al., 2018; Muñoz-Braceras et al., 2019; Yeshaw et al., 2019.
TMX1	ER, MAM (palmitoylated)	TEM, Ca^{2+} transfer	Unknown			Raturi et al., 2016
TG2	Cytoplasm (MAM)	TEM, Proximity ligation assay, Immunofluorescence	GRP75	Posttranslational modification		D'Eletto et al., 2018

ATAD3A, ATPase family AAA domain-containing protein 3A; BAP31, B-cell receptor-associated protein 31; CISD2, CDGSH iron-sulfur domain-containing protein 2; CKAP4, cytoskeleton-associated protein 4; Drp1, dynamin-related protein 1; EMC, endoplasmic reticulum membrane protein complex; ER, endoplasmic reticulum; FATE1, fetal and adult testis-expressed transcript protein; Fis1, fission protein 1; FKBP8, FK506-binding protein 8; FUNDC1, FUN14 domain-containing protein 1; GIMAP5, GTPase immunity-associated protein family member 5; GRP75, glucose-regulated protein 75; IMM, inner mitochondrial membrane; INF2, Inverted formin 2; IP3R, inositol 1,4,5-trisphosphate receptor; MAM, mitochondria-associated membrane; MERCS, mitochondria–endoplasmic reticulum contact site; Mfn2, mitofusin 2; Miga2, mitoguardin 2; MITOL, Mitochondrial ubiquitin ligase; Mul1, mitochondrial ubiquitin protein ligase 1; Mul1, mitochondrial E3 ubiquitin protein ligase 1; OMM, outer membrane of mitochondria; PDZD8, PDZ domain-containing protein 8; PM, plasma membrane; PS2, presenilin 2; Reep1, receptor expression-enhancing protein 1; RHOT1, Ras homolog family member T1; RMDN3, regulator of microtubule dynamics protein 3; RRBP1, ribosome-binding protein 1; SLC25A46, solute carrier family 25 member 46; SPLICS, split GFP-based contact site sensors; SYNJ2BP, synaptojanin-2-binding protein; TEM, transmission electron microscopy; TG2, transglutaminase type 2; TMX1, thioredoxin-related transmembrane protein 1; TMX1, transmembrane protein 1; Tom7, translocase of outer membrane 7; VAPB, VAMP-associated protein B; VDAC, voltage-dependent anion channel; VPS13A, vacuolar protein sorting-associated protein 13 A.

or RMDN3 reduced MERCSs in human HEK293 cells (Stoica et al., 2014). The role of RMDN3 in MERCS formation was also shown in cerebellar Purkinje cells (Fecher et al., 2019). Knocking down either VAPB or RMDN3 caused a significant delay but only slight decrease in the mitochondrial Ca^{2+} uptake (De vos et al., 2012) and stimulated the induction of autophagy flux (Gomez-Suaga et al., 2017). Recently, the OMM protein mitoguardin 2 (Miga2) was also reported to interact with VAPA and VAPB (Freyre et al., 2019) and proposed to increase MERCS formation at least in flies (Xu et al., 2020). VAP-interacting protein vacuolar protein sorting-associated protein 13 A (VPS13A) has also been reported to localize to MERCSs and participate in their stabilization (Kumar et al., 2018; Muñoz-Braceras et al., 2019; Yeshaw et al., 2019). Interestingly, a recent study showed that RMDN3 recruits the oxysterol-binding protein (OSBP)-related proteins ORP5 and ORP8, which transfer phosphatidylinositol (PI) and phosphatidylserine (PS) at ER–plasma membrane (PM) contact sites (Chung et al., 2015; Moser von Filseck et al., 2015), to MERCSs (Galmes et al., 2016). Consistent with that, ORP5 and ORP8 are proposed to mediate PS transport, likely *via* the non-vesicular lipid transfer, at MERCSs (Rochin et al., 2019).

The OMM-localized fetal and adult testis-expressed transcript protein (FATE1) known as an antiapoptotic protein may also contribute to ER–mitochondria tethering. Overexpression of FATE1 partly decreased MERCSs as identified by TEM and confocal microscopy and also reduced Ca^{2+} uptake by

mitochondria (Doghman-Bouguerra et al., 2016). EMD/Emerin is a potential interactor of FATE1 in the ER; however, the role of EMD in MERCS formation has not been investigated.

Posttranslational palmitoylation is found in several proteins localizing at MERCSs. The heterozygous KO of the redox-sensitive oxidoreductase thioredoxin-related transmembrane protein 1 (TMX1) decreased the average length of MERCSs as analyzed by TEM (Raturi et al., 2016). Importantly, the recruitment of TMX1 to MERCSs requires palmitoylation at the cytosolic domain (Roth et al., 2009; Lynes et al., 2012; **Figure 1**). Recruitment of the ER chaperone calnexin to MERCSs also requires palmitoylation (Lynes et al., 2012). While the palmitoylation of TMX1 is required for proper Ca^{2+} uptake from the ER to mitochondria, the ER-resident protein cytoskeleton-associated protein 4 (CKAP4) requires palmitoylation for sequestering VDAC2 from IP3R, which results in a decrease of MERCSs (Harada et al., 2020).

A proteomic analysis of the intersection between OMM and ERM-resident proteins obtained from ascorbate peroxidase (APEX)-mediated proximity biotinylation and subsequent mass spectrometry (MS) analysis identified the synaptojanin-2-binding protein (SYNJ2BP)–ribosome-binding protein 1 (RRBP1) complex as a potential tether that specifically regulates mitochondria–rough ER contact sites (Hung et al., 2017). TEM analysis showed that SYNJ2BP overexpression increased contacts between mitochondria and rough ER but not between mitochondria and smooth ER. In line with this, a recent report showed that RRBP1 is resident in mitochondria–rough ER contacts in mouse liver and works as a regulator of these contacts (Anastasia et al., 2021). The list of proteins identified in the intersection confirmed the localization of known MERCS proteins, even though many MERCS proteins, such as PDZD8, VAPs, and IP3Rs, listed in both ERM and OMM proteins are excluded from the intersection list because they also localized outside of MERCSs.

Recently, two split-pair proximity labeling enzymes, Contact-ID and Split-TurboID, were applied for the direct mapping of proteins localizing at MERCSs (Cho et al., 2020; Kwak et al., 2020). Although these methods are less sensitive than other methods, proteins identified with these methods are reliably localized to MERCS. Contact-ID identified FK506-binding protein 8 (FKBP8) as a novel MERCS-localizing protein. Indeed, knocking down FKBP8 reduces MERCSs in the TEM analysis and also diminishes mitochondrial Ca^{2+} uptake (Kwak et al., 2020).

Disease Association of Mitochondria–Endoplasmic Reticulum Contact Site Proteins

Genome-wide association studies have identified numerous gene mutations associated with neurological diseases. Among those, a significant number of mutations are found in genes related to MERCS formation, such as Mfn2, receptor expression-enhancing protein 1 (Reep1), solute carrier family 25 member 46 (SLC25A46), ATPase family AAA domain-containing protein 3A (ATAD3A), and CDGSH iron-sulfur domain-containing protein 2 (CISD2). Mutations in a genomic region coding an ER-resident protein Reep1 is associated with hereditary spastic paraplegias (HSPs) and distal hereditary motor neuropathy. A split-Renilla Luciferase 8 (RLuc8) reassembly assay suggested that Reep1 facilitates MERCS formation (Lim et al., 2015). The disease-associated *Reep1* mutations impair REEP1's ability to facilitate MERCSs, implying the relationship between HSP pathology and Reep1 function in MERCS formation (Lim et al., 2015).

A recent study using fibroblasts obtained from a patient suffering from Leigh syndrome identified a homozygous missense mutation in the genomic region coding for the mitochondrial protein SLC25A46. The study also proposed that SLC25A46 interacts with the conserved ER membrane protein complex (EMC) at MERCSs (Janer et al., 2016). Interestingly, EMC is suggested to be involved in MERCS formation in yeast (Lahiri et al., 2014). Moreover, it was shown that loss of SLC25A46 altered mitochondrial phospholipid composition, implying that SLC25A46 also plays a role in promoting lipid transfer at MERCSs (Janer et al., 2016). Further studies are still required to elucidate the function of SLC25A46 and EMC in MERCS formation in mammalian cells.

Another disease-associated gene, the inner mitochondrial membrane (IMM)-localized protein ATAD3A, has also been proposed to participate in MERCS formation (Issop et al., 2015; Baudier, 2018). Although the exact structure of ATAD3A remains unknown, a recent report proposed that the N-terminus of ATAD3A may insert into the OMM and associate with the ER (Issop et al., 2015). Thereby, ATAD3A may regulate the interactions among the IMM, OMM, and ERM.

Finally, another disease-related gene coding for a MERCS-regulating protein is CISD2, which is a causative gene associated with Wolfram syndrome. A recent study showed that MERCS formation and Ca^{2+} uptake in mitochondria are upregulated in patient-derived fibroblasts (Rouzier et al., 2017). In mouse white adipose tissues and fibroblasts, CISD2 is proposed to interact with GTPase immunity-associated protein (IMAP) family member 5 (GIMAP5) at MERCSs and modulates mitochondrial Ca^{2+} uptake (C. H. Wang et al., 2014).

MITOCHONDRIA–ENDOPLASMIC RETICULUM CONTACT SITE PROTEINS AT OTHER ORGANELLE CONTACT SITES

The recent development of high-speed super-resolution microscopy revealed that the ER contacts various organelles (Valm et al., 2017). Interestingly, some of the MERCSs regulating ER-resident proteins are also found at other organelle contact sites, which implies that those proteins mediate crosstalk among multiple types of organelle contacts.

A major common function of the membrane contact sites is non-vesicular lipid transfer. In this regard, VAPA and VAPB play essential roles in diverse contact sites by transferring phospholipids and ceramides. VAP proteins interact with FFAT motifs of protein partners located on the opposing membrane or the ERM (H. Wu et al., 2018). Besides RMDN3 (PTPIP51) at MERCSs, VAP proteins form complexes with proteins such as Nir2, ceramide transferase 1 (CERT), and

OSBP at the ER–Golgi contacts, and OSBP, StAR-related lipid transfer protein 3 (STARD3), Protrudin, and ORP1L at the ER–endolysosome contacts.

As mentioned above, ORP5 and ORP8, which promote the exchange of PI and PS at EM–PM contacts, also localize to MERCSs (Galmes et al., 2016). Further ORP5 is suggested to localize to ER–lipid droplet contacts and regulates the exchange of phosphatidylinositol-4-phosphate (PI4P) and PS at these contacts (Du et al., 2020).

Another example of a lipid-binding MERCS protein found in other organelle contact sites is PDZD8. Although it is still controversial if PDZD8 localizes to lysosomal-associated membrane protein 1 (LAMP1)-positive lysosomes, overexpressed PDZD8 directly interacts with Protrudin and GTP-bound Rab7, both of which localize to late endosomes (Guillén-Samander et al., 2019; Elbaz-Alon et al., 2020; Shirane et al., 2020). Interestingly, overexpressed PDZD8 and Rab7 colocalize at the three-way junction of ER, endosomes, and mitochondria, thereby inducing the association of the endosome and mitochondria. Furthermore, a recent study indicates that PDZD8 participates in the VAP complex (Cabukusta et al., 2020), which implies PDZD8's roles in multiple different organelle contact sites. Since overexpression of MERCS proteins can disrupt their localization and therefore their functions, future studies will need to elucidate the location of *endogenous* PDZD8 among those contact sites. This statement is true for most proteins studied at MERCSs. The rapid development of clustered regularly interspaced short palindromic repeats (CRISPR)-Cas9-mediated knockin strategies (as used for PDZD8 in Hirabayashi et al., 2017) in various cell types will be a key step in cell biology of MERCS protein complexes.

VPS13A is yet another lipid-binding MERCS protein that localizes to additional MCSs. Yeast Vps13 resides at mitochondria–vacuole contacts (vacuole and mitochondria patches; v-CLAMPs) and ER–vacuole contacts (nuclear–vacuole junction; NVJ) and has a redundant role with the ERMES complex. It has been hypothesized that Vps13 creates an alternative lipid transport route between the ER and mitochondria through other organelles (Lang et al., 2015; Petrungaro and Kornmann, 2019). Consistent with this idea, the mammalian orthologs of Vps13, VPS13A, and VPS13C, have been reported to possess the ability to transfer glycerophospholipids between membranes *in vitro* (Kumar et al., 2018). Furthermore, VPS13A has been reported to localize at mitochondria–endosome/lysosome contacts and ER–lipid droplet contacts as well as MERCSs, whereas VPS13C is distributed to ER–endosome contacts and ER–lipid droplet contacts, loss of which causes mitochondrial dysfunction (Lesage et al., 2016; Kumar et al., 2018). These reports imply the function of VPS13 family proteins in lipid transport at multiple MCSs, although they also play distinct roles at each contact site, such as MERCS formation, autophagy induction, and regulation of lipid droplet motility (Muñoz-Braceras et al., 2015, 2019; Kumar et al., 2018; Yeshaw et al., 2019). Since both VPS13A and VPS13C are recruited to the ER *via* the FFAT motif (Kumar et al., 2018; Yeshaw et al., 2019), it is plausible that their localization at ER–other organelle contacts might be regulated through the interaction with VAPs. It also has been shown that VPS13A interacts with Rab7 (Muñoz-Braceras et al., 2019), which may result in VPS13A's recruitment to mitochondria–endosome contacts.

Mitochondria also form contact sites with organelles other than the ER. Several MERCS-localized mitochondrial proteins have also been reported to reside at other organelle contact sites. Mfn2 localizes at the contact sites between mitochondria and the lysosome-related organelle of pigment cells melanosome (Daniele et al., 2014). Considering that Fzo1, a yeast homolog of Mfn, is suggested to reside at mitochondria–peroxisome contacts (Shai et al., 2018), Mfns might participate in the contact formation between mitochondria and other various organelles. The mitochondria–lysosome contacts mark at the site of mitochondrial fission. At this fission site, Fis1 recruits the Rab7 GTPase-activating protein TBC1 domain family member 15 (TBC1D15), which results in untethering of the contacts (Wong et al., 2018). This suggests that Fis1 localizes at the mitochondria–lysosome contact sites, as well as at MERCSs.

CONCLUSION

In recent years, owing to advances in microscopy and the development of new biochemical tools, the list of proteins involved in the regulation of MERCSs has been dramatically expanded. Given that PDZD8 remains the only identified mammalian ortholog of the ERMES core subunits (Mmm1), it is conceivable that the mammalian ER and mitochondria tethering protein complexes have not directly evolved from the yeast ERMES complex. Therefore, MERCSs might have evolved various cell type-specific roles in mammals, which are just beginning to be explored. Provided that the properties of MERCS proteins, such as domain structure, size, and localization, are quite diverse, it is plausible to assume that they work at different subdomains of MERCSs, different steps of MERCS formation, or in different cell types. This complex regulation of MERCSs might be required for the precise control of biochemical reactions in response to the various cellular demands unique to each cell type. Since many MERCS proteins also reside at other organelle contact sites, investigation of the dynamic localization of endogenous, as opposed to overexpressed, proteins in a variety of cellular contexts will improve our understanding of the complex spatiotemporal regulation of MERCSs and pave the way to reveal the physiological roles of these contact sites.

AUTHOR CONTRIBUTIONS

Both authors wrote the manuscript. Both authors contributed to the article and approved the submitted version.

ACKNOWLEDGMENTS

We apologize to the many scientists whose work we were not able to credit owing to space restrictions. We thank Drs. Franck Polleux and Heike Blockus for comments on the manuscript.

REFERENCES

Abrisch, R. G., Gumbin, S. C., Wisniewski, B. T., Lackner, L. L., and Voeltz, G. K. (2020). Fission and fusion machineries converge at ER contact sites to regulate mitochondrial morphology. *J. Cell Biol.* 219:e201911122. doi: 10.1083/jcb.201911122

AhYoung, A. P., Jiang, J., Zhang, J., Dang, X. K., Loo, J. A., Zhou, Z. H., et al. (2015). Conserved SMP domains of the ERMES complex bind phospholipids and mediate tether assembly. *Proc. Natl. Acad. Sci. U S A.* 112, E3179–E3188. doi: 10.1073/pnas.1422363112

Anastasia, I., Ilacqua, N., Raimondi, A., Lemieux, P., Ghandehari-Alavijeh, R., Faure, G., et al. (2021). Mitochondria-rough-er contacts in the liver regulate systemic lipid homeostasis. *Cell Rep.* 34:108873. doi: 10.1016/j.celrep.2021.108873

Bartok, A., Weaver, D., Golenár, T., Nichtova, Z., Katona, M., Bánsághi, S., et al. (2019). IP3 receptor isoforms differently regulate ER-mitochondrial contacts and local calcium transfer. *Nat. Commun.* 10:3726. doi: 10.1038/s41467-019-11646-3

Baudier, J. (2018). ATAD3 proteins: brokers of a mitochondria-endoplasmic reticulum connection in mammalian cells. *Biol. Rev.* 93, 827–844. doi: 10.1111/brv.12373

Becker, T., Wenz, L. S., Thornton, N., Stroud, D., Meisinger, C., Wiedemann, N., et al. (2011). Biogenesis of mitochondria: dual role of Tom7 in modulating assembly of the preprotein translocase of the outer membrane. *J. Mol. Biol.* 405, 113–124. doi: 10.1016/j.jmb.2010.11.002

Böckler, S., and Westermann, B. (2014). Mitochondrial ER contacts are crucial for mitophagy in yeast. *Dev. Cell.* 28, 450–458. doi: 10.1016/j.devcel.2014.01.012

Bosc, C., Broin, N., Fanjul, M., Saland, E., Farge, T., Courdy, C., et al. (2020). Autophagy regulates fatty acid availability for oxidative phosphorylation through mitochondria-endoplasmic reticulum contact sites. *Nat. Commun.* 11:4056. doi: 10.1038/s41467-020-17882-2

Cabukusta, B., Berlin, I., van Elsland, D. M., Forkink, I., Spits, M., de Jong, A. W. M., et al. (2020). Human VAPome analysis reveals MOSPD1 and MOSPD3 as membrane contact site proteins interacting with FFAT-Related FFNT motifs. *Cell Rep.* 33:108475. doi: 10.1016/j.celrep.2020.108475

Cho, K. F., Branon, T. C., Rajeev, S., Svinkina, T., Udeshi, N. D., Thoudam, T., et al. (2020). Split-TurboID enables contact-dependent proximity labeling in cells. *Proc. Natl. Acad. Sci. U S A.* 117, 12143–12154. doi: 10.1073/pnas.1919528117

Chung, J., Torta, F., Masai, K., Lucast, L., Czapla, H., Tanner, L. B., et al. (2015). PI4P/phosphatidylserine countertransport at ORP5- and ORP8-mediated ER - plasma membrane contacts. *Science* 349, 428–432. doi: 10.1126/science.aab1370

Cieri, D., Vicario, M., Giacomello, M., Vallese, F., Filadi, R., Wagner, T., et al. (2018). SPLICS: a split green fluorescent protein-based contact site sensor for narrow and wide heterotypic organelle juxtaposition. *Cell Death Differ.* 25, 1131–1145. doi: 10.1038/s41418-017-0033-z

Cosson, P., Marchetti, A., Ravazzola, M., and Orci, L. (2012). Mitofusin-2 independent juxtaposition of endoplasmic reticulum and mitochondria: an ultrastructural study. *PLoS One.* 7:e46293. doi: 10.1371/journal.pone.0046293

Cremer, T., Neefjes, J., and Berlin, I. (2020). The journey of Ca^{2+} through the cell – pulsing through the network of ER membrane contact sites. *J. Cell Sci.* 133:jcs249136. doi: 10.1242/jcs.249136

Csordás, G., Golenár, T., Seifert, E. L., Kamer, K. J., Sancak, Y., Perocchi, F., et al. (2013). MICU1 controls both the threshold and cooperative activation of the mitochondrial Ca^{2+} uniporter. *Cell. Metabol.* 17, 976–987. doi: 10.1016/j.cmet.2013.04.020

Daniele, T., Hurbain, I., Vago, R., Casari, G., Raposo, G., Tacchetti, C., et al. (2014). Mitochondria and melanosomes establish physical contacts modulated by Mfn2 and involved in organelle biogenesis. *Curr. Biol.* 24, 393–403. doi: 10.1016/j.cub.2014.01.007

De Brito, O. M., and Scorrano, L. (2008). Mitofusin 2 tethers endoplasmic reticulum to mitochondria. *Nature* 456, 605–610. doi: 10.1038/nature07534

De vos, K. J., Mórotz, G. M., Stoica, R., Tudor, E. L., Lau, K. F., Ackerley, S., et al. (2012). VAPB interacts with the mitochondrial protein PTPIP51 to regulate calcium homeostasis. *Hum. Mol. Genet.* 21, 1299–1311. doi: 10.1093/hmg/ddr559

Doghman-Bouguerra, M., Granatiero, V., Sbiera, S., Sbiera, I., Lacas-Gervais, S., Brau, F., et al. (2016). FATE 1 antagonizes calcium- and drug-induced apoptosis by uncoupling ER and mitochondria. *EMBO Rep.* 17, 1264–1280. doi: 10.15252/embr.201541504

Du, X., Zhou, L., Aw, Y. C., Mak, H. Y., Xu, Y., Rae, J., et al. (2020). ORP5 localizes to ER-lipid droplet contacts and regulates the level of PI(4)P on lipid droplets. *J. Cell Biol.* 219:e201905162. doi: 10.1083/jcb.201905162

D'Eletto, M., Rossin, F., Occhigrossi, L., Farrace, M. G., Faccenda, D., Desai, R., et al. (2018). Transglutaminase type 2 regulates ER-mitochondria contact sites by interacting with GRP75. *Cell. Rep.* 25, 3573–3581. doi: 10.1016/j.celrep.2018.11.094

Elbaz-Alon, Y., Guo, Y., Segev, N., Harel, M., Quinnell, D. E., Geiger, T., et al. (2020). PDZD8 interacts with protrudin and Rab7 at ER-late endosome membrane contact sites associated with mitochondria. *Nat. Commun.* 11:3645. doi: 10.1038/s41467-020-17451-7

Ellenrieder, L., Opaliłski, Ł, Becker, L., Krüger, V., Mirus, O., Straub, S. P., et al. (2016). Separating mitochondrial protein assembly and endoplasmic reticulum tethering by selective coupling of Mdm10. *Nat. Commun.* 7:13021. doi: 10.1038/ncomms13021

Fecher, C., Trovò, L., Müller, S. A., Snaidero, N., Wettmarshausen, J., Heink, S., et al. (2019). Cell-type-specific profiling of brain mitochondria reveals functional and molecular diversity. *Nat. Neurosci.* 22, 1731–1742. doi: 10.1038/s41593-019-0479-z

Filadi, R., Greotti, E., and Pizzo, P. (2018). Highlighting the endoplasmic reticulum-mitochondria connection: focus on mitofusin 2. *Pharmacol. Res.* 128, 42–51. doi: 10.1016/j.phrs.2018.01.003

Filadi, R., Greotti, E., Turacchio, G., Luini, A., Pozzan, T., and Pizzo, P. (2015). Mitofusin 2 ablation increases endoplasmic reticulum-mitochondria coupling. *Proc. Natl. Acad. Sci. U S A.* 112, E2174–E2181. doi: 10.1073/pnas.1504880112

Filadi, R., Greotti, E., Turacchio, G., Luini, A., Pozzan, T., and Pizzo, P. (2016). Presenilin 2 modulates endoplasmic reticulum-mitochondria coupling by tuning the antagonistic effect of mitofusin 2. *Cell Rep.* 15, 2226–2238. doi: 10.1016/j.celrep.2016.05.013

Filadi, R., Leal, N. S., Schreiner, B., Rossi, A., Dentoni, G., Pinho, C. M., et al. (2018). TOM70 sustains cell bioenergetics by promoting IP3R3-mediated ER to mitochondria Ca^{2+} transfer. *Curr. Biol.* 28, 369–382. doi: 10.1016/j.cub.2017.12.047

Freyre, C. A. C., Rauher, P. C., Ejsing, C. S., and Klemm, R. W. (2019). MIGA2 links mitochondria, the ER, and lipid droplets and promotes De novo lipogenesis in adipocytes. *Mol. Cell.* 76, 811–825. doi: 10.1016/j.molcel.2019.09.011

Friedman, J. R., Lackner, L. L., West, M., DiBenedetto, J. R., Nunnari, J., and Voeltz, G. K. (2011). ER tubules mark sites of mitochondrial division. *Science* 334, 358–362. doi: 10.1126/science.1207385

Galmes, R., Houcine, A., Vliet, A. R., Agostinis, P., Jackson, C. L., and Giordano, F. (2016). ORP5/ORP8 localize to endoplasmic reticulum–mitochondria contacts and are involved in mitochondrial function. *EMBO Rep.* 17, 800–810. doi: 10.15252/embr.201541108

Garofalo, T., Matarrese, P., Manganelli, V., Marconi, M., Tinari, A., Gambardella, L., et al. (2016). Evidence for the involvement of lipid rafts localized at the ER-mitochondria associated membranes in autophagosome formation. *Autophagy* 12, 917–935. doi: 10.1080/15548627.2016.1160971

Gincel, D., Zaid, H., and Shoshan-Barmatz, V. (2001). Calcium binding and translocation by the voltage-dependent anion channel: a possible regulatory mechanism in mitochondrial function. *Biochem. J.* 358, 147–155.

Gomez-Suaga, P., Paillusson, S., Stoica, R., Noble, W., Hanger, D. P., and Miller, C. C. J. (2017). The ER-mitochondria tethering complex VAPB-PTPIP51 regulates autophagy. *Curr. Biol.* 27, 371–385. doi: 10.1016/j.cub.2016.12.038

Guillén-Samander, A., Bian, X., and de Camilli, P. (2019). PDZD8 mediates a Rab7-dependent interaction of the ER with late endosomes and lysosomes. *Proc. Natl. Acad. Sci. U S A.* 116, 22619–22623. doi: 10.1073/pnas.1913509116

Guo, Y., Li, D., Zhang, S., Yang, Y., Liu, J. J., Wang, X., et al. (2018). Visualizing intracellular organelle and cytoskeletal interactions at nanoscale resolution on millisecond timescales. *Cell* 175, 1430–1442. doi: 10.1016/j.cell.2018.09.057

Hailey, D. W., Rambold, A. S., Satpute-Krishnan, P., Mitra, K., Sougrat, R., Kim, P. K., et al. (2010). Mitochondria supply membranes for autophagosome biogenesis during starvation. *Cell* 141, 656–667. doi: 10.1016/j.cell.2010.04.009

Hamasaki, M., Furuta, N., Matsuda, A., Nezu, A., Yamamoto, A., Fujita, N., et al. (2013). Autophagosomes form at ER-mitochondria contact sites. *Nature* 495, 389–393. doi: 10.1038/nature11910

Harada, T., Sada, R., Osugi, Y., Matsumoto, S., Matsuda, T., Hayashi-Nishino, M., et al. (2020). Palmitoylated CKAP4 regulates mitochondrial functions through an interaction with VDAC2 at ER-mitochondria contact sites. *J. Cell. Sci.* 133:jcs249045. doi: 10.1242/jcs.249045

Hirabayashi, Y., Kwon, S. K., Paek, H., Pernice, W. M., Paul, M. A., Lee, J., et al. (2017). ER-mitochondria tethering by PDZD8 regulates Ca^{2+} dynamics in mammalian neurons. *Science* 358, 623–630. doi: 10.1126/science.aan6009

Hung, V., Lam, S. S., Udeshi, N. D., Svinkina, T., Guzman, G., Mootha, V. K., et al. (2017). Proteomic mapping of cytosol-facing outer mitochondrial and ER membranes in living human cells by proximity biotinylation. *Elife* 6:e24463. doi: 10.7554/eLife.24463

Issop, L., Fan, J., Lee, S., Rone, M. B., Basu, K., Mui, J., et al. (2015). Mitochondria-associated membrane formation in hormone-stimulated leydig cell steroidogenesis: role of ATAD3. *Endocrinology* 156, 334–345. doi: 10.1210/en.2014-1503

Iwasawa, R., Mahul-Mellier, A. L., Datler, C., Pazarentzos, E., and Grimm, S. (2011). Fis1 and Bap31 bridge the mitochondria-ER interface to establish a platform for apoptosis induction. *EMBO J.* 30, 556–568. doi: 10.1038/emboj.2010.346

Janer, A., Prudent, J., Paupe, V., Fahiminiya, S., Majewski, J., Sgarioto, N., et al. (2016). SLC25A46 is required for mitochondrial lipid homeostasis and cristae maintenance and is responsible for Leigh syndrome. *EMBO Mol. Med.* 8, 1019–1038. doi: 10.15252/emmm.201506159

Jeong, H., Park, J., Jun, Y., and Lee, C. (2017). Crystal structures of Mmm1 and Mdm12–Mmm1 reveal mechanistic insight into phospholipid trafficking at ER-mitochondria contact sites. *Proc. Natl. Acad. Sci. U S A.* 114, E9502–E9511. doi: 10.1073/pnas.1715592114

Jeong, H., Park, J., and Lee, C. (2016). Crystal structure of Mdm12 reveals the architecture and dynamic organization of the ERMES complex. *EMBO Rep.* 17, 1857–1871. doi: 10.15252/embr.201642706

Kopec, K. O., Alva, V., and Lupas, A. N. (2010). Homology of SMP domains to the TULIP superfamily of lipid-binding proteins provides a structural basis for lipid exchange between ER and mitochondria. *Bioinformatics* 26, 1927–1931. doi: 10.1093/bioinformatics/btq326

Kornmann, B., Currie, E., Collins, S. R., Schuldiner, M., Nunnari, J., Weissman, J. S., et al. (2009). An ER-mitochondria tethering complex revealed by a synthetic biology screen. *Science* 325, 477–481. doi: 10.1126/science.1175088

Kornmann, B., Osman, C., and Walter, P. (2011). The conserved GTPase Gem1 regulates endoplasmic reticulum-mitochondria connections. *Proc. Natl. Acad. Sci. U S A.* 108, 14151–14156. doi: 10.1073/pnas.1111314108

Kumar, N., Leonzino, M., Hancock-Cerutti, W., Horenkamp, F. A., Li, P. Q., Lees, J. A., et al. (2018). VPS13A and VPS13C are lipid transport proteins differentially localized at ER contact sites. *J. Cell. Biol.* 217, 3625–3639. doi: 10.1083/JCB.201807019

Kwak, C., Shin, S., Park, J. S., Jung, M., My Nhung, T. T., Kang, M. G., et al. (2020). Contact-ID, a tool for profiling organelle contact sites, reveals regulatory proteins of mitochondrial-associated membrane formation. *Proc. Natl. Acad. Sci. U S A.* 117, 12109–12120. doi: 10.1073/pnas.1916584117

Lahiri, S., Chao, J. T., Tavassoli, S., Wong, A. K. O., Choudhary, V., Young, B. P., et al. (2014). A conserved endoplasmic reticulum membrane protein complex (EMC) facilitates phospholipid transfer from the ER to mitochondria. *PLoS Biol.* 12:1001969. doi: 10.1371/journal.pbio.1001969

Lang, A. B., John Peter, A. T. A. T., Walter, P., and Kornmann, B. (2015). ER-mitochondrial junctions can be bypassed by dominant mutations in the endosomal protein Vps13. *J. Cell. Biol.* 210, 883–890. doi: 10.1083/jcb.201502105

Lee, I., and Hong, W. (2006). Diverse membrane-associated proteins contain a novel SMP domain. *FASEB J.* 20, 202–206. doi: 10.1096/fj.05-4581hyp

Lee, S., Lee, K. S., Huh, S., Liu, S., Lee, D. Y., Hong, S. H., et al. (2016). Polo kinase phosphorylates miro to control ER-mitochondria contact sites and mitochondrial Ca^{2+} homeostasis in neural stem cell development. *Dev. Cell.* 37, 174–189. doi: 10.1016/j.devcel.2016.03.023

Lesage, S., Drouet, V., Majounie, E., Deramecourt, V., Jacoupy, M., Nicolas, A., et al. (2016). Loss of VPS13C function in autosomal-recessive parkinsonism causes mitochondrial dysfunction and increases PINK1/Parkin-dependent mitophagy. *Am. J. Hum. Genet.* 98, 500–513. doi: 10.1016/j.ajhg.2016.01.014

Lewis, S. C., Uchiyama, L. F., and Nunnari, J. (2016). ER-mitochondria contacts couple mtDNA synthesis with mitochondrial division in human cells. *Science* 353:aaf5549. doi: 10.1126/science.aaf5549

Lim, Y., Cho, I. T., Schoel, L. J., Cho, G., and Golden, J. A. (2015). Hereditary spastic paraplegia-linked REEP1 modulates endoplasmic reticulum/mitochondria contacts. *Annal. Neurol.* 78, 679–696. doi: 10.1002/ana.24488

Lynes, E. M., Bui, M., Yap, M. C., Benson, M. D., Schneider, B., Ellgaard, L., et al. (2012). Palmitoylated TMX and calnexin target to the mitochondria-associated membrane. *EMBO J.* 31, 457–470. doi: 10.1038/emboj.2011.384

Manor, U., Bartholomew, S., Golani, G., Christenson, E., Kozlov, M., Higgs, H., et al. (2015). A mitochondria-anchored isoform of the actin-nucleating spire protein regulates mitochondrial division. *ELife* 4:e08828. doi: 10.7554/eLife.08828

Meisinger, C., Wiedemann, N., Rissler, M., Strub, A., Milenkovic, D., Schönfisch, B., et al. (2006). Mitochondrial protein sorting: differentiation of β-barrel assembly by tom7-mediated segregation of Mdm10. *J. Biol. Chem.* 281, 22819–22826. doi: 10.1074/jbc.M602679200

Modi, S., López-Doménech, G., Halff, E. F., Covill-Cooke, C., Ivankovic, D., Melandri, D., et al. (2019). Miro clusters regulate ER-mitochondria contact sites and link cristae organization to the mitochondrial transport machinery. *Nat. Commun.* 10:4399. doi: 10.1038/s41467-019-12382-4

Moser von Filseck, J., Čopič, A., Delfosse, V., Vanni, S., Jackson, C. L., Bourguet, W., et al. (2015). Phosphatidylserine transport by ORP/Osh proteins is driven by phosphatidylinositol 4-phosphate. *Science* 349, 432–436. doi: 10.1126/science.aab1346

Muñoz-Braceras, S., Calvo, R., and Escalante, R. (2015). TipC and the chorea-acanthocytosis protein VPS13A regulate autophagy in *Dictyostelium* and human HeLa cells. *Autophagy* 11, 918–927. doi: 10.1080/15548627.2015.1034413

Muñoz-Braceras, S., Tornero-Écija, A. R., Vincent, O., and Escalante, R. (2019). VPS13A is closely associated with mitochondria and is required for efficient lysosomal degradation. *Dis. Model. Mech.* 12:dmm036681. doi: 10.1242/DMM.036681

Murley, A., Lackner, L. L., Osman, C., West, M., Voeltz, G. K., Walter, P., et al. (2013). ER-associated mitochondrial division links the distribution of mitochondria and mitochondrial DNA in yeast. *ELife* 2:e00422. doi: 10.7554/eLife.00422

Nagashima, S., Takeda, K., Ohno, N., Ishido, S., Aoki, M., Saitoh, Y., et al. (2019). MITOL deletion in the brain impairs mitochondrial structure and ER tethering leading to oxidative stress. *Life Sci. Alliance* 2:e201900308. doi: 10.26508/lsa.201900308

Naon, D., Zaninello, M., Giacomello, M., Varanita, T., Grespi, F., Lakshminaranayan, S., et al. (2016). Critical reappraisal confirms that Mitofusin 2 is an endoplasmic reticulum-mitochondria tether. *Proc. Natl. Acad. Sci. U S A.* 113, 11249–11254. doi: 10.1073/pnas.1606786113

Nguyen, T. T., Lewandowska, A., Choi, J. Y., Markgraf, D. F., Junker, M., Bilgin, M., et al. (2012). Gem1 and ERMES do not directly affect phosphatidylserine transport from ER to mitochondria or mitochondrial inheritance. *Traffic* 13, 880–890. doi: 10.1111/j.1600-0854.2012.01352.x

Patron, M., Checchetto, V., Raffaello, A., Teardo, E., VecellioReane, D., Mantoan, M., et al. (2014). MICU1 and MICU2 finely tune the mitochondrial Ca^{2+} uniporter by exerting opposite effects on MCU activity. *Mol. Cell.* 53, 726–737. doi: 10.1016/j.molcel.2014.01.013

Petrungaro, C., and Kornmann, B. (2019). Lipid exchange at ER-mitochondria contact sites: a puzzle falling into place with quite a few pieces missing. *Curr. Opin. Cell. Biol.* 57, 71–76. doi: 10.1016/j.ceb.2018.11.005

Petrungaro, C., Zimmermann, K. M., Küttner, V., Fischer, M., Dengjel, J., Bogeski, I., et al. (2015). The Ca^{2+}-dependent release of the Mia40-induced MICU1-MICU2 dimer from MCU regulates mitochondrial Ca^{2+} uptake. *Cell Metabol.* 22, 721–733. doi: 10.1016/j.cmet.2015.08.019

Prudent, J., Zunino, R., Sugiura, A., Mattie, S., Shore, G. C., and McBride, H. M. (2015). MAPL SUMOylation of Drp1 stabilizes an ER/mitochondrial platform required for cell death. *Mol. Cell.* 59, 941–955. doi: 10.1016/j.molcel.2015.08.001

Puri, R., Cheng, X. T., Lin, M. Y., Huang, N., and Sheng, Z. H. (2019). Mul1 restrains Parkin-mediated mitophagy in mature neurons by maintaining ER-mitochondrial contacts. *Nat. Comm.* 10. doi: 10.1038/s41467-019-11636-5

Rapizzi, E., Pinton, P., Szabadkai, G., Wieckowski, M. R., Vandecasteele, G., Baird, G., et al. (2002). Recombinant expression of the voltage-dependent anion channel enhances the transfer of Ca^{2+} microdomains to mitochondria. *J. Cell Biol.* 159, 613–624. doi: 10.1083/jcb.200205091

Raturi, A., Gutiérrez, T., Ortiz-Sandoval, C., Ruangkittisakul, A., Herrera-Cruz, M. S., Rockley, J. P., et al. (2016). TMX1 determines cancer cell metabolism as a thiolbased modulator of ER-mitochondria Ca^{2+} flux. *J. Cell Biol.* 214, 433–444. doi: 10.1083/jcb.201512077

Rizzuto, R., Brini, M., Murgia, M., and Pozzan, T. (1993). Microdomains with high Ca^{2+} close to IP3-sensitive channels that are sensed by neighboring mitochondria. *Science* 262, 744–747. doi: 10.1126/science.8235595

Rochin, L., Sauvanet, C., Jääskeläinen, E., Houcine, A., Kivelä, A., Xingjie, M. A., et al. (2019). Orp5 transfers phosphatidylserine to mitochondria and regulates mitochondrial calcium uptake at endoplasmic reticulum - mitochondria contact sites. *bioRxiv* 2019:695577. doi: 10.1101/695577

Roth, D., Lynes, E., Riemer, J., Hansen, H. G., Althaus, N., Simmen, T., et al. (2009). A di-arginine motif contributes to the ER localization of the type I transmembrane ER oxidoreductase TMX4. *Biochem. J.* 425, 195–208. doi: 10.1042/BJ20091064

Rouzier, C., Moore, D., Delorme, C., Lacas-Gervais, S., Ait-El-Mkadem, S., Fragaki, K., et al. (2017). A novel CISD2 mutation associated with a classical wolfram syndrome phenotype alters Ca^{2+} homeostasis and ER-mitochondria interactions. *Hum. Mol. Genet.* 26, 1599–1611. doi: 10.1093/hmg/ddx060

Schauder, C. M., Wu, X., Saheki, Y., Narayanaswamy, P., Torta, F., Wenk, M. R., et al. (2014). Structure of a lipid-bound extended synaptotagmin indicates a role in lipid transfer. *Nature* 510, 552–555. doi: 10.1038/nature13269

Scorrano, L., De Matteis, M. A., Emr, S., Giordano, F., Hajnóczky, G., Kornmann, B., et al. (2019). Coming together to define membrane contact sites. *Nat. Commun.* 10:1287. doi: 10.1038/s41467-019-09253-3

Shai, N., Yifrach, E., Van Roermund, C. W. T., Cohen, N., Bibi, C., Ijlst, L., et al. (2018). Systematic mapping of contact sites reveals tethers and a function for the peroxisome-mitochondria contact. *Nat. Commun.* 9:1761. doi: 10.1038/s41467-018-03957-8

Shirane, M., Wada, M., Morita, K., Hayashi, N., Kunimatsu, R., Matsumoto, Y., et al. (2020). Protrudin and PDZD8 contribute to neuronal integrity by promoting lipid extraction required for endosome maturation. *Nat. Commun.* 11:4576. doi: 10.1038/s41467-020-18413-9

Stoica, R., De Vos, K. J., Paillusson, S., Mueller, S., Sancho, R. M., Lau, K. F., et al. (2014). ER-mitochondria associations are regulated by the VAPB-PTPIP51 interaction and are disrupted by ALS/FTD-associated TDP-43. *Nat. Commun.* 5:3996. doi: 10.1038/ncomms4996

Stroud, D. A., Oeljeklaus, S., Wiese, S., Bohnert, M., Lewandrowski, U., Sickmann, A., et al. (2011). Composition and topology of the endoplasmic reticulum-mitochondria encounter structure. *J. Mol. Biol.* 413, 743–750. doi: 10.1016/j.jmb.2011.09.012

Sugiura, A., Nagashima, S., Tokuyama, T., Amo, T., Matsuki, Y., Ishido, S., et al. (2013). MITOL regulates endoplasmic reticulum-mitochondria contacts via Mitofusin2. *Mol. Cell* 51, 20–34. doi: 10.1016/j.molcel.2013.04.023

Szabadkai, G., Bianchi, K., Várnai, P., De Stefani, D., Wieckowski, M. R., Cavagna, D., et al. (2006). Chaperone-mediated coupling of endoplasmic reticulum and mitochondrial Ca^{2+} channels. *J. Cell Biol.* 175, 901–911. doi: 10.1083/jcb.200608073

Valm, A. M., Cohen, S., Legant, W. R., Melunis, J., Hershberg, U., Wait, E., et al. (2017). Applying systems-level spectral imaging and analysis to reveal the organelle interactome. *Nature* 546, 162–167. doi: 10.1038/nature22369

Vance, J. E. (1990). Phospholipid synthesis in a membrane fraction associated with mitochondria. *J. Biol. Chem.* 265, 7248–7256. doi: 10.1016/S0021-9258(19)39106-9

Wang, C. H., Chen, Y. F., Wu, C. Y., Wu, P. C., Huang, Y. L., Kao, C. H., et al. (2014). Cisd2 modulates the differentiation and functioning of adipocytes by regulating intracellular Ca^{2+} homeostasis. *Hum. Mol. Genet.* 23, 4770–4785. doi: 10.1093/hmg/ddu193

Wang, P. T. C., Garcin, P. O., Fu, M., Masoudi, M., St-Pierre, P., Panté, N., et al. (2015). Distinct mechanisms controlling rough and smooth endoplasmic reticulum contacts with mitochondria. *J. Cell Sci.* 128, 2759–2765. doi: 10.1242/jcs.171132

Wong, Y. C., Ysselstein, D., and Krainc, D. (2018). Mitochondria-lysosome contacts regulate mitochondrial fission via RAB7 GTP hydrolysis. *Nature* 554, 382–386. doi: 10.1038/nature25486

Wu, H., Carvalho, P., and Voeltz, G. K. (2018). Here, there, and everywhere: the importance of ER membrane contact sites. *Science* 361, eaan5835. doi: 10.1126/science.aan5835

Wu, S., Lu, Q., Wang, Q., Ding, Y., Ma, Z., Mao, X., et al. (2017). Binding of FUNDC1 with inositol 1,4,5-trisphosphate receptor in mitochondria-associated endoplasmic reticulum (ER) membranes maintains mitochondrial dynamics and function in hearts in vivo. *Circulation* 136, 2248–2266. doi: 10.1161/CIRCULATIONAHA.117.030235

Wu, W., Lin, C., Wu, K., Jiang, L., Wang, X., Li, W., et al. (2016). FUNDC 1 regulates mitochondrial dynamics at the ER –mitochondrial contact site under hypoxic conditions. *EMBO J.* 35, 1368–1384. doi: 10.15252/embj.201593102

Xu, L., Wang, X., Zhou, J., Qiu, Y., Shang, W., Liu, J. P., et al. (2020). Miga-mediated endoplasmic reticulum– mitochondria contact sites regulate neuronal homeostasis. *ELife* 9, 1–26. doi: 10.7554/eLife.56584

Yamano, K., Tanaka-Yamano, S., and Endo, T. (2010). Tom7 regulates Mdm10-mediated assembly of the mitochondrial import channel protein TOM40. *J. Biol. Chem.* 285, 41222–41231. doi: 10.1074/jbc.M110.163238

Yeshaw, W. M., van der Zwaag, M., Pinto, F., Lahaye, L. L., Faber, A. I. E., Gómez-Sánchez, R., et al. (2019). Human VPS13A is associated with multiple organelles and influences mitochondrial morphology and lipid droplet motility. *ELife* 8, 1–37. doi: 10.7554/eLife.43561

Conflict of Interest: The authors declare that the research was conducted in the absence of any commercial or financial relationships that could be construed as a potential conflict of interest.

frontiers in Cell and Developmental Biology

REVIEW
published: 24 June 2021
doi: 10.3389/fcell.2021.664788

Functions of Oxysterol-Binding Proteins at Membrane Contact Sites and Their Control by Phosphoinositide Metabolism

Fubito Nakatsu and Asami Kawasaki*

Department of Neurochemistry and Molecular Cell Biology, Niigata University School of Medicine and Graduate School of Medical/Dental Sciences, Niigata, Japan

Lipids must be correctly transported within the cell to the right place at the right time in order to be fully functional. Non-vesicular lipid transport is mediated by so-called lipid transfer proteins (LTPs), which contain a hydrophobic cavity that sequesters lipid molecules. Oxysterol-binding protein (OSBP)-related proteins (ORPs) are a family of LTPs known to harbor lipid ligands, such as cholesterol and phospholipids. ORPs act as a sensor or transporter of those lipid ligands at membrane contact sites (MCSs) where two different cellular membranes are closely apposed. In particular, a characteristic functional property of ORPs is their role as a lipid exchanger. ORPs mediate counter-directional transport of two different lipid ligands at MCSs. Several, but not all, ORPs transport their lipid ligand from the endoplasmic reticulum (ER) in exchange for phosphatidylinositol 4-phosphate (PI4P), the other ligand, on apposed membranes. This ORP-mediated lipid "countertransport" is driven by the concentration gradient of PI4P between membranes, which is generated by its kinases and phosphatases. In this review, we will discuss how ORP function is tightly coupled to metabolism of phosphoinositides such as PI4P. Recent progress on the role of ORP-mediated lipid transport/countertransport at multiple MCSs in cellular functions will be also discussed.

Keywords: ORPs, phosphoinositide, membrane contact site (MCS), lipid transfer protein (LTP), PI4P, phosphatidylserine (PS), cholesterol, lipid countertransport

OPEN ACCESS

Edited by:
Yasunori Saheki, Nanyang Technological University, Singapore

Reviewed by:
Bruno Mesmin, Université Côte d'Azur, France

****Correspondence:***
Fubito Nakatsu
nakatsu@med.niigata-u.ac.jp

Specialty section:
This article was submitted to Membrane Traffic, a section of the journal Frontiers in Cell and Developmental Biology

Received: *06 February 2021*
Accepted: *06 May 2021*
Published: *24 June 2021*

Citation:
Nakatsu F and Kawasaki A (2021) Functions of Oxysterol-Binding Proteins at Membrane Contact Sites and Their Control by Phosphoinositide Metabolism. Front. Cell Dev. Biol. 9:664788. doi: 10.3389/fcell.2021.664788

INTRODUCTION

Lipids have multiple essential roles, including serving as building blocks for cellular membranes, storing energy, and regulating signaling and membrane dynamics/trafficking. In eukaryotes, most, but not all, lipids are synthesized at the endoplasmic reticulum (ER) and then must be correctly delivered to the places where they exert diverse functions (van Meer and de Kroon, 2011; Santos and Preta, 2018). In addition, lipids often move and change their location even during their metabolic or catabolic processes (van Meer et al., 2008). Thus, lipids rely on their transport systems for accomplishing their diverse and complex tasks in biological systems.

Lipids are transported within cells via membrane carriers (vesicles) along secretory and endocytic membrane trafficking pathways (van Meer et al., 2008; Vance, 2014; Stefan et al., 2017). In addition to vesicular transport, lipids are also transported in a vesicle-independent manner

(Holthuis and Levine, 2005; Lev, 2012; Reinisch and Prinz, 2021). Non-vesicular lipid transport is mediated by so-called lipid transfer proteins (LTPs) (Holthuis and Menon, 2014; Wong et al., 2019). LTPs contain a hydrophobic cavity that sequesters lipid molecules from aqueous cytosolic environments, and in this way, they mediate lipid transport between cellular membranes (Wong et al., 2017). Although LTPs are technically able to transport lipids to any accessible place by freely moving in the cytosol, they often do so at membrane contact sites (MCSs). MCSs are places where there is close apposition of cellular membranes (generally 10–30 nm, but the distance differs depending on the type of MCSs) (Helle et al., 2013; Eisenberg-Bord et al., 2016; Scorrano et al., 2019). Accumulating evidence indicates that the ER, which is widely distributed throughout the cell, forms MCSs with most of the organelles or the plasma membrane (PM), and these MCSs serve as zones for non-vesicular lipid transport (Phillips and Voeltz, 2015; Wu et al., 2018; Balla et al., 2019; Prinz et al., 2019; Bohnert, 2020). A number of LTPs have been reported to localize at MCSs and, thus, mediate the transport of a variety of lipid ligands (Wong et al., 2017, 2019).

In this review, we provide an overview of recent progress on understanding the role of oxysterol-binding protein (OSBP)-related proteins (ORPs) (Raychaudhuri and Prinz, 2010; Olkkonen, 2015; Pietrangelo and Ridgway, 2018), a large family of LTPs. Particular focus is placed on their lipid transport function at MCSs and their role in cellular processes in mammals. Given that ORP functions are closely coupled to phosphatidylinositol 4-phosphate (PI4P) metabolism, we will begin with background information as well as recent findings on PI4P, followed by ORP family functions, with the overall goal of an in-depth discussion on the physiological significance of lipid transport at MCSs mediated by ORPs and phosphoinositides.

PHOSPHATIDYLINOSITOL 4-PHOSPHATE

Phosphatidylinositol 4-Phosphate Metabolism in the Cell

Phosphoinositides are a minor group of phospholipids that represent 10–15% of total phospholipids in the cell (Vance, 2014). The inositol ring in their headgroup is exposed to the cytosol, and its 3, 4, or 5 position can be phosphorylated or dephosphorylated to create seven distinct phosphoinositide species (Balla, 2013). Those phosphoinositides are unevenly distributed in the cell (Di Paolo and De Camilli, 2006). For instance, $PI(4,5)P_2$ is concentrated at the PM, while PI4P, its major precursor, is distributed more widely (see below for details). $PI(3,4,5)P_3$ is also localized at the PM, but its level transiently increases locally under certain conditions. Such spatial and temporal distribution of each phosphoinositide species, which determines the identity of cellular membranes, is tightly controlled, mostly based on the action of their metabolic phosphoinositide kinases or phosphatases that localize in distinct cellular compartments (Di Paolo and De Camilli, 2006; Balla, 2013).

PI4P, which is mono-phosphorylated at the 4-position of the inositol ring, is one of the most abundant phosphoinositides in eukaryotes. Its *de novo* synthesis is mediated by phosphatidylinositol 4-kinases (PI4Ks) that phosphorylate phosphatidylinositol (PI), the substrate, at the 4 position of the inositol ring (Balla, 2013). In mammals, there are four PI4Ks: two type III PI4Ks (PI4K3α and PI4K3β) and two type II PI4Ks (PI4K2α and PI4K2β) (Balla and Balla, 2006; Boura and Nencka, 2015). As a side note, type I PI4K turned out to be PI3K, and thus, no type I PI4Ks exists at present. The cellular distribution of PI4P is primarily determined by the localization as well as the site of action of its responsible kinases. PI4P is mainly distributed at the PM, the Golgi, and endosomes/lysosomes, and those pools of PI4P are synthesized by PI4K3α, PI4K3β, and PI4K2α or PI4K2β, respectively (**Figure 1**). A pool of PI4P at autophagosomes has also been demonstrated (**Figure 1**) (Albanesi et al., 2015; Wang et al., 2015; Judith et al., 2019; De Tito et al., 2020).

Phosphatidylinositol 4-Kinases

PI4K3α localizes at the PM with the help of other regulatory proteins including EFR3A, EFR3B, TTC7A, TTC7B, FAM126A, FAM126B, and TMEM150A (Nakatsu et al., 2012; Baskin et al., 2015; Bojjireddy et al., 2015; Chung et al., 2015a). Biochemical as well as genetic evidences show that PI4K3α is required for PI4P production at the PM, and other PI4Ks are unable to compensate for this kinase, suggesting a distinct and non-overlapping function of PI4Ks (Nakatsu et al., 2012). PI4K3β localizes at the Golgi where it produces PI4P (Wong et al., 1997; Antonietta De Matteis et al., 2005). Several proteins, including Arf1 (Godi et al., 1999), ACBD3 (Sasaki et al., 2011) and PKD (Hausser et al., 2005), are reported to support its Golgi localization and function. Both type II PI4Ks, PI4K2α and PI4K2β, localize at endosomes or late endosomes/lysosomes and produce a pool of PI4P at those membranes (Balla and Balla, 2006). PI4K2α and PI4K2β localize at the endosomal membranes *via* palmitoylation (Balla et al., 2002; Barylko et al., 2009; Lu et al., 2012). PI4K2α has been shown to localize and generate a pool of PI4P at the *trans*-Golgi network (TGN) as well (Wang et al., 2003). PI4K2α and PI4K3β have been shown to associate with the autophagosomes, where they contribute to the generation of the pool of PI4P (Albanesi et al., 2015; Wang et al., 2015; Judith et al., 2019; De Tito et al., 2020).

PI4Ks were reported to localize in the nucleus and generate a pool of PI4P (reviewed in Chen et al., 2020). Recent findings have revealed the presence of PI, the precursor of PI4P, at the outer membrane of the mitochondria (Pemberton et al., 2020b; Zewe et al., 2020). In addition, functional involvement and localization of the TGN-derived vesicles containing PI4P, which is synthesized by PI4K3β, have been observed at the ER–mitochondria MCSs (Nagashima et al., 2020). However, no direct evidence for the existence of PI4P or PI4Ks at the mitochondria has been reported.

Phosphatidylinositol 4-Phosphate Phosphatases

Metabolic degradation of PI4P (i.e., dephosphorylation) is controlled by the suppressor of actin (Sac)-domain containing

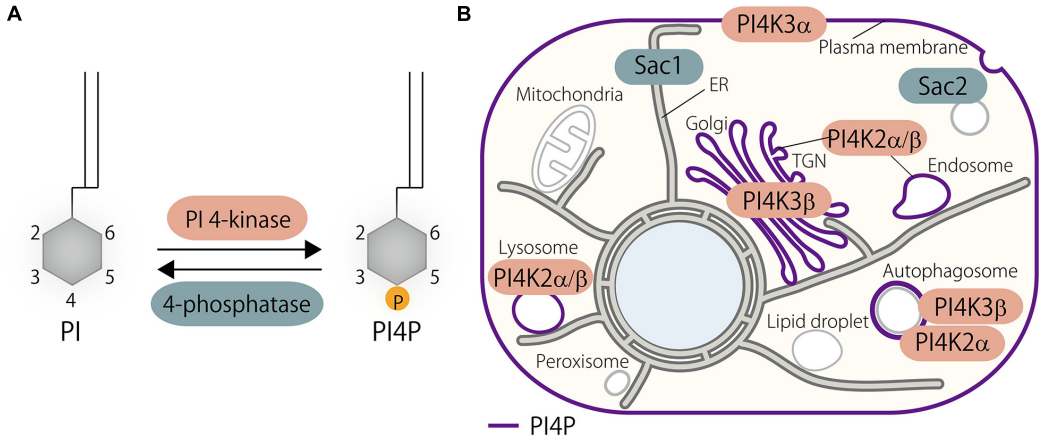

FIGURE 1 | Phosphatidylinositol 4-phosphate (PI4P) metabolism in the cell. **(A)** *De novo* PI4P synthesis is catalyzed by PI 4-kinases that phosphorylate phosphatidylinositol (PI) at the D4 position of the inositol ring. Dephosphorylation of PI4P is mediated by 4-phosphatases. **(B)** Distribution of PI4P and its kinases and phosphatases in the mammalian cell. PI4P is synthesized at the plasma membrane (PM), Golgi, and endosomes/lysosomes by PI4K3α, PI4K3β, and PI4K2α/β, respectively. PI4K2α and possibly PI4K3β as well contribute to the generation of a pool of PI4P at autophagosomes. Metabolic degradation of PI4P is mediated by PI4P phosphatases such as Sac1 and Sac2/INPP5F. PI, phosphatidylinositol; PI4P, phosphatidylinositol 4-phosphate; TGN, *trans*-Golgi network.

phosphoinositide phosphatase family. The Sac phosphatase domain family in mammals consists of five members including Sac1, Sac2/INPP5F, Sac3/Fig4, Synaptojanin1, and Synaptojanin2, which all contain the Sac domain, a phosphoinositide phosphatase domain (Hsu and Mao, 2013). Sac1 is the major phosphatase that controls PI4P metabolism in the cell (Del Bel and Brill, 2018), although it dephosphorylates PI3P and PI(3,5)P_2 in addition to PI4P (Guo et al., 1999; Nemoto et al., 2001). Sac1 is a type II transmembrane protein that localizes at the ER, but translocates to Golgi via COPII-mediated transport at the nutrient-limiting condition (Blagoveshchenskaya et al., 2008). Several pieces of evidence suggest that Sac1 dephosphorylates PI4P on the ER membranes and that it is transported from other membranes to the ER via MCSs (see below). This "in cis" action of Sac1 keeps the levels of PI4P low at the ER and, thus, critically contributes to the ORP-mediated lipid countertransport by creating a concentration gradient of this lipid between the ER and other membranes, which will be described later in detail. However, the "in trans" action of Sac1, in which it dephosphorylates PI4P on the PM or the Golgi membranes, was also reported (Stefan et al., 2011; Dickson et al., 2016; Venditti et al., 2019a).

Sac2/INPP5F and synaptojanins contribute to the metabolism of a pool of PI4P in the endocytic pathway. Synaptojanins have a 5-phosphatase domain that dephosphorylates PI(4,5)P_2 in addition to the Sac1 domain (McPherson et al., 1996). The well-known site of action of synaptojanins is at the clathrin-coated pits. Synaptojanins are recruited to the clathrin-coated pits where they sequentially dephosphorylate PI(4,5)P_2-PI4P-PI via 5-phosphatase and 4-phosphatase enzymatic activities (Mani et al., 2007; Cao et al., 2017). Likewise, Sac2/INPP5F is also recruited to the late phase of endocytic structures (Hsu et al., 2015; Nakatsu et al., 2015; Levin et al., 2017). Sac2/INPP5F interacts with OCRL, a 5-phosphatase that is also recruited to clathrin-coated pits (Pirruccello and De Camilli, 2012). OCRL has a 5-phosphatase domain but lacks a 4-phosphatase domain. Thus, OCRL dephosphorylates PI(4,5)P_2 to PI4P, and then Sac2/INPP5F dephosphorylates PI4P to PI during endocytosis. Thus, OCRL and Sac2/INPP5F function as a split-synaptojanin to cooperatively dephosphorylate PI(4,5)P_2 to PI (Nakatsu et al., 2015). A recent finding suggests a role of Sac2/INPP5F in the exocytic pathway (Nguyen et al., 2019).

ORP FAMILY PROTEINS

ORPs are a family of LTPs that are highly conserved in eukaryotes (Olkkonen, 2015; Pietrangelo and Ridgway, 2018). Seven members in yeast and 12 members in humans have been identified, suggesting a requirement for multiple players that cover diverse cellular functions (Lehto et al., 2001; Raychaudhuri and Prinz, 2010). The 12 known ORPs in mammals are subdivided into six groups according to their sequence homology and domain organization: OSBP and ORP4 in group I, ORP1 and ORP2 in group II, ORP3, ORP6, and ORP7 in group III, ORP5 and ORP8 in group IV, ORP9 in group V, and ORP10 and ORP11 in group VI (**Figure 2**). Mounting evidence demonstrates that ORPs regulate a variety of cellular functions including, but not limited to, lipid transport, membrane/organelle trafficking, and signaling.

Functional Domains in ORPs

Oxysterol-Binding Protein-Related Domain

Several domains or motifs are conserved in this family. One common feature of the ORP family members is the lipid-harboring domain called oxysterol-binding protein-related domain (ORD). Originally, OSBP, the first identified member of the ORP family, was identified as a cytosolic OSBP (Taylor et al., 1984). This study led to the discovery of the larger ORP family that commonly has an ORD as a lipid-transfer

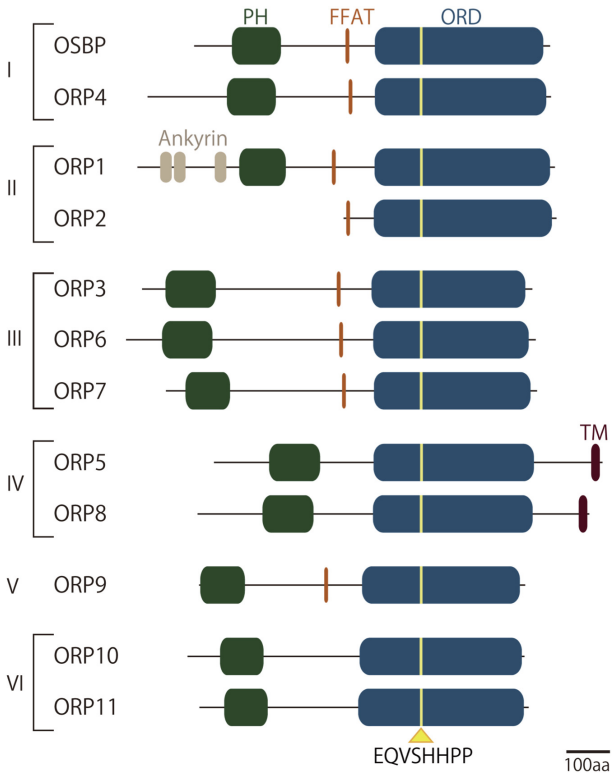

FIGURE 2 | Domain structures of oxysterol-binding protein-related protein (ORP) family proteins. Schematic cartoon representing the domain structures of ORP family proteins in mammals. ORPs in mammals are subdivided into six groups according to their sequence homology and domain organization. They have a well-conserved lipid-binding domain called oxysterol-binding protein-related domain (ORD), in which a consensus lipid-binding motif EQVSHHPP is located. Most but not all of ORPs possess a PH domain that binds phosphoinositides such as PI4P and/or PI(4,5)P_2 in the target membranes. Endoplasmic reticulum (ER) targeting determinants such as the FFAT (two phenylalanines in acidic tract)-motif, which is recognized by ER-resident membrane protein VAPA or VAPB, or membrane anchoring domain facilitates the localization of ORPs at membrane contact sites (MCSs) between the ER and other membranes. ORD, oxysterol-binding protein-related domain; FFAT, two phenylalanines in acidic tract.

or lipid-sensing domain. Subsequent studies of OSBP as well as other ORPs revealed that the ORD accommodates not only oxysterols but also other lipids (Raychaudhuri and Prinz, 2010; de Saint-Jean et al., 2011; Maeda et al., 2013; Olkkonen, 2015; Pietrangelo and Ridgway, 2018). Structural analysis of the ORD from Osh4, one of the well-characterized ORPs in yeast, revealed a β-barrel-like structure, containing a hydrophobic pocket that accommodates oxysterol or cholesterol, and a lid-like structure that closes the pocket (Im et al., 2005). The 3-hydroxylgroup of the sterol is positioned at the bottom of the pocket, and the side chain is covered by the N-terminal lid. To date, the lipid ligands for ORDs include oxysterols, cholesterol, and phospholipids such as phosphoinositides, phosphatidylserine (PS), and/or phosphatidylcholine (PC). ORDs from all ORPs contain the well-conserved residues EQVSHHPP, a consensus lipid-binding motif located near the entrance of the pocket. Given that the tandem histidine residues are responsible for the binding to the head group of PI4P, the ORP family might be structurally adapted to harbor PI4P as a common ligand (de Saint-Jean et al., 2011; Tong et al., 2013).

Membrane Targeting Domains/Motif

Most ORPs possess a Pleckstrin homology (PH) domain (Lemmon, 2008) in their N-terminal portion that mediates membrane association. Many of them have been characterized to have a high affinity to phosphoinositides such as PI4P and/or PI(4,5)P_2. Since phosphoinositides are the critical determinants of cellular membrane identity (Di Paolo and De Camilli, 2006), recognition of such lipids by a PH domain is a key process for localization and, hence, MCS formation by ORPs. They also often have another determinant that associates with the ER. The FFAT (two phenylalanines in acidic tract) motif is recognized by ER-resident membrane protein vesicle-associated membrane protein (VAMP)-associated protein A or B (VAPA or VAPB) with their major sperm protein (MSP) domain (Loewen et al., 2003). The FFAT motif is present in many other LTPs that function at MCSs (Murphy and Levine, 2016). Another ER-associating structure is the membrane spanning domain in ORP5 and ORP8, which enables ER localization on its own. These ER-anchoring determinants help bridge the ER and target membranes at MCSs, where they mediate lipid transfer functions.

Lipid Transfer Regulation by ORPs

A major function of ORPs is to transfer their lipid ligands between cellular membranes (Raychaudhuri and Prinz, 2010). Their lipid transfer activity has been extensively studied *in vitro* (Wong et al., 2017). Purified ORD protein has been shown to extract lipids from artificial liposomal membranes. When mixed with two different liposomes, the ORD is able to transfer lipids from one liposome to another (Pietrangelo and Ridgway, 2018). In the cellular context, most, but not all, ORPs have been shown to mediate lipid transfer between cellular membranes. The mode of lipid transfer is either shuttling between two different membrane compartments that have certain distance or direct transfer at MCSs (Wong et al., 2019).

An interesting nature of ORPs is their lipid exchange activity. OSBP or its yeast counterpart Osh4/Kes1 was initially demonstrated to be a sterol transfer protein (Raychaudhuri et al., 2006; Ngo and Ridgway, 2009). Indeed, they transfer cholesterol (or ergosterol in yeast) between membranes both *in vitro* and in live yeast. However, de Saint-Jean et al. (2011) elegantly demonstrated that Osh4/Kes1 transfers not only sterol, but also PI4P via its ORD. Its crystal structure showed that the ORD of Osh4/Kes1 accommodates either sterols (cholesterol, ergosterol, and oxysterols) or PI4P. An interesting point was that Osh4/Kes1 mediates exchange of sterol and PI4P between two different liposomes containing either lipid. Subsequently, the same group extended this idea to demonstrate that OSBP mediates countertransport of PI4P and cholesterol at MCSs between the ER and Golgi (Mesmin et al., 2013). ORP5 and ORP8 have also been demonstrated to mediate countertransport of PI4P and PS at ER–PM MCSs

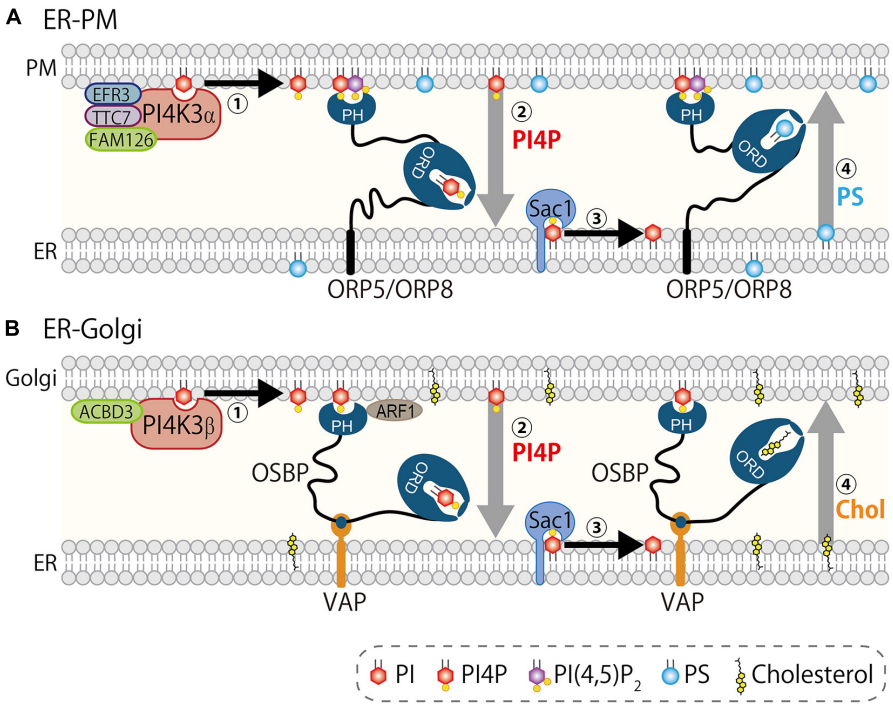

FIGURE 3 | PI4P-driven lipid countertransport at MCSs. PI4P drives lipid countertransport mediated by ORP5/8 at ER–PM MCSs **(A)** and by OSBP at ER–Golgi MCSs **(B)**. **(A)** PI4K3α complex including EFR3A/B, TTC7A/B, and FAM126A/B synthesizes and concentrates PI4P at the PM (step 1). ORP5/8, both of which are anchored to the ER, form MCSs via interaction with PI4P and $PI(4,5)P_2$ by PH domain, and transport PI4P (driver-ligand) from the PM to the ER (step 2). Sac1 dephosphorylates PI4P to PI, which keeps the concentration of PI4P low at the ER (step 3). ORP5/8 transport PS (cargo-ligand) from the ER to the PM. **(B)** PI4K3β generates PI4P upon recruitment to the Golgi by regulatory proteins including Arf1 (step 1). Oxysterol-binding protein (OSBP) is recruited to the ER–Golgi MCSs *via* PH domain that interacts with PI4P and ACBD3 and/or Arf1 on the Golgi membranes and FFAT-motif that binds vesicle-associated membrane protein (VAMP)-associated protein A/B (VAPA/B). Then, OSBP mediates transport of PI4P (driver-ligand) from the Golgi to the ER (step 2). Sac1 hydrolyzes PI4P to PI (step 3). OSBP transports cholesterol (cargo-ligand) to Golgi (step 4). Synthesis and hydrolysis of PI4P by PI4Ks and Sac1 establishes a concentration gradient of this lipid between the ER and the PM/Golgi, which determines the flow of driver-ligand PI4P to the ER and counterflow of cargo-ligands from the ER.

by our group (Chung et al., 2015b) (**Figure 3**). In this lipid countertransport, differing amounts of PI4P between the ER and other membranes such as Golgi or PM is the driving force. PI4P is continuously synthesized at the PM or Golgi by PI4K3α or PI4K3β, respectively, while it is metabolically degraded at the ER by Sac1. This enzymatic regulation establishes a concentration gradient of PI4P between the ER and the PM or Golgi. Given that the ORD accommodates only one lipid molecule at a time (Im et al., 2005), the ORD picks up PI4P at the PM or Golgi and transfers it down a concentration gradient to the ER where Sac1 hydrolyzes it to PI. This PI4P flow empowers backward transfer of another lipid, PS for ORP5/8 or cholesterol for OSBP, from the ER to the PM or Golgi (**Figure 3**). This PI4P-driven lipid countertransport is further ensured by the mechanism by which these ORPs establish MCSs. OSBP or ORP5/8 forms MCSs via PH domain-mediated recognition of PI4P (with the help of other factors such as Arf1 or $PI(4,5)P_2$ (see below for details), which guarantees the concentration gradient of this lipid at the MCSs. The PI4P metabolic cycle generated by its kinases and phosphatase is tightly coupled to the ORP function, and this functional partnership supports PI4P-driven lipid countertransport at MCSs by ORPs (Mesmin and Antonny, 2016).

LIPID TRANSPORT BY ORPs AT MEMBRANE CONTACT SITES

The ER, the site of the synthesis of most of lipids, is now known to make MCSs with most of the organelles or the PM where ORPs mediate transport or countertransport of lipids. Accumulating evidence demonstrates that ORP family proteins are widely localized at distinct MCSs and operate their own lipid transport/countertransport function (**Figure 4** and **Table 1**). Furthermore, the tight regulation of such ORP function by phosphoinositides has also become evident. This section provides an overview of the role of ORPs in lipid transport or exchange at MCSs and their contributions to cellular biological processes. How phosphoinositides, such as PI4P, regulate ORP function will also be discussed.

Endoplasmic Reticulum–Plasma Membrane Membrane Contact Sites

ORP5/8

ORP5 and ORP8, which belong to group IV of the ORP family, have similar characteristics of domain structures (**Figure 2**). Both proteins have a PH domain, a coiled-coil domain, a linker region,

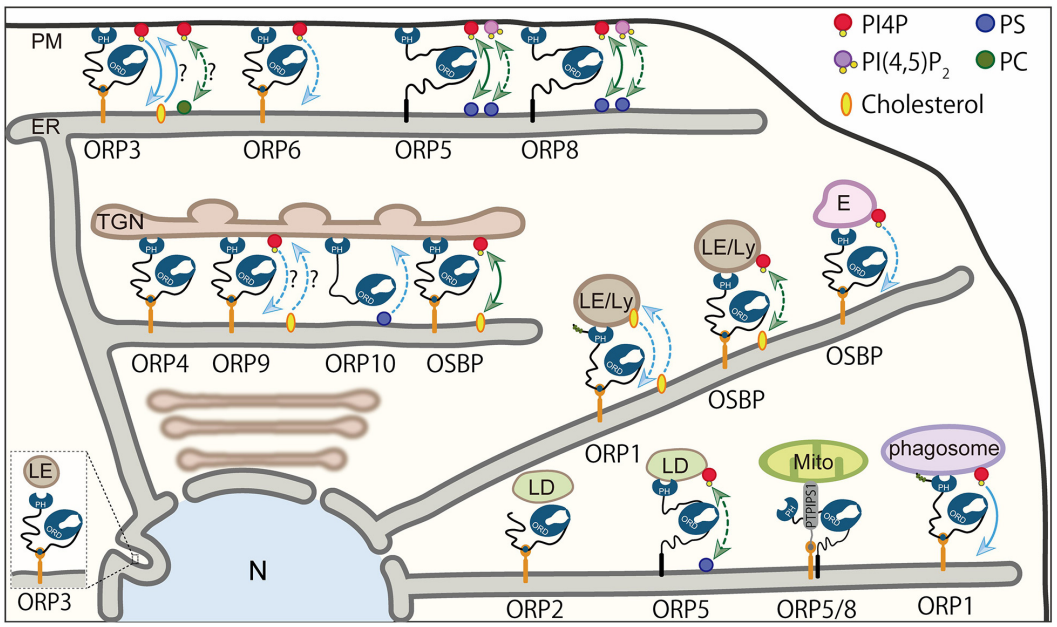

FIGURE 4 | Lipid transport/countertransport mediated by ORPs at MCSs. Summary of ORPs mediating transport or countertransport of lipids at MCSs. At the ER–PM MCSs, ORP5 and ORP8 mediate countertransport of PI4P and PS driven by PI4P metabolic cycle. They have been proposed to act as $PI(4,5)P_2$/PS exchangers. ORP3 and possibly ORP6 mediate PI4P transport to the ER, while ORP3 may transport PC or cholesterol from the ER in exchange for PI4P. At the ER–Golgi MCSs, OSBP is an exchanger of PI4P and cholesterol. ORP10 has been suggested to mediate PS transport from the ER. The function of ORP4 and ORP9 as transporters/exchangers is unknown. At the MCSs between the ER and endosomes, late endosomes, or lysosomes, OSBP functions as a PI4P transporter or PI4P/cholesterol exchanger. ORP1 acts as a sensor or transporter of cholesterol and a transporter of PI4P. At the ER–lipid droplet (LD) MCSs, ORP5 has been proposed to be a PI4P/PS exchanger. The role of ORP2 as a transporter/exchanger at the ER–LD MCSs is unknown. At the ER–mitochondria MCSs, ORP5 and ORP8 may or may not be exchangers/transporters for PI4P and PS. Blue arrows indicate "transport," whereas green arrows show "countertransport." Solid lines are used if the transport or countertransport of the indicated lipids has been demonstrated by loss-of-function or gain-of-function analysis in an acute manner (e.g., acute inhibition or manipulation of ORP proteins). Dashed lines are used if the transport or countertransport of the indicated lipids has been suggested by loss-of-function or gain-of-function analysis in a chronic manner [e.g., chronic inhibition (knock-down or knock-out) or overexpression of ORP proteins]. ER, endoplasmic reticulum; E, endosomes; LE/Ly, late endosomes/lysosomes; Mito, mitochondria; N, nucleus; PM, plasma membrane; TGN, *trans*-Golgi network.

an ORD, and a membrane-spanning domain. Unlike other ORPs, ORP5 and ORP8 anchor to the ER *via* a membrane-spanning domain located at the C-terminus. The PH domain of ORP5 or ORP8 recognizes PI4P and/or $PI(4,5)P_2$ in the PM with different preferences, thereby making an MCS between the ER and the PM (Chung et al., 2015b; Ghai et al., 2017; Sohn et al., 2018). It has been demonstrated that the ORD of ORP5/8 specifically harbors PI4P or PS and transfers them between liposomes *in vitro*. Intriguingly, the transfer of PS from donor to acceptor liposomes was strongly enhanced if another lipid ligand PI4P was present in the acceptor side, and the opposite combination also showed the same tendency, indicating an exchange activity of the ORP8 ORD (Chung et al., 2015b). In addition to PI4P and PS, the ORP5 ORD was shown to transport dehydroergosterol (DHE) *in vitro*, and this DHE transport was partially inhibited in the presence of PI4P in the donor liposomes (Du et al., 2011) (see the section "Endoplasmic Reticulum–Endosome/Lysosome/Autophagosome/Phagosome Membrane Contact Cites" for more details). In the cellular context, ORP5/8 exchanges PS with PI4P between the ER and the PM. Functional ablation of PI4K3α (the PI4P supplier at the PM) or Sac1 (the PI4P remover at the ER) disrupted the countertransport of those lipids, confirming that ORP5/8-mediated lipid countertransport is tightly coupled to the PI4P metabolic flow between the PM and the ER (Chung et al., 2015b) (**Figure 3**). This ORP5/8-mediated PI4P-driven lipid countertransport enables PS supply from the ER to the PM against its concentration gradient. Similarly, PI4P-driven PS transport at ER–PM MCSs has also been demonstrated in yeast (Moser von Filseck et al., 2015).

Several studies showed the regulation of PM $PI(4,5)P_2$ by ORP5 and ORP8. Results from Sohn et al. (2018) support the role of ORP5/8 in exchanging PS with PI4P at ER–PM MCSs. In this study, BRET imaging quantitative assay was used to show that ORP5/8 controls $PI(4,5)P_2$ levels by tuning the amount of its precursor PI4P, and this is basically controlled by their localization to the MCSs via the PH domain. The ORP5 PH domain requires both PI4P and $PI(4,5)P_2$ for localization at ER–PM MCSs. However, the ORP8 PH domain strongly depends on $PI(4,5)P_2$ for its MCS localization, although PI4P is still required even when $PI(4,5)P_2$ production is increased. In the situation where $PI(4,5)P_2$ is highly produced at the PM, PI4P levels become low due to ORP8 localization at the MCSs, thereby limiting PI4P availability for $PI(4,5)P_2$ conversion by PIPKs. They proposed that this is a rheostat mechanism for tightly controlling the $PI(4,5)P_2$ levels in a narrow range

(**Figure 5**). ORP5 might be a housekeeper for PI4P and $PI(4,5)P_2$ (and PS) homeostasis at the PM in the steady-state condition, while ORP8 could be a regulator for more stimulatory situations that might require tight regulation of $PI(4,5)P_2$ (e.g., Ca^{2+} regulation, cell migration, receptor activation, or membrane ruffling).

In contrast, another study by the Yang group (Ghai et al., 2017) proposed a different model for the regulation of $PI(4,5)P_2$ by ORP5 and ORP8. They demonstrated that localization of ORP5 and ORP8 is dependent on $PI(4,5)P_2$, but not on PI4P, and this is due to the binding property of their PH domains to $PI(4,5)P_2$, but not to PI4P. Furthermore, the driver-ligand of the ORP5/8 ORD was proposed to be $PI(4,5)P_2$. In an *in vitro* lipid transport assay, they showed that the ORP8 ORD efficiently transports $PI(4,5)P_2$, and its concentration gradient between two liposomes enhanced the PS exchange. Consistent with this idea, PM $PI(4,5)P_2$ levels increased by knockdown of ORP5/8. These authors proposed that ORP5 and ORP8 are $PI(4,5)P_2$/PS exchangers in a $PI(4,5)P_2$-driven mechanism. Their conclusion regarding the role of ORP5 and ORP8 in controlling $PI(4,5)P_2$ levels at the PM agreed with that of the Balla group, but the underlying mechanism differed. Because of the efficient *in vitro* $PI(4,5)P_2$ transfer activity in addition to a strong dependency on $PI(4,5)P_2$ for PM localization, the localization and function of ORP5/8 appear to be PI4P-independent. In the PI4P-driven model (**Figure 3**), PI4P is transported from the PM to the ER where it is hydrolyzed by the PI4P phosphatase Sac1, and this PI4P metabolic cycle generates the PI4P concentration gradient that drives lipid countertransport by ORP5 and ORP8 (Chung et al., 2015b). However, in the case of the $PI(4,5)P_2$-driven model, how $PI(4,5)P_2$ is metabolically degraded at the ER to create the concentration gradient of this lipid is still unknown. The authors mentioned that INPP5E might be involved in this process, but there is no evidence showing that INPP5E localizes at the ER and hydrolyzes $PI(4,5)P_2$ there. Instead, INPP5K, an ER-localized 5-phosphatase reported to hydrolyze $PI(4,5)P_2$ and $PI(3,4,5)P_3$, is a candidate, although the site of action of INPP5K has been proposed to be not only the ER, but also other membranes, including the PM, nucleus, and autolysosomes (Gurung et al., 2003; Ijuin and Takenawa, 2003; Hung et al., 2009; Dong et al., 2018; Ramos et al., 2020; McGrath et al., 2021).

ORP5/8-mediated countertransport and its relationship with the PI4P–$PI(4,5)P_2$–PS metabolic axis was further reported. A recent yeast study (Nishimura et al., 2019) showed that an osh-mediated lipid exchange mechanism generates a local domain containing unsaturated PS and sterol that promotes the localization and activation of PIPK, leading to $PI(4,5)P_2$ production. This study further points to the functional relationship between PI4P/PS exchange and $PI(4,5)P_2$ regulation. Additionally, a relationship between PS metabolism and MCS formation was also reported (Sohn et al., 2016) in studies of PSS1 (Kuge et al., 1991) and PSS2 (Kuge et al., 1997), the two PS synthases whose genetic mutation leads to Lenz–Majewski syndrome (Lenz and Majewski, 1974). The ER-localized enzyme PSS1 or PSS2 catalyzes PS production using PC or phosphatidylethanolamine (PE), respectively, as a substrate.

TABLE 1 | Oxysterol-binding protein-related proteins (ORPs) that mediate transport or countertransport of lipids at membrane contact sites (MCSs).

ORPs	Lipid transfer activity *in vitro* [A]	Localization at ER MCS (lipids transferred or exchanged)[B]	References
OSBP	PI4P/DHE	ER-Golgi **(PI4P/Sterol),** ER-endosome (PI4P), ER-LE/Ly (PI4P/Cholesterol)	Mesmin et al. (2013, 2017), Dong et al. (2016), Goto et al. (2016), Lim et al. (2019)
ORP1	DHE	ER-LE/Ly (Cholesterol), ER-phagosome **(PI4P)**	Eden et al. (2016), Zhao and Ridgway (2017), Dong et al. (2019), Levin-Konigsberg et al. (2019)
ORP2	$PI(4,5)P_2$/DHE	ER-LD	Weber-Boyvat et al. (2015b)
ORP3	?	ER-PM **(PI4P)**	Weber-Boyvat et al. (2015a), D'Souza et al. (2020), Gulyás et al. (2020)
ORP4	Cholesterol	ER-Golgi	Wyles et al. (2007), Charman et al. (2014), Pietrangelo and Ridgway (2018)
ORP5	PI4P/PS, $PI(4,5)P_2$/PS, DHE	ER-PM **(PI4P/PS),** ER-PM ($PI(4, 5)P_2$/PS), ER-LD (PI4P/PS), ER-Mito	Chung et al. (2015b), Galmes et al. (2016), Ghai et al. (2017), Sohn et al. (2018)
ORP6	?	ER-PM (PI4P)	Mochizuki et al. (2018)
ORP7	?	?	
ORP8	PI4P/PS, $PI(4,5)P_2$/PS	ER-PM **(PI4P/PS),** ER-PM ($PI(4,5)P_2$/PS), ER-Mito	Chung et al. (2015b), Galmes et al. (2016), Ghai et al. (2017), Sohn et al. (2018)
ORP9	Cholesterol	ER-Golgi	Ngo and Ridgway (2009), Venditti et al. (2019b)
ORP10	?	ER-Golgi (PS)	Venditti et al. (2019b)
ORP11	?	?	

[A]Lipids were transported or exchanged between liposomes in vitro. The exchanged lipids are separated by slash (/).
[B]Lipids demonstrated to be transported or exchanged in intact cells are shown in parentheses. The exchanged lipids are separated by slash (/).
*[B]Lipids shown in **bold** font: transport or exchange of the indicated lipids has been demonstrated in loss-of-function or gain-of-function analysis in an acute manner (e.g., acute inhibition or manipulation of ORP proteins).*
[B]Lipids shown in regular font: transport or exchange of the indicated lipids has been suggested in loss-of-function or gain-of-function analysis in a chronic manner [e.g., chronic inhibition (knock-down or knock-out) or overexpression of ORP proteins].
?, Unknown.

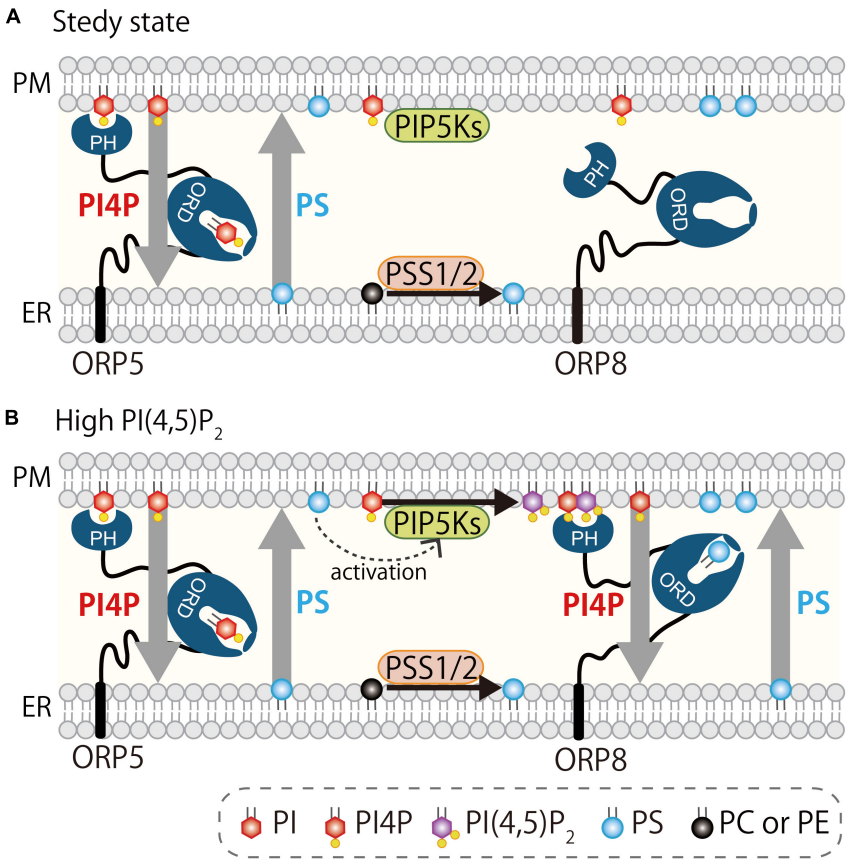

FIGURE 5 | Regulation of PI4P and PI(4,5)P_2 at the PM by oxysterol-binding protein-related proteins 5 and 8. **(A)** At steady state, ORP5 localizes at the ER–PM MCSs *via* binding to PI4P and PI(4,5)P_2. **(B)** When PI(4,5)P_2 is high at the PM, ORP8 is strongly recruited to the PM via preferential binding to PI(4,5)P_2 and mediates countertransport of PI4P and PS. This reduces PI4P levels at the PM and thus contributes indirectly to reducing PI(4,5)P_2 levels by limiting its precursor. ORP8-mediated countertransport of PS to the PM may facilitate the activation of PIPKs (Nishimura et al., 2019).

Their enzyme activity was shown to be inhibited by the end product PS, and the mutation responsible for this feedback inhibition, which caused Lenz–Majewski syndrome, leads to PS accumulation in the ER (Sousa et al., 2014). Inhibition of PI4K3α by the specific inhibitor A1 decreases the PM PI4P levels, and this results in the inhibition of PS synthesis by approximately 50%. This is likely a homeostatic regulation because PS synthesis needs to be slowed down in a situation where PI4P-driven PS transport is slow. In fact, expression of the PSS1 disease mutant, which reflects a disease condition where PS accumulated at the ER, led to a reduction of ORP8 membrane association as well as a decrease in PM PI4P levels (Sohn et al., 2016). Collectively, PI4P-driven lipid countertransport mediated by ORP5 and ORP8 is tightly coupled to homeostasis of lipids such as PI4P, PI(4,5)P_2, and PS at the PM and the ER (Balla et al., 2019, 2020; Pemberton et al., 2020a; Santos et al., 2020) (**Figure 5**).

ORP3

ORP3 is categorized in group III, together with ORP6 and ORP7 (**Figure 2**). ORP3 contains a typical cytosolic ORP family domain architecture, such as a PH domain, FFAT-motif, and ORD. ORP3 is basically cytosolic at steady state, but translocates to the ER–PM MCSs upon PKC activation and Ca^{2+} influx (Weber-Boyvat et al., 2015a; Gulyás et al., 2020). ORP3 associates with the ER via FFAT motif-mediated binding to VAP, and it appears to be phosphorylation dependent (Lehto et al., 2005; Weber-Boyvat et al., 2015a). The PM association of ORP3 is mediated by its PH domain that recognizes PI4P and PI(4,5)P_2 (Gulyás et al., 2020). Such phosphorylation-dependent binding of ORP3 to VAP and the PM might imply that phosphorylation may induce a conformational change that unmasks the PH domain and FFAT-motif. Colocalization of ORP3 with ORP6 or ORP8 at the ER–PM MCSs has been reported (Weber-Boyvat et al., 2015a; Mochizuki et al., 2018). ORP3-mediated ER–PM MCS formation has been linked to cellular processes such as Ca^{2+} regulation, adhesion, and migration (Machaca, 2020). A recent study (D'Souza et al., 2020) provided a mechanistic insight into how ORP3 controls focal adhesion dynamics. Those studies indicate the following scenario. Store-operated Ca^{2+}entry (SOCE) by STIM1-Orai1 axis activates PKC and then induces the ORP3 translocation to the ER–PM MCSs where STIM1 and Orai1 also localize. This ORP3 translocation occurs around the focal adhesion where ORP3 recruits the

guanin exchange factor IQSec1 that activates Arf5, thereby promoting the disassembly of focal adhesion at the rear front of the cell. How ORP3-mediated lipid transport/countertransport is involved in those processes, however, is still unclear. This is because the ligand(s) of the ORD have not been firmly identified. However, an imaging study showing a strong reduction of PI4P, but not of $PI(4,5)P_2$, $PI(3,4,5)P_3$, or PS, at the PM after acute recruitment of ORP3 to the ER–PM MCS, suggests PI4P as a ligand of the ORP3 ORD (Gulyás et al., 2020). Other cargo-ligand(s) could be PC or cholesterol (D'Souza et al., 2020; Gulyás et al., 2020). However, whether ORP3 is indeed an exchanger of those candidate ligands has not been clearly demonstrated and, thus, needs further investigation.

ORP6

ORP6 is another member in group III (**Figure 2**). Like ORP3, ORP6 also shows a typical domain architecture such as N-terminal PH domain, FFAT-motif, and ORD. Mochizuki et al. (2018) demonstrated that ORP6 colocalized with ORP3 or extended synaptotagmins (E-Syts), but not with ORP5, at the ER–PM MCSs in neuronal cells such as Neuro2A or primary cerebellar granule cells. The ORP6 PH domain binds PI4P, $PI(4,5)P_2$, and phosphatidic acid (PA) in a membrane lipid strip assay. ORP6 knockdown led to an increase in PM PI4P detected by the OSBP PH domain probe, suggesting that ORP6 contributes to the PI4P turnover at the PM. However, whether ORP6 mediates transport or countertransport of lipids is still unclear, as well as its contribution to cell physiology.

Endoplasmic Reticulum–Golgi Membrane Contact Sites

OSBP

OSBP is the founding member of the ORP family (Raychaudhuri and Prinz, 2010) (**Figure 2**). The domain architecture is PH domain, FFAT-motif, and ORD, the typical ORP family domain structure. OSBP represents both a cytosolic pool and membrane-bound status. Initially, OSBP was shown to associate with the Golgi including the TGN, but also with endosomes or lysosomes in later studies. The membrane targeting of OSBP is mediated by PH domain as is the case for other ORPs. According to an *in vitro* liposome-binding assay, the OSBP PH binds PI4P and $PI(4,5)P_2$ (Rameh et al., 1997; Levine and Munro, 1998). However, a study using yeast as a model (Levine and Munro, 2002) showed the OSBP PH domain localizes in the Golgi, and this Golgi localization was abolished upon deletion of the PI4-kinase *pik1* (the yeast ortholog of mammalian PI4K3β that synthesizes PI4P at the Golgi). The deletion of the PIP-kinase *mss4* [the yeast ortholog of mammalian PIPKs that generates $PI(4,5)P_2$], however, did not abolish the Golgi localization of the OSBP PH domain, indicating that PI4P is the key to Golgi localization *in situ*. Furthermore, the OSBP PH domain also interacted with the GTP-bound form of Arf1, the small GTPase that controls membrane association of Golgi proteins (Levine and Munro, 2002). Arf1 also controls recruitment to the Golgi of PI4K3β, the PI4K responsible for the synthesis of a pool of PI4P at this organelle (Godi et al., 1999). PI4K2α, another PI4K that synthesizes PI4P at endosomes and the TGN (Wang et al., 2003), is also shown to provide a pool of PI4P at the TGN for OSBP recruitment (Mesmin et al., 2017). Thus, the OSBP PH domain recognizes both PI4P and GTP-Arf1. This coincident detection mechanism ensures the targeting of OSBP to the Golgi, and thus, OSBP localizes at ER–Golgi MCSs with the FFAT motif captured by VAP at the ER.

The OSBP ORD has been demonstrated to exchange PI4P and cholesterol between the ER and Golgi (Mesmin et al., 2013). This idea, basically, came from a study by de Saint-Jean et al. (2011) using osh4 as a model. Extraction of fluorescent ergosterol DHE by Osh4p, which was previously shown to bind sterol in its ORD, was inhibited by PI4P, but not by many other lipids tested. This was due to the surprising ability of the osh4 ORD to solubilize PI4P by itself. In fact, crystal structural analysis clearly revealed that osh4 specifically harbors PI4P or cholesterol in its ORD. The acyl chain of PI4P is inserted deep inside the pocket, and the head group of PI4P is positioned near the entrance that contains the conserved sequence containing tandem histidines. Additionally, a series of elegant *in vitro* lipid transport experiments demonstrated that osh4 exchanges sterol with PI4P between liposomes (de Saint-Jean et al., 2011).

The study above led to the discovery of OSBP function at ER–Golgi MCSs. Mesmin et al. (2013) demonstrated that OSBP exchanges cholesterol and PI4P at ER–Golgi MCSs. Mechanistically, OSBP extracts PI4P from the Golgi membranes and transfers it to the ER, and this PI4P flow along its gradient ensures the back transfer of cholesterol against the gradient by OSBP (**Figure 3**). Functionally, OSBP has been estimated to mediate one-third to two-thirds of cholesterol transport by consuming approximately half of the total cellular PI4P, according to an acute pharmacological inhibition study (Mesmin et al., 2017) using the chemical OSW-1 (Burgett et al., 2011). Such inhibition of OSBP led to a roughly fourfold increase in PI4P levels at the TGN and a roughly twofold increase in whole cells. A recent study using a different inhibitor also reported a similar effect (Péresse et al., 2020). These data suggest the physiological contribution of OSBP in the regulation of PI4P and cholesterol at the TGN. However, another study demonstrated no major impact on PI4P levels at the TGN by OSBP knockdown or addition of 25-hydroxycholesterol (Goto et al., 2016). Chronic inhibition by knockdown (in contrast to acute inhibition) as well as a cell type difference might be the reasons for the apparently different results. Regarding the 25-hydroxycholesterol, no inhibitory (but even a slight stimulatory) effect on the OSBP-mediated PI4P transport between liposomes has been demonstrated (Mesmin et al., 2017). This could be a possible explanation for the very minor effect of this lipid on the PI4P levels in the TGN. Collectively, OSBP regulates PI4P levels at the TGN.

ORP4

ORP4 belongs to group I, together with OSBP (**Figure 2**). ORP4 has a PH domain, FFAT motif, and ORD, and there is a short isoform containing only an ORD. ORP4 has been detected in the brain, kidneys, heart, skeletal muscles, and spleen by Northern blot analysis of human tissues (Wang et al., 2002), as well as in the brain and testis by Western blot analysis of

mouse tissues (Udagawa et al., 2014). The PH domain bound to PI4P in a membrane lipid strip assay, as well as in a liposome-binding assay (Charman et al., 2014). In CHO cells, the PH domain of ORP4 weakly associated with the Golgi. The purified protein containing the ORP4 ORD binds 25-hydroxycholesterol to extract and transfer cholesterol between liposomes (Charman et al., 2014). ORP4 was shown to interact with OSBP and localizes to the Golgi in an OSBP-dependent manner, suggesting that ORP4 functions at the ER–Golgi MCSs with OSBP (Wyles et al., 2007; Pietrangelo and Ridgway, 2018). However, whether ORP4 mediates transport or countertransport of PI4P and/or cholesterol is unknown. ORP4 has been implicated in several cancers, including leukemia, as a signaling regulator; however, its role as an LTP in MCSs is unclear (Fournier et al., 1999; Silva et al., 2001; Henriques Silva et al., 2003; Zhong et al., 2016).

ORP9

ORP9 is the sole member in group V (**Figure 2**). The domain structure of the full-length long form is a typical one containing a PH domain, FFAT motif, and ORD. The short isoform lacking the PH domain has also been reported. The ORP9 PH domain binds mono-phosphorylated phosphoinositides according to a lipid membrane overlay assay and cosediments with liposomes containing PI4P (Ngo and Ridgway, 2009). Purified full-length ORP9 proteins extract cholesterol and PI4P, but not oxysterol or PS, from liposomes *in vitro* and transfer cholesterol between liposomes (Ngo and Ridgway, 2009; Liu and Ridgway, 2014). This cholesterol transfer activity is enhanced if the donor liposomes also contain PI4P, and this enhancement is dependent on its PH domain, suggesting that such enhancement is due to the efficient targeting of purified ORP9 proteins to the donor liposomes by PH domain (Ngo and Ridgway, 2009). Whether ORP9 exchanges PI4P and cholesterol is still unknown. ORP9 localizes partially at the TGN and does not colocalize with PI4K3β. ORP9 knockdown in HeLa cells did not alter the PI4P levels in the TGN, as assessed by immunofluorescence staining with anti-PI4P antibody (Liu and Ridgway, 2014). A recent study demonstrated a role of ORP9 in the integrity of ER–TGN MCSs as its depletion in addition to simultaneous depletion of OSBP affects the formation of ER–TGN MCSs assessed by FLIM (fluorescence lifetime imaging) (Venditti et al., 2019b).

ORP10

ORP10 is a member of group VI, and it has a PH domain and an ORD, but lacks a FFAT motif (**Figure 2**). ORP10 is reported to localize at the Golgi *via* its PH domain. The ORD of ORP10 has been shown to extract PS from liposomes (Maeda et al., 2013). Venditti et al. (2019b) demonstrated that ORP10 localized at the MCSs between the ER and TGN. ORP10 depletion in HeLa cells affects the integrity of ER–TGN MCSs and leads to reduced PS levels in the Golgi, suggesting its role as a PS transporter. The residues involved in binding to PI4P and PS in the ORP5/8 ORD are well conserved in ORP10, and mutations in these residues were shown to abolish the ability to rescue the integrity of the MCSs in ORP10-deficient cells. These results suggest that ORP10 might be a lipid exchanger. However, a lipid exchange function of ORP10 has not been demonstrated.

Endoplasmic Reticulum–Endosome/Lysosome/Autophagosome/Phagosome Membrane Contact Sites

OSBP

OSBP has been reported to localize at MCSs other than the Golgi. Dong et al. (2016) demonstrated the function of OSBP at ER–endosome MCSs. OSBP knockdown as well as VAPA/VAPB deletion leads to endosomal PI4P accumulation and then actin reorganization such as the loss of stress fibers and WASH-dependent actin comet formation. OSBP-mediated transport of PI4P from endosomes to the ER contributes to the negative regulation of PI4P at endosomes. Sobajima et al. (2018) showed the function of OSBP at the MCSs between endosomes and the TGN, but not the ER. OSBP interacts with RELCH, a novel Rab11-GTP effector, and tethers recycling endosomes to the TGN by the OSBP–RELCH-Rab11 complex. This complex meditates the transfer of cholesterol from recycling endosomes to the TGN (Sobajima et al., 2018). Another study (Lim et al., 2019) also indicates the role of OSBP-mediated cholesterol transport at ER–lysosome MCSs. OSBP was found to supply cholesterol to lysosomes *via* ER–lysosome MCSs. This pool of cholesterol in the limiting membrane of lysosomes triggers the activation of mTORC1, the master regulator of growth, via Rag GTPases as well as the amino acid permease SLC38A9 (Castellano et al., 2017). In fact, OSBP inhibition by the chemical inhibitor OSW1 or shRNA-mediated knockdown reduced cholesterol accumulation on the lysosomal-limiting membranes in cells lacking Niemann Pick C type 1 (NPC1), thereby suppressing the hyperactivation of mTORC1 (Lim et al., 2019). The studies described above all indicate an important role of OSBP as a transporter, but not as a *bona fide* exchanger, of lipid ligands at several MCSs. Despite the fact that OSBP is an exchanger of PI4P and cholesterol at the ER and Golgi, whether and how such exchange activity of OSBP support those functions at the MCSs other than Golgi is currently unclear.

ORP5

ORP5 has been suggested to functionally contribute to the cholesterol transport from late endosomes/lysosomes to the ER (Du et al., 2011). Purified ORP5 ORD mediates transfer of DHE between liposomes, and this activity is partially inhibited by PI4P, but not by PI3P, PI5P, or $PI(4,5)P_2$, suggesting a possibility of ORP5 as a cholesterol transporter. Transiently expressed full-length ORP5 or its ORD was co-immunoprecipitated with either exogenously expressed or endogenous NPC1. Their association might be direct or indirect. Knockdown of ORP5, but not of ORP8, resulted in accumulation of cholesterol in the limiting membrane of late endosomes/lysosomes and impairment of cholesterol transfer from those organelles to the ER (evaluated by ACAT-mediated cholesterol esterification at the ER). The authors suggest that ORP5 may function with NPC1 as a cholesterol

transporter *via* MCSs between the ER and lysosomes, although such MCS formation has not been demonstrated to date.

ORP1

ORP1, which belongs to group II together with ORP2, exists in long (L) and short (S) forms (**Figure 2**). ORP1L contains ankyrin repeats in addition to other typical domains for ORPs such as a PH domain, FFAT-motif, and ORD. ORP1S encodes only an ORD but lacks other domains. Purified PH domain of ORP1L binds weakly $PI(3,4)P_2$, $PI(3,5)P_2$, and $PI(3,4,5)P_3$ in liposome-binding assay (Johansson et al., 2005). ORP1L binds Rab7 *via* ankyrin repeats (Johansson et al., 2005) as well as VAP *via* FFAT motif and, hence, localizes at the MCSs between the ER and late endosomes/lysosomes or autophagosomes. The ORP1 ORD binds oxysterol, cholesterol, and PI4P (Vihervaara et al., 2011; Zhao and Ridgway, 2017; Zhao et al., 2020). Dong et al. (2019) reported that the ORD binds all of the phosphoinositides with a similar extent compared with DHE but does not bind PS. Lipid transfer activity of the ORP1 ORD has also been demonstrated (see below). However, its exchange activity has not been reported to date.

Cholesterol Transport by ORP1

Dong et al. (2019) reported that the purified ORP1 ORD protein transports cholesterol or DHE between liposomes *in vitro*, and its transfer activity is enhanced in the presence of $PI(3,4)P_2$ or $PI(4,5)P_2$ in the acceptor liposomes. However, the backward transfer of those phosphoinositides was not detected. Another study by Zhao and Ridgway (2017) reported that extraction of cholesterol from liposomes by purified full-length ORP1 protein was inhibited by the addition of PI4P, but not other phosphoinositides including $PI(4,5)P_2$, to the liposomes. Consistent with this result, ORP1 protein extracts isotope-labeled PI4P from liposomes. Thus, these *in vitro* studies suggest that the ORP1 ORD is able to transport cholesterol, but may not transport phosphoinositides. In the cellular extent, ORP1L has been shown to mediate transport of cholesterol or PI4P (see below) at late endosome–ER MCSs. In the absence of exogenous low-density lipoprotein (LDL), which can be a source of late endosomal cholesterol *via* endocytosis, ORP1L mediates cholesterol transport to late endosomes from the ER, the site of its synthesis (Eden et al., 2016). This cholesterol transport can be driven by countertransport of PI4P in theory, but such countertransport has not yet been reported. Other studies also support the cholesterol transport, but its direction is opposite. Zhao and Ridgway (2017) demonstrated that accumulation of cholesterol in late endosomes in ORP1L-deficient HeLa cells was rescued by expression of wild-type, but not of mutants lacking the ORD or FFAT motif, suggesting that ORP1L mediates transfer of LDL-derived cholesterol from late endosomes to the ER along its concentration gradient. This ORP1L-mediated cholesterol transfer requires NPC1, which delivers LDL-cholesterol to the limiting membranes of late endosomes. Surprisingly, the mutant ORP1L, which is unable to bind PI4P due to disruption of the conserved PI4P-binding histidine residues in its ORD, did not rescue the cholesterol accumulation phenotype. This implies possible involvement of PI4P in the cholesterol transport, although it is difficult to reconcile at this moment how PI4P contributes to this cholesterol regulation. Dong et al. (2019) also supported the idea that ORP1L mediates cholesterol transport from late endosomes to the ER. Consistent with their *in vitro* data showing that the cholesterol transport activity of ORP1L is enhanced by $PI(3,4)P_2$ or $PI(4,5)P_2$, inhibition of $PI(3,4)P_2$ synthesis by PI3KC2β on late endosomes (Marat et al., 2017) phenocopies the cholesterol transport defect. Collectively, ORP1L functions as a cholesterol transporter with or without the help of phosphoinositides, but its transport might be bi-directional between the ER and late endosomes/lysosomes depending on the cholesterol concentration.

Phosphatidylinositol 4-Phosphate Transport by ORP1

PI4P transport by ORP1L has been demonstrated at the MCSs between the ER and phagosomes. Phagosomes are endocytic organelles that engulf extracellular materials including microorganisms and apoptotic cells, and eventually fuse with lysosomes that degrade them. It has recently been demonstrated that ORP1L localizes at the MCSs between the ER and phagolysosomes, the mature phagosomes, where it mediates transport of PI4P from phagolysosomes to the ER (Levin-Konigsberg et al., 2019). The disappearance of PI4P from phagolysosomes, evaluated by live imaging, was delayed in ORP1L KO RAW 264.7 cells, and this delay was rescued by reexpression of wild-type ORP1L but not of the PI4P-binding mutant or the FFAT motif mutant. This ORP1L-mediated PI4P transport contributes to the segregation and concentration of this lipid into a domain that recruits the SKIP–ARL8B–kinesin complex (*via* PI4P binding of SKIP PH domain) leading to tubulation and fission of PI4P-positive membranes of phagolysosomes. Given that membrane-associated free cholesterol increases with phagosome maturation (Rai et al., 2016), such ORP1L-mediated PI4P transport to the ER might be coupled to back-transfer of cholesterol to the phagolysosomes. This interesting possibility needs further investigation.

Cholesterol Sensing by ORP1

ORP1L has been shown to control dynamics of late endosomes/lysosomes as a cholesterol sensor. Rab7 is a small GTPase that localizes at those organelles and controls a variety of their functions including subcellular positioning (Zerial and McBride, 2001; Cabukusta and Neefjes, 2018). ORP1L localizes at late endosomes/lysosomes *via* its PH domain and binding to Rab7 as an effector. Rab7 also recruits another effector RILP (Cantalupo et al., 2001; Jordens et al., 2001), which is the adaptor protein connecting Rab7 to the dynein–dynactin motor complex by binding to the light intermediate chain of dynein (Schroeder et al., 2014) and $p150^{Glued}$ subunit of dynactin (Johansson et al., 2007). Interaction of Rab7–ORP1L–RILP to the dynein–dynactin motor complex, thus, determines the positioning of late endosomes/lysosomes, but this interaction is controlled by ORP1L-mediated cholesterol sensing. When the cholesterol levels are high in the limiting membrane of late endosomes, ORP1L accommodates cholesterol, leading

to a conformation that does not allow it to bind VAP and, thus, to form MCSs with the ER. This, in turn, allows RILP to interact with the dynein–dynactin complex, and then late endosomes/lysosomes are clustered at the perinuclear area due to minus end-directed movement on microtubules. In a condition where cholesterol levels are low in late endosomes/lysosomes, ORP1L does not bind cholesterol in its ORD, leading to a conformational change in ORP1L so that it binds to VAP through the FFAT motif and forms MCSs with the ER. Then RILP no longer binds the dynein–dynactin complex, thereby leading to more scattered peripheral localization of late endosomes (Rocha et al., 2009). Thus, ORP1L controls late endosome/lysosome positioning depending on cholesterol levels *via* connecting or disconnecting those organelles to microtubules *via* promoting or inhibiting the binding capacity of RILP to the dynein–dynactin motor complex. Similar regulation was also reported for autophagosomes (Wijdeven et al., 2016). How lipid transport or countertransport activity of ORP1L contributes to such positioning control of late endosomes/lysosomes is still unclear.

ORP3

ORP3 has been reported to localize at the MCSs between late endosomes and the nuclear envelope (NE), whose outer membrane is continuous with the ER membrane. Extracellular vesicles such as exosomes or microvesicles are taken up *via* endocytosis by recipient cells, and their contents (e.g., nucleic acids, proteins, or lipids) are then delivered into the cytosol or other compartments (Raposo and Stoorvogel, 2013; van Niel et al., 2018). However, the underlying mechanism of the delivery of EV components is not completely understood (Mathieu et al., 2019). Rappa et al. (2017) demonstrated that EV components are transported along the endocytic pathway to a subset of Rab7-positive late endosomes, which are located in the nucleoplasmic reticulum in a deep nuclear envelope invagination. A subsequent study by the same group showed that such late endosomes contact the outer nuclear membranes in nuclear envelope invagination through tethering by ORP3 and VAPA. Functional ablation of ORP3 or VAPA (but not VAPB) leads to malformation of NE-late endosome MCSs in the nucleoplasmic reticulum and inhibits the transport of EV components such as CD9 or nucleic acids into the nucleoplasm, suggesting that ORP3-mediated MCSs contribute to delivering EV contents to the nucleus (Santos et al., 2018). Given that the nucleoplasmic reticulum is involved in Ca^{2+} regulation (Echevarría et al., 2003), the localization and function of ORP3 at the NE-late endosome MCSs may also be coupled to Ca^{2+} regulation, as shown at the ER–PM MCSs (Weber-Boyvat et al., 2015a; D'Souza et al., 2020; Gulyás et al., 2020). However, the targeting mechanism and lipid transport function of ORP3 in moving EV components into the nucleus remains unknown.

Endoplasmic Reticulum–Lipid Droplet Membrane Contact Sites

ORP2

ORP2 is a member of group II (**Figure 2**). It has an FFAT motif and ORD, but lacks a PH domain. The ORP2 ORD binds oxysterol, cholesterol, and phosphoinositides such as PI4P, $PI(4,5)P_2$, $PI(3,5)P_2$, and $PI(3,4,5)P_3$ *in vitro* (Xu et al., 2001; Hynynen et al., 2005, 2009; Suchanek et al., 2007). ORP2 has been suggested to function at the lipid droplets (LDs). ORP2 localizes to the surface of LDs or MCSs between the ER and LDs. Loss of function studies suggest that ORP2 may control triacylglycerol metabolism as well as lipolysis in LDs (Weber-Boyvat et al., 2015b). How ORP2 targets the LDs, however, is unclear. A recent study showed the association of ORP2 with the COPI machinery, which has been demonstrated to transport proteins to the LDs (Soni et al., 2009; Wilfling et al., 2014). ORP2 might utilize COPI to target LDs. Whether and how ORP2 exerts its function as a lipid transporter/exchanger is also unknown.

ORP5

ORP5, but not ORP8, is shown to localize and function at the ER–LD MCSs. ORP5 localizes LDs upon oleate loading, and its localization is mediated by ORD. Mutations in the lipid binding residues of ORP5 ORD abolished its localization, suggesting that PI4P/PS transport activity is required for the LD targeting. ORP5 knockdown increased the size of LDs, although no morphological change was reported in the previous study by the same group (Du et al., 2011). ORP5 knockdown also leads to an increase in PI4P and a decrease in PS on the LD surface. PI4K2α, but not other PI4Ks, was responsible for the generation of a pool of PI4P on LDs in ORP5 KD cells. ORP5 has been proposed to control the function of LDs *via* PI4P/PS countertransport, which is similar to that at the ER–PM MCSs but is supported by a different kinase, PI4K2α. However, direct evidence of the PI4P/PS exchange at the ER–LD MCSs *in situ* seems to be rather weak. It is quite interesting to find that ORP5 has a pleiotropic function as a PI4P/PS exchanger at multiple MCSs. However, many questions remain elusive. What is the physiological significance of PS transport to LDs? How does PI4K2α, which is a palmitoylated endosomal protein (Balla et al., 2002; Balla and Balla, 2006), contribute to the synthesis of the pool of PI4P on LDs? How is the localization (and hence the MCS formation) of ORP5, which does not require its PH domain, precisely controlled? Answering those questions may advance our understanding of ORP5 functions as well as novel aspects of LD biology.

Endoplasmic Reticulum–Mitochondria Membrane Contact Sites

ORP5/8

ORP5 as well as ORP8 seem to have pleiotropic functions at multiple MCSs. ORP5 and ORP8 have been shown to localize at the ER–mitochondria MCSs (Galmes et al., 2016). Immunofluorescence staining and immunogold electron microscopy revealed the localization of both ORP5 and ORP8 at the MCSs between the ER and mitochondria in HeLa cells. Fractionation experiments showing the enrichment of

ORP5 and ORP8 in mitochondria−associated ER membranes (MAMs) also support their localization at the ER–mitochondria MCSs. Localization of ORP5/8 to the ER–mitochondria MCSs does not require their PH domain but, instead, requires their novel binding partner, protein tyrosine phosphatase-interacting protein-51 (PTPIP51). PTPIP51 is the mitochondrial outer membrane protein that localized at the ER–mitochondria MCSs *via* interaction with VAPB and is involved in Ca^{2+} regulation at the mitochondria (Stoica et al., 2014). The ORD of ORP5 and ORP8 interacts with PTPIP51, and this interaction is required for their localization to the MCSs. Interestingly, though, the ORD mutant that abolishes PS binding cannot localize at the MCSs due to loss of binding to PTPIP51. Given that PS is transported to mitochondria to be converted to PE, ORP5/8 may contribute to PS transport to this organelle for PE synthesis. However, whether ORP5 and ORP8 mediate countertransport of PI4P and PS has not been confirmed. Nevertheless, the presence of PI, the precursor of PI4P, in the mitochondrial membrane was reported (Pemberton et al., 2020b; Zewe et al., 2020). Furthermore, the presence of PI4P-containing vesicles at the ER–mitochondria MCSs was also recently reported, although this pool of PI4P was provided via vesicular transport from the TGN after synthesis by PI4K3β (Nagashima et al., 2020). These observations suggest an interesting possibility of a direct involvement of PI4P in PS transport to mitochondria mediated by ORP5 and ORP8. These important aspects of whether and how ORP5/8 and PI4P contribute to such a process need further investigations.

DISCUSSION

In eukaryotes, more than 1,000 species of lipid molecules are coordinated to support fundamental cellular activities. In order to be fully functional, each lipid must be correctly positioned at the right place at the right time. Non-vesicular lipid transport by LTPs, including ORPs, controls such spatiotemporal positioning of lipids in cells (Holthuis and Menon, 2014). LTPs transfer their own set of lipid ligands between cellular membranes. ORPs, originally identified as oxysterol-binding proteins, have now been characterized as sensors or transporters of multiple lipids at MCSs. Biochemical studies as well as structural analysis have demonstrated that ORPs have a multiple-ligand repertoire including not only cholesterol but also phospholipids such as phosphoinositides, PS, and/or PC. Moreover, ORPs widely localized at multiple MCSs in cells to mediate transport of their own different lipid ligands, suggesting a functional diversity of ORPs to handle numerous cellular processes.

A unique functional property of ORPs is the lipid countertransport function at MCSs. Several, but not all, ORPs have been shown to exchange two different lipids: PI4P as a common driver-ligand and another lipid as a cargo-ligand. In the case of ORP5/8, they form ER–PM MCSs where PI4P and $PI(4,5)P_2$ are enriched, and transport PI4P along its concentration gradient to the ER where PI4P is dephosphorylated by the PI4P phosphatase Sac1 (Chung et al., 2015b; Ghai et al., 2017; Sohn et al., 2018). This PM-to-ER flow of PI4P ensures the ER-to-PM counter-directional transport of the cargo-ligand PS against its concentration gradient. PI4K3α and Sac1 generate a concentration gradient of PI4P, the driver of this lipid countertransport, while ORP5/8 are the operators of lipid exchange at MCSs.

Although a better understanding of the role of ORPs as lipid transporters/exchangers at MCSs is emerging, many questions arise and remain unanswered. First, we do not know whether all ORPs act as lipid exchangers. As described above, some ORPs function as lipid exchangers in a PI4P-dependent manner. Considering that PI4P is distributed at cellular membranes such as the PM, Golgi, endosomes, and lysosomes (Hammond et al., 2014) (**Figure 1**), PI4P-driven lipid countertransport would be widely operated by ORPs at MCSs between those PI4P-containing membranes and the ER. In fact, structural analysis has suggested that PI4P might be the common ligand of ORPs (Tong et al., 2013; Antonny et al., 2018). Nevertheless, some ORPs have shown no lipid exchange activity and behave as transporters or sensors of lipids, suggesting that all ORPs may not necessarily be an exchanger. Second, the dynamic nature of ORPs at MCSs need to be understood. From a metabolic standpoint, cellular lipids must be under tight control in their quantity, quality, and distribution in response to changes in cellular status. How do ORPs dynamically change their localization at MCSs? How is their lipid transport/countertransport activity regulated? Such questions, especially in the context of cellular lipid homeostasis, would be important issues. Third, technical and methodological advancement will greatly help our understanding of the role of ORPs. Detection or analysis of lipids at organellar levels by imaging techniques will continue to provide useful information. Manipulation of lipids as well as ORP proteins in cells by chemical biology or some other genetic techniques will also give us novel insights. Last but not the least, the physiological significance of ORP-mediated lipid transport/countertransport in the regulation of lipid metabolism as well as some other processes must be further investigated. In particular, how such lipid countertransport at MCSs directly regulates specific cellular functions other than lipid metabolism remains elusive. In addition, the physiological role of ORPs at tissue or animal levels is largely unknown. The physiological importance of the intracellular lipid transport/countertransport by LTPs is underscored by human diseases caused by defects in such regulation. As the connection between malfunctions of intracellular lipid transport and various human diseases becomes progressively evident, a comprehensive understanding of the role of intracellular lipid transport is increasingly important.

AUTHOR CONTRIBUTIONS

FN and AK wrote the manuscript and prepared the figures. Both authors contributed to the article and approved the submitted version.

REFERENCES

Albanesi, J., Wang, H., Sun, H. Q., Levine, B., and Yin, H. (2015). GABARAP-mediated targeting of PI4K2A/PI4KIIα to autophagosomes regulates PtdIns4P-dependent autophagosome-lysosome fusion. *Autophagy* 11, 2127–2129. doi: 10.1080/15548627.2015.1093718

Antonietta, De Matteis, M., Di Campli, A., and Godi, A. (2005). The role of the phosphoinositides at the Golgi complex. *Biochim. Biophys. Acta Mol. Cell Res.* 1744, 396–405. doi: 10.1016/j.bbamcr.2005.04.013

Antonny, B., Bigay, J., and Mesmin, B. (2018). The oxysterol-binding protein cycle: burning off PI(4)P to transport cholesterol. *Annu. Rev. Biochem.* 87, 809–837. doi: 10.1146/annurev-biochem-061516-044924

Balla, A., and Balla, T. (2006). Phosphatidylinositol 4-kinases: old enzymes with emerging functions. *Trends Cell Biol.* 16, 351–361. doi: 10.1016/j.tcb.2006.05.003

Balla, A., Tuymetova, G., Barshishat, M., Geiszt, M., and Balla, T. (2002). Characterization of type II phosphatidylinositol 4-kinase isoforms reveals association of the enzymes with endosomal vesicular compartments. *J. Biol. Chem.* 277, 20041–20050. doi: 10.1074/jbc.M111807200

Balla, T. (2013). Phosphoinositides: tiny lipids with giant impact on cell regulation. *Physiol. Rev.* 93, 1019–1137. doi: 10.1152/physrev.00028.2012

Balla, T., Kim, Y. J., Alvarez-Prats, A., and Pemberton, J. (2019). Lipid dynamics at contact sites between the endoplasmic reticulum and other organelles. *Annu. Rev. Cell Dev. Biol.* 35, 85–109. doi: 10.1146/annurev-cellbio-100818-125251

Balla, T., Sengupta, N., and Kim, Y. J. (2020). Lipid synthesis and transport are coupled to regulate membrane lipid dynamics in the endoplasmic reticulum. *Biochim. Biophys. Acta Mol. Cell Biol. Lipids* 1865:158461. doi: 10.1016/j.bbalip.2019.05.005

Barylko, B., Mao, Y. S., Wlodarski, P., Jung, G., Binns, D. D., Sun, H. Q., et al. (2009). Palmitoylation controls the catalytic activity and subcellular distribution of phosphatidylinositol 4-kinase IIα. *J. Biol. Chem.* 284, 9994–10003. doi: 10.1074/jbc.M900724200

Baskin, J. M., Wu, X., Christiano, R., Oh, M. S., Schauder, C. M., Gazzerro, E., et al. (2015). The leukodystrophy protein FAM126A (hyccin) regulates PtdIns(4)P synthesis at the plasma membrane. *Nat. Cell Biol.* 18, 132–138. doi: 10.1038/ncb3271

Blagoveshchenskaya, A., Cheong, F. Y., Rohde, H. M., Glover, G., Knödler, A., Nicolson, T., et al. (2008). Integration of Golgi trafficking and growth factor signaling by the lipid phosphatase SAC1. *J. Cell Biol.* 180, 803–812. doi: 10.1083/jcb.200708109

Bohnert, M. (2020). Tether me, tether me not-dynamic organelle contact sites in metabolic rewiring. *Dev. Cell* 54, 212–225. doi: 10.1016/j.devcel.2020.06.026

Bojjireddy, N., Guzman-Hernandez, M. L., Reinhard, N. R., Jović, M., and Balla, T. (2015). EFR3s are palmitoylated plasma membrane proteins that control responsiveness to G-protein-coupled receptors. *J. Cell. Sci.* 128, 118–128. doi: 10.1242/jcs.157495

Boura, E., and Nencka, R. (2015). Phosphatidylinositol 4-kinases_ function, structure, and inhibition. *Exp. Cell Res.* 337, 136–145. doi: 10.1016/j.yexcr.2015.03.028

Burgett, A. W. G., Poulsen, T. B., Wangkanont, K., Anderson, D. R., Kikuchi, C., Shimada, K., et al. (2011). Natural products reveal cancer cell dependence on oxysterol-binding proteins. *Nat. Chem. Biol.* 7, 639–647. doi: 10.1038/nchembio.625

Cabukusta, B., and Neefjes, J. (2018). Mechanisms of lysosomal positioning and movement. *Traffic* 19, 761–769. doi: 10.1111/tra.12587

Cantalupo, G., Alifano, P., Roberti, V., Bruni, C. B., and Bucci, C. (2001). Rab-interacting lysosomal protein (RILP): the Rab7 effector required for transport to lysosomes. *EMBO J.* 20, 683–693. doi: 10.1093/emboj/20.4.683

Cao, M., Wu, Y., Ashrafi, G., McCartney, A. J., Wheeler, H., Bushong, E. A., et al. (2017). Parkinson sac domain mutation in synaptojanin 1 impairs clathrin uncoating at synapses and triggers dystrophic changes in dopaminergic axons. *Neuron* 93, 882.e5–896.e5. doi: 10.1016/j.neuron.2017.01.019

Castellano, B. M., Thelen, A. M., Moldavski, O., Feltes, M., van der Welle, R. E. N., Mydock-McGrane, L., et al. (2017). Lysosomal cholesterol activates mTORC1 via an SLC38A9-Niemann-Pick C1 signaling complex. *Science* 355, 1306–1311. doi: 10.1126/science.aag1417

Charman, M., Colbourne, T. R., Pietrangelo, A., Kreplak, L., and Ridgway, N. D. (2014). Oxysterol-binding protein (OSBP)-related protein 4 (ORP4) is essential for cell proliferation and survival. *J. Biol. Chem.* 289, 15705–15717. doi: 10.1074/jbc.M114.571216

Chen, M., Wen, T., Horn, H. T., Chandrahas, V. K., Thapa, N., Choi, S., et al. (2020). The nuclear phosphoinositide response to stress. *Cell Cycle* 19, 268–289. doi: 10.1080/15384101.2019.1711316

Chung, J., Nakatsu, F., Baskin, J. M., and De Camilli, P. (2015a). Plasticity of PI4KIIIα interactions at the plasma membrane. *EMBO Rep.* 16, 312–320. doi: 10.15252/embr.201439151

Chung, J., Torta, F., Masai, K., Lucast, L., Czapla, H., Tanner, L. B., et al. (2015b). Intracellular transport. *PI*4P/phosphatidylserine countertransport at ORP5- and ORP8-mediated ER-plasma membrane contacts. *Science* 349, 428–432. doi: 10.1126/science.aab1370

de Saint-Jean, M., Delfosse, V., Douguet, D., Chicanne, G., Payrastre, B., Bourguet, W., et al. (2011). Osh4p exchanges sterols for phosphatidylinositol 4-phosphate between lipid bilayers. *J. Cell Biol.* 195, 965–978. doi: 10.1083/jcb.201104062

De Tito, S., Hervás, J. H., van Vliet, A. R., and Tooze, S. A. (2020). The golgi as an assembly line to the autophagosome. *Trends Biochem. Sci.* 45, 484–496. doi: 10.1016/j.tibs.2020.03.010

Del Bel, L. M., and Brill, J. A. (2018). Sac1, a lipid phosphatase at the interface of vesicular and nonvesicular transport. *Traffic* 19, 301–318. doi: 10.1111/tra.12554

Di Paolo, G., and De Camilli, P. (2006). Phosphoinositides in cell regulation and membrane dynamics. *Nature* 443, 651–657. doi: 10.1038/nature05185

Dickson, E. J., Jensen, J. B., Vivas, O., Kruse, M., Traynor-Kaplan, A. E., and Hille, B. (2016). Dynamic formation of ER-PM junctions presents a lipid phosphatase to regulate phosphoinositides. *J. Cell Biol.* 213, 33–48. doi: 10.1083/jcb.201508106

Dong, J., Du, X., Wang, H., Wang, J., Lu, C., Chen, X., et al. (2019). Allosteric enhancement of ORP1-mediated cholesterol transport by PI(4,5)P2/PI(3,4)P2. *Nat. Commun.* 10, 829–816. doi: 10.1038/s41467-019-08791-0

Dong, R., Saheki, Y., Swarup, S., Lucast, L., Harper, J. W., and De Camilli, P. (2016). Endosome-ER contacts control actin nucleation and retromer function through VAP-dependent regulation of PI4P. *Cell* 166, 408–423. doi: 10.1016/j.cell.2016.06.037

Dong, R., Zhu, T., Benedetti, L., Gowrishankar, S., Deng, H., Cai, Y., et al. (2018). The inositol 5-phosphatase INPP5K participates in the fine control of ER organization. *J. Cell Biol.* 217, 3577–3592. doi: 10.1083/jcb.201802125

D'Souza, R. S., Lim, J. Y., Turgut, A., Servage, K., Zhang, J., Orth, K., et al. (2020). Calcium-stimulated disassembly of focal adhesions mediated by an ORP3/IQSec1 complex. *eLife* 9:1381. doi: 10.7554/eLife.54113

Du, X., Kumar, J., Ferguson, C., Schulz, T. A., Ong, Y. S., Hong, W., et al. (2011). A role for oxysterol-binding protein-related protein 5 in endosomal cholesterol trafficking. *J. Cell Biol.* 192, 121–135. doi: 10.1083/jcb.201004142

Echevarría, W., Leite, M. F., Guerra, M. T., Zipfel, W. R., and Nathanson, M. H. (2003). Regulation of calcium signals in the nucleus by a nucleoplasmic reticulum. *Nat. Cell Biol.* 5, 440–446. doi: 10.1038/ncb980

Eden, E. R., Sanchez-Heras, E., Tsapara, A., Sobota, A., Levine, T. P., and Futter, C. E. (2016). Annexin A1 tethers membrane contact sites that mediate ER to endosome cholesterol transport. *Dev. Cell* 37, 473–483. doi: 10.1016/j.devcel.2016.05.005

Eisenberg-Bord, M., Shai, N., Schuldiner, M., and Bohnert, M. (2016). A tether is a tether is a tether: tethering at membrane contact sites. *Dev. Cell* 39, 395–409. doi: 10.1016/j.devcel.2016.10.022

Fournier, M. V., Guimarães, da Costa, F., Paschoal, M. E., Ronco, L. V., Carvalho, M. G., et al. (1999). Identification of a gene encoding a human oxysterol-binding protein-homologue: a potential general molecular marker for blood dissemination of solid tumors. *Cancer Res.* 59, 3748–3753.

Galmes, R., Houcine, A., van Vliet, A. R., Agostinis, P., Jackson, C. L., and Giordano, F. (2016). ORP5/ORP8 localize to endoplasmic reticulum-mitochondria contacts and are involved in mitochondrial function. *EMBO Rep.* 17, 800–810. doi: 10.15252/embr.201541108

Ghai, R., Du, X., Wang, H., Dong, J., Ferguson, C., Brown, A. J., et al. (2017). ORP5 and ORP8 bind phosphatidylinositol-4, 5-biphosphate (PtdIns(4,5)P 2) and regulate its level at the plasma membrane. *Nat. Commun.* 8:757. doi: 10.1038/s41467-017-00861-5

Godi, A., Pertile, P., Meyers, R., Marra, P., Di Tullio, G., Iurisci, C., et al. (1999). ARF mediates recruitment of PtdIns-4-OH kinase-beta and stimulates synthesis of PtdIns(4,5)P2 on the Golgi complex. *Nat. Cell Biol.* 1, 280–287. doi: 10.1038/12993

Goto, A., Charman, M., and Ridgway, N. D. (2016). Oxysterol-binding protein activation at endoplasmic reticulum-golgi contact sites reorganizes phosphatidylinositol 4-phosphate pools. *J. Biol. Chem.* 291, 1336–1347. doi: 10.1074/jbc.M115.682997

Gulyás, G., Sohn, M., Kim, Y. J., Varnai, P., and Balla, T. (2020). ORP3 phosphorylation regulates phosphatidylinositol 4-phosphate and Ca2+ dynamics at plasma membrane-ER contact sites. *J. Cell. Sci.* 133:jcs237388. doi: 10.1242/jcs.237388

Guo, S., Stolz, L. E., Lemrow, S. M., and York, J. D. (1999). SAC1-like domains of yeast SAC1, INP52, and INP53 and of human synaptojanin encode polyphosphoinositide phosphatases. *J. Biol. Chem.* 274, 12990–12995. doi: 10.1074/jbc.274.19.12990

Gurung, R., Tan, A., Ooms, L. M., McGrath, M. J., Huysmans, R. D., Munday, A. D., et al. (2003). Identification of a novel domain in two mammalian inositol-polyphosphate 5-phosphatases that mediates membrane ruffle localization. The inositol 5-phosphatase skip localizes to the endoplasmic reticulum and translocates to membrane ruffles following epidermal growth factor stimulation. *J. Biol. Chem.* 278, 11376–11385. doi: 10.1074/jbc.M209991200

Hammond, G. R. V., Machner, M. P., and Balla, T. (2014). A novel probe for phosphatidylinositol 4-phosphate reveals multiple pools beyond the Golgi. *J. Cell Biol.* 205, 113–126. doi: 10.1083/jcb.201312072

Hausser, A., Storz, P., Märtens, S., Link, G., Toker, A., and Pfizenmaier, K. (2005). Protein kinase D regulates vesicular transport by phosphorylating and activating phosphatidylinositol-4 kinase IIIβ at the Golgi complex. *Nat. Cell Biol.* 7, 880–886. doi: 10.1038/ncb1289

Helle, S. C. J., Kanfer, G., Kolar, K., Lang, A., Michel, A. H., and Kornmann, B. (2013). Organization and function of membrane contact sites. *Biochim. Biophys. Acta* 1833, 2526–2541. doi: 10.1016/j.bbamcr.2013.01.028

Henriques Silva, N., Vasconcellos Fournier, M., Pimenta, G., Pulcheri, W. A., Spector, N., da Costa, et al. (2003). HLM/OSBP2 is expressed in chronic myeloid leukemia. *Int. J. Mol. Med.* 12, 663–666.

Holthuis, J. C. M., and Levine, T. P. (2005). Lipid traffic: floppy drives and a superhighway. *Nat. Rev. Mol. Cell Biol.* 6, 209–220. doi: 10.1038/nrm1591

Holthuis, J. C. M., and Menon, A. K. (2014). Lipid landscapes and pipelines in membrane homeostasis. *Nature* 510, 48–57. doi: 10.1038/nature13474

Hsu, F., and Mao, Y. (2013). The Sac domain-containing phosphoinositide phosphatases: structure, function, and disease. *Front. Biol.* 8:395–407. doi: 10.1007/s11515-013-1258-y

Hsu, F., Hu, F., and Mao, Y. (2015). Spatiotemporal control of phosphatidylinositol 4-phosphate by Sac2 regulates endocytic recycling. *J. Cell Biol.* 209, 97–110. doi: 10.1083/jcb.201408027

Hung, C.-S., Lin, Y.-L., Wu, C.-I., Huang, C.-J., and Ting, L.-P. (2009). Suppression of hepatitis B viral gene expression by phosphoinositide 5-phosphatase SKIP. *Cell. Microbiol.* 11, 37–50. doi: 10.1111/j.1462-5822.2008.01235.x

Hynynen, R., Laitinen, S., Käkelä, R., Tanhuanpää, K., Lusa, S., Ehnholm, C., et al. (2005). Overexpression of OSBP-related protein 2 (ORP2) induces changes in cellular cholesterol metabolism and enhances endocytosis. *Biochem. J.* 390, 273–283. doi: 10.1042/BJ20042082

Hynynen, R., Suchanek, M., Spandl, J., Bäck, N., Thiele, C., and Olkkonen, V. M. (2009). OSBP-related protein 2 is a sterol receptor on lipid droplets that regulates the metabolism of neutral lipids. *J. Lipid Res.* 50, 1305–1315. doi: 10.1194/jlr.M800661-JLR200

Ijuin, T., and Takenawa, T. (2003). SKIP negatively regulates insulin-induced GLUT4 translocation and membrane ruffle formation. *Mol. Cell Biol.* 23, 1209–1220. doi: 10.1128/mcb.23.4.1209-1220.2003

Im, Y. J., Raychaudhuri, S., Prinz, W. A., and Hurley, J. H. (2005). Structural mechanism for sterol sensing and transport by OSBP-related proteins. *Nature* 437, 154–158. doi: 10.1038/nature03923

Johansson, M., Lehto, M., Tanhuanpää, K., Cover, T. L., and Olkkonen, V. M. (2005). The oxysterol-binding protein homologue ORP1L interacts with Rab7 and alters functional properties of late endocytic compartments. *Mol. Biol. Cell* 16, 5480–5492. doi: 10.1091/mbc.e05-03-0189

Johansson, M., Rocha, N., Zwart, W., Jordens, I., Janssen, L., Kuijl, C., et al. (2007). Activation of endosomal dynein motors by stepwise assembly of Rab7-RILP-p150Glued, ORP1L, and the receptor betalll spectrin. *J. Cell Biol.* 176, 459–471. doi: 10.1083/jcb.200606077

Jordens, I., Fernandez-Borja, M., Marsman, M., Dusseljee, S., Janssen, L., Calafat, J., et al. (2001). The Rab7 effector protein RILP controls lysosomal transport by inducing the recruitment of dynein-dynactin motors. *Curr. Biol.* 11, 1680–1685. doi: 10.1016/s0960-9822(01)00531-0

Judith, D., Jefferies, H. B. J., Boeing, S., Frith, D., Snijders, A. P., and Tooze, S. A. (2019). ATG9A shapes the forming autophagosome through Arfaptin 2 and phosphatidylinositol 4-kinase IIIβ. *J. Cell Biol.* 218, 1634–1652. doi: 10.1083/jcb.201901115

Kuge, O., Nishijima, M., and Akamatsu, Y. (1991). A Chinese hamster cDNA encoding a protein essential for phosphatidylserine synthase I activity. *J. Biol. Chem.* 266, 24184–24189. doi: 10.1016/s0021-9258(18)54410-0

Kuge, O., Saito, K., and Nishijima, M. (1997). Cloning of a Chinese hamster ovary (CHO) cDNA encoding phosphatidylserine synthase (PSS) II, overexpression of which suppresses the phosphatidylserine biosynthetic defect of a PSS I-lacking mutant of CHO-K1 cells. *J. Biol. Chem.* 272, 19133–19139. doi: 10.1074/jbc.272.31.19133

Lehto, M., Hynynen, R., Karjalainen, K., Kuismanen, E., Hyvärinen, K., and Olkkonen, V. M. (2005). Targeting of OSBP-related protein 3 (ORP3) to endoplasmic reticulum and plasma membrane is controlled by multiple determinants. *Exp. Cell Res.* 310, 445–462. doi: 10.1016/j.yexcr.2005.08.003

Lehto, M., Laitinen, S., Chinetti, G., Johansson, M., Ehnholm, C., Staels, B., et al. (2001). The OSBP-related protein family in humans. *J. Lipid Res.* 42, 1203–1213. doi: 10.1016/s0022-2275(20)31570-4

Lemmon, M. A. (2008). Membrane recognition by phospholipid-binding domains. *Nat. Rev. Mol. Cell Biol.* 9, 99–111. doi: 10.1038/nrm2328

Lenz, W. D., and Majewski, F. (1974). A generalized disorders of the connective tissues with progeria, choanal atresia, symphalangism, hypoplasia of dentine and craniodiaphyseal hypostosis. *Birth Defects Orig. Artic Ser.* 10, 133–136.

Lev, S. (2012). Nonvesicular lipid transfer from the endoplasmic reticulum. *Cold Spring Harb. Perspect. Biol.* 4:a013300. doi: 10.1101/cshperspect.a013300

Levin, R., Hammond, G. R. V., Balla, T., De Camilli, P., Fairn, G. D., and Grinstein, S. (2017). Multiphasic dynamics of phosphatidylinositol 4-phosphate during phagocytosis. *Mol. Biol. Cell* 28, 128–140. doi: 10.1091/mbc.E16-06-0451

Levine, T. P., and Munro, S. (1998). The pleckstrin homology domain of oxysterol-binding protein recognises a determinant specific to Golgi membranes. *Curr. Biol.* 8, 729–739. doi: 10.1016/s0960-9822(98)70296-9

Levine, T. P., and Munro, S. (2002). Targeting of Golgi-specific pleckstrin homology domains involves both PtdIns 4-kinase-dependent and -independent components. *Curr. Biol.* 12, 695–704. doi: 10.1016/s0960-9822(02)00779-0

Levin-Konigsberg, R., Montaño-Rendón, F., Keren-Kaplan, T., Li, R., Ego, B., Mylvaganam, S., et al. (2019). Phagolysosome resolution requires contacts with the endoplasmic reticulum and phosphatidylinositol-4-phosphate signalling. *Nat. Cell Biol.* 21, 1234–1247. doi: 10.1038/s41556-019-0394-2

Lim, C.-Y., Davis, O. B., Shin, H. R., Zhang, J., Berdan, C. A., Jiang, X., et al. (2019). ER-lysosome contacts enable cholesterol sensing by mTORC1 and drive aberrant growth signalling in Niemann-Pick type C. *Nat. Cell Biol.* 21, 1206–1218. doi: 10.1038/s41556-019-0391-5

Liu, X., and Ridgway, N. D. (2014). Characterization of the sterol and phosphatidylinositol 4-phosphate binding properties of Golgi-associated OSBP-related protein 9 (ORP9). *PLoS One* 9:e108368. doi: 10.1371/journal.pone.0108368

Loewen, C. J. R., Roy, A., and Levine, T. P. (2003). A conserved ER targeting motif in three families of lipid binding proteins and in Opi1p binds VAP. *EMBO J.* 22, 2025–2035. doi: 10.1093/emboj/cdg201

Lu, D., Sun, H. Q., Wang, H., Barylko, B., Fukata, Y., Fukata, M., et al. (2012). Phosphatidylinositol 4-Kinase IIÎ ± Is palmitoylated by golgi-localized palmitoyltransferases in cholesterol-dependent manner. *J. Biol. Chem.* 287, 21856–21865. doi: 10.1074/jbc.M112.348094

Machaca, K. (2020). Ca2+ signaling and lipid transfer "pas a deux" at ER-PM contact sites orchestrate cell migration. *Cell Calc.* 89:102226. doi: 10.1016/j.ceca.2020.102226

Maeda, K., Anand, K., Chiapparino, A., Kumar, A., Poletto, M., Kaksonen, M., et al. (2013). Interactome map uncovers phosphatidylserine transport by oxysterol-binding proteins. *Nature* 501, 257–261. doi: 10.1038/nature12430

Mani, M., Lee, S. Y., Lucast, L., Cremona, O., Di Paolo, G., De Camilli, P., et al. (2007). The dual phosphatase activity of synaptojanin1 is required for both efficient synaptic vesicle endocytosis and reavailability at nerve terminals. *Neuron* 56, 1004–1018. doi: 10.1016/j.neuron.2007.10.032

Marat, A. L., Wallroth, A., Lo, W.-T., Müller, R., Norata, G. D., Falasca, M., et al. (2017). mTORC1 activity repression by late endosomal phosphatidylinositol 3,4-bisphosphate. *Science* 356, 968–972. doi: 10.1126/science.aaf8310

Mathieu, M., Martin-Jaular, L., Lavieu, G., and Théry, C. (2019). Specificities of secretion and uptake of exosomes and other extracellular vesicles for cell-to-cell communication. *Nat. Cell Biol.* 21, 9–17. doi: 10.1038/s41556-018-0250-9

McGrath, M. J., Eramo, M. J., Gurung, R., Sriratana, A., Gehrig, S. M., Lynch, G. S., et al. (2021). Defective lysosome reformation during autophagy causes skeletal muscle disease. *J. Clin. Invest.* 131:e135124. doi: 10.1172/JCI135124

McPherson, P. S., Garcia, E. P., Slepnev, V. I., David, C., Zhang, X., Grabs, D., et al. (1996). A presynaptic inositol-5-phosphatase. *Nature* 379, 353–357. doi: 10.1038/379353a0

Mesmin, B., and Antonny, B. (2016). The counterflow transport of sterols and PI4P. *Biochim. Biophys. Acta* 1861, 940–951. doi: 10.1016/j.bbalip.2016.02.024

Mesmin, B., Bigay, J., Moser, von Filseck, J., Lacas-Gervais, S., Drin, G., et al. (2013). A four-step cycle driven by PI(4)P hydrolysis directs sterol/PI(4)P exchange by the ER-Golgi tether OSBP. *Cell* 155, 830–843. doi: 10.1016/j.cell.2013.09.056

Mesmin, B., Bigay, J., Polidori, J., Jamecna, D., Lacas-Gervais, S., and Antonny, B. (2017). Sterol transfer, PI4P consumption, and control of membrane lipid order by endogenous OSBP. *EMBO J.* 36, 3156–3174. doi: 10.15252/embj.201796687

Mochizuki, S., Miki, H., Zhou, R., Kido, Y., Nishimura, W., Kikuchi, M., et al. (2018). Oxysterol-binding protein-related protein (ORP) 6 localizes to the ER and ER-plasma MCS sites and is involved in the turnover of PI4P in cerebellar granule neurons. *Exp. Cell Res.* 370, 601–612. doi: 10.1016/j.yexcr.2018.07.025

Moser, von Filseck, J., Čopič, A., Delfosse, V., Vanni, S., Jackson, C. L., et al. (2015). Intracellular transport. Phosphatidylserine transport by ORP/Osh proteins is driven by phosphatidylinositol 4-phosphate. *Science* 349, 432–436. doi: 10.1126/science.aab1346

Murphy, S. E., and Levine, T. P. (2016). VAP, a versatile access point for the endoplasmic reticulum: review and analysis of FFAT-like motifs in the VAPome. *Biochim. Biophys. Acta* 1861, 952–961. doi: 10.1016/j.bbalip.2016.02.009

Nagashima, S., Tábara, L.-C., Tilokani, L., Paupe, V., Anand, H., Pogson, J. H., et al. (2020). Golgi-derived PI(4)P-containing vesicles drive late steps of mitochondrial division. *Science* 367, 1366–1371. doi: 10.1126/science.aax6089

Nakatsu, F., Baskin, J. M., Chung, J., Tanner, L. B., Shui, G., Lee, S. Y., et al. (2012). PtdIns4P synthesis by PI4KIIIα at the plasma membrane and its impact on plasma membrane identity. *J. Cell Biol.* 199, 1003–1016. doi: 10.1083/jcb.201206095

Nakatsu, F., Messa, M., Nández, R., Czapla, H., Zou, Y., Strittmatter, S. M., et al. (2015). Sac2/INPP5F is an inositol 4-phosphatase that functions in the endocytic pathway. *J. Cell Biol.* 209, 85–95. doi: 10.1083/jcb.201409064

Nemoto, Y., Wenk, M. R., Watanabe, M., Daniell, L., Murakami, T., Ringstad, N., et al. (2001). Identification and characterization of a synaptojanin 2 splice isoform predominantly expressed in nerve terminals. *J. Biol. Chem.* 276, 41133–41142. doi: 10.1074/jbc.M106404200

Ngo, M., and Ridgway, N. D. (2009). Oxysterol binding protein-related Protein 9 (ORP9) is a cholesterol transfer protein that regulates Golgi structure and function. *Mol. Biol. Cell* 20, 1388–1399. doi: 10.1091/mbc.e08-09-0905

Nguyen, P. M., Gandasi, N. R., Xie, B., Sugahara, S., Xu, Y., and Idevall-Hagren, O. (2019). The PI(4)P phosphatase Sac2 controls insulin granule docking and release. *J. Cell Biol.* 218, 3714–3729. doi: 10.1083/jcb.201903121

Nishimura, T., Gecht, M., Covino, R., Hummer, G., Surma, M. A., Klose, C., et al. (2019). Osh proteins control nanoscale lipid organization necessary for PI(4,5)P2 synthesis. *Mol. Cell* 75, 1043.e8–1057.e8. doi: 10.1016/j.molcel.2019.06.037

Olkkonen, V. M. (2015). OSBP-related protein family in lipid transport over membrane contact sites. *Lipid Insights* 8s1, 1726–1729. doi: 10.4137/LPI.S31726

Pemberton, J. G., Kim, Y. J., and Balla, T. (2020a). Integrated regulation of the phosphatidylinositol cycle and phosphoinositide-driven lipid transport at ER-PM contact sites. *Traffic* 21, 200–219. doi: 10.1111/tra.12709

Pemberton, J. G., Kim, Y. J., Humpolickova, J., Eisenreichova, A., Sengupta, N., Tóth, D. J., et al. (2020b). Defining the subcellular distribution and metabolic channeling of phosphatidylinositol. *J. Cell Biol.* 219, 213–234. doi: 10.1083/jcb.201906130

Péresse, T., Kovacs, D., Subra, M., Bigay, J., Tsai, M.-C., Polidori, J., et al. (2020). Molecular and cellular dissection of the oxysterol-binding protein cycle through a fluorescent inhibitor. *J. Biol. Chem.* 295, 4277–4288. doi: 10.1074/jbc.ra119.012012

Phillips, M. J., and Voeltz, G. K. (2015). Structure and function of ER membrane contact sites with other organelles. *Nat. Publ. Group* 17, 69–82. doi: 10.1038/nrm.2015.8

Pietrangelo, A., and Ridgway, N. D. (2018). Bridging the molecular and biological functions of the oxysterol-binding protein family. *Cell. Mol. Life Sci.* 75, 3079–3098. doi: 10.1007/s00018-018-2795-y

Pirruccello, M., and De Camilli, P. (2012). Inositol 5-phosphatases: insights from the Lowe syndrome protein OCRL. *Trends Biochem. Sci.* 37, 134–143. doi: 10.1016/j.tibs.2012.01.002

Prinz, W. A., Toulmay, A., and Balla, T. (2019). The functional universe of membrane contact sites. *Nat. Rev. Mol. Cell Biol.* 0, 1–18. doi: 10.1038/s41580-019-0180-9

Rai, A., Pathak, D., Thakur, S., Singh, S., Dubey, A. K., and Mallik, R. (2016). Dynein clusters into lipid microdomains on phagosomes to drive rapid transport toward lysosomes. *Cell* 164, 722–734. doi: 10.1016/j.cell.2015.12.054

Rameh, L. E., Arvidsson, A. K., Carraway, K. L., Couvillon, A. D., Rathbun, G., Crompton, A., et al. (1997). A comparative analysis of the phosphoinositide binding specificity of pleckstrin homology domains. *J. Biol. Chem.* 272, 22059–22066. doi: 10.1074/jbc.272.35.22059

Ramos, A. R., Ghosh, S., Suhel, T., Chevalier, C., Obeng, E. O., Fafilek, B., et al. (2020). Phosphoinositide 5-phosphatases SKIP and SHIP2 in ruffles, the endoplasmic reticulum and the nucleus: an update. *Adv. Biol. Regul.* 75:100660. doi: 10.1016/j.jbior.2019.100660

Raposo, G., and Stoorvogel, W. (2013). Extracellular vesicles: exosomes, microvesicles, and friends. *J. Cell Biol.* 200, 373–383. doi: 10.1083/jcb.201212113

Rappa, G., Santos, M. F., Green, T. M., Karbanová, J., Hassler, J., Bai, Y., et al. (2017). Nuclear transport of cancer extracellular vesicle-derived biomaterials through nuclear envelope invagination-associated late endosomes. *Oncotarget* 8, 14443–14461. doi: 10.18632/oncotarget.14804

Raychaudhuri, S., and Prinz, W. A. (2010). The diverse functions of oxysterol-binding proteins. *Annu. Rev. Cell Dev. Biol.* 26, 157–177. doi: 10.1146/annurev.cellbio.042308.113334

Raychaudhuri, S., Im, Y. J., Hurley, J. H., and Prinz, W. A. (2006). Nonvesicular sterol movement from plasma membrane to ER requires oxysterol-binding protein-related proteins and phosphoinositides. *J. Cell Biol.* 173, 107–119. doi: 10.1083/jcb.200510084

Reinisch, K. M., and Prinz, W. A. (2021). Mechanisms of nonvesicular lipid transport. *J. Cell Biol.* 220:e202012058. doi: 10.1083/jcb.202012058

Rocha, N., Kuijl, C., van der Kant, R., Janssen, L., Houben, D., Janssen, H., et al. (2009). Cholesterol sensor ORP1L contacts the ER protein VAP to control

Rab7-RILP-p150 Glued and late endosome positioning. *J. Cell Biol.* 185, 1209–1225. doi: 10.1083/jcb.200811005

Santos, A. L., and Preta, G. (2018). Lipids in the cell: organisation regulates function. *Cell. Mol. Life Sci.* 75, 1909–1927. doi: 10.1007/s00018-018-2765-4

Santos, M. F., Rappa, G., Karbanová, J., Kurth, T., Corbeil, D., and Lorico, A. (2018). VAMP-associated protein-A and oxysterol-binding protein-related protein 3 promote the entry of late endosomes into the nucleoplasmic reticulum. *J. Biol. Chem.* 293, 13834–13848. doi: 10.1074/jbc.RA118.003725

Santos, N. C., Girik, V., and Nunes-Hasler, P. (2020). ORP5 and ORP8: sterol sensors and phospholipid transfer proteins at membrane contact sites? *Biomolecules* 10:928. doi: 10.3390/biom10060928

Sasaki, J., Ishikawa, K., Arita, M., and Taniguchi, K. (2011). ACBD3-mediated recruitment of PI4KB to picornavirus RNA replication sites. *EMBO J.* 31, 754–766. doi: 10.1038/emboj.2011.429

Schroeder, C. M., Ostrem, J. M. L., Hertz, N. T., and Vale, R. D. (2014). A Ras-like domain in the light intermediate chain bridges the dynein motor to a cargo-binding region. *eLife* 3:e03351. doi: 10.7554/eLife.03351

Scorrano, L., De Matteis, M. A., Emr, S., Giordano, F., Hajnóczky, G., Kornmann, B., et al. (2019). Coming together to define MCS sites. *Nat. Commun.* 10, 1287–1211. doi: 10.1038/s41467-019-09253-3

Silva, N. H., Pimenta, G., Pulcheri, W. A., Fournier, M. V., Spector, N., da Costa, et al. (2001). Detection of messenger RNA in leukocytes or plasma of patients with chronic myeloid leukemia. *Oncol. Rep.* 8, 693–696. doi: 10.3892/or.8.3.693

Sobajima, T., Yoshimura, S.-I., Maeda, T., Miyata, H., Miyoshi, E., and Harada, A. (2018). The Rab11-binding protein RELCH/KIAA1468 controls intracellular cholesterol distribution. *J. Cell Biol.* 217, 1777–1796. doi: 10.1083/jcb.201709123

Sohn, M., Ivanova, P., Brown, H. A., Tóth, D. J., Varnai, P., Kim, Y. J., et al. (2016). Lenz-Majewski mutations in PTDSS1 affect phosphatidylinositol 4-phosphate metabolism at ER-PM and ER-Golgi junctions. *Proc. Natl. Acad. Sci. U.S.A.* 113, 4314–4319. doi: 10.1073/pnas.1525719113

Sohn, M., Korzeniowski, M., Zewe, J. P., Wills, R. C., Hammond, G. R. V., Humpolickova, J., et al. (2018). PI(4,5)P2 controls plasma membrane PI4P and PS levels via ORP5/8 recruitment to ER-PM contact sites. *J. Cell Biol.* 217, 1797–1813. doi: 10.1083/jcb.201710095

Soni, K. G., Mardones, G. A., Sougrat, R., Smirnova, E., Jackson, C. L., and Bonifacino, J. S. (2009). Coatomer-dependent protein delivery to lipid droplets. *J. Cell Sci.* 122, 1834–1841. doi: 10.1242/jcs.045849

Sousa, S. B., Jenkins, D., Chanudet, E., Tasseva, G., Ishida, M., Anderson, G., et al. (2014). Gain-of-function mutations in the phosphatidylserine synthase 1 (PTDSS1) gene cause Lenz-Majewski syndrome. *Nat. Genet.* 46, 70–76. doi: 10.1038/ng.2829

Stefan, C. J., Manford, A. G., Baird, D., Yamada-Hanff, J., Mao, Y., and Emr, S. D. (2011). Osh proteins regulate phosphoinositide metabolism at ER-plasma membrane contact sites. *Cell* 144, 389–401. doi: 10.1016/j.cell.2010.12.034

Stefan, C. J., Trimble, W. S., Grinstein, S., Drin, G., Reinisch, K., De Camilli, P., et al. (2017). Membrane dynamics and organelle biogenesis-lipid pipelines and vesicular carriers. *BMC Biol.* 15:102. doi: 10.1186/s12915-017-0432-0

Stoica, R., De Vos, K. J., Paillusson, S., Mueller, S., Sancho, R. M., Lau, K.-F., et al. (2014). ER-mitochondria associations are regulated by the VAPB-PTPIP51 interaction and are disrupted by ALS/FTD-associated TDP-43. *Nat. Commun.* 5, 3996–3912. doi: 10.1038/ncomms4996

Suchanek, M., Hynynen, R., Wohlfahrt, G., Lehto, M., Johansson, M., Saarinen, H., et al. (2007). The mammalian oxysterol-binding protein-related proteins (ORPs) bind 25-hydroxycholesterol in an evolutionarily conserved pocket. *Biochem. J.* 405, 473–480. doi: 10.1042/BJ20070176

Taylor, F. R., Saucier, S. E., Shown, E. P., Parish, E. J., and Kandutsch, A. A. (1984). Correlation between oxysterol binding to a cytosolic binding protein and potency in the repression of hydroxymethylglutaryl coenzyme A reductase. *J. Biol. Chem.* 259, 12382–12387. doi: 10.1016/s0021-9258(18)90757-x

Tong, J., Yang, H., Yang, H., Eom, S. H., and Im, Y. J. (2013). Structure of Osh3 reveals a conserved mode of phosphoinositide binding in oxysterol-binding proteins. *Structure* 21, 1203–1213. doi: 10.1016/j.str.2013.05.007

Udagawa, O., Ito, C., Ogonuki, N., Sato, H., Lee, S., Tripvanuntakul, P., et al. (2014). Oligo-astheno-teratozoospermia in mice lacking ORP4, a sterol-binding protein in the OSBP-related protein family. *Genes Cells* 19, 13–27. doi: 10.1111/gtc.12105

van Meer, G., and de Kroon, A. I. P. M. (2011). Lipid map of the mammalian cell. *J. Cell. Sci.* 124, 5–8. doi: 10.1242/jcs.071233

van Meer, G., Voelker, D. R., and Feigenson, G. W. (2008). Membrane lipids: where they are and how they behave. *Nat. Rev. Mol. Cell Biol.* 9, 112–124. doi: 10.1038/nrm2330

van Niel, G., D'Angelo, G., and Raposo, G. (2018). Shedding light on the cell biology of extracellular vesicles. *Nat. Rev. Mol. Cell Biol.* 19, 213–228. doi: 10.1038/nrm.2017.125

Vance, J. E. (2014). Phospholipid synthesis and transport in mammalian cells. *Traffic* 16, 1–18. doi: 10.1111/tra.12230

Venditti, R., Masone, M. C., Rega, L. R., Di Tullio, G., Santoro, M., Polishchuk, E., et al. (2019a). The activity of Sac1 across ER–TGN contact sites requires the four-phosphate-adaptor-protein-1. *J. Cell Biol.* 218, 783–797. doi: 10.1083/jcb.201812021

Venditti, R., Rega, L. R., Masone, M. C., Santoro, M., Polishchuk, E., Sarnataro, D., et al. (2019b). Molecular determinants of ER-Golgi contacts identified through a new FRET-FLIM system. *J. Cell Biol.* 218, 1055–1065. doi: 10.1083/jcb.201812020

Vihervaara, T., Uronen, R.-L., Wohlfahrt, G., Björkhem, I., Ikonen, E., and Olkkonen, V. M. (2011). Sterol binding by OSBP-related protein 1L regulates late endosome motility and function. *Cell. Mol. Life Sci.* 68, 537–551. doi: 10.1007/s00018-010-0470-z

Wang, C., JeBailey, L., and Ridgway, N. D. (2002). Oxysterol-binding-protein (OSBP)-related protein 4 binds 25-hydroxycholesterol and interacts with vimentin intermediate filaments. *Biochem. J.* 361, 461–472. doi: 10.1042/0264-6021:3610461

Wang, H., Sun, H. Q., Zhu, X., Zhang, L., Albanesi, J., Levine, B., et al. (2015). GABARAPs regulate PI4P-dependent autophagosome:lysosome fusion. *Proc. Natl. Acad. Sci. U.S.A.* 112, 7015–7020. doi: 10.1073/pnas.1507263112

Wang, Y. J., Wang, J., Sun, H. Q., Martinez, M., Sun, Y. X., Macia, E., et al. (2003). Phosphatidylinositol 4 phosphate regulates targeting of clathrin adaptor AP-1 complexes to the Golgi. *Cell* 114, 299–310. doi: 10.1016/s0092-8674(03)00603-2

Weber-Boyvat, M., Kentala, H., Lilja, J., Vihervaara, T., Hanninen, R., Zhou, Y., et al. (2015a). OSBP-related protein 3 (ORP3) coupling with VAMP-associated protein A regulates R-Ras activity. *Exp. Cell Res.* 331, 278–291. doi: 10.1016/j.yexcr.2014.10.019

Weber-Boyvat, M., Kentala, H., Peränen, J., and Olkkonen, V. M. (2015b). Ligand-dependent localization and function of ORP-VAP complexes at membrane contact sites. *Cell. Mol. Life Sci.* 72, 1967–1987. doi: 10.1007/s00018-014-1786-x

Wijdeven, R. H., Janssen, H., Nahidiazar, L., Janssen, L., Jalink, K., Berlin, I., et al. (2016). Cholesterol and ORP1L-mediated ER contact sites control autophagosome transport and fusion with the endocytic pathway. *Nat. Commun.* 7, 11808–11814. doi: 10.1038/ncomms11808

Wilfling, F., Thiam, A. R., Olarte, M.-J., Wang, J., Beck, R., Gould, T. J., et al. (2014). Arf1/COPI machinery acts directly on lipid droplets and enables their connection to the ER for protein targeting. *eLife* 3:e01607. doi: 10.7554/eLife.01607

Wong, K., Meyers, R., and Cantley, L. C. (1997). Subcellular locations of phosphatidylinositol 4-kinase isoforms. *J. Biol. Chem.* 272, 13236–13241. doi: 10.1074/jbc.272.20.13236

Wong, L. H., Čopič, A., and Levine, T. P. (2017). Advances on the transfer of lipids by lipid transfer proteins. *Trends Biochem. Sci.* 42, 516–530. doi: 10.1016/j.tibs.2017.05.001

Wong, L. H., Gatta, A. T., and Levine, T. P. (2019). Lipid transfer proteins: the lipid commute via shuttles, bridges and tubes. *Nat. Rev. Mol. Cell Biol.* 20, 85–101. doi: 10.1038/s41580-018-0071-5

Wu, H., Carvalho, P., and Voeltz, G. K. (2018). Here, there, and everywhere: the importance of ER membrane contact sites. *Science* 361:eaan5835. doi: 10.1126/science.aan5835

Wyles, J. P., Perry, R. J., and Ridgway, N. D. (2007). Characterization of the sterol-binding domain of oxysterol-binding protein (OSBP)-related protein 4 reveals a novel role in vimentin organization. *Exp. Cell Res.* 313, 1426–1437. doi: 10.1016/j.yexcr.2007.01.018

Xu, Y., Liu, Y., Ridgway, N. D., and McMaster, C. R. (2001). Novel members of the human oxysterol-binding protein family bind phospholipids and

regulate vesicle transport. *J. Biol. Chem.* 276, 18407–18414. doi: 10.1074/jbc.M101204200

Zerial, M., and McBride, H. (2001). Rab proteins as membrane organizers. *Nat. Rev. Mol. Cell Biol.* 2, 107–117. doi: 10.1038/35052055

Zewe, J. P., Miller, A. M., Sangappa, S., Wills, R. C., Goulden, B. D., and Hammond, G. R. V. (2020). Probing the subcellular distribution of phosphatidylinositol reveals a surprising lack at the plasma membrane. *J. Cell Biol.* 219, 253–219. doi: 10.1083/jcb.201906127

Zhao, K., and Ridgway, N. D. (2017). Oxysterol-binding protein-related protein 1L regulates cholesterol egress from the endo-lysosomal system. *Cell Rep.* 19, 1807–1818. doi: 10.1016/j.celrep.2017.05.028

Zhao, K., Foster, J., and Ridgway, N. D. (2020). Oxysterol-binding protein-related protein 1 variants have opposing cholesterol transport activities from the endolysosomes. *Mol. Biol. Cell* 31, 793–802. doi: 10.1091/mbc.E19-12-0697

Zhong, W., Yi, Q., Xu, B., Li, S., Wang, T., Liu, F., et al. (2016). ORP4L is essential for T-cell acute lymphoblastic leukemia cell survival. *Nat. Commun.* 7, 12702–12714.

Conflict of Interest: The authors declare that the research was conducted in the absence of any commercial or financial relationships that could be construed as a potential conflict of interest.

Advantages of publishing in Frontiers

OPEN ACCESS
Articles are free to read for greatest visibility and readership

FAST PUBLICATION
Around 90 days from submission to decision

HIGH QUALITY PEER-REVIEW
Rigorous, collaborative, and constructive peer-review

TRANSPARENT PEER-REVIEW
Editors and reviewers acknowledged by name on published articles

Frontiers
Avenue du Tribunal-Fédéral 34
1005 Lausanne | Switzerland

Visit us: www.frontiersin.org
Contact us: frontiersin.org/about/contact

REPRODUCIBILITY OF RESEARCH
Support open data and methods to enhance research reproducibility

DIGITAL PUBLISHING
Articles designed for optimal readership across devices

FOLLOW US
@frontiersin

IMPACT METRICS
Advanced article metrics track visibility across digital media

EXTENSIVE PROMOTION
Marketing and promotion of impactful research

LOOP RESEARCH NETWORK
Our network increases your article's readership